WELCOME TO THE CONFERENCE ON ADVANCES IN FUNCTIONAL MATERIALS 2016

Overview

After the grand success of the 1st edition of AFM-2015 conference, we, the Conference Co-chairs and the organizing committee welcome you again to the 2nd International Conference on Advances in Functional Materials (AFM 2016) that is going to be held at International Convention Center (ICC) from August 8-11, 2016 at the beautiful Jeju Island of South Korea.

The objective of this international event is to present and share up to date researches and findings in the field of functional materials science. The conference will provide a platform for the researchers to find global partners for future collaboration. More than 1500 abstracts have been received from all over the world. A large number of participants including scientists, engineers, educators and students from all over the world will attend this event.

In order to maintain the quality of the presented work the abstracts have been reviewed by international researchers carefully to maintain the quality of the work presented. Likewise, full length manuscripts will undergo peer review system and only accepted manuscripts will be published in Elsevier journal Materials Research Bulletin (Impact Factor: 2.435).

In addition, the participants of the conference will also be able to attend the talks from our highly reputed Plenary and Keynote Speakers from all over the world.

The venue of the conference is always carefully chosen for you to spend quality and enjoyable time on and off the conference. Jeju Island is an ideal location for a convention combined with leisure and recreation. Magnificent nature, abundant tourist assets, convenient access and lodgings-a warm and friendly people: Jeju is a worldly renowned resort in terms of its recreation and tourism. AFM 2016 is going to be held at this gorgeous island in a top-notch convention center: ICC JEJU.

We are warm-heartedly extending our welcome to you and hope that you will join us in Jeju Island for a stimulating Conference, a friendly gathering amongst friends and simply a good time.

Co-Chairs

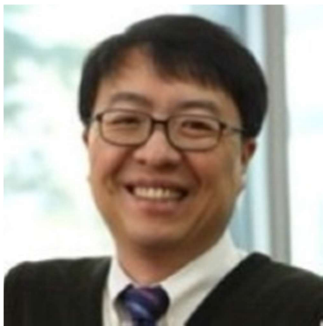

PROF. DAE JOON KANG
Sungkyunkwan University, Korea

PROF. TAE JIN KIM
Stony Brook University, USA

PROF. IMRAN SHAKIR
King Saud University, KSA

Advisory Committee

Co-Chairs

Prof. Dae Joon Kang (Sungkyunkwan University, Jangan-gu Suwon, Korea)
Prof. Tae Jin Kim (Stony Brook University, Stony Brook, USA)
Prof. Imran Shakir (King Saud University, Saudi Arabia)

International Advisory Committee

Dr. Zhong Lin Wang (Georgia Tech, USA)
Prof. Hui-Ming Cheng (Chinese Academy of Sciences, China)
Dr. Kazuhiro Takanabe (King Abdullah University of Science and Technology (KAUST))
Prof. Vivek Polshettiwar (Tata Institute of Fundamental Research (TIFR), India)
Prof. Arindam Ghosh (Indian Institute of Science, India)
Prof. Li Zhang (The Chinese University of Hong Kong)
Prof. Rizwan Raza (COMSATS, Pakistan)
Prof. Jason Jieshan Qiu (Dalian University of Technology, China)
Dr. Abbas Amini (University of Western Sydney, Australia)
Dr. Jose Rodriguez (Brookhaven National Laboratory Upton, NY, USA)
Dr. Rajeev S. Assary (Argonne National Laboratory, Lemont IL, USA)
Prof. Bin Zhu (KTH, Stockholm, Sweden)
Prof. N. Ali (Chairman CNC Coatings, UK)
Prof. Mohamed Bououdina (University of Bahrain)
Prof. Jean-Marie Basset (Director, KAUST Catalysis Research Center)
Prof. Fuat Celik (Rutgers University, New Jersey, USA)
Prof. Chang-Yong Nam (Brookhaven National Lab, BNL)
Prof. Xiangfeng Duan (University of California Los Angeles)
Dr. Arun Kumar (Amity University, Noida, India)
Dr. Michael De Volder (University of Cambridge, UK)

Local Advisory Committee

Prof. Hyeon Suk Shin, **Committee Head** (Ulsan National Institute of Science and Technology, Korea)
Prof. Kwanghee Lee (Gwangju Institute of Science & Technology - GIST, Korea)
Prof. In Sik Nam (Pohang University of Science and Technology, Korea)

PLENARY SPEAKERS

1. Prof. Klaus Mullen — Max Planck Institute of Polymeric Research, Germany
2. Professor Tal MargaLith — University of California, Santa Barbara (UCSB)

Prof. Klaus Mullen

Director, Max Planck Institute of Polymeric Research, Germany

Brief Biography: *Klaus Müllen's broad research interests range from the development of new polymer-forming reactions, including methods of organometallic chemistry, to the chemistry and physics of small molecules, graphenes, dendrimers and biosynthetic hybrids. His work further encompasses the formation of multi-dimensional polymers with complex shape-persistent architectures, nanocomposites, and molecular materials with liquid crystalline properties for electronic and optoelectronic devices*

Abstract Title: Graphene Nanoribbons and Graphene Molecules as Multitalents of Material Science

Graphenes and graphene nanoribbons (GNRs) are praised as multifunctional wonder materials and rich playgrounds for physicists. Indeed, GNRs hold promise as a new family of semiconductors which are superior to classical conjugated polymers. Above all, graphene as a two-dimensional polymer and GNRs are true challenges for materials synthesis. Herein, we present, both, "bottom-up" precision synthesis and "top-down" fabrication protocols toward graphene. Further, GNRs are synthesized by conventional polymer synthesis in solution and by on-surface synthesis under STM-control. The resulting materials properties cover an enormous breadth, indicating utility from batteries, supercapacitors, oxygen reduction catalysts, photodetectors and sensors to semiconductors. Field effect transistors are built from GNRs even including single-molecule devices. Another question is whether graphene holds promise for robust technologies. An attempt will be made at providing answers.

Nature 2010, 466, 470; Nature Chem. 2011, 3, 61; Nature Nanotech. 2011, 6, 226; Nature Chem. 2012, 4, 699; Angew. Chem. Int. Ed. 2012, 51, 7640; Adv. Polym. Sci. 2013, 262, 61; Nature Nanotech. 2014, 9, 182; Nature Nanotech. 2014, 9, 131; Nature Chem. 2014, 6, 126; Nature Commun. 2014, DOI:10.1038/ncomms5973; Nature Nanotech. 2014, 9, 896; Nature Commun. 2014, DOI:10.1038/ncomms5253; Adv. Mater. 2015, 27, 669; ACS Nano 2015, 9, 1360; Angew. Chem. Int. Ed. 2015, 54, 2927; J. Am. Chem. Soc. 2015, 137, 6097; Nature Commun. 2015, DOI: 10.1038/ncomms8992; Nature Commun. 2015, DOI: 10.1038/ncomms8655; Nature 2016, accepted; Science 2016, accepted.

Professor Tal MargaLith

University of California, Santa Barbara (UCSB)

Brief Biography: *Executive Director for Technology of the Solid State Lighting & Energy Electronics Center. Tal's new joint position, shared between SSLEEC and the California NanoSystems Institute (CNSI), is designed to enhance technology outreach and corporate relations while also developing new multi-PI and multi-campus initiatives for science and engineering at UCSB. Tal received his PhD in Materials from UCSB in 2002. He has 18 years of GaN experience, most recently serving as the Director of Process Engineering at Soraa, Inc.*

Abstract Title: From Nobel Prize Winning LEDs to Next Generation Laser Lighting: Solid State Lighting at UC Santa Barbara

In 2014, Prof. Shuji Nakamura was awarded the Nobel Prize in Physics for his invention of the blue light emitting diode (LED). Prof. Nakamura's invention paved the way for a solid-state lighting revolution; the deployment of clean and long-lasting lighting sources that are 20 times more efficient than the Edison bulb. Moreover, Prof. Nakamura built on his success with LEDs and demonstrated the first violet laser in 1996. This talk will explore the path taken by Prof. Nakamura that led to his groundbreaking discoveries, and will look ahead to new ways at addressing some of the remaining challenges faced by LEDs, namely laser-based solid-state lighting.

KEY NOTE SPEAKERS

1.	Prof. Zhong Jin	Nanjing University, China
2.	Prof. Xiangfeng Duan	University of California, Los Angeles, USA
3.	Prof. Rodney Ruoff	UNIST, Korea
4.	Prof. Jiaxing Huang	Northwestern University, Evanston, USA
5.	Prof. Yu Huang	University of California, Los Angeles, USA
6.	Prof. Kian Ping Loh	National University of Singapore
7.	Prof. Lain-Jong Li	King Abdullah University of Science and Technology, KSA
8.	Prof. Yongbing Xu	Nanjing University, China and York University, UK
9.	Prof. Manish Chhowalla	Rutgers University, USA

Professor Zhong Jin

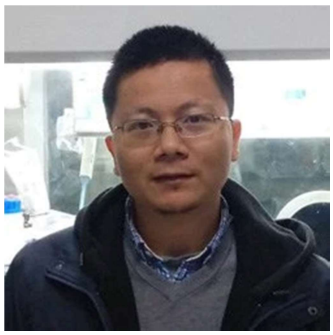

School of Chemistry and Chemical Engineering, Nanjing University, China

Abstract Title: Rational Design of Carbon/Inorganic Nanostructures for Efficient Energy Conversion and Storage

Zhong Jin, 1,* Jie Liu 1,2

[1] Key Laboratory of Mesoscopic Chemistry of MOE and Collaborative Innovation Center of Chemistry for Life Sciences, School of Chemistry and Chemical Engineering, Nanjing University, Nanjing, Jiangsu 210093, China

[2] Department of Chemistry, Duke University, Durham, NC 27708, USA

* Corresponding author: zhongjin@nju.edu.cn

Nanostructures composed of carbon and inorganic materials (transition metal oxides, chalcogenides, carbides... etc.) can exhibit high conductivity, porosity, flexibility, electrochemical and catalytic performances. For high-efficiency energy storage and conversion (such as solar cells, photo-/electro-catalysis and secondary batteries), it is of great importance to rationally design and fabricate ordered carbon/inorganic hybrid nanostructures. In the past 2 years, our newly-built research group has worked on the construction of 3D hierarchical carbon/inorganic based architectures with precisely-designed components and structures for energy applications, such as: (1) Flexible solar-power harvesting and storage integrated devices [1]. (2) High-efficiency electro- and photo-catalysts for hydrogen and oxygen evolution reactions [2-3]. (3) Active material encapsulated mesoporous carbon matrix as high-performance anodes and cathodes for lithium and sodium ion batteries [4-9].

References

[1] Liang, J.; Zhu, G.; Jin, Z.*; Liu, J.*; et al. 2016, submitted.

[2] Ma, L.; Jin, Z.*; Liu, J.*; et al. ***Nano Energy***, 2016, 24, 139.

[3] Liu, H.; Jin, Z.*; Liu, J.*; et al. 2016, submitted.

[4] Wang, Y.; Chen. R.; Jin, Z.*; Liu, J.*; et al. ***Energy Storage Materials***, 2016, 4, 103.

[5] Chen, T.; Jin, Z.*; Liu, J.*; et al. ***Nano Energy***, 2016, 20, 305.

[6] Sun, P.; Jin, Z.*; Liu, J.*; et al. ***Nanoscale***, 2016, 8, 7408.

[7] Chen, T.; Jin, Z.*; Liu, J.*; et al. ***Journal of Materials Chemistry A***, 2015, 3, 9510.

[8] Ma, L.; Chen. T.; Jin, Z.*; Liu, J.*; et al. ***Journal of Power Sources***, 2016, minor revision.

[9] Zhu, G.; Jin, Z.*; Liu, J.*; et al. 2016, submitted.

Professor Xiangfeng Duan

Professor in Department of Chemistry and Biochemistry,
University of California, Los Angeles, USA

Abstract Title: 2D Electronics and Optoelectronics: Opportunities and Challenges

Xiangfeng Duan

Department of Chemistry and Biochemistry, California Nanosystems Institute, University of California, Los Angeles, CA 90095, USA

Two-dimensional materials such as graphene and MoS_2 have attracted intense interest as alternative electronic materials in the post-silicon era. Graphene features exceptionally high carrier mobility but is limited by its semimetal nature and cannot be used for transistors with sufficient on-off ratio. Two-dimensional semiconductors (2DSCs) such as MoS_2 exhibit an intrinsic band gap and can enable transistors with high on-off ratio, but are limited by relatively low carrier mobility and poor on-current density. Despite intense interest and effort to date, it remains an open question whether 2DSC transistors can offer competitive performance matching up to exceeding that of the silicon devices.

To achieve a high performance (high on-current) device requires (1) a pristine channel with high carrier mobility, (2) an optimized contact with low contact resistance and (3) a short channel length. The simultaneous optimization of these parameters is of considerable challenge for the atomically thin 2DSCs since the typical low contact resistance approaches either degrade the electronic properties of the channel or are incompatible with the fabrication of short channel devices. Here I will review various strategies for optimizing these factors, and discuss how these strategies can be combined together to achieve high performance 2D transistors. In particular, I will discuss a unique approach towards high-performance MoS_2 transistors using a physically assembled nanowire as a lift-off mask for creating ultra-short channel devices with pristine MoS_2 channel and self-aligned low resistance metal/graphene/MoS_2 hybrid contact, and demonstrate sub-100 nm MoS_2 transistors with a record-high on-current density comparing well with that of silicon devices. We will also discuss possible strategies to further push the limit of 2D transistors. Lastly, we will discuss a new design of 2D-material-based vertical transistors that can enable new device functions or unprecedented combination of device performance and flexibility and a series of tunable photonic devices. I will conclude with a brief summary of the current challenges and future opportunities in 2D electronics.

Professor Rodney Ruoff

Director, Center for Multidimensional Carbon Materials (CMCM), Institute for Basic Science (IBS), UNIST, Korea

Abstract Title: Diamane and Diamond

Rodney S. Ruoff
Ulsan National Institute of Science & Technology (UNIST)
Ulsan 689-798, Republic of Korea

'Diamane' means ultrathin (few atom thick) sp^3-bonded carbon films. The conversion to diamane of 'AB-stacked few layer graphene' has been shown by others by density functional theory calculations to be possible through the formation of sufficient C-H (or C-F) bonds on the two free surfaces. We [1] then considered "nG/M", where nG represents n layers of AB-stacked graphene and M a metal substrate having an interface with the n^{th} graphene layer, and found for configurations [up to about 8-layer graphene on Cu(111) or Ni(111) or Co(00001)] that the metal surface could stabilize the conversion to diamane if the top surface was functionalized with roughly 25-30% of the C atoms having C-H (or C-F) bonds. We undertook this set of calculations because we grow AB-stacked graphene on metal substrates by chemical vapor deposition. Calculations have also been reported for the conversion of few layer hexagonal boron nitride (hBN) in the AA' stacking configuration (the typical layer stacking of h-BN), again by the atoms in the top and bottom surfaces of the multilayer hBN bonding to H or F, to a wurtzite-type BN (in an ultrathin layer). This is (also) of interest because the cubic phase of BN is the more stable phase and bulk wurtzite cannot readily be made. These methods of converting layered graphene or layered h-BN to allotropes having tetrahedral bonding represent a new pathway for such a conversion, to be contrasted with conversion by high pressure, or synthesis by plasma-enhanced chemical vapor deposition. After suggesting the potential importance of experimentally pursuing diamane(s) 4 years ago in a perspectives article, we are now pursuing these types of materials at UNIST, in the CMCM.

Professor Jiaxing Huang

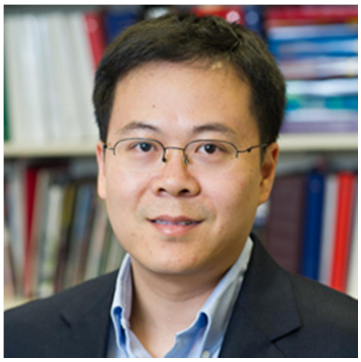

Professor in Department of Materials Science and Engineering, Northwestern University, Evanston, USA

Abstract Title: Self-dispersed crumpled graphene balls in oil for friction and wear reduction

Jiaxing Huang

Department of Materials Science and Engineering, Northwestern University

Email: Jiaxing-huang@northwestern.edu

Aggregation is a major problem for ultrafine particle additives in lubricant oil because it reduces the effective particle concentrations, prevents particles from entering the contact area of working surfaces, and leads to unstable tribological performance. Molecular ligands can help the particles to disperse, but they tend to degrade under the harsh tribological conditions. Therefore, self-dispersed particles without the need for surfactant are highly desirable. Here I will discuss, for the first time to our knowledge, such type of ultrafine particles made of crumpled, paper-ball-like graphene, which indeed can self-disperse in lubricant oil, and exhibit stable and superior tribological performances.

Professor Yu Huang

Henry Samueli School of Engineering and Applied Science, Materials Science and Engineering, University of California, Los Angeles, USA

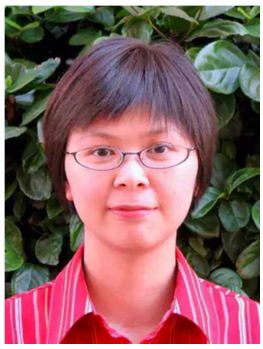

Abstract Title: Surface Engineered High-Performance Catalysts

Department of Materials Science and Engineering, University of California, Los Angeles, CA 90095-1595, http://yhuang.seas.ucla.edu

e-mail: yhuang@seas.ucla.edu

Noble metal-based nanocrystals have played important roles in heterogeneous catalysts due to their high activity and chemical stability. The high cost of noble metals, however, created roadblocks for the large volume production of noble metal catalysts for many applications. Improving the catalytic activity or the efficiency of noble metal usage, and prolong the life-time of a noble metal based catalysts are solutions to these challenges. On a nanocatalyst, the composition, atomic coordination, and strains of the top surface layers eventually determine its performance in catalytic reactions. Slight changes in the surface structure of catalytic materials for example, such as increase in the number of accessible surface adsorption sites or generating uniform surfaces with abundant specific defects, can have large impacts on the catalytic stability and activity. In this presentation I will share our recent efforts on tuning the surface compositions and structures of noble metal catalysts to improve both catalytic activity and stability.

Professor Kian Ping Loh

National University of Singapore

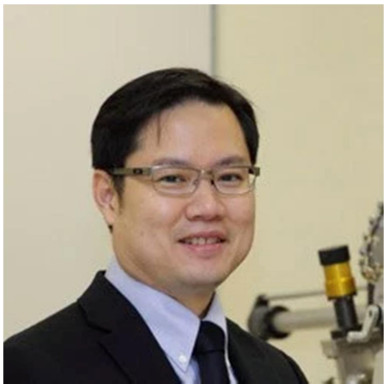

Abstract Title: The 1T' phase, 1-D and 2-D Sub-Stoichiometric Phases of MoS_2

Kian Ping Loh*

Department of Chemistry and Centre for Advanced 2D Materials, National University of Singapore

*E-mail: chmlohkp@nus.edu.sg

Tailoring the dimension of nanomaterials to achieve precise tuning of optical, electronic and catalytic properties have been the major goals of researchers for decades. Two dimensional metal chalcogenides of the MX_2 (M=Mo, W and Ti, X= Se, Te) family represent the ultimate control of material dimension in the vertical direction, and exhbits unique quantum confined optoelectronic properties. Depending on the distribution of electrons in the d orbitals, MoS_2 can convert between the 2H and 1T polymorphs. The 1T-MoS_2 polymorphs have attracted intense interests because the metallicity suggests the possibilities of catalytically active basal planes, as well as enhanced electrical contact properties. However the stability of the 1T/1T' phase is often short-lived. Herein, we report on strategies to enhance the air-stability of the 1T' phase and exploit its use in catalysis. We also show that the conversion to 1T' phase induces nanoscale phase conversion in MoS2, which enhances its cycle stability and rate capability in rechargeable lithium batteries.

At the 1-D level, MoS_2 quantum wires display quasi one-dimensional metallic state and novel ferromagnetic behavior that is tunable by its width and edge configurations. Unlike graphene nanoribbons which have been successfully synthesized using bottom–up molecular techniques, there are scant reports on the growth of MoS_2 nanoribbons. Herein, we report two novel phases of sub-stochiometric MoS_2 (MoSx) grown on Au (111) and Cu (111), respectively. We performed the templated growth of well-aligned, sub-stoichiometric MoS_x molecular wire on Au(111) vicinal surface. Interestingly, we observed the dynamic assembly of MoS_x molecular wires and its phase transition into stoichiometric MoS_2 nanoribbon. On Cu (111) surfaces, we studied the growth of a novel MoS_x 2-D phase which shows catalytic activities for the oligomerization of small molecules on its basal planes. Due to the in-plane rotational freedom and greater diversity of bonding arrangements in MoS_2, a plethoras of different polytypes may be possible when the structural assembly is mediated by metal substrate. Thus a whole new class of alternative 2D structures, uniquely different to the classical chalcogenides in terms of electronic and physical properties, may be possible.

Professor Lain-Jong Li

Principal Investigator & Associate Professor, King Abdullah University of Science and Technology, Saudi Arabia

Abstract title: Growth and Applications of Two-Dimensional Transition Metal Dichalcogenides

Lain-Jong Li

Physical Sciences and Engineering Division, King Abdullah University of Science and Technology, Thuwal, 23955-6900, Kingdom of Saudi Arabia

Atomically thin 2D Transition metal dichalcogenide (TMD) materials provide a wide range of basic building blocks with unique electrical, optical, and thermal properties which do not exist in their bulk counterparts. Our recent demonstration in vapor phase growth of TMD monolayer [1] has stimulated the research in growth and applications [2]. In this presentation, I would start with the discussion on the synthesis and characterizations of crystalline MoS2 and WSe2 monolayers. These layer materials can be transferred to desired substrates, making them suitable building blocks for constructing multilayer stacks for various applications [3].

Heterostructures of 2D materials formed by vertical stacking have been realized recently via transfer of their exfoliated flakes, where their properties are dominated by the stacking orientation and strength of interlayer coupling. The method to determine valence band and conduction band alignment for various TMD materials is proposed [4]. Another very attractive structure is the lateral heterostructure, where the atomically sharp p-n junction exhibits diode properties and a large strain exhibits at the junction region which offers tenability in electronic structures. The direct growth of such lateral heterostructures is shown below (Figure 1) [5]. These unique 2D heterostructures have abundant implications for many potential applications.

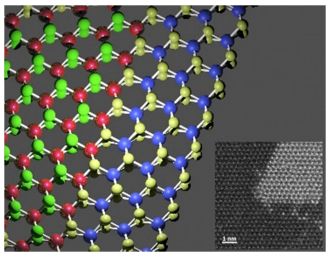

Fig. 1 Lateral heterostructure of MoS_2 and WSe_2 monolayers

TMD materials are also promising materials for post-Si electronics, where their ultra-thin body structure may be able to serve for 5 nm technology nodes [6] and a 10 nm channel length of transistor based on MoS_2 few layers is demonstrated [7].

References

[1] Y.-H. Lee et al. Adv. Mater. 24, 2320 (2012)

[2] M. Chhowalla et al. Nature Chem. 5, 263-275 (2013)

[3] C.-H. Chen et al. Adv. Mater. 26,4838 (2014)

[4] M.-H. Chiu et al. Nature Comm. 6, 7666 (2015)

[5] M.-Y. Li et al. Science 349, 524 (2015)

[6] M.C. Chen et al. IEDM (2015)

[7] K.H. Li et al VLSI (2016)

Professor Yongbing Xu

Director of York-Nanjing Joint Center, Nanjing University, China and York University, UK

Abstract Title: The Next Generation Spintronics with Hybrid and 2D Materials

Yongbing Xu,[1, 2], Wenqing Liu,[1, 2] Liang He,[1] Xuefeng Wang,[1] Jun Du[1], Biao You[1], Xuezhong Ruan[1], Fengqiu Wang[1], Edmond Turcuand[1] and Rong Zhang[1]

[1]York-Nanjing Joint Center for Spintronics and Nano Engineering (YNJC), School of Electronics Science and Engineering, Nanjing University, Nanjing 210093, China

[2]Spintronics and Nanodevice Laboratory, Department of Electronics, University of York, York YO10 5DD, UK Email:yongbing.xu@york.ac.uk, web site: http://www.ynjc.org/

The first generation spintronics based on the giant magneto-resistance effect (GMR, the 2007 Nobel Prize) in the magnetic multilayers has already generated huge impact to the mass data storage industries. The next generation spintronics based on magnetic-semiconductor hybrid structures and 2D materials aims to develop new spin based devices such as spin transistors and spin logic, which will not just improve the existing capabilities of electronic transistors, but will have new functionalities [1]. These spin devices have the potential to integrate both data storage and processing, enabling future computers to run faster and at the same time consume less power. In this talk, we will report our studies of the magnetic/semiconductor, Graphene and TI based spintronic materials and devices. We have established that high quality epitaxial Fe films can be achieved in both GaAs(100) and InAs(100) surfaces with bulk like spin moment and enhanced orbital moments down to monolayers thicknesses [2]. While there is a robust room temperature magnetization of the interfacial Co, the magnetic moments of the interfacial Ni is strongly diminished down to 5 K due to hybridization of the Ni d(eg) and GaAs sp3 states [3]. The epitaxial growth of half metallic oxide/III-V semiconductor hybrid structures such as Fe3O4/GaAs(100) Fe3O4/MgO/GaAs(100) and Fe3O4/GaN has recently been demonstrated using the post-growth annealing technique. The system shows an interesting epitaxial relationship with the unit cell of the Fe3O4 rotated by 45° to match that of GaAs(100) substrate. The nanoscale Fe3O4 films show a significant unquenched orbital moment, which may come from the breaking of the symmetry at the interfaces in this low dimension system [4]. We have recently demonstrated that Fe/Graphene interfaces are ferromagnetic down to monolayers [5]. We have observed the enhancement of magnetic ordering of transition metal doped TIs via the proximity to ferrimagnetic insulator YIG and firstly demonstrated the unique 'abnormal' proximity effect of TIs [6]. We studied the atomic scale mechanism of the magnetism in the transition-metal-doped TIs, showing the effect of the antiferromagnetic dimer in this technologically important system [7]. We have also prepared a series of new Sm-doped Bi2Se3 MTIs, which exhibit ferromagnetism up to about 52 K. All evidence suggests that Sm-doped Bi2Se3 is a promising Magnetic TI candidate with high-mobility [8]. We have also

demonstrated a photoconductive gain of ~10^5 electrons per photon in a carbon nanotube–graphene hybrid due to efficient photocarriers generation and transport within the nanostructure, leading the way for a potential ultrafast all-carbon spin-optoelectronic device [9]. While the fabrication and transport studies of lateral SET have attracted greatly attentions, there are few studies of vertical devices. Very recently, we have demonstrated two-terminal electrical spin injection and detection in an in-situ fabricated Fe/GaAs/Fe hybrid vertical spin-valve (SV) [10], which may offer the opportunity for the future 3D integration.

1. "Handbook of Spintronics", Yongbing Xu, David Awschalom and Junsaku Nitta (Eds.), Springer, 2016, ISBN 978-94-007-6892-5,
2. J. S. Claydon et al, Phys. Rev. Lett., 93 (3), 037206 (2004).
3. W Liu et al, ACS applied materials & interfaces 8 (9), 5752 (2016).
4. WQ Liu et al, Applied Physics Letters 104 (14), 142407
5. W. Q. Liu et al, Sci. Rep. , 5, 11911 (2015)
6. W. Q. Liu et al, Nano Letts. 15, 764 (2015).
7. W. Q. Liu et al, ACS Nano Vol. 9, 10237 (2015).
8. T Chen et al, Advanced Materials 27 (33), 4823-4829, (2015)
9. Y.D Liu, Nature Communications 6, Article number: 8589 doi:10.1038/ncomms9589, 2015
10. J. Wong et al, Sci. Rep. , 2016, in press

This work is supported by the State Key Program for Basic Research of China (Grants No. 2014CB921101, 2013CB934600 and 2011CB921404), NSFC (Grants No. 61274102, 61474061, 21473168, 11174244, 51390474, and 11234011) and UK STFC.

Professor Manish Chhowalla

Associate Department Chair Materials Science and Engineering, Rutgers University, USA

Abstract Title: Phase-engineered low-resistance contacts for ultrathin MoS2 transistors and catalysis

Manish Chhowalla, Rutgers University

Ultrathin molybdenum disulphide (MoS_2) has emerged as an interesting layered semiconductor because of its finite energy bandgap and the absence of dangling bonds. However, metals deposited on the semiconducting 2H phase usually form high resistance (0.7 k□ µm–10 k□ µm) contacts, leading to Schottky-limited transport. In this study, we demonstrate that the metallic 1T phase of MoS_2 can be locally induced on semiconducting 2H phase nanosheets, thus decreasing contact resistances to 200–300 □-µm at zero gate bias. Field-effect transistors (FETs) with 1T phase electrodes fabricated and tested in air exhibit mobility values of ~50 $cm^2 V^{-1} s^{-1}$, subthreshold swing values below 100 mV per decade, on/off ratios of $>10^7$, drive currents approaching ~100 µA $µm^{-1}$, and excellent current saturation. The deposition of different metals has limited influence on the FET performance, suggesting that the 1T/2H interface controls carrier injection into the channel. An increased reproducibility of the electrical characteristics is also obtained with our strategy based on phase engineering of MoS_2. In addition to FETs, we also show that the catalytic activity of MoS_2 towards the hydrogen evolution reaction can be improved by phase engineering low resistance contacts. We show that the activity of the 2H basal planes of monolayered MoS_2 nanosheets can be made comparable to state-of-the-art catalytic properties of metallic edges and the 1T phase by improving electrical coupling between the substrate and the catalyst so that electron injection from the electrode and transport to the catalyst active site is facilitated.

Session Chairs

SYMPOSIUM S1

Prof. W. Hong Yeo (Virginia Commonwealth University)
Prof. Michael De Volder (University of Cambridge)
Prof. Donghyeon Ryu (New Mexico Tech)
Prof. Anna Laromaine (ICMAB-CSIC)
Prof. Yi Zhang (Sun Yat-sen (Zhongshan) University)
Prof. Hua Wu (ETH Zurich)
Prof. Alexandra Palla Papavlu (National Institute for Lasers, Plasma and Radiation Physics)
Prof. Denis Sabirov (Russian Academy of Sciences)
Prof. Suhe Wang (University of Michigan)
Prof. Jatinkumar Dave (Nirma University)
Prof. Dharmendra Sharma (Nirma University)
Prof. Saliza Azlina (Universiti Tun Hussein Onn Malaysia)
Prof. Pragya Shandilya (MNNIT Allahabad)
Prof. Songjing Li (Harbin Institute of Technology, China)
Prof. Palani Lyamperumal Anand (IIT, Indore, India)

SYMPOSIUM S2

Prof. Kaleem Abbas (Sungkyunkwan University)
Prof. Ir. Wong Yew Hoong (University of Malaya)
Prof. Iren Kuznetsova (Kotel'nikov Institute of Radio Engineering and Electronics of RAS)
Prof. Radchada Buntem (Silpakorn University)
Prof. Christian Teichert (Institute of Physics, Montanuniversitaet Leoben)
Prof. Saibal Mitra (Missouri State University)
Prof. Huynh Van Ngoc (Sungkyunkwan University)

SYMPOSIUM S3

Prof. Wanliang Shan (University of Nevada)
Prof. Eugenia Eftimie Totu (University Politehnica of Bucharest, Romania)
Prof. Jayaramudu Tippabattini (Inha University)
Prof. Dongpeng Yan (Beijing Normal University)
Prof. Azzuliani Supangat (University of Malaya)

SYMPOSIUM S4

Prof. Irina Petreanu (Institute for Cryogenic and Isotopic Technologies, Romania)
Prof. Winie Tan (Universiti Teknologi MARA)
Prof. Sergey Sinebryukhov (Institute of Chemistry FEB RAS)

SYMPOSIUM S5

Prof. Jun Ma (Huazhong University of Science and Technology)
Prof. Ja-Hyoung Ryu (Ulsan National Institute of Science & Technology)
Prof. Saithip Pakapongpan (National Sci. & Tech Development Agency)
Prof. Jae-Ho Han (Korea University)
Prof. Uraiwan Waiwijit (National Electronics and Computer Tech. Center)
Prof. Emily Hyde (University of Newcastle)

SYMPOSIUM S6

Prof. Rodica Zavoianu (University of Bucharest)
Prof. Changzeng Yan (Nanjing University, China)
Prof. Huynh Van Ngoc (Sungkyunkwan University)

SYMPOSIUM S7

Prof. Jing Sun (Chinese Academy of Sciences)
Prof. Hyesung Park (Ulsan National Institute of Science & Technology)
Prof. Hongwei Zhu (Tsinghua University)
Prof. Kian Ping Loh & PLain-Jong Li (NUS, KAUST)
Prof. Hyeon-Jin Shin (SAIT)
Prof. Manish Chhowalla (University of Rutgers)
Prof. Hyunseob Lim (Ulsan National Institute of Science and Technology - UNIST)
Prof. Changzeng Yan (Nanjing University, China)

Symposia 1

Advances in Multifunctional Composite materials

- Synthesis and characterization of Composite materials
- Dielectric, Ferroelectric and Piezoelectric materials
- Electrostrictive and Magnetostrictive Materials.
- Shape-memory alloy (SMA), (smart metal, memory metal, memory alloy, muscle wire, smart alloy)
- Theoretical/Modelling/Computer Simulations Of Functional Materials
- Nano and mesostructured materials
- Carbon and metal oxide based composite materials
- Superconducting and magnetic materials
- Others

Index Page

A novel antistatic pearlescent pigment based on mica-titanium@graphene composite

Yan Wang, Miaomiao Liu, Yangqiao Liu, Jianqiang Luo, Xiaoyu Lu, Jing Sun*

State Key Laboratory of High Performance Ceramics and Superfine Microstructures, Shanghai Institute of Ceramics, Chinese Academy of Sciences, Shanghai 200050, China

Abstract

In this work, a novel graphene-based mica-titanium complex-conductive pearlescent pigment has been designed to decrease electrical resistivity without affect the pearlescent effect by introducing transparent conductive shell. The MT@GO composite was synthesized by using homogenous precipitation method. The MT@rGO pigment was prepared under N_2 atmosphere at 500^{o}C for 5 min to reduce GO and the MT silver pearlescent effect was almost not decreased. TEM spectra results show that the TiO_2 layer of MT is coated by carbon shell layer obviously. The weight loss of TG-DTA around 500^{o}C show that the carbon content is about 2.2% in the MT@rGO composite. The I_D/I_G increasing in Raman scattering spectroscopy and C1s peak of XPS spectra results prove that GO is reduced to rGO after N_2 annealed. At last the electric resistivity of the composites were measured by volume resistivity measurement under 40 MPa/cm^2 and 100 MPa/cm^2 separately, which suggest the conductivity of MT@rGO pigments increase by the increasing of measure pressure and compared with MT@GO under the same pressure significantly. Our graphene@MT complex-conductive pigment can not only improve the electric property of pigments, but also enrich the family of pigments and apply a new idea for functional pearlescent pigment.

Keywords: graphene, mica titanium pigments, complex-conductive pearlescent pigment, antistatic.

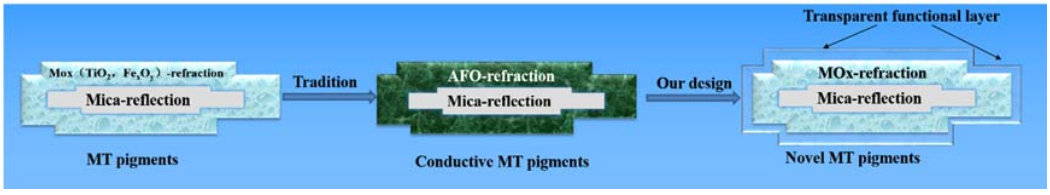

Scheme 1. Structure comparison of conductive MT pigments.

* Corresponding author. Tel: +86-21-52412722; Fax: +86-21-52413122
E-mail address: jingsun@mail.sic.ac.cn (Jing Sun).

Fibre orientation and Surface Conformity effect on tribological Behaviour of C/C composites

Parshant Kumar, V.K. Srivastava
Department of Mechanical Engineering, Indian Institute of Technology (BHU)
Varanasi-221005, U.P., India

Abstract

Carbon carbon (C/C) composites are generally used for aircraft brake discs due to their low density and good thermal, mechanical and tribological properties. The density of C/C composites is generally less than 2 g/cm^3 even after densification. The tribological behaviour of carbon carbon (C/C) composites had been investigated to a greater extent. But most of the investigation deals with the parallel orientation of the fibres and fully conformal surfaces. The effect of perpendicular fibre orientation and surfaces with low conformity are not investigated much. This article deals with the investigation of tribological behaviour of C/C with different orientation of fibres and surface conformity.

Functional nickel /porous carbon nanocomposite for active catalytic oxidation of MC-LR in aqueous solution

Wan-Kuen Jo[a*], S. Karthikeyan[a,b*], Seung-ho shin[c] , Jun-ho Lee[d], Migyeong Kim[a], and G.Sekaran[b]*

[a] *Department of Environmental Engineering, Kyungpook National University, Daegu*

702-701, South Korea. E-mail: wkjo@knu.ac.kr; karthik.keyan02@gmail.com.

[b] *Environmental Technology Division, Council of Scientific & Industrial Research (CSIR),*

Central Leather Research Institute (CLRI), Chennai 600 020, India. E-mail:

ganesansekaran@gmail.com; Tel: +91-44-24911386.

[c]*Department of Health Environment, Deagu Health College, 15 Youngsong-Ro, Buk-Gu, Deagu 702-722, Korea.*

[d]*GyeongSangBukdo Government Public Institute of Health and Environment, Yeongcheon, Kyungpook,770-800, Korea.*

ABSTRACT

The present investigation relates to distorted nickel nanoparticle doped nanoporous carbon (Ni/NPC) matrix for the destruction of *Microcystine–LR* in aqueous solution at neutral (pH) conditions. The novelty lies on the development of nano nickel doped nano porous carbon (NPC) using pretreated nano porous carbon as the precursor. Nano nickel doped NPC catalyst has high capacity to generate hydroxyl radical to destruction of toxic Microcystine–LR in aqueous solution. The synthesized catalyst was characterized various technique such as BET surface area, X-ray Powder Diffraction (XRD), Scanning Electron Microscopy (SEM), Energy-dispersive X-ray spectroscopy, Transmission electron microscopy(TEM) and X-ray photoelectron spectroscopy (XPS). This Ni/NPC catalyst applied to oxidative destruction of toxin contaminated water/wastewater with less consumption of hydrogen peroxide at ambient conditions. The new process does not generate secondary metal pollution during the destruction of Microcystine–LR from water/wastewater.

Keywords: Nickel/porous carbon, Heterogeneous catalyst, Oxidation, Microcystine–LR

References:

1. Karthikeyan, S., Dionysiou, D.D., Lee, A.F., Suvitha, S., Maharaja, P., Wilson, K. and Sekaran, G., 2016. *Catalysis Science & Technology*. **DOI:** 10.1039/C5CY00888C.

2. Kim, Byung-Joo, Kyong-Min Bae, Hye-Min Lee, Shin-Jae Kang, and Soo-Jin Park(2015). Journal of Nanomaterials, http://dx.doi.org/10.1155/2015/546720.

Title: Graphene Aerogel - Recovery of Heavy Crude Oil from Contaminated Sand

Name: E. V. Lau; W. K. Cheong
School of Engineering, Monash University Malaysia, Jalan Lagoon Selatan, 47500 Bandar Sunway, Selangor, Malaysia

Oil spills on land are a common problem in the petroleum industry, as there are many ways where oil can spill and contaminate the land. Due to the difficulty in separation of heavy oil from oil-wet sands as well as the use of large volumes of solvents for the separation process, many researches have been conducted using various solvents and surfactants at high temperatures.Today, with new advancements in materials, the synthesis of graphene aerogel presents one of the world's lightest materials, with an extraordinarily low density. The low density, in combination with the hydrophobic properties of graphene sheets, makes graphene aerogel a promising candidate for oil absorption. Recent studies have shown successful results in recovering oil from water using various forms and synthesis of graphene and graphene aerogel, including graphene-carbon nanotube aerogels, magnetic graphene foam, functionalized graphene aerogel and nanoporous grapheme. While these studies have shown that the various forms of graphene and graphene aerogel are successful in removing oil from water, there are no studies to-date which adopts this material to remove oil from sand, particularly from oil-wet sand. This problem is complicated as oil adheres strongly to sand, and is more difficult to separate. Thus, this study aims at investigating the feasibility of using the graphene aerogel to remove and recover oil from oil-wet sands, using the traditional batch extraction modified with graphene aerogel stirrers as seen in Figure 1. (232 words)

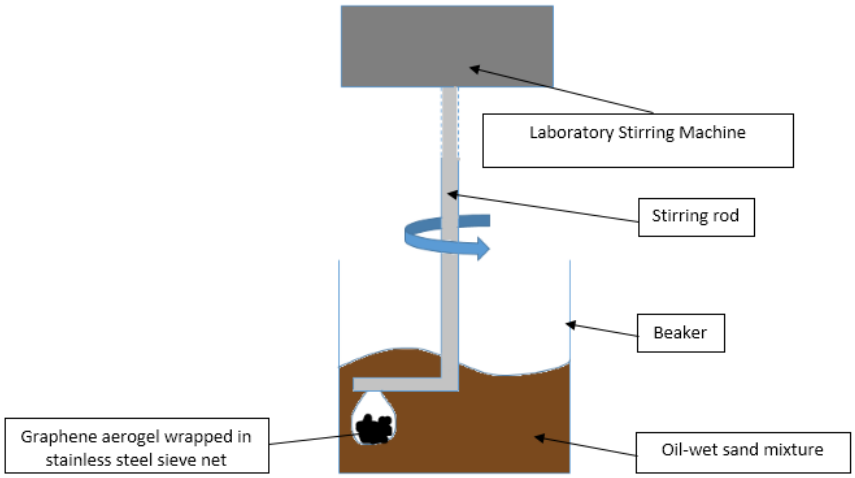

Figure 1. Schematic of mechanical stirrer with attached graphene aerogel for oil removal from contaminated sand

Biography

Dr. Lau has completed her PhD at the age of 28 years from Nottingham University Malaysia Campus. She is currently a Senior Lecturer at Monash University Malaysia. She has published 9

ISI-indexed journals, and have a total citation of 183 (Scopus) since 2009. (43 words)

Presenting author details

Full name: Dr. Lau Ee Von
Contact number: +6012-3566339
Twitter account: -
Linked In account: Ee Von Lau
Session name/ number:
Category: (Oral presentation/ ~~Poster presentation~~)

High-performance Graphene Field Effect Transistors based on Chemical Vapor Deposition Growth h-BN as Dielectric Layer

Huynh Van Ngoc and Dae Joon Kang

Department of Physics, Sungkyunkwan University, Republic of Korea

Hexagonal boron nitride (h-BN) has emerged as an exceptional dielectric material for graphene field effect transistors (GFETs).[1] GFETs exploiting mechanically exfoliated h-BN dielectrics exhibited an order of magnitude improvement in device mobility, reduced carrier in-homogeneity, lower extrinsic doping, reduced chemical reactivity, and improved high-bias performance when compared with devices with conventional oxide dielectrics. Chemical vapor deposition (CVD) based synthesis of high-quality graphene and h-BN over a large-area is currently the most widely used. However, the CVD grown h-BN dielectric has not been demonstrated for high-performance GFETs. This is mainly due to problems associated with a contamination issue in a thin poly(methyl methacrylate) (PMMA) assisted transfer of CVD-grown 2D materials from a growth substrate to a target substrate for the optical and electronic devices fabrication. The residues from incomplete etching of PMMA on the surface of transferred 2D materials, being contaminants, are then trapped at the surface of the transferred 2D materials, which leads to degradation of intrinsic characteristics of 2D materials. This limits further study of heterostructure of 2D materials using layer-by-layer transferring methods.[2,3] In this work, we report a successful development of a facile transfer technique for 2D materials by adding a water-soluble PVA layer in-between PMMA and 2D materials grown on a rigid substrate. This technique allows not only effective transfer to a target substrate with a high degree of freedom but also etching-free PMMA-assisted transfer while minimizing the effects of contamination on the overall device performance. We demonstrate that GFETs based on CVD grown graphene and h-BN dielectric layer showed excellent electrical properties. GFETs transferred by this process exhibits a negative shift of charge neutrality point close to zero and both graphene and graphene/h-BN FETs showed greater mobility, current modulation and smaller hysteretic than GFETs prepared via a conventional PMMA assisted transfer. Our results demonstrate the transferred 2D materials are of high quality, and that the developed transfer method is so versatile that multilayer stacking of heterostructure of graphene and h-BN can be reliably performed in a wafer scale. This facile transfer technique presents great potential for future research and development for flexible and transparent devices based on graphene/h-BN heterostructures in a wafer scale.

References

1. Banszerus *et al.* Sci. Adv. 1-6, 2015.
2. Yang *et al. Small* **11**, 175-181, 2015.
3. Garcia *et al. Nano Lett.* **12**, 4449-4454, 2012.

Laser direct writing of hybrid carbon-oxide nanostructures: towards original sensing applications

Alexandra Palla Papavlu[1,2], Mihaela Filipescu[2], Maria Dinescu[2], Alexander Wokaun[1], Thomas Lippert[1]

[1] Energy and Environment Research Department, Paul Scherrer Institute, 5232 Villigen PSI, Switzerland

[2] Lasers Department, National Institute for Lasers, Plasma and Radiation Physics, 077125 Magurele, Romania

*alexandra.palla-papavlu@psi.ch (***presenting and corresponding author)**

1-dimensional materials, i.e. carbon nanotubes (CNT), in particular single-walled CNT have unique electrical and structural properties, which make them useful in various applications, including sensors. Herein we describe new applications of 1dimensional sensor materials that have been opened up through the use of lasers.

One suitable technique for the deposition of different materials onto various types of non-conventional substrates with high spatial resolution (a few microns) is laser-induced forward transfer (LIFT). In LIFT, a laser beam is focused through a transparent support plate onto the backside of a photodegradable polymer (triazene polymer) thin film coated with the material to be transferred. Each single laser pulse promotes the transfer of the thin film material onto a receiver substrate that is usually placed parallel and facing the thin film at a short distance. The triazene polymer layer, also called dynamic release layer (DRL) or sacrificial layer, has the purpose to improve the process efficiency and to reduce the risk of damaging the layer to be transferred.

In this work, the developments in DRL assisted LIFT of complex materials i.e. carbon nanotubes and hybrid carbon nanostructures (nanoparticle decorated CNT and carbon nanowalls) for applications as recognizing elements in miniaturized chemiresistor devices are sumarized.

As the functionality of such sensors depends on the applied laser source, target material, and transfer geometry, first an optimization of the process parameters is reported. In addition, the real-time study of the process by shadowgraphy gives various insights into the dynamic of the process and can be used to optimize the transfer.

Following a morphological and structural characterization of the active material, the performance, i.e. the sensitivity, resolution, and response time of the laser-printed devices was evaluated by exposure of the sensor arrays to different toxic vapors. Different sensitivities and selectivity to the selected analytes i.e. acetone, ethanol, ammonia, etc. have been measured thus proving the feasibility of LIFT for applications in sensors.

Keywords: CNT, SnO_2, lasers, patterns, pixels

Synthesis of Zinc Oxide/Graphene Composite for Electrochemical Detection of Amines

Jianping Du[1], Siyuan He[1], Ruihua Zhao[2], Jinping Li [1]

[1] Taiyuan University of Technology, Shanxi China

[2] Shanxi Kunming Tobacco Limited Liability Company, Taiyuan, Taiyuan China.

E-mail: dujp518@163.com;

Metal oxide semiconductors have wide application in photocatalysis and solar cell. Recently, the application of metal oxide in gas sensing field has drawn increased interest. It is reported that metal oxide can be used to detect gases and volatile organic compounds (VOCs), such as aldehydes, acetone and some amines.[1-3] However, low-concentration amines in solution have potential threat to human health. So it is necessary to develop a novel material used for detection of volatile amines by sample method.

Here, graphene-doped zinc oxide composites (ZOG) were synthesized and their ability of amines detection by electrochemical system was also studied. The results indicate that ZOG exhibits high selectivity of volatile amines, and doped graphene lead to an enhanced sensitivity, implying the zinc oxide/graphene composites have potential application using electrochemical method for detection of low-concentration amines.

Keywords: zinc oxide, graphene, composite, electrochemical sensing

[1] GIBERTIA, A., CAROTTA, M. C., FABBRI, B., GHERARDI, S., GUIDI, V., MALAGU, C. 2013. High-Sensitivity Detection of Acetaldehyde. Sens. Actuators B Chem., 174, 402-405

[2] DU, J. P., YAO, H. L., ZHAO, R. H., WANG, H. Y., XIE, Y. J. 2014. Surfactant-Controllable Synthesis of Prism- and Lamella-like ZnO and Their Gas Sensing. Mater. Lett., 136, 427-430.

[3] DU, J. P., ZHAO, R. H., XIE, Y. J., LI, J. P. 2015. Size-controlled Synthesis of SnO_2 Quantum Dots and Their Gas-sensing Performance. Appl. Sur. Sc., 346, 256-262

The effects of hydrocarbon for the long-CNT growth and quality

Jin Gyu (Park)[1], Shelby (Green)[1], Liyu (Dong)[1], Zhiyong (Liang)[1]

[1]High-Performance Materials Institute, Florida State University, 2005 Levy Ave, Tallahassee, FL 32310

jgpark@fsu.edu

Continuous growth of long carbon nanotube (CNT) is a key issue for developing high-performance CNT nanocomposites. . In this research, floating catalyst method was adopted for continuous CNT growth and different organic solvents, acetone, ethanol and isopropanol, were used for hydrocarbon source along with selected catalysts. Higher temperature (> 1200 °C) growth gives continuous drawing of double-walled CNT or few-walled CNT based on transmission electron microscope. Long-CNT was drawn continuously with motor and it gives additional alignment to form CNT fiber. Electrical and mechanical properties of CNT fiber were measured and the results were used to understand CNT length-property relationship as well as the effect of CNT quality on properties. CNT fiber grown from acetone gives higher physical properties compared to other hydrocarbon based CNTs. All the physical properties were improved after densification of CNT fiber. Properties after composite fabrication with resin system were measured as well and compared with CNT yarn

Keywords: long-CNT synthesis, composite,

Improvement of Electrical Properties of Natural Rubber Composite by Chemically Modified Graphite from Metal Smelting Industry

Pattharaporn Wipatkrut, Sirilux Poompradub*

Department of Chemical Technology, Faculty of Science, Chulalongkorn University, Bangkok, Thailand 10330

E Mail/Contact Detail: pattharap.w@gmail.com, sirilux.p@chula.ac.th

Conductive polymers have significantly received attention due to ease of processing, low cost, wide range of electrical properties and lightweight compared with metal. However, the limitation of polymer is low conductivity for practical application. In order to tackle this problem, polymer composite material with conducting solid like metal, carbon black and graphene has been received interest due to its excellent electrical, mechanical and thermal properties. In this work, graphene was chosen to improve the electrical property of natural rubber (NR) vulcanizate. Graphene was obtained from chemical exfoliation via oxidation and reduction processes of graphite waste from metal smelting industry. All materials, i.e. graphite, graphite oxide (GO) and graphene (obtained by L-ascorbic acid reduction: graphene-V and thermal reduction: graphene-T) were then characterized by X-ray photoelectron spectroscopy (XPS), fourier transform infrared spectroscopy (FTIR), X-ray diffraction spectroscopy (XRD), transmission electron microscopy (TEM) and four-point probe. The obtained results showed that the oxygen contents in graphene were significantly decreased compared to those in GO. In addition, XPS and FTIR spectra of graphene showed the decrease in intensity of hydroxyl groups (C–OH), carbonyl groups (C=O), epoxy/ether groups (C-O) and carboxylate carbon group (O-C=O). The morphology of graphene from TEM images confirmed that the stacks of graphene sheets were exfoliated into the single-layer sheets. The electrical conductivity of graphene both in graphene-V and graphene-T were significantly increased and the electrical conductivity of graphene-T was higher than that of graphene-V. Then, graphene were mixed with NR and curing agents to produce the conducting rubber composites. The percolation thresholds of rubber composites using conducting fillers (graphene-V, graphene-T and conductive carbon black as a reference) were appeared at 5 parts by weight per hundred parts of rubber (phr) of conducing fillers with the conductivity of 8.22 S/cm, 11.04 S/cm and 14.17 S/cm,

respectively. Accordingly, graphene prepared in this study can be used as the conductivity filler for replacement of conducting carbon black, which was obtained from the combustion of petroleum. Finally, the mechanical properties in terms of modulus, tensile strength and hardness of graphene/NR composites were comparable to those of conducting carbon black/NR composites.

Keywords: Graphene, L-ascorbic acid, Natural rubber, Electrical conductivity

[1] HUANG, X., QI, X., BOEY, F. & ZHANG, H. 2012. Graphene-Based Composite. *Chemical Society Reviews,* 41, 666-686.
[2] HUMMERS, W. & OFFEMAN, R. 1958. Preparation of Graphitic Oxide. *Journal of the American Chemical Society*, 80 (6), 1339–1339.
[3] FERNÁNDEZ-MERINO, M., GUARDIA, L., PAREDES, J., VILLAR-RODIL, S., SOLÍS- FERNÁNDEZ, P., MATÍNEZ-ALONSO, A., & TASCÓN, J. 2010. Vitamin C is an Ideal Substitute for Hydrazine in the Reduction of Graphene Oxide Suspensions. *Journal of Physical Chemistry C,* 114, 6426-6432.

Anodizing properties of ZrO_2 coated aluminum foils in 2-methy-1, 3-propanediol and boric acid mixed solution

Kaiqiang Zhang, Sang-Shik Park*

School of Nano Materials Engineering, Kyungpook National University,
Gyeongbuk 742-711, Republic of Korea
Presenting author: zhangkaiqiangjack@gmail.com *Corresponding author: parkss@knu.ac.kr

Abstract

ZrO_2-Al_2O_3 composite oxide films are a promising dielectric material for future use in capacitors. These films are prepared by ZrO_2 coating on etched Al foils and anodizing. The anodizing for high voltage Al foils has been carried out exclusively in aqueous boric acid solution. But when Al foils are anodized above about 700V, boric acid solution is not suitable due to the occurrence of micro arc in foil surface by low resistivity. In order to inhibit the micro-arc discharge, 2-methy-1, 3-propanediol (MPD) was mixed with boric acid solution. In this study, we discussed that the effects of MPD concentration in boric acid solution on anodizing behavior and electrical properties of ZrO_2 coated Al foils. The thickness of the oxide layer was decreased and the withstanding voltage of samples increased with increasing the MPD concentration. The formation rate of oxide layer was decreased as the concentration of MPD is increase above 20 volume %. MPD-boric acid solution could effectively inhibit the micro-arc discharge. The samples anodized in 30 % MPD-boric acid solution showed 50% higher capacitance than those anodized in only boric acid solution. MPD-boric acid solution could effectively increase the withstanding voltage and specific capacitance of Al foils.

Acknowledgments

This work was supported by a grant (15RTRP-B067917-03) from the Railroad Technology Research Program funded by the Ministry of Land, Infrastructure, and Transport of the Korean government.

Development of solid state crystal growth (SSCG) technology and seed-free SSCG of $K_{0.5}Na_{0.5}NbO_3$ single crystals

M.H. Jiang[a, b,*]; H.Z.Guo[b]; G.H. Rao[a]; Z.F. Gu[a]; G. Cheng[a]; X.Y. Liu[a]; J.W. Zhang[a]; C.A. Randall[b]

[a] Guangxi Key Laboratory of Information Materials, Department of Materials Science and Engineering, Guilin University of Electronic Technology, Guilin, Guangxi 541004, P. R. China

[b] Center for Dielectrics and Piezoelectrics, Materials Research Institute, The Pennsylvania State University, University Park, Pennsylvania,16802, USA

Abstract: Based on the solid state crystal growth (SSCG) method, a seed-free solid-state crystal growth (SFSSCG) method was developed. Large $K_{0.5}Na_{0.5}NbO_3$ (KNN) lead-free piezoelectric single crystals were obtained by the SFSSCG method, which is a traditional sintering grain growth process, doped with doping low content of $LiBiO_3$. Using this seed free method, these single crystals can be, either easily or reproducibly, prepared by traditional grain growth process. The largest dimension of the single crystals obtained 11 × 9 × 3 mm^3, which has a dimension comparable to the macroscopic scale single crystals. These KNN single crystals have a high-quality single-crystalline structure with an orthorhombic perovskite phase without any secondary phase. In order to better investigate such an abnormal crystal growth phenomenon, a comprehensive study is presented here regarding to the crystal growth kinetics and the electrical properties.

Keywords: Single crystal; piezoelectric materials; seed-free solid state growth (SFSSCG); potassium sodium niobate (KNN)

*Corresponding authors:
Jiang Minhong，Guangxi Key Laboratory of Information Materials, Department of Materials Science and Engineering, Guilin University of Electronic Technology, Guilin, Guangxi 541004, P. R. China, Email: jmhsir@tom.com.

Effect of Electrical Properties of Dielectric Elastomer on Electromechanical Response for Actuator Application

Sumonman Niamlang[1*], Nopanan Boonchu [1] , Anuvat Sirivat[2]

[1] Department of Material and Metallurgical Engineering, Faculty of Engineering, Rajamangala University of Technology Thanyaburi, Klong 6, Thanyaburi, Pathumthani 12110

[2]The Petroleum and Petrochemical College, Chulalongkorn University, Phatumwan, Bangkok, 10330, Thailand

* E-mail : sumonman.n@en.rmutt.ac.th

In this research 7 kinds of dielectric elastomers were used, as actuator materials such as styrene acrylic rubber (SAR), acrylic rubber (AR), styrene butadiene rubber (SBR), butadiene rubber (BR), nitrile rubber (NBR), styrene-isoprene-styrene rubber (SIS), and styrene-butadiene-styrene rubber (SBS).

The permeability was calculated from capacitance of dielectric elastomer which was measured by LCR meter at frequency of 10 Hz – 2 MHz. The permeability of SAR, AR, BR, SBR, NBR, SIS and SBS is 6.75×10^{-6}, 6.24×10^{-6}, 4.69×10^{-6}, 4.54×10^{-6}, 3.47×10^{-6}, $2.32 \times 10^{-6}$and 1.56×10^{-6}, respectively. To determine the electromechanical properties, the storage modulus (G') at frequency of 0- 100 rad/s, 1% strain and electric field strength of 0 and 1500 V/mm were measured by the Parallel Plate Melt Rheometer under linear viscoelastic regime. When external electric field was applied, the G' increased because the induced dipole moments are generated and tend to interact each other. Higher shear force is required to deform elastomer [1]. The electromechanical response ($\Delta G' = G'_E - G'_0$) is 4.4×10^6, 0.95×10^6 , 1.19×10^6, 0.094×10^6, -0.015×10^6 and -0.10×10^6 Pa for SAR, AR, BR, SBR, NBR, SIS and SBS, respectively. Higher permeability of elastomer shows stronger polarizability thus stronger interaction between induced dipole moment are generated [2].

The bending response was studied by dipping elastomer in silicone oil between copper electrode under electric field strength of 0 - 1,000 V/mm When external electric field was applied the elastomer was bended toward cathode electrode and degree of bending increase

with increasing electric field strength. The dielectrophoresis force (F_d) increases with increasing electric field strength [3]. The dipole moments were generated and interacted with cathode electrode thus elastomer was bended toward cathode electrode. Higher electric field strength, stronger dipole moments were generated higher degree of bending was observed [4].

When external electric field is applied, the G′ of elastomers increase and F_d of elastomers are generated. Thus these dielectric elastomers can be used in actuator applications under controlling electric field strength.

Keywords: Dielectric elastomer, Electromechanical response, Dielectric constant, Dielectrophoresis force

[1] BAR-COHEN Y. 2009 Electroactive polymer (EAP) actuators for future humanlike robots. *Proc. SPIE 7287, Electroactive Polymer Actuators and Devices (EAPAD)*, 728703.

[2] KOFOD G., SOMMER-LARSEN P. 2005 Silicone dielectric elastomer actuators; finite-elasticity model of actuation. *Sens Act A Phys*, 122, 273-283.

[3] NIAMLANG, S., SIRIVAT, A. 2008 Dielectrophoresis force and deflection of electroactive poly(p-phenylene vinylene)/polydimethylsiloxane blends. *Smart Mater Struct*, 17, 1-8.

[4] CARPI F., ROSSI DD., KORNBLUH R., PELRINE R., SOMMER-LARSEN P. 2008 Dielectric elastomer as electromechanical transducers: fundamentals, materials, devices, models and applications of an emerging electroactive polymer technology. *1st edition Academic Press.*

Investigation on the Sensor Characteristics and Their Improvements of the PNN-PZT/Epoxy Paint for Impact Monitoring

MyeongCheol (Kang)[1], Lae-Hyong (Kang)[1*]

[1]Department of Mechatronics Engineering, and LANL-CBNU Engineering Institute-Korea, Chonbuk National University, 567 Baekje-daero, Deokjin-gu, Jeonju-si, Jeollabuk-do 54896, Republic of Korea.

Presenting author's e-mail : mckang@jbnu.ac.kr

Corresponding author's e-mail : reon.kang@jbnu.ac.kr

Authors' group has investigated on the piezoelectric characteristics of paint sensor with $Pb(Ni_{1/3}Nb_{2/3})O_3$-$Pb(Zr, Ti)O_3$(PNN-PZT), one of the soft type piezoelectric ceramic. The sensitivity of the paint sensor depends on the piezoelectric powder. Therefore, in order to improve the piezoelectricity of the PNN-PZT, we optimized the sintering temperature of it with different wt% of spacer powders. Three sintering temperature conditions (1,000, 1,100, and 1,200^{0}C) were considered and we found that the grain size of the ceramic increases as the sintering temperature increases. The spacer powder(100~500 wt%) was used to prevent evaporation of Pb during the high temperature sintering process. Paint sensor was fabricated by PNN-PZT and epoxy resin with 50:50 wt%, and the electrodes were coated by silver paste on both sides of paint sensor specimen. After that, poling treatment was performed by applying high DC voltage at 4kV/mm for 30 min at room temperature to activate the paint as an impact sensor. The sensitivity of the paint sensor was measure by comparing corresponding output voltage from the paint sensor with the impact force from the impact hammer. As a result, he paint sensor with the optimal (higher piezoelectricity) PNN-PZT showed higher sensitivity than the other paint sensors.

Keywords: PNN-PZT, paint sensor, piezoelectric ceramic, impact monitoring

ACKNOLEDGEMENT

This research was supported by Leading Foreign Research Institute Recruitment Program through the National Research Foundation of Korea funded by the Ministry of Science, ICT and Future Planning. (2011-0030065)

[1] S. Mahajan, O. P. Thakur, and C. Prakash, Effect of Sintering Temperature on Structural and Piezoelectric Properties of PNN-PZT Ceramics, DEF. SCI. J., 57, 23-28

[2] J. Du, J. Qiu, K. Zhu, H. Ji, Enhanced piezoelectric properties of $0.55Pb(Ni_{1/3}Nb_{2/3})O_3$-$0.135PbZrO_3$-$0.315PbTiO_3$ ternary ceramics by optimizing sintering temperature, J. Electroceram., 32, 234-239

[3] D. H. Han, L. H. Kang, J. Thayer, C. Farrar, Manufacturing Method for Sensor-Structure Integrated Composite Structure, Composites Research, 28, 155-161

Microwave Dielectric Properties of $NiAl_2O_3$ Ceramics for Ultra Wideband Antenna

A. Rahman[1*], M.T. Islam[2], A. Rahman[1], M. R. I. Faruque[1] and M.J. Singh[2]

[1]Center for Space Science, Universiti Kebangsaan Malaysia,
43600 UKM Bangi, Selangor, Malaysia
[2]Department of Electrical, Electronic and Systems Engineering,
Faculty of Engineering and Built Environment, Universiti Kebangsaan Malaysia,
43600 UKM Bangi, Selangor, Malaysia

Corresponding author: E-mail: ashu_rahman@yahoo.com

Abstract

In this paper, an attempt has been made to fabricate and analyze the characterization and dielectric properties of $NiAl_2O_3$ ceramics prepared by sol-gel method for ultra-wideband (UWB) communication. In wireless communication the wide and multiband antennas is prerequisite to support more users and to provide information with the higher transmission data rate. Microwave dielectric ceramics play an important role in the modern communication system as an antenna substrate. Materials with high dielectric permittivity, minimum dielectric loss and low temperature coefficient are the prerequisite to achieve microwave devices in small dimension along with minimum loss and high temperature stability [1]. Several researches had been carried out to develop suitable dielectric materials to reduce the dimension and system steadiness of the antenna. The planar antenna offers numerous advantages such as; compact in size, easy to fabricate, low spectral power density, compatible to microwave circuitry and stable radiation characteristics. Various microwave dielectric ceramics (MDC) e.g. $MgZnTiO_3$–$CaNdTiO_3$, $(Mg_{(1-x)}Co_x)_2SnO_4$, $MgCoTiO_3$-NaNd,TiO_3, $ZnTa_2O_6$-TiO_2, $MgCoTiO_3$-NaNd, Al_2O_3 were introduced to use as microwave devices. MDC receiving much attention with good future potential due to their unique electrical properties. Besides, the device made from MDC and operating in the microwave and millimetre-wave technologies should be able to reduce the resources of electromagnetic wave [2]. To support this statement, researchers reported that in the case of microwave substrate and patch antenna application, the resource of electromagnetic wave can be solved using the materials with dielectric constant [3]. Structural and morphological properties of $NiAl_2O_3$ nanoparticle powders are investigated by X-ray diffraction (XRD) analysis and field emission scanning electron microscopy (SEM). XRD analysis confirmed the formation of face centred cubic spinel structure of $NiAl_2O_3$ ceramics. SEM reveals the surface morphology of the ceramics. The dielectric properties are measured using dielectric assessment kit as a function of frequency between 1 GHz to 10 GHz. A dielectric constant (ε_r) of 4.8 and loss tangent ($tan\delta$) of 0.04 are obtained for $NiAl_2O_3$ ceramics. In the literature, several techniques have been introduced to design UWB antenna [4, 5]. The design of

an efficient, compact and light weigt antenna for wideband application is still a major challenge. The performance of the patch antenna is measured using the Agilent vector network analyzer (VNA). In this paper, the measured results show a remarkable achievement of 117% bandwidth with a bandwidth ratio of 3.85:1. The impedance bandwidth increases by 11.2% without any modification of the ground plane. The overall dimension of the antenna also reduces significantly. The overall performance validates the synthesized ceramic as a promising candidate for application in a microstrip patch antenna.

Keywords: Dielectric properties, Microwave Dielectric Ceramics, Sol-gel method, Ultra Wideband Antenna.

References:

[1] Y.C. Chen, Y.N. Wang, W.C. Lee, Enhancement microwave dielectric properties of $La(Mg_{0.5}Sn_{0.5})O_3$ ceramics by substituting La^{3+} with Sm^{3+}, Journal of Physics and Chemistry of Solids. 73 (2) (2012) 296-301.

[2] X. Ye, W. Lei, W.Z. Lu, Microwave dielectric characteristics of Nb_2O_5 added 0.9 Al_2O_3–0.1 TiO_2 ceramics, Ceramics International. 35 (6) (2009) 2131-2134.

[3] T. Tsunooka, M. Androu, Y. Higashida, H. Sugiura, H. Ohsato, Effects of TiO_2 on sinterability and dielectric properties of high-Q forsterite ceramics, Journal of the European Ceramic Society. 23 (14) (2003) 2573-2578.

[4] Azim, R., Islam, M.T. and Misran, N., 2011. Design of a Planar UWB Antenna with New Band Enhancement Technique. Applied Computational Electromagnetics Society Journal, 26(10).

[5] Azim, R., Islam, M.T. and Misran, N., 2013. Microstrip line-fed printed planar monopole antenna for UWB applications. Arabian Journal for Science and Engineering, 38(9), pp.2415-2422.

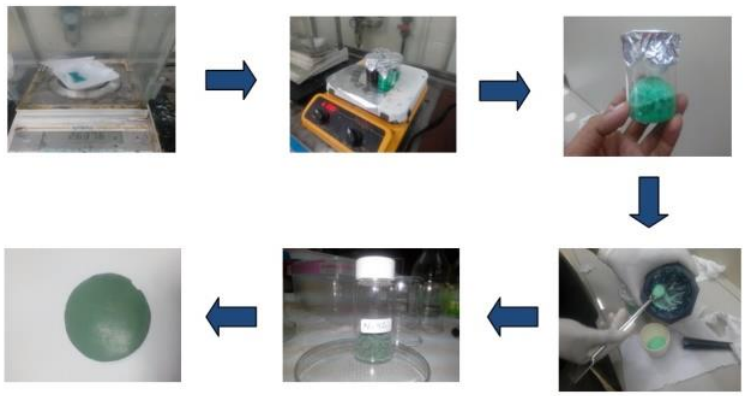

Nanocellulose based piezoelectric sensors

S. Tuukkanen[1], M. Viehrig[1], S. Rajala[1] and P. Kallio[1]

[1]Tampere University of Technology (TUT), Department of Automation Science and Engineering, P.O. Box 692, FI-33101 Tampere, Finland.

*E-Mail:*sampo.tuukkanen@tut.fi

Cellulose based nanomaterials, generally known as nanocellulose [1], are interesting renewable bio-based nanomaterials which have potential applications in material sciences, electronics and biomedical engineering and diagnostic. A strong ability to form light-weight, highly porous, entangled networks makes nanocellulose suitable substrate or membrane material for various applications, such as supercapacitors [2,3].

It was proposed already in 1950's, that wood has piezoelectric properties initiating from the highly crystalline assemblies of cellulose chains [4]. Experimental evidence of the piezoelectricity of cellulose nanocrystals (CNC) was reported only very recently [5,6]. Cellulose nanofibrils (CNF), produced by a mechanical homogenizing process from cellulose fibers, contain both crystalline and amorphous regions. CNC can be obtained from CNF by removal of amorphous regions using hydrolysis e.g. in sulfuric acid.

Here, we report the experimental results on piezoelectricity of nanocellulose films prepared using different methods. The piezoelectric sensitivity of prepared sensor elements is measured using in-house built measurement setup equipped with a mechanical shaker and charge amplifier [7]. A randomly oriented CNF film (prepared by pressure filtering from aqueous CNF dispersion) showed piezoelectric sensitivities of 2-7 pC/N [8,9], which is between the piezoelectric coefficients of quartz (2.3 pC/N) and polyvinylidenefluoride (PVDF, -30 pC/N). Initial results from the nanocellulose based composite films gives promises for biomedical applications of nanocellulose based piezoelectric sensors.

Keywords: Nanocellulose, piezoelectric sensor, cellulose nanofibrils, polyvinylidenefluoride

[1] MOON, R. J., MARTINI, A., NAIRN, J., SIMONSEN, J. & YOUNGBLOOD, J. 2011. Cellulose nanomaterials review: structure, properties and nanocomposites. *Chem Soc Rev*. 40(7), 3941-3994.

[2] TUUKKANEN, S., LEHTIMAKI, S., JAHANGIR, F., ESKELINEN, A.-P., LUPO, D. & FRANSSILA, S. 2014. Printable and disposable supercapacitor from nanocellulose and carbon nanotubes. In: *Proceedings of the 5th Electronics System-Integration Technology Conference (ESTC)*. IEEE; 1-6.

[3] TORVINEN, K., LEHTIMÄKI, S., KERÄNEN J. T., SIEVÄNEN, J. , VARTIAINEN, J., HELLÉN, E., LUPO, D., & TUUKKANEN, S. 2015. Pigment-cellulose nanofibril composite and its application as a separator-substrate in printed supercapacitors. *Electron Mater Lett*., 11(6), 1040-1047.

[4] FUKADA, E. 1955. Piezoelectricity of Wood. *J Phys Soc Japan*., 10, 149-154.

[5] CSOKA, L., HOEGER, I. C., ROJAS, O. J., PESZLEN, I., PAWLAK, J. J. & PERALTA, P. N. 2012. Piezoelectric effect of cellulose nanocrystals thin films. *ACS Macro Lett*., 1(7), 867-870.

[6] FRKA-PETESIC, B., JEAN, B. & HEUX, L. 2014. First experimental evidence of a giant permanent electric-dipole moment in cellulose nanocrystals. *EPL (Europhysics Lett*., 107(2), 28006.

[7] RAJALA, S., METTANEN, M. & TUUKKANEN, S. 2015. Structural and Electrical Characterization of Solution-Processed Electrodes for Piezoelectric Polymer Film Sensors. *IEEE Sens J*. (Accepted for publication).

[8] RAJALA, S., VUORILUOTO, M., ROJAS, O. J., FRANSSILA, S. & TUUKKANEN, S. 2015. Piezoelectric sensitivity measurements of cellulose nanofibril sensors. In: *XXI IMEKO 2015 World Congress "Measurement in Research and Industry" Conference Proceedings*. 2-6.

[9] TUUKKANEN, S. & RAJALA, S. 2015. A Survey of Printable Piezoelectric Sensors. In: *Proceedings of IEEE Sensors 2015 Conference*., 1426-1429.

Properties of $BaTiO_3$-Al_2O_3 composite oxide prepared by sol-gel coating and anodizing for high-voltage electrolytic capacitor

Lian Xiang, Sang-Shik Park*

School of Nano Materials Engineering, Kyungpook National University,
Gyeongbuk 742-711, Republic of Korea
Presenting author: xianglian93@163.com *Corresponding author: parkss@knu.ac.kr

ABSTRACT

$BaTiO_3$ films were coated on high-voltage etched aluminum foils by vacuum infiltration using sol. The specimens coated with $BaTiO_3$ films were annealed under 450–600 ℃, and then repeated for serval cycles (n=0, 1, 2, 4, and 8 cycles), finally anodized at 100–900 V. The specimens were analyzed by X-ray diffraction, field emission scanning electron microscopy, and field emission transmission electron microscopy. The results shown that the tunnels of the specimens had a multi-layer structure, which consisted of an Al_2O_3 outer layer, a $BaTiO_3$-Al_2O_3 composite oxide middle layer, and an aluminum hydrate inner layer. The withstanding voltages, leakage current and specific capacitance of specimens were also measured. The specimens can withstand the expected voltage and maintain the relatively low leakage current. The specific capacitances of the $BaTiO_3$-coated specimens are all increased comparing to specimens without $BaTiO_3$ coating. The $BaTiO_3$-Al_2O_3 composite oxide films were successfully formed on high-voltage etched aluminum foils by vacuum infiltration and anodizing. The results suggested that composite oxide films could be used in order to enhance the specific capacitance and withstanding voltage of anode Al foils.

Acknowledgments

This work was supported by a grant (15RTRP-B067917-03) from the Railroad Technology Research Program funded by the Ministry of Land, Infrastructure, and Transport of the Korean government.

Recent Progress in High-Performance Intrinsic Ultralow-k Polyimide Films

Yi Zhang*, Chao Qian, Runxin Bei, Yiwu Liu, Zhenguo Chi, Siwei Liu, Jiarui Xu

Key Laboratory for Polymeric Composite and Functional Materials of Ministry of Education, Guangdong Engineering Technology Research Center for High-Performance Organic and Polymer Photoelectric Functional Films, GDHPPC Lab, State Key Laboratory of Optoelectronic Materials and Technologies, School of Chemistry and Chemical Engineering, Sun Yat-Sen University, Guangzhou 510275, P. R. China

E Mail: ceszy@mail.sysu.edu.cn

The search for new low-k dielectric materials has always been dictated by industrial needs, resulting in a strong connection between fundamental research and technology. And the acquisition of intrinsic ultralow-k materials remains one of the most important bottlenecks restricting the leapfrog development of the microelectronics industry. Here we introduce recent advance in the research of high-performance intrinsic ultralow-*k* polyimide films in our lab, by considering the polarizability and the free-volume theory from the molecular level. The intrinsic ultralow-*k* property was obtained by the molecular design and the control of the steric and aggregation structure of the polymers, which led to the formation of uniform distributed free-volume holes with sizes at the Ångström scale, measured by positron annihilation lifetime spectroscopy (PALS). Such a strategy is beneficial for lowering the *k* value and simultaneously maintaining the overall properties of polyimide, such as excellent mechanical properties, thermal properties, and good processing properties.

Keywords: Intrinsic ultralow-k, polyimide, high-performance, progress

*The financial support by the National 973 Program of China (2014CB643605), the National 863 Program of China (2015AA033408), the National Natural Science Foundation of China (51373204, 51173214, 51233008, J1103305), the Science and Technology Project of Guangdong Province (No. 2015B090915003), the Doctoral Fund of the Ministry of Education of China (20120171130001), and the Fundamental Research Funds for the Central Universities are gratefully acknowledged.

Research on structure characteristics of micro compound vibration generator

Yan Zhen

Mechanic & Electronic College, Agricultural University of Hebei, Baoding, China

Abstract: With the rapid development and application of WSN, power supply mode of traditional cell and wired power are difficult to satisfy the special requirement of panel point. Micro energy harvesting device of small volume, high efficiency, without confine to environment condition is received much concern. We try to enhance energy harvesting efficiency as target. A new structure type, combined type micro vibration generator is put forward, and analysis and design technology of improving the vibration energy conversion density is studied. Piezoelectric and electromagnetic power generation technology are integrated in a micro electrical mechanical system, and the key technology of machine-electric-magnetic coupled modeling, analysis and optimization design are researched. Considering the micro piezoelectric, micro electromagnetic basic theory to improve the power generation efficiency of the whole system. The effective way to reduce the fatigue limit and expand the frequency range of the micro generator is explored by using the structure of the distributed mass. The validity of system modeling, analysis and design theory is verified by experiment. The results show that in the same volume, compared with the piezoelectric vibration generator, the compound vibration generator increases the power of 80%, while the electromagnetic vibration generator is increased by 160%. The compound vibration generator has both high stable and energy conversion efficiency.

Study on smart actuator based on piezoelectric polymers bimorphs

Y.Z. Liu[1,a], Y. Sun[1,b],F.L. Zeng[1,c]

[1]Harbin Institute of Technology, Department of Astronautic Science and Mechanics, Harbin, China.

[a]liuyizhi@hit.edu.com, [b]sunyi@hit.edu.cn, [c]zengfanlin@hit.edu.cn

- Clearly state the contact details (e-mail, affiliation, country) of the presenting author

Presenting author:

Y.Z. Liu, liuyizhi@hit.edu.com, Harbin Institute of Technology, Harbin, China.

- Indicate your preference on the mode of presentation (Oral or Poster)

Oral presentation

Abstract:

Poly(vinylidene fluoride) (PVDF) is extensively used in smart structure sensors, actuators and transducers because of its good piezoelectric and pyroelectric properties. At present, PVDF as a novel material has been used in space. However, the use of PVDF was badly affected by atomic oxygen from Low Earth Orbit. These conditions combined with the need for lower cost and lighter weight necessitates the design of multi-functional and space-survivable materials.

In our previous works[1-3], PVDF has been prepared by the solvent evaporation method and POSS (Polyhedral oligomeric silsesquioxane) as nanofiller was also added to enhance superior properties such as oxygen permeability and mechanical strength. That POSS was incorporated into PVDF matrix is to enhance the mechanical properties of piezoelectric polymer.The morphology, crystallization, and piezoelectric and mechanical properties (including nanoindentation, nanoscratch, and nanotensile testing) of the composites have been investigated. The mechanical and polarization properties can be remarkably increased and ensured by addition of POSS. The piezoelectric coefficients of

PVDF were 14 Pc/N, 12 Pc/N and 11 Pc/N with POSS additions of 3 wt%, 5 wt% and 8 wt% respectively.

Single sheets of PVDF don't have very large displacements when voltages are applied even if the value of d33 of PVDF were tested 32 PC/N, so other things such as bimorphs are created. In this work, Bimorphs of electroded PVDF sheets were prepared by putting electrodes on both sides and glued two sheets together so that the poled directions are in the same direction. we have tried to get the metallic electrodes as thin as possible maximize the flexibility of the bimorphs. Equal but opposite electric fields are then applied to the two sheets. One of the sheets shrinks in length and the other expands causing the bimorph to bend.

When electric voltage (0-1500V) was applied, displacements of bimorphs preduced. And displacements increased with increasing AC voltages.

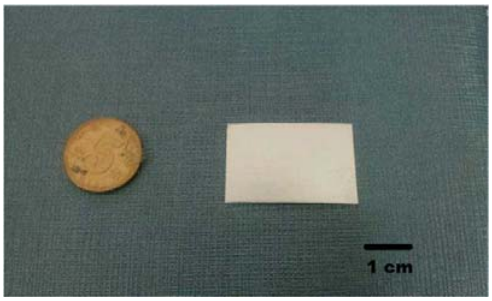

Figure 1. PVDF

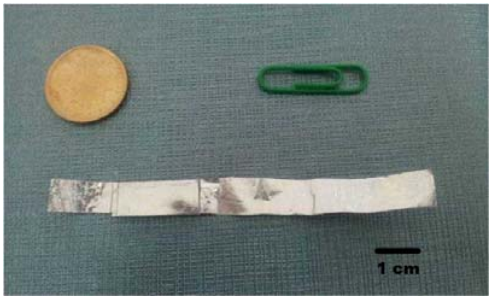

Figure 2. Bimorphs of electroded PVDF sheets

Figure 3. Series of photographs showing the bimorphs of PVDF sheets

[1] Y.Z. Liu, Y. Sun, F. Zeng, Y. Chen, Q. Li, B. Yu, and W. Liu. Polym. Eng. Sci.,7, 53, 2012.

[2] Y.Z. Liu, Y. Sun, F. Zeng, and Y. Chen. Int. J. Electrochem. Sci, 8: 5688-5697, 2013.

[3] F.L. Zeng, Y.Z. Liu, Y. Sun, E. Hu, and Y. Zhou. J.Polym. Sci. B: Polym.Phys., 23,50: 1597-1611, 2012.

Study on the arc piezoelectric composite oscillator

In this study, in order to expand piezoelectric oscillator bandwidth and beam opening angle, a new piezoelectric oscillator structure with matching layer on the surface of the arc piezoelectric composite material is presented. The vibration characteristics of a new arc piezoelectric composite material are investigated by means of finite element analysis (FEA) and experimental measurement.

Firstly, the single arc piezoelectric ceramic composite material is modeled and simulated in air by FEA. Then the relationships between the resonant frequency and thickness, width, average radius are researched, the results show that the thickness is the main factor that affects the resonance frequency of vibration.

Secondly, the arc piezoelectric ceramic composite material with the matching layer is modeled and simulated in air and water by FEA, in which the matching layer is composed of aluminum powder and epoxy resin. By selecting different component matching layers and thickness, the changes of the resonance frequency, bandwidth and transmitting voltage response of the piezoelectric oscillator are analyzed. In the simulation process, the selected mass fraction of aluminum powder are 10%, 30%, 45% and 60% respectively, by comparing the four sets of data to optimize the matching layer parameters, the result of simulation shows that when the mass fraction of aluminum powder is of 45%, the piezoelectric oscillator bandwidth presents the largest, and the maximum bandwidth reaches 55 kHz.

Finally, the experiment is carried out, the arc composite piezoelectric oscillator is designed by using the optimized matching layer structure, with the mass fraction of aluminum powder is of 45%, and the thickness of the matching layer is 8.5mm. The result of the experiment shows the transmitting voltage response bandwidth (biggest transmitting voltage response decreases 3 dB) of arc piezoelectric vibrator is 57 kHz. And the bandwidth of the piezoelectric oscillator is increased by 3 times after adding the matching layer. The experimental results are in accordance with the simulation results. The results show that the finite element simulation is feasible. Meanwhile the errors between the simulation and experiment are analyzed.

Keywords: arc piezoelectric composite oscillator; matching layer; transmitting voltage response; expand bandwidth

Tests on Piezoelectric Materials Qualification on Structural Health Monitoring of Space Vehicles

Daniela (ENCIU)[1], Ioan (URSU)[1]

[1] INCAS – National Institute for Aerospace Research "Elie Carafoli"
B-dul Iuliu Maniu 220, Bucharest 061136, Romania

enciu.daniela@incas.ro

In the paper is presented a complex tests program in which smart structures specimens defined by aluminium discs with bonded piezo active sensors are subjected to laboratory simulated harsh conditions of outer space. The purpose of these tests was to show, for the first time in our best knowledge, that an already classic intelligent material, namely piezo material used as piezo wafer active sensor (PWAS), is capable of survivability and operation in simultaneous conditions of high temperature variations, from cryogenic (-200^0 C) to high temperatures (about $+200^0$ C), and in the presence of cosmic type radiation (the calculated 23.5 kGy integral irradiation dose), and so validate a structural health monitoring (SHM) technology based on electromechanical impedance spectroscopy (EMIS) method in view of a possible transfer to the spacecraft [1]-[4]. The SHM technology is defined as the adopted strategy in order to identify the damages that occur in the structure. Indeed, the PWASs are used as both actuator and sensor in order to identify the occurrence of a local mechanical damage by using the EMIS method. This method is based on the piezoelectric effect: the PWAS, excited by an electrical signal, generates elastic waves which propagate through the investigated structure. The generated waves capture the presence of any mechanical modification in the structure and modify the EMIS signature. Moreover, to avoid false alarm, in article is presented a procedure for distinguishing between the reversible effects of environmental conditions and the irreversible effects of mechanical damages on the EMIS signature.

Keywords: Piezoelectric wafer active sensor, smart material, structural health monitoring, electromechanical impedance spectroscopy method

References

[1] MANCINI, S., TUMINO, G. & GAUDENZI, P. 2006. Structural health monitoring for future space vehicles. *Journal of Intelligent Material Systems and Structures*, 17, 577-585.

[2] RUGINA, C., ENCIU, D. & TUDOSE, M. 2015. Numerical and experimental study of circular disc electromechanical impedance spectroscopy signature changes due to structural damage and sensor degradation. *Structural Health Monitoring - an International Journal*, 14(6), 663-681.

[3] RUGINA, C., TOADER, A., GIURGIUTIU, V. & URSU, I. 2013. The electromechanical impedance method for structural health monitoring of thin circular plates. *Proceedings of the Romanian Academy, Series A*, 15(3), 272-282.

[4] TOADER, A., URSU, I. & ENCIU, D. 2015. New Advances in Space SHM Project. *INCAS Bulletin*, 7(1), 65-80.

Pulsed Laser Deposition of Multiferroic Complex Oxide Superlattices

Author(s): Gail J Brown[1], John Jones[1], Krishnamurthy Mahalingam[1], Zhongqiang Hu[1], Larry Grazulis[1], Yalin Lu[2]

Affiliation(s): [1]Materials & Manufacturing Directorate, Air Force Research Laboratory; [2]Physics Department, US Air Force Academy

$Bi_5Fe_{0.5}Co_{0.5}Ti_3O_{15}$ (BFCTO) ceramics exhibits a naturally forming layered structure of perovskite-like layers separated by Bi_2O_2 layers. The material has a four-layer unit cell, and presents a remarkable coexistence of ferroelectricity (FE) and ferromagnetism (FM) above room temperature (RT). The measured 2*Pr* and 2*Mr* are 13 ¹C/cm2 and 7.8*m*emu/g, respectively, and the material's magnetic transition temperature is *»* 345 ±C. These bulk ceramic properties led to an interest in further exploring the material's potential for electronic and photonic applications when deposited in thin films. For this study, thin films were fabricated using pulsed laser deposition with a single bulk ceramic target. A systematic study of PLD deposition parameters was performed for films grown on LAO, LSAT and Silicon substrates. The thin films were characterized by a variety of techniques such as XRD, AFM, XTEM, XPS and PFM to study the impact of deposition conditions on the structural and morphological qualities of the films. The thin films replicated the oxide superlattice structure formed in the bulk ceramic targets.

Ultraviolet to near-infrared dielectric functions and ferroelectric polydomain structures of $K_{0.5}Na_{0.5}Nb_{1-x}Mn_xO_{3-\delta}$ nanocrystalline films for potential optoelectronic applications

Qinglin Deng, Jinzhong Zhang, Zhigao Hu* and Junhao Chu

Department of Electronic Engineering, East China Normal University, Shanghai 200241, China.

**E-mail: zghu@ee.ecnu.edu.cn*

Lead-free ferroelectric $K_{0.5}Na_{0.5}NbO_3$-based films are undoubtedly one of the most promising materials for miniaturized devices such as ferroelectric memory, detector and electro-optic devices. Recently, interest in the optical properties and domain behavior of these films has surged for potential optoelectronic applications. Spectroscopic ellipsometry is a powerful and nondestructive tool that allows us to simultaneously obtain the thickness and optical parameters without Kramers–Krönig transformation.[1] Piezoresponse force microscopy techniques were widely adopted to probe and manipulate the domains at the nanoscale.

In this Talk, the Adachi's dielectric function model and a four-phase layered model were used at the first time to fit the ellipsometric spectra of high-quality $K_{0.5}Na_{0.5}Nb_{1-x}Mn_xO_{3-\delta}$ (KNNM*x*) films, which have the optimal ferroelectric properties when x=0.06 (KNNM0.06), for extracting optical parameters in the photon energy range of 1.5–5.5 eV.[2] The optical band gap (E_g) slightly decreases, while the high-frequency dielectric constant (ε_∞) linearly increases with increasing Mn concentration. Moreover, temperature dependent optical dispersion behavior of the KNNM0.06 film has been investigated from 300 K to 800 K. The analysis of E_g and the extinction coefficient (k) reveals the correlation between optical properties and structural phase transition. In addition, the well-defined rectangular phase hysteresis loop reflects good piezoresponse properties of the KNNM0.06 film, which mainly shows the distinct in-plane (180^o) nano-domains. After the application of the +2 V field, switching of the in-plane polarization (IPP) domain was evident. In consideration of the excellent optical and electrical properties of the KNNM0.06 film, we proposed a model to design the nonvolatile ferroelectric random-access memory (NVFRAM). Besides, it can be a novel idea to develop KNNM0.06-based films for potential multifunctional applications, for instance, co-doping with rare earth elements and used for ultraviolet detector.

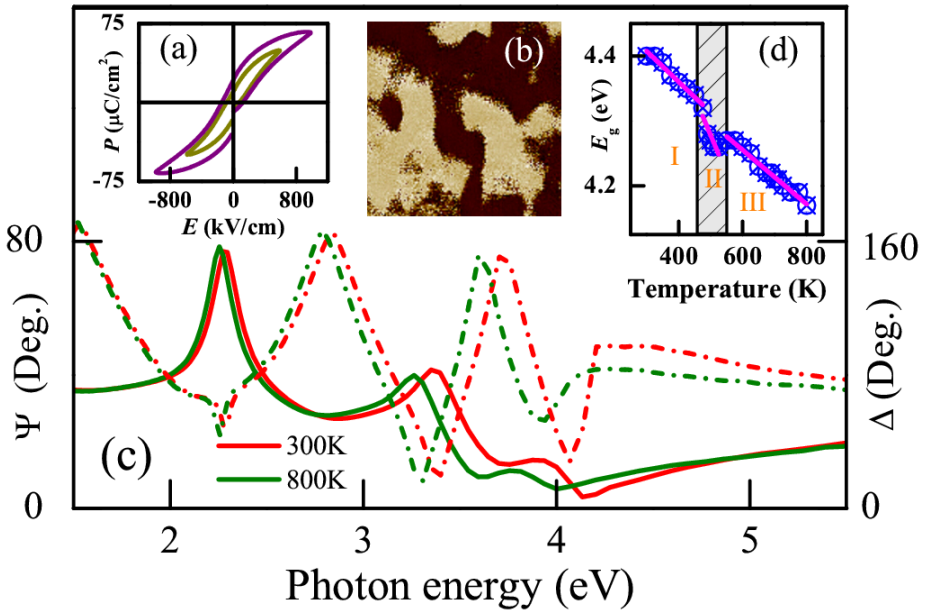

Fig.1 Polarization–electric field loops (a), phase of IPP signal (b), temperature dependent experimental ellipsometric spectra (c) and E_g evolution as a function of temperature (d) for the KNNM0.06 film.

Keywords: lead-free, ferroelectric, ellipsometric spectra, fitting model, polar domain

[1] ZHANG, J. Z., TONG, W.-Y., ZHU, J. J., XU, J. Y., DUAN, Z. H., XU, L. P., HU, Z. G., DUAN, C.-G., MENG, X. J., ZHU, Z. Q. & CHU, J. H. 2015. Temperature Dependent Lattice Dynamics and Electronic Transitions of $0.93Pb(Zn_{1/3}Nb_{2/3})O_3$-$0.07PbTiO_3$ Single Crystals: Experiment and Theory. *Phys. Rev. B*, 91, 085201.

[2] DENG, Q. L., ZHANG, J. Z., HUANG, T., XU, L. P., JIANG, K., LI, Y. W., HU, Z. G. & CHU, J. H. 2015. Optoelectronic Properties and Polar Nano-Domain Behavior of Sol–Gel Derived $K_{0.5}Na_{0.5}Nb_{1-x}Mn_xO_{3-\delta}$ Nanocrystalline Films with Enhanced Ferroelectricity. *J. Mater. Chem. C*, 3, 8225-8234.

Varifocal Lens with Plasticized Poly(vinyl chloride) Gel

Eun-Jae Shin[1], Myoung Yeo[1], Jin Woo Bae[2], Sang-Youn Kim[1]

[1]Interaction Laboratory, Advanced Technology Research Centre, Korea University of Technology and Education, 1800 Chungjeollo, Byeongcheon-Myeon, Cheonan-City 330-708, Chungnam Province, Korea.

[2]Department of Advanced Materials Engineering for Information and Electronics, Kyung Hee University, Yongin, Gyeonggi-do 446-701, Korea.

E Mail : ejshin@koreatech.ac.kr / sykim@kut.ac.kr

This paper proposes a transparent and electroactive polymer gel for a varifocal microlens. The proposed electroactive polymer gel, consisting of non-ionic poly(vinyl chloride) and dibutyl adipate, is reconfigured in response to the applied voltage. Based on this effect, we fabricate a microlens whose curvature is altered under variable input voltages, and thus the variation of its focal length and zoom effect was observed consequently. Furthermore, as soon as applied voltage is removed, the proposed electroactive polymer gel showed rapid restoration to initial configuration. Therefore, the focal length of the proposed plasticized PVC gel lens can be considerably changed in real-time under an applied electric field. The focal length remarkably increases from 3.8 mm up to 14.3 mm with increasing applied voltages from 300 V to 800 V. Because of its transparent, compact, and electroactive characteristics, the proposed plasticized PVC gel microlens can be easily inserted into small electronic devices, such as digital cameras, cell phones, and other portable optical devices.

Keywords: non-ionic PVC/DBA (nPVC) gel, creep deformation, dielectric property, varifocal lens

Acknowledgements

This research was supported by a grant of the Korea Health Technology R&D Project through the Korea Health Industry Development Institute (KHIDI), funded by the Ministry of Health & Welfare, Republic of Korea (grand number : HI14C0765). This research was

also supported by the Dual Use Program Cooperation Center (Development of tactile display device for Virtual reality-based flight simulator, 12-DU-EE-03).

Varifocal Lens with Plasticized Poly(vinyl chloride) Gel

Eun-Jae Shin[1], Myoung Yeo[1], Jin Woo Bae[2], Sang-Youn Kim[1]

[1]Interaction Laboratory, Advanced Technology Research Centre, Korea University of Technology and Education, 1800 Chungjeollo, Byeongcheon-Myeon, Cheonan-City 330-708, Chungnam Province, Korea.

[2]Department of Advanced Materials Engineering for Information and Electronics, Kyung Hee University, Yongin, Gyeonggi-do 446-701, Korea.

E Mail : ejshin@koreatech.ac.kr / sykim@kut.ac.kr

This paper proposes a transparent and electroactive polymer gel for a varifocal microlens. The proposed electroactive polymer gel, consisting of non-ionic poly(vinyl chloride) and dibutyl adipate, is reconfigured in response to the applied voltage. Based on this effect, we fabricate a microlens whose curvature is altered under variable input voltages, and thus the variation of its focal length and zoom effect was observed consequently. Furthermore, as soon as applied voltage is removed, the proposed electroactive polymer gel showed rapid restoration to initial configuration. Therefore, the focal length of the proposed plasticized PVC gel lens can be considerably changed in real-time under an applied electric field. The focal length remarkably increases from 3.8 mm up to 14.3 mm with increasing applied voltages from 300 V to 800 V. Because of its transparent, compact, and electroactive characteristics, the proposed plasticized PVC gel microlens can be easily inserted into small electronic devices, such as digital cameras, cell phones, and other portable optical devices.

Keywords: non-ionic PVC/DBA (nPVC) gel, creep deformation, dielectric property, varifocal lens

Acknowledgements

This research was supported by a grant of the Korea Health Technology R&D Project through the Korea Health Industry Development Institute (KHIDI), funded by the Ministry of Health & Welfare, Republic of Korea (grand number : HI14C0765). This research was

also supported by the Dual Use Program Cooperation Center (Development of tactile display device for Virtual reality-based flight simulator, 12-DU-EE-03).

Colossal Dielectric Permittivity in (Y^{3+} and Nb^{5+}) Doped TiO_2 Ceramics

Theeranuch Nachaithong[1,2], Pinit Kidkhunthod[3], Prasit Thongbai[2,4*], Santi Maensiri[5]

[1]Materials Science and Nanotechnology Program, Faculty of Science, Khon Kaen University, Khon Kaen 40002, Thailand.

[2]Nanotec–KKU Center of Excellence on Advanced Nanomaterials for Energy Production and Storage, Khon Kaen 40002 ,Thailand.

[3]Synchrotron Light Research Institute (Public Organization), 111 University Avenue, Muang District, Nakhon Ratchasima 30000, Thailand.

[4]Integrated Nanotechnology Research Center (INRC), Department of Physics, Faculty of Science, Khon Kaen University, Khon Kaen 40002, Thailand.

[5]Institute of Science, School of Physics, Suranaree University of Technology, Nakhon Ratchasima 30000, Thailand.

[*]*Email: pthongbai@kku.ac.th*

Recently, a novel dielectric material with excellent–performance with high dielectric permittivity (ε′) and low dielectric loss tangent (tanδ) was reported in (In^{3+} and Nb^{5+}) co-doped rutile-TiO_2 [1]. In this work, the dielectric properties of (Y^{3+} and Nb^{5+}) co-doped TiO_2 ceramics prepared by a glycine nitrate process were investigated. A main rutile–TiO_2 phase and dense ceramic microstructure were obtained in $(Y_{0.5}Nb_{0.5})_xTi_{1-x}O_2$ ceramics with x=0.025 and 0.05. By using SEM mapping of all elements (Ti, O, Y, and Nb), it was found that the dopants were homogeneously dispersed in both the grain and grain boundary. The sintered ceramics exhibited very high ε′ of ≈10^4-10^5 with nearly independent on frequency in the range of 10^2-10^7 Hz. Interestingly, a low tanδ value was slightly dependent on frequency. X–ray absorption near edge structure (XANES) confirmed the presence of Ti^{3+} ions, which was induced by Nb^{5+} doping ions. The colossal dielectric properties were caused by the formation of large defect–dipole clusters of localized electrons induced by co–doping ions.

Keywords: Colossal dielectric permittivity, loss tangent, rutile-TiO_2, electrical properties.

[1] HU, W., LIU, Y., WITHERS, R. L., FRANKCOMBE, T. J., NORÈN, L., SNASHALL, A., KITCHIN, M., SMITH, P., GONG, B., CHEN, H., SHIEMER, J., BRINK, F. & WONG-LEUNG, J. 2013. Electron-pinned Defect-dipoles for High-Performance Colossal Permittivity Materials. *Nat Mater*, 12, 821-826.

Dielectric, ferroelectric, and large field-induced strain properties of $LiNbO_3$-Modified $BiFeO_3$–$BaTiO_3$ Ceramics

Rizwan Ahmed Malik[1], Ali Hussain[1], Adnan Maqbool[1], Tae Kwon Song[1], Won-Jeong Kim[2] and Myong-Ho Kim[1,*]

[1]School of Advanced Materials Engineering, Changwon National University, Gyeongnam 641-773, Republic of Korea
[2]Department of Physics, Changwon National University, Gyeongnam 641-773, Republic of Korea

(**rizwanmalik@yahoo.com and mhkim@changwon.ac.kr**)

In this work, a new lead-free piezoelectric ceramics, (1–x) ($0.67BiFeO_3$ – $0.33BaTiO_3$) – x $LiNbO_3$ abbreviated as BF-BT-LN (x = 0.00–0.030), were fabricated by conventional solid state method. It was found that the incorporation of $LiNbO_3$ into BF-BT system caused no significant change in crystal structure. However, an obvious variation in microstructure was observed. The x = 0.015 composition showed enhanced ferroelectric and electric field-induced strain properties with dynamic piezoelectric constant Smax/Emax = d^*_{33} = 440 pm/V at a relatively low field of 4 kV/mm, along with a high Curie temperature T_c = 392°C. Large electric-field induced strain at low driving field combine with high T_c makes this system suitable for high temperature piezoelectric devices.

Keywords: Lead-free, piezoelectricity, Ferroelectricity, BiFeO3, Field-induced strain

* Corresponding author. Tel: +82 55 213 3719, Fax: +82 55 262 6486
Email Address: mhkim@changwon.ac.kr (Myong-Ho Kim)

Enhanced dielectric and piezoelectric characteristics of 0-3 high-content ceramic/epoxy nanocomposite thin films doped with multi-wall carbon nanotubes

H.J. Kim[1], B. Yeon[1,2], and K.M. Lee[2]

[1]Nano Convergence Sensor Research Section, Electronics and Telecommunications Research Institute, Daejeon, Republic of Korea

[2]Department of Material Science and Engineering, Korea University of Technology and Education, Cheonan-si, Republic of Korea

E Mail : nolawara@etri.re.kr

Recently, flexible piezoelectric nanocomposites have received a great deal of attention for sensors, actuators and transducers in variety areas [1-2]. Especially, 0-3 piezoelectric nanocomposites have many advantages of better flexibility, easier manufacturing and lower cost, compared to other types of nanocomposites. However, it still has critical drawbacks of poorer piezoelectric and dielectric properties since the piezoelectric ceramic particles within a polymer matrix are hard to be fully polarized. In this paper, we focus our attention on the effects of CNTs on the dielectric and piezoelectric properties of 0-3 high-content PZT/epoxy nanocomposite thin films. The 0-3 $Pb(Zr_{1/2}Ti_{1/2})O_3$-($Pb(Zn_{1/3}Nb_{2/3})O_3$-$Pb(Ni_{1/3}Nb_{2/3})O_3$) (PZT)/epoxy nanocomposites were fabricated with 81 wt.% (~40 vol.%) of PZT ceramic particles and 19 wt.% of epoxy resins based on low viscosity diglycidyl ether of bisphenol F type by casting process. And CNTs-doped PZT/epoxy nanocomposite films were investigated with various volume fractions of CNTs up to 0.4 wt.%. The fabricated CNTs-doped PZT/epoxy nanocomposite thin film had just about 45 μm thickness and had hardly residual pores, voids, and any other defects in the matrix. From the experimental electrical conductivity and dielectric constant characteristics, it was shown that the electrical conductivity of the film slowly increases with the increase of the CNTs below 0.08 wt.% and then abruptly increases in the CNTs contents above 0.08 wt.%. Moreover, the dielectric constant and dielectric loss characteristics of the nanocomposites also increased along with the CNTs contents, similar to the electrical conductivity tendencies. These results can be expalined by percolation theory that these abrupt increases of electrical conductivity and dielectric loss of the composites are attributed to the infinite

conductive network of percolated CNTs. The measured piezoelectric charge and voltage coefficients of the nanocomposite were in good agreement with the conclusion obtained from the conductivity and dielectric properties of the CNTs-doped PZT/epoxy nanocomposites. The d_{33} and g_{33} values of the nanocomposite with 0.07 wt.% CNTs were respectively 68 pC/N and 434 mV·m/N, which are respectively 2.5 and 2.2 times higher than that of pure PZT/epoxy nanocomposite. These piezoelectric characteristics reveal that the small contents of CNTs additives can improve the conductivity of the nanocomposites and thereby help them polarize easier. However, more CNTs above 0.08 wt.% result in higher dielectric loss and electrical conductivity in the PZT/epoxy nanocomposite, which cannot polarize the nanocomposite effectively. As a result, it is obvious that a very small amount of CNTs can improve the poling efficiency of the high-content PZT/epoxy nanocomposite thin films and induce higher dielectric and piezoelectric properties of them.

Keywords: Carbon nanotube, Nanocomposite, Conductivity, Dielectric constant, Piezoelectric property

[1] CHUN, J., Kang, N.R., Kim, J.Y., Noh, M.S., Kang, C.Y., Chai, D., Kim, S.W., Wang, Z.L., Baik, J.M. 2015. Highly Anisotropic Power Generation in Piezoelectric Hemispheres Composed Stretchable Composite Film for Self-powered Motion Sensor. *Nano Energy*, 11, 1-10.

[2] Xu, S., Yeh, Y.W., Poirier, G., McAlpine, M.C., Register, R.A., Yao, N., 2013. Flexible Piezoelectric PMN-PT Nanowire-based Nanocomposite and Device. *Nano Lett.*, 13, 2393-2398.

Improved Dielectric Properties of 0-3 PZT/Epoxy Nanocomposite with Soft Polymer Matrix

B. R (Yeon)[1,2], H. J (Kim)[1], K. M (Lee)[2]

[1]Nano Convergence Sensor Research Section, Electronics and Telecommunications Research Institute, Daejeon, Republic of Korea.

[2]Department of Material Science and Engineering, Korea University of Technology and Education, Cheonan-si, Republic of Korea.

nolawara@etri.re.kr

Piezoelectric nanocomposites with 0-3 connectivity have received a great deal of attention for sensors, actuators and transducers.[1] Generally, the 0-3 piezoelectric nanocomposites consisting of a particulate piezoelectric ceramic randomly dispersed within a polymer matrix have several advantages of their good flexibility and large-scale production. However, they still have critical drawbacks such as poor piezo- and di-electric properties and too higher driving voltages compared to the sintered piezoelectric ceramics. This paper reports that piezo- and di-electric properties of the flexible 0-3 lead zirconate titanate/epoxy resin polymer (PZT/Epoxy) nanocomposite film can be improved by mechanical elasticity of the used epoxy matrix. The piezoelectric nanocomposite were realized with a very high PZT volume fraction of 89 wt.% to achieve a beneficial higher piezoelectric coefficients. To produce the PZT/epoxy piezoelectric nanocomposites, PZT particles were initially mixed in the prepared epoxy resin mixture using a motorized pestle and mortar at 600 rpm for 3 h. Then, the hardener was added and the composite pastes were again mixed at 600 rpm for 5 min. The PZT/epoxy pastes were sequentially casted onto a silver-coated Polyethylene Naphthalate (PEN) substrate by the size of 25x25 mm^2 using a doctor blade applicator [ZUA2000 Universal Applicator, Zhentner Testing Instruments], and followed by defoaming in vacuum for 15 h. Defoaming process in vacuum is very important because nanocomposites with a high loading of PZT powders have problems of poor mechanical and piezoelectric properties by their pores and voids formed during mixing and curing

process. After the defoaming, the piezoelectric nanocomposite films were dried at 130℃ for 4 h, and completed by the silver electrode coating and curing at 100℃ for 30 min. In order to investigate the effects of the polymer matrix on the dielectric and piezoelectric properties of the nanocomposite, we compared the characteristics of the nanocomposite dispersed into the epoxy matrix mixed with 2 different ratios. From the FE-SEM images of the fabricated nanocomposites, it was shown that the nanocomposite film is uniform and well-dispersed. And, the experimental dielectric and piezoelectric properties showed that the nanocomposite film with softer polymer matrix can obtain the higher dielectric and piezoelectric value respectively, regardless of PZT volume fractions. The capacitances of the nanocomposites with 2 different epoxy matrixes were 3.29 nF (for a softer matrix) and 1.24 nF (for a harder matrix) at 1 kHz, respectively, under an oscillating voltage of 1 V. As a result, it is obvious that the piezo- and di-electric properties of the 0-3 piezoelectric nanocomposite can be improved by decreasing the mechanical stiffness of the polymer matrix, due to the increasing the effective mechanical strain of the nanocomposite film.

Keywords: nanocomposite, piezoelectric, dielectric, epoxy matrix

[1] Babu, I. and G. de With, *Highly flexible piezoelectric 0–3 PZT–PDMS composites with high filler content.* Composites Science and Technology, 2014. **91**: p. 91-97.

Improved Dielectric Properties of PVDF Composites by Employing Mg–Doped $La_{1.9}Sr_{0.1}NiO_4$ Nanoparticles as Filler

Keerati Meeporn[1], Prasit Thongbai[1,2*]

[1]Materials Science and Nanotechnology Program, Faculty of Science, Khon Kaen University, Khon Kaen 40002, Thailand.

[2]Integrated Nanotechnology Research Center (INRC), Department of Physics, Faculty of Science, Khon Kaen University, Khon Kaen 40002, Thailand.

[*]*Email: pthongbai@kku.ac.th; prasitphysics@hotmail.com*

In recent years, Ceramics-Polymer composite materials have been widely studied because of the need for flexible polymer matrix materials with high dielectric permittivity for supporting the rapid progress of electronic industry [1]. In this work, a composite with enhanced dielectric permittivity (ε′) is realized by employing Mg-doped $La_{1.9}Sr_{0.1}NiO_4$ nanoparticles (LSNMO-NPs) as an inorganic filler and poly (vinylidene fluoride) (PVDF) as a polymer matrix. The LSNMO ceramic was used as filler owing to its high $\varepsilon' \approx 10^5$-$10^6$ with relatively low loss tangent (tanδ) compared to the un-doped $La_{1.9}Sr_{0.1}NiO_4$ ceramic. LSNMO-NPs fillers were prepared by a combustion method using a urea as fuel. LSNMO-NPs/PVDF composites were prepared by liquid-phase assisted dispersion and hot-pressing method. Microstructure analysis revealed that LSNMO-NPs were dispersed well in the PVDF matrix. The abrupt changes in ε′ and tanδ of LSNMO-NPs/PVDF composites were observed at a critical volume fraction of LSNMO-NPs. These finding indicated the formation of percolation networks of LSNMO-NPs. The ε′ value of the polymer composite with volume fraction of 50% LSNO was 503.73 at 1 kHz, which was ~50 times higher than that of pure PVDF (ε′~10). The enhanced ε′ of the LSNMO-NPs/PVDF composites with low LSNMO-NPs loading content was attributed to the large value of ε′ of filler, while the great enhanced ε′ in the high loading content LSNMO-NPs/PVDF composites was well described by the percolation theory.

Keywords: PVDF, dielectric permittivity, loss tangent, polymeric composite

[1] ARBATTI, M., SHAN, X. & CHENG, Z. 2007. Ceramic-Polymer Composites with High Dielectric Constant. *Adv Mater*, 19, 1369-1372.

Improvement of Dielectric Properties of 3-Phase Polymer Nanocomposites : $BaTiO_3$-Ag/PVDF

Kanyapak Silakaew[1,2], Prasit Thongbai[2,3]

[1]Materials science and Nanotechnology Program, Faculty of Science, Khon Kaen University, Khon Kaen 40002, Thailand.

[2]Nanotec-KKU Center of Excellence on Advanced Nanomaterials for Energy Production and Storage, Khon Kaen 40002 ,Thailand.

[3]Integrated Nanotechnology Research Center (INRC), Department of Physics, Faculty of Science, Khon Kaen University, Khon Kaen 40002, Thailand.

Phone: +66 43-203166, Fax: +66 43-202374, E-mail: pthongbai@kku.ac.th

Poly(vinylidene fluoride) (PVDF) is a promising polymeric dielectric material due to its flexibility and high dielectric constant (ε′) compared to other polymeric materials. Unfortunately, ε′ of PVDF is still too low for practical application (ε′≈10). Recently, enhancement of the dielectric properties of PVDF has been intensively investigated [1,2]. In this work, $BaTiO_3$-Ag/PVDF nanocomposites were synthesized by using $BaTiO_3$-Ag hybrid particles as filler in the PVDF matric. Nanoparticles of Ag were growth on the surface of $BaTiO_3$ nanoparticles with sizes of ≈100 nm. $BaTiO_3$-Ag hybrid particles were dispersed very well in the PVDF matric. It was found that ε′ increased with increasing volume fraction of $BaTiO_3$-Ag. A rapid change in ε′ was observed, while the loss tangent (tanδ) was kept too low. Notably, a great enhanced ε′ value of ≈246.97 with very low tanδ of ≈0.04 was successfully achieved in the (f=0.521)$BaTiO_3$-Ag/PVDF nanocomposites. The results demonstrated that better dielectric properties can be achieved from the BT-Ag/PVDF nanocomposites.

Keywords: Dielectric constant, poly(vinylidene fluoride), $BaTiO_3$–Ag

[1] YU, K., WANG, H., ZHOU, Y.C., BAI, Y.Y., NIU, Y.J., J. 2013. Enhanced dielectric properties of $BaTiO_3$/poly(vinylidene fluoride) nanocomposites for energy storage applications. *Appl. Phys*, 113, 034105.

[2] HUANG, X.Y., JIANG, X.Y., XIE, L.Y. 2009. Ferroelectric polymer/silver nanocomposites with high dielectric constant and high thermal conductivity. *Appl. Phys. Lett*, 95, 242901.

Investigation of dielectric properties of artificial multiferroic structures based on barium strontium titanate

A. A. Semenov[1], A. I. Dedyk[1], Yu. V. Pavlova[1], I. L. Myl'nikov[1], P. Yu. Belyavskii[1], A. A. Nikitin[1], O. V. Pakhomov[2], A.A. Stashkevich[2,3]

[1]St. Petersburg State Electrotechnical University

LETI, Prof. Popova str. 5, St. Petersburg, 197376 Russia

[2]ITMO University, International Laboratory "MultiferrLab",

Kronverkskii pr. 49, St. Petersburg, 197101 Russia

[3]Universite Paris 13,

Sorbonne Paris Cite, 93430 Villetaneuse, France

semalexander@gmail.com

Multiferroics, i.e. materials or heterostructures that possess more than one ferroic parameter have been intensively studied during the last two decades both theoretically and experimentally. A revival of interest to them has been mainly driven by such important potential applications as data storage devices, in which advantage is taken of new functionalities originating from coupling of two constituent ferroic phases. The multiferroics are divided into two major categories, namely, the intrinsic/natural materials and extrinsic/artificial ones. The aim of this work is to investigate the dielectric properties of the both categories based on $Ba_xSr_{1-x}TiO_3$ (BSTO). The extrinsic multiferrioc structures were obtained in a form of bi-layers made of single crystal yttrium-iron garnet (YIG) and BSTO films. The intrinsic structures were obtained in a form of Mn-doped BSTO films with relatively high doping rate in the range of 10-20 wt%. For the experimental investigations the planar capacitors were formed on surfaces of the structures and the capacitance-voltage characteristics were measured. The influence of different substrates on the properties of the structures was investigated. The following parameters for the bi-layers

$Ba_{0.6}Sr_{0.4}TiO_3$-YIG were observed in the experiments: the temperature of the phase transition between ferroelectric and paraelectric states was 265 K; the relative dielectric permittivity at 300 K and zero bias was 1910; the dielectric loss tangent at 300 K and zero bias was 0.017; the electric field tunability at 300 K and 30 V/μm was 1.43; the half-width the ferromagnetic resonance line was 0.55 Oe. The $Ba_{0.5}Sr_{0.5}TiO_3$ films with 15 wt% of Mn doping deposited on sapphire substrate had the following parameters: the temperature of the phase transition between ferroelectric and paraelectric was 190 K; the relative dielectric permittivity at 300 K and zero bias was 650; the dielectric loss tangent at 300 K and zero bias was 0.001; the electric field tunability at 300 K and 30 V/μm was 2.05. The additional 3 % and 6 % tunings of the dielectric permittivity by external magnetic field of 2000 Oe was demonstrated for the extrinsic and intrinsic structures, respectively.

Keywords: multiferroics, barium strontium titanate, yttrium-iron garnet, manganese doping

Modulating and Tuning the Relative Permittivity of Dielectric Materials at the Unit Cell Level: Simulation and Experimental Verification

Li Zhang [1 *], King Ho Li [1, 2 *], Eng-Kee Chua [3], Man Siu Tse [1, 3], Ooi Kiang Tan [1, 3] and Kye-Yak See [3]

[1] Temasek Laboratories @ NTU, Nanyang Technological University, Singapore

[2] School of Mechanical & Aerospace Engineering, Nanyang Technological University, Singapore

[3] School of Electrical & Electronic Engineering, Nanyang Technological University, Singapore.

*li_zhang@ntu.edu.sg/holdenli@ntu.edu.sg

Dielectric materials with appropriate relative permittivity, coupled with low dielectric loss, low moisture absorption, as well as suitable mechanical stiffness have seen wide applications in electromagnetic (EM) devices and packages [1]. However, the desirable permittivity may not be readily available in nature and is usually difficult to be tailored precisely. We hereby predict and experimentally achieve the flexible tuning of the permittivity for dielectric materials as inspired by the recent developments in metamaterials [2], whereby repeating patterns at sub-wavelength scales can be arranged on the host materials to allow alteration of the EM properties. A series of composite dielectric plates with permittivity in the range of 3-8 were fabricated successfully by uniformly dispersing different volumes of bimodal TiO_2 powders into polypropylene polymer matrix. The permittivity of the composites was measured using transmission line method and the result was in good agreement with the Lichtenecker model (n=0.08) and effective medium theory (n=0.18) in the frequency range of 2.60-3.95 GHz. The corresponding loss tangent was also much lower as compared to the commercial products. To further enhance the tuning ability of the permittivity with greater flexibility, sub-wavelength holes with different diameters were drilled on the composite dielectric plates based on the concept of metamaterials. The resultant permittivity of these modified composite dielectric plates conformed well to the simulation results based on 5 × 5 × 5 mm^3 unit cells by CST STUDIO SUITE® software, with near-isotropic EM responses insensitive to the polarization of the incident EM wave. A potential scheme to implement

a dielectric gradient index (GRIN) lens with discretized shells of varying permittivity has finally been demonstrated by utilizing the fabricated modified composite dielectric plates to effectively improve the directivity of broadband EM generation devices in microwave range. The applications of these materials can be easily extended to other microwave or optical devices including cloaks, lenses, and beam shifters.

Keywords: permittivity, nanocomposite, hole, metamaterial, GRIN lens

[1] SEBASTIAN, M. T. & JANTUNEN, H. 2010. Polymer–Ceramic Composites of 0–3 Connectivity for Circuits in Electronics: A Review. International Journal of Applied Ceramic Technology, 7, 415-434.

[2] SMITH, D. R., MOCK, J. J., STARR, A. F. & SCHURIG, D. 2005. Gradient index metamaterials. Physical Review E, 71, 036609.

Phase transition behaviour and electrical properties of lead-free modified BNKT piezoelectric ceramics

Pichitchai Butnoi[1], Supalak Manotham[1], Pharatree Jaita[1, 2], Ratabongkot Sanjoom[1], Gobwute Rujijanagul[1, 3]
[1]Department of Physics, Faculty of Science, Chiang Mai University, Chiang Mai, 50200, Thailand
[2] Science and Technology Research Institute, Chiang Mai University, Chiang Mai, 50200, Thailand
[3]Materials science research center Faculty of Science, Chiang Mai University, Chiang Mai, 50200, Thailand
E-Mail p.butnoi@gmail.com

In this present work, complex lead-free piezoelectric ceramics with the composition of $Bi_{0.5}(Na_{0.40-x}K_{0.10}La_x)(Ti_{1-y}Zr_y)O_3$ were synthesized using a solid state reaction technique. Effects of co-doping of La and Zr on the phase evolution, microstructure, dielectric, ferroelectric and piezoelectric properties were systematically investigated. XRD analysis indicated that all samples exhibited a single perovskite structure. The microstructure of all ceramics was changed by the additives. Furthermore, dielectric properties of ceramics were determined in order to study of phase transition behavior of the system. The additives produced a change in phase transition and ferroelectric behaviors. These changes also influenced the electric field-induced strain response for the studied system. Based on our results, some compositions of the modified ceramics presented better electrical properties as compared to the unmodified sample. The co-doping approach is may be an alternative way to improve the piezoelectric properties of BNKT-based ceramics or other lead-free ceramics.

Keywords: BNKT, Electrical properties, Piezoelectric, co-doping, lead-free ceramics

Acknowledgments

This work was supported by the Thailand Research Fund (TRF, BRG5680002), National Research University Project under Thailand's Office of the Higher Education Commission, The National Research Council of Thailand, 50th CMU anniversary Ph.D. Program Chiang Mai University, Department of Physics and Materials Science, Faculty of Science and Graduate School, Chiang Mai University. Science and Technology Research Institute, Chiang Mai University, Thailand is also acknowledged.

Piezoelectric Properties of Textured NKLNT Ceramics

Moon-Jung Choi[1,2], Jong-Gyeon Ahn[2], Soon-Jong Jeong[2], In-Sung Kim[2], Jaesung Song[2], Tae Kwon Song[1], Min-Soo Kim[2]

[1]Dept. of Ceram. Sci. & Eng., Changwon National University, Rep. of Korea.

[2]Battery Research Center, Korea Electrotechnology Research Institute, Rep. of Korea.

E Mail : minsoo@keri.re.kr

$(Na_{0.51}K_{0.47}Li_{0.02})(Nb_{0.8}Ta_{0.2})O_3$ (NKLNT), lead-free piezoelectric ceramics were reported to have excellent electro-mechanical responses by controlling the microstructure. In addition, it was reported that the piezoelectric properties of textured NKN-based ceramics, manufactured via reactive template grain growth (RTGG), approached those of $Pb(Zr,Ti)O_3$ ceramics closely. In this study, textured NKLNT ceramics were manufactured from $NaNbO_3$ (NN) templates of various sizes via RTGG. The effect of NN template size was investigated in regard to the degree of orientation and the piezoelectric properties of NKLNT. A planar NN template was prepared via the topochemical microcrystal conversion method, and its size was controlled by adding excess Na_2CO_3 to $Bi_{2.5}Na_{3.5}Nb_5O_{18}$ precursor. The NN template size increased with the amount of Na_2CO_3. XRD analyses exhibited peaks typically inherent in the perovskite structure in all the specimens and the intensity of the {h00} peak was significantly increased in tape-cast NKLNT as compared with that in the one prepared via the solid-state method. The piezoelectric properties of crystal-oriented NKLNT were even better than those of non-oriented ones. Although oriented NKLNT changed its piezoelectric properties according to the size of the NN template, which was related to a change in the degree of orientation, the non-oriented NKLNT did not. The results showed the influence of the size of template on the degree of orientation and the piezoelectric properties of crystal-oriented NKLNT. Thus, additional attention should be paid to the size and the morphology of the template, not only to the composition of the doping system, employed in crystal-oriented NKN-based ceramics.

Keywords: Lead-free, piezoelectric, materials, NKLNT, reactive templated grain growth

Processing parameter influence on electrical properties of modified BNKT based ceramics

Ratabongkot Sanjoom[1], Pharatree Jaita[1,2], Tawee Tunkasiri[1,2], Denis Sweatman[1,2], Gobwute Rujijanagul[1, 2]

[1]Department of Physics and Materials Science, Faculty of Science, Chiang Mai University, Chiang Mai, 50200, Thailand
[2]Science and Technology Research Institute, Chiang Mai University, Chiang Mai 50200, Thailand

E-mail: noon_bongkot@yahoo.com

In this work (1-x)(0.80$Bi_{1/2}Na_{1/2}TiO_3$–0.20$Bi_{1/2}K_{1/2}TiO_3$)-0.03$SrTiO_3$, was prepared by a conventional solid-state reaction method. Optimum sintering temperature was found to be 1125°C for 2 h. Diffèrent fring rates were performed to obtained the optimum properties. X-ray diffraction analysis revealed that all samples exhibited a single perovskite structure with a mixture of rhombohedral and tetragonal phase. The firing rates affected to the dielectric properties such as maximum dielectric constant at T_m and depolarization temperature (T_d). This parameter also influenced on the ferroelectric and piezoelectric propertties of the studied ceramics where large electric field-induced strains and normalized strain coefficient were obtained for some conditions.

Keywords: *Electrical properties, BNKT based ceramics, Piezoelectric*

Acknowledgments

This work was supported by the Thailand Research Fund (TRF, BRG5680002), National Research University Project under Thailand's Office of the Higher Education Commission, The National Research Council of Thailand, 50th CMU anniversary Ph.D. Program Chiang Mai University, Department of Physics and Materials Science, Faculty of Science and Graduate School, Chiang Mai University. Science and Technology Research Institute, Chiang Mai University, Thailand is also acknowledged.

Stress Analysis of Sandwich Composite Beam Induced by Piezoelectric Layer

Shiuh-Chuan Her[1], Han-Yung Chen[1]

[1]Dept. of Mechanical Engineering, Yuan Ze University, Chung-Li, Taiwan.

*E Mail (***presenting and corresponding author's)** mesch@saturn.yzu.edu.tw

In this investigation, a piezoelectric layer is embedded in the host structure to form a sandwich composite structure. An electric voltage is applied to the piezoelectric layer, resulting in the bending effect on the sandwich composite beam. An analytical model based on the beam theory and compatibility condition is presented to determine the stresses of the sandwich beam with the piezoelectric layer as an actuator. The theoretical prediction is validated with the finite element result. Good agreement is achieved between the present approach and the finite element method. The influences of the embedded depth and Young's modulus of the piezoelectric layer on the stress distribution of the sandwich composite beam are investigated through a parametric study. Numerical results show that the maximum stresses in the top and bottom layers are tensile stresses and decreasing with the increase of the embedded depth, while the maximum stress in the PZT layer is compressive stress.

Keywords: **sandwich composite beam, piezoelectric actuator, beam theory, compatibility condition.**

Switching processes in thin ferroelectric films

A.S. Sidorkin, L.P. Nesterenko, B.M. Darinskii, A.A. Sidorkin, E.V. Vorotnikov,

H. T. Nguyen

Voronezh State University, University Sq. 1, Voronezh, Russia, 394006

nhatminhcon2013@gmail.com

The influence of size effects on phase transitions, dielectric and switching characteristics of thin ferroelectric films on examples of lead titanate $PbTiO_3$ and lead zirconate-titanate $Pb(Zr_{0.5}Ti_{0.5})O_3$ thin films with various thicknesses was studied. The conducted investigations have shown that with decreasing the thin film thickness the phase transition temperature and the smearing level of phase transition are increased. The domain contribution to the dielectric constant is proportional to the ratio of film thickness to lattice constant or the thickness of the surface of nonferroelectric layer. With decreasing the thin film thickness the value of coercive field increases. With the growth of the value of the electric field the activation mode of domain walls motion in weak fields is replaced by the regime of viscous motion of domain walls in strong fields. In this case the boundary between these different types of domain wall motion increases with decreasing film thickness and removal shift from the Curie point temperature. The reason for both the observed effects is an increase in the coercive field with decreasing film thickness due to growth in the volume concentration of defects and the interaction energy of the domain walls with defects in removing deep into the ferroelectric phase.

For weak fields the deviation from a strictly exponential dependence of the velocity of the domain walls V on the external field was found that can be compensated by emergence of the exponent in the activation dependence $V \sim \exp [-C / E^{\mu}]$, where C - constant, and μ - the so-called dynamic exponent. It is shown that with decreasing film thickness the increase in the value μ for the investigated films is observed, wherein for lead titanate, this exponent is more than for lead zirconate-titanate with the same thickness. With increasing temperature approaching the Curie point the coefficient μ decreases. It is shown that the observed increase of the dynamic exponent μ with decreasing the film thickness can be related to experimentally observed growth of the level of orientation of crystallites in polycrystalline film.

For strong fields the experimental values of the time switch is designed mobility of the domain walls for different thicknesses of the studied films, which decreases with decreasing film thickness that can be connected with increasing in the concentration of surface defects.

It was found that all synthesized films are characterized by the presence of the internal bias field the value of which depends on the substrate and the electrode material.

Keywords: Ferroelectric films*, *domain wall, coercive field, dynamic exponent.

Magnetic Microwires with Tunable Electric Polarization as Embedded Sensing Elements

Larissa V. Panina[1,2], Dmitriy P. Makhnovskiy[3], Abdukarim Dzhumazoda[1], Mohamed M. Salem[1,4], Alexander T. Morchenko[1], Vladimir G. Kostishyn[1]

[1]National University of Science and Technology, MISIS, Moscow 119991, Russia

[2]Institute for Design Problems in Microelectronics RAS, Moscow 124681, Russia

[3]Robat Ltd, UK

[4]Physics Department, Faculty of Science, Tanta University, Tanta 31527, Egypt

E-mail: lpanina@plymouth.ac.uk, elshshtawy@science.tanta.edu.eg,

Miniature sensors with remote wireless operation are required in many technological areas including structural health monitoring, smart composites, embedded biosensors, etc. Microwave technologies have a high potential for remote sensing applications. Here we propose to utilize magnetic microwires as embedded sensors operating at microwave frequencies (1-10 GHz). The sensor operation is based on tunable electric polarization due to large modulation of the wire surface impedance (known as magnetoimpedance effect [1]). Recently, the research topic on microwave interacting with ferromagnetic materials or metamaterials is intensively developing. The main areas of applications are identified as sensor materials [2] and microwave shielding systems [3].

In order to realize efficient tunable properties, magnetic microwires of CoFeSiB composition in amorphous state are considered. The absence of the crystalline structure is very useful since it is possible to induce a required magnetic anisotropy through magnetoelastic interaction. For microwave applications, the domain structure in the outer shell is important. For sensing applications, a circumferential or helical anisotropy is preferable, which can be established in Co-rich alloys with negative magnetostriction. For such wires, the remagnetisation behaviour in an axial magnetic field less than the effective anisotropy field is almost linear, without hysteresis and with very high susceptibility. The external stress and temperature substantially modify the magnetic anisotropy and the magnetization processes.

Tunable soft magnetic properties of amorphous microwires result in unique high frequency behavior, namely, giant magnetoimpedance. At MHz frequencies, MI is utilized in various magnetic and stress sensors. At GHz frequency, the MI effect can be used to control the scattering of electromagnetic waves from microwires with application to tunable electromagnetic composites and embedded sensors. The use of metal inclusions in microwave applications is often justified by their larger electric polarisability in comparison with dielectrics. This enables one to obtain a strong response even from a single inclusion. Here we demonstrate that scattering from a ferromagnetic microwire showing large MI effect at microwaves can be modulated with low frequency magnetic field and the amplitude of this modulation near the antenna resonance can sensitively change with application of the external stress or temperature. The modelling is based on solving the scattering problem from a cylindrical wire with the impedance boundary conditions. The modelling results agree well with the experimental data.

Keywords: magnetic microwires; magnetoimpedance; tunable electric polarization; embedded sensor.

[1] L. V. PANINA and K. MOHRI, 1994 Magneto-Impedance Effect in Amorphous Wires ,*Appl. Phys. Letters* 65, 1189

[2] D. P. MAKHNOVSKIY, L. V. PANINA, C. GARCIA, A. P. ZHUKOV, and J. GONZALEZ, 2006 Experimental demonstration of tunable scattering spectra at microwave frequencies in composite media containing CoFeCrSiB glass-coated amorphous ferromagnetic wires and comparison with theory *Phys. Rev. B: Condens. Matter*, 74, 064205

[3] QIN F. X., PENG H. X., PANKRATOV N., PHAN M. H., PANINA L. V., IPATOV M. , ZHUKOVA V., ZHUKOV A. , GONZALEZ J. 2010 Exceptional electromagnetic interference shielding properties of ferromagnetic microwires enabled polymer composites. *J. Appl. Phys.* 108, 044510.

Magnetoelectric Element for Energy Harvesting Devices

R.V.Petrov[1], M.I.Bichurin[1], A.S.Tatarenko[1], Su-Chul Yang[2]

[1]Novgorod State University, Veliky Novgorod, 173003, Russia.

[2]Department of Chemical Engineering, Dong-A University, Hadan 840, SahaGu, Busan 604-701, South Korea.

E Mail/ alexandr.tatarenko@novsu.ru

The paper is devoted to the study of the magnetoelectric (ME) element, which operates in the resonant bending mode and intended for use in energy harvesting devices. ME effect which was studied in detail in [1] can be used to generate energy [2]. Earlier the case of using the ME element at the resonant axial mode was considered in [3]. It was investigated an element with dimensions 40x10x0.5 mm and composition of PZT-Metglas. In the axial resonance mode of 41 kHz the magnetoelectric coefficient was of 1.32 V/(cm□Oe) at an output current of 205 microamps. For more efficient application of ME element in the energy harvesting devices it is necessary to provide the most possible low-frequency resonant mode of ME element. It is known that the resonant bending mode may provide the most low-frequency resonance regime. The resonance excited in ME element at the frequency of several hundred Hertz will already be acceptable for the creation of ME generators and other highly effective energy harvesting devices. Such ME element can be applied, for example, in wind-turbine magnetoelectric plants, ME hydrogenerators, ME turbogenerators, and the electrical equipment intended for converting the mechanical energy of the primary engines in electric one.

Keywords: Magnetoelectric element; bending mode; energy harvesting device

[1] BICHURIN M.I., PETROV V.M., and PRIYA S. Magnetoelectric Multiferroic Composites. *In: Ferroelectrics - Physical Effects / Ed. Mickaël Lallart.* - *InTech*, 2011. P. 277-302.

[2] R.V. PETROV, N.A. KOLESNIKOV, M.I. BICHURIN. Magnetoelectric alternator. *Energy Harvesting and Systems*, 2015 (in print)

[3] M. BICHURIN, N. KOLESNIKOV, R. PETROV, S. ALEKSIĆ. Magnetoelectric energy source. *Proceeding of 12th International Conference on Applied Electromagnetics - ΠΕС 2015,* August 31 – September 02, 2015, Niš, Serbia.

Stress-Sensitive Magnetization Process in Amorphous Glass-Coated Microwires for Embedded Sensor Applications

M. M. Salem[1,3], M. G. Nematov[1], A. Udin[1], L. V. Panina[1,2], A. T. Morchenko[1]

[1]National University of Science and Technology, MISIS, Moscow 119991, Russia

[2]Institute for Design Problems in Microelectronics RAS, Moscow 124681, Russia

[3]Physics Department, Faculty of Science, Tanta University, Tanta 31527, Egypt

E-mail: elshshtawy@science.tanta.edu.eg, lpanina@plymouth.ac.uk

Testing internal stress/strain condition of polymer composite materials is of high importance in structural health monitoring. A number of sensing methods have been used for stress measurements inside composites but each technology has some drawbacks so considerable efforts are made to develop innovative approaches. In the present work, the method of monitoring the internal stresses consists in embedding a soft magnetic microwire into a polymer matrix and measuring its harmonic spectra when the wire is remagnetized. The microwire with a diameter of 10-100 microns is covered by glass and is in amorphous state, which allows a specific magnetic anisotropy to be establish. Since the main source of the anisotropy is magnetostrictive interaction the wire magnetic state and magnetization processes may be highly sensitive to stress. When the microwire is remagnetized the sharp voltage is induced which is characterized by high frequency harmonics. The amplitude of these harmonics sensitively depends on various stresses. This property can be used for stress monitoring inside composite materials.

Ferromagnetic microwires with positive magnetostriction are characterized by almost rectangular hysteresis loop measured in a magnetic field along the microwire axis [1-2]. The magnetization takes place by axial domain propagation which generates a sharp voltage signal producing high harmonics. The detection of high harmonics is possible with enhanced signal-to-noise ratio since the common noise and 1/f noise are greatly suppressed at high frequencies. The harmonic amplitude depends on external parameters, such as stress, strain and temperature. Enhanced stress sensitivity is seen in the case when the magnetostriction constant can change a sign under stress effect. Therefore, these wires can be used as wireless sensors with remote

interrogation and can be placed on the surface or inside materials. We demonstrate that the ratio of harmonic amplitude may also sensitively depend on tensile and torsion stress which can be used directly for structural health monitoring.

It would be useful to compare several embedded sensing methods which are similar to our method either by the geometry of inclusions or some physical principles. The undisputed leader in non-destructive testing of composites is the method using embedded optical fibres [3]. Along with the high sensitivity, the optical method can also measure a wide range of parameters such as strain, temperature, pressure, etc. The drawback of this technology occurs due to a need of protecting coating so the overall size of the sensing element is large. Magnetic microwires in glass coating can be made as small as several microns which is comparable with structural fibers (glass or carbon). The other advantage of using magnetic microwires as embedded sensors is related with the tunability of the response, small cost and relatively simple signal processing.

Keywords: magnetoimpedance; microwires; magnetic sensors; stress

[1] A. ZHUKOV and V. ZHUKOVA 2009. Magnetic properties and applications of ferromagnetic microwires with amorphous and nanocrystalline structure *Nova Science Publishers, New York*

[2] M. VAZQUEZ, H. CHIRIAC, A. ZHUKOV, L. PANINA, T. UCHIYAMA 2011. On the state-of-the-art in magnetic microwires and expected trends for scientific and technological studies *Phys. Status Solidi*, 208, 493-501

[3] K. PETERS 2011. Polymer optical fiber sensors - a review *Smart Mater.* Struct. 20, 013002-013018

Hydrothermal Synthesis of Core-shell Magnetostrictive Nanoparticles for Self-bisa Magnetoelectric Effect

Su-Chul Yang[1], M.I.Bichurin[2]

[1]Department of Chemical Engineering, Dong-A University, Hadan 840, SahaGu, Busan 604-701, South Korea.

[2]Novgorod State University, Veliky Novgorod, 173003, Russia.

E Mail/ scyang@dau.ac.kr

Recently, multiferroic materials have been interested for potential applications due to its unique characteristics exhibiting two or more ferroic orders such as ferroelectric, ferromagnetic or ferroelastic. Among multiferroic materials, magnetoelectric (ME) composites exhibit direct coupling between the ferroelectric and ferromagnetic order parameters so that it can be used for high-sensitive magnetic field sensors, communication components and electric-write/magnetic-read memory devices. [1, 2] From the multiferroic ME composites, both direct and converse ME responses were induced as change in electric polarization in response to applied magnetic field and as change in magnetization in response to applied electric field, respectively. Particularly, the productive ME responses were induced under very low magnitudes of magnetic field or electrical field utilizing high sensitive electrical devices. In this study, we focused on synthesis of core-shell magnetostrictive particles possessing high built-in magnetic field ($H_{\text{built-in}}$) which can induce remenant magnetostriction for self-bias ME applications. [3, 4] The cobalt nanoparticles as a core material were synthesized by room-temperature reaction method. Then shell materials of $NiFe_2O_4$, $ZnFe_2O_4$, and $CoFe_2O_4$ were respectively coated on Co core particles by hydrothermal method. In order to investigate materials effect on M-H hysteresis of core-shell magnetic particles, XRD, HR-TEM, EDS, SEAD, VSM characterizations were conducted.

[1] J. Ma, J. Hu, Z. Li, C.-W. Nan, *Advanced Materials* **2011**, *23*, 1062.
[2] L. Yan, Y. Yang, Z. Wang, Z. Xing, J. Li, D. Viehland, *Journal of Materials Science* **2009**, *44*, 5080.
[3] S. C. Yang, K.-H. Cho, C.-S. Park, S. Priya, *Applied Physics Letters* **2011**, *99*.
[4] S.-C. Yang, C.-S. Park, K.-H. Cho, S. Priya, *Journal of Applied Physics* **2010**, *108*.

Magnetic resonance in bilayers of ferrite and functionally graded piezoelectric

M. I. Bichurin[1], V. M. Petrov[1], A. F. Saplev[1], A. S. Tatarenko[1], D. G. Melnichuk[1], and Su-Chul Yang[2]

[1]Novgorod State University, 41 B.S.-Peterburgskaya, Veliky Novgorod 173003, Russia
[2]Department of Chemical Engineering, Dong-A University, Hadan 840, SahaGu, Busan 604-701, South Korea.

E Mail/ alexandr.tatarenko@novsu.ru

The particular purpose of this paper is theoretical modeling of magnetoelectric (ME) interactions at ferromagnetic resonance (FMR) in a bilayer of a ferrite and a through-thickness compositionally graded piezoelectric. The ME effect is known to consist in inducing the polarization by an applied magnetic field and, vice versa, in inducing the magnetization by an applied electric field. This effect in a magnetostrictive-piezoelectric laminate results from mechanical deformation [1]. Applying a dc electric field to the piezoelectric layer gives rise to strains that are transferred into ferrite component and induce a uniaxial magnetic anisotropy and a shift in the magnetic resonance field [2]. In case of piezoelectric which is assumed to be compositionally graded in thickness direction, the thickness-dependent strains contribute to the flexural deformations of magnetic layer. Thus FMR line appears to be shifted and inhomogeneously broadened due to flexure. For theoretical modeling of the applied electric field induced shift of magnetic resonance line and additional line width, we solve the equation of motion of magnetization.

$$\partial \boldsymbol{M}/\partial t = -\gamma\,[\boldsymbol{M}, \boldsymbol{H}_{eff}], \qquad (1)$$

where effective field is given by $\boldsymbol{H}_{eff} = -\partial ({}^{m}W)/\partial \boldsymbol{M}$ with ${}^{m}W$ being the free-energy density of a ferrite, M is magnetization. The free-energy density of a single crystal ferrite includes magnetic crystallographic anisotropy, form anisotropy and magnetoelastic anisotropy. The stress components that enter into the expression for magnetoelastic

energy are assumed to be induced by applied electric field. To find these stress components we solve the elasticity equations and material equations for the ferrite and piezoelectric layers. For taking into account the flexural deformations, the longitudinal strain of the layers should be considered as linear functions of the vertical coordinate z_j: ${}^jS_1 = {}^jS_{10} + z_j/R$ where ${}^jS_{10}$ is the centroidal strain along the length direction (x-axis) and R is the radius of curvature, z_j is counted off from the middle plane of j-layer ($i=m, p$ with m and p corresponding to magnetic and piezoelectric layer). The obtained model is applied to a specific case of yttrium iron garnet/PZT with through-thickness variation of piezoelectric coefficient. Our previous model indicated that bending the sample gives rise to a decrease in the strength of ME interaction and predicted a strong microwave ME interaction when the piezoelectric phase volume fraction is sufficiently high, the piezoelectric layer has strong piezoelectric coupling, and the magnetic phase has high magnetostriction [3]. In addition, the present study shows that using the functionally graded piezoelectric with through-thickness variation of piezoelectric coefficient leads to an additional line shift and broadening of ferromagnetic absorption. The phenomena are of interest for FMR-based filters with variable bandwidth. The unique feature of suggested devices is the electrical tunability.

Keywords: Functionally graded materials, magnetoelectric coupling, magnetic resonance

[1] Bichurin M.I. and Petrov V.M. (2014), *Modeling of Magnetoelectric Effects in Composites*. Springer, Springer Series in Materials Science, Book 201.

[2] Bichurin M. I., Kornev I. A., Petrov V. M., Tatarenko A. S., and Kiliba YU. V. (2001) Theory of magnetoelectric effects at microwave frequencies in a piezoelectric/magnetostrictive multilayer composite. *Phys. Rev. B,* 64, 094409 (1-6). DOI: http://dx.doi.org/10.1103/PhysRevB.64.094409

[3] Bichurin M.I., Petrov V.M., and Galkina T.A. (2009) Microwave magnetoelectric effects in bilayer of ferrite and piezoelectric. *Eur. Phys. J. Appl. Phys,*. 45, 30801 (1-5). DOI: 10.1051/epjap/2009013

3D Carbon Nanotubes Structures for Advanced Functional Materials

Michael De Volder[1]

[1]University of Cambridge, Department of Engineering, IfM.

mfld2@cam.ac.uk / 17 Charles Babbage Rd, CB3 0FS, Cambridge, UK

Carbon nanotubes (CNTs) have been investigated intensively during the past two decades because of their excellent electrical, thermal, and mechanical properties [1]. However, these assets are only measured in individual CNTs, whereas most advanced functional materials require the assembly of tens to millions of these nanoparticles into one structure. Unfortunately, the properties of such CNT aggregates are often disappointing compared to the constituent nanoparticles. In order to leverage the full potential of CNTs for AFM applications, it is key to control the nanotube arrangement at both the micro and nanoscale [2].

This work presents new methods for arranging nanotubes with unprecedented control over their microscale arrangement using top-down lithographic techniques. More precisely, we found a method to induce local changes in CNT synthesis rates, which allows to shape the nanotubes into bending pillars, helices, trusses and other complex structures in high throughput. Further, all nanotubes are aligned within each structure, and the surface chemistry of the structures can be tailored to the requirements of the application. We will discuss how these structures can be used to fabricate smart surfaces with anisotropic properties as well as for structural mechanic and energy storage applications.

Keywords: Carbon Nanotubes, Nano and mesostructured materials, NEMS

[1] M De Volder, S Tawfick, R Baughman, A Hart, Carbon nanotubes: present and future commercial applications, Science 339 (6119), 535-539, 2013

[2] M De Volder, S Park, S Tawfick, A Hart, Strain-engineered manufacturing of freeform carbon nanotube microstructures, Nature Communications 5, 2014

AFM applications for analysis of friction and wear of nanomaterials

Aleks Laihtman, Akexey Moshkovich, Igor Lapsker, Lev Rapoport

Holon Institute of Technology, Holon 5810201, Israel

Inorganic fullerene-like WS_2 and MoS_2 nanoparticles (*IF*) with structures closely related to (nested) carbon fullerenes and nanotubes showed that *IF* added to oil, coatings and polymer matrixes lubricating appear superior properties to those of layered commercially available WS_2 and MoS_2 solid lubricant powders in a definite range of operating conditions. To elucidate the tribological mechanisms involved, a careful analysis of the mating surfaces and the lubricating medium by a number of experimental techniques was carried out. For this purpose atomic force microscopy (AFM); scanning electron microscopy (SEM); transmission electron microscopy (TEM); X-ray photoelectron spectroscopy (XPS), and X-ray powder diffraction (XRD) were used. In the present work primary attention has been devoted to the study of friction and wear of the *IF*- WS_2 and MoS_2 nanoparticles mainly by AFM.

The analysis of the *IF* nanoparticles showed that most, if not all pristine nanoparticles were closed and hollow, having nearly spherical shape. The average size of the *IF*-WS2 particles was close to 120 nm, while it was about 50 nm for *IF*-MoS_2. It was found that these nanoparticles are capable of withstanding a severe hydrostatic pressure, caused by compression. Detailed structural studies revealed a deformation of the *IF* nanoparticles and breakage of their outer shells under compression. The surface topography of the samples before and after the friction tests was studied with SPM DI Dimension 3100.

Friction and wear of steel and ceramic pairs lubricated with oil+ *IF* lubricant have been studied. The similarity in the behavior of steel and ceramic pairs was found to be due to the filling of the valleys, grooves and gaps of rubbed surfaces with the *IF* nanoparticles and their layers. High contact pressure under friction with oil+*IF* lubricant leads to squeezing out of the oil and tight sticking of broken shells of destroyed *IF* nanoparticles on the rubbed surfaces. On the base of AFM, SEM, TEM and XPS analysis it was concluded that the islands of destroyed *IF* nanoparticles could provide improved tribological properties of the contact under severe contact conditions.

AFM applications for analysis of friction and wear of nanomaterials

Aleks Laihtman, Akexey Moshkovich, Igor Lapsker, Lev Rapoport

Holon Institute of Technology, Holon 5810201, Israel

Inorganic fullerene-like WS_2 and MoS_2 nanoparticles (*IF*) with structures closely related to (nested) carbon fullerenes and nanotubes showed that *IF* added to oil, coatings and polymer matrixes lubricating appear superior properties to those of layered commercially available WS_2 and MoS_2 solid lubricant powders in a definite range of operating conditions. To elucidate the tribological mechanisms involved, a careful analysis of the mating surfaces and the lubricating medium by a number of experimental techniques was carried out. For this purpose atomic force microscopy (AFM); scanning electron microscopy (SEM); transmission electron microscopy (TEM); X-ray photoelectron spectroscopy (XPS), and X-ray powder diffraction (XRD) were used. In the present work primary attention has been devoted to the study of friction and wear of the *IF*- WS_2 and MoS_2 nanoparticles mainly by AFM.

The analysis of the *IF* nanoparticles showed that most, if not all pristine nanoparticles were closed and hollow, having nearly spherical shape. The average size of the *IF*-WS2 particles was close to 120 nm, while it was about 50 nm for *IF*-MoS_2. It was found that these nanoparticles are capable of withstanding a severe hydrostatic pressure, caused by compression. Detailed structural studies revealed a deformation of the *IF* nanoparticles and breakage of their outer shells under compression. The surface topography of the samples before and after the friction tests was studied with SPM DI Dimension 3100.

Friction and wear of steel and ceramic pairs lubricated with oil+ *IF* lubricant have been studied. The similarity in the behavior of steel and ceramic pairs was found to be due to the filling of the valleys, grooves and gaps of rubbed surfaces with the *IF* nanoparticles and their layers. High contact pressure under friction with oil+*IF* lubricant leads to squeezing out of the oil and tight sticking of broken shells of destroyed *IF* nanoparticles on the rubbed surfaces. On the base of AFM, SEM, TEM and XPS analysis it was concluded that the islands of destroyed *IF* nanoparticles could provide improved tribological properties of the contact under severe contact conditions.

Characteristics of activated carbon derived from bacterial cellulose and its application as a catalyst support

Khamkeaw, Phanthang, Jongsomjit, Phisalaphong

Chemical Engineering Research Unit for Value Adding of Bioresources, Department of Chemical Engineering, Faculty of Engineering, Chulalongkorn University, Phayathai Rd., Patumwan, Bangkok, 10330, Thailand.

E Mail arnon.k1231@gmail.com and muenduen.p@chula.ac.th

Bacterial cellulose (BC) was investigated as a novel material for preparing activated carbons. BC was dried by heating and it was carbonized with a chemical activation process using phosphoric acid (H_3PO_4) as an activating agent at different temperatures (400, 500 and 600 °C). The properties of the activated carbons were characterized by X-ray diffraction (XRD), scanning electron microscopy (SEM), N_2-physisorption, Fourier transform infrared spectroscopy (FT-IR) and thermal gravimetric (TGA). The obtained activated carbons showed mesoporous structure (pore size diameter 23-25 nm) with high surface area (1237 – 1818 m^2/g), and large pore volume (0.78 – 1.13 cm^3/g). In addition, the BC activated carbons were used as catalyst support for sulfuric acid catalyst in ethanol dehydration. It was found that the ethylene selectivity and the ethanol conversion at about 80% could be obtained. The experimental results indicated that the BC activated carbons have superior properties comparable with those of commercial activated carbon; consequently it can provide superior performance as catalyst support.

Keywords: Activated carbon, bacterial cellulose, activated carbon, ethanol dehydration, sulfuric acid catalyst

Effect of reprocessing on functional groups on detonation nanodiamond surface

Q. Zou, M.Z. Wang*, J.M. Li, L. Wang, J.Q. Zhang, Y.C. Zhao

College of Mechanical Engineering, State Key Laboratory of Metastable Materials Science and Technology, Yanshan University, Qinhuangdao 066004, Hebei, P.R. China

E-mail 1465314@qq.com, Tel./Fax.:+86-335-8061671

Abstract: Effect of reprocessing using mixed solution of potassium permanganate and concentrated sulfuric acid, in the air, in hydrogen, in vacuum and in Ar gas on the functional groups on detonation nanodiamond surfaces was studied in this work. An X-ray diffractometer (XRD), a high resolution transmission electron microscope (HRTEM), a fourier transform infrared spectroscope (FTIR) and a differential scanning calorimeter (DSC) were used to investigate the microstructures, properties and surface states of the nanodiamond before and after being processed. The results showed that the shape of the nanodiamond particles was spherical or elliptical; the average grain size was approximately 5 nm; the initial oxidation temperature in the air was about 550 ℃; the graphitization temperature in hydrogen, in vacuum and in Ar was about 284 ℃, 1146 ℃ and 1184 ℃. The surfaces of the nanodiamond before being processed mainly contained a lot of functional groups, such as －OH, －CH_3, －CH_2, CO_2, －C=O, －COOH and －C－O－C. CO_2 had been removed from the surfaces of the nanodiamond after being processed in hydrogen. Moreover, reprocessing in hydrogen could avoid the second absorption of the processed nanodiamond in the air.

Keywords: nanodiamond; reprocessing; functional group; surface state

Effects of hydrostatic pressure and aluminum concentration on the phonon-assisted cyclotron resonance in asymmetrical semi-parabolic quantum well

Tran Cong Phong[a], Huynh Vinh Phuc[b]

[a)] Vietnam Institute of Educational Sciences, 101 Tran Hung Dao, Hanoi 10000, Vietnam
[b)] Division of Theoretical Physics, Dong Thap University, Dong Thap 93000, Vietnam

The combined effect of hydrostatic pressure, aluminum concentration, temperature, and confinement frequency of an asymmetrical semi-parabolic quantum well (ASPQW) on the phonon-assisted cyclotron resonance (PACR) via two-photon absorption process is investigated theoretically. While the analytical expression for the magneto-optical absorption coefficient (MOAC) is obtained by relating it to the transition probability for the absorption of photons, the half width at half maximum (HWHM) of the resonant peaks is gained by the profile method. The numerical results are calculated for typical GaAs/GaAlAs quantum well. The obtained results show that MOAC and HWHM are significantly dependent on hydrostatic pressure, aluminum concentration, temperature, and confinement frequency in both one and two-photon processes. Our results give a new capacity for optical device applications since the magneto-optical properties of the GaAs/GaAlAs ASPQW can be modified by changing these parameters.

Encapsulation and Antibacterial Activity of *Citrus hystrix* Oil Using Expanded Liquid Sub-critical CO_2

Noorrasyidah Mohd. Sarmin. [a,b], Masturah Markom[a*], Mohd. Fuat Abdul Razak[c], and Mazita Mohd. Diah[b]

*[a] Department of Engineering and Build Environment, National University of Malaysia, 43600 UKM, Bangi Selangor, MALAYSIA
[b] Industrial Biotechnology Research Centre, SIRIM Berhad, 1 Persiaran Dato' Menteri, P.O Box 7035, 40700 Shah Alam, Selangor, MALAYSIA
[c] Infectious Disease Research Centre, Institute for Medical Research (Ministry of Health Malaysia), Kuala Lumpur, MALAYSIA
E-mail : masturahmarkom@ukm.edu.my

The *Citrus hystrix* essential oil (CHO) has potential in medicinal or cosmeceutical industry due to its antibacterial activity. However, encapsulation process is required to ensure long shelf life and stability of the essential oil. The objective of this research is to investigate the encapsulation process using sub-critical CO_2 and its optimization by Response Surface Method (RSM). Three key factors, namely the pressure (30-80 bar), temperature (40-60˚C) and resident time (10-60 minutes) were studied for the microencapsulation. The optimum results were at 54.14 bar, temperature 59.65˚C and resident time 58 minutes to produce 549.4 nm particle size and 38.2% yield. The antibacterial activity of CHO particles against *Propionibacterium acnes*) was tested using disc-diffusion method, which showed promising results compared to the unencapsulated CHO.

Keyword: Citrus hystrix; essential oil; CO_2 - expanded liquid; minimum inhibitory concentration

Hybrid mesoporous SBA-15 with active organic species and molecularly imprinted cavities in the framework wall

Hang Huo[1], Kaifeng Lin[2], Yanqiu Jiang[3]

[1,2,3]School of Chemistry and Chemical Engineering, Harbin Institute of Technology,

Harbin 150001, China

[1]15B907001@hit.edu.cn , [2]linkaifeng@hit.edu.cn

Recently, hybrid mesoporous organosilica materials containing active organic species have been widely used as nanoreactors for various reactions. The large pore volume and surface area of these mesoporous silica provide ample room to locate the organic species on the surface and/or in the framework walls. Several researches indicate that some of the pore mouths are blocked by organic species when they are tethered in the channel pores, rendering those pores inaccessible to reactants due to the diffusion limitation. It seems that incorporation of the active organic species in the mesopore framework is a practical strategy to overcome the weakness by making all of the pores unblocked. However, it should be taken into account that the access of the reactants to the active sites may be somewhat limited in the case of the incorporated mesoporous silicas as the active sites can be buried in the framework wall of solids. In our work, a series of hybrid mesoporous SBA-15 materials containing organic base species incorporated into the mesopore framework have been successfully prepared via combination of molecularly imprinted technique and one-pot co-condensation route, in which molecularly imprinted cavities in the mesoporous organosilica wall are created by using a newly prepared organosilicon source. The catalyst showed improved catalytic activity and high turnover frequency values in the Knoevenagel reactions, owing to the high accessibility of these active framework species to the reactants via the unblocked mesopore channels and/or the molecularly imprinted cavities in the mesopore walls. Meanwhile, the catalyst was robust and can be reused up to 6 times without loss of activity and selectivity, pointing to their high stability of the base species incorporated in the framework wall.

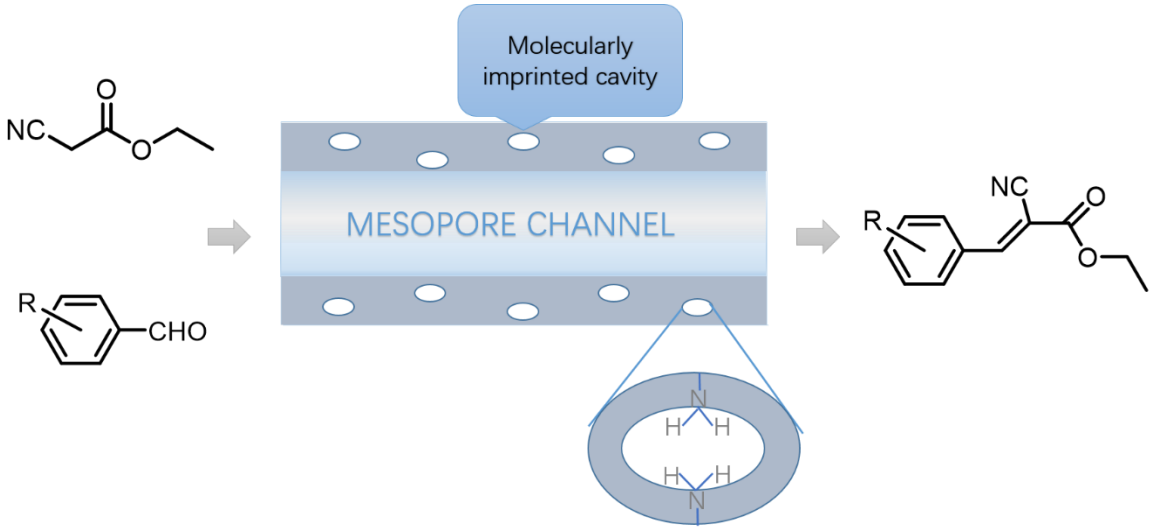

Scheme 1 Knoevenagel reactions conducted in the mesopore channels of the molecularly imprinted mesoporous organosilica

Keywords: Hybrid SBA-15; Molecularly imprinted cavity; Heterogeneous Knoevenagel reactions.

[1] MARGELEFSKY, E. L., BENDJERIOU, A., ZEIDAN, R. K., DUFAUD, V. & DAVIS, M. E. 2008. Nanoscale Organization of Thiol and Arylsulfonic Acid on Silica Leads to a High Active and Selective Bifunctional, Heterogeneous Catalyst. *J. Am. Chem. Soc.*, 130, 13442-13449.

[2] HUANG, Y. L., XU, SH. & VICTOR, S.-Y. LIN. 2011. New Strategy for Enantioselective Heterogeneous Catalysis: Immobilization of both Metal Nanoparticles and Chiral Modifiers on Mesoporous Silica Nanoparticles. *ChemCatChem.*, 3, 690-694.

[3] JENNIFER, E. L., LGOR, L. M. & GEOFFREY, A. O. 2011. Molecularly Imprinted Mesoporous Organosilica. *ACS Nano*, 5, 2277-2287.

Large-scale assembly of nanorods and anisotropic optical properties

Jongwook Kim[1], Jean-Pierre Boilot[1], Jacques Peretti[1], Thierry Gacoin[1]

[1] Department of Physics, Ecole Polytechnique, Palaiseau, 91128, FRANCE

Presenting and corresponding author: jong-wook.kim@polytechnique.edu

Synthesis and assembly of anisotropic nanocrystals is a key issue towards devices performing anisotropic functional properties such as birefringence, ferromagnetism, and polarized luminescence. Although a variety of synthesis and self-assembly techniques have been developed, extending the organized domain size to the device scale is not straightforward. Moreover, dynamic control of the assembled structure in the soft matter state is highly challenging. We present a novel method to overcome such difficulties by exploiting spontaneous liquid crystalline (LC) assembly of colloidal nanorods. We prepared charge-stabilized ligand-free suspension of $LaPO_4$ nanorods, which exhibits purely entropic LC phase behavior (isotropic↔nematic↔columnar) [1]. In this system, an efficient optical Kerr effect was observed which is directly applicable as a thermally stable Kerr cell. Also, a shear-directed assembly technique assisted by the thixotropy of the rod suspension was developed to fabricate transparent inorganic thin film wave retarders performing high level of birefringence (Δn = 0.13) [2]. Theoretical study reveals that such a high Δn is accessed by an optimal combination of intrinsic and form birefringence together [3]. Another remarkable feature of $LaPO_4$, when doped with europium, is independently polarized photoluminescence bands, which becomes a three-dimensional orientation marker useful in bio-imaging and microfluidic measurement.

Keywords: Nanorod, assembly, liquid crystal, birefringence, polarized luminescence

[1] Kim, J. et al. *Adv. Funct. Mater.* **22**, 4949-4956, (2012).

[2] Kim, J. et al. *Adv. Mater.* **25**, 3295-3300, (2013).

[3] Kim, J. *et al. Appl. Phys. Lett.* **105**, 061102, (2014).

Multi structures using bacterial cellulose films

Muling Zeng, Anna May-Masnou, Anna Roig, Anna Laromaine

Institut de Ciència de Materials de Barcelona, Campus UAB, 08193 Bellaterra, Spain.

Cellulose from microbial origin, commonly known as bacterial cellulose (BC), is becoming a commodity material since it incorporates desirable structural properties for biomedical applications. Here, we present the production and characterization of bacterial cellulose (BC) films of less than a hundred microns thick produced by Gluconacetobacter bacteria. These thin films are processed using three different drying methods: 1) room temperature, 2) freeze drying and 3) supercritical drying. The different processes confer the cellulose films a hierarchical porous network, high purity and crystallinity, flexibility and strength (high Young modulus at room and elevated temperatures) and large water holding capacity that can be tailored and controlled for different applications.

In this work, we used BC films as a platform to incorporate magnetic functionality by the incorporation of iron oxide nanoparticles and gold nanoparticles as potential catalysts. Using the microwave-assisted method in a rapid and cost effectively manner, we magnetically coated the whole structure of our BC films uniformly. By evaluating different precursor´s concentrations and taking advantage of the different drying methods, we achieved magnetic bacterial films with different magnetic strength. We obtained magnetic, flexible and robust BC composites within a few minutes in a clean, easy and reproducible method.

We present different options to increase the complexity of these BC films, including the attachment of metallic or oxide nanoparticles, or patterning the BC films with different hydrophobic domains.

Novel Soft Chemical Synthesis Method of Functional Ceramic Materials

Kenji Toda[1], Ayano Toda[1], Sun-Woog Kim[1,2], Takuya Hasegawa[1], Mizuki Watanabe[1], Kazuyoshi Uematsu[1], Mineo Sato[1] Tadashi Ishigaki[1], Emiko Kawakami[3], Junko Koide[3], Masako Toda[3], Yoshiaki Kudo[3], Toshiyuki Masui[4], Takaki Masaki[5] and Dae Ho Yoon[5]

[1]Niigata University, 8050 Ikarashi 2-nocho, Niigata 950-2181, Japan.

[2]Sejong University, Gwangjin-gu, Seoul 05006, Republic of Korea.

[3]N-Luminescence Corporation, 8867-3 Ikarashi 2-nocho, Niigata 950-2101, Japan.

[4]Tottori University, 4-101 Koyama-cho Minami, Tottori 680-8550, Japan.

[5]Sungkyunkwan University, Kyunggi-do 400-746, Republic of Korea

E Mail/ ktoda@eng.niigata-u.ac.jp

Recently, we developed novel soft chemical synthesis method, water assisted solid state reaction (WASSR) method [1,2]. This simple method can synthesized the functional ceramic materials just by mixing of raw materials added a small amount of water (about 10 wt%) at low temperature below 373 K. For example, we successfully synthesized numerous ceramic materials, such as (Cs,Rb)VO_3, YVO_4:Eu^{3+}, $BiVO_4$, $LiCoO_2$, $SrMoO_4$, $BaTiO_3$, $LaPO_4$:Ce^{3+},Tb^{3+} and $NaEuMo_2O_8$ at low temperature below 373 K by the WASSR method. In this study, we report the advantages of WASSR method as novel soft chemical synthesis method and also discuss the reaction mechanism.

Keywords: Soft Chemistry, Solid State Reaction, Ionic Diffusion, Water

[1] KANEKO, T., KIM, S. W., TODA, A., UEMATSU, K., ISHIGAKI, T., TODA, K., SATO, M., KOIDE, J., TODA, M., KUDO, Y., MASAKI. T. & YOON, D. H., 2015. Synthesis of YVO4 nano particles by novel room temperature synthesis method. *Science of Advanced Materials*, 7, 1502-1505.

[2] TODA, K., KIM, S. W., HASEGAWA, T., WATANABE, M., KANEKO, T., TODA, A., ITADANI, A., SATO, M., UEMATSU, K., ISHIGAKI, T., KOIDE, J., TODA, M., KUDO, Y., MASAKI. T. & YOON, D. H., 2016. Novel Soft Chemical Synthesis Methods of Ceramic Materials. *Key Engineering Materials*, 690, 268-271.

Optical and Electronic Dual-Function Tuning of Ag Nanoparticles to Enhance UV-Emissions of n-ZnO Nanorods/p-GaN Heterojunction Light-Emitting Diodes

Yung-Chi Yao[1], Zu-Po Yang[2], Jung-Min Hwang[1,3], Yi-Lun Chuang[1], Jing-Yu Haung[1], Jinn-Kong Sheu[4], Meng-Tsan Tsai[5], Ya-Ju Lee[1*]

[1]Institute of Electro-Optical Science and Technology, National Taiwan Normal University, 88, Sec. 4, Ting-Chou Road, Taipei 116, Taiwan.

[2]Institute of Photonic System, National Chiao Tung University, 301, Gaofa 3rd Road, Tainan 711, Taiwan.

[3]Advanced Lighting Technology Department, Green Energy and Environment Research Laboratories, Industrial Technology Research Institute (ITRI), Hsinchu 310, Taiwan.

[4]Department of Photonics, National Cheng Kung University, 1, University Rd, Tainan 701, Taiwan.

[5]Department of Electrical Engineering, Chang Gung University, 259, Wen-Hwa 1st Rd, Taoyuan 33302, Taiwan.

E Mail: ycyao@ntnu.edu.tw/ Fax: +886-2-86631954; Tel: +886-2-77346719

[*]E Mail: yajulee@ntnu.edu.tw/ Fax: +886-2-86631954; Tel: +886-2-77346733

ZnO nanorods (NRs) [1-3] and Ag nanoparticles (NPs) [4-7] are known for enhancing the luminescence of light-emitting diodes (LEDs) through high directionality of waveguide mode transmission and efficient energy transfer of localized surface plasmon (LSP) resonances, respectively. Recently, one-dimensional NRs have been implemented to improve carrier injection efficiency through nanosized heterojunctions. Additionally, the highly homogenous crystallinity inherently present in the ZnO NRs, which can be synthesized by the hydrothermal method [8-10] or other fabrication schemes [11,12], provides excellent transportation paths for injected electrons and serves as the escaping routes for trapped light to enhance the light extraction efficiency. The other increasingly studied nanostructure is the LSPs in noble metal nanoparticles due to its unique ability to enhance the photoluminescence (PL) and/or electroluminescence (EL) intensity of LED devices [5-7, 13-16]. This enhancement is due to energy transition from excitons in active region

(e.g. InGaN/GaN multiple quantum-wells) to LSP resonant modes of metal NPs, either through near-field coupling [17-20] (to enhance the internal quantum efficiency) or far-field coupling [21] (to enhance the light extraction efficiency), depending on the degree of spatial overlap of the extended LSP resonant modes and exciton's wavefunction (which is mainly determined by the distance of the LSP-exciton). Although either the ZnO NRs or the metal NPs have been well recognized with strongly optical coupling effects so that can enhance the LED's luminescence, their hybridization and possible influence on the device performances are barely discussed. In this work, we demonstrated Ag NPs-incorporated n-ZnO NRs/p-GaN heterojunctions by facilely hydrothermally growing ZnO NRs on Ag NPs-covered GaN, in which the Ag NPs were introduced and randomly distributed on the p-GaN surface to excite the LSP resonances. Compared with the reference LED, the light-out power of the near-band-edge (NBE) emission (ZnO, λ=380 nm) of our hybridized structure is increased almost 1.5−2 times and can be further modified in a controlled manner by varying the surface morphology of the surrounding medium of the Ag NPs. The improved light-output power is mainly attributed to the LSP resonance between the NBE emission of ZnO NRs and LSPs in Ag NPs. We also observed different behavior in the EL spectra as the injection current increased for the treatment and reference LEDs. This observation might be attributed to the modification of the energy band diagram for introducing Ag NPs at the interface between n-ZnO NRs and p-GaN. Our results pave the way for developing advanced nanostructured LED devices with high luminescence efficiency in the UV emission regime.

Keywords: Nanorods, noble metal nanoparticles, localized surface plasmon, heterojunctions, light-emitting diodes

[1] LAI, E., KIM, W. & YANG. P. 2008. Vertical Nanowire Array-Based Light Emitting Diodes. *Nano Res.*, 1, 123-128.

[2] JEONG, H., PARK, D. J., LEE, H. S., KO,Y. H., YU, J. S., CHOI, S.-B., LEE, D.-S., SUH, E.-K. & JEONG, M. S. 2014. Light-Extraction Enhancement of a GaN-Based LED Covered with ZnO Nanorod Arrays. *Nanoscale*, 6, 4371-4378.

[3] YE, B.-U., KIM, B. J., SONG, Y. H., SON, J. H., YU, H. K., KIM, M. H., LEE, J.-L. & BAIK, J. M. 2012. Enhancing Light Emission of Nanostructured Vertical Light-Emitting Diodes by Minimizing Total Internal Reflection. *Adv. Funct. Mater.*, 22, 632-639.

[4] GU, X., QIU, T., ZHANG, W. & CHU, P. K. 2011. Light-Emitting Diodes Enhanced by Localized Surface Plasmon Resonance. *Nanoscale Res. Lett.*, 6, 199 (12pp).

[5] YEH, D.-M., HUANG, C.-F., CHEN, C.-Y., LU, Y.-C. & YANG, C. C. 2008. Localized Surface Plasmon-Induced Emission Enhancement of a Green Light-Emitting Diode. *Nanotechnology*, 19, 345201 (4pp).

[6] FADIL, A., IIDA, D., CHEN, Y., MA, J., OU, Y., PETERSEN, P. M. & OU, H. 2014. Surface Plasmon Coupling Dynamics in InGaN/GaN Quantum-Well Structures and Radiative Efficiency Improvement. *Sci. Rep.*, 4, 6392 (7pp).

[7] KWON, M.-K., KIM, J.-Y., KIM, B.-H., PARK, I.-K., CHO, C.-Y., BYEON, C. C. & PARK, S.-J. 2008. Surface-Plasmon-Enhanced Light-Emitting Diodes. *Adv. Mater.*, 20, 1253-1257.

[8] LI, Q., KUMAR, V., LI, Y., ZHANG, H., MARKS, T. J. & CHANG, R. P. H. 2005. Fabrication of ZnO Nanorods and Nanotubes in Aqueous Solutions. *Chem. Mater.*, 17, 1001-1006.

[9] HUA, G., ZHANG, Y., YE, C., WANG, M. & ZHANG, L. 2007. Controllable Growth of ZnO Nanoarrays in Aqueous Solution and Their Optical Properties. *Nanotechnology*, 18, 145605 (6pp).

[10] Kim, K.-K., Lee, S.-D., Kim, H., Park, J.-C., Lee, S.-N., Park, Y., Park, S.-J. & Kim, S.-W. 2009. Enhanced Light Extraction Efficiency of GaN-Based Light-Emitting Diodes with ZnO Nanorod Arrays Grown Using Aqueous Solution. *Appl. Phys. Lett.*, 94, 071118 (3pp).

[11] ZHONG, J., CHEN, H., SARAF, G., LU, Y., CHOI, C. K., SONG, J. J., MACKIE, D. M. & SHEN, H. 2007. Integrated ZnO Nanotips on GaN Light Emitting Diodes for Enhanced Emission Efficiency. *Appl. Phys. Lett.*, 90, 203515 (3pp).

[12] ZHONG, J., MUTHUKUMAR, S., CHEN, Y., LU, Y., NG, H. M., JIANG, W. & GARFUNKEL, E. L. 2003. Ga-Doped ZnO Single-Crystal Nanotips Grown on Fused Silica by Metalorganic Chemical Vapor Deposition. *Appl. Phys. Lett.*, 83, 3401-3403.

[13] LIU, W. Z., XU, H. Y., WANG, C. L., ZHANG, L. X., ZHANG, C., SUN, S. Y., MA, J. G., ZHANG, X. T., WANG, J. N. & LIU, Y. C. 2013. Enhanced Ultraviolet Emission and Improved Spatial Distribution Uniformity of ZnO Nanorod Array Light-Emitting Diodes via Ag Nanoparticles Decoration. *Nanoscale*, 5, 8634-8639.

[14] OKAMOTO, K., NIKI, I., SHVARTSER, A., NARUKAWA, Y., MUKAI, T. & SCHERER, A. 2004. Surface-Plasmon-Enhanced Light Emitters Based on InGaN Quantum Wells. *Nat. Mater.*, 3, 601-605.

[15] QIAO, Q., SHAN, C.-X., ZHENG, J., ZHU, H., YU, S.-F., LI, B.-H., JIA, Y. & SHEN, D.-Z. 2013. Surface Plasmon Enhanced Electrically Pumped Random Lasers. *Nanoscale*, 5, 513-517.

[16] ZHANG, C., MARVINNEY, C. E., XU, H. Y., LIU, W. Z., WANG, C. L., ZHANG, L. X., WANG, J. N., MA, J. G. & LIU, Y. C. 2015. Enhanced Waveguide-Type Ultraviolet Electroluminescence from Zno/Mgzno Core/Shell Nanorod Array Light-Emitting Diodes via Coupling with Ag Nanoparticles Localized Surface Plasmons. *Nanoscale*, 7, 1073-1080.

[17] GONTIJO, I., BORODITSKY, M., YABLONOVITCH, E., KELLER, S., MISHRA, U. K. & DENBAARS, S. P. 1999. Coupling of InGaN Quantum-Well Photoluminescence to Silver Surface Plasmons. *Phys. Rev. B*, 60, 11564-11567.

[18] NEOGI, A., LEE, C.-W., EVERITT, H. O., KURODA, T., TACKEUCHI, A. & YABLONOVITCH, E. 2002. Enhancement of Spontaneous Recombination Rate in a Quantum Well by Resonant Surface Plasmon Coupling. *Phys. Rev. B*, 66, 153305 (4pp).

[19] LU, C.-F., LIAO, C.-H., CHEN, C.-Y., HSIEH, C., KIANG, Y.-W. & YANG, C. C. 2010. Reduction in the Efficiency Droop Effect of a Light-Emitting Diode through Surface Plasmon Coupling. *Appl. Phys. Lett.*, 96, 261104 (3pp).

[20] JANG, L.-W., JEON, D.-W., KIM, M., JEON, J.-W., POLYAKOV, A. Y., JU, J.-W., LEE, S.-J., BAEK, J.-H., YANG, J.-K. & LEE, I.-H. 2012. Investigation of Optical and Structural Stability of Localized Surface Plasmon Mediated Light-Emitting Diodes by Ag and Ag/SiO_2 Nanoparticles. *Adv. Funct. Mater.*, 22, 2728-2734.

[21] DANG, S., LI, C., JIA, W., ZHANG, Z., LI, T., HAN, P., & XU, B. 2012. Improvement of Light Extraction Efficiency of GaN-Based Light-Emitting Diodes Using Ag Nanostructure and Indium Tin Oxide Grating. *Opt. Express*, 20, 23290-23299.

PDA Nanoparticles for Detoxification

Maling Gou

State Key Laboratory of Biotherapy and Cancer Center, West China Hospital, Sichuan University, and Collaborative Innovation Center for Biotherapy

NO.17 People's South Road Section 3, Chengdu, Sichuan, 610041, P.R. China

goumaling@scu.edu.cn/ +86 13880640692

Polydiacetylene (PDA) is known as a sensor material whose color (blue-to-red) and fluorescence (non-to-fluorescent) changes in response to environmental cues[1-3]. Here, we discovered that the PDA nanoparticles can sense, capture and neutralize pore-forming toxins for its cellular membrane-mimetic surface and the conjugated structure, which inspired us to apply it to detoxification. We have designed and completed a "PDA-PFTs" vaccine to efficiently induce a specific immune response in the body for the PDA nanoparticles could neutralize pore-forming toxins without damaging their antigenic epitopes. Meanwhile, we used synthetic PDA nanoparticles that act like artificial hepatocytes to "recellularize" decellularized liver scaffold, creating a liver-mimetic device[4]. This device was proved to selectively cleanse the blood of pore-forming toxins and did not significantly affect the normal component of blood. Furthermore, we presented a liver-inspired three-dimensional (3D) detoxification device which was created by 3D printing of designer hydrogels with PDA nanoparticles installed in the hydrogel matrix[5]. Our results showed that this bio-mimetic detoxification device could neutralize the virulence of pore-forming toxins at 100% rate.

All in all, PDA nanoparticles have made a breakthrough in the developments of novel vaccine or extracorporeal detoxification device and we anticipate their more clinical application in the future.

Keywords: PDA, 3D printing, Liver, Detoxification, Vaccine

[1] LU, Y., YANG, Y., SELLINGER, A., LU, M., HUANG, J., FAN, H., HADDAD, R., LOPEZ, G., BURNS, A. R., SASAKI, D. Y., SHELNUTT, J., BRINKER, C. J. 2001. Self-Assembly of Mesoscopically Ordered Chromatic Polydiacetylene/Silica Nanocomposites. *Nature*, 410, 913-917.

[2] WANG, X., SUN, X., HU, P., ZHANG, J., WANG, L., FENG, W., LEI, S., YANG, B., CAO, W. 2013. Colorimetric Sensor Based on Self-Assembled Polydiacetylene/Graphene-Stacked Composite Film for Vapor-Phase Volatile Organic Compounds. *Adv Funct Mater*, 23, 6044-6050.

[3] CHEN, X., ZHOU, G., PENG, X., YOON, J. 2012. Biosensors and Chemosensors Based on the Optical Responses of Polydiacetylenes. *Chem Soc Rev*, 41, 4610-4630.

[4] XU, F., KANG, T., DENG, J., LIU, J., CHEN, X., WANG, Y., OU, Y., DU, T., TANG, H., XU, X., CHEN, S., DU, Y., SHI, Y., QIAN, Z., WEI, Y., DENG, H., GOU, M. 2016, Functional Nanoparticles Activate a Decellularized Liver Scaffold for Blood Detoxification. *Small*.

[5] GOU, M., QU, X., ZHU, W., XIANG, M., YANG, J., ZHANG, K., WEI, Y., CHEN, S. 2014. Bio-inspired Detoxification Using 3D-printed Hydrogel Nanocomposites. *Nat Commun*, 5, 3774.

Shear-Driven Aggregation of Binary Colloids for Homogeneous Distribution of Nanoparticles in a Matrix

Xia Meng, Xinxin Sheng, Hua Wu, Massimo Morbidelli

Institute for Chemistry and Bioengineering, Department of Chemistry and Applied Biosciences, ETH Zurich, 8093 Zurich, Switzerland.

E Mail: *hua.wu@chem.ethz.ch*

Nanocomposite materials are widely used in many fields such as biomedicine, dental and bone implants, therapeutics delivery, diagnostics and treatment, membrane performance enhancement, solid-state lighting and photovoltaic devices. In these applications there is often a challenging issue how one can homogeneously distribute nanoparticles (NPs) in a matrix, avoiding their agglomeration, for which a general methodology cannot be found in the literature. In this work, we propose a methodology for preparing composite materials where B NPs are homogeneously and randomly distributed inside a matrix of A NPs. It is based on intense shear-driven aggregation [1-6] of binary colloids composed of A and B NPs, without using any additives. Its feasibility has been demonstrated using two stable binary colloids composed of (1) polystyrene (PS) particles and poly-methyl methacrylate (PMMA) particles, and (2) graphene oxide (GO) sheets and poly-vinylidene fluoride (PVDF) NPs. In the first case, the PS particles alone undergo the shear-driven aggregation (shear-active), while the PMMA particles alone do not (shear-inactive). It is found that the shear-driven aggregation of the binary colloids does occur, and the formed clusters are composed of both the “shear-active” PS and “shear-inactive” PMMA particles. The SEM picture demonstrates that the PMMA particles are homogeneously and randomly distributed among the PS particles in the clusters. Similar results are also obtained in the second case , gelation of the shear-active PVDF NPs are able to homogeneously capture and distribute the shear-inactive GO sheets inside the PVDF NP gel matrix. All the results confirm the feasibility of the proposed methodology. Mechanism leading to the aggregation of the binary colloids has been proposed based on the experimental observations.

Keywords: binary colloid, shear-driven, aggregation, nanocomposite, graphene oxide

[1] WU, H., ZACCONE, A., TSOUTSOURA, A., LATTUADA, M. & MORBIDELLI, M. 2009. High shear-induced gelation of charge-stabilized colloids in a microchannel without adding electrolytes. *Langmuir,* 25**,** 4715-4723.

[2] ZACCONE, A., WU, H., GENTILI, D. & MORBIDELLI, M. 2009. Theory of activated-rate processes under shear with application to shear-induced aggregation of colloids. *Phys. Rev. E,* 80**,** 051404.

[3] XIE, D. L., WU, H., ZACCONE, A., BRAUN, L., CHEN, H. Q. & MORBIDELLI, M. 2010. Criticality for shear-induced gelation of charge-stabilized colloids. *Soft Matter,* 6**,** 2692-2698.

[4] ZACCONE, A., GENTILI, D., WU, H., MORBIDELLI, M. & DEL GADO, E. 2011. Shear-driven solidification of dilute colloidal suspensions. *Phys. Rev. Lett.,* 106**,** 138301.

[5] XIE, D. L., LAMPROU, A., STORTI, G., MORBIDELLI, M. & WU, H. 2012. Shear-induced gelation of soft strawberry-like particles in the presence of polymeric P(BA-b-AA) surfactants. *Phys. Chem. Chem. Phys.,* 14**,** 14374-14382.

[6] MENG, X., WU, H. & MORBIDELLI, M. 2015. Kinetics and cluster morphology evolution of shear-driven aggregation of well-stabilized colloids. *Langmuir,* 31**,** 1113-1119.

Structural and XPS Studies of SiO_2-Ag Core-Shell Nanocomposite Synthesized Using Nonsurfactant Surface Modification

M. A. Salim[1], H. Misran[1]

[1]Nanoarchitechtonic Laboratory, College of Engineering, Universiti Tenaga Nasional, Jalan IKRAM-UNITEN, 43000 Kajang Selangor, Malaysia.

Halina@uniten.edu.my

SiO_2-Ag core-shell nanocomposite has attracted great research interest for application in various fields due to its excellent optical properties and as an antibacterial agent. The properties of SiO_2-Ag core-shell nanocomposite are highly dependent on particles size and morphology. Based on size-tuning optimization condition obtained from statistical analyses, SiO_2 sphere at ca. 300 nm were synthesized by our group using palm oil derived fatty alcohol (PODFA) as reported [1]. Thus, in this study, the surface of obtained SiO_2 sphere were successfully coated with Ag nanoparticles using nonsurfactant surface modification technique using PODFA and ammonia as surface modification agents [1, 2]. The morphology of SiO_2-Ag core-shell nanocomposite was characterized using field emission scanning electron microscopy (FE-SEM) and transmission electron microscopy (TEM). Nanoparticles with size ca. 10-50 nm were observed on spherical silica (ca.300 nm) suggested the successful attachment of Ag element. Sharp peaks attributable to the face-centered cubic (FCC) structure of metallic Ag nanoparticles was observed in X-ray diffraction (XRD) pattern. The X-ray photoelectron spectroscopy (XPS) exhibited the existence of spin orbit component of Ag3d peaks at 367 eV and 373 eV, respectively. The binding energy (BE) of Si-Ag and Si-O-Si bonds were observed at ca. 99 eV and 530 eV. Figure 1 shows the XPS spectra of bare SiO_2 and SiO_2-Ag core-shell nanocomposite. The results obtained in the present work suggested the feasibility of employing PODFA and ammonia as potential nonsurfactant surface modifiers in synthesizing SiO_2-Ag core-shell nanocomposite.

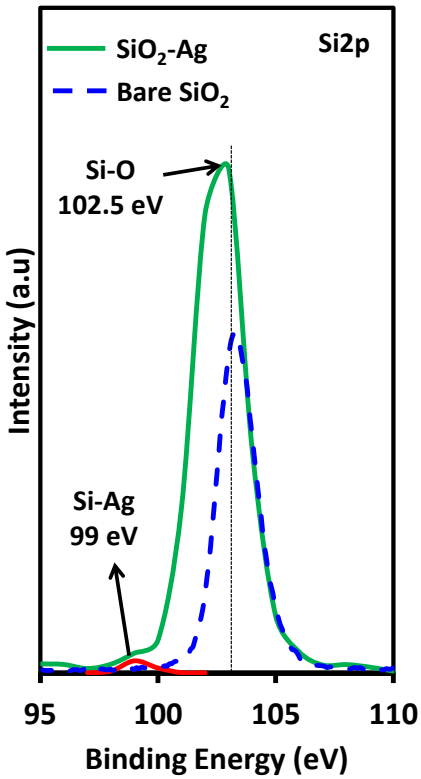

Figure 1: XPS Si2p spectra of bare SiO_2 and SiO_2-Ag samples.

Keywords: Surface modification, SiO_2-Ag core-shell, nanocomposite, XPS

[1] SALIM, M. A., MISRAN, H., OTHMAN, S. Z., SHAH, N. N. H. & RAZAK, N. A. A. 2013. Renewable Decyl-alcohol Templated Synthesis of Si-Cu core-shell Nanocomposite. *IOP Conf. Series: Earth and Environmental Science*, 16, 012054.

[2] SALIM, M. A., MISRAN, H., OTHMAN, S. Z., MAHADI, N., PAUZI, N. I. M. & MANAP, A. 2015. Synthesis and Characterizations of SiO_2-Ag Core-Shell Nanostructure Using Fatty Alcohols as Surface Modifiers. *Applied Mechanics and Materials*, 773-774, 199-203.

Synthesis and application of mesostructured materials for energy storage and conversion

Qiang Wu, Zhiyang Lyu, Tao Sun, Hongwei Lai, Xizhang Wang, Zheng Hu

Key Laboratary of Mesoscopic Chemistry of MOE, School of Chemistry and Chemical Engineering, Nanjing University, Nanjing 210093, China.

Email: wqchem@nju.edu.cn

The research on the mesoscale science is “the next big(ger) thing” of the scientific world [1] and the development of mesostructured materials for energy applications is one of the priority research directions [2]. The mesostructured materials that are assembled by nanostructured building blocks with particular manners possess the characters of hierarchical arrangement and multiscale pore structure, which endow them with large surface area, short ion solid-state diffusion path and good accessibility to electrolyte. This kind of materials could be promising in energy applications.

Recently, we synthesized the mesostructures of 3D hierarchical carbon nanocages (hCNC) with high surface area, good graphitization degree and multiscale pore structures, which showed large specific capacitance and high rate as the electrodes for supercapacitors [3,4]. Sulfur can be filled into the nanocages with high loading (~80 wt%), and the designed S@hCNC composite presented large capacity, high-rate capability and long cycle life in lithium-sulfur batteries [5]. By using the hCNC as the support, alloyed Co-Mo nitride electrocatalysts were constructed, which combined the merits of cobalt nitride and molybdenum nitride, showing high activity comparable to that of cobalt nitride and progressively enhanced stability with the increase in the Mo ratio for the oxygen reduction reaction in acidic medium [6]. In addition, the construction of the mesostructured metal oxides can greatly boost their energy storage performance. These progresses suggest that the mesostructured materials have bright prospect in energy storage and conversion.

Keywords: Mesostructures, energy storage and conversion, carbon nanocages, metal oxides, electrode design

[1] Service, R. F. 2012. The Next Big(ger) Thing, *Science*, 335, 1167.

[2] Hemminger, J. et al. 2012. *From Quanta to the Continuum: Opportunities for Mesoscale Science,* A report from the Basic Energy Science Advisory Committee, US Department of Energy, Sept. 2012 (Downloaded at www.meso2012.com).

[3] Xie, K., Qin, X. T., Wang, X. Z., Wang, Y., Tao, H. S., Wu, Q., Yang, L. J. & Hu, Z. 2012. Carbon Nanocages as Supercapacitor Electrode Materials, *Adv. Mater.*, 24, 347-352.

[4] Zhao, J., Lai, H. W., Lyu, Z. Y., Jiang, Y. F., Xie, K., Wang, X. Z., Wu, Q., Yang, L. J., Jin, Z., Ma, Y. W., Liu, J. & Hu, Z. 2015. Hydrophilic Hierarchical Nitrogen-Doped Carbon Nanocages for Ultrahigh Supercapacitive Performance, *Adv. Mater.*, 27, 3541-3545.

[5] Lyu, Z. Y., Xu, D., Yang, L. J., Che, R. C., Feng, R., Zhao, J., Li, Y., Wu, Q., Wang, X. Z. & Hu, Z. 2015. Hierarchical Carbon Nanocages Confining High-Loading Sulfur for High-Rate Lithium-Sulfur Batteries, *Nano Energy*, 12, 657-665.

[6] Sun, T., Wu, Q., Che, R. C., Bu, Y. F., Jiang, Y. F., Li, Y., Yang, L. J., Wang, X. Z. & Hu, Z. 2015. Alloyed Co-Mo Nitride as High-Performance Electrcatalyst for Oxygen Reduction in Acidic Medium, *ACS Catal.*, 5, 1857-1862.

Abstract AFM 2016

Transparent aerogels from nematic nanofibrillated carboxyl celluloses covalently equipped with carbon dots of high quantum yield: First steps towards bio-based true volumetric 3D displays

S. Plappert, S. Quraishi, T. Rosenau, F. Liebner*

University of Natural Resources and Life Sciences Vienna, Division of Chemistry of Renewable Resources, Konrad-Lorenz-Strasse 24, 3430 Tulln an der Donau, Austria

**falk.liebner@boku.ac.at*

Fluorescence caused by quantum confinement of excitons is one of the unique and versatile response phenomena of quantum dots (QD) towards low energy photons. It is a feature attractive for many applications including QD laser, solar cells, chemo-sensing, bio-sensing of active compounds, or tracing of cancer cells.

QDs homogeneously dispersed in a transparent matrix can be used to generate adressable «active elements» transparent in *off* state but either opaque or luminous in *on* state. These immobilized elements (voxels) can be activated by pulsed IR laser light forming a visual representation of an object in three physical dimensions as opposed to the planar image of traditional screens, thus providing ultimate physiological depth cues. As the color gamut of QDs is much greater than that of the common RGB standard, 3D color images of high brilliance can be created using an ensemble of randomly dispersed QDs of different photoluminescence covering the whole range of the visible light.

Following our previous works on transparent, monolithic aerogels from nematic liquid-crystalline, nanofibrillated TEMPO-oxidized cellulose reinforced by percolating networks of PMMA and on fluorescent cellulose aerogels covalently equipped with $(ZnS)_x(CuInS_2)_{1-x}/ZnS$ (core/shell) quantum dots, this paper communicates the results of an ongoing study investigating approaches towards grafting of different types of surface functionalized carbon dots onto transparent, highly porous yet mechanically robust aerogels from nematic liquid-crystalline suspensions of nanofibrillated carboxyl cellulose derivatives.

Four different types of carbon dots (CDs) were prepared by microwave-assisted thermolysis from different organic precursors. Aiming at the synthesis of CDs equipped with surface amino groups for grafting the CDs onto the respective carboxyl cellulose derivatives via classic EDC/NHS chemistry, each set of precursor compounds consisted therefore of both a carbon and an nitrogen source. Investigation of the photoluminescence properties revealed relatively high quantum yields (≤ 30%) and good pH stability for all synthesized CDs allowing for grafting onto the respective cellulose derivatives prior to the acidic gelation step.

CD coupling via NHS/EDC chemistry prior to gel formation has been confirmed to be superior with regard to homogeneity of CD distribution compared to loading of CDs into monolithic hydrogels. Reinforcement of all types of CD-modified carboxyl cellulose gels with percolating networks of PMMA as accomplished by combined $scCO_2$ anti-solvent precipitation (7.5 MPa, 40°C) and $scCO_2$ drying (9.5 MPa, 40°C, 3h) afforded mechanically robust, hydrophobic and largely transparent (400-750 nm) aerogels. Grafting of CDs prior to the PMMA reinforcement step strongly reduces the photoluminescence presumably through coating of cellulosic nanofibrils.

BSA-stabilized gold fluorescent nanocluster for sensitive and selective detection of lead (II) and melamine in aqueous solution

Che-Yu Lee, Nai-Yue Hsu, and Yang-Wei Lin*

Department of Chemistry, National Changhua University of Education, Changhua, Taiwan

Address correspondence to these authors at Department of Chemistry, National Changhua University of Education, Changhua City, PO Box 500, Taiwan; Fax: +886-4-721-1190; E-mail: linywjerry@cc.ncue.edu.tw

Abstract

In this work, a sensitive and selective fluorescence assay by using fluorescent BSA-stabilized gold nanoclusters (BSA-AuNCs) was proposed for the determination of lead (II) and melamine in aqueous solution. The fluorescence of the BSA-AuNCs was quenched through a Pb^{2+}-mediated interparticle aggregation mechanism, and thus the change in fluorescence at 660 nm was dependent on the Pb^{2+} ion concentration. In addition, the fluorescence of the BSA-AuNCs was also quenched based on the high-affinity metallophilic Hg^{2+}-Au^{+} interaction, while the fluorescence of the BSA-AuNCs restored when melamine was added and coordinated with Hg^{2+}. Under

optimal conditions (0.1 × BSA-Au NCs; 50 mM phosphate buffer at pH 7.0), the limit of detection for Pb^{2+} ions and melamine at a signal-to-noise ratio of 3 was 0.48 μM and 2.9 μM, respectively. Our present approach is simpler, faster, and more cost-effective than other techniques for the detection of Pb^{2+} ions in environmental water samples (pond and seawater) and that of melamine in milk samples

Keywords: microwave, gold nanocluster, Pb^{2+}, melamine, fluorescence quenching/antiquenching

Filter-free spectrometer on-a-chip based on nano-structured Silicon photo-detector array

Hyun Seung (Lee)[1,3], Inho (Kim)[1], Won Mok (Kim)[1], Seok-Joo (Byun)[2], Byeong-Kwon (Ju)[3], Taek-Sung (Lee)[1,4,*]

[1]Center for Electronic Materials, Korea Institute of Science and Technology, Hwarang-ro 14-gil 5, Seongbuk-gu, Seoul, 02792, Rep. of Korea.

[2]INSIDEOPTICS Co. LTD, Geongneung-ro 232, Nowon-gu, Seoul, 01811, Rep. of Korea.

[3]School of Electrical Engineering, Korea University, Anam-dong 5-ga, Seongbuk-gu, Seoul, 02841, Rep. of Korea.

[4]Smart Farm Solution(SFS) Convergence Research Team, KIST Gangneung Institute of Natural Products, Saimdang-ro 679, Gangneung-si, Gangwon-do, 25451, Rep. of Korea.

t14472@kist.re.kr / *tslee@kist.re.kr* *

Conventional miniature spectrometers which take a role of the core of mobile and wearable devices have its intrinsic size limitation due to the wavelength discriminating components such as diffraction grating, interferometer. Filter-based miniature spectrometers are allowed to fabricate on-a-chip by implementing multiple filters directly onto pixels of the photo-detectors (PDs). However the transmitted light through the filter would result in a reduction in its intensity and it would cause problems to weaken the sensitivity of the spectrometers.

In this work, a concept of a spectrometer on-a-chip without filters or any dispersive optics was simulated. Also a concept prototype of a filter-free spectrometer on-a-chip was fabricated and tested. It comprised of multiple nano-structured Silicon PD array with digital-signal-processing (DSP) method. DSP algorithm play a role as a reduction the requirements of a delta-function-like spectrum shape without overlapping within the individual PDs and is possible to fabricate the devices for low-cost process. Each PD which was composed of different shape of nano-structure had unique its light absorption spectrum by the optical properties of the nano-structured semiconducting materials. This could enable both functions of a filter and a PD in a single structure as well as to enhance

the photon efficiency by removing the filter on the detector. The calculations of the optical absorption in the nano-structured Si PD were carried out by rigorous coupled-wave analysis (RCWA) method and it was assumed that all of the PDs were restored by the DSP. Based on a discrete linear system model, a series of estimators for spectrum recovery was applied. Nano-structured Si PD arrays for the concept prototype were fabricated with laser interference lithography (LIL) method and etching process. The device was measured by using various light sources having different spectral distribution.

Keywords: Spectrometer on-a-chip, Nano-structured materials, RCWA, Laser interference lithograph

Periodic Mesoporous Organosilica Modified with Poly(ethylene oxide) and Amine-containing Silanes for Gas Adsorption

Sora Sim, Dongjoo Yoon, Eun-Bum Cho

Department of Fine Chemistry, Seoul National University of Science and Technology, Seoul 01811, Korea.

E-mail address: echo@seoultech.ac.kr

Periodic mesoporous organosilica was prepared using 1,4-bis(triethoxysilyl)benzene (BTEB) in the presence of a poly(ethylene oxide)-*b*-poly(D,L-lactic acid-*co*-glycolic acid)-*b*- poly(ethylene oxide) triblock copolymer (PLGE) template under acidic conditions. Moreover, the benzene-silica framework wall was modified with isocyannurate (ICS)-containing organosilane and polyethylene oxide chains inside the pore wall. Also, the surface of mesoporous wall was functionalized with an amine-containing organosilane. The ICS-containing mesoporous benzene-silica was prepared with co-condensation method and poly(ethylene oxide) chain was located inside the pore wall by thermal treatment of 250 ^{o}C for 3 h under flowing nitrogen gas. Amine-functionalization was made by post-grafting method on the mesoporous surface. Small angle X-ray scattering and nitrogen adsorption isotherms showed highly ordered hexagonal (*p*6*mm*) mesostructured and high surface area. The amount of ICS-containing organosilane was adjusted up to 25 mol% still maintaining the ordered mesostructured. Solid-state ^{13}C and ^{29}Si CP-MAS NMR showed ICS moiety linked with silica bonds as well as poly(ethylene oxide) chains. Amine groups on the mesoporous surface were also confirmed with solid-state NMR spectra. Carbon dioxide uptake on the mesoporous organosilica materials were investigated using a TGA microbalance at 25 ^{o}C under 1 atm.

Keywords: mesoporous organosilica, benzene-silica, isocyanurate, poly(ethylene oxide)

[1] SIM, K., LEE, N., KIM, J., CHO, E.-B., GUNATHILAKE, C. & JARONIEC, M. 2015. *ACS Applied Materials & Interfaces, 7*, 6792-6802.

Preparation of electrically conductive bucky-sponge using CNT-cement : Conductivity control using room temperature ionicliquids

Ju Hyun (Kim)[1], Ueon Sang (Shin) [1,2]

Presenting author should be underline

[1] Department of Nanobiomedical Science Dankook University, Cheonan, Chungnam 330-714, Korea

[2]Institute of Tissue Regeneration Engineering (ITREN), Dankook University, Cheonan, Chungnam 330-714, Korea

E Mail/ : magic8136@dankook.ac.kr and usshin12@dankook.ac.kr

We present CNT bucky-sponges prepared using CS-NH2/CNT-cement (CNT nanohybrid molecules individually wrapped with chitosan molecules) as a construction material and an imidazolium based room temperature ionic liquid (RTIL) as a liquid porogen. The nano-sized and micro-sized pores with various width (respectively, about <20 nm and 20–300 μm) were controllably produced by increasing the amount of RTIL used (from 1 to 5 g). It was confirmed by SEM characterization that both types of pores coexist within the CNT frameworks with chitosan skin. Total pore volumes calculated from the volume increaseof the sponge samples ranged in percentage from 89 to 98. Porosity of the CNT bucky-sponges, caused by the micro-pores and measured with a mercury porosimeter, ranged between 5 and 28% controlled by theamount of RTIL used. BET surface area and volume resistivity of the CNT sponges were in the ranges of,respectively, 19.7–94.5 m^2/g and 0.022–3.22Ωcm. The prepared CNT sponges showed important characteristics indicating broad applicability as a conductive polymer framework, drug carrying scaffold,catalyst support, oil adsorbents, and molecular sieve membrane.

Keywords: CNT bucky-sponges, Room temperature ionic liquids, Electrically conductive sponges.

Studies on Self-Assembly of Block Copolymers in Aqueous Solution using SANS and SAXS

Tae-Hwan Kim*, Eunhye Kim, Young-Soo Han

Neutron Science Division, Research Reactor Utilization Department, Korea Atomic Energy Research Institute 1045 Daedeok-daero, Yuseong-gu, Daejeon, 305-353, Korea

(taehwan@kaeri.re.kr/Tae-Hwan Kim)

Amphiphilic block copolymers form various micellar nanostructures such as sphere, cylinder, and lamellae in aqueous solution and their phase behaviors are easily tunable by controlling the external conditions (additives, temperature or pH). Particularly, since the Pluronic triblock copolymers (PEO_m-PPO_n-PEO_m) are highly biocompatible, they provide a wide range of potential applications in biotechnology such as drug delivery systems. Regarding to the change of external conditons, however, the self-assembled nanostructures of the Pluonic block copolymers has not been fully exploited yet, which provides key information for the practical application of block copolymers. Here, we have studied the self-assembled nanostructure of block copolymers in aqueous solution by changing the various external conditions using small angle neutron and X-ray scattering. In this presentation, we will present a variety of nanostructures of Pluronic triblock copolymers with different concentration, temeprature and additives, which are applicable to nano- and bio-materials.

Keywords: Block Copolymer, Self-Assembly, Nanostructure, SANS, SAXS

Thermo-magnetic stability of carboxylic adsorption on magnetic Fe_3O_4 nanoparticles for hyperthermia

W. Zhang[a,*], Z.C. Lin[a], X.P. Zhang[b], L. Luo [a], Z.D. Zeng[a], Q. Huang[a], Z.F. Hu[a], L. Zhuang[c]

a School of Physics and Optoelectronic Engineering, Guangdong University of Technology, Guangzhou 510006, People's Republic of China

b Cancer Institute and hospital, Guangzhou Medical University, Guangzhou, 510182, People's Republic of China

c Institute for Solar Energy Systems, State Key Laboratory of Optoelectronic Materials and Technologies, Sun Yat-Sen University, Guangzhou, 510275, People's Republic of China

Abstract: Monodispersed Fe_3O_4 magnetic particles adsorpted with amylase (Citric Acid ,carboxymethyl chitosan and β -Cyclodextrin) was prepared by means of co-precipitation method. The absorption characters of samples were investigated by FTIR, TG and VSM. It was found that the COOH groups of amylase reacted with the surface OH groups of Fe_3O_4 particles resulting in the formation of the iron carboxylate to adsorb onto Fe_3O_4. Furthermore, the inductive heating property of the Fe_3O_4 magnetic nanoparticles in an alternating current magnetic field was investigated and the thermo-magnetic stabilities around induction heating are discussed.

Key words: Fe_3O_4, Adsorption, Heating effect, Carboxylic, hyperthermia

* Corresponding author. Tel.: +86 20 39322265; Fax: +86 20 39322265.
E-mail addresses: Weizh55@aliyun.com

A Novel Thin Film Nitinol Covered Stent for Treating Atherosclerotic Carotid Artery Stenosis

Mahdis Shayan[1], Brian T. Jankowitz[2], and Youngjae Chun[1,3,4]

[1]Department of Industrial Engineering, University of Pittsburgh, Pittsburgh, PA, USA

[2]Department of Neurological Surgery, University of Pittsburgh Medical Center, Pittsburgh, PA, USA

[3]Department of Bioengineering, University of Pittsburgh, PA, USA

[4]McGowan Institute for Regenerative Medicine, University of Pittsburgh and University of Pittsburgh Medical Center, PA, USA

Email : yjchun@pitt.edu, Phone : +1-310-310-0622, and Fax : +1-412-624-9831

Stroke and carotid artery atherosclerotic disease represents a significant disease burden in the United States, showing the third most common cause of mortality [1]. Recently, endovascular treatment became more popular in vascular disease management due to its less invasive and more cost-effective nature compared with the open surgery. The endovascular approach uses balloon angioplasty and placement of stents with the separate embolic protection filter devices, where the filter is not so effective in reducing periprocedural complications [2]. Advancements in stent graft technologies for carotid artery stenosis are limited by the lack of a suitable, biocompatible material for the covering of the embolic protection stent. Therefore, we introduce a novel thin film nitinol (TFN) and develop the carotid artery embolic protection stent that is non-thrombogenic and ultra-low profile, as well as capable of continuously preventing intra-/post-operative distal embolization with the optimized TFN covering.

We have demonstrated *in vitro* efficacy of the TFN covered embolic protection stents using various size of fuorescent micro particles and biodegradable polymer coating that mimic the carotid artery stenosis environment. Total five different types of micro-patterned TFN coverings (i.e., 15-44% porosity with diamond and ellipse patterns) were used to investigate the optimal pore size and geometry for the embolic protection. The diamond patterned TFN showed superior protection capability (>85-90%) compared with the ellipse patterns (78-87%). Both *in vitro* and *in vivo* biocompatibility studies were

also performed to demonstrate superior in cytotoxicity, cell growth behavior, and thromboresistance of the superhydrophilic TFN [3]. *In vitro* platelet adhesion study of the superhydrophilic TFN demonstrated no significant platelet adhesion (0-3 per mm^2) and no platelet aggregation ($p < .05$) after 180 min of platelet contact, while the ePTFE samples showed evidence of dense platelet aggregation of >100 platelets per mm^2 [4]. This finding confirms that treatment of TFN to increase surface hydrophilicity significantly reduces platelet adhesion and may reduce or eliminate thrombosis. *In vivo* study with swine model has also demonstrated that the devices covered with superhydrophilic TFN with a 30x60μm diamond pattern (i.e., 17% porosity) had moderate neointimal growth with well-organized cell architecture and little evidence of ongoing inflammation [5]. These findings do suggest that pore geometry and porosity of micro-patterned TFN can be optimized to achieve the successful embolic protection for the dislodgement of the carotid artery stenosis, as well as the desired biological response i.e. neointimal growth and thrombosis, suggesting a high potential for future endovascular device for treating atherosclerotic carotid artery stenosis.

Keywords: atherosclerotic, carotid artery stenosis, thin film nitinol, stent, superhydrophilic

[1] SOBIESZCZYK & BECKMAN, J. 2006. Carotid artery disease. *Circulation*, 114, e244-e247.

[2] ANSEL, G. M. & JAFF, M. R. 2008. Carotid stenting with embolic protection: evolutionary advances. *Expert Review of Medical Devices*, 5, 427-436.

[3] CHUN, Y., LEVI, D. S., MOHANCHANDRA, K., & CARMAN, G. P. 2009. Superhydrophilic surface treatment for thin film NiTi vascular applications. *Materials Science and Engineering: C*, 29, 2436-2441.

[4] TULLOCH, A. W., CHUN, Y., LEVI, D. S., MOHANCHANDRA, K. P., CARMAN, G. P., LAWRENCE, P. F., & RIGBERG, D. A. Super hydrophilic thin film nitinol demonstrates reduced platelet adhesion compared with commercially available endograft materials. 2010. *Journal of Surgical Research*, 171, 317-322.

[5] CHUN, Y., LEVI, D. S., MOHANCHANDRA, K. P., FISHBEIN, M., & CARMAN, G. P. 2010. Novel micro-patterning processes for thin film NiTi vascular devices. *Smart Materials and Structures*, 19, 105021.

Mechanical Behavior of a Microstructured Thin Film Nitinol

Yanfei Chen[1], Connor Howe[2], Youngjae Chun[1, 3], Woon-Hong Yeo[2, 4]

[1]Department of Industrial Engineering, University of Pittsburgh, Pittsburgh, PA 15261, USA.

[2]Department of Mechanical and Nuclear Engineering, Virginia Commonwealth University, VA 23284, USA.

[3]Department of Bioengineering, University of Pittsburgh, PA 15261, USA.

[4]Center for Rehabilitation Science and Engineering, Virginia Commonwealth University, VA 23298, USA.

Email : whyeo@vcu.edu, Phone : 1-804-827-3517, and Fax : 1-804-827-7030

A cerebral aneurysm occurs as a result of a weakened blood vessel, which allows blood to flow outside the normal path into a sac or a ballooned section (Brisman et al., 2006). The risk of leaking or rupturing from aneurysms results in a high morbidity and mortality rates. While an endovascular coiling procedure has been widely used to treat cerebral aneurysm because of its less invasive nature compared with surgical clipping, there is a fairly high rate of post-operative recanalization (~37%) or regrowth due to persistent blood flow into the aneurysm, specifically for the patients with wide-neck or giant aneurysms (Raymond et al., 2003). Recent advancement shows that a new device, called a "flow-diverter", can divert blood flow away from the aneurysm sac by placing a cylindrical porous structure inside the vessel (Wong et al., 2011). This new approach effectively reduces the intrasaccular blood flow, resulting in gradual localized thrombosis formation of the aneurysm over time and subsequently complete occlusion within the sac. There are a few commercial flow-diverters, based on a metal wire braided structure, such as pipeline embolization device, surpass flow-diverter, and silk flow-diverter. More recently, a new type of flow-diverter has been developed based on a highly stretchable thin layer of nitinol (i.e., thin film nitinol: TFN) (Chun et al., 2010). While this new device has demonstrated the efficacy in in vitro and in vivo settings, there are no significant studies investigating the mechanical safety of such devices in bending and stretching, considering the use in irregular, curved blood vessels in neurovascular anatomy. The main contribution

of this paper is to study the mechanical behaviors and structural safety of a microstructured TFN membrane through the computational and experimental studies (both in vivo and in vitro). The combination of mechanical modeling and the corresponding experiment establish the fundamental aspects of the uniaxial/biaxial stretching and bending mechanics of the microfabricated TFN flow-diverter. The result shows a hyper-elastic behavior of the TFN with a negligible strain change up to 180° in bending and over 500% in circumferential stretching, which is ideal for the deployment in the neurovascular curved arteries. The computational study determines the optimal joint locations between the film and stent frame. *In vitro* experimental test qualitatively demonstrates the mechanical flexibility of the flow-diverter with multi-modal bending. *In vivo* micro X-ray and histopathology study results show that the flow-diverter can be conformally deployed in the curved blood vessel of a swine model without any significant complications or abnormalities.

Keywords: Thin film nitinol, flow-diverter, microfabrication, computational mechanics, and in vivo animal study.

References

BRISMAN, J. L., SONG, J. K. & NEWELL, D. W. 2006. Cerebral aneurysms. *New England Journal of Medicine,* 355**,** 928-939.

CHUN, Y., LEVI, D., MOHANCHANDRA, K., FISHBEIN, M. & CARMAN, G. 2010. Novel micro-patterning processes for thin film NiTi vascular devices. *Smart Materials and Structures,* 19**,** 105021.

RAYMOND, J., GUILBERT, F., WEILL, A., GEORGANOS, S. A., JURAVSKY, L., LAMBERT, A., LAMOUREUX, J., CHAGNON, M. & ROY, D. 2003. Long-term angiographic recurrences after selective endovascular treatment of aneurysms with detachable coils. *Stroke,* 34**,** 1398-1403.

WONG, G. K., KWAN, M. C., NG, R. Y., SIMON, C. & POON, W. 2011. Flow diverters for treatment of intracranial aneurysms: current status and ongoing clinical trials. *Journal of Clinical Neuroscience,* 18**,** 737-740.

3D Graphene Foam/Polydimethylsiloxane as a Novel Flexible Heating Element

Kata Jaruwongrungsee, Ditsayut Phokharatkul, Thitima M. Daniels, Adisorn Tuantranont, Anurat Wisitsoraat

National Electronics and Computer Technology Center (NECTEC),

112 Thailand Science Park, Phahon Yothin Rd., Klong Luang, Pathumthani, Thailand.

E-mail: anurat.wisitsoraat@nectec.or.th

3D graphene foam is a novel material with high thermal and electrical conductivity and should be highly promising for electric heating applications. However, there is no report of its applications in electric heating due to poor physical integrity. In this work, graphene foam (GF) and polydimethylsiloxane (PDMS) composite has been proposed as a novel flexible heating element. The GF is formed on nickel (Ni) foam template by chemical vapor deposition (CVD) using acetylene carbon source (3 sccm) and hydrogen gas carrier (24 sccm) at 700°C for 3 minutes followed by fast cooling. Next, silver paste was applied at contact area on graphene/Ni foam and graphene/PDMS composite was then formed by dip coating the graphene foam into PDMS solution and dried in an oven at 70°C for 12 hour. The nickel foam template was then removed everywhere except the contact area by chemical etching in a hot hydrochloric acid at 80°C for 12 hour. An infrared camera (IR-camera), the 2-dimentional temperature-measuring instrument, has been used to study the heating characteristic of this device. As the experimental results, the GF-PDMS has the excellent heating-cooling properties, high efficiency, uniformity and flexibility. The maximum working of the flexible heater is as high as 290°C. Thus, this GF-PDMS is an attractive heating structure for various thermal applications.

Keywords: graphene, polydimethylsiloxane, flexible, heater, infrared.

[1] ZHAO Y.-H., WU Z.-K., BAI S.-L., 2015. Study on thermal properties of graphene foam/graphene sheets filled polymer composites. *Composite A: Appl. Sci. Manufact.,* 72, 200-206.

A Coupled Resonator Inspired Antenna for Low SAR Wireless Applications

Touhidul (Alam)[1, 3], Mohammad Tariqul (Islam)[1], Mohammad Rashed Iqbal (Faruque)[2]

[1]Department of Electrical, Electronic and Systems Engineering.

[2] Space Science Centre (ANGKASA),

Universiti Kebangsaan Malaysia, 43600, UKM, Bangi, Selangor D. E., Malaysia

[3] Dept. of Computer Science & Engineering,

International Islamic University Chittagong (IIUC), Bangladesh

E Mail : touhid13@siswa.ukm.edu.my

rashed@ukm.edu.my

A coupled resonator based multiband antenna is presented for low specific absorption rate (SAR) wireless applications. The antenna consists of a rectangular resonator with partial ground plane. The proposed antenna reveals multiband characteristics, which can operates at PCS 1900, WCDMA, Bluetooth, WLAN 2400, WiMAX 2.5 and WLAN 5 GHz frequency band applications. The antenna is fabricated on bio-plastic materials with overall electrical dimension of 0.15 λ × 0.08 λ× 0.0096 λ at 1.2 GHz lower frequency band. A metamaterial inspired dual frequency bands antenna has been proposed for mobile applications in [1], which can cover DCS, GSM1800, WCDMA, and Bluetooth frequency bands with dimension of 50×50×1.6 mm^3. Alam *et al.* proposed metamaterial unit cell based antenna for wireless mobile application with the 0.26 λ × 0.26 λ× 0.0084 λ at 1.6 GHz lower frequency band [2]. The perceptible novelties revealed in this proposed antenna are achieving multiband frequency with appreciable reduction of electromagnetic absorption.

Keywords: Antenna, coupling resonator, metamaterial, specific absorption rate, wireless applications

[1] SHARMA, S.K. AND CHAUDHARY, R.K., 2015. Dual band metamaterial inspired antenna for mobile applications. *Microwave and Optical Technology Letters*, 57(6), 1444-1447.

[2] Alam, T., Faruque, M.R.I. and Islam, M.T., 2015. Specific absorption rate reduction of multi-standard mobile antenna with double-negative metamaterial. *Electronics Letters*, 51(13), 970-971.

A graphene-based fiber for detecting multiple kinds of deformations and its use in wearable sensing

As wearable sensors have been increasingly employed in modern life, such as kinesthetic sensing, personal health monitoring, smart prosthetics/robotics, and human-computer interaction, materials scientists and engineers have devoted great enthusiasm and efforts to developing flexible and wearable sensors, especially mechanical sensors for monitoring various human activities. Though considerable progress has been made, there still exist two formidable challenges: one is the combination of high sensitivity to small strain and broad sensing range; the other is the capability of detecting multiple deformation forms with a single device.

Here we devise a graphene-based fiber sensor with “compression spring” structure. The fiber not only achieves ultrahigh sensitivity (detection limit of 0.2% strain) and wide working range (up to 100% strain) in strain sensing, but also exhibits superb performance in the detection of bending and torsion deformation, due to the microstructure variation under different mechanical stimulus. We integrate the fibers into wearable sensors and manage to realize capturing of full-range human activities, from as subtle as speech recognition, pulse recording, and sleep quality evaluation, to vigorous human motions (like walking, jogging and jumping), thus greatly advancing the state of the art in wearable sensing. Interestingly, by virtue of the fiber sensor’s ability to detect multiple deformation forms, we also succeed in tracing intricate movement combinations (like stepping, waist side-bending, and elbow rotation) of a robot in real time, “Gangnam style” dance as an example in our work.

Also noteworthy is that the fabrication strategy of the graphene-based fiber is facile, scalable, and low-cost, which we believe sets the stage for the practical and widespread applications in our daily life.

Reference:

Cheng Y, Wang R, Sun J, et al. **A Stretchable and Highly Sensitive Graphene-Based Fiber for Sensing Tensile Strain, Bending, and Torsion**. *Advanced Materials*, **2015**, 27(45): 7365-7371.

A high thrust screw type piezoelectric ultrasonic motor with three-wavelength exciting mode

Tinghai Cheng[1, 2*], Liang Wang[1], Yingting Wang[1], Hongwei Zhao[2], Haibo Gao[3*]

[1]*School of Mechatronic Engineering, Changchun University of Technology, Changchun, Jilin, 130012, China*

[2] *School of Mechanical Science and Engineering, Jilin University, Changchun, Jilin, 130025, China*

[3]*School of Mechatronic Engineering, Harbin Institute of Technology, Harbin, Heilongjiang, 150080, China*

(*E-mail: chengtinghai@163.com, gaohaibo@hit.edu.cn)

As one type of ultrasonic motors, the screw type piezoelectric ultrasonic motor adopts screw pairs to transfer movement between the stator and screw output shaft，which can be applied in the micro electro mechanical system (MEMS) [1-2]. In the previous researches, the mechanical output was achieved with single wavelength driving and the output thrust is generally several Newton. There has application restricts in large load condition due to the lower output thrust [3-4]. To increase the output thrust, a high thrust screw type piezoelectric ultrasonic motor with three-wavelength exciting mode is presented in this paper.

The structure and exciting mode of the novel motor are shown in Fig.1. The motor consists of a stator and a screw output shaft. The stator contains 12 PZT plates and a hollow metal elastomer with internal thread. These PZT plates are bonded to flat surfaces on the outside of metal elastomer at 30 degree spacing, which constitute exciting group A(A_1 ~ A_6) and exciting group B (B_1 ~ B_6). The standing wave vibrations S_A and S_B with three crests and troughs are generated by exciting signals $U_0 \sin\omega t$ and $U_0 \sin(\omega t+\varphi)$, respectively. When the phase shift between exciting groups A and B is 90^o, a three-wavelength travelling wave can be synthesized by standing wave vibrations S_A and S_B. Thus the screw output shaft is rotated directly to realize the forward output motion. The movement direction can be reversed with a 270^o phase-shift signal.

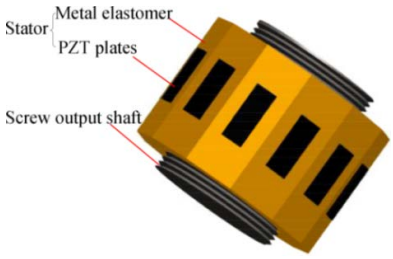

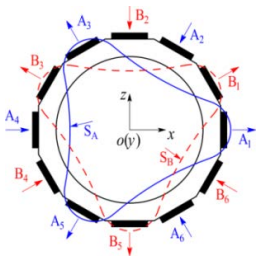

(a) **S**tructure schematic drawings of the motor. (b) Exciting mode of the motor.

FIG.1 Structure and exciting mode of piezoelectric ultrasonic motor.

The prototype was fabricated and its photograph is shown in Fig.2. The testing results of load characteristics are shown in Fig.3, the output velocity of the prototype decreases with the increasing of load. It also can be seen that the maximum output power is 14.56 mW. The force density of the motor is 365.85 N/kg.

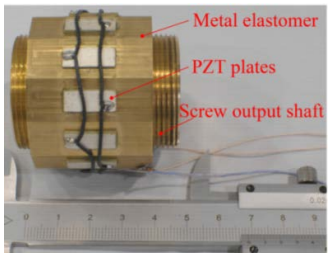

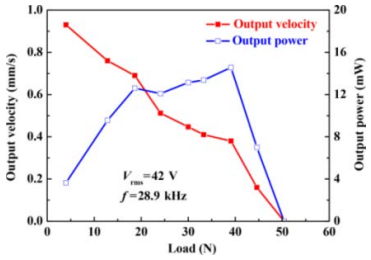

FIG.2 Photograph of prototype motor. FIG.3 Load characteristics of the motor.

Keywords: piezoelectric ultrasonic motor, screw, rotary-linear motion, exciting mode

[1] HENDERSON, D. A., 2006. Simple Ceramic Motor Inspiring Smaller Products. *10th International Conference on New Actuators*, 14-16, June, Bremen, Germany, 1-4.

[2] HO, S. T. & CHIU, W. H., 2016. A Piezoelectric Screw-Driven Motor Operating in Shear Vibration Modes. *Journal of Intelligent Material Systems and Structures*, 27(1) 134–145.

[3] CHU, X. C., WANG, J. W., YUAN, S. M., LI, L. T. & CUI, H. C.,2014. A Screw-Thread-Type Ultrasonic Actuator Based on a Langevin Piezoelectric Vibrator. *Review of Scientific Instruments*, 85(6), 1-4.

[4] NICHOLAS, A. P., TAKEYOSHI, O.,MARCO, A. Z. & CAMERON, N. R., 2012. Synchronization of Epicardial Crawling Robot with Heartbeat and Respiration for Improved Safety and Efficiency of Locomotion. *The International Journal of Medical Robotics*, 8(1), 97-106.

A Study on Characteristics of the Carbon Nano Tube/Epoxy Strain Sensor integrated in the Structure

Dae-Hyun (Han)[1], Lae-Hyong (Kang)[1*]

[1]Department of Mechatronics Engineering, and LANL-CBNU Engineering Institute-Korea, Chonbuk National University, 567 Baekje-daero, Deokjin-gu, Jeonju-si, Jeollabuk-do 54896, Republic of Korea.

Presenting author's e-mail : dh.han@jbnu.ac.kr

Corresponding author's e-mail : reon.kang@jbnu.ac.kr

In this study, a new type of the strain sensor, composed of carbon nano tube (CNT) and epoxy resin, was developed to use at harsh environments by integrating in the structure. The strain sensor embedded in the structure can successfully perform and maintain the sensing function when the sensor is exposed in low and high temperature or under impact condition. Various sensor patterns were engraved in the acrylic cantilever beam by using laser cutting machine in order to find the optimal sensor pattern. Then, the CNT/Epoxy sensors composed of different mixing ratio (CNT:Epoxy) were filled in the engraved pattern to check the effect of mixing ratio on the sensitivity. Finally, the CNT/Epoxy strain sensor integrated cantilever beam was successfully measured the strain according to various loading conditions.

Keywords: Carbon Nano Tube (CNT), epoxy resin, optimization, strain sensor

Acknowledgement

This research was supported by Leading Foreign Research Institute Recruitment Program through the National Research Foundation of Korea funded by the Ministry of Science, ICT and Future Planning. (2011-0030065)

[1] ZHANG, W., SUHR, J., & KORATKAR, N. 2006. Carbon nanotube/polycarbonate composites as multifunctional strain sensors. *J. Nanosci. Nanotechnol*, 6, 4, 960-964.

Dendrimer Antibody Conjugate to Target and Image Cancer Cells

Otis J[1], Zong H[1], Kotylar A[1], Yin A[1], Bhattacharjee S[1], Wang H[2], Baker Jr. J[1], Wang S[1]

[1]Michigan Nanotechnology Institute for Medicine and Biological Sciences, Department of Internal Medicine, Division of Allergy, University of Michigan, 4031A BSRB, Ann Arbor, Michigan 48109, USA.

[2]Department of Radiology, Shanghai General Hospital, Shanghai Jiao Tong University School of Medicine, P.R.China

Corresponding author's email: shidasui@umich.edu

Although many breast and lung cancers overexpress human epidermal growth factor receptor-2 (HER-2), no methods exist currently for effective and early *in vivo* detection of HER-2-positive cancers. To address this problem, we designed and tested novel nano-imaging agents that contain gold nanoparticles (AuNPs) and gadolinium (Gd), conjugated with the humanized anti-HER-2 antibody (1).

Generation-5 (G5) polyamidoamine (PAMAM) dendrimers were selected as a backbone for the nano-imaging agent due to their unique size, high ratio of surface groups to molecule and bio-functionality (2). G5-PAMAM dendrimers were first chemically modified to encapsulate AuNPs and Gd, and then Herceptin-azide was conjugated to Au-G5-Gd through click chemistry to prepare Au-G5-Gd-Herceptin. Finally, the Au-G5-Gd-Herceptin was tested against a series of cell lines *in vitro.*

Our results demonstrated that the Au-G5-Gd-Herceptin was able to bind exclusively to cells overexpressing HER-2, with subsequent internalization into cells. However, non-targeted AuNP and Gd containing G5 neither bound nor internalized into cells overexpressing HER-2. The specificity of this conjugate for cells over-expressing HER-2 suggests that this approach could provide a basis from which to develop nano-diagnostic agents designed for early detection of HER-2-positive cancers by computerized tomography and magnetic resonance image, or for the development of a nano-therapeutic agent delivering therapeutic treatment specifically to HER2-positive cells.

Keywords: Anti-HER2-antibody, Gold nanoparticles, Imaging agent, Targeting

[1] SHUKLA , R., THOMAS, T. P., PETERS, J. L., DESAI, A. M., KUKOWSKA-LATALLO, J., PATRI, A. K., KOTLYAR, A. & BAKER, J. R. 2006. HER2 Specific

Tumor Targeting with Dendrimer Conjugated Anti-HER2 mAb. *Bioconjugate Chemistry*. 17, 1109-1115.

[2] MULLEN DG, FANG M, DESAI A, BAKER J. R., ORR B. G. & BANASZAK HOLL M. M. 2010. A Quantitative Assessment of Nanoparticle−Ligand Distributions: Implications for Targeted Drug and Imaging Delivery in Dendrimer Conjugates. *ACS Nano*. 4, 657-670.

Deposition of thin composited films of fluoropolymer and metal nanoparticles having surface plasmon resonance

A.I. Safonov[1], V.S. Sulyaeva[2], N.I. Timoshenko[1], S.V. Starinskiy[1]

[1]Kutateladze Institute of Thermophysics SB RAS, Ave. Lavrentyev, 1, Novosibirsk, 630090, Russia.

[2]Nikolaev Institute of Inorganic Chemistry SB RAS, Ave. Lavrentyev, 3, Novosibirsk, 630090, Russia.

safonov@itp.nsc.ru

It has been shown that structure and composition of thin films determine their optical properties [1]. Furthermore, the presence of nanosized elements on the surface often cause effects that changes the optical properties [2]. Recently great interest has been placed on nano-sized elements of noble metals due to their specific response to infrared and visible radiation which excite localized plasmons. This effect is the most noticeable in metal nanostructures [3]. The incorporation of these nanostructures within biosensors [4] for the visualization of cell structures [5], targeted delivery of medicines [6], photothermolysis of cancer cells [7], and higher efficiency of solar elements [8] has triggered the development of new methods to obtain and study structures with plasmonic properties.

The usage of thin nanostructured metal films is hindered due to their quick surface contamination [9]. Oxidation, sulfidation and nanoparticle coalescence in the coatings are likely to cause its properties to change. It is possible to solve these problems by encapsulating metal nanoparticles inside a polymer matrix. Furthermore, the dielectric layer created by the polymer matrix provides the possibility of greater control of the plasmonic effects.

The given investigation presents the results of developing the method to obtain metal nanoparticles in a fluoropolymer (PTFE) matrix and studies the properties of these films. The method consists in deposition of two thin layers: metal (Au, Cu) and fluoropolymer. The first layer from the metal is deposited by vacuum gas-jet method and the second

layer is the thin fluoropolymer film by hot wire CVD (HWCVD). After deposition of some of the resulting composites were annealed at various temperatures. As a result of a thin metal film or nanostructured metal film were obtained nanoparticles encapsulated inside fluoropolymer matrix. The method allows controlling the size and concentration of the metal nanoparticles in fluoropolymer matrix. The composites of metal nanoparticles of different average size and fluoropolymer on the glass, quartz glass and silicon substrates were deposited.

The optical properties of deposited coatings were examined. The samples have the surface plasmon resonance in the various areas of wavelengths. The surface morphology of obtained composite coatings was observed by the method of the scanning electron microscopy (SEM). The calculations of optical properties were carried out by the full Mie theory method. The results of this research are of interests in the production of coatings for solar cells, sensors and other electronic devices.

The reported study was partially supported by RFBR, research project No. 15-38-20411a.

Keywords: thin film, surface plasmon resonance, metal nanoparticles, fluoropolymer, solar cell

[1] WANG, X. F., ZHAO, M., CHEN, K. P., NOLTE, D. D., WANG, X., CHEN, K., ZHAO, M. & NOLTE, D. D. 2010. Refractive index and dielectric constant evolution of ultra-thin gold from clusters to films. *Opt. Express*, 18, 24858-24867.

[2] MESKINIS, S., CIEGIS, A., VASILIAUSKAS, A., TAMULEVICIENE, A., SLAPIKAS, K., JUSKENAS, R., NIAURA, G., TAMULEVICIUS, S. 2014. Plasmonic properties of silver nanoparticles embedded in diamond like carbon films: Influence of structure and composition. *Applied Surface Science*, 317, 1041-1046.

[3] KULADEEP, R., JYOTHI, L., ALEE, K. S., DEEPAK, K. L. N. & RAO, D. N. 2012. Laser-assisted synthesis of Au-Ag alloy nanoparticles with tunable surface plasmon resonance frequency. *Opt. Mater. Express*, 2, 161-172.

[4] STUART, D. A., HACS, A. J., YONZON, C. R., HICKS, E. M. & VAN DUYNE, R. P. 2005. Biological applications of localised surface plasmonic phenomenae. *IEE Proc. Nanobiotechnol,* 152, 13-32.

[5] STEWART, M. E., ANDERTON, C. R., THOMPSON, L. B., GRAY, S. K., ROGERS, J. A. & NUZZO, R. G. 2008. Nanostructured plasmonic sensors. *Chem. Rev.,* 108, 494-521.

[6] ZHOU, W., GAO, X., LIU, D. & CHEN X. 2015. Gold Nanoparticles for In Vitro Diagnostics. *Chem. Rev.*, 115, 10575–10636.

[7] JAIN, P. K., EL-SAYED, I. H. & EL-SAYED, M. A. 2007. Au nanoparticles target cancer. *Nano Today*, 2, 18-29.

[8] MIN, G., ZI, O., BAOHUA J., STOKES, N., XI, C., NARGES, F., LI X., MICHAEL JAMES VENTURA, M. J. & SHI, Z. 2012. Nanoplasmonics: a frontier of photovoltaic solar cells. *Nanophotonics*, 1, 235–248.

[9] MAIER, S. 2007. Plasmonics: Fundamentals and Applications. *Springer*, 224.

Effect of Isothermal Aging on Interfacial Reaction between Sn-2.5Ag-0.8Cu-0.5Sb Lead-Free Solders and Copper Substrate

Saliza Azlina (Osman)[1], Mohamad Subri (Abdul Samad)[1], Rabiatul Adawiyah (Mohamed Anuar)[1], Wan Nur Azrina (Wan Muhammad)[1], Shahrul Azmir (Osman)[1]

Presenting author should be underline

[1]Faculty of Mechanical and Manufacturing Engineering, Universiti Tun Hussein Onn Malaysia, 86400 Batu Pahat, Johor, Malaysia

E Mail/ Contact Détails : salizaz@uthm.edu.my

The electronic packaging industries has shifted to green technology by replacing leaded-solder with lead-free solder in order to fulfill the European Restriction of Hazardous Substance (RoHS) compliance. Among lead-free solders, Sn-Ag-Cu solder alloys family are the most attractive and popular solders to replace lead-base solder because it offers better properties and quite similar properties to lead-base solder [1-4]. Although, the intermetallic compounds coarsening effect during isothermal aging makes their usage are restricted [5]. Consequently, many lead-free solder alloy systems with additional alloying elements such as Ag, In, Cu, Zn, Bi, Ni and Sb have been developed and their microstructures, mechanical properties and wettability have been reported [6]. Numerous researchers have tried to use antimony (Sb) as a minor element in lead-free solder to improve their thermal resistance, mechanical properties and wetting properties of the solder materials. Moreover, Sb also can inhibit IMC growth and refined the grain structure, but it raises slightly the melting point of Sn-Ag solder system [5-9]. Besides that, the addition of 0–10 wt. % Sb was affect the shear strength and fracture behavior of the solder. It also has been reported that the strength of the solder increases as the amount of added Sb increases, then a high amounts of Sb also can decrease the volume fraction of Ag_3Sn in the solder and effectively ease the Ag_3Sn coarsening effect during isothermal storage [10]. Therefore, this study investigates the effect of isothermal aging on interfacial reaction between Sn-2.5Ag-0.8Cu-0.5Sb lead-free solders and copper substrate. The reliability test of the solder joint also will be assessed through lap-shear test. In this study, ball-grid-array (BGA) of Sn-2.5Ag-0.8Cu-0.5Sb (SACSb250805) with size diameter of 500µm was used

during reflow soldering process. Reliability of solder joint has been assessed by performing solid state isothermal aging at 150 ºC with aging duration of 250, 500, 1000 and 2000 hours and also lap-shear test to examine the strength of solder joint using low load tensile test machine. Several characterization techniques will be conducted including image analyzer, optical microscope, field emission scanning electron microscopy and energy dispersive x-ray analysis to characterize the intermetallic formed. The results revealed that after reflow soldering process, the Cu_6Sn_5 intermetallic compound (IMC) is formed at interface meanwhile after exposed in isothermal aging, a new layer of IMC was formed underneath the Cu_6Sn_5 IMC known as Cu_3Sn. Besides that, no antimony (Sb) element has been detected in the intermetallic compounds formed at the interface. The thickness of intermetallic compounds was found to be increase with increasing the aging duration. In addition, aging duration also resulted in an increase in thickness and changed the morphology into more spherical, dense and large grain size. Lap-shear test was discovered the samples was subjected into isothermal aging process at 2000 hours was failed earlier than exposed at 250 hours. Meanwhile, reflowed sample showed stronger solder joint compared to isothermal aging which exposed at 250 hours.

Keywords: Soldering, lead-free solder, intermetallic compound, lap-shear test, aging

1) WEDIANTI SHUALDI, BADARIAH BAIS, IBRAHIM AHMAD, GHAZALI OMAR AND AISHAH ISNIN. 2011. Nanoindentation Characterization of Sn-Ag-Sb/Cu Substrate IMC Layer Subject to Thermal Aging. Proceeding of 2011 IEEE Regional Symposium on Micro and Nanoelectronics (RSM) 28-30 Sept. 2011, 220-223
2) CHEN, B.L. & LI, G.Y. 2004. Influence of Sb on IMC growth in Sn–Ag–Cu–Sb Pb-Free Solder Joints in Reflow Process. Thin Solid Films 462 – 463, 395 – 401
3) WANG, C-H., WEN, C-C., & LIN, C-Y. 2016. Solid-state interfacial reactions of Sn and Sn-Ag-Cu solders with an electroless Co(P) layer deposited on a Cu substrate. Journal of Alloys and Compounds 662, 475-483

4) ZENG, G., GAO, L., XUE, S., DAI, W., ZHANG, L., & LUO, J. 2010. A Review on the Interfacial Intermetallic Compounds between Sn–Ag–Cu Based Solders and Substrates. Journal of Materials Science: Mater Electron 21:421–440
5) LEE, H-T., LEE, F-F., HONG, T-F., & CHEN, H-W. 2008. Effect of In addition on Sn-Ag-Sb lead-free solder system. Proceeding of International Conference on Electronic Materials and Packaging, 2008. 22-24 Oct. 2008, 191 – 194.
6) MAHMUDI, R., & MAHIN-SHIRAZI, S. 2011. Effect of Sb Addition on the Tensile Deformation Behavior of Lead-Free Sn–3.5Ag Solder Alloy. Materials and Design 32, 5027–5032
7) LI, G.Y., CHEN, B.L., SHI, X.Q., STEPHEN C.K., & WONG, Z.F. Wang. 2006. Effects Of Sb Addition On Tensile Strength of Sn–3.5Ag–0.7Cu Solder Alloy And Joint. Thin Solid Films 504, 421 – 425
8) CHEN, B.L., & LI G.Y. 2004. Influence of Sb on IMC growth in Sn–Ag–Cu–Sb Pb-Free Solder Joints in Reflow Process. Thin Solid Films 462 – 463, 395 – 401
9) MA, X., WANG, F., QIAN, Y., & YOSHIDA F., "Development of Cu–Sn Intermetallic Compound at Pb-free solder/Cu joint Interface," Materials Letters, vol. 57, 3361-3365.
10) LEE, HT. HU, S.Y., HONG, T.F., & CHEN, Y.F. 2008. The Shear Strength and Fracture Behavior of Sn–Ag–xSb solder joints with Au/Ni–P/Cu UBM. J Electron Mater 37:867–73

Effects of Temperature and Electric Field on Upconversion Luminescence in Er^{3+} /Yb^{3+} co-Doped PSZT Ceramics

Qiu Sun[1], Zhikai Liu[1], Xiangqun Chen[2*], Teizhu Xin[2]

[1] School of Chemical Engineering and Technology, Harbin Institute of Technology, Harbin 150001, PR China

[2] Department of Materials Physics and Chemistry, School of Materials Science and Engineering, Harbin Institute of Technology, Harbin 150001, PR China

Presenting author chenxq@hit.edu.cn

corresponging author chenxq@hit.edu.cn

Er^{3+} /Yb^{3+} co-doped $Pb_{0.8}Sr_{0.2}(Zr_{0.6}Ti_{0.4})O_3$ (PSZT) ceramics were prepared by solid state sintering route at the 1230 ^oC for 2 h in oxygen atmosphere. Er^{3+} /Yb^{3+} co-doped PSZT ceramics were characterized by X-ray diffraction patterns (XRD) and scan electron microscopy (SEM) images. Er^{3+} /Yb^{3+} co-doped PSZT ceramics emit green light and red light, which correspond to $^2H_{11/2}$, $^4S_{3/2}$ and $^4F_{9/2}$ to $^4I_{15/2}$ transitions of Er^{3+} ions, respectively. Effect of Yb^{3+} content on the upconversion luminescence intensity of Er^{3+} /Yb^{3+} co-doped PSZT ceramics was investigated systematically. 1% Er^{3+}/5% Yb^{3+} PSZT (1E5Y-PSZT) ceramics showed the highest upconversion luminescence intensity at the room temperature. In the temperature range of 323-453 K, the maximum sensitivities of about $0.0047K^{-1}$ and $0.0011K^{-1}$ for 1E5Y-PSZT ceramics were obtained by using green and red emission, respectively. Both the dielectric and ferroelectric properties of 1E5Y-PSZT ceramics were observed. The remnant polarization of 1E5Y-PSZT ceramics was 5.01 $\mu C/cm^2$. The upconversion luminescence intensity of 1E5Y-PSZT ceramics also was influenced by the external electric field, which decreased above the coercive field of 5.89 kv/cm. The higher temperature revolution

and fluorescence efficiency of Er^{3+} /Yb^{3+} co-doped PSZT ceramic indicated that it is promising for applications in optical temperature sensors.

Keywords: PSZT ceramics, thermal sensitivity, dielectric properties, ferroelectric properties

[1] DU, P., LUO, L., LI, W., & YUE, Q. 2014. Upconversion Emission in Er-doped and Er/Yb-codoped Ferroelectric $Na_{0.5}Bi_{0.5}TiO_3$ and Its Temperature Sensing Application. *J. Appl. Phys.* 116, 14102-112904.
[2] GAO, F., ZHANG, Q., DING, G., QIN, N., & BAO, D. 2011. Strong Upconversion Photoluminescence and Large Ferroelectric Polarization in Er^{3+}–Yb^{3+}–W^{6+} Triply Substituted Bismuth Titanate Thin Films Prepared by Chemical Solution Deposition. *J. Am. Ceram. Soc.* 94, 3867-3870.
[3] HAO, J.,VZHANG, Y. & WEI, X. 2011. Electric-Induced Enhancement and Modulation of Upconversion Photoluminescence in Epitaxial $BaTiO_3$:Yb/Er Thin Films. *Angew. Chem. Int. Ed.* 50, 6876-6880.
[4] SAVCHUK, O. A., CARVAJAL, J. J., PUJOL, M. C., BARRERA, E. W., MASSONS, J., AGUILO, M., & DIAZ, F. 2015. Ho, Yb: $KLu(WO_4)_2$ Nanoparticles: A Versatile Material for Multiple Thermal Sensing Purposes by Luminescent Thermometry. *J. Phys. Chem. C*. 119, 18546−18558.

Experimental Study of Polyethylene Pyrolysis and Combustion over HZSM-5, HUSY, and MCM-41

Que (Huang)[1], Changcheng (Liu)[1], Ruichao (Wei)[1], Jian (Wang)[1]

[1]State Key Laboratory of Fire Science, University of Science and Technology of China, Hefei, China.

*E Mail/ Contact Détails (***huangque@mail.ustc.edu.cn; wangj@ustc.edu.cn)**

The effects of temperatures, catalysts, and catalyst contents on polyethylene (PE) pyrolysis were investigated by using single-photon ionization time-of-flight mass spectrometry (SPI-TOFMS). The mass spectra of pyrolyzed PE and PE/catalysts from 300 °C to 800 °C illustrate that the pyrolysis reactions were apparently promoted and varied by introducing HZSM-5, HUSY, and MCM-41. The pyrolysis products of PE were grouped into alkenes, dienes, and aromatics mainly including benzene, toluene and xylene (BTX). As microporous catalysts, HZSM-5 and HUSY were found to accelerate the BTX formation at 400 °C, which could not be observed for pure PE until 800 °C. With the existence of MCM-41, only alkenes were produced below 600 °C, indicating the selectivity of mesoporous catalyst. Moreover, the time-evolved profiles of each species could be obtained by virtue of the online detection capability of SPI-TOFMS. We found that pyrolysis processes could to be accelerated by adding catalysts, and different degradation mechanism could be proposed according to the time-dependent profiles of major pyrolysis products of PE and PE/catalysts. Principal components analysis (PCA) was finally employed to identify the main factors with influence on the products distribution. Analytical results showed that the yield of the majority of products could be affected by different experimental conditions, that the type of catalysts makes the most significant influence. Furthermore, as the pyrolysis and combustion products are relevant to the fire risk, the impact of different types of catalysts on fire hazard of PE was studied by using the cone calorimeter. The results indicated that the time to ignition (TTI) and the peak heat release rate (pHRR) were changed remarkably. It is worth noting that with the addition of MCM-41, the pHRR is the minimum.

Keywords: Photoionization mass spectrometry; polyethylene; catalyst; cone calorimeter; heat release rate

Gelled Ethanolamine as a Propellant and Its Rheology

Jyoti (B.V.S)[1], Seung Wook (Baek)[1]

[1]Division of Aerospace Engineering, School of Mechanical, Aerospace and Systems Engineering

Korea Advanced Instituted of Science and Technology (KAIST)

291 Daehak-ro, Yuseong-Gu, Daejeon 34141, Republic of KOREA.

*E Mail : jyotiv@kaist.ac.kr, swbaek@kaist.ac.kr (***Presenting, corresponding author's)**

ABSTRACT: The augmentation and modification for better performance, safety and to accommodate the growing mission requirements the advanced propellants would be essential. At the same time in modern propulsion system eco-friendly propellant technology has become a potential replacement for conventional solid and liquid propellants where environmental friendly, safety, energy management, high performance and efficient propellant packing are the main concerns. In present study efforts are made to convert ethanolamine base fuel which is consider as less toxic and eco-friendly in comparison to other conventional liquid fuels for rocket propulsion application into a gel phase and performed few rheology studies. In order to design gel propulsion rocket engine; gel formulation and propellant rheological property studies are essential. The gelling agent selected and used for gelation was agarose and hybrid pairs of agarose+PVP, agarose+SiO_2, PVP+SiO_2 after a several sets of gelation experiments. Hybrid pairs were used inorder to produce a substantial yield stress and viscoelasticity in the ethanolamine gel propellant. Rheology flow study was performed under the shear rate range of 1-1000 s^{-1}. The result shows that the formulated ethanolamine gel is shear-thinning and thixotropic fluids at operating temperature (room temperature) and a moderate effect of gellant and hybrid pair can be observed on thixotropic behavior of the gel system. Different models (Direct method, Powerlaw and Herschel-Bulkley Model) were used for better understanding of gel rheology in terms of thixotropy and yield stress. The reason thixotropy studies are important because it help us to understand the phenomenon like viscoelastic nature of gel to some extent through gel micro structural network such as; network structural breakdown and rebuilding in response to the shear rate which is very essential for designing a propulsion injection system. Further detail

understanding can be obtained through dynamic sweep study. At the same time yield stress study gives a detail understanding about the gel stability hence safe storage, handling and transportation of the propellant and also for investigating the initiating flow in a material, such as in pumping. Most of the propellants used in current liquid propulsion system is not only toxic but also carcinogenic and non-ecofriendly hence requires special storage systems and care in their handling and transportation. Additional disadvantages related to liquid propulsion system are leakage, sedimentation of energetic metal particles, throttling and sloshing related problems which can be overcome by gel propellant based propulsion system.

Keywords: Propellant, Ethanolamine, Gel, Rheology, Thixotropy

Acknowledgements

This work was supported by a National Research Foundation of Korea (NRF) grant funded by the Korea government (MEST) (No. 2014R1A2A2A01007347). Dr. Jyoti was also supported by the Korean Research Fellowship Program funded by the Ministry of Science, ICT and Future Planning through the National Research Foundation of Korea (No. 2015H1D3A1061637).

References

[1] GUPTA, B.L., VARMA, M. & MUNJAL, N.L. 1986. Rheological studies on virgin and metalized unsymmetrical dimethyl hydrazine gelled systems. *Propellants, Explosives, Pyrotechnics* 1986, 11, 45–52.

[2] MUNJAL, N.L., GUPTA, B.L. & VARMA, M. 1985. Preparative and mechanistic studies on unsymmetrical dimethyl hydrazine - red fuming nitric acid liquid propellant gels. *Propellants, Explosives, Pyrotechnics*, 10 , 111–7.

[3] NATAN, B. & RAHIMI, S. 2002. The status of gel propellants in year 2000. *International Journal of Energetic Materials and Chemical Propulsion*, 5 , 172-94.

[4] RAHIMI, S., PETERZ, A. & NATAN, B. 2007. On shear rheology of gel propellants. *Propellants, Explosives, Pyrotechnics*, 32, 165-174.

[5] TEIPEL, U. & FORTER-BARTH, U. 2007. Rheological behavior of nitromethane gelled with nanoparticles. *J. Propul. Power* , 21, 40-3.

[6] VARMA, M., GUPTA, B.L. & PANDEY, M. 1996. Formulation & storage studies on hydrazine based gelled propellants. *Defence Science Journal*, 46, 435–42.

[7] BEAK, G. & KIM, C. 2011. Rheological properties of carbopol containing nanoparticles. *Journal of Rheology*, 55 , 313-30.

[8] SANTOS, P.H.S., ARNOLD, R., ANDERSON, W.E., CARIGNANO, M.A. & CAMPANELLA, O.H. 2010. Characterization of JP-8/SiO2 and RP-1/SiO2 gels, *Engineering Letters*, 18, 41-7.

[9] BOTCHU JYOTI, V.S. & SEUNG WOOK BAEK. 2014. Rheological characterization of metalized and non-metalized ethanol gel propellants, *Propellant, Explosives and Pyrotechnics*, 39, 866-873.

[10] BOTCHU JYOTI, V.S. & SEUNG WOOK BAEK. 2015. Formulation and comparative study of rheological properties of loaded and unloaded ethanol-based gel propellants, *Journal of Energetic Materials*, 33, 125-139.

[11] BOTCHU JYOTI, V.S. & SEUNG WOOK BAEK. 2016. Rheological characterization of ethanolamine gel propellant, *Journal of Energetic Material*, 34, 260-278.

InGaAs/GaAs/Graphene microtubes fabricated by rolled-up nanotechnology on GaAs (100) Substrate

Guoming Mao, Qi Wang*, Qing Mi, Bingfei Liu, Hao Liu and Xiaomin Ren

State Key Laboratory of Information Photonics and Optical Communications, Beijing University of Posts and Telecommunications, Beijing 100876, China

E Mail : wangqi@bupt.edu.cn; heroamao@bupt.edu.cn

Graphene has been continuously becoming an attractive 2D material due to its special and unusual properties. Meanwhile, III-V semiconductor microtubes fabricated by rolled-up nanotechnology have aroused great attention and tremendous research interest. Obviously, the combination of graphene and III-V semiconductor self-rolled-up microtubes will bring new physics phenomenon and potential applications in microfluidics, biology, electronics, optoelectronics and integrated optics. In this study, we successfully fabricated InGaAs/GaAs/Graphene self-rolled-up microtubes on GaAs (100) substrate. As-fabricated microtubes were characterized by scanning electron microscope (SEM) and micro-Raman. It shows that the graphene tightly adheres to the inner wall and the microtubes are high-quality, uniform, smooth and crackles.

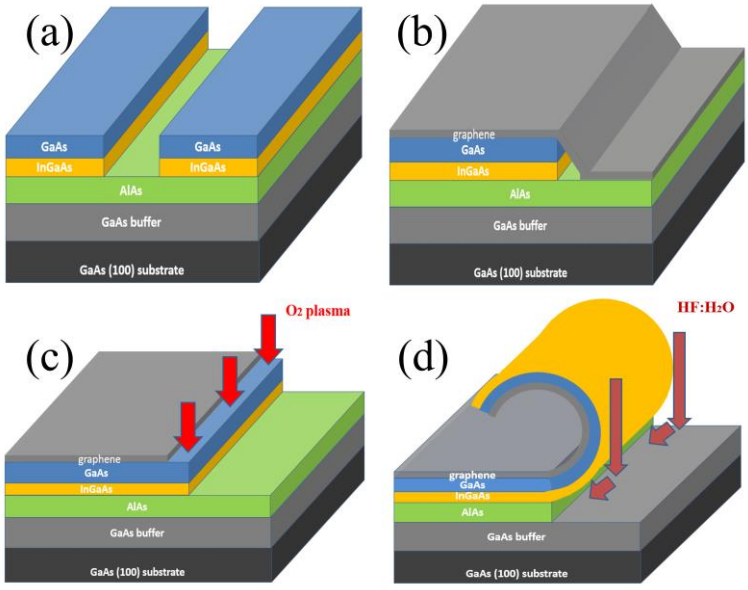

Fig. 1. Process flows for InGaAs/GaAs/Graphene microtubes: (a) Wet etching into AlAs forms the rectangular mesas. (b) Transferring CVD-grown single-layer or double-

layer graphene with size of 1cm×1cm onto the top of the wafer. (c) Dry etching of graphene by oxygen (O_2) plasma exposes one edge of the mesa. (d) Wet etching of AlAs sacrificial layer releases the layer stacks rolling into microtubes.

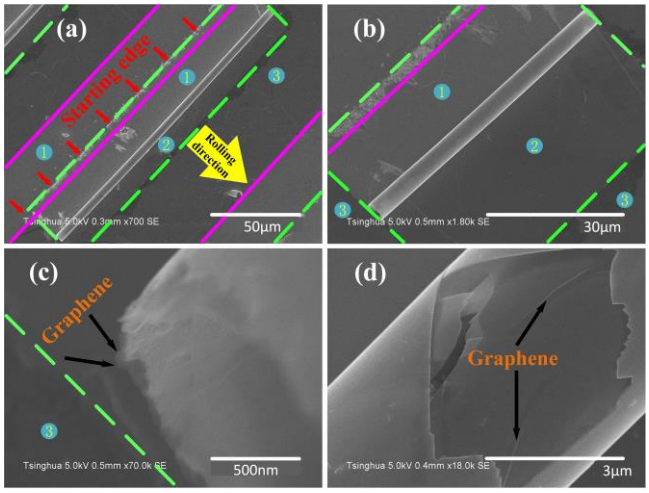

Fig. 2. (a-b) SEM images of single InGaAs/GaAs/Graphene microtubes with length of 180μm and 50μm. (c) Magnified SEM image of the opening of microtube of 50μm in length. (d) Magnified image of the broken middle part of a single microtube. Graphene tightly adhering to the inner wall of microtube was exposed. The green dash lines show the border of rectangular mesas, the purple solid lines show the borders of the stripes formed after the secondary photolithography. Regions labeled 1-3 in (a-c) represent GaAs, graphene on InGaAs/GaAs bilayer and graphene on AlAs, respectively.

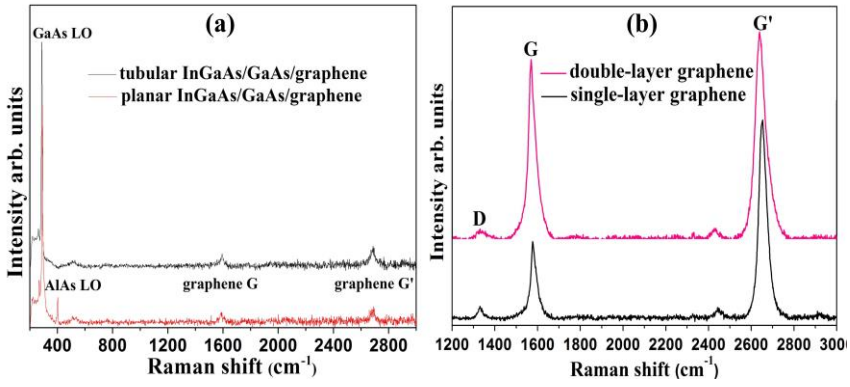

Fig. 3. (a) Raman spectra of planar and tubular InGaAs/GaAs/Graphene heterojunctions. (b) Raman spectra of single-layer or double-layer graphene in microtube.

Ion Exchange Membrane based on Engineering Plastics with Low Cost and High Selectivity for Vanadium Redox Flow Battery

Sung-Hee Roh[1], Gun-Oh Moon[2], Ho-Young Jung[2,*]

[1]College of General Education, Chosun University,
309 Pilmoon-daero, Dong-gu, Gwangju, 61452, Republic of Korea
[2]Department of Environment & Energy Engineering, Chonnam National University,
77 Yongbong-ro, Buk-gu, Gwangju, 61186, Republic of Korea

Vanadium redox flow battery (VRFB) is now expected to successfully combine with the renewable energy sources, such as wind power, and solar cells, in order to store the large-capacity electric power. Here, the developments of key components, such as membrane, electrode, and bipolar plate are very critical for the commercialization of VRFB systems. Specifically, Nafion membrane has been conventionally used for the ionic exchange membrane of VRFB. However, it has high production cost and high vanadium permeation during the operation of VRFB system. To address these issues for the long-term operation of VRFB, new candidate for the polymer electrolyte membrane in VRFB is introduced in this study. Specifically, sulfonated poly(phenylene oxide) (sPPO) are prepared for vanadium redox flow batteries (VRFBs). The key idea of this work is to combine high proton conducting property and low vanadium permeability of sPPO. The membranes are characterized by water uptake, dimensional change, proton conductivity, vanadium ion permeability, and cross-sectional morphology. Proton conductivity of sPPO membrane significantly increased with the increase of ion exchange capacity, while vanadium permeability changed only a little, resulting in higher proton selectivity against vanadium ion transport. The VRFBs employing the sPPO membranes exhibit significant improvements in discharge capacity and energy efficiency (EE) in comparison with those based on the Nafion 211 membrane. Therefore, the sPPO membrane can be useful for VRFB applications and evaluated the feasibility of commercial production using a pilot casting machine in the lab.

Acknowledgement

This work was supported by the Energy Efficiency & Resources Core Technology Program of the Korea Institute of Energy Technology Evaluation and Planning (KETEP), granted financial resource from the Ministry of Trade, Industry & Energy, Republic of Korea. (No. 20153030031670)

Microstructure and Strain Distribution of Stepwise and Graded $Si_{1-x}Ge_x$ Epitaxy

Sangmo Koo[1], Sun-Wook Kim[2], Hyunchul Jang[1] and Dae-Hong Ko[1]

[1]Department of Materials Science and Engineering, Yonsei University, Seoul, Korea

[2]Samsung Electron. Co., Ltd., Hwasung, Korea

dhko@yonsei.ac.kr

Strain engineering is an effective way to enhance p-channel field-effect transistor (pFET) drive current. Epitaxial $Si_{1-x}Ge_x$ embedded source/drain (S/D) with larger Ge concentration generates higher compressive stress in the channel region [1]. However, defect generation such as dislocations or stacking faults resulting from the strain relaxation limits the Ge concentration to a certain value. In addition to crystal structure of epitaxy, the importance of strain measurement and analysis becoming more important since strain engineering is being applied to MOSFETs. Recent studies have reported on strain evolution in $Si_{1-x}C_x$ upon dry oxidation by Nano Beam Diffraction (NBD) method [2]. In this study, epitaxial $Si_{1-x}Ge_x$ layers were selectively grown by using ultrahigh vacuum chemical vapor deposition (UHV-CVD) on the bare and patterned Si wafers. The SEG of $Si_{1-x}Ge_x$ by UHV-CVD shows a characteristic trend during growth. During the UHV-CVD SEG process, the growth of the $Si_{1-x}Ge_x$ layer from the (110) side wall is minimal. In applying a unique characteristic of UHV-CVD, $Si_{1-x}Ge_x$ layers were grown in a stepwise manner. Crystallinity and strain distribution were examined for each step of the $Si_{1-x}Ge_x$ layering process in an attempt to determine how epitaxial $Si_{1-x}Ge_x$ films are grown and how they affect Si channels in terms of strain. Based on this study of stepwise growth, we applied graded $Si_{1-x}Ge_x$ with the objective of modulating strain engineering.

Keywords: selective epitaxial growth, stepwise growth, $Si_{1-x}Ge_x$, graded $Si_{1-x}Ge_x$

[1] Kim, S. W., Byeon, D. S., Jang, H., Koo, S. M., Lee, H. J., & Ko, D. H. 2014. Strain characterization of fin-shaped field effect transistors with SiGe stressors using nanobeam electron diffraction. *Applied Physics Letters*, *105*(8), 083104.

[2] Kim, S. W., Yoo, J. H., Koo, S. M., Lee, H. J., & Ko, D. H. 2013. Strain behavior of epitaxial Si 1− x C x films on silicon substrates during dry oxidation. *Thin Solid Films*, *546*, 226-230.

Optimum Design, Analysis and Manufacturing of Blade - Body for Unmanned Aerial Vehicles with 3D Printer (FDM)

Yuksel Korkmaz[1,2,C], Direncan Boyraz[1], Cemil Yigit[1], Osman Iyibilgin[1,2], Fehim Findik[2,3]

[1] Sakarya University, Eng. Faculty, Mechanical Eng. Dept. Sakarya/Turkey

[2] Sakarya University, BIMAS-RC, Sakarya/Turkey

[3] Sakarya University, Technology Faculty, Metallurgy & Materials Eng. Dept. Sakarya/Turkey

[C] Corresponding Author: Tel: **+90 5322621453**, e-mail: **ykorkmaz@sakarya.edu.tr**

Abstract

Unmanned aerial vehicles (UAV) have begun to be used in almost every field in the recent years. Especially increased payload capacity widens the area of usage of these vehicles. In this study, the design and the optimization for a high performance aerodynamic blade and body will be performed to increase the payload capacity for low speed multi rotor unmanned aerial vehicles.

Three different blade profiles will be analyzed for different angles of attack at low Reynolds numbers using FLUENT. Optimal blade profile and angle of attack will be determined from the graphs of lift coefficient, drag coefficient and angle of attack (C_L-α, C_L/C_D- α). The solid model of the blade and body will be created with SOLIDWORKS based on the data obtained from the graphs. These models will be manufactured using the 3D (FDM) printer. Optimum blade-body design will be determined based on the data obtained from the tests that will be conducted on the model. Unlike other current studies, this project aims to design a high performance blade structure and body structure suitable to the blade. In this way, the most suitable blade geometry and body design will be determined for the work to be done. At the end of this study, an optimum blade and body will be designed and the prototype will be manufactured based on the data obtained from the results of the analyses. Optimum blade and body geometry will be selected after comparing the data obtained from the analysis and the experimental studies conducted on the prototype. The changes to be made on the body will be in the limited range but they depend on the blade geometry.

The evaluation of the data obtained from the analysis and the experimental studies will be used for the development and modeling of a complex structure.

Keywords: Unmanned aerial vehicle, blade design, Finite Element Analysis, Optimization, Efficiency.

Phtoactive materials. Advances in third generation.

D. Bahnemann [1,2], A.A. Murashkina [1], A.V. Rudakova[1], A.V. Emeline[1]

[1]Laboratory "Photoactive Nanocomposite Materials", Saint-Petersburg State University, Saint-Petersburg, Russia.

[2] Institut fuer Technische Chemie, Gottfried Wilhelm Leibniz Universitat Hannover, Hannover, Germany.

E Mail: alexei.emeline@spbu.ru

To overcome three major challenges existing for photoactive materials: higher activity, higher sensitivity to the visible light, and higher selectivity in heterogeneous photoreactions, a new concept of the third generation of photoactive materials has been proposed recently [1]. The concept is based on the nanoconstruction of heterostructured materials as a combination of materials with different properties that results in improvement of the functional characteristics of the nanocomposite materials and enhancement of required reaction pathways comparing to the side processes. In this presentation a review of the concept and recent advances in the studies related to the third generation of photoactive materials performed in the Laboratory "Photoactive Nanocomposite Materials" of SPbSU and elsewhere in the world is given. The major attention focuses on the heterostructured materials realizing Z-scheme of two-photon excitation and charge separation, enhancement of the surface activity due to the effect of the surface localized plasmon resonance, and application of up-conversion materials to achieve higher spectral sensitivity of hybrid photoactive materials.

Keywords: photoactive materials, photocatalysis, solar energy conversion, heterostructures, surface localized plasmon resonance

[1] N. SERPONE, A.V. EMELINE, Semiconductor Photocatalysis — Past, Present, and Future Outlook. *J. Phys. Chem. Lett.*, 2012, 3 (5), 673–677.

Study of wettability transition of laser textured stainless steel surface with low temperature annealing

Chi-Vinh (Ngo)[1], Kyong-Min (Lee) [1] and Doo-Man (Chun)[1]

[1]School of Mechanical Engineering, University of Ulsan, Ulsan, Korea

E Mail: *ngochivinh@gmail.com*

dmchun@ulsan.ac.kr

Superhydrophobic metallic surfaces have evoked great interest in researchers for their important applications in anti-icing, anti-corrosion, liquid transportation, and other fields[1, 2]. To create a superhydrophobic surface on stainless steel, laser texture and a relatively long time exposure of several weeks under ambient air have been used[3]. To accelerate the process time for wettability change from hydrophilicity to superhydrophobicity, a simple post process after laser texture was proposed. In this research, grid patterns was firstly fabricated on stainless steel by a nanosecond laser, then additional low temperature annealing was used. Study on effect of step size of grid pattern to process time was also investigated. This post process demonstrated that the process time was reduced from several weeks to within several days.

Keywords: superhydrophobic metallic surface, nanosecond laser ablation, surface modification, low temperature annealing, grid pattern.

[1] LIU, K. & JIANG, L. 2011. Metallic surfaces with special wettability. *Nanoscale,* 3**,** 825-838.

[2] SIMPSON, J. T., HUNTER, S. R. & AYTUG, T. 2015. Superhydrophobic materials and coatings: a review. *Reports on Progress in Physics,* 78**,** 086501.

[3] KENAR, H., AKMAN, E., KACAR, E., DEMIR, A., PARK, H., ABDUL-KHALIQ, H., AKTAS, C. & KARAOZ, E. 2013. Femtosecond laser treatment of 316L improves its surface nanoroughness and carbon content and promotes osseointegration: An in vitro evaluation. *Colloids and Surfaces B: Biointerfaces,* 108**,** 305-312.

Thin film of photo resist assisted 3D photo chemical machining

Photo chemical machining (PCM) is usually associated with production of 2D components from thin sheet metal. Until now few attempts has been made to produce 3D components using Photo chemical machining. Present work is an attempt to develop novel 3D photochemical machining process by different chemical reaction rate on thin film photo resist using color photo tool. The examination of UV Light as depth of penetration in thin film of photo resist was carried out by using different colored photo tool. The response of thin film photoresist to different color photo tool has been resulted as different depths of etching for Inconel 718 substrate. The experimental results shows maximum depth of etching observed at the area exposed under violet color photo tool and minimum depth of etching observed at area exposed under red color photo tool.

Keywords: Thin film, photo resist, colored Photo tool, Photochemical Machining, Inconel, 718, ultraviolet light.

A Study on Basic Characteristics of ML/CPW Composite Open stub Employing SiO_2 Thin-Film on RFIC

Hyun-Soo Oh, Soo-Jeong Kim, Young Yun

d)Dep. Of Radio Communication Engineering, Korea Maritime and Ocean University
727, Taejong-ro, Busan, 606-791 Korea

ohs8415@kmou.ac.kr

In this paper, basic RF characteristics of ML / CPW (microstrip line / coplanar waveguide) composite open stub employing SiO_2 thin-film were studied for application to miniaturization of RF filter on Si RFIC. The novel transmission line showed wavelength much shorter than conventional transmission line. Concretely, wavelength of transmission line employing SiO_2 thin-film showed 60.5% length reduction of conventional one. In addition, for application to RF filter, Q value of open stub employing TFTL was 7.6, respectively, while the Q value of conventional open stub was 2.5. Using the open stub employing TFTL, a highly miniaturized harmonic rejection filter was fabricated on silicon substrate. The filter exhibited a comparatively good harmonic suppression characteristic at n×16.5 GHz, and its size was 0.1 mm^2, which was only 7% of the conventional filter on silicon substrate.

Keywords:Open stub, Thin-Film Transmission Line (TFTL), RF characteristics, harmonic rejection filter, harmonic suppression characteristic

Acknowledgement

This work was supported by the National Research Foundation of Korea (NRF) grant funded by the Korea government (MSIP) (2014R1A2A1A11049844).

[1] J. H. Jeong, K. J. Son and Y. Yun, "Basic Study on RF Characteristics of Thin-Film Transmission Line Employing ML/CPW Composite Structure on Silicon Substrate and Its Application to a Highly Miniaturized Impedance Transformer", *Transactions on Electrical and Electronic Materials*, Vol. 16, No. 1, pp.10-15, Feb., 2015.

Preparation of the Carbon/Silica composites with the anti-oxidation treatment

Chun Su Kim[1], Sung Chan Lim[2], Jong Sung Won[3], Song Hee Kang[4], Won Gi Jo[5], Hyeon Soo Lim[6], Chi Hong Joo[7] , Seung Goo Lee[1*]

[1]Chungnam National University, Daejeon, South Korea

[2]Nexcoms Co. Ltd., Daejeon, South Korea

seisyu@cnu.ac.kr (preseinting author's) / lsgoo@cnu.ac.kr (corresponding author's)

To develop the high temperature composite materials, carbon fiber preform reinforced silica composites were prepared by using the sol-gel process. It is important to protect the carbon fiber surface from the oxidation during high temperature sintering for the preparation of the carbon/silica composite. In this study, to improve the anti-oxidation property, carbon fiber preform was coated with silicon carbide (SiC). The SiC coating layers were obtained by impregnating the carbon fiber preform in the polycarbosilane (PCS, precursor of SiC) and followed by drying and sintering process. As a precursor of the silica gel, tetraethyl orthosilicate (TEOS) was used. To increase the degree of matrix impregnation of the carbon fiber preform, optimum conditions of the gelation-time and viscosity of silica gel were investigated. Also to increase the silica impregnation in the composites, re-impregnation of the carbon preform in the silica sol. Thermal and morphological properties of the Carbon/Silica composites were investigated by using a thermogravimetric analysis (TGA) and a scanning electron microscope (SEM), respectively. Silica content in the composites gradually increased according to re-impregnation process. It is concluded that SiC coating was effective to improve the anti-oxidation properties of the carbon preform and the Caron/Silica composites

The work presented in this paper was supported by Research Funds of the Dual Use Technology Program from the Civil Military Technology Cooperation Center of the Agency for Defense Development.

.

Keywords: Carbon fiber reinforced composites, Silica matrix, Sol-gel process, TEOS

[1] J. Magnan, R. Pailler, Y. Le Petitcorps, L. Maillé, A. Guette & J. Marthe, E. Philippe, 2013. Fiber-reinforced Ceramic Matrix Composites Processed by a Hybrid Technique based on Chemical Vapor Infiltration, Slurry Impregnation and Spark Plasma Sintering: Journal of the European Ceramic Society, 33(1), 181-190

[2] Jae Jun Lee, Young Woong Kim, Woon-Jo Cho, In Tae Kim, Hae-June Je & Jae-Gwan Park. 1999. Preparation of Silica Films by Sol-gel Process: Journal of the Korean Ceramic Society, 36(9), 893-900

[3] Jérôme Magnant, Laurence Maillé, René Pailler, Jean-Christophe Ichard, Alain Guette, Francis Rebillat & Eric Philippe. 2012. Carbon Fiber/Reaction-bonded Carbide Matrix for Composite Materials-Manufacture and Characterization: Journal of the European Ceramic Society, 32(16), 4497-4505

[4] Dae Hyun Kim, Ki Chang Song, Jae Shik Chung, Bum Suk Lee. 2007. Preparation of Hard Coating Solutions using Colloidal Silica and Glycidoxypropyl Preparation of Hard Coating Solutions using Colloidal Silica and Glycidoxypropyl: Korean Chemical Engineering Research, 45(5), 442-447

[5] S. M. Latifi, M. H. Fathi & M. A. Golozar. 2011. Preparation and Characterisation of Bioactive Hydroxyapatite–Silica Composite Nanopowders via Sol–gel Method for Medical Applications: Advances in Applied Ceramics, 110(1), 8-14

Bone Regeneration In Rat Femur Using Porous and Bioactive Bone Cement: Histological Analysis

M. Puska[1], N. Moritz[1], H. Leminen[2], A.J. Aho[1], P.K. Vallittu[1,2]

[1]Turku Clinical Biomaterial Centre – TCBC, University of Turku, Turku, Finland

[2]Dept of Prosthetic Dentistry and Biomaterials Science, University of Turku, Finland

Contact details: Dr Mervi Puska, Turku Clinical Biomaterial Centre – TCBC, Lemminkäisenk. 2, 20520 Turku, Finland, tel. +358-2-3338388, email: mervi.puska@utu.fi

Objective: Polymethylmethacrylate (PMMA) based bone cements are used as substitutes in trauma surgery [1-3]. Conventional PMMA bone cement does not allow bone ingrowth into the cement layer [4]. Thus, new bone formation is limited to the interface between the bone cement and the bone. The aim was to study the biological behavior of modified (i.e. porous and bioactive) PMMA bone cement [5] in rat *femur*. The bone formation on the outermost surface and porous inner structure of modified bone cement was performed using histological analysis.

Experimental: Animal experiments were performed according to the license (#ESAVI/4379/04.10.03/2012) for animal experimentation allocated by the Labanimal care and use committee. The implants were manufactured either from commercially available PMMA based bone cement (Palacos®R) or from the modified version of Palacos® R containing porosity forming a hybrid co-monomer and bioactive glass (BAG S53P4 (BonAlive®) particulate Ø~315 – 1000 µm fraction) [5]. Six parallel implantations (N=6) of both groups were employed in the midshaft of rat *femur*. The bone defect healing process was evaluated on histological analysis at 8 weeks, postoperatively.

Results, accomplishments and their significance: According the microscopical analysis of of modified bone cement, the significant signs of bone ingrowth were observed. Also, it was observed the formation of reactive layers on bioactive glass granules. The difference in new bone formation inside the implant material between the modified bone cement and

conventional bone cement was obvious. In the case of conventional PMMA, the implant did not contain bone ingrowth. In fact, it was mainly encapsulated by fibrotic connective tissue on the implant surface. After modified bone cement being implanted in rat *femur*, a distinct interconnected porosity containing bone ingrowth was observed. Bioactive glass granules of modified bone cement seems to guide the reparative growth of the natural bone and likely encourages undifferentiated cells to become active osteoblasts.

Advancement over previous work: The results demonstrated performance of bone ingrowth into the modified bone cement that formed a direct contact with bone tissue. This phenomenon was not observed in the case of conventional bone cement.

Acknowledgements: Pobi Concept Ltd. (Turku, Finland) is acknowledeged for financial support of this research. This study was carried out at the Central Animal Laboratory of the University of Turku.

Keywords: Bioactivity, bone graft, composite, polymeric material, porous structure

[1] BOUZA, C., LOPEZ, T., MARGO, A., NAVALPOTRO, L., AMATE J.M. 2006. Efficacy and safety of balloon kyphoplasty in the treatment of vertebral compression fractures: a systematic review. Eur Spine J, 15, 1050–1067.

[2] DIEPPE, P., BASLER, H.D., CHARD, J., CROFT, J., DIXON, J., HURLEY, M., LOHMANDER, S., RASPE, H. 1999. Knee replacement surgery for osteoarthritis: effectiveness, practice variations, indications and possible determinants of utilization. Rheumatology, 38, 73-83.

[3] LEWIS, G. 2008. Alternative acrylic bone cement formulations for cemented arthroplasties: present status, key issues, and future prospects. J Biomed Mater Res B Appl Biomater, 84, 301-319.

[4] PUSKA, M., KOKKARI, A., NÄRHI, T., VALLITTU, P. 2003. Mechanical properties of oligomer-modified acrylic bone cement. Biomaterials, 24, 417-425.

[5] PUSKA, M., MORITZ, N., AHO, A., VALLITTU, P.K. 2015. Morphological and mechanical characterization of composite bone cement containing polymethylmethacrylate matrix functionalized with trimethoxysilyl and bioactive glass. J Mech Behav Biomed Mater, 21, 11-20.

Effect of sandblasting on shear bond strength between glass-infiltrated zirconia core and ultralow-fusing porcelain veneer

Ji-won Kim[1], Eun-Kyung Lim[1], Gye-Jeong Oh[2], Sang-Won Park[1]

[1]Department of Prosthodontics, Dental Science Research Institute,
School of Dentistry, Chonnam National University, Gwangju, Republic of Korea.
[2]RIS Foundation for Advanced Biomaterial, School of Dentistry,
Chonnam National University, Gwangju, Republic of Korea.

Presenting author: *cupid0621@naver.com. Tel: 82-62-530-5840*
Corresponding author: *psw320@chonnam.ac.kr. Tel: 82-62-530-5842*

Objectives: The purpose of this study was to evaluate the influence of sandblasting treatment on the shear bond strength (SBS) between glass-infiltrated zirconia core and ultralow-fusing porcelain veneer.

Materials and methods: Forty-eight zirconia disks (15 x 2.4mm) were divided into four groups: no treated zirconia (group Z); glass-infiltrated zirconia (group ZG); ZirLiner-coated zirconia (group ZZ); glass-infiltrated and sandblasted zirconia (group ZGS). A cylinder of ultralow-fusing veneer porcelain (6x4 mm) was fired on each core. All specimens were subjected to SBS test using a universal testing machine. Scanning electron microscopy (SEM) was used to examine the surface of specimen cores and cross-sectional microstructure of the specimens. Energy dispersive spectroscopy (EDS) was used to evaluate the chemical composition of the core surfaces. The data were statistically analyzed using one-way ANOVA and Turkey's HSD test.

Results: SBS value of group ZGA (3.94±2.4 MPa) was significantly lower than that of other groups. No significant differences were detected among group ZZ (12.54±1.65MPa), group Z (11.84±1.93 MPa), and group ZG (11.44±1.67 MPa).

Conclusion: Sandblasting treatment decreased bonding strength between glass-infiltrated zirconia core and ultra-low fusing porcelain veneer.

Key words: Glass infiltration, Sandblasting, Shear bond strength, Ultralow-fusing porcelain.

Gel Spinning of Functionalized Core-sheath Hybrid Silk Fiber with High Tensile Strength

Pui Fai (NG), B. (FEI)*

Institute of Textiles & Clothing, Hong Kong Polytechnic University, Hong Kong, China.

Presenting author. E-mail : joanne.yu.ng@connect.polyu.hk

**Corresponding author. E-mail : tcfeib@polyu.edu.hk. Tel : +852 27664795*

Silkworm silk has attracted great attention for its superior mechanical properties due to its unique protein chain sequence [1], and is known in textile industry for thousands of years. In the recent decades, regenerated silk fibroin-based materials with desired properties are of considerable interest among the field of polymer science. Regeneration of silk fibroin (SF) fibers have been successfully prepared via wet spinning [2] or electrospinning [3], of which harmful organic solvents are usually involved.

The current study is aimed to identify the feasibility of gel spinning of SF-based opto-functional microfibers in a more eco-friendly way. Regenerated core-sheath microfibers composed of silk fibroin (SF) and opto-functional materials are processed via co-axial gel spinning. Calcium chloride-formic acid ($CaCl_2$-FA) is used for dissolving SF in the sheath phase [4], and aqueous carrageenan solution containing different loadings of opto-functional materials is used as the core phase. Subsequent immersion process of the as-spun fibers is performed in water for 2 days, allowing fiber crystallization and the removal of core carrageenan matrix. The outermost SF sheath can serve as a protective layer for the core materials from the external environment.

Gel spinning technique enables the fabrication of high strength microfiber with a high degree of molecular orientation from liquid crystalline silk fibroin. Also, it is of particular interest for those core materials that are unable to form fibers by themselves.

Investigation will be conducted to analyze in detail the morphologies, structures and the mechanical performances of the as-spun fibers using scanning electron microscopy (SEM),

Fourier-transformed infrared spectroscopy (FTIR), X-ray diffraction (XRD), differential scanning calorimetry (DSC) and universal testing machine (UTM).

Keywords: Carrageenan, core-sheath, gel spinning, microfiber, silk fibroin

[1] BINI. E., KNIGHT, D. P. & KAPLAN, D. L. 2004. Mapping Domain Structures in Silks from Insects and Spiders Related to Protein Assembly. J. Mol. Biol., 335, 27-40.

[2] CHUNG, D. E. & UM, I. C. 2014. Effect of Molecular Weight and Concentration on Crystallinity and Post Drawing of Wet Spun Silk Fibroin Fiber. Fibers Polym., 15, 153-160.

[3] ZHOU, J., CAO, C. & MA, X. 2009. A Novel Three-dimensional Tubular Scaffold Prepared from Silk Fibroin by Electrospinning. Int. J. Biol., Macromol., 45, 504-510.

[4] ZHANG, F., LU, Q., YUE, X., ZUO, B., QIN, M., LI, F., KAPLAN, D. L. & ZHANG, X. 2015. Regeneration of High-quality Silk Fibroin Fiber by Wet Spinning from CaCl2-Formic Acid Solvent. Acta Biomater., 12, 139-145.

Miniaturized RF Devices Employing Periodic Structure on Polyether Sulfone Thin Film Substrate for application to flexible MMIC

Young Yun, Soo-Jeong Kim, Hyun-Soo Oh

d) Dep. Of Radio Communication Engineering, Korea Maritime and Ocean University
727, Taejong-ro, Busan, 606-791 Korea

yunyong@kmou.ac.kr

In this work, the TLEPS (transmission line employing periodic structure) was fabricated on PES (polyether sulfone) substrate, and its RF characteristics were investigated. The TLEPS on PES substrate showed wavelength much shorter than conventional coplanar waveguide on PES. Using the TLEPS, highly miniaturized RF devices were fabricated on PES substrate. Concretely, the size of the impedance transformer employing TLEPS was 0.45 mm^2, which was 57.5 % of the size of the transformer fabricated by conventional coplanar waveguide on PES substrate. The size of the branchline coupler employing TLEPS was 3.94×2.92 mm^2, which was 61.3 % of the size of the conventional one on PES substrate. The size of the Wilkinson power divider employing TLEPS was 3.53×2.38 mm^2, which was 59.2 % of the size of the conventional one on PES substrate. According to measured results, excellent RF performances were observed from the RF devices employing TLEPS on PES substrate.

Keywords: RF devices, periodic structure, polyether sulfone, flexible, MMIC

Acknowledgement

This work was supported by the National Research Foundation of Korea (NRF) grant funded by the Korea government (MSIP) (2014R1A2A1A11049844)

[1] Young Yun, Jang-Hyeon Jeong, Hong-Seung Kim, and Nak-Won Jang "Basic RF Characteristics of Fishbone-type Transmission Line Employing Comb-type Ground Plane (FTLCGP) on PES substrate for Application to Flexible Passive Circuit", ETRI Journal, vol. 37, No.1, pp.128-137, February, 2015

Photoluminescence of Mn^{4+} Activated Monoclinic Na_3AlF_6

Thomas Jansen*, David Böhnisch, Florian Baur, and Thomas Jüstel*

Department of Chemical Engineering, Münster University of Applied Sciences, Stegerwaldstrasse 39, 48565 Steinfurt, Germany

*Corresponding authors: t.jansen@fh-muenster.de; tj@fh-muenster.de

Mn^{4+} activated luminescent materials have attracted much attention recently. Especially alkaline metal hexafluorides, such as $K_2SiF_6:Mn^{4+}$ or $K_2TiF_6:Mn^{4+}$, can emit light in the red region under blue or near UV excitation and meet thus the efficiency and color quality of future "warm white" phosphor converted LEDs (pc-LED) [1]. However, Mn^{4+} photoluminescence (PL) in the well-known monoclinic mineral cryolite (Na_3AlF_6) [2] has not been shown in literature so far. According to *Zhu et al.* we applied the cation-exchange method in order to synthesize Mn^{4+} doped Na_3AlF_6 for the first time [3]. $Na_3AlF_6:Mn^{4+}$ exhibits efficient red photoluminescence peaking at 627 nm, which can be assigned to the $^2E_g \rightarrow {}^4A_{2g}$ intraconfigurational transition of Mn4+ ([Ar]3d^3 configuration) within the $[MnF_6]^{2-}$ octahedra on the aluminum site in the cryolite host structure. Photoluminescence properties, such as temperature dependence of the PL intensity and luminescence lifetime are presented in comparison with the well-established phosphor $K_2SiF_6:Mn^{4+}$ (PSF). Additionally, luminous efficacy and colour rendering values of simulated warm white emitting pcLEDs comprising a dichromatic phosphor blend involving $Na_3AlF_6:Mn^{4+}$ are calculated and compared to the performance of those warm white emitting pcLEDs comprising PSF.

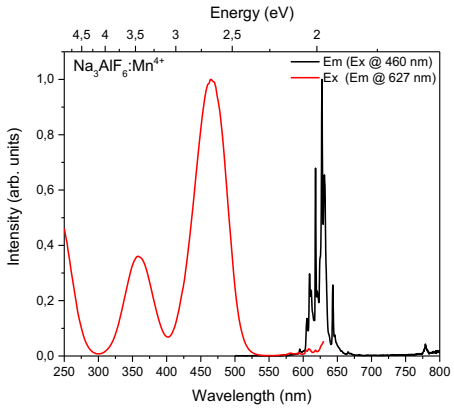

Fig. 1 Photoluminescence excitation (red) and emission (black) spectrum of $Na_3AlF_6:Mn^{4+}$

Keywords: Mn^{4+} phosphor, Fluorides, Cryolite, warm white pcLEDs

References

[1] A.A. Setlur, E.V. Radkov, C.S. Henderson, J.-H. Her, A.M. Srivastava, N. Karkada, M.S. Kishore, N.P. Kumar, D. Aesram, A. Deshpande, B. Kolodin, L.S. Grigorov, U. Happek, Chem. Mater. **22** (2010) 4076.
[2] Q. Zhou, B.J. Kennedy, J. Solid State Chem. **177** (2004) 654.
[3] H. Zhu, C.C. Lin, W. Luo, S. Shu, Z. Liu, Y. Liu, J. Kong, E. Ma, Y. Cao, R.-S. Liu, X. Chen, Nat. Com. **5** (2014) 4312.

Point-Of-Care Applications of Surface-Enhanced Raman Scattering Paper Sensor using Successive Ionic Layer Absorption and Reaction-Synthesized Plasmonic Nanoparticles

W. Kim[1], H.K. Park[1,2], and S. Choi[1,2]

[1]Department of Medical Engineering, Graduate School, Kyung Hee University, Seoul, 02447, Korea.

[2]Department of Biomedical Engineering, College of Medicine, Kyung Hee University, Seoul, 02447, Korea.

E Mail/ wskim731@khu.ac.kr and medchoi@khu.ac.kr

Two different types of surface-enhanced Raman scattering (SERS) paper strips were developed for point-of-care (POC) bio-sensing applications based on plasmonic gold nanoparticles (AuNPs) and silver nanoparticles (AgNPs) directly deposited on paper using the successive ionic layer absorption and reaction (SILAR) approach. SERS is a powerful fingerprinting technique to identify the biochemical composition to provide molecule-specific information. In particular, it has become as a potentially powerful diagnostic tool for investigation of biofluids and their chemical components due to rapid, non-destructive, label-free analysis with traces of biospecimens [1]. Plasmonic nanoparticles have been suggested as an alternative process that provides facile, low-cost fabrication with controllable size and shape through the reaction conditions. In particular, AuNPs and AgNPs provides a superior SERS perfomrance due to the formation of localized surface plasmon resonances (LSPR).

In POC applications, the paper having positive characteristics of lightweight, flexible, economical, harmless, and portable has been become more attractive as a platform for rapid diagnostic test. Most studies to develop the paper-based SERS sensors used the dropping and dipping methods of plasmonic nanoparticles [2,3]. However, these methods require some equipment or complicated and tedious processing times, for synthesizing and depositing the nanoparticles on paper. Also, indirect deposition method using pre-made nanoparticles does not produce a uniform distribution on paper.

Therefore, this study presents a SERS sensor, generated by plasmonic AgNPs and AuNPs deposited directly in paper through the SILAR approach, allowing to control the size of nanoparticle or film via multiple repetitions of the chemical reactions [4]. Additionally, it does not require external equipment for synthesis of the nanoparticles. The potential of this sensor was evaluated through human cervical fluid for clinical diagnosis of human papillomavirus (HPV) infection using AuNPs [5] and three indistinguishible eye diseases in the initial stage [6].

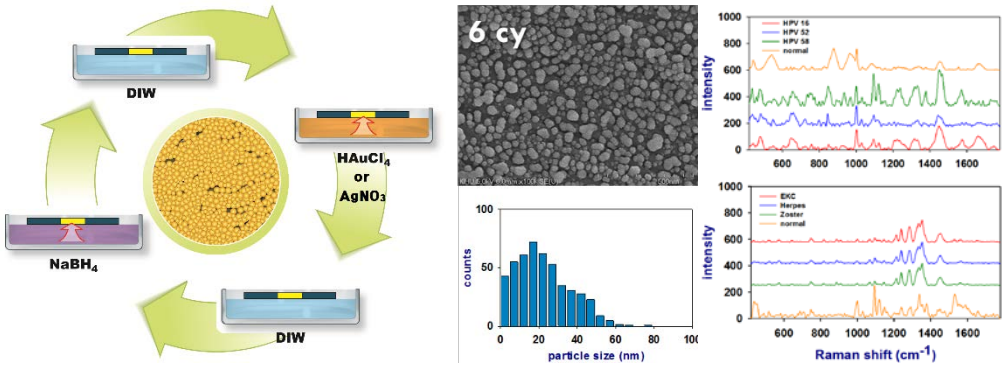

Keywords: SERS, SILAR, plasmonic gold and silver nanoparticles, paper, biofluids

[1] KNEIPP, J., KNEIPP, H., KNEIPP, K., 2008. SERS-a single-molecule and nanoscale tool for bioanalytics. *Chem. Soc. Rev.*, 37, 1052–1060.

[2] NGO, Y.H., LI, D., SIMON, G.P., GARNIER, G., 2012. Gold nanoparticle-paper as a three-dimensional surface enhanced Raman scattering substrate. *Langmuir*, 28, 8782–8790.

[3] BI, L., DONG, J., XIE, W., LU, W., TONG, W., TAO, L., QIAN, W., 2013. Bimetallic gold-silver nanoplate array as a highly active SERS substrate for detection of streptavidin/biotin assemblies. *Anal. Chim. Acta.*, 805, 95–100.

[4] KOROTCENKOV, G., GULINA, L.B., CHO, B., BRINZARI, V., TOLSTOY, V.P., 2014. Synthesis by successive ionic layer deposition (SILD) methodology and

characterization of gold nanoclusters on the surface of tin and indium oxide films. *Pure Appl. Chem.*, 86, 801–817.

[5] KIM, W., KIM, Y.H., PARK, H.K., CHOI, S., 2015. Facile fabrication of a silver nanoparticle-immersed, surface-enhanced Raman scattering-imposed paper platform through successive ionic layer absorption and reaction for on-site bioassays. *ACS Appl. Mater. Interfaces*, 7, 27910–27917.

[6] KIM, W., LEE, J.C., PARK, H.K., SHIN, J.H., CHOI, S., 2016. Label-free optical bio-sensing paper strip for the early detection of keratoconjunctival infections: power-free synthesizable fabrication. Submitted to *Biosens. Bioelectron.*

Preparation and characteristic of high-entropy alloy (AlCrNbSiTiV)N thin film

Ho Chang[1], Shih-Wen Huang[1], Chun-Yao Hsu[2]

[1]Graduate Institute of Manufacturing Technology, National Taipei University of Technology, No. 1, Sec.3, Zhongxiao E. Rd., Taipei 10608, Taiwan

[2]Department of Mechanical Engineering, Lunghwa University of Science and Technology, No.300, Sec.1,Wanshou Rd., Taoyuan City, 33306,Taiwan

f10381@ntut.edu.tw

The study uses vacuum arc melting method to prepare AlCrNbSiTiV, a high-entropy alloy target material having 6 kinds of equal-mole elements. The study further employs DC sputtering deposition to prepare a thin films of high-entropy alloy (AlCrNbSiTiV)N. In addition, Taguchi method with mixed orthogonal arrays of L9 (34) was used to acquare the effects of sputtering deposition parameters on the microstructure and mechanical performance of the prepared (AlCrNbSiTiV)N thin film. Experimental result show that the prepared (AlCrNbSiTiV)N thin films have Nb_5N_3 phase and amorphous structure. In addition, DC power is the most important process parameters for the hardness of the prepared (AlCrNbSiTiV)N thin films. Furthermore, the prepared (AlCrNbSiTiV)N thin film has hardness of surface roughness of 21.30 Gpa, Young's modulus of 235.56Gpa, friction coefficient of 0.4 and wear rate of $6.25x10^{-6}mm^3/mN$ and surface roughness of 2.165nm (Ra) under the the optimization process.

Keywords: DC sputtering deposition, high-entropy alloy, hardness, wear rate, roughness

[1] HSIEH, M. H., TSI, M. H., SHEN, W. J. & YEH, J.W. 2013. Structure and properties of two Al–Cr–Nb–Si–Ti high-entropy nitride coatings.*Surface and Coatings Technology*, 221, 118-123.

Abstract

In the previous research, we have already reported that Cu wires of the resistivity of about eighteen times of pure copper, resistors, the laminated capacitors and circuits on the front and back of the substrate can be formed and implanted in a POM (thermoplastic resin friendly to the global environment) substrate by using a laser assisted powder jet implantation method. This technique is performed without a mask.

In this paper, we report that Cu wires of low resistivity (about three times of the pure copper, about sixth part of the good conductive paste) can be formed and implanted in the POM substrate by this method using mixed powder of copper and a small amount of carbon (reducing agent). The value of this resistivity by this technique is lower than the value by a laser assisted ink jet method. Furthermore, we report that the resistivity of the implanted copper wire can be reduced by vibrating the substrate in this forming process.

Abstract

In the previous research, we have already reported that Cu wires of the resistivity of about eighteen times of pure copper, resistors, the laminated capacitors and circuits on the front and back of the substrate can be formed and implanted in a POM (thermoplastic resin friendly to the global environment) substrate by using a laser assisted powder jet implantation method. This technique is performed without a mask.

In this paper, we report that Cu wires of low resistivity (about three times of the pure copper, about sixth part of the good conductive paste) can be formed and implanted in the POM substrate by this method using mixed powder of copper and a small amount of carbon (reducing agent). The value of this resistivity by this technique is lower than the value by a laser assisted ink jet method. Furthermore, we report that the resistivity of the implanted copper wire can be reduced by vibrating the substrate in this forming process.

Abstract

In the previous research, we have already reported that Cu wires of the resistivity of about eighteen times of pure copper, resistors, the laminated capacitors and circuits on the front and back of the substrate can be formed and implanted in a POM (thermoplastic resin friendly to the global environment) substrate by using a laser assisted powder jet implantation method. This technique is performed without a mask.

In this paper, we report that Cu wires of low resistivity (about three times of the pure copper, about sixth part of the good conductive paste) can be formed and implanted in the POM substrate by this method using mixed powder of copper and a small amount of carbon (reducing agent). The value of this resistivity by this technique is lower than the value by a laser assisted ink jet method. Furthermore, we report that the resistivity of the implanted copper wire can be reduced by vibrating the substrate in this forming process.

Study on performance of ceramizable silicone rubber composite

Jiuqiang Song[1], Yan Qin[1], Liangdian Liu[1], Xinyi Li[1]

[1]Key Laboratory of Special Functional Materials, Wuhan University of Technology, Luoshi road NO.122, Wuhan, China, 430070

E-mail: qinrock@sina.com

Abstract: As a kind of fire retardant material, ceramizable silicone rubber composite has made a wide range of applications in the field, and expected to have a further value. In this paper, ceramizable silicone-based composite was prepared by using VMQ as matrix, Kaolin as additives, low melting point glass powder and Zinc borate as alternative solvent, and high silica glass fiber as reinforcing material. the ceramifying reaction can occur at high temperature and become a self-supporting structure of the ceramic body. TG-DSC test showed that thermal stability was significantly improved as Kaolin added. When the addition of Kaolin was 40wt%, the residual rate was 50.23%, while the pure VMQ was 37.33%. As low melting point glass powder added, the TG-DSC analysis showed that T5 and Tmax of the material were both reduced a lot. The T5 was lowered to 660.15K from 690.15K, and Tmax is reduced in the range of 323.15~343.15K, even dropped from 785.55K to 720.05K. SEM results showed that Kaolin/frits/VMQ start the organic-inorganic transition at 1073.15K, the surface is intact and there is no obvious cracks or voids. Scanning electron microscopy analysis showed within the softening temperature range, there were many continuous molten pellets, which were proved glass powder by EDS, they helped to bond the matrix and additives. Zinc borate was added as an alternative solvent to prepare the ceramizable silicone rubber composites. By TG-DSC analysis, residual increased to 57.63wt% as the addition of ZB was 15wt%, which was higher than Kaolin/frits/VMQ. T5 and Tmax were slightly lower, but don't as obvious as Kaolin/frits/VMQ was. SEM showed the interior part became dense, homogeneous lattice-shaped from about 873.15K, and more obvious at higher temperature, and showed significant change in densification at 1073.15K. There appeared some new molten liquid phase at 1273.15K, and were proved "eutectic" by EDS spectrum

analysis, which could combine silica with Kaolin filler well, act as a “bridging” effect, and that could cured under ignition point, the ceramic structure could formed after the strip cooling, and the maximum strength was obtained at this temperature. In this case, the structure was complete and the surface crack is minimal. High silica glass fiber was added as a reinforcing material, which can effectively improve the thermodynamic property of silicone rubber. When glass powder was added, the residual rate increased from 54.00% to 63.00%, and the other group which added ZB also increased from 57.63% to 65.12%. The flexural strength of two groups were both improved significantly after 873.15K, and the maximum were 1.89MP, 2.01MPa, which increased 1.19MPa, 1.22MPa, compared with fiber enhanced before.

Keywords: ceramifying reaction, methyl vinyl silicone rubber, Kaolin, heat-resistant

[1] Dvornic P R, Lenz R W. High temperature siloxane elastomers[M]. Wepf, 1990.

[2] Silicon-containing polymers: the science and technology of their synthesis and applications[M]. Springer Science & Business Media, 2001.

[3] Ariagno D., Barruel P., Viale A. Heat-vulcanisable organopolysiloxanes, intended for coating of electrical cables[P]. European Patent: EP 0467800,1995-3-1.

[4] Alexander G., Cheng Y. B., Burford R. P., et al. Fire-resistant silicone polymer compositions[P]. U.S. Patent: 7652090, 2010-1-26.

[5] Osman M., Atallah A., Muller, et al. Reinforcement of poly(dimethylsiloxane) networks by mica [J]．Polymer，2001，42(15)：6545-6556

[6] Ariagno D, Barruel P, Viale A. Compositions Organopolysiloxanes Vulcanisables à chaud, Utilisables Notamment Pour Le RevêTement de cables électriques[P]. EPO: EP 0467800B1, 1995-05-01.

[7] Breck D•W. Zeolite molecular Sieves[M]. 1974: 314~315

[8] Zbigniew Pedzich, Dariusz M Bielinsk, Jan Dul. Microstructure of Ceramic Phase for Ceramizable Silicone rubber Based Composites[A]. 4th International Symposium on Advanced Ceramics. Osaka, Japan:2010-11-14

[9] Siska Hamdani, Claire Longuet, José-Marie Lopez-Cuesta, et al. Calcium and a luminium-based fillers as flame-retardant additives in silicone matrices. I. Blend

preparation and thermal properties[J]. Polymer Degradation and Stability, 2010, 95:1911-1919.

[10] Siska Hamdani-Devarennes, Audrey Pommier, Claire Longuet, et al. Calcium and aluminium- based fillers as flame- retardant additives in silicone matrices II. Analyses on composite resid ues from an indus trial-based pyrolysis test[J]. Polymer Degradation and Stability, 2011, 96:1562-1572.

[11] L. G. Hanu, G. P. Simon, J. Mansouri, R. P. Burford, Y. B. Cheng. Development of polymer-ceramic composites for improved fire resistance[J]. Journal of Materials Processing Technology, 2004,153-154:401-407.

[12] J. Mansouri, R. P. Burford, Y. B. Cheng, L. G. Hanu. Formation of strong ceramified ash from silicone-based compositions[J]. Journal of Materials Science, 2005, 40: 5741-5749.

[13] Jaleh Mansouri, Chris A. Wood, Katherine Roberts, Yi-Bing Cheng, Robert P. Burford. Investigation of the caramifying process of modified silicone-silicate compositions[J]. journal of Materials Science. 2007, 42: 6046-6055.

[14] Cao E, Cui X, Wang K, et al. Improving properties of ceramic silicone rubber composites using high vinyl silicone oil[J]. Journal of Applied Polymer Science, 2015. 132(19)

[15] Yu L, Zhou S, Zou H, et al. Thermal stability and ablation properties study of aluminum silicate ceramic fiber and acicular wollastonite filled silicone rubber composite[J]. Journal of Applied Polymer Science, 2014, 131(1)：

[16] Dong Yang, Wei Zhang, Benzheng Jiang, et al. Ceramization and oxidation behaviors of silicone rubber ablative composite under oxyacetylene flame[J]. Ceramics International, 2013,39: 1575-1581.

[17] Xiang Zhang, Rutie Liu, Xiang Xiong, Zhaoke Chen. Mechanical properties and ablarion behavior of ZrB_2-SiC ceramic fabricated by spark plasma sintering[J]. International Journal of Refractory Matals and Hard Materials. 2015, 48: 120-125.

[18] V. S. Minaev,V. Z. Petrova, S. P. Timoshenkov, et al. Glass formation and glass-forming ability of melts in AIIO–B_2O_3binary systems (AIIO = BeO, MgO, CaO, SrO, BaO, ZnO,CdO). Glass Physics and Chemistry. 2004, 30(3): 215~225

[19] Y. C. Lee, W. H. Lee, F. S. Shieu. Microwave dielectric properties and microstructures of $Ba_2Ti_9O_{20}$-based ceramics with $3ZnO–B_2O_3$ addition. Journal of the European Ceramic Society.2005, 25: 3459~3468

[20] J. R. Kim, D. W. Kim, H. S. Jung, et al. Low-temperature sintering and microwave dielectric properties of $Ba_5Nb_4O_{15}$ with ZnB_2O_4 glass. Journal of the European Ceramic Society. 2006, 26:2105~2109

[21] Hamdani S., Longuet C., Perrin D., et al. Flame retardancy of silicone-based materials[J]. Polymer Degradation and Stability, 2009, 94 (4): 465-495.

[22] Alexander G, Cheng Y B, Burford R P, et al. Fire-resistant Silicone Polymer Compositions[P]. US: USP 7652090B2. 2010-01-26

[23] NIES N, HULBERT P. Zinc borate of low hydration and method for preparing same:US, 3649172[P].1972-3-14.

[24] WU Z P, Hu Y C, SHU W Y. Effect of ultrafine zinc borate on the smoke suppression and toxicity reduction of a low-density polyethylene/in tumescent f lame-retardant system [J]. Journal of Applied Polymer Science ,2010, 117(1):443-449.

[25] Camino G, Lomakin S M, Lazzari M. Polydimethylsiloxane thermal degradation Part 1. Kinetic aspects. Polymer, 2001,42(6):2395-3402

[26] F. Laoutid, L. Bonnaud, M. Alexandre, J.-M. Lopez-Cuesta, Ph. Dubois. New prospects in flame retardant polymer materials: From fundamentals to nanocomposites[J]. Materials Science and Engineering. 2009, 100-125.

[27] Mansouri J., Burford R. P., Cheng Y. B. Pyrolysis behaviour of silicone-based ceramifying composites[J]. Materials Science and Engineering: A, 2006, 425(1): 7-14.

Temperature rise for electrodes of Carbon Nanospheres in the charge/discharge process

B.C. Chen[a], C.Y. Ho [b,*] , J. W. Yu[b], M. Y. Wen[c] and V. H. Lin[b]

[a]Department of Chinese medicine, Buddhist Dalin Tzu Chi General Hospital, Chiayi 622, Taiwan

[b]Department of Mechanical Engineering, Hwa-Hsia Institute of Technology, New Taipei City 235, Taiwan

[c]Department of Mechanical Engineering, Cheng Shiu University, Kaohsiung 833, Taiwan

Abstract

Temperature is one of important factors affecting the life time, efficiency and performance for li-ion batteries. Over high temperature possibly leads to expansion, burning, and even explosion of li-ion batteries. Temperature rise is obvious for li-ion battery in the charge/didcharge process. Nanospheres are usually employed as the supercapacitor electrodes due to the high ratio of area to volume. The performance and quality of batteries are influenced by the temperature rise of the electrodes made up of these carbon materials in the charge/discharge process. This paper investigates temperature rise for electrodes of carbon nanospheres in the charge/discharge process. Using the ballistic-diffusive transient heat transfer equation, this study computes the temperature fields in carbon nanospheres and compares its results with the available measured data.

*Corresponding author

The NIR photo-stimulated persistent luminescence and mechanism of $SrAl_2O_4:Eu^{2+}$ and Dy^{3+} phosphors

Haibo Liu, Li Luo* ,Baoyu huang, Chunlong Han,Wei Zhang

School of Physics and Optoelectronic Engineering, Guangdong University of Technology,

Waihuan Xi Road, No.100, Guangzhou 510006, People's Republic of China.

Abstract

Long lasting phosphors are a kind of very important and usable materials. Some long lasting phosphors can be excited by sun light so that they can save solar energy in daytime and release the stored solar energy slowly at night through emitting luminescence. They have been widely used in weak light illumination and safety signage field. Some of the investigation shows that photostimulated persistent Luminescence was observed in some long lasting phosphors. Photostimulated persistent luminescence refers to persistent luminescence under the stimulation of a low energy photon after the excitation with high-energy radiation. Using this kind of phenomenon, optical information storage can be carried on, broadening the application field of long lasting phosphors from weak light illumination and safety signage to optical information and high energy beam survey. In conventional photostimulable storage phosphors, the stored optical information is usually read out as a transient luminescence which vanishes after the excitation stops. Unlike the transient luminescence, photostimulated persistent Luminescence phosphors exhibit a long lasting luminescence, making it possible to replace traditional photostimulable storage phosphors in novel storage device, high energy beam survey as well as image and optical information storage. In recent years, new photostimulable persistent phosphors gradually became the research hot spot. In this work, long persistent luminescence phosphor with high bright green emission of SrAl2O4: Eu2+, Dy3+ (SED) were synthesized by a solid state reaction method. The excitation and emission spectrums, persistent luminescence, thermo-luminescence (TL), NIR photo-stimulated spectrum and NIR photo-stimulated persistent luminescence (PSPL) decay curve were reported. The emission and persistent luminescence all contributed to characteristic emission (4f65d1–4f7) of Eu2+. The thermo-luminescence revealed two traps in the crystal and the trap depth are evaluated at 0.796 eV and 1.306 eV respectively. The NIR photo-stimulated spectrum and NIR-PSPL indicated the range of write-in and read-out were 330-470 nm and 630-850 nm respectively. Peaks of the write-in and read-out energies are located at 430 nm and 760 nm. The SED phosphor displays obvious photo-stimulated luminescence properties, indicating its potential in using as optical storage phosphor.

Key words: $SrAl_2O_4:Eu^{2+}$, Dy^{3+}, NIR photo-stimulated persistent luminescence, storage phosphor

* Corresponding author. Tel.:+86-13527789917

Understanding the enhanced ductility of TiAl alloys using a hybrid study of in-situ TEM experiment and molecular dynamics

Seong-Woong Kim[1,*], Seung-Hwa Ryu[2], Young-Sang Na[1] and Seung-Eon Kim[1]
[1]Light Metal Division, Korea Institute of Materials Science, Changwon 642-831, South Korea
[2]Department of Mechanical Engineering, Korea Advanced Institute of Science and Technology, Daejeon 305-701, South Korea
[*]*Corresponding author's Tel: 82-55-280-3837, E-mail: mrbass@kims.re.kr*

An in-situ transmission electron microscopy study was conducted at room temperature in order to understand an underlying mechanism on room temperature ductility of TiAl alloys. Also, melecular dynamics simulation was conducted to calculate the stacking fault energy of TiAl alloys and to show which deformation mode is dominant. From the quantitative in-situ TEM experiements, it was found that the γ lamellar of TiAl alloys having room temperature ductility was deformed by slip (Fig. 1). However, the γ lamellar of TiAl alloys without room temperature ductility was deformed by deformation twin (Fig. 2). The difference in deformation mode was explained by stacking fault energy of the TiAl alloys which was calculated by molecular dynamics. The TiAl alloy with low stacking fault energy was deformed by deformation twin (Fig. 2) whereas the TiAl alloy with high stacking fault energy was deformed by dislocation slip (Fig. 1). Furthermore, the role of lamellar orientation of tensile direction on deformation behavior was examined using Schmid factor of each orientation.
Finally, we proposed the important microstructural factors to have room temperature ductility of TiAl alloys.

Keywords: *TiAl, in-situ TEM, molecular dynamics, ductility, deformation*

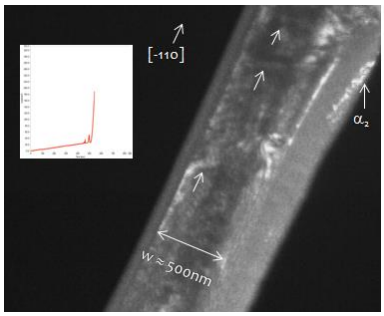

Fig. 1. Dark field image of alloy having room temperature ductility taken during in-situ TEM experiment. White arrows are indicating dislocations.

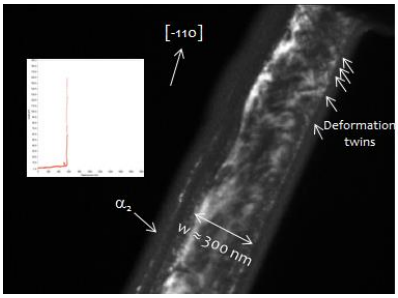

Fig. 2. Dark field image of alloy having no room temperature ductility taken during in-situ TEM experiment. White arrows are indicating deformation twins.

A Numerical Study of Crack Tip Hydrostatic Stress Fields in Plastically Compressible Hardening Solids

Shushant Singh, Debashis Khan, S.K.Panda

Department of Mechanical Engineering, Indian Institute of Technology (BHU) Varanasi

E-Mail: shushantsingh1986@gmail.com: Contact no: +91-9259232929

Abstract: Even though in classical plasticity theory the effect of hydrostatic stress is neglected, many materials exhibit pressure-sensitive flow strength with plastic volumetric change and in such materials volumetric strains are usually closely related to the pressure sensitivity. As well in such materials the distribution of hydrostatic stress is very closely related to the pattern of plastic deformation in front of a crack. In the present study, the effect of plastic compressibility and soft elasticity, i.e., a relatively small value of the ratio of Young's modulus to yield strength on plain strain mode I crack tip hydrostatic stress field for two different bilinear hardening and plastically compressible solids is investigated. The load level has been assumed to be small enough so that small scale yielding condition prevails. Figures 1 and 2 illustrate the hydrostatic stress distribution in front of the crack tip of materials B and D in both incompressible and compressible conditions, respectively, (Mohan *et al*.;2013). It is reflected from these figures that, for both the materials B and D the shape and position of the maximum hydrostatic stress contour with respect to the crack tip are different in case of compressible condition as compared to the incompressible situation. It is to be interestingly noted here that in case of material D (whose hardness slope is less) in compressible condition, the shape of the hydrostatic contour is very peculiar. As well in compressible condition, the movement of the contour of maximum hydrostatic stress is more in positive x direction.

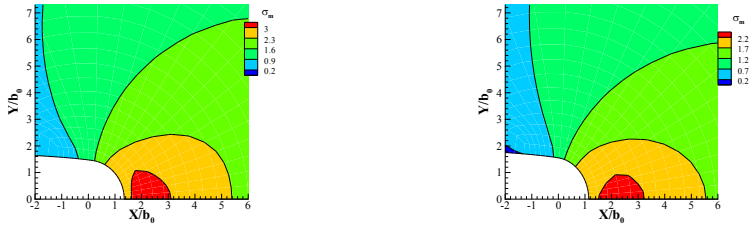

(a) (b)

Fig 1: Hydrostatic stress distribution at the crack tip for material B with normalized *J*-integral = 2.25; a) Incompressible, b) Compressibility $(\alpha_p) = 0.25$

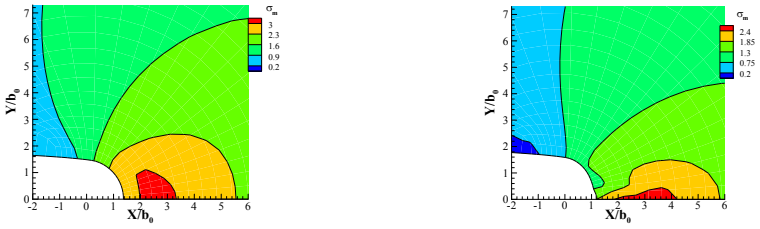

(a) (b)

Fig 2: Hydrostatic stress distribution at the crack tip for material D with normalized *J*-integral = 2.25; a) Incompressible, b) Compressibility $(\alpha_p) = 0.25$

Next, figure 3 describes the effect of elastic stiffness on the hydrostatic stress distribution in front of the crack tip of material D in incompressible condition. It is revealed here that the peak value and the contour of maximum hydrostatic stress increase with increase in the value of the ratio of Young's modulus to yield strength.

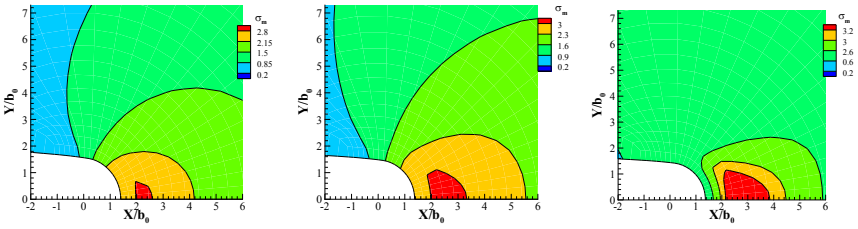

(a) (b) (c)

Fig 3: Hydrostatic stress distribution at the crack tip for material D, normalized *J*-integral = 2.25 and incompressible condition; a) $E/\sigma_0 = 50$, b) $E/\sigma_0 = 100$, c) $E/\sigma_0 = 200$

Keywords: Crack tip hydrostatic stress, Compressible solids, Finite Deformation, Finite Element Method.

References:

[1] MOHAN, N., CHENG, J., GREER, J.R., NEEDLEMAN, A., (2013) Uniaxial tension of a class of compressible solids with plastic non-normality, J. Appl. Mech., 80, 040912-1-8.

Analysis of non-isothermal kinetics via generalized rate constant method

A.S. Portnyagin[1,2], A.P. Golikov[2]

[1] Far Eastern Federal University, Vladivostok, Russia

[2] Institute of chemistry of Far Eastern Branch of Russian Academy of Sciences, Vladivostok, Russia

E Mail/ Contact Détails : arsuha@gmail.com, 89241234400,

159, prosp.100-letiya Vladivostoka, Vladivostok 690022, Russia

Experimental techniques of thermal analysis are widely used in characterization of solids; in particular, they enable one to trace processes occurring during thermal treatment of the material [1]. Investigations of thermic decomposition, functional material degradation and heterogeneous chemical reactions are conducted most effectively by non-isothermal methods. Information about dynamics of such processes allows aimed selection of conditions for fabrication of more effective functional materials. Methods of temperature-programmed reactions are convenient instruments in researchers toolbox for obtaining such information. Most frequently used variations of this group of methods are temperature programmed reduction and oxidation (TPR and TPO) that caused by the importance of reduction or oxidation steps in catalyst or material production cycle [2]. Despite the great advance in experimental setup and accuracy, analysis of the temperature programmed reaction data is carried out very approximately. Such inaccurate analysis leads to mistakes that make results less confident. For example, activation energy of iron oxide reduction varies from 18 to 246 $kJ*mol^{-1}$ that caused not only by different composition and particle sizes of the solid material but also due to inaccurate data analysis. In this work we suggest new method for kinetic parameter identification which requires minimal amount of *a priory* knowledge about the reaction process. Suggested method is based on the special approach that is comprised of preliminary identification of the temperature function of generalized reaction constants and treatment of obtained function using various model assumptions of chemical kinetics (Arrhenius equation, solid-state kinetics, etc.). Presented approach was implemented to the kinetic analysis of iron (III) oxide TPR under different heating rates

(3-20 ºC*min^{-1}). Excellent fit and stability of suggested method to shifting and shape changing of experimental curve were proved by low (down to 25.8 Pa^2) values of variance. Small range of calculated values of kinetic parameters also evidence high stability of suggested method.

Keywords: optimizing synthesis, temperature programmed reduction, iron oxide, spline approximation.

[1] WUNDERLICH, B. 2005. Thermal Analysis of Polymeric Materials, Springer, Berlin, 894 p.

[2] GERVASINI, A. 2013. Temperature Programmed Reduction/Oxidation (TPR/TPO) Methods, in: AUROUX, A. (Ed.), Calorimetry and Thermal Methods in Catalysis, Springer, p. 561.

Analysis of the Forces on Infantry Rifle Housing via Finite Element Method

Osman Iyibilgin[1,2,C] , Ismail Hakki Serdar[1], Yuksel Korkmaz[1,2]

[1] Sakarya University, Eng. Faculty, Mechanical Eng. Dept. Sakarya/Turkey

[2] Sakarya University, BIMAS-RC, Sakarya/Turkey

[C] Corresponding Author: Tel: **+90 5332417860**, e-mail: **ibilgin@sakarya.edu.tr**

Abstract:

The aim of the working principle of the infantry rifle, to explode the cartridge within the barrel housing, locking cartridge mechanism head in an appropriate tolerance and to eject the empty cartridge by the help of barrel gas pressure which reduced to the safe value after firing. The explosion of the cartridge in a safe manner and ejecting of empty cartridge depend directly on the head space dimensions and barrel material. There are three different weapon mechanisms including sudden retrodriving, retrodriving and gas operational to eject the empty cartridge automatically by weapon mechanism. In this study, the obtained behaviors of cartridge housing is investigated depending on the different materials and head space dimension as a result of the firing of ammunition in a gas operated gun.

The aim of this study is to determine the head space tolerance which could operate safely in a rifle operating with a gas piston system that uses a 7,62x51 NATO normal cartridge for brass housing and to observe the behavior of housing after the firing and to analyze the change of the head space measurement when the housing material is steel. Furthermore, the properties of removability from the barrel are examined comparing with the housing contact pressure values between steel and brass barrel (housing). During the firing of ammunition, the bursting pressure and temperature after the explosion are experimentally determined. The pressure and temperature data obtained from the experimental studies are defined in finite element model and performed analysis. As a result of the performed studies, for the same dimensional barrel it is observed that instead of brass, using steel material, the tolerance of head space increased but the contract pressure between barrel and housing. According to the analysis results, it was determined that the service life of the rifle will be increase with the increment of head space dimensions depending on the head space tolerance and the empty cartridge will easily be removed from the rifle when using the brass material instead of steel housing .

Keywords: Finite Element (FE) Analysis, cartridge cases, explicit, efficiency

Density Functional Theory of Graphene/Metallophthalocyanines: Electronic Structure of CuPc, NiPc, and CoPc on Graphene

A. Jomphoak[1,2], R. Maezono[2], T. Onjun[1]

[1]Sirindhorn International Institute of Technology (SIIT), Thammasat University, Pathum Thani 12121, Thailand

[2]Japan Advanced Institute of Science and Technology (JAIST), Nomi, Ishikawa 923-1292, Japan

Email: thawatchai@siit.tu.ac.th

The structure of metallophthalocyanines (MPcs) molecule is schematically constructed by inserting a metal atom at the center of organic groups, where the metal ion at the center can strongly affect the whole molecular structure by illuminating a delicate balance of the interactions that governs synthesis of the composite materials. Self-consistency simulations for a molecular structure, bond length and angle, formation, stability, and adsorption energies of graphene/MPcs composite material are carried out using Materials Studio software package with LDA/PWC and GGA/PBE functionals. In this work, it focuses on Copper phthalocyanine (CuPc), nickel phthalocyanine (NiPc), and cobalt phthalocyanine (CoPc). Bond lengths and angles obtained with the different functionals used in this work are provided as electronic supplementary material. After the structural optimization with LDA/PWC functional, it was found that the distance between a graphene layer and CuPc, NiPc, and CoPc are 3.155 Å, 3.139 Å, and 2.784 Å, recpectively. Similarly, using GGA/PBE functional, the larger values, but the same trend, is found as the distance between a graphene layer and CuPc, NiPc, and CoPc are 3.690 Å, 3.481 Å, and 3.277 Å, respectively. The GGA/PBE functional yields slightly longer bond lengths than those of LDA/PWC functionals, a tendency that is typical for organic compounds. Among these formations, CoPc is the shortest interplane distances between MPcs and a graphene layer. It is also known that the system with the higher reactivity and potential in the charge transport must have a lower value for HOMO-LUMO gap, and for graphene/CoPc is much lower than those for graphene or CuPc or NiPc which is in agreement for both results from PWC and PBE functionals. This indicates an enhancement of reactivity in the graphene/CoPc structure, resulting in a potential candidate for a better charge transport material. It is also found that the adsorption of CoPc on graphene layer is a spontaneous process with the shortest distance between the two layers.

The presence of CoPc on graphene decreases the HOMO−LUMO gap and, therefore, it increases a reactivity compared to isolated CoPc or graphene. Thus, CoPc enhances charge transport on graphene making this graphene/CoPc a high quality transparent conductive material.

Keywords: DFT, CuPc, NiPc, CoPc, Graphene

Effect of the Size of Iron Core on the Coercive Field and Magnetization of Core/Shell Fe/Fe_3O_4 Nanoparticles

Sergei (Anisimov)[1], Leonid (Afremov)[1], Ilia (Ilyushin)[1]

[1]Far Eastern Federal University, Vladivostok, Russia.

ahriman25@gmail.com

Size effects hold a prominent place among the diversity of magnetic properties of the core/shell nanoparticles [1-4]. The aim of this work is to study the dependence of the hysteresis characteristics of the core/shell Fe/Fe_3O_4 nanoparticles on the size of iron core.

The calculation of the coercive field H_c, saturation magnetization I_s and remanent saturation magnetization I_{rs} is carried out within the framework of the model of two-phase nanoparticles developed by us [5]:

1. Uniformly magnetized ellipsoidal nanoparticle with volume V and elongation Q contains a uniformly magnetized ellipsoidal core with volume $v = \varepsilon V$ and elongation q.
2. The axes of crystallographic anisotropy and major axes of core and shell are parallel to each other and aligned along the axis Oz.
3. Spontaneous magnetization vectors of phases lie in the same plane with the external magnetic field and axis Oz.

Results of modeling of the dependence of the hysteresis properties of the system of core/shell Fe/Fe_3O_4 nanoparticles on sizes of their cores carried out using the formal description developed by us [5] are shown on the figures 1 and 2. It is clearly seen, that the increase of the size of iron core results in growth of the coercive field, saturation magnetization and remanent saturation magnetization and closely resemble the experimental results [3]. Moreover, to compare with the experimental results of the reference [4], we calculated the dependence of the normalized coercive field $h_c = H_c/H_{c\,max}$ on the relative volume of the shell $1 - \varepsilon$ of nanoparticles.

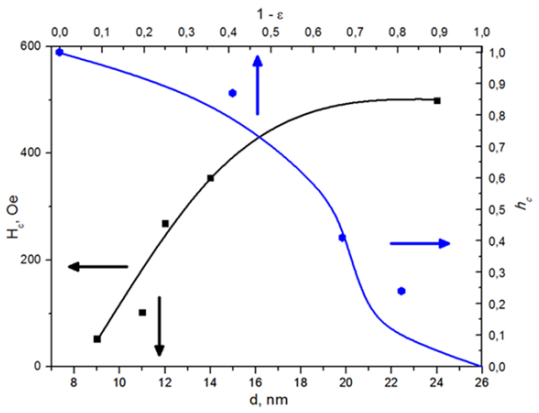

Fig. 1. Dependence of the coercive field H_c on the size of nanoparticles (black line). Dependence of the normalized coercive field h_c on the relative volume of the shell $1-\varepsilon$ of nanoparticle (blue line). Black squares show the experimental values of H_c [3], and blue dots represent h_c [4].

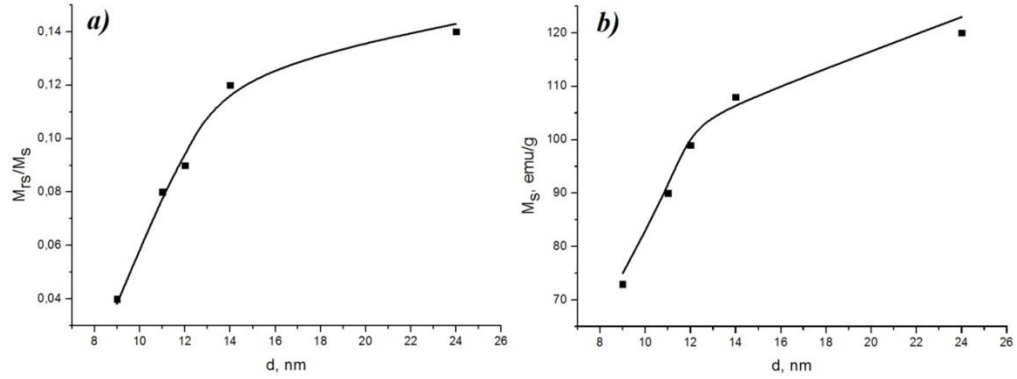

Fig. 2. a) Dependence of the remanent saturation magnetization to saturation magnetization ratio on the size of core/shell nanoparticles; b) dependence of the saturation magnetization on the size of the core/shell nanoparticles. Dots show the experimental results [3].

Keywords: Magnetism, modeling, hysteresis properties, core/shell nanoparticles

[1] KOLHATKAR, A. G., JAMISON, A. C., LITVINOV, D. WILLSON, R. C. & RANDALL LEE, T. 2013. Tuning the Magnetic Properties of Nanoparticles. *Int. J. Mol. Sci.*, 14, 15977-16009.

[2] YANG, C., HOU, Y. L. & GAO, S. 2014. Nanomagnetism: Principles, Nanostructures, and Biomedical Applications. *Chin. Phys. B*, 23, 057505.

[3] KAUR, M., McCLOY, J. S., JIANG, W., YAO, Q. & QIANG, Y. 2012. Size Dependence of Inter- and Intracluster Interactions in Core-Shell Iron-Iron Oxide Nanoclusters. *J. Phys. Chem. C*, 116, 12875-12885.

[4] ZENG, H., LI, J., WANG, Z. L., SUN, S. & LIU, J. P. 2004. Tailoring Magnetic Properties of Core/Shell Nanoparticles. *Applied Physics Letters*, 85, 792-794.

[5] AFREMOV, L. L. & ILYUSHIN, I. G. 2013. Effect of Mechanical Stress on Magnetic States and Hysteresis Characteristics of a Two-Phase Nanoparticles System. *Journal of Nanomaterials*, 2013, 15p.

Investigation on Mechanical properties of Activated Carbon by Molecular Simulation Method

Po-Yu Yang[1,a], Hsin-Tsung Chen*[,2,b], Shin-Pon Ju[1,3,c], Siou-Mei Huang [1,d]

[1]Department of Mechanical and Electro-Mechanical Engineering, National Sun Yat-sen University, Kaohsiung 80424, Taiwan

[2]Department of Chemistry and Center for Nanotechnology, Chung Yuan Christian University, Chungli 32023, Taiwan

[3]Department of Medicinal and Applied Chemistry, Kaohsiung Medical University, Kaohsiung 807, Taiwan

[a] winniebird0519@gmail.com, [b] htchen@cycu.edu.tw, [c] jushin-pon@mail.nsysu.edu.tw,

[d] j93341enny@gmail.com

By taking the advantages of molecular dynamics (MD) simulations with the Adaptive Intermolecular Reactive Empirical Bond Order (AIREBO) potential [1] and Reactive force field (Reaxff)[2], the MD tensile simulations were systematically applied to the activated carbon (AC) materials with different pore sizes, and the AC fracture mechanism and the relationship between the mechanical properties and the AC pore size were drawn in this study.

Keywords: Activated carbon, mechanical property, tensile simulation

[1] S. J. Stuart, A. B. Tutein, and J. A. Harrison, "A reactive potential for hydrocarbons with intermolecular interactions," *The Journal of Chemical Physics*, vol. 112, pp. 6472-6486, 2000.

[2] A. C. Van Duin, S. Dasgupta, F. Lorant, and W. A. Goddard, "ReaxFF: a reactive force field for hydrocarbons," *The Journal of Physical Chemistry A,* vol. 105, pp. 9396-9409, 2001.

Modeling of damping force due to magnetic fluids on the depression of self-excited pressure oscillations in a hydraulic jet pipe servo-valve

Songjing Li* Wei Zhang Jinghui Peng

Department of Fluid Control and Automation,
Box 3040 Science and Technology Park,
Harbin Institute of Technology,
No. 2 Yikuang Street, Nangang District, Harbin, China, 150001
Email: lisongjing@hit.edu.cn
Tele: +86-13796635768

Abstract

High frequency self-excited pressure oscillations and noise, appearing often in hydraulic servo-valves, may deteriorate the stability of the valves and the performance of hydraulic control systems. The aim of this paper is to investigate the influence of magnetic fluids and to build the mathematical models of damping force due to magnetic fluids on the depression of self-excited pressure oscillations and noise appearing in a hydraulic jet pipe servo-valve. Due to the properties of high saturation magnetization and large viscosity when exposed to a magnetic field, as a functional fluid, magnetic fluids are applied in the servo-valve torque motor to exert damping and resistance to the valve in this paper. Construction of the hydraulic jet pipe servo-valve is introduced and the forces due to magnetic fluids on the torque motor armature are studied with the finite element analysis method. The pressure oscillations and noise inside the servo-valve are tested and analyzed using FFT method. Tested and analyzed results are compared when magnetic fluids are applied or not in the servo-valve. Good depression effects due to magnetic fluids on the self-excited pressure oscillations and noise inside the valve are shown by the comparison of the results.

Keywords: magnetic fluids, damping force, pressure oscillations, servo-valve, jet pipe

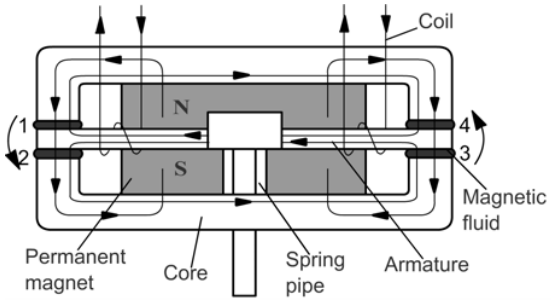

Figure 1 Torque motor with magnetic fluids

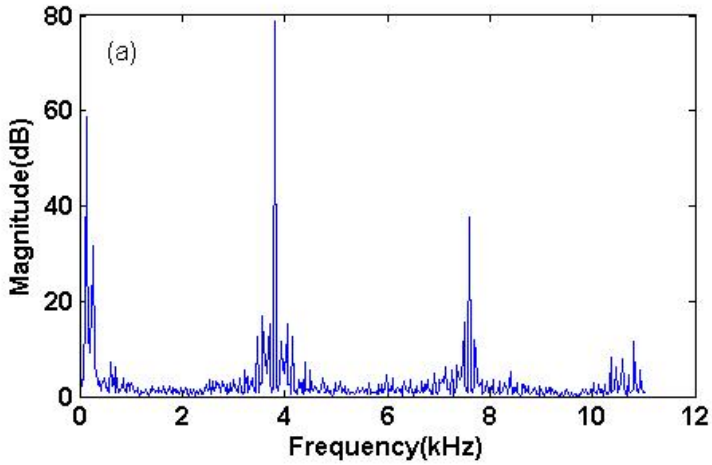

(a)Without magnetic fluids

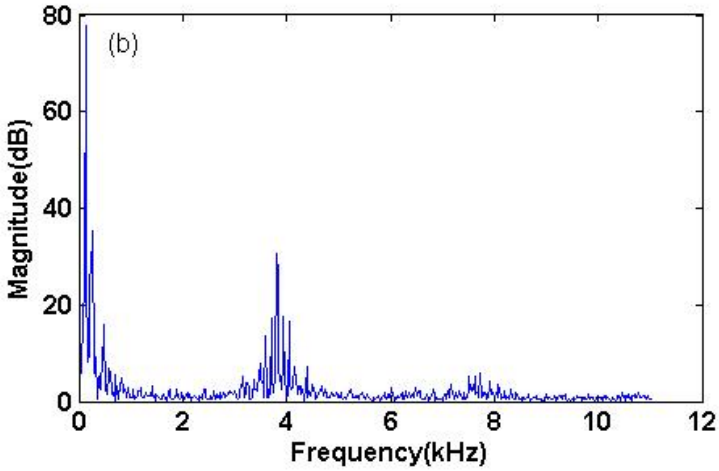

(b) With magnetic fluids

Figure 2 FFT analysis results of tested noise wave signals

Modeling of the Oxidation of Magnetite Core/Shell Nanoparticles

Leonid (Afremov)[1], Ilia (Iliushin)[1], Maria (Shmykova)[2]

[1]Far Eastern Federal University, Vladivostok, Russia.

futted@gmail.com

Study of the effect of the single-phase oxidation on the magnetic properties of the titanomagnetites has been carried out within the framework of the model of Shcherbakov and Gribov. The detailed description of this model is presented in [1, 2]. In our model of core/shell-nanoparticles [3] the single-phase oxidation can be considered as two mutually complementary processes: the growth of the fully oxidized envelope ($z = 1$) and the simultaneous increase in the degree of oxidation z of the core of a titanomagnetite nanoparticle. For modeling we used the dependence of the spontaneous magnetization on the oxidation degree z, described in the reference [4], and the theoretical dependence of the crystallographic anisotropy constants: $K_a(z) = K_a(0)[I_s(z)/I_s(0)]^{10}$. During the calculations we used the values of the size distribution function shown in the reference [5]. Magnetic characteristics of the two-phase nanoparticles system are obtained via the hysteresis loops, calculated using formal description described in detail in the reference [6].

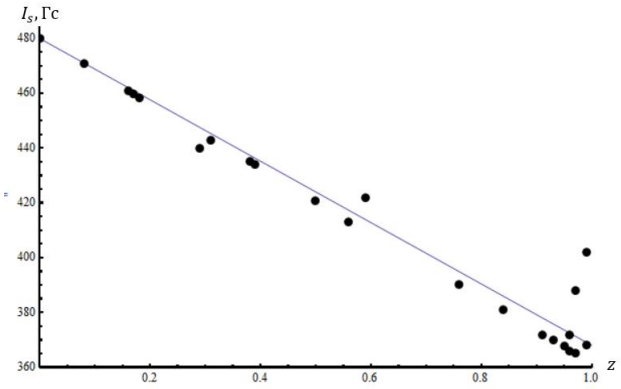

Figure 1. Dependence pf the saturation magnetization I_s on the oxidation degree z. Dots representing the experimental results from the reference [7]

Figure 1 show the dependence of the saturation magnetization on the oxidation degree. As it was expected, saturation magnetization linearly decrease with growth of z due to the linear dependence of the saturation magnetization on the oxidation degree z. the results of

calculation is in a good agreement with the experimental data [7]. The dependence of the coercive field of the magnetite nanoparticles on the oxidation degree is shown on the figure 2a. It is clearly seen, that theoretical curve goes lower than experimental one. It is due to the fact that we have not included the particles with sizes over 100 nm, assuming their amount negligible. At the same time, some portion of the nanoparticles with sizes below 100 nm can be in superparamagnetic state that leads to the lower theoretical values of the coercive field and remanent saturation magnetization to saturation magnetization ratio (figure 2b).

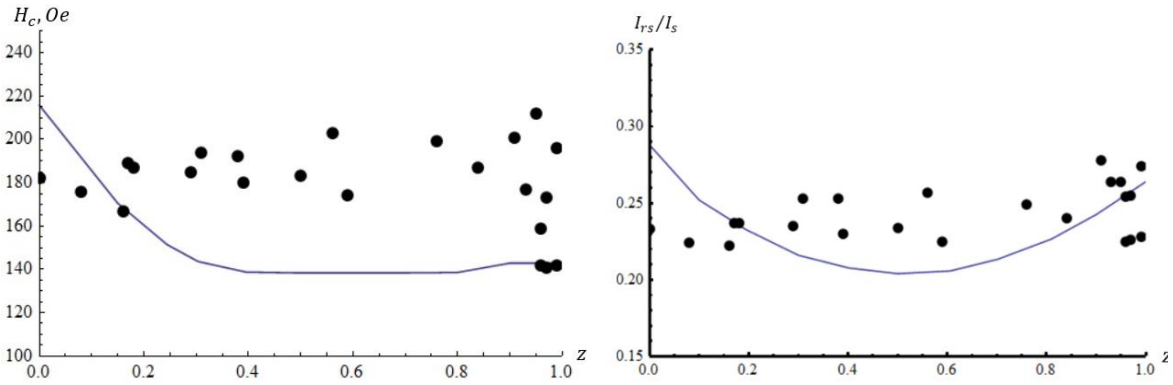

Figure 2. Dependences of the coercive field H_c (a) and the remanent saturation magnetization to saturation magnetization ratio on the oxidation degree z (b) of magnetite. Dots representing the experimental values from the reference [7].

Thus, the modeling of the effect of the processes of single-phase oxidation on the hysteresis characteristics of the system of magnetite nanoparticles, conducted within the framework of the model of two-phase nanoparticles [3] shown that: a) spontaneous saturation magnetization is decreasing with an increase of the oxidation degree of nanoparticles; b) oxidation of magnetite have a little effect on the coercive field H_c and I_{rs}/I_s ratio. The modeling results closely resemble the experimental results [7].

Keywords: Titanomagnetites, hysteresis characteristics, magnetic properties, modeling, oxidation.

[1] SHCHERBAKOV, V. P. 1982. The role of the kinetics in the oxidation of titanomagnetite grains. *Izv. USSR Academy of Sciences. Ser. Phis*., 5, 43-49.

[2] SHCHERBAKOV, V. P. & GRIBOV, S. K. 1986. The theory of oxidation of titanomagnetite grains in the diffusion coefficient, which depends strongly on the degree of oxidation. *Izv. USSR Academy of Sciences, Physics of the Earth*, 4, 105-112.

[3] AFREMOV, L. L. & ILYUSHIN, I. G. 2013. Effect of Mechanical Stress on Magnetic States and Hysteresis Characteristics of a Two-Phase Nanoparticles System. *Journal of Nanomaterials*, 2013, 15p.

[4] READMAN, P.W. & O'REILLY, W. 1972. Magnetic Properties of Oxidized (Cation-Deficient) Titanomagnetites (Fe, Ti,)3O4. *J. Geomag. Geoelectr*., 24, 69-90.

[5] OZDEMIR, O. & DUNLOP, D. J. 2010. Hallmarks of maghemitization in low-temperature remanence cycling of partially oxidized magnetite nanoparticles. *J. Geophys. Res*., 115, B02101.

[6] AFREMOV, L. L., IL'YUSHIN, I. G. & ANISIMOV, S. V. 2015. Modeling the Implications of Chemical Transformations for the Magnetic Properties of a System of Titanomagnetite Nanoparticles. *Izv. Physics of the Solid Earth*, 51, 613-621.

[7] GE, K., WILLIAMS, W., LIU, Q. & YU, Y. 2015. Effects of the core-shell structure on the magnetic properties of partially oxidized magnetite grains: Experimental and micromagnetic investigations. *Geochem. Geophys. Geosyst.*, 15, 2021–2038.

Predicting the mechanical and electrical properties of polyvinylidene fluoride/carbon nanotubes nanocomposites by molecular simulation

Hui-Lung Chen[1*,a],Shin-Pon Ju[2,3,b], Jenn-Sen Lin[4,c], Chen-Yun Lin [2,d]

[1]Department of Chemistry and Institute of Applied Chemistry, Chinese Culture University, Taipei, 111, Taiwan

[2]Department of Mechanical and Electro-Mechanical Engineering, National Sun Yat-sen University, Kaohsiung 80424, Taiwan

[3]Department of Medicinal and Applied Chemistry, Kaohsiung Medical University, Kaohsiung 807, Taiwan

[4]Department of Mechanical Engineering, National United University, Miaoli 36003, Taiwan.

E Mail/ Contact Détails: [*]chl3@faculty.pccu.edu.tw, yun19930731@gmail.com

Polyvinylidene fluoride (PVDF) is a polymer with high mechanic property[1] and strong piezoelectricity material while under strong eletric field due to induced net dipole moment[2]. This study predicted the mechanical and piezoelectric properties of PVDF/CNT composites by molecular dynamics (MD) simulation [4] with the polymer consistent force field (PCFF). The tensile test simulations were applied to predict the mechanical properties of PVDF/CNT composites including Young's modulus and mechanical strength with different mixing ratio. The piezoelectric properties of PVDF/CNT composites were calculated by GULP module in Material Studio 7.0 package[6]. By taking advantage of this molecular simulation procedure, the fast and comparable predictive properties of PVDF/SWCNT composites were performed and provide a pathway for reducing the cost and researth time in the related experiments.

Keywords: PVDF, CNT, piezoelectric, LAMMPS, molecular dynamics

1. Vinogradov, A. and F. Holloway, *Electro-mechanical properties of the piezoelectric polymer PVDF*. Ferroelectrics, 1999. **226**(1): p. 169-181.
2. Liu, Z., et al., *Piezoelectric properties of PVDF/MWCNT nanofiber using near-field electrospinning.* Sensors and Actuators A: Physical, 2013. **193**: p. 13-24.

3. Manna, S. and A.K. Nandi, *Piezoelectric β polymorph in poly (vinylidene fluoride)-functionalized multiwalled carbon nanotube nanocomposite films.* The Journal of Physical Chemistry C, 2007. **111**(40): p. 14670-14680.
4. Xue-Ming, S. and W. Jia-Ying, *Simulated Annealing Method.* Chinese Journal of Engineering Geophysics, 2007. **3**: p. 001.
5. Plimpton, S., P. Crozier, and A. Thompson, *LAMMPS-large-scale atomic/molecular massively parallel simulator.* Sandia National Laboratories, 2007. **18**.
6. Bennett, T., *Nanochemistry Research Institute-Capabilities.* 2009.

Predicting the mechanical properties of Polymethyl methacrylate /Ag nanoparticle composites by molecular simulation

Shin-Pon Ju [1,2*], Hui-Lung Chen[3], Jenn-Sen Lin[4], Che-Wei Shih [1]

[1] Department of Mechanical and Electro-Mechanical Engineering, National Sun Yat-sen University, Kaohsiung 80424, Taiwan

[2] Department of Medicinal and Applied Chemistry, Kaohsiung Medical University, Kaohsiung 807, Taiwan

[3] Department of Chemistry and Institute of Applied Chemistry, Chinese Culture University, Taipei, 111, Taiwan

[4] Department of Mechanical Engineering, National United University, Miaoli 36003, Taiwan

E Mail/ Contact Détails : [*]jushin-pon@mail.nsysu.edu.tw, xyz20054071022@gmail.com

The simulated-annealing basin-hopping (SABH) method[1] was applied to constructed the stable structures of Polymethyl methacrylate/Ag nanoparticle (PMMA/AgNP) composites, which can reflect the real sample configurations in the corresponding experiments. The SABH results indicated that both PMMA/AgNP composite and pristine PMMA material exhibit isotropic amorphous structures and PMMA/AgNP composite exhibit higher density than pristine PMMA. These stable structures of PMMA/AgNP composite were further used to predict composite mechanical properties at different temperatures by molecular dynamics (MD) simulation for the tensile test. From the stress-strain curves, the PMMA/AgNP composites exhibit higher Young's modulus and Poisson ratio than pristine PMMA in different weight and volume fraction of Ag nanoparticle. All the molecular mechanics calculations were performed by Large-scale Atomic/Molecular Massively Parallel Simulator (LAMMPS)[2] and the prediction of stable structures and mechanical properties were in agreement with experiments. In this study, a reliable simulation procedure had been provided and may be applied to other polymer/nanoparticle systems in future.

Keywords: Polymethyl methacrylate, Basin-Hopping method, nanoparticle, LAMMPS

[1] David, J. W, & Jonathan P. K. D, 1997. Global Optimization by Basin-Hopping and the Lowest Energy Structures of Lennard-Jones Clusters Containing up to 110 Atoms. *J Chem Phys A,*101, 5111-5116.

[2] Shengfeng, C, & Gary S. G . 2013. Molecular dynamics simulations of evaporation-induced nanoparticle assembly. *J Chem Phys,* 138, 064701.

Stress field around oval shaped hole in functionally graded plate with through-thickness material properties variation

Jatin (Dave)[1], Dharmendra (Sharma)[2]

[1]Mechanical Engineering Department, Institute of Technology, Nirma University, Ahmedabad, Gujarat, 382481, India.

[2]Faculty of Technology and Engineering, The M. S. University of Baroda, Vadodara, Gujarat, 390001, India.

[1]dave.jatin.m@gmail.com (91-8347025899), [2]dss_iit@yahoo.com, (91-9879472897)

In Mechanical, Civil, aerospace and other related applications, plate type components are widely used. The plates are made from isotropic or composite material to achieve some advantages like ultimate strength, weight-to-strength ratio, wear and corrosion resistance etc. A functionally graded (FG) plate is recent research area in the domain of anisotropic material and may be useful in structural application in future. A hole or cut-out present in a component (e.g pressure vessel, container, automobile body parts), facilitate operational or service need. The stress concentration around such holes are higher than other region and may fail the part when it is subjected to loading environment. Many researchers have contributed to give analytical solution to find stress concentration around a hole in isotropic plate and composite plate. Very few research work is available to determine stress field around a hole in FG plate as per the best of author's knowledge.

The present work addressed the issue of determining stress field around oval shaped hole in infinite FG plate. The through-thickness material property variation is considered from the mid-plane of the plate. Muskhelishvili's complex variable method is used to formulate analytical equations and solving stress functions. A mapping functions is derived from the parametric equations and gives shapes like circle, ellipse, square, rectangle, eye shape and many other variance depends on shape and size constant. Arbitrary biaxial loading condition is used in general boundary conditions. A condition of single valued-ness of out-of-plane displacement is incorporated to solve stress functions. Effect of hole geometry, material properties and loading conditions is studied. The results obtained using present method are compared with existing literature and are in close agreement.

Keywords: functionally graded, complex variable method, oval shaped hole, stress field

[1] MUSKHELISHVILI, N. I. 1962. Some basic problems of mathematical theory of elasticity. 2nd English ed. *The Netherlands: Noordhoff International Publishing*.

[2] SAVIN G. 1961. Stress concentration around holes. *New York: Pregamon Press.*

[3] LEKHNITSKII S. 1968. Anisotropic plates. *New York: Gordon and Breach science publishers.*

[4] SHARMA D. S. 2015. Stress analysis of infinite laminated composite plate with a polygonal hole. *European J of Mechanics – A/Solids*, 54, 44 – 52.

[5] BECKER W. 1991. A complex potential method for the plate problems with bending extension coupling. *Archive Appl Mech*; 61, 318 – 326.

[6] CHEN P., SHEN Z. 2003. Stress resultants and moments around holes in unsymmetrical composite laminates subjected to remote uniform loading. *Mechanics Research Communication*, 30, 79-86.

[7] YANG Q., GAO C. F., CHEN W. 2010. Stress analysis of a functional graded material plate with a circular hole. *Archive of Applied Mechanics*, 80(8), 895-907.

[8] KUBAIR D., BHANU-CHANDAR B. 2008. Stress concentration factor due to a circular hole in functionally graded panels under uniaxial tension. *Int J Mech Sci*, 50, 732–742.

[9] DAVE J. M., SHARMA D. S. 2016. Stresses and moments in through-thickness functionally graded plate weakened by circular/elliptical cut-out, Int J Mech Sci, 105, 146–157.

Stresses and moments around rectangular hole in through - thickness functionally graded plate

Jatin (Dave)[1], Dharmendra (Sharma)[2]

[1]Mechanical Engineering Department, Institute of Technology, NirmaUniversity, Ahmedabad, Gujarat, 382481, India.

[2]Faculty of Technology and Engineering, The M. S. University of Baroda, Vadodara, Gujarat, 390001, India.

[1]dave.jatin.m@gmail.com (91-8347025899), [2]dss_iit@yahoo.com, (91-9879472897)

The openings and holes in plate or component are made to satisfy operational and design requirements. When such component is subjected to different loading conditions, the stresses and moments around the hole boundaries may increases beyond safe limits and results into failure of components.The analytical formulations for isotropic material and composite plate having a hole is available. A functionally graded (FG) plate is a new concept in the field of anisotropic material and may prove itself advantageous in structural applications. As per best of author's knowledge, few researchers have attempted to problem of finding stresses around a hole in FG plate.

In this work, a functionally gradedplate with through-thickness material property variation from the mid-plane is considered having a rectangular hole at the centre. Muskhelishvili's complex variable method is used to obtain solutions of stress functions. A conformal mapping is used to determine size of the hole. Arbitrary biaxial loading conditions is employed to avoid superposition and condition of single valued-ness of out-of-plane displacement is used to solve stress functions. Effect of hole geometry, material properties and loading conditionson stresses and moments around the hole is studied in this work. Some of the results obtained using present formulations are compared with existing literature and found in good agreement.

Keywords: complex variable method, functionally graded plate, through-thickness, stress and moments, hole

[1] MUSKHELISHVILI, N. I. 1962. Some basic problems of mathematical theory of elasticity. 2nd English ed. *The Netherlands: Noordhoff International Publishing*.

[2] SAVIN G. 1961. Stress concentration around holes. *New York: Pregamon Press.*

[3] LEKHNITSKII S.1968. Anisotropic plates. *New York: Gordon and Breach science publishers*.

[4] SHARMA D. S. 2015. Stress analysis of infinite laminated composite plate with a polygonal hole. *European J of Mechanics – A/Solids*, 54, 44 – 52.

[5] BECKER W. 1991. A complexpotentialmethod for the plate problemswithbending extension coupling. *Archive ApplMech*; 61, 318 – 326.

[6] CHEN P., SHEN Z.2003. Stress resultants and moments around holes in unsymmetrical composite laminates subjected to remote uniform loading. *Mechanics Research Communication*, 30, 79-86.

[7] YANG Q., GAO C. F., CHEN W. 2010. Stress analysis of a functional graded material plate with a circular hole. *Archive of Applied Mechanics*, 80(8), 895-907.

[8] KUBAIR D., BHANU-CHANDAR B. 2008. Stress concentration factor due to a circular hole in functionally graded panels under uniaxial tension. *Int J MechSci*, 50, 732–742.

[9] DAVE J. M., SHARMA D. S.2016.Stresses and moments in through-thickness functionally graded plate weakened by circular/elliptical cut-out, IntJMechSci, 105, 146–157.

Structural Integrity of Stretchable Electrodes Based on Mogul Structure in a Thermal Environment

You-Joon (Song)[1], Han-Byeol (Lee)[2], Nae-Eung (Lee)[2], Youn-Jea (Kim)[3]

[1]Graduate School of Mechanical engineering, Sungkyunkwan University
2066 Seobu-ro, Suwon 16419, Republic of Korea

[2]School of Advanced Materials Science & Engineering, Sungkyunkwan University
2066 Seobu-ro, Suwon 16419, Republic of Korea

[3]School of Mechanical Engineering, Sungkyunkwan University
2066 Seobu-ro, Suwon 16419, Republic of Korea

yjkim@skku.edu

Stretchable electronics have been attracted a treat interest in potential applications that require reliable operation under mechanical deformation. To realize the flexible electronics, making a success of stretch ability in devices requires a deeper understanding of nano-scale materials and mechanics. The electrical peroformance of stretchable electrode is affected by thermal condition and stretching. In this regard, many research institutions have strived to develop the stretchable electrode which endures certain thermal condition and stretchability. Thin film thickness affects thermal endurances and stretchability. In this study, the relationship among the thickness, thermal condition and stress was analyzed. Since the electrical performnace is preserved until the film is broken, it is possible to derive the electrical performance through the stress distribution. The stress and strain distribution investigated by numerical analysis showed good agreement with the experimental results for the reference model. The results are graphically depicted for operating condtion.

Keywords: Mogul-pattern, Electrical performance, Stretchable electrode, Stress distribution

[1] ROGERS, A. J., SOMEYA, T. & HUANG, Y. 2010. Materials and Mechanics for Stretchable Electronics, Journal of Science, 327, 1603-1607.

[2] KIM, D. H., SONG, J., CHOI, W. M., KIM, R. H., LIU, Z., HUANG, Y. Y., HWANG, K. C., ZHANG, Y. W. & ROGERS, J. A. 2008. Materials and noncoplanar mesh designs for integrated circuits with linear elastic responses to extreme mechanical deformations, Journal of PNAS, 105, 18675-18680.

Study on advancement in machining of shape memory alloys: A mini review

Bisaria[1], Shandilya[2]

[1,2]Department of Mechanical Engineering, Motilal Nehru National Institute of TechnologyAllahabad, Allahabad and 211004, India

pragya20@mnnit.ac.in

This review paper is focused on the advancement in machining of shape memory alloys (SMAs). This review paper highlights the methods of manufacturing and utility of various SMAs into different sectors such as aerospace, biomedical, automobile etc. The numerous conventional machining processes for SMAs and the problem associated with these processes are studied under this review paper. This review paper explores different advance machining processes for machining of shape memory alloys.

Keywords: Shape memory alloys, pseudoelasticity, wedm, surface integrity

Damping effect of the smart energy dissipated system for the protection of isolated bridges against near-fault seismic excitations

Chen Ling-kun[1,2], Li Qiao[1], Zhang Ming[2], Jiang Li-zhong[3]

(1. Southwest Jiaotong University School of Civil Engineering Chengdu 610031 China; 2. College of Civil Science and Engineering, Yangzhou University, Jiangsu, Yangzhou 225127 China; 3. National Engineering Laboratory for High-Speed Railway Construction, Central South University, Changsha, PR China)

Abstract: Optimization of isolation system involves a trade-off between the isolation efficiency and isolator displacement to ensure optimal performance. Quite often, the latter aspect is overruled, even though, large isolator displacements are known to be linked with adverse consequences. Especially for the railway bridge, because the most crucial problem is displacement of bridge deck, if the displacement of bridge deck is of little larger than about the 1/800 of the beam span, the train will derailed. Actually, a conventional seismic isolation system is usually a long-period dynamic system, it may easily incur an excessive seismic response when subjected to near-fault earthquakes, which usually contain strong long-period wave components. In order to analysis this near-fault isolation problem, this paper investigates a numerical analysis process of a smart isolation system, which is installed in the high-speed railway bridge. The spatial analysis model of a vehicle-bridge system under high-speed vehicles is set up. Theoretical results have demonstrated that in either a near-fault or a far-field earthquake, the PSIS with the isolation system is very effective in suppressing simultaneously the isolator displacement and the acceleration response of the isolated object.

Keywords: damping effect; energy dissipated system; high-speed railway bridge; lead rubber bearings; near-fault earthquake

Finite element model of welded joint for study the residual stresses considering a time-independent cyclic plasticity approach

Ruben Lostado Lorza[1], Pedro Villanueva Roldan[2], Marina Corral Bobadilla[1], Maria Angeles Martinez Calvo[1], Fatima Somovilla Gomez[1], Roberto Fernandez Martinez[3]

[1]Mechanical Engineering Department, University of La Rioja, Logroño, Spain.

[2]Rural Engineering Depart. and Projects, Public University of Navarre, Pamplona, Spain.

[3] Department of Electrical Engineering, University of The Basque Country UPV/EHU, Bilbao, Spain

ruben.lostado@unirioja.es, roberto.fernandezm@ehu.es

Due to the intense concentration of heat in a reduced area when the Gas Metal Arc Welding (GMAW) is used for joining mechanical components, the regions near the weld line are subjected to severe thermal cycles. These thermal cycles generates changes in the microstructure, inhomogeneity in the distribution of the phases and variations in the mechanical properties. Also, the region close to the weld line being heated tends to be in compression and the region being cooled tends to be in compression, which can be considered as a strain-stress cycle. According to Pilipenko [1], the material is being exposed to elastic compression and then, reaching the yield limit, the material undergoes plastic deformation followed by elastic unloading. In addition, these thermal cycles generates the apparence of residual stresses, which should be avoided in mechanical welded components. These residual stresses are usually determined by several methods, which are usually classified as among destructive, semi destructive and non-destructive techniques [2]. In addition, the modeling and optimization of welded joints through the Finite Element Method (FEM) has been widely used in recent decades [3]. This paper proposed a Finite Element model which considers the plastic-strain-range memorization based on Time-independent Cyclic Plasticity for a Butt joint with single V-groove. The Chaboche model proposed in this work [4] combines the isotropic hardening rule to describe the cyclic hardening and the nonlinear kinematic hardening to capture the proper characteristic of cyclic plasticity for a welded joint. An agreement between the principal stresses obtained by the FE model and those obtained experimentally by using the semi-

destructive hole drilling method [5] demonstrates that the Chaboche model proposed could be used to model the effect of strain-stress cycle according to Pilipenko theory.

Keywords: Time-Independent Cyclic Plasticity, Chaboche Model, Residual Stresses, Finite Element Method, Gas Metal Arc Welding

[1] PILIPENKO, A. 2001. Computer simulation of residual stress and distortion of thick plates in multielectrode submerged arc welding: Their mitigation techniques.

[2] OLABI, A.G., LOSTADO, R., BENYOUNIS, K.Y. 2014. Welding and Bonding Technologies. *Reference Module in Materials Science and Materials Engineering. Comprehensive Materials Processing*, 6, 193-212

[3] LOSTADO R., FERNANDEZ R., MAC DONALD B.J., VILLANUEVA P.M. 2015. Combining Soft Computing Techniques and Finite Element Method for the Design and Optimization of Complex Welded Products. *Integrated Computer-Aided Engineering*, 22, 153-170.

[4] CHABOCHE, J.L. 1989. Constitutive Equations for Cyclic Plasticity and Cyclic Viscoplasticity. *International Journal of Plasticity*, 5, 247-302.

[5] ASTM Standard E 837. Determining Residual Stresses by the Hole-Drilling Strain-Gage Method.

Study of tensile strength and toughness in AISI 304 bidirectional continuous reinforcement fibers metal matrix composite

Ignacio Eguia Cambero[1], Ruben Lostado Lorza[1], Maria Angeles Martinez Calvo[1], Fatima Somovilla Gomez[1], Marina Corral Bobadilla[1], Roberto Fernandez Martinez[2]

[1]Mechanical Engineering Department, University of La Rioja, Spain.

[2]Department of Electrical Engineering, University of The Basque Country UPV/EHU, Bilbao, Spain

ruben.lostado@unirioja.es, roberto.fernandezm@ehu.es

Metal Matrix Composite (MMC) is made by dispersing a reinforcing material embedded and completely continuous into a monolithic material or metal matrix [1]. This paper shows a study of a composite material formed by an aluminium matrix reinforced with bidirectional continuous fibers of AISI 304 stainless steel with three different diameters and wire spacing. The wire diameters studied were 0.26, 0.32 and 0.8 mm, while the wires spacing studied were 1.12, 1.41, and 2.828 mm respectively. All MMC was manufactured by immersing the AISI 304 continuous fibers in the molten aluminum matrix. A radiographic study was developed with the aim of assessing the correct integration of both materials to form the MMC. In addition, a finite element model of the MMC was developed in order to know the distribution of the stresses inside of the bidirectional continuous fibers. A Tensile and toughness tests were developed to know the load capacity of the MMC obtained in comparison with aluminum metal matrix without its bidirectional continuous fibers. In this case, the combination of wire diameter-wire spacing of 0.8-2.828 mm. shows an increase in tensile strength of 46% regarding to unreinforced aluminum. Moreover, the combination of 0.32-1.41 mm demonstrated an increase in toughness of 55% while the combination of 0.26-1.12 demonstrated an increase in toughness of 71.5% both regarding to unreinforced aluminum. From the finite element analysis is observed that the maximum stress obtained for the aluminium is situated close to the perpendicular fibers. By contrast, the maximum stress obtained for the stainless steel is situated in the longitudinal fibers. The results obtained were satisfactory, achieving the improvement of both mechanical properties studied by using the three types of reinforcements proposed.

Keywords: Metal Matrix Composite (MMC), Bidirectional Continuous Fibers, Stainless steel AISI 304, Mechanical Properties, Finite Element Analysis.

[1] MATTHEWS, de FL., RAWLINGS, Rees D. 1999. Composite materials: engineering and science. Elsevier.

Theory of Thermal Expansion of Kondo Lattice Materials

R. Konno[1], N. Hatayama[1]

[1]Kindai Technical College 7-1 Kasugaoka, Nabari-shi 518-0459 Japan.

*E Mail/ r-konno@ktc.ac.jp (***presenting and corresponding author's)**

We investigated thermal expansion of the Kondo lattice model theoretically. Hanzawa and Ohara derived the Ginzburg-Landau free energy based on the periodic Coqblin and Schrieffer model in a half-filled conduction band. They also derived the full free energy. However, an unanswered question is how thermal expansion behaves at elevated temperatures. We succeeded to obtain analytical expressions of thermal expansion at very low temperatures, and near the Kondo temperature, based on the full free energy. At very low temperatures, thermal expansion has an exponential behavior. Near the Kondo temperature, thermal expansion has a T-linear dependence. The thermodynamic Gruneisen's relation is automatically satisfied.

Keywords: Kondo lattice, thermal expansion, Kondo temperature (Maximum Five)

[1] HANZAWA K., & OHARA K. 2007. Asymptotic local moment formation in the Kondo lattice: *Phys. Rev. B, 76*, 184407.

Investigations on the Influence of Substrate Temperature towards the Thermo-mechanical behavior of the CuAlNi/PI Bimorph

Akash K[1], Palani I A[1,2*],

[1]Opto-Mechatronics Lab, Department of Mechanical Engineering, Indian Institute of Technology, Indore, Madhya Pradesh
[2]Centre for Material Science and Engineering, Indian Institute of Technology, Indore, Madhya Pradesh

*palaniia@iiti.ac.in, Contact no: +91 9009356097,

Shape memory alloy/Polyimide bimorphs are flexible films which are more suitable for microactuators, as it can be pre-strained and thus avoiding the training required for SMA's. Cantilever made out of SMA/PI bimorphs developed through sputtering was studied in detail (Kotnur et al. 2013; Kotnur et al. 2014). Recently NiTi/Polyimide composite actuated using a 1.5 V battery as a wing of dragonfly, has paved way for further more microactuators (Ishida 2015; Ishida & Sato 2008). Conversely, CuAlNi shape memory alloy have excellent properties such as high heating and cooling rate, high energy efficiency, high damping capacity and low cost (Lojen et al. 2013; Yuan et al. 2015). However poor ductility and workability, due to inter granular cracking acts as major limitations, which leads to poor cyclic behavior (Dimitris C. Lagoudas 2008).

In this research an attempt has been made to develop CuAlNI/PI bimorph using thermal evaporation at various substrate temperatures and studying their thermo-mechanical behavior. Thermal evaporation acts as a simple and cost effective technique, which can be used in large area depositions also. Cu-Al-Ni/Polyimide bimorph has been developed through direct thermal evaporation method on flexible pre-strained, 50µm thick kapton polyimide sheet. Various substrate temperatures ranging from 50 °C – 200 °C have been used for deposition. The influence of substrate temperature on the structural, morphological and life cycle fatigue of the developed structures has been analyzed. The bimorph structures without any post-processing and training, displayed two way displacement where the return was achieved with the influence of flexible substrate. SEM, XRD and Temperature vs. resistance measurement were used to characterize the bimorph's phase transition temperature. The phase transformation temperature from martensite to austenite was found to be A_s = 215 °C and A_f = 240 °C. To investigate the

maximum displacement, the bimorph was actuated using a substrate heater and maximum displacement of 19 mm observed from the edge of the bimorph.

In addition, to probe suitability of the bimorph in MEMS application, joule heating was used for the analysis of thermo-mechanical behavior. The schematic measurement setup shown in figure 1 (a) consists of Laser displacement sensor, K-type thermocouple, data acquisition system and programmable power supply. Three different voltages 2V, 2.5V and 3V were used for the analysis. Figure 1(b) shows the maximum displacement achieved during with different

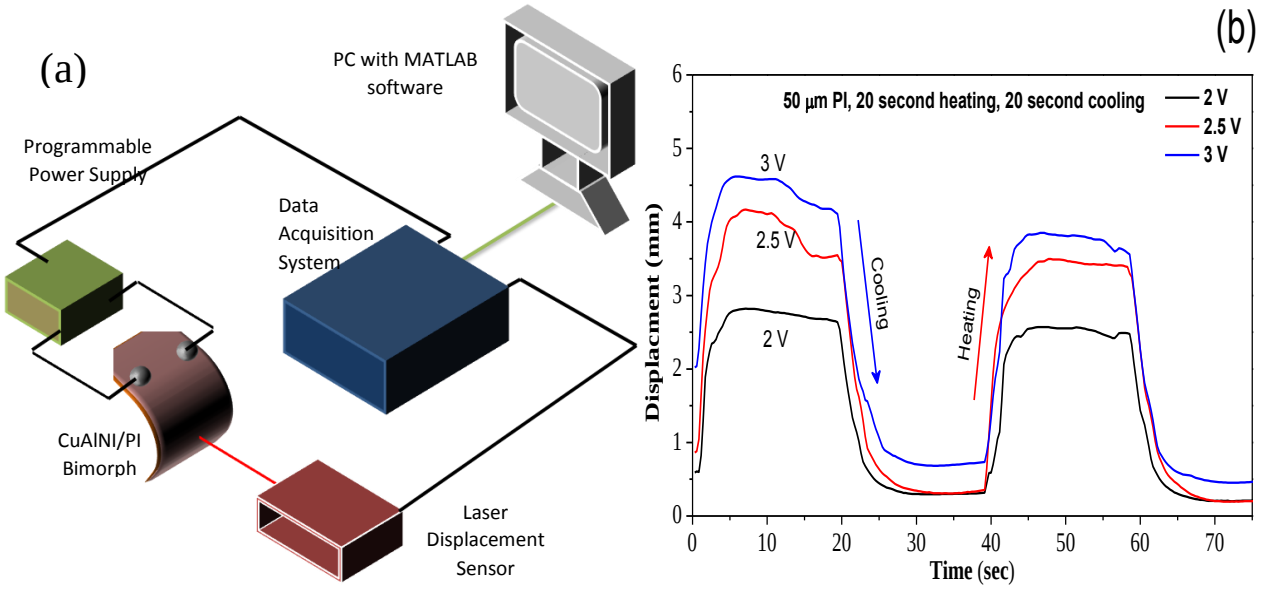

Figure 1 (a) Experimental setup for life cycle analysis (b) Maximum displacement plot at three different voltages for samples deposited without substrate heating

voltages for samples deposited without substrate heating.

Thus it was observed that, at a frequency of 0.5 Hz, the film deposited with substrate heating at 50°C, 100 °C and 200 °C showed a maximum displacement of 0.5, 0.7, 0.8 mm, whereas substrate heating at 150 °C showed a maximum displacement of 1.1 mm with 3 V. There was no reduction in displacement of any bimorphs even after fifty cycles. However the fatigue life and the material properties are to be studied in detail to have a better understanding.

Keywords: Shape Memory Alloys, Thermal Evaporation, Cu-Al-Ni/Polyimide, Thermo-mechanical behavior, Life cycle.

References

Dimitris C. Lagoudas, 2008. *Shape Memory Alloys: Modeling and Engineering Applications*,

Ishida, A., 2015. Ti–Ni–Cu/polyimide composite-film actuator and simulation tool. *Sensors and Actuators A: Physical*, 222, pp.228–236. Available at: http://linkinghub.elsevier.com/retrieve/pii/S0924424714005196.

Ishida, A. & Sato, M., 2008. Ti-Ni-Cu shape-memory alloy thin film formed on polyimide substrate. *Thin Solid Films*, 516(21), pp.7836–7839.

Kotnur, V.G. et al., 2014. Shape memory NiTi thin films deposited at low temperature. *Surface and Coatings Technology*, 258, pp.1145–1151.

Kotnur, V.G., Tichelaar, F.D. & Janssen, G.C. a M., 2013. Sputter deposited Ni-Ti thin films on polyimide substrate. *Surface and Coatings Technology*, 222, pp.44–47. Available at: http://dx.doi.org/10.1016/j.surfcoat.2013.01.058.

Kuribayashi, K. & Fujii, T., 1998. A new micro SMA thin film actuator prestrained by polyimide. *MHA'98. Proceedings of the 1998 International Symposium on Micromechatronics and Human Science. - Creation of New Industry - (Cat. No.98TH8388)*, 2, pp.165–170.

Lojen, G., Gojić, M. & Anžel, I., 2013. Continuously cast Cu-Al-Ni shape memory alloy - Properties in as-cast condition. *Journal of Alloys and Compounds*, 580, pp.497–505.

Weir, P.E. et al., 2008. (12) Ulllted States Patent. , 2(12).

Yuan, B. et al., 2015. Effect of directional solidification and porosity upon the superelasticity of Cu–Al–Ni shape-memory alloys. *Materials & Design*, 80, pp.28–35. Available at: http://linkinghub.elsevier.com/retrieve/pii/S0261306915002393.

Zardetto, V. et al., 2011. Substrates for flexible electronics: A practical investigation on the electrical, film flexibility, optical, temperature, and solvent resistance properties. *Journal of Polymer Science, Part B: Polymer Physics*, 49(9), pp.638–648.

Development of high B_s amorphous alloys with super high ferromagnetic element content

Anding Wang[1,a], Pingbo Chen[1,b], Chengliang Zhao[1,c], Chuntao Chang[1,d], Xinmin Wang[1,e], Run-wei Li[1,f]

[1]Key Laboratory of Magnetic Materials and Devices, Ningbo Institute of Materials Technology & Engineering, Chinese Academy of Sciences, Ningbo, Zhejiang 315201, China.

[a]anding@nimte.ac.cn, [b]chenpingbo@nimte.ac.cn, [c]zhaocl@nimte.ac.cn, [d]ctchang@nimte.ac.cn, [e]jbmgwang@yahoo.co.jp, [f]runweili@nimte.ac.cn

Keywords: Amorphous alloys; Magnetic properties; Amorphous-forming ability.

In the numerous glassy alloy systems, soft-magnetic alloys based on the ferromagnetic elements Fe, Co, Ni and their combination have attracted more interests for their high soft-magnetic performances After decades of development, the production equipment and technology of amorphous soft-magnetic alloy ribbon as well as transformer become mature gradually providing a fundamental guarantee for the large area promotion. However, the commonly used Metglas alloys ($Fe_{78-80}Si_9B_{11-13}$) developed 30 years ago exhibit comparatively lower saturation flux density (B_s) which hinders the miniaturization and reduction of noise[1]. However, the obtaining of high Bs are always at the expense of the amorphous-forming ability (AFA) wich are crucial parameter of manufacturability. Accordingly, breakthrough of the ferromegnetic element content limitation and development of new amorphous alloys with high Bs and adequate AFA are greatly required. In our recent work, high Fe content $Fe_{83}C_1(Si,B,P)_{16}$ amorphous alloys with excellent magnetic properties and high AFA were successfully developed by composition designing and adjusting [2]. Here we will exhibit the roles of minor Co and Ni additions in formation and properties of $Fe_{83}Co_aNi_b(C,Si,B,P)_{17-a-b}$ alloys. As a result, the addition of Co and Ni can effectively increase the limitation of ferromagnetic element content. $Fe_{83}(Co,Ni)_{3-4}(C,Si,B,P)_{12-13}$ alloys with super high ferromagnetic element content which can be easily prepared by single melt spinning method are successfully developed. Interestingly, the ferromagnetic element content is almost equal to that of high Si electrical steel (≈95 wt%). The alloys with minor addition of Co and Ni exhibit high B_s of 1.7 T and excellent soft magnetic properties. The mechanisms of good magnetic properties, high AFA and good ductility for these amorphous alloys were also discussed. The integration of excellent soft-magnetic properties and good manufacturability makes these high Bs alloys promising soft-magnetic materials for industrial applications.

References

[1] Y. Ogawa, M. Naoe, Y. Yoshizawa, R. Hasegawa, J. Magn. Magn. Mater., 304 (2006) E675-E677.
[2] A. Wang, C. Zhao, H. Men, A. He, C. Chang, X. Wang, R.-W. Li, J. Alloys Compd., 630 (2015) 209-213.

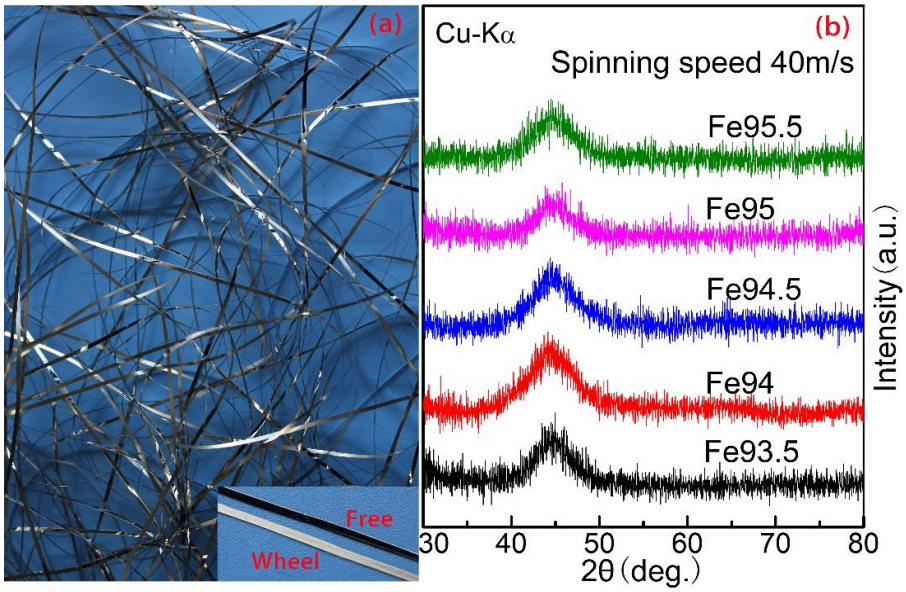
(a)
Free
Wheel
(b)
Cu-Kα
Spinning speed 40m/s
Fe95.5
Fe95
Fe94.5
Fe94
Fe93.5
Intensity (a.u.)
30
40
50
60
70
80
2θ (deg.)

Effect of calcination atmosphere on the structural and magnetic properties of $ZnFe_2O_4$ nanoparticles prepared by Sol-Gel method

Amir Zelati[1*], Ahmad Amirabadizadeh[2], Houshang Safarpour[2]

[1]*Department of Electrical Eng., Technical Faculty of Ferdows, University of Birjand, Iran*
[2]*Department of Physics, Faculty of Science, University of Birjand, Iran*

Abstract

In this report, $ZnFe_2O_4$ nanoparticles were prepared by using Sol-Gel method. To study the effect of calcination atmosphere on the structural and magnetic properties of $ZnFe_2O_4$, the prepared nanoparticles were calcined at 600 ^{0}C in three different atmospheres, Argon, Oxygen and air.

Transmission Electron Microscopy (TEM) and X–Ray Diffraction (XRD) were used for structural characterization and Vibrating Sample Magnetometer (VSM) was used for studying magnetic properties of the samples. XRD analyses show formation of the spinel structure for the samples calcined in Ar and air atmosphere while spinel structure has not been formed in the sample calcined in the O_2 atmosphere. The crystallite sizes were estimated from 30 nm to 60 nm by using Scherrer's formula. Nano-size of the particles were confirmed by TEM results. VSM measurements show that by changing the calcination atmosphere from air to argon the magnetic behavior of the sample vary from paramagnetism to ferrimagnetism. M_{max}, M_r and H_c of the samples were measured by VSM.

* Corresponding Author:
Amir Zelati, PhD in Solid State Physics, Assistant Professor
Email: azelati@birjand.ac.ir; a_zelati@yahoo.com
Tell: +98 915 304 7550

Exotic magnetic order in multiferroic $Mn_{0.85}Co_{0.15}WO_4$ investigated by resonant magnetic x-ray scattering

J. Herrero-Martin[1,2], C. Mazzoli[3], A. N. Dobrynin[4], P. Bencok[4], P. Steadman[4], R. Fan[4], A. A. Mukhin[5], V. Skumryev[6], and J. L. García-Muñoz[2]

[1]ALBA Synchrotron Light Source, Cerdanyola del Vallès, Spain
[2]Institut de Ciència de Materials de Barcelona, ICMAB-CSIC, E-08193 Bellaterra, Spain
[3]Dpto. Fisica, Politecnico di Milano, Milano, Italy
[4]Diamond Light Source, Didcot, Oxfordshire, United Kingdom
[5]Probkhorov General Physics Institute, Russian Academy of Science, Moscow, Russia
[6]Departament de Fisica, Universitat Autònoma de Barcelona, Bellaterra, Spain

jherrero@cells.es

Tuning synthesis towards the induction of magnetic frustration and complex magnetic orders breaking the spatial inversion symmetry is regarded as an effective way of producing multiferroic (MF) and magnetoelectric (ME) materials. $MnWO_4$ and the $(Mn,Co)WO_4$ extended family are reference models for the study of the mutual interaction between spins and polar orders. The introduction of Co favors a strong competition between its magnetocrystalline anisotropy (McA) and Mn-Mn exchange interactions, stabilises the characteristic ferroelectric (FE) behavior of $MnWO_4$ at low temperatures (T), and uplifts the T-x phase diagram richness with the appearance of new FE phases and magnetic structures. Moreover, this family of MFs is intrinsically inhomogeneous since the two different magnetic ions (Mn and Co) occupy the same crystallographic position [1-3].

Employing resonant magnetic soft x-ray scattering (RMSXS) we have investigated in detail the magnetic order in a MF crystal with the $Mn_{0.85}Co_{0.15}WO_4$ critical composition above its FE transition, focusing on the well-known collinear AF4 phase. Thanks to RMSXS chemical selectivity we have demonstrated that Co moments arrange antiferromagnetically following their own strong uniaxial McA, although the collinear order of Mn spins point to a different direction [4]. This implies intrinsic remarkable deviations of the spin arrangement at the local scale from the average description provided by neutron diffraction. These element-resolved magnetic results call for reexamining the phase diagram of this model family of MFs. The occurrence of a similar non-collinearity of ordered spins from different magnetic ions must be investigated in other mixed compounds with competing anisotropic interactions.

Keywords: magnetism, multiferroic, synchrotron radiation, resonant magnetic x-ray scattering

[1] TANIGUCHI K. et al 2008, Phys. Rev. Lett., 101, 207205
[2] SONG Y.-S. et al 2010, Phys. Rev. B, 82, 214418
[3] URCELAY-OLABARRIA I. et al 2015, Phys. Rev. B, 91, 104429
[4] HERRERO-MARTIN J. et al 2015, Phys. Rev. B, 91, 220403(R)

Non-homogeneity of crystallization behavior and magnetic properties of high B_s FeSiBCu nanocrystalline soft magnetic alloys

Anding Wang[1,a], Tao Liu[1,b], Aina He[1,c], Chuntao Chang[1,d], Xinmin Wang[1,e], Run-wei Li[1,f]

[1]Key Laboratory of Magnetic Materials and Devices, Ningbo Institute of Materials Technology & Engineering, Chinese Academy of Sciences, Ningbo, Zhejiang 315201, China.

[a]anding@nimte.ac.cn, [b]zhaocl@nimte.ac.cn, [c]menhe@nimte.ac.cn, [d]ctchang@nimte.ac.cn, [e]jbmgwang@yahoo.co.jp, [f]runweili@nimte.ac.cn

Keywords: Nanocrystalline alloys; Magnetic properties; Non-homogeneity.

For nanocrystalline soft-magnetic alloys, it is crucial to form homogeneous embedding structure of α-Fe grains with ultrafine size and random orientation by controlling crystallization process[1]. It has been proved that the α-Fe primary phase precipitated in the solidification process plays important roles in increasing the density and refining the grain size during the subsequent annealing process[2]. However, the distribution and size of α-Fe primary phase in the ribbon sample is affected by the cooling rate gradient and technological parameters. Better understanding of the crystallization behavior and its effect on magnetic properties are important for further improvements of performance and manufacturability. In our recent work, the non-homogeneity of crystallization behavior and magnetic properties of high B_s FeSiBCu nanocrystalline alloys were studied systematically. It is found that three layers with different microstructure (shown in Fig.1) were formed along the cross-section direction during the solidification process. Second crystal nucleus formed in the layer with low density of primary phase near the wheel side during annealing treatment. α-Fe primary phase and second crystal nucleus grow non-uniformly in the normal annealing process. The non-homogeneity of the α-Fe primary phase lead to different and asynchronized crystallization processes (shown in Fig.2), which weaken the competing effects between grains as well as increase the average grain size and width of the grain-size distribution. The ribbon preparation parameters dependences of density and distribution of primary phase were determined. The formation mechanism of the primary phase in the melt-spun sample were also revealed, by investigating the non-uniform microstructure of the as-spun sample and analyzing the kinetics and thermodynamic of the solidification process. These results will provide a theoretical basis for the design of composition and heat treatment process.

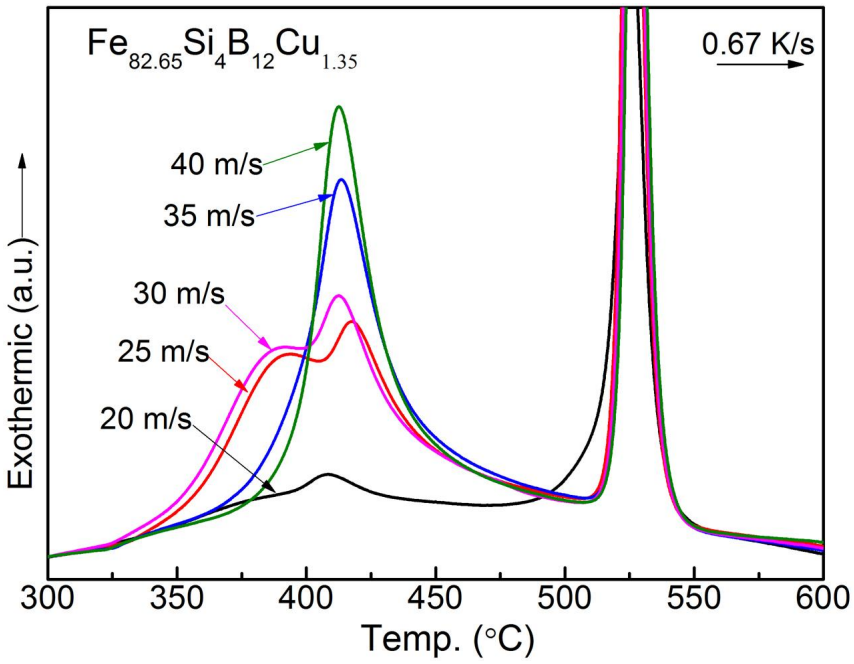

Fig.1 DSC curves of $Fe_{82.65}Si_4B_{12}Cu_{1.35}$ alloy ribbons prepared with different wheel speed.

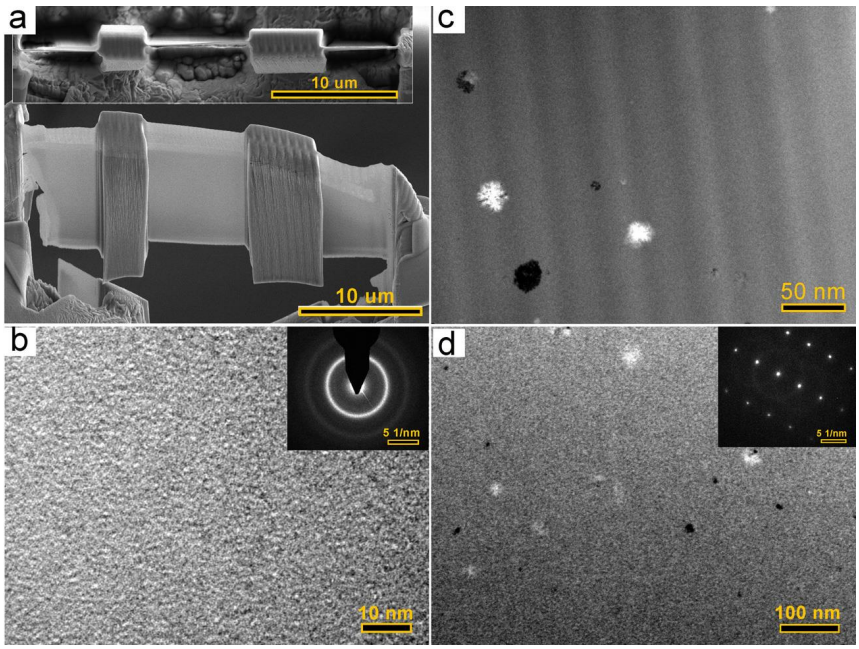

Fig.2 (a) TEM sample for cross-section observation. (b-d) TEM images of different layers.

References

[1] G. Herzer, Acta Mater., 61 (2013) 718-734.
[2] M. Ohta, Y. Yoshizawa, M. Takezawa, J. Yamasaki, IEEE Trans. Magn., 46 (2010) 203-206

Tunable competition and possible coexistence of magneto-electric phases in a charge ordered manganite

S. Dash

Dept. of Physics and Astronomy, National Institute of Technology Rourkela, Rourkela, Odisha, India-769008.

E-Mail : **dsuryanarayan@gmail.com**

The magnetoelectric (ME) effect, i.e., cross control of magnetization (electric polarization) by an external electric (magnetic) field, may introduce a new design principle for novel spin devices. However, it has been a long-standing challenge to enhance the magnetoelectric effect. There are two known magnetoelectric effects: a conventional linear magnetoelectric effect in a centrosymmetry-broken magnet and a recently explored nonlinear magnetoelectric effect associated with a magnetic phase transition. To enhance the ME signal, effective control of a phase competition has recently been revealed as a promising approach. Here, we report the magnetic field control of the distinct ME phases in a charge ordered magnet $Pr_{0.75}Na_{0.25}MnO_3$, in which an antiferromagnetic (AFM) phase is competing with a ferromagnetic (FM) phase. Charge ordered magnetic compounds are a far more promising class of materials with potentially large magnetoelectric coupling. The material is prepared by wet chemical route at low sintering time and temperature in order to maintain the Na stoichiometry. The phase purity and structure is well studied through different techniques. The temperature evolution of resistivity and dielectric shows anomaly at charge ordering (CO) transition. With rise in temperature raises the dielectric parameter upto CO and then decreases. The rise in this region is probably due to the formation of polar regions. However, at different frequency, the slope change in dielectric permittivity and peak in loss tangent are uncorrelated signifies this system to be a relaxor. The magnetic field dependent dielectric behavior is highly correlated but in contrast to their resistivity. Surprisingly, the dielectric parameter follows the magnetic signal. The variation of dielectric permittivity with field is intrinsically associated with the coexisting phases of contrasting order. However, the ground state of this system is proved to be ferromagnetic. Using suitably experimental protocol the magnetic phases as well as electronic phases can

be tuned effectively at low magnetic field vis-à-vis to enhance the ME signal. Moreover, the FM in the proximity of AFM phase enhance the functionality of this materials with a several order in the ME parameter. The apparent change in ME signal in accordance with macroscopic phase competition are modelled through Maxwell's dynamical theory. We envisage that this short of studies will renders valuable information for other materials which shows similar behavior.

Keywords: Magnetoelectric, manganite, competing phase, functional, spin device

[1] DAGOTTO, E., 2003. Nanoscale Phase Separation and Colossal Magnetoresistance (Springer-Verlag, Berlin, 2003), and references therein.

[2] DASH, S., BANERJEE, A., & CHADDAH, P., 2013. Magnetodielectric response of coexisting phases in half doped manganites. *JAP*, 113, 17D912.

[3] SATOH, T., KIKUCHI, Y.,MIYANO,K.,& JIRÁK.Z., 2002, Irreversible photoinduced insulator-metal transition in the Na-doped manganite $Pr_{0.75}Na_{0.25}MnO_3$., Phys. Rev. B 65, 125103

[4] LANDAU, L. D., 1960. Electrodynamics of Continuous Media, 2nd ed. (Pergamon Press, 1960), pp. 42–44.

[5] COHEN, R. W., CODY, G. D. COUTTS, M. D. & ABELES, B. 1973, Optical Properties of Granular Silver and Gold Films, Phys. Rev. B 8, 3689-3701

Effect of Ca and CaO on the synthesis of $Nd_2Fe_{14}B$ particles by reduction-diffusion process

Dongsoo Kim[1,2], Jongbin Ahn[1,2], Chuljin Choi[2]

[1]Convergence research center for development of mineral resources, Korea Institute of Geoscience and Mineral Resources, 124, Gwahakro, Yuseonggu, Daejeon, 34132, Korea

[2]Powder & Ceramics Division, Korea Institute of Materials Science, 797, Changwondaero, Seongsangu, Changwon, Gyeongnam, 51508, Korea

dskim@kims.re.kr/ +82-42-868-3839

Since Nd-Fe-B magnet was first discovered by Sagawa et al. [1], many kinds of methods have been developed to fabricate magnetic powders, such as powder metallurgical, rapidly quenching and reduction-diffusion (R-D) processes. Nowadays, powder metallurgical and rapidly quenching methods are commonly used. But both of them need several processes for obtaining fine particles and increase the production cost due to the use of high purity of metals as raw materials. Compared with these methods, main advantages of R-D process are the use of a relatively inexpensive Nd oxide as raw material and the direct production of fine alloy powder suitable for further procedures. In this study, a novel route to prepare Nd-Fe-B magnetic particles by utilizing spray drying and reduction-diffusion process was proposed. Precursors were prepared by spray drying method from the aqueous solutions containing Nd salt, Fe salt and boric acid with stoichiometric ratio. The spray dried particles were desalted at 800 ℃ for 2 hours in air, followed by ball milling. In order to reduce iron oxides, heat treatment of the milled powders was performed under H_2 atmosphere. Then, Calcium (Ca) as a reducing agent in R-D process was mixed with powders obtained by H_2 reduction in appropriate ratio. The R-D of the compacts was carried out at 1000 ℃ for 3 hours in Argon (Ar) atmosphere. For the effective washing, the compact was pulverized to coarse granules and the granules were washed with water several times to achieve $Nd_2Fe_{14}B$ powders. The phases and the magnetic properties of the particles were examined with X-ray diffractometer, Scanning electron microscopy and vibrating sample magnetometer. XRD patterns of each step in this procedure as shown in Fig. 1 depicted that precursors obtained by spray

drying was amorphous structure due to volatile compounds and physical adsorption of elements. They were crystallized into oxides of Nd and Fe through desalting at 800 ℃. And then ball milling was performed to triturate the aggregates after desalting. As shown in Fig. 1, Fe oxides were reduced to α-Fe by heat treatment in H_2 atmosphere. After mixing and compacting with reduced powders in H_2 and exceeded Ca and CaO granules, R-D process was carried out. CaO was added in R-D step for the stabilization of reduction reaction and also for the effective disintegration with water in washing step. $Nd_2Fe_{14}B$ particles were formed and CaO and unreacted Ca were remained. This result was similar to that from the reference by Kim et al. [2]. The final step of washing was performed using water to wash out CaO for 1–3 hours. (BH)max of the washed powders reached to 13.6 MGOe after washing for 1 hour with de-ionized water. To reduce nonmagnetic phase, the ball milling under an ethanol was added into the washing step. The final magnetic property was enhanced to 16.7 MGOe of (BH)max as shown in Fig. 2. This demonstrates that our process is a promising route for fabrication of Nd-Fe-B magnetic powders, especially for recycling of the Nd magnets.

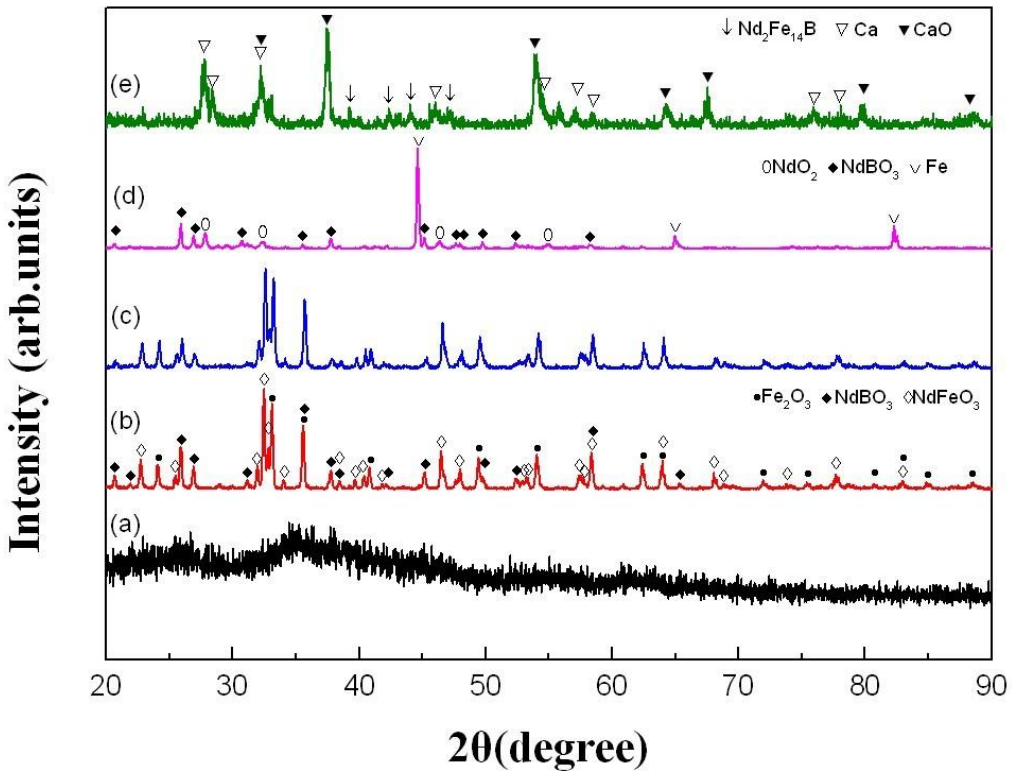

Fig. 1. XRD patterns of powders after (a) spray-drying, (b) desalting, (c) ball milling, (d) H_2 reduction and (e) Ca reduction

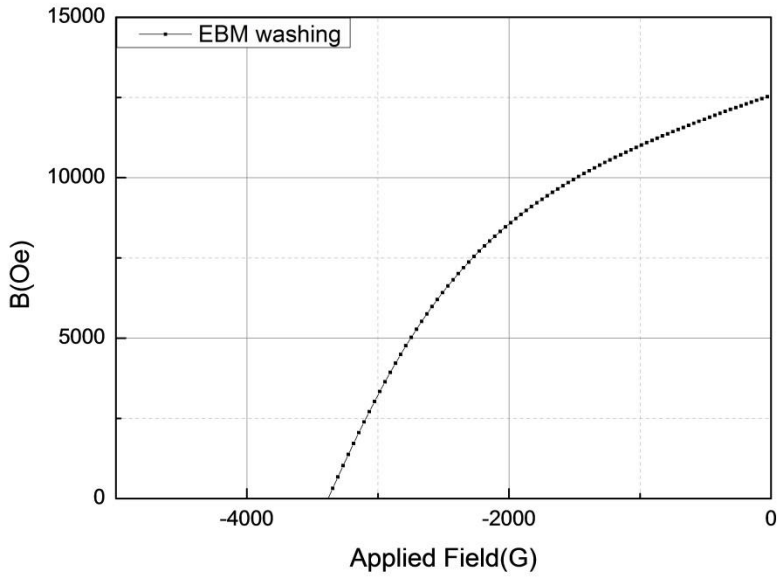

Fig. 2. Demagnetization curve of $Nd_2Fe_{14}B$ powder after ethanol balling milling and washing process

Keywords: Nd-Fe-B powders, Spray Drying, CaO, Reduction-Diffusion, Washing

[1] M. SAGAWA, S. FUJIMURA, M. TOGAWA, H. YAMAMOTO, Y. MATSUUEA, 1984. New material for permanent magnets on a base of Nd and Fe. *J. Appl. Phys.*, 55, 2083-2087.

[2] C.Q. CHEN, D. KIM, C.J. CHOI, 2014. Influence of Ca amount on the synthesis of $Nd_2Fe_{14}B$ particles in reduction-diffusion process. *J. Mag. Mag. Mater.*, 355, 180-183.

Formation of CoFe-based bulk metallic glasses with high thermoplastic formability

Qikui Man[a,b], Diana Estevez[a,b], Zhe Li[a,b], Yaqiang Dong[a,b], Chuntao Chang[a,b,*] Xinmin Wang[a,b], Run-Wei Li[a,b]

[a] *Key Laboratory of Magnetic Materials and Devices, Ningbo Institute of Materials Technology and Engineering, Chinese Academy of Sciences, Ningbo 315201, China*

[b] *Zhejiang Province Key Laboratory of Magnetic Materials and Application Technology, Ningbo Institute of Materials Technology and Engineering, Chinese Academy of Sciences, Ningbo 315201, China*

[*] Corresponding authors: Chuntao Chang*

Tel.: +86-574-87911392

Fax: +86-574-87911392

E-mail address: ctchang@nimte.ac.cn

Postal address: Key Laboratory of Magnetic Materials and Devices, Ningbo Institute of Materials Technology and Engineering, Chinese Academy of Sciences, No. 1219 Zhongguan West Road, Zhenhai District, Ningbo 315201, P. R. China.

Abstract

A new class of CoFeNbMB (M=Er, Tb, Y, Dy) bulk metallic glasses with a large supercooled liquid region is reported. Optimized quinary alloys exhibit supercooled liquid regions reaching 130 K and critical casting diameters up to 4 mm. It was found that the small addition of Er, Tb, Y and Dy leads to the significant extension of the supercooled liquid region as well as the increase of glass forming ability. At room temperature, this bulk metallic glass system exhibits high strength and Vickers hardness over 4300 MPa and 1147, as well as good soft-magnetic properties. However, the compressive behavior can completely change to Newtonian flow when temperature rises up to glass transition temperature. The high thermal stability of this glassy alloy system offers an enough processing window to thermoplastic forming (TPF), and the strong processing ability was examined by simple micro-replication experiments. It is demonstrated that the TPF formability on length scales ranging down to nanometers can be achieved in the selected experimental condition. Furthermore, nearly full density bulk samples have been fabricated by the powder metallurgy technique. These bulk metallic glasses with high thermal stability, good mechanical properties, high thermoplastic formability and good soft-magnetic properties could have potential for use in engineering applications.

***Keywords*:** Metallic glass; Thermoplastic forming; Glass transition and crystallization; Mechanical properties; Magnetic properties.

A Dual-polarized Metamaterial-based Cloak

Islam[1], Faruque[1], Islam[2]

[1]Space Science Centre (ANGKASA),

[2]Dept. of Electrical, Electronic and Systems Engineering,

Universiti Kebangsaan Malaysia

E Mail: rashed@ukm.edu.my

After the invention of metamaterial, it is being utilized in many interesting fields of electromagnetic arena including cloak design. An electromagnetic cloak can hide an object electromagnetically. Usually a good cloak reduces the normalized scattering width (NSW) of an object below one [1]. An object can be hidden electromagnetically if it does not scatter wave in any direction. Previously few studies were performed on metamaterial-based cloak. However, most of the cloaks were cylindrical in shape. Very few metamaterial-based non-cylindrical cloaks were proposed in the literature but their cloaking performances were not demonstrated for dual polarized operations and wideband applications. Recently, in [2], a two-component near zero refractive index (NZRI) metamaterial-based rectangular single layer cloaks was proposed but cloak operation was not proven for dual polarization. Moreover, their cloak not operates for multi-band or wideband region. Another, metasurface based cloak was claimed in [3] for dual incident polarization but it was applicable for C-band only. Moreover, it was a cylindrical-shaped cloak. In this study, a design of a new metamaterial for dual polarized electromagnetic cloaking operation is presented. Initially, a bare-H-shaped metamaterial unit cell was designed on FR-4 substrate material. The metamaterial exhibits an epsilon-negative property in the certain region of C- and X-band of microwave spectra. Experimental transmittance for the metamaterial is provided. The metamaterial was then utilized in designing a rectangular-shaped electromagnetic invisibility cloak. The cloak hides a metal cylinder for dual polarized operation. Scattering reduction technique was adopted for performing the cloaking operation. The cloak shows normalized scattering width below one from the frequency of 5.04GHz to 9.47 GHz that covers certain region of C- and X-band of microwave spectra. It is a promising design for its single layer, multi-band and dual polarized cloaking operation.

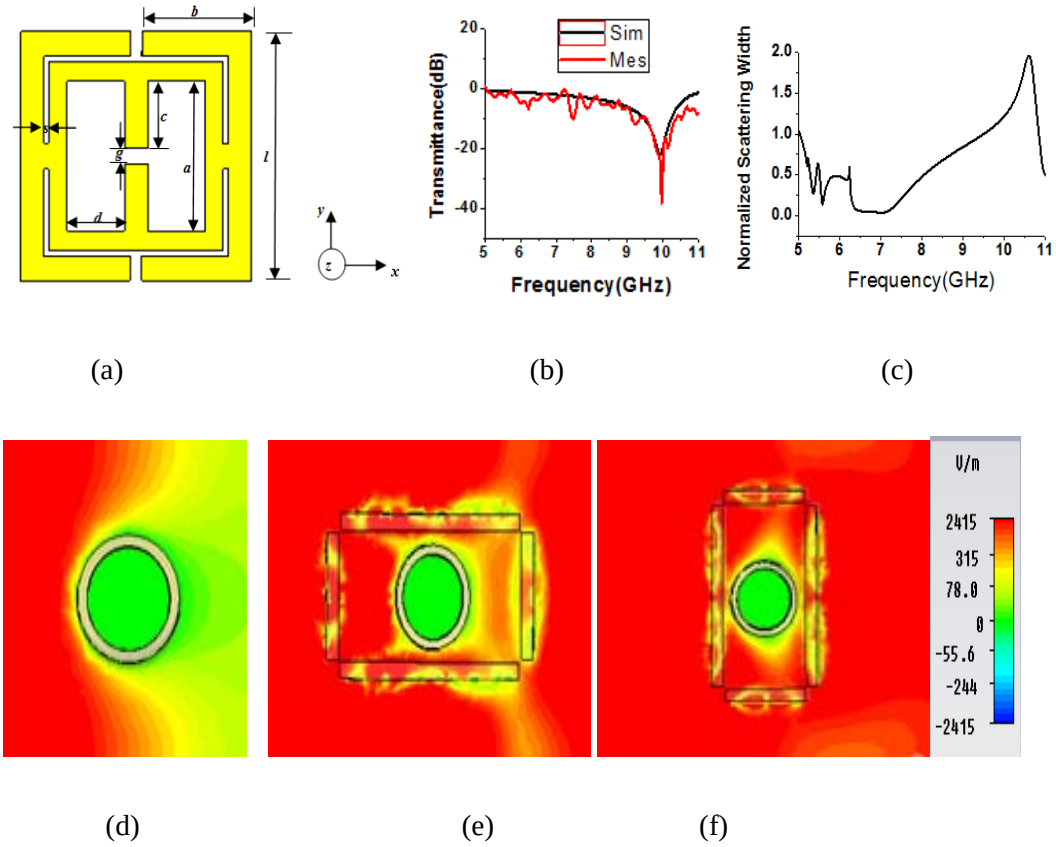

(a) (b) (c)

(d) (e) (f)

Figure: (a) metamaterial unit cell with parameter *a=6, b=4.77, c=2.77, d=2.50, s=0.2, g=0.66, l=10* all in mm scale 20X20 mm^2 substrate (b) transmittance of the metamaterial unit cell (c) NSW of cloaked and uncloaked object (d) E-field distribution of bare object (e) E-field distribution of cloaked object from horizontal side (f) E-field distribution of cloaked object from vertical side

Keywords: cloak, metamaterial, dual-polarization

[1]. WANG, X., CHEN, F., & SEMOUCHKINA, E. 2013.Implementation of low scattering microwave cloaking by all-dielectric metamaterials. IEEE Microwave and Wireless Component Letters, 23, 63–65.

[2]. ISLAM, S. S., FARUQUE, M.R. I., & ISLAM, M. T. 2015. A two-component NZRI metamaterial based rectangular cloak. AIP Advances, 5, Article ID 107116:1-9.

[3]. MONTI, A., SORIC, J.C. & ALU, A. 2015. Anisotropic mantle cloaks for TM and TE scattering reduction. IEEE Transactions on Antenna and Propagation, 63, 1775-1787.

APTES modified Cellulose Nanocrystals-reinforced Vinyl Epoxy Resin: Fabrication and Mechanical Properties

L. Thompson, M. Nikzad, I. Sbarski, J. Miller, A. Yu

Faculty of Science, Engineering and Technology; Swinburne University of Technology, Melbourne, Australia

Abstract

A new surface modification route for Cellulose Nanocrystals (CNC) is implemented using an aminopropyltriethoxysilane (APTES) solution to improve their dispersion within a Vinyl Ester resin. The objective is to enhance mechanical properties of the vinyl ester based nanocomposites reinforced with functionalised CNC nano particles. Nano-scale dispersion of the CNC particles proves to be a key factor in maximising mechanical properties of the matrix and keeping the nanofiller content to an optimal minimum. Surface functionalization of CNC particles by APTES has been effective in converting their native hydrophilic nature into hydrophobic one necessary for dispersion in an organic network.

Tensile strength and modulus of the matrix was found to have peaked around 1-1.15% w/v loading of the CNC particles whereas higher loading had negative impact on the properties due to agglomeration of the nano particles and formation of micro inclusions.

Dynamic Mechanical Analysis (DMA) showed an approximate 1 GPa rise in the storage modulus of the CNC reinforced vinyl ester matrix compared to the neat resin. Loss modulus of the matrix of the rubbery phase beyond 100 °C remained unaffected indicating little or no impact on the complex viscosity of the resultant composite at lower loading of CNC nanoparticles.

APTES based surface treatment of CNC particles is shown as a promising route to enhance dispersion of these nano particles as reinforcing fillers in vinyl ester based composite structures for use in a myriad of industrial applications.

Biomechanical evaluation of the load-bearing fiber-reinforced composite plates intended for the treatment of long bone fractures

Moritz N[1], Mattila R[1], Vallittu PK[1]

[1]Department of Biomaterials Science, Institute of Dentistry, University of Turku, Turku, Finland and Biocity Turku Biomaterials Research Program, Turku Clinical Biomaterial Centre – TCBC and City of Turku Welfare Division, Itäinen Pitkäkatu 4B (PharmaCity), FI-20520 Turku, Finland

Contact information: Niko Moritz, Email niko.moritz@utu.fi, Tel. +358 2 333 8227

Objectives: The state of the art treatment for long bone fractures includes the application of metallic cortical screws and/or locking head screws in a locking compression plate (LCP) through open reduction and internal fixation. Nevertheless, metallic implants have intrinsic drawbacks. Low fatigue resistance, unfavorable load distribution and interference with diagnostic imaging are among them.

Fiber-reinforced composite (FRC) technology developed at the University of Turku is based on bisphenol-A-glycidyldimethacrylate (BisGMA) and triethyleneglycoldimethacrylate (TEGDMA) polymer matrix reinforced with E-glass fibers. This FRC material combines the benefits of lower elastic modulus, high strength and adequate fatigue resistance.

The overall objective of this work was to develop novel load-bearing FRC plates which could potentially replace the metallic counterparts. In particular, this study was dedicated to the biomechanical testing of FRC plate prototypes before their implantation in a large animal model in a weight-bearing bone (femur in the minipig).

Experimental: Commercially available human stainless steel LCP plates (Synthes) with a length of 116 mm served as controls. The plates were bent to a curvature radius of ~ 290 mm. Implants mimicking the shape of the control LCP plate were manufactured from the FRC. The plates had a sandwich structure with a core made of unidirectional fibers covered on both (interior and

exterior) surfaces by two layers of braiding. Biomechanical testing was performed according to ISO 9585 standard (4-point bending). Experimental groups are shown in Table 1.

Results, accomplishments significance and advancement over previous research:

Table 1. Results of the biomechanical test

Parameter	**Experimental groups**			
	FRC plates without holes (n=7)	FRC plates with 6 holes (n=6)	Control LCP plates with 6 holes (n=5)	minipig femurs (n=5)
Cross-sectional area [mm^2]	105.7	105.7	70.2	169.6
F_{max} (Proof load) [kN]	7.9	4.2	7.3	5.4
Deflection at F_{max} [mm]	5.5	5.1	3.7	4.3
Strength at F_{max} [MPa]	602	322	1431	40.7
Stiffness [Nm^2]	21.4	11.4	27.5	22.2
Bending moment [Nm]	53.6	28.6	46.5	37.3
Flexural modulus [GPa]	30.7	16.5	142	2.9

As expected, drilling of holes weakened the FRC structure; however, the strength of the plate was 8-fold higher compared to that of the minipig femur.

FRC implants based on BisGMA-TEGDMA, have gained significant interest in recent years. In craniofacial reconstructions, FRC implants have been successfully used to treat large size bone defects [1]. Various types of FRC implants were investigated for non-load bearing [2, 3] and load-bearing implant applications [4, 5].

This is the first study to address the mechanical properties of BisGMA-TEGDMA based FRC plates intended for the treatment of long bone fractures. The proposed FRC plates are suitable for implantation in a large animal model in a weight-bearing bone.

Keywords: Fiber-reinforced composite, load-bearing, implant, bone

[1] AITASALO, K.M., PIITULAINEN, J.M., REKOLA, J., VALLITTU, P.K. 2014. Craniofacial Bone Reconstruction With Bioactive Fiber-Reinforced Composite Implant. *Head Neck*,36,722-728.

[2] TUUSA, S.M., PELTOLA, M.J., TIRRI, T., LASSILA, L.V., VALLITTU, P.K. 2007. Frontal Bone Defect Repair with Experimental Glass-Fiber-Reinforced Composite with Bioactive Glass Granule Coating. *J Biomed Mater Res B Appl Biomater*, 82, 149-155.

[3] TUUSA, S.M-R., PELTOLA, M.J., TIRRI, T., PUSKA, M.A., RÖYTTÄ, M., AHO, H., SANDHOLM, J., LASSILA, L.V.J., VALLITTU, P.K. 2008. Reconstruction of Critical Size Calvarial Bone Defects in Rabbits with Glass-Fibre-Reinforced Composite with Bioactive Glass Granule Coating. *J Biomed Mater Res B Appl Biomater*, 84, 510-519.

[4] ZHAO, D.S., MORITZ, N., LAURILA, P., MATTILA, R., LASSILA, L.V.J, STRANDBERG, N., MÄNTYLÄ, T., VALLITTU, P.K., ARO, H.T. 2009. Development of a Multi-Component Fiber-Reinforced Composite Implant for Load-Sharing Conditions. *Med Eng Phys*, 31, 461-469.

[5] MORITZ, N., STRANDBERG, N., ZHAO, D.S., MATTILA, R., PARACCHINI, L., VALLITTU, P.K., ARO, H.T. 2014. Mechanical Properties and In Vivo Performance of Load-Bearing Fiber-Reinforced Composite Intramedullary Nails with Improved Torsional Strength. *J Mech Behav Biomed Mater*, 40C,127-139.

Cross-Linking vs. Reduction: How to Improve the Mechanical Performance of Graphene Oxide/Polyvinyl Alcohol Composite Film

Cheng-an (Tao), Hao (Zhang), Fang (Wang), Jian (Huang), Jianfang (Wang)*

College of Science, National University of Defense Technology, Changsha, 410073, P. R. China.

Tca02@mails.thu.edu.cn;Wangjianfang@nudt.edu.cn

Polymer composites have attracted a great deal of attention from industrial and academic fields because of their improved properties benefiting from the reinforcement of nanofillers[1]. Graphene oxide (GO), which consists of a two-dimensional carbon skeleton sheet bearing lots of hydrophilic oxygen-containing groups, can be readily dispersed in water as individual sheets to form stable colloidal suspensions[2]. Meanwhile, benefit from these oxygen funntional groups, GO sheets can interact strongly with polar groups of polymers to form GO/polymer composites. Recently, it's reported that GO is an effective mechanical reinforcement nanofiller for polymer composites. The reduction of GO can further improve the mechanical property of its composite. And the cross-linking interaction between polymer matrix and GO also can increase the mechanical performance. But how to influence the mechanical performance of the composite when reduction marries with cross-linking has not been explored.

Herein, GO/Polyvinyl Alcohol(PVA) composite films (denoted as GO/PVA) were prepared by simple solution mixing method. GO/PVA composite film was reduced by soaking in HI solution, the product was denoted as GO/PVA-Red. While the cross-linked GO/PVA (GO/PVA-CL) composite was obtained by soaking GO/PVA film in glutaraldehyde solution. Moreover, GO/PVA-Red and GO/PVA-CL were cross-linked and reduced respectively to yield GO/PVA-Red-CL and GO/PVA-CL-Red composite film. The mechanical performance of above-mentioned various GO/PVA composite films were investigated. Take the GO/PVA composite with 20wt% GO content as an example, the tensile strength of GO/PVA can be increased by 33.2% (from 59.6 MPa to 79.4 MPa) through HI reduction, while improved by 63.9% through cross-linking. It indicates that cross-linking has more effect than reduction on the mechanical property of GO/PVA composite film. When the GO/PVA composite has been cross-linked thoroughly, the GO

sheets were constrained tightly. So GO is hard to be reduced, and accordingly, the enhancement of the tensile strength is only 6.3%. The tensile strength of GO/PVA-Red-CL was up to 112.8 MPa, which is higher than that of GO/PVA-CL-Red, which is produced by cross-linked first and reduced then. It indicates that the order of cross-linking and reduction can also affect the performance of the produced composite. The reasonably comprehensive use of reduction and cross-linking presents a new approach to develop graphene-based composite materials with high mechanical performance and other great properties.

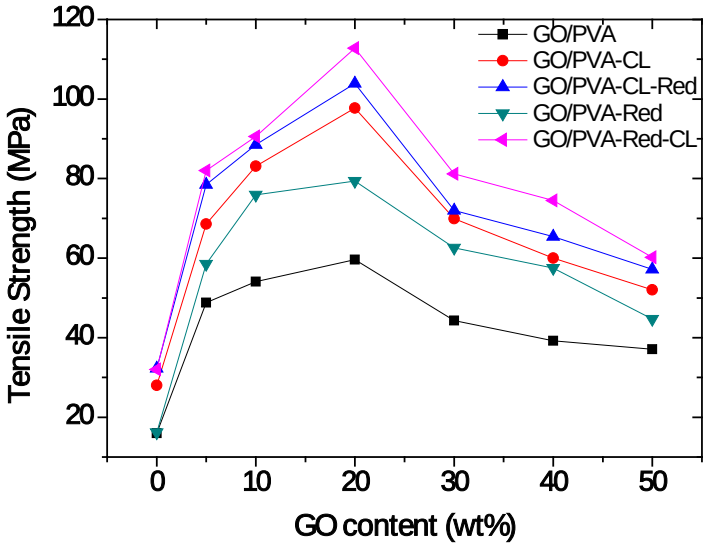

Fig.1 Tensile strength of various GO/PVA composite films

Keywords: Graphene, composite, mechanical, polymer, film

[1] TAO, C., WANG, J., QIN, S., LV, Y., LONG, Y., ZHU, H. & JIANG, Z. 2012. Fabrication of pH-Sensitive Graphene Oxide-Drug Supramolecular Hydrogels as Controlled Release System. *J. Mater. Chem.*, 22, 24856-24861.

[2] TAO, C., ZOU, X., HU, Z., LIU, H. & WANG, J. 2014. Chemically Functionalized Graphene/Polymer Nanocomposites as Light Heating Platform. *Polymer Composites*, DOI: 10.1002/pc.23303.

Development of copper metal matrix hybrid composite and its mechanical properties

Manvandra Kumar Singh[1]*, Rakesh Kumar Gautam[1]
[1]Indian Institute of Technology (Banaras Hindu University)-Varanasi, 221005, U.P. (India)
Corresponding Author's Email- *mksingh.rs.mec13@itbhu.ac.in, (Mob. No. +91-9532235509)*

Abstract

Since copper has very nice electrical, thermal and corrosion resistance properties but it does not have good mechanical and tribological properties, so this work is totally inclined towards the advancement of these inferior properties of copper. So to fulfill these requisite properties of copper the stir casting technique is used to develop such copper metal matrix hybrid composite. Commercial copper is taken as matrix materials and tungsten carbide (WC), boron carbide (B_4C) and boron nitride (BN) are taken as reinforcement with some weight percentage. The characterizations of this developed copper hybrid composite is done with the help of X-rays diffraction, optical microscope and Scanning electron microscope to assure that this develop hybrid composite is containing the reinforcements with phases. The density of the hybrid composite is lower than its matrix it is because of the reinforcement of some lower dense materials but the tensile strength and hardness much better than its matrix even its compressive strength is too much better than its matrix this is due the reinforcement of harder materials and involving some strengthening mechanism. So this work is fruitful to achieve those requisite properties of copper.

Keywords: *Stir Casting, Metal Matrix Composite, Tensile Strength, Hardness, Density, etc.*

[1] HANSANG KWON, SEUNGCHAN CHO, MARC LEPAROUX and AKIRA KAWASAKI, "Dual nano particulate-reinforced aluminum matrix composite materials". Nanotechnology 23 (2012) 225704 (9pp).

[2] C.S. RAMESH, R. NOOR AHMED, M.A. MUJEEBU, M.Z. ABDULLAH, "Development and performance analysis of novel cast copper–SiC–Gr hybrid composites". Materials and Design 30 (2009) 1957–1965.

Effect of the Metallic Particles on the Mechanoluminescence Properties of Cu-doped ZnS

Donghyeon Ryu[1*] and George Hoover[1]

[1] Department of Mechanical Engineering, New Mexico Tech, 801 Leroy Place, Socorro, NM 87801

[*]*Email: donghyeon.ryu@nmt.edu*

Copper-doped ZnS (ZnS:Cu) crystals are known to exhibit photoluminescence (PL) and mechanoluminescence (ML) and have strong potential as a next generation light source, sensor, and energy harvester. While PL of ZnS:Cu is explained well, ML mechanism of ZnS:Cu is not completely understood [1-3]. Chandra *et al.* [2, 4] explained that the ML light emission of ZnS:Cu was due to the hole-electron recombination at Cu^{+}-doping sites, which was forced by the local piezoelectric effect. Shin *et al.* [3] recently indicated the importance of the presence of Al coating on ZnS:Cu crystals. It was known that the band bending due to Schottky barrier between Al and ZnS:Cu resulted in built-in potential gradient, which helped electron transition from Fermi level of Al to ZnS:Cu conduction band. ML light was emitted when the electrons and holes are combined at Cu^{+}-doping sites.

The research objective is to investigate the effect of metallic particles interfacing with ZnS:Cu crystals on the ML properties of ZnS:Cu crystals. ZnS crystals and ZnS:Cu crystals without any metallic coating (ZnS:Cu) were synthesized. Preliminary studies were conducted to compare the fluorescence and crystalline structures of the synthesized ZnS and nm-ZnS:Cu crystals to the commercial Al-coated ZnS:Cu (Al-ZnS:Cu) crystals. First, it was shown that both ZnS:Cu and Al-ZnS:Cu crystals exhibited similar excitation and fluorescence peaks at 320 nm and 455 nm, respectively. Similar peaks indicate that there is no effect of Al coating on the fluorescence properties. On the other hand, the excitation and fluorescence peaks occurred at 280 nm and 430 nm, respectively, in ZnS crystals. The different peaks between ZnS and ZnS:Cu seem to be due to the presence of Cu^{+}-doping. Second, X-ray diffractometer (XRD) revealed that both ZnS:Cu and Al-ZnS:Cu crystals commonly have cubic ZnS crystalline structures based on the three peaks

at 28.6°, 47.8°, and 56.7°, which correspond to (111), (220), and (311) lattice planes, respectively. Due to smaller size of the ZnS:Cu crystals (diameter = ~800 nm) than the Al-ZnS:Cu (diameter = ~23 μm), the XRD peaks of ZnS:Cu crystals were more broadened than the Al-coated one.

In this study, the ML properties of ZnS:Cu will be investigated when interfaced with metallic particles and compared with the ML properties of Al-ZnS:Cu. Metallic particles will be blended together with ZnS:Cu in elastomeric polydimethylsiloxane (PDMS) to prepare elastomeric test specimens. As a reference specimen, Al-ZnS:Cu/PDMS composites will be also prepared. These test specimens will be subjected to the cyclic loadings at various strain levels. ML light emission of the test specimens will be characterized using a video camera to quantify light emission by conducting image processing as done by Ryu *et. al* [5]. Furthermore, the environment effects on the ML properties of the ZnS:Cu/PDMS composites will be studied.

Keywords: Cu-doped ZnS, metallic particles, mechanoluminescence

[1] UMMARTYOTIN, S., BUNNAK, N., JUNTARO, J., SAIN, M. & MANUSPIYA, H. 2012. Synthesis and Luminescence Properties of Zns and Metal (Mn, Cu)-Doped-Zns Ceramic Powder. *Solid State Sciences,* 14(3), 299-304.

[2] CHANDRA, B. P., CHANDRA, V. K. & JHA, P. 2015. Piezoelectrically-Induced Trap-Depth Reduction Model of Elastico-Mechanoluminescent Materials. *Physica B: Condensed Matter,* 46138-48.

[3] SHIN, S. W., OH, J. P., HONG, C. W., KIM, E. M., WOO, J. J., HEO, G.-S. & KIM, J. H. 2016. Origin of Mechanoluminescence from Cu-Doped Zns Particles Embedded in an Elastomer Film and Its Application in Flexible Electro-Mechanoluminescent Lighting Devices. *ACS Applied Materials & Interfaces,* 8(2), 1098-1103.

[4] CHANDRA, B. P., CHANDRA, V. K. & JHA, P. 2015. Elastico-Mechanoluminescence and Crystal-Structure Relationships in Persistent Luminescent Materials and Ii–Vi Semiconductor Phosphors. *Physica B: Condensed Matter,* 46362-67.

[5] RYU, D., CASTAÑO, N. & VEDERA, K., *Mechanoluminescent Composites Towards Autonomous Impact Damage Detection of Aerospace Structures*, in *10th International Workshop on Structural Health Monitoring*, F.-K. Chang, Editor. 2015, DEStech Publications: Stanford, CA.

Electrophysical Properties of Ferroelectric Nanocomposites Nanocrystalline Cellulose – Sodium Nitrite

Nguyen H.T., Milovidova S.D., Sidorkin A.S., Rogazinskaya O.V.

Voronezh State University, Voronezh, Russia.

sidorkin@phys.vsu.ru

Recently, a numerous studies of the properties of composites with reinforcing matrix in the form of nanocrystalline cellulose (NCC) have appeared in the field of physical materials science. Due to the large number of parallel nanochannels of 50-100 nm width due to the presence of active polar groups OH^- on their surface, the matrix NCC possesses a high sorption capacity with respect to water, liquids and nanoparticles also. Authors of the present work in previous studies [1,2] showed the ability of creating composites based on matrix NCC with triglycine sulfate (TGS). The expansion of ferroelectric phase in this composite up to 5 - 7 ºC as compared to single-crystal TGS (T_C = +49 ºC) was found.In addition, a significant dispersion of dielectric constant conditioned by Maxwell-Vagner polarization was found in the frequency range from 10^{-3} – 10^3 Hz [2].

For the purpose of getting a deeper understanding of possible mechanisms of the influence of different matrices on behavior of ferroelectric composites, in the present work, the electrophysical properties on the composite based on the matrix with Sodium Nitrite ($NaNO_2$) in the frequency range of 10^{-3} – 10^6 Hz at different temperatures from room temperature to the possible maximum heating temperature for NCC (170 ºC) including the phase transition temperature of the bulk $NaNO_2$ (+165 ºC) have been investigated. The conducted investigations showed that in this composite in the studied temperature range including the phase transition of the bulk $NaNO_2$, an increase of dielectric constant with increasing temperature was found as observed for nanoparticles $NaNO_2$ introduced into matrices such as Al_2O_3, Si and glasses. The obtained values of dielectric constant for the composite based on NCC with $NaNO_2$ are close to those of composites based on other nanoporous matrices such as Al_2O_3, Si and glasses with

$NaNO_2$, unlike the composite NCC+TGS, for which the values of dielectric constant are small as compared to the composites based on the specified matrices with TGS inclusion [2].The obtained behavior can be related to a strong interaction between groups OH^- in NCC and TGS. This interaction in the composite NCC+$NaNO_2$ doesn't exist due to the absence of hydrogen bonds in $NaNO_2$. In addition, the investigation of dielectric relaxation at low and infra-low frequencies showed a significant dispersion with giant dielectric constant, that is presumably associated with Maxwell-Vagner polarization conditioned by charge accumulation at the boundaries of nanoparticles $NaNO_2$ with NCC.

Keywords: Ferroelectric nanocomposites, phase transition, dielectric relaxation

[1] MILOVIDOVA,S.D., ROGAZINSKAYA,O.V., SIDORKIN,A.S., NGUYEN, H.T., GROHOTOVA,E.V., POPRAVKO, N.G. 2014. Dielectric Properties of Composites Based on Nanocrystalline Cellulose and Triglycine Sulfate. *Ferroelectrics*, 469, 116-119.

[2] NGUEN, KH. T., MILOVIDOVA,S.D., SIDORKIN,A.S.,ROGAZINSKAYA,O. V. 2015. Dielectric Properties of Composites Based on Nanocrystalline Cellulose with Triglycine Sulfate. *Physics of the Solid State*, 57, 503-506.

Explorations of New Compounds in the Pb-NO_3-BO_3 System

Jiang-Gao Mao* and Jun-Ling Song

***Sate Key Laboratory of Structure chemistry, Fujian Institute of Research on the Structure of Matter, Chinese Academy of Sciences,* Yangqiao Xilu, Fuzhou, P. R. China 350002**

E-mail address: mjg@fjirsm.ac.cn

Since B^{3+} can adopt both planar trigonal BO_3 and tetrahedral BO_4 coordination geometries, metal borates exhibit very rich structure chemistry, ranging from various isolated B–O clusters to 1D, 2D and 3D borate networks.[1] They are also important second order non-linear optical (NLO) crystals.[2] According to the anionic group theory, the NLO property of the borate materials could be significantly enhanced if we can increase the density of the π-conjugated planar triangular groups.[2] Recently we have been exploring metal mixed anion compounds containing two different types of π-conjugated planar triangular units (BO_3 and NO_3 groups), five lead(II) borate-nitrate compounds were obtained by using a facile hydrothermal synthetic techniques,[3-4] namely, $[Pb_3(B_3O_7)](NO_3)$ **(1)**, $Pb_2(BO_3)(NO_3)$ (**2**), $[Pb_6(\mu_4\text{-}O)_4(BO_3)](NO_3)$ (**3**), $H[Pb_6(\mu_3\text{-}O)_2(BO_3)_2](NO_3)_3$ (**4**) and $H[Pb_8(\mu_4\text{-}O)_3(\mu_3\text{-}O)(BO_3)_2](NO_3)_3$ (**5**).

$[Pb_3(B_3O_7)](NO_3)$ (**1**) with a space group *Pnma* features a 3D lead(II) borate cationic network structure in which $(B_3O_7)^{5-}$ anions are bridged by lead(II) cations, the nitrate anions remain isolated and located at the small voids of the cationic network. The structure of $Pb_2(BO_3)(NO_3)$ (**2**) with a polar space group $P6_3mc$ contains honeycomb $[Pb_2(BO_3)]_\infty$ layers with non-coordination $[NO_3]^-$ anions located at the interlayer space. The structures of centrosymmetric compounds **3**-**5** feature three different types of lead(II) oxo borate layers that are separated by nitrate anions. The 2D $[Pb_6(\mu_4\text{-}O)_4(BO_3)]^+$ layer parallel to the *ab* plane in **3** is built from 1D $[Pb_6(\mu_4\text{-}O)_4]^{4+}$ chains along the *a* axis and bridging borate anions. The 2D $H[Pb_6(\mu_3\text{-}O)_2(BO_3)_2]^{3+}$ layer in **4** is formed by "isolated" Pb^{2+} and tetranuclear $[Pb_4(\mu_3\text{-}O)_2]^{4+}$ clusters interconnected by bridging BO_3 groups. The $[Pb_8(\mu_4\text{-}O)_3(\mu_3\text{-}O)(BO_3)_2]^{2+}$ (011) layer in **5** composed of two types of lead(II) oxo chains, namely, 1D chains of $[Pb_4(\mu_4\text{-}O)_2]^{4+}$ and 1D chains of $[Pb_4(\mu_4\text{-}O)(\mu_3\text{-}O)]^{4+}$.

The polar $Pb_2(BO_3)(NO_3)$ (**2**) shows a remarkable strong SHG response of ~9.0 times that of potassium dihydrogen phosphate (KDP) and the material is also phase-matchable. The large SHG coefficient of $Pb_2(BO_3)(NO_3)$ arises from the synergistic effect of the stereo-active lone-pairs on Pb^{2+} cations and parallel alignment of π-conjugated BO_3 and NO_3 units.

Keywords: Lone pair electrons; borate; nitrate; SHG materials; crystal structures

REFERENCES

[1] Becker, P. Adv. Mater., 10 (1998) 979-992.
[2] C. T. Chen, Y. B. Wang, B. C. Wu, K. C. Wu, W. L. Zeng, L. H. Yu, Nature, 373 (1995) 322-324.
[3] J.-L. Song, C.-L. Hu, X. Xu, F. Kong, J.-G. Mao, Angew. Chem. Int. Ed., 54 (2015) 3679 –3682.
[4] J.-L. Song, C.-L. Hu, X. Xu, F. Kong, J.-G. Mao, Inorg. Chem., 52 (2013) 8979-8986.
[5] J.-L. Song, X. Xu, C.-L. Hu, F. Kong, J.-G. Mao, CrystEngComm.,17(2015) 3953-3960.

Fabrication and Magnetic Purification of Magnetic Core PEI-Silica Shell Particles

Emily D.E.R. (Hyde)[1], Frances (Neville)[2], Roberto (Moreno-Atanasio)[1]

[1]School of Engineering, The University of Newcastle, Callaghan, New South Wales 2308, Australia.

[2]School of Environment & Life Sciences, The University of Newcastle, Callaghan, New South Wales 2308, Australia.

E Mail/ Emily.Hyde@uon.edu.au

Magnetic core silica shell particles combine the ease of surface functionalization and the high thermal, mechanical and relative chemical stability of the silica shell with the convenience of magnetic separation. Such particles have attracted considerable research attention due to their large range of applications in fields such as catalysis, drug delivery, absorption and separation.

Biomimetic silica synthesis methods produce silica particles in a more environmentally friendly manner compared to traditional silica production. Moreover, greater morphological control is possible when utilizing biomimetic processes in place of traditional silica synthesis routes. Previous work [1] has utilized the biomimetic polypeptide, polyethylenimine (PEI), to catalyze the formation of a silica coating on the surface of ferromagnetic particles.

The objective of this study was to develop PEI-initiated silica coating techniques through performing systematic variations in the sequence and manner of reagent addition, thus optimizing the PEI-silica coating method. This work demonstrates how biomimetic silica shells retain the advantages of traditionally synthesized magnetic core silica shell particles while gaining the additional benefits of bio-inspired synthesis for the first time. PEI-silica coated iron carbonyl particles were characterized via scanning electron microscopy, energy dispersive X-ray spectroscopy and Fourier Transfer Infrared spectroscopy. The methods studied produced a number of different silica coatings including a multicore-silica gel, singular core rough silica surface and partial silica

coatings, which may prove useful for different applications. The magnetic separation process used during the washing of the core-shell particles was determined to successfully eliminate the undesired coreless silica particle by-product from the core-shell product. Therefore, we achieved a degree of purification that makes these core-shell particles useful for potential applications requiring specific surface interactions and the ease of magnetic separation.

Keywords: Magnetic core-shell particles; biomimetic silica synthesis

[1] NEVILLE, F. & MORENO-ATANASIO, R. 2012. Magnetic interactions of core-shell composite particles: A combined experimental and simulation approach. In *Chemeca 2012: Quality of life through chemical engineering: 23-26 September 2012, Welling, New Zealand*. Engineers Australia, Barton, A.C.T., pp. 727-737.

Flexible Silica Aerogel Composites Strengthened with Phosphoric Acid Modified Aramid Fibers

Zhi Li, Song He, Lunlun Gong, Congcong Li, Hui Yang, Xudong Cheng*

University of Science and Technology of China, Hefei, Anhui 230027, PR China

E-Mail/ Contact Details: Presenting author: lizhi89@mail.ustc.edu.cn.

**Corresponding author: chengxd@ustc.edu.cn, Tel.: +86 0551 63606957.*

With the advantages of extremely low density, low thermal conductivity and high specific surface area, silica aerogels can be used in extensive fields. However, the actual applications have been hindered seriously due to the inherent fragility and low strength of silica aerogels (Kistler, 1932; Hüsing and Schubert, 1998). Extensive research shows that using fibers as reinforcements to generate silica aerogel composites is one of the most effective way to solve the fragile nature of silica aerogels in which the current reinforcements concentrate on inorganic fibers (Kim et al., 2008; Yuan et al., 2012; Li et al., 2013; Motahari and Abolghasemi, 2015) The introduced inorganic fibers can improve the compressive strength of silica aerogel composites but do nothing to improve the flexibility owing to the brittleness of inorganic fibers themselves.

In this work, using organic fibers to reinforce silica aerogel was proposed and aramid fibers were chose as reinforcements. Aramid fibers reinforced silica aerogel composites were successfully prepared presenting a low density, low thermal conductivity and nice flexibility. In consideration of the interface bonding between aerogel matrix and aramid fibers, phosphoric acid (PA) was adopted to enhance the fibrillar structure of aramid fibers. The microstructure of the composites strengthened with the PA modified aramid fibers (MAF/aerogels) showed a favorable interfacial adhesion with the aramid fibers inlaying in the aerogel matrix and the porous nanostructures wrapping around the aramid fiber. Mechanical tests including the large deflection bend and compression tests demonstrated a good flexibility and elasticity of the MAF/aerogels. As the fiber content increased, it was found that the thermal

conductivity approximated linear increase slightly with a small slope of 6.09×10^{-4} W m^{-1} K^{-1} and the minimum thermal conductivity could reach 0.023 W m^{-1} K^{-1}, while the density of the composites fluctuated around 0.141 g cm^{-3}. At optimum of the fiber content being 6.04%, the composites presented the minimum elastic modulus of 0.083 MPa indicating the best elastic performance. TG-DSC analysis revealed that the thermal stability was up to approximately 300 ℃ which was mainly depended on the thermostability of the pure silica aerogel.

In sum, the characteristics mentioned above turned out that the as-prepared PA modified aramid fibers reinforced silica aerogel composites conquered the fragile nature and presented many excellent properties including low density, low thermal conductivity and nice flexibility which indicated huge application prospects in heat preservation field, sound insulatiocn, adsorption, etc.

Keywords: Aramid fibers, silica aerogels, nanocomposites, flexibility, thermal properties

[1] Hüsing, N., Schubert, U., 1998. Aerogels—Airy Materials: Chemistry, Structure, and Properties. Angew. Chemie Int. Ed. 37, 22–45.

[2] Kim, C.Y., Lee, J.K., Kim, B.I., 2008. Synthesis and pore analysis of aerogel-glass fiber composites by ambient drying method. Colloids Surfaces a-Physicochemical Eng. Asp. 313, 179–182.

[3] Kistler, S.S., 1932. Coherent Expanded Aerogels and Jellies. Nature 5, 600–603.

[4] Li, X., Wang, Q., Li, H., Ji, H., Sun, X., He, J., 2013. Effect of sepiolite fiber on the structure and properties of the sepiolite/silica aerogel composite. J. Sol-Gel Sci. Technol. 67, 646–653.

[5] Motahari, S., Abolghasemi, A., 2015. Silica Aerogel – Glass Fiber Composites As Fire Shield for Steel Frame Structures 27, 1–7.

[6] Yuan, B., Ding, S., Wang, D., Wang, G., Li, H., 2012. Heat insulation properties of silica aerogel/glass fiber composites fabricated by press forming. Mater. Lett. 75, 204–206.

Formation of wrinkled-structure on the surface of microspheres by controlling the self-assembling of nanosilica

Nanami HANO[1], Makoto TAKAFUJI[1]*, Zhenghe XU[2], Hirotaka IHARA[3,4]*

[1]Department of Applied Chemistry and Biochemistry, Kumamoto University, Kumamoto, Japan.
[2]Department of Chemical and Materials Engineering, University of Alberta, Edmonton, Canada.
[3]Department of Nanoscience and Technology, Kumamoto University, Kumamoto, Japan.
[4]Kumamoto Institute for Photo-Electro Organics (PHOENICS), Kumamoto, Japan.
takafuji@kumamoto-u.ac.jp, *ihara@kumamoto-u.ac.jp*

Surface microstructure of materials is of importance to various applications. The surface of lotus leaf is an excellent example of water-repellent material found in nature, which is based on the unique hierarchical surface structure. Such examples in nature give us hints for new materials with specific surface property. In fact, water-repellent materials imitating lotus leaf have already been developed. Materials with wrinkled surface have potentials for a wide range of applications such as optical devices, electronics and biological devices. Several methods such as chemical oxidation [1] and UV irradiation [2] on the surface were reported to create wrinkled-surface on the flat surface. In this paper, we demonstrate to fabricate the wrinkled-structure on the surface of microspherical polymer particles by controlling the self-assembling of silica nanoparticles. We have reported microspherical hybrid particles with silica nanoparticles-covered surface by using modified suspension polymerization [3]. During the polymerization, silica nanoparticlesdispersed in polymerizable monomer were condensed at the surface of monomer droplet and strongly immobilized on the surface of polymer microsphere through covalent bonds. When excess amounts of silica nanoparticles (average size = 30 nm) were used, silica nanoparticles crowded at the surface of polymer core to form wrinkled-structure. This is probably due to pushing up the surface by condensation of self-assembled silica nanoparticles. FE-SEM observations indicated that the wrinkled surface was composed of silica nanoparticles. Interestingly, the depth and the distance between folds of wrinkled-structure could be controlled by the preparation conditions such as initial concentration of silica nanoparticles. In this presentation, we will display the various wrinkled-surface on the polymer microspheres and their surface properties such as wettability and reflectance and reflectivity.

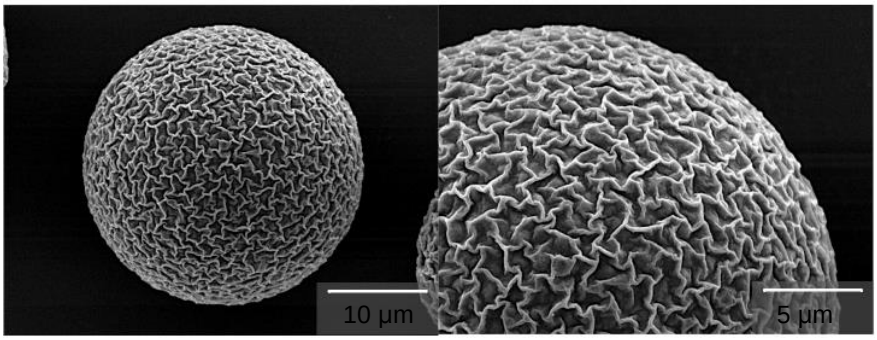

Figure 1 SEM images of the microsphere with wrinkled-structure.

Keywords: Core-Shell microsphere, wrinkled-surface, suspension polymerization

[1] YIN, J., HAN, X., CAO, Y. & LU, C. 2014. Surface Wrinkling on Polydimethylsiloxane Microspheres via Wet Surface Chemical Oxidation. *Sci. Rep.*, 4, 5710.

[2] ANA, C. T., JOAO, P. C., PEDRO, P., PEDRO, B., PAULO, I. T. & MARIA, H. G. 2012. Hierarchical wrinkling on elastomeric Janus spheres. *J. Mater. Chem.*, 22, 22044-22049.

[3] UCHIMURA, A., KUBOTA, S., YAMADA, S., WAKIYA, T., TAKAFUJI, M., SHIROSAKI, T., NAGAOKA, S. & IHARA, H. 2011. Facile and versatile method for preparing core-shell microspheres with controlled surface structures based on silica particles-monolayer. *Mater. Chem. Phys.*, 129, 871-880.

Gelatin-Bacterial Cellulose Composite Sponge Thermally Cross-Linked with Glucose

Suchata Kirdponpattara[1], Charuk Prathuangyukhan[1], Napawan Kongsakun[1],
Sasithorn Kongruang[2], Muenduen Phisalaphong[3]
[1]Department of Chemical Engineering, Faculty of Engineering,
King Mongkut's University of Technology North Bangkok, Bangsue, Bangkok, Thailand
[2]Department of Biotechnology, Faculty of Applied Science,
King Mongkut's University of Technology North Bangkok, Bangsue, Bangkok, Thailand
[3]Department of Chemical Engineering, Faculty of Engineering,
Chulalongkorn University, Phyathai, Bangkok, Thailand

suchata.k@eng.kmutnb.ac.th

Bacterial cellulose (BC) is a suitable supplement to improve elasticity and water adsorption capacity (WAC) of gelatin sponge. BC is highly pure network structure synthesized by bacteria. Many unique properties of BC have been reported such as high mechanical strength, high crystallinity, high hydrophilicity and non-toxicity [1]. Applications of dried gelatin has been limited [2], especially in tissue engineering and biomedical fields, due to its brittleness. Moreover, gelatin must be cross-linked to prevent dissolution in aqueous medium. In this research, glucose was used as a cross-linking agent because of its non-toxicity and low price.

The objective of this research is to fabricate gelatin-bacterial cellulose composite sponge by thermally cross-linking with glucose. Freeze drying technique was carried out to fabricate sponge-like structure. The parameters of cross-linking condition, such as amount of cross-linking agent, cross-linking temperature and cross-linking time, were optimized. In addition, the effect of weight ratio between gelatin and BC on sponge structure was also studied.

The result demonstrated that toxicity of the composite sponge increased with increasing of glucose content because of the side product of Maillard's reaction and caramelization reaction [3]. The degree of cross-linking was affected by the cross-linking temperature and time. Development of sponge-like structure, and enhancements of WAC and elasticity of the composite sponge were observed with increasing of BC supplementation. However, the stability of the composite sponge in water decreased with increasing of BC weight ratio.

Gelatin-bacterial cellulose composite could be further modified to apply in bone tissue engineering as a bioscaffold.

Keywords: Gelatin, bacterial cellulose, glucose, composite, cross-linking

[1] FU, L., ZHANG, J., & YANG, G. 2013. Present Status and Applications of Bacterial cellulose-Based Materials for Skin Tissue Repair. *Carbohydrate Polymer*, 92, 1433-1442.
[2] TAOKAEW, S., SEETABHAWANG, S., SIRIPONG, P., & PHISALAPHONG, M. 2013. Biosynthesis and Characterization of Nanocellulose-Gelatin Films. *Materials*, 6, 782-794.
[3] CAPUANO, E., & FOGLIANO, V. 2011. Acrylamide and 5-Hydroxymethylfurfural (HMF): A Review on Metabolism, Toxicity, Occurrence in Food and Mitigation Strategies. *Food Science and Technology*, 44, 793-810

Hybrid Two-step Preparation of Nano-sized MgAl Layered Double Hydroxides for CO_2 Adsorption

Xiani Huang[1], XiaogangYang[1,*], Guang Li[1], Collins I. Ezeh[1]

[1] Department of Mechanical Engineering

University of Nottingham Ningbo

University Park, Ningbo 315100. P.R. China

Corresponding author: Email : Xiaogang.Yang@nottingham.edu.cn / Tel: +86-574-88182419 Presenting author : Email : Xiani. Huang@nottingham.edu.cn

This paper reports the results obtained by using a hybrid two-step preparation approach for sythesising the MgAl layered double hydroxide (MgAl LDHs) used for CO_2 adsorption. The hybrid two-step preparation consists of the step applying ultrasonic processing (first step) and the following step of co-precipation (second step). The synthesized samples that have been characterized by the XRD have clearly shown that the LDHs forms a typical layered double hydroxide structure and no other impurities were identified in the compound. The SEM and TEM analysis also confirms that the size distribution of the synthesized MgAl LDHs is relatively uniform (with an average size of approximate 100 *nm*) and layered structure is clearly visible. The BET characterization indicates that such LDHs has a large surface area (235 m^2g^{-1}), which makes it a promising adsorbent material for CO_2 capture in practical application. The effect of the rate of addition of $Mg(NO_3)_2$&$Al(NO_3)_3$ on improvement of the CO_2 capture capacity of MgAl LDHs was also investigated. It has been demonstrated that the highest capture capacity reaches to 0.76 mmol g^{-1} on the conditions that pure CO_2 gas is adopted with the temperature of 80^{O}c and the pressure of 1 atm.

Key words: MgAl LDHs, CO_2 adsorption, ultrasonic nucleation, co-precipation

[1] WANG, Q., GAO, Y.S., LUO, J.Z., ZHONG, Z.Y., BORGNA, A., GUO, Z.H., O'Hare, D. 2013. Synthesis of nano-sized spherical $Mg_3Al–CO_3$ layered double hydroxide as a high-temperature CO_2 adsorbent. *RSC Advances*, 3, 3414-3420.

Hydrothermally Synthesized Ternary Heterostructured $MoS_2/Al_2O_3/g\text{-}C_3N_4$ Photocatalyst

S.V. Prabhakar Vattikuti[1]*, Chan Byon1

[1]School of Mechanical Engineering, Yeungnam University, Gyeongsan, South Korea, 712-749

* Corresponding Authors/ E-mail: vsvprabu@gmail.com

TEL: +82-10-4017-8527, FAX: +82-53-810-4627

A multifaceted ternary $MoS_2/Al_2O_3/g\text{-}C_3N_4$ heterostructure has been prepared from a simple and facile hydrothermal method having good photocatalytic performance for the degradation of crystal violet (CV) dye under visible light irradiation. As a result of wide structural features for charge separation mechanism, the formation of the ternary heterojunction remarkably affects the photocatalytic activity of pure MoS_2. Thus, the best result for the binary system was obtained for 60 wt% MoS_2-40 wt% Al_2O_3 system. In addition, the incorporation of $g\text{-}C_3N_4$ leads to a further enhancement on the photocatalytic activity when it is specifically done as ternary system. The ternary $MoS_2/Al_2O_3/g\text{-}C_3N_4$ heterostructure displays 14.5 times and 3.1 times higher than binary photocatalysts MoS_2/Al_2O_3 and $MoS_2/g\text{-}C_3N_4$ respectively. More significantly, the ternary composite also demonstrates a good photostability and reusability. $g\text{-}C_3N_4$ is produced during the photocatalytic process, which may serve as the electron transfer mediator at the interface of $MoS_2/Al_2O_3/g\text{-}C_3N_4$. The effective photocatalytic mechanism of charge separation of the ternary system was proposed to be responsible for the enhancement of visible light photocatalytic activity, whereas the surface properties were key factors for the photodegradation of CV dye.

Keywords: Photocatalyst, ternary, hydrothermal, coupled semiconductor, heterostructure

Improved Thermoelectric Properties of CNT-Dispersed-Bi_2Te_3 Composites Processed by Molecular-Level Mixing

Kyung Tae Kim[1*], Taesik Min[1,2], Injoon Son[2]

[1] *Powder Technology Department, Korea Institute of Materials Science, 797 Changwon-daero, Seongsan-gu, 642-831 Changwon, Gyeongnam, Republic of Korea*
[2] *Department of Materials Science and Metallurgical Engineering, Kyungpook National University, 80 Daehakro, Buk-gu, 702-701 Daegu, Republic of Korea*

[*] *e-mail of presenting author: ktkim@kims.re.kr*

Bismuth telluride (Bi_2Te_3)-based alloys are very promising for practical applications in waste heat recovery or active cooling/heating system because of superior energy conversion efficiency at ambient temperature. However, the application field of this material does not become larger than expected due to the limited TE conversion efficiency, defined as the dimensionless figure-of-merit, *ZT* which is calculated from $T(\alpha^2/\rho\kappa)$, where *T* is the absolute temperature, α is the Seebeck coefficient, and ρ and κ are respectively the electrical resistivity and thermal conductivity.

In this study, carbon nanotubes (CNTs) were utilized as dispersion agent for Bi_2Te_3 matrix in order to achieve high ZT value. The CNTs are expected to be suitable for embedding in the thermoelectric matrix materials due to superior physical and chemical properties. Thus, we suggest a novel procedure to fabricate a CNT-dispersed bismuth telluride matrix composite, in which CNTs are homogeneously dispersed in the bismuth telluride matrix powders. Carbon nanotubes-dispersed Bi_2Te_3 matrix (CNT/Bi_2Te_3) composites were synthesized by using molecular-level mixing, followed by spark plasma sintering process. It was found that the homogeneous dispersion of CNTs is guaranteed by interfacial oxygen atoms present at the CNT/Bi_2Te_3 interface. In addition, the influence of Se addition on the thermoelectric properties of CNT/binary Bi_2Te_3 composite was investigated in this study. The obtained maximum ZT value of the CNT/Bi_2Te_3, $Bi_2(Se,Te)_3$ composite is found to be 1.8 and 1.9 times, respectively, higher than that of n-type Bi_2Te_3 without incorporation of CNTs, which elucidates the effect of CNTs in the thermoelectric matrix materials. These results indicate that a synthetic process utilized in this study is very profitable for dispersion of CNTs in the bismuth telluride matrix thermoelectric composite. Furthermore, both effect of CNT addition and matrix doping are found to be key factors to provide synergistically improved thermoelectric performances of bismuth telluride based composites.

Laser fabrication of 3-D part having variable porosity densities

Seong Hoon Lee[1], Sang Wook Han[1], Tae Woo Hwang[1], Young Hoon Moon[1*]

[1*] School of Mechanical Engineering, Pusan National University, Busan 609-735, Korea

E Mail : shlee@pusan.ac.kr, TEL : +8251-510-1672,
[*]E Mail : yhmoon@pusan.ac.kr, TEL : +8251-510-2472, FAX : +8251-512-1722

The processing method to fabricate 3-D part having variable porosity densities is proposed and investigated in this study. To fabricate the porosity-graded part, powders having different morphologies and particle sizes are laser processed at various processing conditions. As the active control of laser power and scan speed are very crucial in laser processing, the combined effects of laser processing parameters with powder materials need to be investigated for the control the porosity densities in laser deposited layer. . Direct laser melting process produces part by solidification of fully molten metallic powder, while laser sintering process consolidates successive layers of powder material on top of each other. For the fabrication of fully dense layer, high laser energy has been applied to achieve complete laser melting. Atomized spherical powders having smaller particle size has been used to enhance full melting. Porous layers have been fabricated at relatively lower laser energy to achieve laser sintering instead of full melting. To obtain target porosity density, the non-spherical powders having different particle sizes have been laser processed and estimated. By using proposed method, part having graded-porosity was successfully fabricated with high reliability.

Keywords: Laser fabrication, porosity-graded, laser sintering, direct laser melting

[1] SURYANARAYANA, C. 2001. Mechanical alloying and milling. *Progress in Materials Science*, 46, 1-184.

[2] YADROITSEV, I., THIVILLON, L., BERTRAND, PH. & SMUROV, I. 2007. Strategy of manufacturing components with designed internal structure by selective laser melting of metallic powder. *Applied Surface Science*. 254. 980-983.

[3] SIMCHI, A. 2006. Direct laser sintering of metal powders: mechanism, kinetics and microstructural features," *Materials Science and Engineering: A*, 428, 148-158.

[4] Li, R., Liu, J., Shi, Y., Du, M. & Xie, Z. 2010. 316L Stainless Steel with Gradient Porosity Fabricated by Selective Laser Melting. *Journal of Materials Engineering and Performance*. 19. 666-671.

Novel acid modification of natural rubber-bacterial cellulose composites

Phomrak, Phisalaphong

Chemical Engineering Research Unit for Value Adding of Bioresources, Department of Chemical Engineering, Faculty of Engineering, Chulalongkorn University, Phayathai Rd., Patumwan, Bangkok, 10330, Thailand.

E-mail adresse: muenduen.p@chula.ac.th (M. Phisalaphong).

Natural rubber (NR) is important materials for a variety of the elastomer industry such as tires, medical gloves, automotive interior parts as well as packaging due to the excellent elastic properties. However, there are some defects such as low strength and abrasion resistance. Moreover, its applications are also limited because of its poor resistance to oil and solvents. Development of fiber-reinforced NR-matrix composites is a promising solution to these problems. In this study, bacterial cellulose (BC) was used as reinforcing agent for NR due to its many advantages including biocompatibility, remarkable mechanical properties, and high hydrophilicity. The nanofiber-network structure of BC provides a large surface area. Additionally, acid modification of composites was used to enhance the compatibility between NR and BC. The natural rubber-bacterial cellulose (NRBC) composite and the acid modified NRBC composite (ANRBC) films were characterized for physical, chemical and biological properties including antimicrobial properties and biodegradability in soil. The ANRBC composite showed significantly improved in mechanical properties, chemical resistance properties and structural stability. The ANRBC composite films had less degree of swelling and were not dissolved in both of nonpolar and polar solvents. However, the modification had almost no effect on its degradability in soil.

Keywords: Natural rubber, bacterial cellulose, composites, acid modification, degradability

Unloaded and Palladium- Loaded WO_3 Nanoparticles by Precipitation/Impregnation Methods for Use as Ethanol Gas Sensors

Sathukarn Kabcum,[a] Anurat Wisitsora-at,[b] Chaikarn Liewhiran,[a] Sukon Phanichphant,[c,*]

[a]*Department of Physics and Materials Science, Faculty of Science, Chiang Mai University, Chiang Mai 50200, Thailand.*
[b]*Nanoelectronics and MEMS Laboratory, National Electronics and Computer Technology Center, Klong Luang, Pathumthani 12120, Thailand.*
[c]*Materials Science Research Center, Faculty of Science, Chiang Mai University, Chiang Mai 50200, Thailand.*

*Fax: +66-53892277, *E-mail: sphanichphant@yahoo.com*

The ultra-rapid gases sensors based on unloaded and 0.25–2.0 wt% Pd–loaded WO_3 nanoparticles were synthesized by the precipitation method and imgregnated using palladium acetylacetonate. Unloaded and 0.25–2.0 wt% Pd–loaded WO_3 nanoparticles were characterized by by X-ray diffraction (XRD), scanning electron microscopy (SEM), energy dispersive X-ray spectroscopy (EDS) and high resolution transmission electron microscopy (HRTEM) techniques. The BET surface area (SSA_{BET}) of the nanoparticles was measured by nitrogen adsorption. The sensing films were prepared by mixing the unloaded and Pd–loaded WO_3 nanoparticles into an organic paste composed of vehicle ethyl cellulose binder and α–terpineol solvent to form a viscous paste. The resulting paste was spin–coated onto Al_2O_3 substrates interdigitated with Au electrodes by spin coating technique to form the sensing films. All sensors were systematically tested with C_2H_5OH gases. The C_2H_5OH gas sensing performances including the change in resistance, sensor response, selectivity, dynamic range, and enhanced time factors were significantly performed at the different operating temperatures ranging from 150–350ºC with various C_2H_5OH gas concentrations in dry air. After sensing test, the morphology and the cross–sectional sensing film (3–5 μm in thickness) were analyzed by SEM and EDS analyses. It was found that 1.5 wt% Pd-loaded WO_3 sensing film showed the highest response of $1.52x10^4$ to 2,000 ppm C_2H_5OH at 350ºC and the shortest response time within 3.8 s. Therefore, an operating temperature of 350ºC was optimal for C_2H_5OH detection. The responses of 1.5 wt% Pd–loaded WO_3 sensing film to other flammable and toxic gases, including CO, NO2, NH3 and H2S, demonstrating Pd–loaded WO_3 sensing film to be highly selective to C_2H_5OH.

Keywords: WO_3 nanoparticles; Precipitation; Impregnation; Pd; Ethanol gas sensors.

Preparation and dynamic compression properties of W-Zr reactive material

Huilan Ren, Xiaojun Liu, Tianbao Ma, Jianguo Ning

State Key Laboratory of Explosion Science and Technology, Beijing Institute of Technology, Beijing 100081, P.R.China

E Mail/ huilanren@bit.edu.cn

Reactive Materials are a new class of energetic materials as a means to increase the lethality of direct-hit or fragmentation warheads, which usually consist of two and more non-explosive solid materials. The reactive material will fragment, react and release high amount of energy fast under impact loading as a result of the high temperature and pressure, and these provide additional means for destruction. The reactive materials are adaptable to a variety of applications such as target damage using structural reactives, propellant/explosive additives and manufacturing. These materials are mainly consisted of thermites, intermetallics, metal/fluorine systems, metastable intermolecular composites (MICs), nano-laminates and metal hydrides [1-3]. Among these, as an important representative of the reactive materials, the intermetallics have gotten widespread attention due to the unique characteristics that not only are the energy reactants, but also work as the structural component. Intermetallics have been studied by numerous researches over the past several decades, such as Ni-Al, Al-W and W-Zr powder system, including initiation and characterization [4-6].

To improve the structural strength and density of this kind composite, in this work, it has been shown a hot-pressing sintering method to fabricate the W-Zr reactive materials mass ratios of Zr:W of 66:34. The compressive mechanical behavior W-Zr was tested at different strain rates by using material testing system and split Hopkinson pressure bar (SHPB). A constant strain rate loading can be obtained by employing the pulse shaping technique and attaching a strain gauge directly to the sample. This research shows that the W-Zr is a kind of brittle high-strength reactive material which is attributed to the W_2Zr sintering product, which could be demonstrated from the microstructure of fracture surfaces by scanning electron microscopy (SEM) with energy dispersive spectrometer

(EDS). The samples produced evidently strong fires under under strong impacting, and High resolution X-ray diffraction (XRD) was performed on the original samples and residues after SHPB test, showing that the Zr is the active component in the reaction with air. It shows a good linear elastic stress-strain curve both under quasi-static and dynamic loading, and its Young's modulus is about 186 GPa, not so sensitive to stain rate. The results show that the failure strain and compressive strength of W-Zr increase with the strain rate increasing, and its compressive strength is approximately 2690MPa at 1000 s^{-1}. These results suggest that the W-Zr reactive material has huge potential to take the place of inert steel as fragments because of its high strength and high energy level, as well as the density close to that of steel.

Keywords: W-Zr, Reactive materials, Mechanics properties, Microstructure, constant strain rate, shock-induced reaction

[1] THADHANI, N. N. 1994. Shock-induced and shock-assisted solid-state chemical reactions in powder mixtures. Journal of Applied Physics, 76: 2129–2138.

[2] ZHANG, X. F., ZHAO, X. N. 2009. Review on multifunctional energetic structural materials. Journal of Energetic Materials, 17(6): 731-739 (in Chinese).

[3] COMMITTEE ON ADVANCED ENERGETIC MATERIALS AND MANUFACTURING TECHNOLOGIES. 2004. Advanced Energetic Materials, The National Academies Press. 32: 20–23.

[4] BENNETT, L. S., SORRELL, F. Y., SIMONSEN, I. K., HORIE, Y., IYER, K. R. 1992. Ultrafast chemical reactions between nickel and aluminum powders during shock loading. Applied Physics Letter. 61: 520-1.

[5] OLNEY, K. L., NESTERENKO, V. F., BENSON, D. J. 2012. Mechanisms of fragmentation of aluminum-tungsten granular composites under dynamic loading. Applied Physics Letter. 100: 191910.

[6] LUO, P. G., WANG, Z. C., JIANG, C. L., MAO, L., LI, Q. 2015. Experimental study on impact-initiated characters of W/Zr energetic fragments. Materials and Design 84: 72-78.

Properties of Nanocomposites Prepared from Hybrids of Silver Nanoparticles and Graphene Nanoplates Dispersed in Epoxy Resins

Gwang Seok Song and Dai Soo Lee

Division of Semiconductor and Chemical Engineering, Chonbuk National University,

Jeonju 54596, South Korea

dslee@jbnu.ac.kr

One-dimensional nanostructured particles such nanowire, nanotubes, nanorods, or nanofibers are expected to play important roles in fabricating nanoscale devices and nanocomposites. Silver nanoparticle (SNP) and silver nanowire (SNW) are considered attractive fillers for various polymers in electronic parts because of its optical polarizability, chemical reactivity, and high thermal/electrical conductivity [1, 2]. In addition, nanocomposites in a readily processable form can be made by the incorporation of nanoparticles into the polymers [3-5]. But, agglomeration of silver nanoparticles takes place easily and efforts to improve the dispersion are necessary. Graphene nanoplate (GNP) is a attractive reinforcements for polymers because of its high thermal and electrical property as well as the high mechanical strength. However, incorporations of GNP into polymers impose difficulties such as the high viscosity at low concentration due to the nature resulting from nano size thickness. To overcome this problem, hybrids of SNP or SNW and GNP dispersed in an epoxy resin were investigated.

Especially, the electrical and rheological properties of simple mixtures of SNP or SNW and GNP and the hybrids of SNP or SNW and GNP dispersed in different epoxy resin were investigated from view point of different interfacial interactions between nanoparticles employing contact angle measurements, rheometry, and electrical resistivity measurements. It was desired that the nanoparticles show fine dispersion in the epoxy resins before the cure while

the nanoparticles undergo flocculation after the cure of the epoxy resins in the nanocomposites to induce efficient percolation of the fillers. In order to achieve such desirable properties, interfacial properties of the nanocomposites could be optimized. It was found that GNPs could prevent agglomeration of silver nanoparticles in the hybrid system. In addition, the hybrid systems showed lower viscosity at the same filler contents in comparison with simple mixtures of SNP or SNW and GNP.

Keywords: hybrid, silver nanoparticle, graphene nanoplate, epoxy resin, nanocomposite

[1] D.I. Tee, M. Mariatti, A. Azizan, C.H. See, K.F. Chong, Compos. Sci. Technol. 67., 2584 (2007).
[2] F. Tan, X. Qiao, J. Chen, H. Wang, Int. J. Adhes. Adhes. 26., 406 (2006).
[3] M. Rong, M. Zhang, H. Liu, H. Zeng, Polymer. 40., 6169 (1999).
[4] Z. Lin, A. Mcnamara, Y. Liu, K.S. Moon, C.P. Wong, Compos. Sci. Technol. 90., 123 (2014).
[5] K.H. Kim, J.H. Kim, Ceram. Int. 40, 5181 (2014).

Rheology and Thermal Properties of Epoxy Resins Containing Mixture of Alumina and Boronnitride or Silver Plate.

Van Dung Mai and Dai Soo Lee

Division of Semiconductor and Chemical Engineering, Chonbuk National University, Deokjin-dong 664-14, Jeonju 561-756, South Korea.

daisoolee@jbnu.ac.kr.

Epoxy resins are widely used for the packaging of electronic devices due to the excellent electrical insulation property and heat resistance. Epoxy molding compound (EMC) is one of good examples for the packaging of various semiconductors. Such packaging materials require efficient heat dissipation to prevent heating and malfunction of the device during the operation of highly integrated devices. Thus, many type of inorganic or metallic fillers of high thermal conductivity can be incorporated into the various epoxy resins. There are many reports on the thermal properties of epoxy resins filled with such fillers as alumina [1], hexagonal boron nitride [2], or silver particles [3] to develop polymer composites of improved thermal conductivity. Processing of the epoxy resins containing large amount of the thermally conductive fillers requires optimizing the rheological properties as well as maximizing the thermal conductivities. In this paper, rheology and thermal conductivity of bis phenol A based epoxy resins containing mixture of alumina and boronnitride or silver plate were investigated. It is postulated that proper mixtures of different fillers are necessary for the efficient heat dissipation of the electronic devices as well as the processing of the composites for the packaging of the electronic devices.

Keywords: epoxy resins, rheology, alumina, silver plate, boron nitride.

[1] Alok, A. & Alok S., Effect of Al_2O_3. 2015 Addition on Thermo-Electrical Properties of Polymer Composites: An Experimental Investigation. *Composites,* 36, 102-112.

[2] Martin D., Spiros T., Emmanuel L. 2015. Boron nitride filled epoxy with improved thermal conductivity and dielectric breakdown strength. *Composites Science and Technology* , 110, 152–158

[3] Yi-Hsiuan Y., Chen-Chi M., Chih-Chun T., Yuan-Li H., Hsi-Wen T., Shie-Heng L. & Ikai W. 2013. Enhanced thermal and mechanical properties of epoxy composites filled with silver nanowires and nanoparticles, *Journal of the Taiwan Institute of Chemical Engineers*, 44, 654–659.

Selective Adsorption Behaviors of Core−shell- and Hollow-structured Mn_2O_3/TiO_2 Composite Microspheres

Hack-Keun Lee, Seung-Woo Lee*

Graduate School of Environmental Eengineering, University of Kitakyushu
Hibikino 1-1, Kitakyushu 808-0135, Japan

hackkeunlee@gmail.com, **leesw@kitakyu-u.ac.jp*

Morphologically controlled inorganic compounds, especially having porous and hierarchical structures, have attracted intensive attention in recent years because of their large surface area and keeping as high as catalytic activity. Most of them could show specific chemical and physical properties and emerge as promising materials in a wide range of applications such as water purification, catalysis, and lithium ion storage. Recently, we proposed a facile method for synthesis of hierarchical core−shell- and hollow-structured Mn_2O_3/TiO_2 anatase microspheres [1]. Titania coating was conducted on the $MnCO_3$ particle surface via liquid phase deposition (LPD). After calcination, BET surface areas of the core−shell and hollow Mn_2O_3/TiO_2 composites were estimated to be 83.6 and 21.4 $m^2\ g^{-1}$, respectively. In this study, we evaluated the adsorption behaviors of the synthesized composites using several organic dye compounds as candidate pollutants in water. The fabricated core–shell and hollow- structured Mn_2O_3/TiO_2 composites showed fast and selective adsorption of dyes, which reflects the morphological features of the composites.

Keywords: Mn_2O_3/TiO_2 composite, Core–shell and hollow structures, Selective adsorption

[1] LEE, H-.K., SAKEMI, D., SELYANCHYN, R., LEE, C-.G. & LEE, S-.W. 2014. Titania Nanocoating on $MnCO_3$ Microspheres via Liquid-Phase Deposition for Fabrication of Template-Assisted Core–Shell- and Hollow-Structured Composites. *ACS Applied Materials & Interfaces*, 6, 57-64.

Self-organization of non-ionic surfactants aggregates in layered materials

Régis Guégan[1]

[1]ISTO, UMR 7327 CNRS-Université d'Orléans, 1A Rue de la Férollerie, 45071 Orléans Cedex 2

regis.guegan@univ-orleans.fr

Amphiphilic molecules own the main feature to form ordered aggregates on interfaces which determine various applications in the area of detergency, ore flotation, oil recovery agents, or composite materials. Among various kinds of amphiphilic molecules, n-$CnH_{2n+1}(OCH_2CH_2)_mOH$ nonionic surfactant (abbreviated as C_nE_m) have received particular attention due to their ability to self-assemble in various liquid crystalline phases above the critical micelle concentration (cmc). The aim of this work is to study the role of the surfactant state in bulk solution for the adsorption onto layered materials (clay minerals, layered double hydroxydes, nanosheets) by focusing on the structure and the dynamics of aggregates. The results obtained by a set of complementary techniques (Small angle X-ray scattering, X-ray diffraction, solid state nuclear magnetic resonance, FTIR, thermo-gravimetry analyses) point out the importance of the bulk phase state of nonionic surfactant for the arrangement of the aggregates confined within the interlayer space of the layered materials [1-3].

Keywords: nanosheets, layered materials, adsorption, composite, surfactants

[1] GUEGAN, R. 2010. *Langmuir*, 26, 19175–19180.

[2] GUEGAN, R. 2013. *Soft Matter*, 9, 10913.

[3] GUEGAN, R., SUEYOSHI, K., ANRAKU, S., YAMAMOTO, S., MIYAMOTO, N., 2016. *ChemComm,* doi: 10.1039/C5CC08948D.

Sol-Gel Based Molecularly Imprinted Polymers: Highly Sensitive Synthetic Receptors Created by Functional Materials

Abuzar Kabir, Rayma Blanco, Javier Mejia, Kenneth G. Furton

International Forensic Research Institute, Department of Chemistry and Biochemistry, Florida International University, Miami, Florida, USA.

E-mail : akabir@fiu.edu; Contact Address: 11200 SW 8th Street, AHC4-215, Miami, FL-33199, USA

Considering the high costs, unreliability and challenges involved in immobilizing biological recognition elements such as antibodies, enzymes on a suitable substrate, substantial research efforts have been focussed in recent years in developing inexpensive, reusable and robust synthetic molecular recognition elements known as molecularly imprinted polymers (MIP). MIPs are tailor-made synthetic recognition materials that possess specific cavities, complimentary to the shape, size, and functional groups of the template molecule used in the imprinting process. Due to the inherent advantages of MIPs, the use of these unique synthetic receptors in resolving critical analytical challenges has been skyrocketed in recent years. MIP utilizes one or multiple functional monomers, a cross-linker, a porogenic solvent, a reaction initiator or catalyst and the template molecule to carry out the polymerization reaction, resulting in a 3-D networks of polymeric sorbent with trapped template molecules inside. Subsequent removal of the template molecules leaves specific binding sites/cavities in the polymer network.

The most popular approach of creating molecularly imprinted polymers, organic synthesis route, suffer from a number of shortcomings which include (a) slow mass transfer kinetics; (b) heterogeneity and low population of high-affinity binding sites; (c) irreversible shrinking and/or swelling when exposed to organic solvents, leading to considerable deformation of the imprinted cavities, and subsequent loss in template recognition capacity; (d) relatively high non-specific adsorption often leads to low imprinting factor (IF) value.

Some of these shortcomings have been addressed in sol-gel synthesis approach which is extremely versatile and possesses substantial advantages such as mild room temperature synthesis conditions, controllable pore size, and high surface area. The rigid, highly cross-linked structure of sol-gel MIPs possesses delicate imprinted sites with high degree of shape, size and functional recognition selectivity. Due to their unique characteristics such as selectivity; physical robustness; thermal, chemical and solvent stability as well as low cost and easy preparation, sol-gel MIPs have drawn increased attention with novel applications in many fields.

Recently, we have developed a facile formulation for creating rapid and efficient sol-gel molecularly imprinted polymers. Utilizing this formulation, a number of MIPs have been created using chloramphenicol, sulfa drugs, diphenylhydramine (DPH), and bisphenol A as templates. The MIPs were characterized by Scanning Electron Microscopy, Fourier Transform Infrared Spectroscopy and nitrogen adsorption porosimetry. The selectivity and sorption capacity of these MIPs were evaluated as solid phase extraction sorbents for monitoring chloramphenicol in milk, diphenylhydramine in environmental water, sulfa drugs in milk, bisphenol A in milk. Relevant analytical data will be presented.

Keywords: Sol-gel, molecularly imprinted polymers, synthetic receptors, functional materials sample preparation

A novel process to fabricate Al/AlN composites

Kon-Bae Lee[1], Seong Hyun Yoo[1], Jae-Pyoung Ahn[2,*], Hyun Joo Choi[1,*]

[1]School of Advanced Materials Engineering, Kookmin University, 77 Jeongneung-ro, Seongbuk-gu, Seoul 136-702, Republic of Korea

[2]Advanced Analysis Center, Korea Institute of Science and Technology (KIST), 39-1 Hawolgok-dong, Wolsong-gil 5, Seongbuk-gu, Seoul 130-650, Republic of Korea

E Mail/ Contact Détails

Presenting author (Seong Hyun Yoo): youssh1119@kookmin.ac.kr
TEL: +82-2-910-5256, FAX: +82-2-910-4320

Corresponding author (Jae-Pyoung Ahn): jpahn@kist.re.kr,
TEL: +82-2-958-5536, FAX: +82-2-958-6974

Corresponding author (Hyunjoo Choi): hyunjoo@kookmin.ac.kr
TEL: +82-2-910-4287, FAX: +82-2-910-4320

Metal matrix composites (MMCs), which exhibit the characteristics of both metallic and ceramic materials, have been studied extensively in the last few decades. The conventional processes used for synthesizing MMCs have major drawbacks, the chief of which are (i) the poor wettability between the reinforcing phase and the matrix metal, and (ii) the limited volume fraction of the reinforcing phase. In order to overcome these problems, a number of different techniques have been introduced, such as mechanical stirring to enhance the wettability, and vacuum or pressure to increase the volume fraction of reinforcing phase. However, these approaches not only result in an increase in the production cost, but also have a detrimental effect on the properties of the fabricated MMCs. This limits the use of MMCs in industrial applications on a large scale.

In this study, we introduce a novel MMC fabrication process that simultaneously overcomes the two above-mentioned problems. Al/AlN composites were fabricated by heat-treatment of Al powder in nitrogen atmosphere. The volume fraction of the AlN phase, which was formed *in situ* during the fabrication reaction, was controlled by varying the amount of carbon additives. The composite was produced by the spontaneous infiltration of molten Al and the process did not involve the use of a vacuum, an external pressure, or an expensive additive such as a reactive element (i.e., Mg, Li, etc.). Therefore, the fabrication cost of MMCs is much lower the other MMC fabrication processes. In addition, because the MMCs are fabricated by the spontaneous infiltration of molten Al, a wide variety of additional reinforcing phases (such as carbides, oxides, borides, and nitrides) can be further incorporated into the metal matrix. Finally, the mechanical and thermal properties of the composite were tailored by the type and volume fraction of reinforcing phases.

Keywords: Metal Matrix Composites, Aluminum, Nitridation, Powder, Carbon

Bioactive glass surface for fiber reinforced composite implants via surface etching by Excimer laser: *in vitro* and *in vivo* results

Kulkova[1], Moritz[1], Huhtinen[2], Mattila[1], Donati[3], Marsich[3], Vallittu[1]

[1]Department of Biomaterials Science, Institute of Dentistry, University of Turku, Turku, Finland and Biocity Turku Biomaterials Research Program, Turku Clinical Biomaterial Centre – TCBC and City of Turku Welfare Division, Turku, Finland

[2]Wihuri Physical Laboratory, Department of Physics, University of Turku, Finland

[3]Department of Life Sciences, University of Trieste, Trieste, Italy

Presenting and Corresponding author : Julia Kulkova, DDS, PhD

E Mail : julkul@utu.fi Contact Détails : Turku Clinical Biomaterials Centre-TCBC

Itäinen Pitkäkatu 4B, FI-20520 Turku, Finland

Tel.:+ 35823338527

Objective

Biostable fiber-reinforced composites (FRC) prepared from bisphenol A –glycidyldimethacrylate dimethacrylate (BisGMA)-based thermosets reinforced with E-glass fibers are promising alternatives to metallic implants [1]. Clinical use of non-load-bearing FRC implants has already commenced in cranial reconstructions [2]. In addition, preclinical studies demonstrated the potential of BisGMA-based FRC implants in load-bearing orthopaedic applications [3, 4]. FRC implants provide physiological load-sharing between implant and host bone and reduce the risk of peri-implant bone resorption [1]. Surface-bound bioactive glass (BG) particles have been shown to improve the osteointegration of the FRC implants [2]. In this study, we used surface etching by Excimer laser to prepare novel BG-based surfaces on FRC implants.

Experimental

A UV-Vis spectroscopic study was performed to outline the differences in the penetration of light between the thermoset matrix and BG. Subsequently, a series of experiments was performed to optimize the Excimer laser etching parameters. The bioactivity was verified by the simulated body fluid (SBF) test. The proliferation of MG63 cells on the surfaces of the laser-etched FRC specimens was investigated. Implants made of FRC with the novel BG-based surface were placed in the cortex of the femoral shaft in minipig. Osteointegration was assessed biomechanically in a push-out test and histologically.

The Results and their significance

The optimal laser etching effect was achieved with the total energy of 175 mJ and the energy density of 0.32 J/cm^2. The SBF test has demonstrated the formation of calcium phosphate on the surface of the laser-etched FRC specimens. In addition, for the laser-ablated specimens, proliferation of MG63 cells was similar to that of the positive control group (Ti6Al4V). Perfect osteointegration was confirmed in the *in vivo* experiment. In fact, the implants were not possible to push out of the cortical bone.

To our knowledge, this is the first study to report the use of this method in relation with the BG-based surfaces. Detachment of BG granules from the FRC implants was previously reported for

load-bearing [3] and non-loadbearing [5] conditions. Extensive interfacial sheer forces which arise in the load-bearing of FRC implants may contribute to the detachment of the BG granules [6]. The presence of loose granules at the implant interface is objectionable as they may act as a rolling surface in the micromotion of the implant [7].

The advancement over previous work

Our previous studies revealed technical challenges in the creation of a feasible surface layer using BG granules [3, 4]. The results of this study have shown that Excimer laser ablation has potential for the creation of a BG-based bioactive surface on FRC-implants.

Keywords

Fiber-reinforced composites; Excimer laser; Laser ablation; Bioactive glass; Intramedullary nail.

References

[1] EVANS, S.L., GREGSON, P.J. 1998. Composite Technology in Load-Bearing Orthopaedic Implants. *Biomaterials*, 19, 1329-1342.

[2] AITASALO, K.M., PIITULAINEN, J.M., REKOLA, J., VALLITTU, P.K. 2014. Craniofacial Bone Reconstruction With Bioactive Fiber-Reinforced Composite Implant. *Head Neck*,36,722-728.

[3] ZHAO, D.S., MORITZ, N., LAURILA, P., MATTILA, R., LASSILA, L.V.J, STRANDBERG, N., MÄNTYLÄ, T., VALLITTU, P.K., ARO, H.T. 2009. Development of a Multi-Component Fiber-Reinforced Composite Implant for Load-Sharing Conditions. *Med Eng Phys*, 31, 461-469.

[4] NEWBONE (Development of load-bearing fibre reinforced composite based non-metallic biomimetic bone implants), EU 6th Framework Programme, NMP, Integrated Project for SMEs, Contract no. 026279, final report, 2010.

[5] TUUSA, S.M., PELTOLA, M.J., TIRRI, T., LASSILA, L.V., VALLITTU, P.K. 2007. Frontal Bone Defect Repair with Experimental Glass-Fiber-Reinforced Composite with Bioactive Glass Granule Coating. *J Biomed Mater Res B Appl Biomater*, 82, 149-155.

[6] MORITZ, N., STRANDBERG, N., ZHAO, D.S., MATTILA, R., PARACCHINI, L., VALLITTU, P.K., ARO, H.T. 2014. Mechanical Properties and In Vivo Performance of Load-Bearing Fiber-Reinforced Composite Intramedullary Nails with Improved Torsional Strength. *J Mech Behav Biomed Mater*, 40C,127-139.

[7] KERÄNEN, P.,ITÄLÄ, A., KOORT, J., KOHONEN, I., DALSTRA, M., KOMMONEN, B., ARO, HT. 2007. Bioactive glass granules as extender of autogenous bone grafting in cementless intercalary implant of the canine femur. *Scand J Surg*, 96, 243-51.

Core-shell structured upconversional luminescent graphene/quantum dots for photodynamic therapy of cancer cells

Seung Yoo Choi, Seung Hoon Beak and Tae Jung Park*

Department of Chemistry, Chung-Ang University, 84 Heukseok-ro, Dongjak-gu, Seoul 06974, Republic of Korea

*E-mail: tjpark@cau.ac.kr

Various methods and materials have been studied for biomedical applications. The materials consisted of upconversion nanoparticles (UCNPs), magnetic nanoparticles (MNPs), and graphene quantum dots (GQDs) exhibited their therapeutic multifunctionalities for imaging-guided analyses. UCNPs have distinctive characteristics accessible to diagnosis and therapy. Thus, cell imagings for verifying apoptosis/necrosis of cancer cells using the upconversional luminescent techniques have been performed. First, GQDs passivated with polyethylene glycol (PEG) on the surface were synthesized. The surface passivation is the most effective functionalization with biomolecular imaging and monitoring and drug delivery system. Sequentially, multi-functional materials by coupling chemistry were attached with ethyl-dimethyl-aminopropylcarbodiimide and N-hydroxy-succinimide on prepared PEG-GQDs. This multifunctional material, GQDs-attached MNP@UCNPs, has a great potential for both imaging (upconversion luminescence and magnetic resonance imaging, MRI) and therapy (photothermal therapy, PTT and photodynamic therapy, PDT) in cancer diagnostics. Furthermore, hematoporphyrin monomethyl ether (HMME) conjugated GQDs-attached MNP@UCNPs nanocomposites were designed due to their intrinsic properties, which are drug abilities from HMME and imaging capability from magnetic resonance/upconverisonal luminescence (MR/UCL). Here, we have developed a noble method and material for the light stability and biocompatibility for biomedical applications.

References

[1] M. Haase, H. Schafer, Upconversion Nanoparticles, *Angew. Chem. Int. Ed*., 50, 5808-5829 (2011)

[2] M. Zhang, S. Shi, J. Meng, X. Wang, H. Fan, Y. Zhu, X. Wang, Y. Qian, Preparation and Characterization of Near-Infrared Luminescent Bifunctional Core/Shell Nanocomposites, *J. Phys. Chem. C*, 112, 2825-2830 (2008)

Keywords: Photoluminescence, Upconversion nanoparticle, Magnetic nanoparticle, Photo-therapy, Graphene quantum dots

Crystallization of Calcium Deficient Hydroxyapatite Nanocrystals on Woven Silk Fibroin Fabricvia Precipitation Process

Piyapong Pankaew[1], Pattarinee Klumdoung[2]

[1]Division of Industrial Materials Science, Faculty of Science and Technology, Rajamangala University of Technology Phra Nakhon, Bangkok 10800, Thailand
[2]Divisionof Physics, Department of Science, Faculty of Science and Technology, Rajamangala University of Technology Krungthep Bangkok 10120, Thailand

E Mai :piyapong.p@rmutp.ac.th

Hydroxyapatite (HAp, $Ca_{10}(PO_4)_6(OH)_2$), a type of calcium phosphate (CP),have been recognized as one of the most promising materials for medical applications due to its excellent biocompatibility and similar chemical properties to bones and teeth [1]. Unfortunately, its clinical application was limited on a high load-bearing implant due to the inherent poor fracture strength and toughness [2]. Silk fibroin (SF), a fibrous protein with β-sheet structure derived from Bombyx mori silk worm, is numerously considered to be the potential biomaterial in implantable biomaterials and scaffolds for tissue engineering due to its low cost, excellent biocompatibility and excellent mechanical performance [5]. Therefore, many researchers have extensively developed SF/HAp composites crosslinking of SF and HAp in order to improve their mechanical and biological characteristics. In the last decades, SF/HAp composites have been developed by mineralization of HAp under regulating of SF through precipitation process [6-8] or immersing in simulated body fluid (SBF) [9-13]. Many authors reported the preparation of SF/HAp nanoparticles by dropping the co-solution of SF and H_3PO_4into $Ca(OH)_2$ suspension or adding $(NH_4)_2HPO_4$ solution into co-solution of SF/$CaCl_2$. In the form of SF/HAp film, Duet al fabricated by precipitation reaction of co-solution of SF/$Ca(NO_3)_2$ and Na_2HPO_4. Yang et al. Observed HAp crystal growth by self-assembly of SF solution in 1.5 times SBF. Particularly there are few reports to propose the growth of HAp nanocrystals on SF fibers by immersing in 1 SBF and 1.5 SBF [12,13]. There are some disadvantages for such preparation methods and in the forms of composites. HAp/SF

composites in the forms of bulk or film are generally of poor mechanical strength. For HAp mineralization through immersing in SBF, it is unfeasible in industrial processes due to its complex procedure, high production cost and long period consumption of at least 7 days to activate HAp crystals on SF surface. Therefore there is an urgent need to develop simpler fabrication techniques and to design the SF/HAp composite forms that can produce grafts to match load bearing requirements of the desired applications.

In the present research, a promising composite had been proposed by crystallization of calcium deficient hydroxyapatite (Ca-def HAp) on woven SF fabrics via rapid precipitation method for future applications on the utilization of bioactivity of Ca-def HAp and strength of SF fiber. This method is expected to lower cost by simpler setup and time-saving preparation. The Ca-def HAp phase interested in this study is expected to improve as bone implant materials because of its higher solubility and more efficient in inducing the bone-like apatite than HAp [13]. Thus this phase may be also utilized for future orthopedic applications with enhanced biological performance. Chicken eggshells are selected as calcium source for crystallizing Ca-def HAp due to their high calcium content and easy procurement. Besides, for long period testing HAp synthesized from eggshells was found with higher bone tissue regenerationthan commercial HAp in a comparison study.

CP crystals were grown on SF fiber templates by precipitation reaction of $Ca(NO_3)_2$; prepared from chicken eggshells, and $(NH_4)_3PO_4$ solutions using NH_4OH solution to adjust the pH of reaction. Firstly, powdered eggshells ($CaCO_3$) were heated at 1300 °C for 4 h to obtain CaO powders. Then, $Ca(NO_3)_2$ solution was prepared by dissolving the obtained CaO powder in 65% HNO_3 solution. Next step, SF fiber templates was immersed in $Ca(NO_3)_2$ solution at room temperature for 30 minutes. The prepared $(NH_4)_3PO_4$ solution with different pH values was poured into the glass dish containing SF fiber templates/$Ca(NO_3)_2$ solution in order to allow nucleation process of CP crystals on surface of SF fiber templates. After being reacted for 1 minute, grown SF fiber templates was removed from the precipitated suspension and was cleaned and left at room temperature until completely dry.The initial Ca/P ratio of $Ca(NO_3)_2$ solution to $(NH_4)_3PO_4$ solution was kept at 1.2 and 1.6 and assigned as CP_1 and CP_2 samples. The

effect of initial pH values of solutions on phase structure and morphology of CP crystals grown on SF fiber templates was investigated at pH of 7, 8 and 9 and assigned as CP_{17}-CP_{19} and CP_{27}-CP_{29} samples. Moreover, two patterns of woven SF fabric model such as plain-woven SF fabric and twill-woven SF fabric are designed and tested for selecting for the better as prototype for future bone implant materials.

A composite material combining of CP crystals and SF fiber templates was successfully prepared via a rapid precipitation technique. SEM results revealed two distinctive morphologies of CP crystals on SF fiber templates: large plates and clusters of nanoparticles. With initial pH of 7 and 8, the crystal feature is plates with its width and length between 2-5 µm and thickness of about 400 nm. When adjust the initial pH to 9, the plate-shaped crystal disappeared and the crystal morphology exhibits clusters of smaller than 100 nm nanoparticles. The mechanisms of CP crystallization can explained as when SF fiber templates are immersed in $CaNO_3$ solution, C-O and N-H groups on SF molecules were preferentially coordinated with calcium (Ca^{2+}) ions after that the occurrence of Ca-SF complexes. When $(NH_4)_3PO_4$ and NH_4OH solutions are dropped into the Ca-SF complex system, Ca^{2+} ions on the SF molecules electrostatically interact with the $PO_4^{3-}$and OH^- groups. More of these ions are further gathered in unit the concentration and are favorable to the growth of CP nuclei on SF surface. After the nucleation, the growth of CP crystals will spontaneously progress from these active nucleation sites. The nucleation generation rate was slowly for low pH values of 7 and 8, resulting in a faster growth rate. Thus the nuclei of CP crystals on SF surface grow slower and will lead to larger crystals until grow into plate-shaped crystal. Oppositely, their nuclei grow faster at high pH of 9 and as the result the formation of nanocrystals.

The Ca/P ratios of CP crystals grown on SF fiber templates, quantitatively calculated using EDX data, are 1.28, 1.31 and 1.52 for samples CP_{17} to CP_{19} and are 1.61, 1.85 and 1.86 for CP_{27} to CP_{29} samples, respectively. Increasing of initial pH value directly causes an increase in concentration of OH^- ions and decreases the amount of HPO_4^{2-} ions substituted into CP crystal by dissociating of HPO_4^{2-} ions into PO_4^{3-} and H^+ ions. As the result, more Ca^{2+}, PO_4^{3-} and OH^- ions are being in corporated into CP crystal and therefore the increase in Ca/P ratio. Calcium deficient hydroxyapatite (Ca-dHAp) is

called for the phase with Ca/P ratio of 1.50-1.67. From all the results above, processing of CP_{19} sample (the initial Ca/P ratio of 1.2 with the initial pH value of 9) is the most optimum condition for CP crystal growth on woven SF fabric for obtaining Ca-def HAp phase and crystal in nanoscale.

For testing the tensile strength of SF fabric models, the tensile strengths of woven SF fabric were about 840 MPa and 470 MPa for plain-weave and twill-weave patterns, respectively. The tensile strength of plain-woven SF fabric is about two times higher than that of twill-woven SF fabric. In plain pattern, the contact area between warp and weft yarns is more due to interlacing of warp and weft yarns by one up and one down, while the fewer interlacings in twills allow the yarns to move more freely. The higher contact friction between warp and weft yarns of plain-weave is therefore more than that of twill-weave and as a result a higher tensile strength of plain woven SF fabric. The plain pattern of woven SF fabric was chosen as the suitable template to grow CP crystal for its highest tensile strength.

The Ca/P ratio of the Ca-def HAp nanocrystals on plain-woven SF fabric was about 1.52 as confirmed with the results of Ca-dHAp phase from XRD and FT-IR. The Ca-def HAp nanocrystals on plain-woven SF fabric showed clusters of about 100 nm nanoparticles; indicating a high surface area for cell attachment and the better cell growth and differentiation.

The overall result is accordingly indicated that the composite combining Ca-def HAp nanocrystals on plain-woven SF fabric could be successfully prepared by rapid precipitation. The method provided with a simpler setup and time-saving preparation and the product has a high potential for high load bearing bone implant applications.

Keywords: crystallization, Calcium deficient hydroxyapatite, silk fibroin, precipitation, fabric-model

[1] DOROZHKIN, S. V. 2010. Nanosized and Nanocrystalline Calcium Ortho-Phosphates. *Acta Biomater*, 6, 715–734.

[2] RAMESH, S., TAN, C. Y., BHADURI, S. B., TENG, W. D. & SOPYAN, I. 2008. Densification Behaviour of Nanocrystalline Hydroxyapatite Bioceramics. *J. Mater. Proc. Technol*, 206, 221-230.

[3] DOROZHKIN, S. V. 2010. Bioceramics of Calcium Orthophosphates. *Biomaterials,*1465-1485.

[4] WANG, T. & DORNER-REISEL, A. 2004. Thermo-Analytical Investigations of the Decomposition of Oxyhydroxyapatite. *Mater Lett*, 58, 3025-3028.

[5] ALTMAN, G. H., DIAZ, F., JAKUBA, C., CALABRO, T., HORAN, R. L., CHEN, J., Lu, H.,RICHMOND, J. & KAPLAN, D. L. 2003. Silk-Based Biomaterials. *Biomaterials,* 24,401-416.

[6] NIU, L., ZOU, R., LIU, Q., LI, Q., CHEN, X. & CHEN, Z. 2010. A Novel Nanocomposite Particle of Hydroxyapatite and Silk Fibroin: Biomimetic Synthesis and Its Biocompatibility. *J. Nanomater*, 729457 (7pp).

[7] WANG, J., YU, F., QU, L., MENG, X. & WEN, G. 2010. Study of Synthesis of Nano-Hydroxyapatite Using a Silk Fibroin Template. *Biomed. Mater*, 5, 041002 (5pp)

[8] FAN, C., LI, J., XU, G., HE, H., YE, X., CHEN, Y., SHENG, X., FU, J. & HE, D. 2010. Facile Fabrication of Nano-Hydroxyapatite/Silk Fibroin Composite Via a Simplified Coprecipitation Route. *J. Mater. Sci*, 45, 5814-5819.

[9] DU, C., JIN, J., LI, Y., KONG, X., WEI, K. & YAO, J. 2009. Novel Silk Fibroin/HydroxyapatiteComposite Films: Structure and Properties. *Mater. Sci. Eng. C.*, 29, 62-68.

[10] LI, Y., CAI, Y., KONG, X., & YAO, J. 2008. Anisotropic Growth of Hydroxyapatite onthe Silk Fibroin Films. *Appl. Surf. Sci*., 255, 1681-1685.

[11] YANG, M., HE, W., SHUAI, Y., MIN, S. & ZHU, L. 2013. Nucleation of Hydroxyapatite Crystals by Self-Assembled Bombyx Mori. Silk Fibroin. *J Polym Sci B Polym Phys*. 51, 742-748.

[12] Takeuchi, A., Ohtsuki, C., Miyazaki, T., Tanaka, H., Yamazaki, M. & Tanihara, M. 2003. Apatite Formation on Silk Fiber in a Solution Mimicking Body Fluid. *J. Biomed. Mater. Res. Part A*, 65, 283-289.

[13] Sukjai, O., Asanithi, P., Limsuwan, S. & Limsuwan, P. 2013. Growth of Hydroxyapatite on Sericin Coated and Non-Sericin Coated Silk Fibers Using Simulated Body Fluid. *IJSRP*, 3, 1-5.

Experimental research on the basic mechanics performance of Inorganic polymer lightweight aggregate concrete

YAO Yuan , ZHOU Kai , CHEN Xiaoye

School of Civil Engineering and Architecture , Wuhan University of Technology , Wuhan, Hubei, 430070 China

Abstract: Inorganic polymer concrete has become one of the hot issues in engineering research, with it's advantages of environmental protection, earlystrength and so on. Inorganic polymer lightweight aggregate concrete(IPLAC) was prepared by using inorganic polymer powder and shale aggregate. With different water binder ratios, it's compressive performance and failure chacharacteristics had been studied in curing period of 28 days. Concrete fragments had been studied by scanning electron microscope. Test results indicate that the inorganic polymer slurry body and aggregate interface bonding closely. The curing rate of IPLAC mixture is faster than that of ordinary lightweight aggregate concrete(OLAC). The compressive strength and splitting tensile strength of IPLAC are both higher than OLAC's, Besides, it's ductility also slightly improved. The water binder ratio within the range of 0.44~0.36, the compressive strength and splitting tensile strength of IPLAC increased with the decrease of water binder ratio. However, as the water binder ratio dropped to a certain value, the compressive strength will no longer have to enhance.

Keywords: ***Inorganic polymer, lightweight aggregate concrete, mechanics performance, experimental research, failure mode***

[1] Davidovits, J. Geopolymers and Geopolymeric materials. 1989. Journal of Thermal Analysis. Cement and Concrete Research, 35, 429-441.

[2] Yuan Hongchang , Jiang Yaozhong. The developmengt of geopolymer and its future of our country. 1998. Journal of the Chinese Ceramic Society, 46-50.

[3] Wang Qing, Liu Lei, Wu Changpeng & Sui Zhitong. Reacher on mechanical

propertity of slag based geopolymer. 2007. Journal of Shenyang Jianzhu University, 23, 73-76.

[4] Palomo, A., Glasser, F. P. Chemically-bonded cementitious materials based on metakaolin. 1992. Br.Ceram.Trans.J, 91, 107-112.

[5] MEHTA, P. K. Greening of the concrete industry for sustainable development. 2002. Concrete International, 23-28.

[6] Fan Xiaochun, Liu Dong, Yan Yan, Yuan Bo & Lu Zhean. Experimental reseach of compressive performance on inorganic polymer concrete pavement at differengt ages. 2012. Concrete, 69-71.

[7] Van Jaarsveld, J.G.S., Van Deventer, J.S.J. & Lorenzen, L. Factors affecting the immobilization of metals in geopolymerized fly ash. Metallurgical and Materials Transactions B;1998. Process Metallurgy and Materials Processing Science, 29, 283-291.

[8] Van Jaarsveld, J.G.S., Van Deventer, J.S.J. Effect of metal contaminants on the formation and properties of waste-based geopolymers. 1998, Cement and concrete Research, 29, 1189-1200.

[9] Wang Gang, Ma Hongwen, Ren Yufeng, Feng Wuwei & Ding Qiuxia. Study on preparation of mineral polymer from fiy ash. 2003. Industrial Minerals Processing, 22, 24-27.

[10] Wang Gang, Ma Hongwen, Feng Wuwei & Ding Qiuxia. The preparation of mineral polymer from potassium-distilled waste residue and fiy ash : an experimental study. 2004. Industrial Minerals Processing, 22, 453-457.

[11] Wu Yonggen, Fu Yawei, Cai Liangcai,Wang Shuotai & Xu Bo. Studies of geopolymer fast-repaired concrete. 2008. Concrete, 9, 98-100.

[12] Davidovits, J. 30 years of seccesses and failures in geopolyment applications. 2002. Geopolymer 2002. Australia : Melbourne University, 2-8.

[13] Huo Junfang. Status quo and develomengt of reseaarch on lightweight aggregate concrete. 2009. Architechnique of Technology, 40, 363-365.

[14] Holm, T. A, Bremner, T, W. State-of-the-art report on high-strength, high-durability structural low-density concrete for applications in severe marine environments. 2000, 1-7.

[15] Song Shaoming. The application and development of light-weight aggregate

concrete in construction of high-rise building and large-span bridges. 2003. Jiangsu Construction, zl, 76-84.

[16] Euroligcon. LWAC materials properties state-of- the-art. 1998, 11-16.

[17] Cheng Li. Reaction mechanisms and the products of three alkali-activated cementations materials. 2004. Journal of Jingmen Technical College, 19, 92-95.

[18]Shao Zheyu, Research of Hydration process and carbonation perfoemance. 2014. Wuhan : Wuhan University of Technology, 10-14.

[19] Ma Xiao. Research on preparation and performance of new type high performance lightweight aggregate concrete based on inorganic polymier cement. 2012. Changsha : Central South University, 6-27,33-36,40-43,63-65,101-112.

[20]Xiang Chunlin. Experimengtal research on mechanics performance of geopolymer concrete. 2011. Wuhan : Wuhan University of Technology, 2-5, 22-25.

[21]Wang Hailong, Shen Xiangdong. Study of early mechanical properties of lightweight aggregate concrete. 2008. Bulletin of the Chinese Ceramic Society, 27,1018-1022.

Fabrication and Characterization of MWCNT/Epoxy Nanocomposite Film Deposited on Aluminum Substrate

Shiuh-Chuan Her[1], Pao-Chu Chien[1]

[1]Dept. of Mechanical Engineering, Yuan Ze University, Chung-Li, Taiwan.

*E Mail (***presenting and corresponding author's)** mesch@saturn.yzu.edu.tw

In this work, multi-walled carbon nanotubes (MWCNTs) reinforced epoxy thin films were deposited on the aluminum substrate by a hot-pressing process. Three-point bending tests were performed to determine the Young's modulus of MWCNT reinforced nanocomposite films. Shear lag model was employed to evaluate the stress distribution and load carrying capability of the nanocomposite film subjected to tensile load. Analytical expressions of the stress distribution and moment transfer of the nanocomposite film subjected to bending moment were derived basing on the beam theory. A close agreement with difference about 6 % was achieved between the theoretical prediction and experimental result. The Young's modulus and load transfer of the naocomposite film is increasing with the increase of the MWCNT content. Compared to the neat epoxy film, nanocomposite film with 1 wt % of MWCNT exhibits an increase of 21 % in both the Young's modulus and load transfer. The addition of MWCNTs into the epoxy matrix shows a significant improvement of the load carrying capability to the nanocomposite film.

Keywords: **multi-walled carbon nanotube, nanocomposite film, load transfer, Shear lag model.**

Fabrication of hydroxyapatite-alumina/ 3 mol% yttria tetragonal zirconia bilayered composite for bone replacement material

Piyapong Pankaew[1], Pattarinee Klumdoung[2]

[1]Division of Industrial Materials Science, Faculty of Science and Technology, Rajamangala University of Technology Phra Nakhon, Bangkok 10800, Thailand
[2]Divisionof Physics, Department of Science, Faculty of Science and Technology, Rajamangala University of Technology Krungthep Bangkok 10120, Thailand

E Mai :piyapong.p@rmutp.ac.th

Hydroxyapatite (HAp) has long been recognized as one of the most potential candidate for hard tissue implants in orthopedic and dental surgeries because of its crystallographical and chemical similarity with human bone and teeth [1]. Unfortunately, due to its poor behaviour towards tensile stresses, its medical applications are limited to nonstressed regions of the skeleton or to regions where compression is the main mechanical load [2]. To widen the field of application of HAp, extensive attempts have been made to counteract its brittleness in tensile loadings.

The development of a bilayer structure ,consisting of HAp as coating and high strength biomaterials as substrate, is one major direction among the various attempts to enable the utilization of low flexural strength HAp in orthopedic and dental implants. The HAp coating can stimulate hard tissue growth which bridges the bilayer implant to bone while the tougher substrate provides fracture substrate. Various processes including laser and induction plasma [3], thermal/plasma spray [4], pulsed laser deposition [5] and chemical vapor deposition have been used to deposite HAp layer on titanium and its alloys. However ,these processes need to be heated up to more high temperature of 1200 C leading to decomposition of HAp phase into tricalcium phosphate (TCP) and tetracalcium phosphate (TTCP) phases [6]. These compounds deteriorate the mechanical properties of HAp and enhance in vivo degradation of the HAp resulting HAp layer slenderizes for long-term implant. Therefore it is not thickness enough to resist

resorbability of HAp which can be as much as 15-30 um per year [7, 8]. Moreover, the residual stress which may be result from coefficient of thermal expansion (CTE) mismatch between coating and substrate causes microcrack leading to the deterioration of the long-term durability and stability of the implant. For deposition based on powder-based slurry system [9, 10], the obtained HAp coating is considerably thin and is poorly bonded to the substrate. In recent year, functionally graded material (FGM) has been proposed to improve the mechanical property of HAp [11-13]. Afzal et al. successfully fabricated HAp-Al_2O_3/Al_2O_3-YSZ/YSZ multilayer via spark plasma sintering (SPS) technique. Results with strong adherence and absence of cracking at interfaces between layers indicate that Al_2O_3 addition into several layers can reduce the mismatch of the coefficient of thermal expansion between HAp and YSZ layers and the match of fracture toughness gradation between composite layers of FGM.

Therefore for our work, we attempt to bond hydroxyapatite-alumina (HAp-Al_2O_3) layer to 3 mol% yttria tetragonal zirconia (TZ-3Y) layer using conventional technique consisting of the die pressing together with pressureless sintering. The simple die pressing combined with normal sintering is chosen in layering the bilayer structures in its green state to be expected a thick HAp-Al_2O_3 outerlayer and strong interfacial bonding between interface layers. The TZ-3Y, which is well-known as bionert and has high flexural strength, is chosen because its coefficient of thermal expansion (CTE) and sintering temperature are closer to HAp. Al_2O_3 is added in HAp matrix to reduce the CTE of HAp as close to TZ-3Y. In order to obtain the desired characteristics of bilayered structure, layer thickness and cosintering temperature on successful fabrication of HAp-Al_2O_3/TZ-3Y bilayer structure are investigated. The mechanical characteristics of the bilayer specimens will be evaluated from indentation technique generated by Vickers indenter.

In the present research, HAp powders were synthesized by the precipitation reaction of $Ca(NO_3)_2$ solutions and $(NH_4)_3PO_4$ solutions using NH_4OH solution to adjust the pH of reaction. As HAp and TZ-3Y have different CTE and sinterbility, the HAp/TZ-3Y green compact is in general difficult to cosinter due to the need to accommodate differential shrinkage upon firing. Furthermore, residual stresses are induced in its

constituent layers during sintering [3]. Since the CTE of HAp is higher than TZ-3Y, the HAp outerlayer is under residual tension, while the TZ-3Y underlayer is under residual compression. Accordingly, exploratory tests were carried out to investigate the suitable relative thickness of the two layers so as to produce a strong bilayered interface and to minimize the residual tension generated in the HAp outerlayer. Firstly an appropriate sintering temperature of the HAp/TZ-3Y green compact was studied. HAp and TZ-3Y monolithic green compacts with 4 mm thick were carried out by single-end die pressing the powders in hollow cylindrical graphite die under 60 MPa pressure into a disc shape of 25.7 mm diameter. They were subsequently fired in air with a heating rate of 2^{o}C/min to four different elevated temperatures (1200, 1250, 1300 and 1350 ^{o}C) for 1 h. The results of diameters and densities of both sintered samples indicated that 1310 ^{o}C should be employed as the sintering temperature of the HAp/TZ-3Y bilayered green compact. The second exploratory test was made by preparing HAp/TZ-3Y bilayered green compacts having the TZ-3Y underlayer thickness fixed at 4 mm whereas the HAp outerlayer thicknesses varied as 3, 4, 5, 6 and 7 mm. Then they were sintered at 1310 ^{o}C for 1 h. It is found that the interface of all sintered HAp/TZ-3Y bilayered composites was strong. However, crackings normal to the HAp outerlayer plane were apparent in the HAp outerlayer for the case in which the thicknesses of the outerlayer green compact prior to sintering were 3 and 4 mm. For the case in which the thicknesses of the outerlayer green compacts were 5, 6 and 7 mm, these normal crackings were unseen, whereas crackings parallel to the bilayered interface were apparent in the HAp outerlayer. The density of parallel crackings increased as the thickness of the outerlayer increased. Accordingly, the results demonstrated that for the TZ-3Y underlayer green compact of 4 mm thick, 5 mm is the most appropriate thickness for the green compact of the HAp outerlayer.

Since crackings parallel to the HAp/TZ-3Y bilayered interface were unable to eliminate, further attempt was made to reduce the CTE mismatch between the HAp and TZ-3Y layers. According to Choi et al. [14], the CTE of HAp can be made to decrease by adding alumina (Al_2O_3) into the HAp. Therefore, Al_2O_3 powders (A) of various amounts (4, 6, 8, 10 and 12 vol %) were added into the HAp matrix. The two powders were dried mixed by milling them in a rotating polyethylene jar with Al_2O_3

balls for 6 h. After sintering at 1310 ^{o}C for 1 h, the HAp- A green compact was found to shrink less than the HAp green compact. In addition, the shrinkage of the HAp-A composite was found to decrease as the amount of Al_2O_3 addition increased. Therefore, it was chosen to use the sintering temperature for the HAp-A/TZ-3Y green compact as 1200 ^{o}C instead of 1310 ^{o}C. Further exploratory test was made to find a suitable amount of Al_2O_3 addition into the HAp matrix so that the HAp-A and TZ-3Y layers can be strongly bonded after cosintering at 1200 ˚C for 1 h. Accordingly, monolithic green compacts of HAp-A composite of five different amounts of Al_2O_3 additions (4, 6, 8, 10 and 12 vol%) were prepared using single-end die pressing. They were subsequently sintered at 1200 ˚C for 1 h. Their diameters were measured and plotted as a function of the amount of Al_2O_3 addition. The results indicated that 10 vol% is an appropriate amount of Al_2O_3 to be added into the HAp matrix due to codiameter of HAp-10A and TZ-3Y specimens. The obtained HAp-10A/TZ-3Y bilayered composite was found to have a weak interface and low consolidation. Therefore its green compacts formed by single-end die pressing were further wet-bag isostatically pressed in oil to 300 MPa pressure to remove any defects associated with the die pressing before sintering at 1200 ˚C for 1 h. The sintered HAp-10A/TZ-3Y bilayer was found to have a better quality than those without isostatically pressing.

The HAp-10A/TZ-3Y bilayered composite was successfully fabricated via the simple pressing technique combined with pressureless sintering. It is found that an addition of 10 vol% Al_2O_3 into the HAp outerlayer is the essential condition to effectively suppress the differences in densification and coefficient of thermal expansion of the two layers during cosintering at 1200 ^{o}C for 1 h. The obtained HAp-10A/TZ-3Y bilayered disc has diameter of 21.0 mm, HAp-10A outerlayer of 4.5 mm thick, and TZ-3Y underlayer of 2.5 mm thick. The density of its HAp-10A outerlayer and TZ-3Y underlayer measured using the Archimedes method are 2.11g/cm^3 (65% theoretical density) and 4.63 g/cm^3 (76% theoretical density), respectively.

The XRD pattern of the powders crushed from its HAp-10A outerlayer revealed no transformation into other new phases, demonstrating that there is no reaction between HAp and Al_2O_3 during sintering at 1200˚C.

The cross-section morphology of HAp-10A/TZ-3Y bilayered composite obtained from the SEM result revealed the porous structure with good interconnectivity. The high porous structure of the bilayered composite provided high surface area for cell attachment, indicative of good cell growth and differentiation. The primary grain sizes of HAp-10A outerlayer and TZ-3Y underlayer were in the range of 1-3 um and 100-500 nm , respectively.

Accordingly, the results presented in this work demonstrated that the HAp-10A/TZ–3Y bilayered composite fabricated by simple technique has thick HAp-Al_2O_3 outerlayer and strong interfacial bonding between interface layers, which can be tailored for specific applications.

Keywords: bilayered composite, hydroxyapatite-alumina, zirconia, bone replacement material

[1] DOROZHKIN, S. V. 2010. Nanosized and Nanocrystalline Calcium Ortho-Phosphates. *Acta Biomater*, 6, 715-734.

[2] KALMODIA, S., GOENKA, S., LAHA, T., LAHIRI, D., BASU, B. & BALANI, K. 2010. Microstructure, Mechanical Properties, and In Vitro Biocompatibility of Spark Plasma Sintered Hydroxyapatite-Aluminum Oxide-Carbon Nanotube Composite. *Mater Sci Eng C*, 30, 1162-1169.

[3] ROY, M., BALLA, V. K., BANDYOPADHYAY, A. & BOSE, S. 2011. Compositionally Graded Hydroxyapatite/Tricalcium Phosphate Coating on Ti by Laser and Induction Plasma. *Acta Biomater*, 7, 866-873.

[4] LI, H., LI, H., WU, Y. & WEI, Q. 2009. Characterization of Plasma Sprayed Hydroxyapatite/ZrO_2 Graded Coating. *Mater Design*, 30, 3920-3924.

[5] SUDA, Y., KAWASAKI, H., OHSHIMA, T., NAKASHIMA, S., KAWAZOE, S. & TOMA, T. 2006. Hydroxyapatite Coatings on Titanium Dioxide Thin Films Prepared by Pulsed Laser Deposition Method. *Thin Solid Films*, 506,115-119.

[6] WANG, T. & DORNER-REISEL, A. 2004. Thermo-Analytical Investigations of the Decomposition of Oxyhydroxyapatite. *Mater Lett*, 58, 3025-3028.

[7] DOROZHKIN, S. V. 2010. Bioceramics of Calcium Orthophosphates. *Biomaterials*, 31, 1465-1485.

[8] SUCHANEK, W. & YOSHIMURA, M. 1998. Processing and Properties of Hydroxyapatite-Based Biomaterials for Use as Hard Tissue Replacement Implants. *J. Mater. Res.,* 13, 94-116.

[9] WANG, Z. Q., XUE, D. F., CHEN, X. X., LU, B. L. & RATAJCZAK, H. 2005. Mechanical and Biomedical Properties of Hydroxyapatite-Based Gradient Coating on Al_2O_3 Ceramic Substrate. *J. Non-Cryst. Solids.,* 351, 1675-1681.

[10] KIM, H. W., YOON, B. H., KOH, Y. H. & KIM, H. E. 2006. Processing and Performance of Hydroxyapatite/Fluorapatite Double Layer Coating on Zirconia by the Powder Slurry Method. *J. Am. Ceram. Soc*., 89, 2466-2472.

[11] GUO, H., KHOR, K. A., BOEY, Y. C. & MIAO, X. 2003. Laminated and Functionally Graded Hydroxyapatite/Yttria Stabilized Tetragonal Zirconia Composites Fabricated by Spark Plasma Sintering. *Biomaterilas,* 24, 667-675.

[12] YANG, J. Z., SULTANA, R., HU, X. Z. & HUANG, Z. H. 2011. Porous Hydroxyapatite Coating on Strong Ceramic Substrate Fabricated by Low Density Slip Coating-Deposition and Coating-Substrate Co-Sintering. *J. Eur. Ceram. Soc.,* 31, 2065-2071.

[13] Afzal, M. A. F., Kesarwani, P., Reddy, K. M., Kalmodia, S., Basu, B. & Balani, K. 2012. Functionally Graded Hydroxyapatite-Alumina-Zirconia Biocomposite: Synergy of Toughness and Biocompatibility. *Mater Sci Eng C,* 32, 1164-1173.

[14] CHOI, J. W., KONG, Y. M. & KIM, H. E. 1998. Reinforcement of Hydroxyapatite Bioceramic by Addition of Ni_3Al and Al_20_3. *J. Am. Ceram. Soc.*, 81, 1743-1748.

Fiber Reinforced Ice (FRI) Utilized as a New One-Time-Use Disposable Material in Metal Forming

Takahiro Ohashi[1]

[1]School of Science and Engineering, Kokushikan University

E-Mail tohashi@kokushikan.ac.jp

In this paper, the author suggests utilization of fiber-reinforced ices (FRIs) as a one-time-use disposable material having comparable crushing strength with conventional metals. In metal forming, low temperature melting materials, such as lead and low temperature melting alloys, are successfully utilized as supports, one-time-use disposable tools and fillings in hollow materials. These low temperature materials are expensive or harmful for the environment and have limited strength. The FRI, which is a composite material of ice matrix and high strength fibers, is effective for the above purpose. The FRIs have following advantageous points:

(1) Water expands when it freezes and it contributes to precision casting of the ice and avoiding blowholes.
(2) Low cost
(3) Environmental friendly
(4) Easy to reuse
(5) Easy to remove
(6) Lower combined heat conductivity than plain ice by using the fibers having low heat conductivity

In this study, the author prepared FRIs using pulp fiber and glass fiber to archive a low temperature melting material with comparable high strength with conventional leads and light metals. The author investigated the thermal conductivity of FRIs using the transient hot-wire method. They then evaluated the crushing strength of the material using compression tests. Specimens were prepared as φ50-46H cylinders and compression rates were 100mm/min and 1mm/min. The experiments were conducted in a constant temperature chamber with -25℃ and -5℃. The crushing strength of FRIs were expressed

as liner functions of fiber ratio and seemed to be subject to the law of mixture well. The crushing strength of normal ice was 3.12MPa and that of the FRI with pulp fiber was up to 21MPa. It is almost same as the maximum strength in strain-stress curve of lead. In this condition, FRIs were observed as brittle. The crushing strength of the FRI with glass fiber was lower than the author expected. The author assumes that it is due to weaker strength of adhesive bonding between ice matrix and glass fiber than that between ice and pulp fiber. In the test in -25℃ with compression rate 1mm/min, the FRIs were observed as ductile. It is reported that normal ice is ductile in the strain rate less than 10^{-4}-10^{-3} s^{-1}[1]. In the test in -5 ℃, it depended on pulp fiber ratio Cw. Ductility of the FRI important when we intend to use it as a filling material in metal forming, therefore we must choose fiber ratio, temperature and deform rate of the FRI in the process with regarding not only required strength but ductility.

Keywords: Fiber reinforced ice, filling medium, one time disposable tool. hollow product

[1] MIZUNO,Y. 1993. Effect of hydrostatic pressure on compressive strength of polycrystalline ice, Low Temperature Science, Ser A, 52, 1-13.

H_2-TPR-XANES study on the reducibility of cobalt in cerium doped cobalt oxide

Yingyot Poo-arporn[1], Surangrat Tonlublao[1], Siwaruk Chotiwan[2], Rungtiva P. Poo-arporn[3]

[1]Synchrotron Light Research Institute, 111 University Avenue, Nakhon Ratchasima 30000, Thailand.

[2]Department of Chemistry, Faculty of Science, Kasetsart University, 50 Ngam Wong Wan Road, Chatuchak, Bangkok 10900, Thailand.

[3]Biological Engineering Program, Faculty of Engineering, King Mongkut's University of Technology Thonburi, 126 Pracha Uthit Road, Bangkok 10140, Thailand.

E Mail/ Contact Détails: yingyot@slri.or.th

Ceriun doped cobalt oxides were prepared by the co-precipitation method using Aerosil as the support, denoted as xCeCo/Aerosil (x = 1, 5 and 10). The structural property of prepared samples was characterized using x-ray absorption near edge structure (XANES). The measurement of Co K-edge XANES and Ce L_3-edge XANE were performed at BL2.2: TRXAS, SLRI, Thailand. By employing an energy dispersive scheme, at BL2.2: TRXAS, XANES spectrum can be obtained simultaneously using a position sensitive detector with the fastest readout speed of 25 ms. This great advantage opens a new opportunity *in situ* XANES experiments such as studies of changes of the electronic structures or the local coordination environments of an atom during a change in thermodynamic conditions. For xCeCo/Aerosil, at various cerium content, the Co K-edge XANES spectra exhibited mixed phases of CoO and Co_3O_4. Liner combination fitting was applied to estimate the phase fraction of cobalt compounds. XANES spectra of Co foil, standard CoO and standard Co_3O_4 were used as the references. By calcinations at 873 K in air, the main structure of cobalt oxide in all cerium contents was CoO. The reducibility of cobalt in xCeCo/Aerosil was further studied by the H_2-temperature programmed reduction (H_2-TPR) coupling with the *in situ* XANES measurement. Using phase fraction plot, at 923 K, it was found that only some parts of cobalt oxide were reduced. The results indicated an insufficient temperature for the total reduction of cobalt

oxide using H_2 gas. The influence of starting structure of cobalt oxide on its reducibility was also examined.

Keywords: in situ XANES, H_2-TPR, cerium oxide, cobalt oxide, reduction

[1] POO-ARPORN, Y., CHIRAWATKUL, P., SAENGSUI, W., CHOTIWAN, S., KITYAKARN, S., KLINKHIEO, S., HORMES, J. & SONGSIRIRITTHIKUL, P. 2012. Time-resolved XAS (Bonn-SUT-SLRI) beamline at SLRI. *J. Synchrotron Radiat.* 19, 937-943.

Lanthanum-based Metal-Organic Frameworks: Synthesis, Characterization and Photosensitivity

Anton Mayeuski[1], Elena Vlasova[2], Yuliya Rozhkova[1], Konstantin Nikitin[1],

Aida Rudakova[1], Alexei Emeline[1]

[1]Saint-Petersburg State University, Saint-Petersburg, 198504 Russia

[2] State University of Chemistry and Technology, Ivanovo, 153000 Russia

arudakova@mail.ru

Metal-organic frameworks (MOFs) as a class of novel porous material have attracted intensive attention during the last two decades.[1,2] Lanthanide-based MOFs have recently gained tremendous attention due to their luminescence properties.[3] The design of the lanthanide MOFs with proper stability and high crystallinity is still a challenging task. Here we present data on synthesis, material characterization of lanthanide metal-organic frameworks with different organic linkers namely benzene 1,4-dicarboxylate (BDC), naphthalene 2,6-dicarboxylate (NDC), and benzene 1,3,5-tricarboxylate (BTC). The processes of photoexcitation of synthesized La-MOFs were investigated by time-resolved diffuse reflectance UV-Vis spectroscopy and EPR spectroscopy. Data obtained may help to discover new ways for application of these compounds as a photosensitive material.

Acknowledgements: The present study was performed within the Project "Establishment of the Laboratory "Photoactive Nanocomposite Materials" No. 14.Z50.31.0016 supported by a Mega-grant of the Government of the Russian Federation.

Keywords: lanthanum based metal-organic framework, La-MOF, synthesis, photoexcitation

[1] ZHOU, H.-C., KITAGAWA, S. 2014. Metal-organic frameworks (MOFs). *Chem. Soc. Rev.*, 43, 5415-5418.

[2] YAGHI, O. M., LI, G., LI, H. 1995. Selective binding and removal of guests in a microporous metal-organic framework. *Nature*, 378, 703-706.

[3] ALLENDORF, M. D., BAUER, C. A., BHAKTA, R. K., HOUK, R. J. T., 2009. Luminescent metal-organic frameworks. *Chem. Soc. Rev.*, 38, 1330–1352.

Magnetic and dielectric properties of BST/BF multiferroic ceramic materials

YABO ZHANG[1], XIYUN HE[2], QIRONG YAO[2], FEIFEI WANG[1], YANXUE TANG[1], ZIYAO ZHOU[3], PINGSUN QIU[2], NIANXING SUN[3], AND DAZHI SUN[1]*

[1]Key Laboratory of Resource Chemistry of Education Ministry, Key Laboratory of Optoelectronic Material and Device, Shanghai Normal University, 100 Guilin Road, Shanghai 200234, China

[2]Shanghai Institute of Ceramics, Chinese Academy of Sciences, 1295 Dingxi Road, Shanghai 20050, China

[3]Department of Electrical and Computer Engineering, Northeastern University, 360 Huntington Avenue, Boston, MA 02115, USA

E-mail: zhangyabo1125@126.com

Contact Détails: Shanghai Normal University, 100 Guilin Road, Shanghai 200234, China

The lead-free multiferroic ceramic of (1-x)$Ba_{0.70}Sr_{0.30}TiO_3$(BST)+x$BiFeO_3$(BFO) was synthesized by a conventional solid-state reaction method. The dielectric, ferroelectric and magnetic properties was studied. The XRD revealed that the ceramic formed a single perovskite structure. The results suggests that the remanent magnetization (Mr) reached to maximum when the BFO content is up to 0.05. The Mr=70memu/g when x=0.05.The rate of the insulation resistance depend on magnetic field of the (1-x)$Ba_{0.70}Sr_{0.30}TiO_3$+x$BiFeO_3$ samples reached 25.6% when x=0.03. The relative dielectric constant was reduced under magnetic field compared with no magnetic field and the change rate is 13.1% as x=0.01. It is indicated that the lead-free multiferroic ceramic of (1-x)$Ba_{0.70}Si_{0.30}TiO_3$+x$BiFeO_3$ exhibited both ferroelectric and magnetic at room temperature. The ferroelectric and magnetic properties are derived from the displacement of magnetic atom iron and the change of the atomic spin state.

Keywords: multiferroic, ceramic, BST, dielectric, BiFeO3

Multifunctional hybrid carbon nanocomposites: carbon nanotubes grown on polyacrylonitrile

Choi, H.[1,2], Hwang, S.[2], Yoo, I.[1], Bae, Y.[1], Jo, H. H. [1], Jeon, M. [1,2]

[1]Department of Nano Science Engineering, Inje University, Gimhae 621-749, Korea

[2]Center for Nano manufacturing, Inje University, Gimhae 621-749, Korea

ihyon@inje.ac.kr

A randomly arranged three-dimensional network has been confirmed in the carbon nanotubes (CNTs) on carbon fibers structure. However, CNTs composites have less freedom of designing a device as a substrate itself has a pre-defined geometry. It is advisable to use a carboneous templating material for CNTs growth that yields highly graphitic carbon needing no further purification, and produces its flexibility for the design and fabrication of a device. In this work, vertically aligned CNTs were grown by chemical vapor deposition on a carbon fiber driven by polyacrylonitrile (PAN) substrates. It was prepared carbon nanofibers with an average diameter of 380 nm from the PAN by thermal processes, namely stabilization, carbonization and graphitization. A 10 nm-thick catalytic layer coating of nickel was added on the graphited-PAN substrates by thermal evaporator deposition. Prior to the onset of nanotube growth, the substrate with the catalyst film was heated to 700℃ in chemical vapor deposition chamber. The acetylene gas (C_2H_2) was then introduced to the chamber to start the growth of CNTs at 900℃. Infrared (IR) spectra can be used to analyze the chemical structure that exists in the fiber. The electrical conductivities of carbon nanocomposites less than 10 ohm/square were determined by a 4-point probes resistivity measurement system. Field emission scanning electron microscopy (FE-SEM) was performed to evaluate the microstructural morphology of the nanotubes grown. The typical lengths of CNTs were observed 700 nm grown on the carbon nanoofibers. Based on our results, suggested carbon nanocomposites may pave the way for carbon to be used in future electronics, such as sensors, secondary battery or wearable electrode developments.

This research was supported by Bio-Mimetic Robot Research Center funded by Defense Acquisition Program Administration (Grant code: UD130070ID)

Keywords: Polyacrolonitril, carbon fiber, carbon nanotube, chemical vapor deposition

[1] RAHAMAN, M.S.A., ISMAIL, A.F. & MUSTAFA, A. 2007. A review of heat treatment on polyacrylonitrile fiber. *Polymer Degradation and Stability*, 92, 1421-1432

Photocatalytic and thermal insulating performances of fiber reinforced hierarchical TiO_2-SiO_2 xerogel composites

Haixun Xu [a, c*], Shanyu Zhao [b], Meng Zheng [a], Jia Jiajia [a], Pinghua Zhu [a,*]

[a.] School of Environmental and Safety Engineering, Changzhou University, Changzhou, Jiangsu 213164, PR China

[b.] Swiss Federal Institute of Materials Science and Technology, CH-8600,Switzerland

c. Institute for Building Materials, Dalian University of Technology, Dalian 116024, PR China

Abstract: Silica based aerogel/xerogel materials have been received ever-growing attentions for versatile applications. However, the widespread applications are narrowed by the inert properties, fragile and brittle nature of silica materials and cumbersome preparation processes. In this paper, we try to introduce the TiO_2 into a silica matix to form photocatalytic hybrid gels and reinforce the TiO_2-SiO_2 composites by the impregnation of various fibrillary reinforcing agents, such as glass, mullite mineral and ceramic fibers, the properties of the reinforced composites were studied systematically in terms of stability of fibers, microstructure, chemical interactions and thermal conductivity, the final xerogel composites display improved monolithic geometry, satisfied thermal conductivity (0.09-0.25 W m^{-1} K^{-1}) and improved photocatalytic performance (85 % removal of model pollutant of methyl orange), which can be expected to be a route to the multi-functional building facades in the future.

Keywords: TiO_2-SiO_2 composite, photocatalytic, thermal conductivity, fiber reinforcement

* Corresponding author: Xu Haixun, Ph.D; E-mail: haixunxu@gmail.com; Zhu Pinghua, Ph.D; E-mail:zph@cczu.edu.cn
This work is financed by the National Natural Scientific Foundation of China (NSFC No. 51308079, 51408073).

Photonic Reactions of Magnetic Multi-Granule Nanoclusters-Polymer Composite induced by Photothermal effect

Bum Chul Park[1], Yu Jin Kim[2], and Young Keun Kim[1,*]

[1]Department of Materials Science and Engineering, Korea University, 145 Anam-ro, Seongbuk-gu, Seoul 02841, Korea

[2]Center for Creative Materials and Components, Korea University, 145 Anam-ro, Seongbuk-gu, Seoul 02841, Korea

p23rd@korea.ac.kr (Bum Chul Park), ykim97@korea.ac.kr (Young Keun Kim),

Magnetite nanoparticles (NPs) combined with polymers produce white light emission under 780 nm multiphoton laser irradiation. Understanding photonic external stimulus-induced conformational changes in magnetite-polymer composites is critical for applications of the magnetite NPs as photothermal agents. Since most research efforts were previously focused on the unique electromagnetic properties of the magnetic NPs, their behaviour under electromagnetic field have been studied very well [1]. However, photonic properties of the magnetite NPs modified by polymers remain unstudied. , while only a few studies on the phenomenological analysis of photothermal and photodynamic therapies in the biomedical field have been reported so far [2]. We demonstrate emission of white light by the multiphoton laser-induced photonic reaction of magnetic multi-granule nanoclusters (MGNCs) with poly(methyl methacrylate) (PMMA), and analyzed the mechanism of reactions via XRD, TEM, NMR, XPS, Raman, PL, UV-Vis spectrometer measurements. As a result of reactions, phase of MGNC was reduced from magnetite(Fe_3O_4) to wustite($Fe_{1-x}O$) owing to phtothermal effect of MGNC and product gas. Laser irradiated magnetite nanoparticle-PMMA composites exhibit fluorescence (with a maximum at 525 nm) owing to the carbon double-bond rearrangements resulting in the oxidation of the polymer. The findings reported in this work suggest that the MGNC-PMMA composites can be potentially used as efficient photothermal and imaging agents in the theranostic application.

Keywords: Magnetic Nanoclusters, Magnetic Nanoparticles-Polymer Composites,

Photothermal effect, Photonic Reaction, White Light Emission

[1] Lee, J. S., Cha, J. M., Yoon, H. Y., Lee, J., Kim, Y. K. 2015. Magnetic multi-granule nanoclusters: A model system that exhibits universal size effect of magnetic coercivity. Sci. Rep., 5, 12135-12141

[2] Dong, W., Li, Y., Niu, D., Ma, Z.; Gu, J., Chen, Y., Zhao, W., Liu, X., Liu, C., Shi, J. 2011. Facile Synthesis of Monodisperse Superparamagnetic Fe_3O_4 Core@hybrid@Au Shell Nanocomposite for Bimodal Imaging and Photothermal Therapy. Adv. Mater., 23, 5392-5397

Photonic Reactions of Magnetic Multi-Granule Nanoclusters-Polymer Composite induced by Photothermal effect

Bum Chul Park[1], Yu Jin Kim[2], and Young Keun Kim[1,*]

[1]Department of Materials Science and Engineering, Korea University, 145 Anam-ro, Seongbuk-gu, Seoul 02841, Korea

[2]Center for Creative Materials and Components, Korea University, 145 Anam-ro, Seongbuk-gu, Seoul 02841, Korea

p23rd@korea.ac.kr (Bum Chul Park), ykim97@korea.ac.kr (Young Keun Kim),

Magnetite nanoparticles (NPs) combined with polymers produce white light emission under 780 nm multiphoton laser irradiation. Understanding photonic external stimulus-induced conformational changes in magnetite-polymer composites is critical for applications of the magnetite NPs as photothermal agents. Since most research efforts were previously focused on the unique electromagnetic properties of the magnetic NPs, their behaviour under electromagnetic field have been studied very well [1]. However, photonic properties of the magnetite NPs modified by polymers remain unstudied. , while only a few studies on the phenomenological analysis of photothermal and photodynamic therapies in the biomedical field have been reported so far [2]. We demonstrate emission of white light by the multiphoton laser-induced photonic reaction of magnetic multi-granule nanoclusters (MGNCs) with poly(methyl methacrylate) (PMMA), and analyzed the mechanism of reactions via XRD, TEM, NMR, XPS, Raman, PL, UV-Vis spectrometer measurements. As a result of reactions, phase of MGNC was reduced from magnetite(Fe_3O_4) to wustite($Fe_{1-x}O$) owing to phtothermal effect of MGNC and product gas. Laser irradiated magnetite nanoparticle-PMMA composites exhibit fluorescence (with a maximum at 525 nm) owing to the carbon double-bond rearrangements resulting in the oxidation of the polymer. The findings reported in this work suggest that the MGNC-PMMA composites can be potentially used as efficient photothermal and imaging agents in the theranostic application.

Keywords: Magnetic Nanoclusters, Magnetic Nanoparticles-Polymer Composites,

Photothermal effect, Photonic Reaction, White Light Emission

[1] Lee, J. S., Cha, J. M., Yoon, H. Y., Lee, J., Kim, Y. K. 2015. Magnetic multi-granule nanoclusters: A model system that exhibits universal size effect of magnetic coercivity. Sci. Rep., 5, 12135-12141

[2] Dong, W., Li, Y., Niu, D., Ma, Z.; Gu, J., Chen, Y., Zhao, W., Liu, X., Liu, C., Shi, J. 2011. Facile Synthesis of Monodisperse Superparamagnetic Fe_3O_4 Core@hybrid@Au Shell Nanocomposite for Bimodal Imaging and Photothermal Therapy. Adv. Mater., 23, 5392-5397

Preparation and Antimicrobial Evaluation of Regenerated Cellulose with Novel Non-water Soluble Polymeric Guanidine Derivatives

Changlin Cao[1], Shiyu Ji[1], Yang Zhang[1], Hong Jin[1], Yumei Zhang[1], Huaping Wang[1]

[1] State Key Laboratory for Modification of Chemical Fibers and Polymer Materials, College of Materials Science and Engineering, Donghua University, Shanghai, 201620, China

Presenting author: email, changlincao@126.com;

Corresponding author: email, zhangym@dhu.edu.cn.

Abstract: It is a direct method to prepare antimicrobial functional cellulose by dissolving antimicrobial agents in the cellulose solution, in which appropriate agents are very important. In this paper, three novel polymeric guanidine derivatives, polyhexamethylene guanidine dodecyl benzene sulfonate (PHGDBS), polyhexamethylene guanidine dodecyl sulfate (PHGDSA) and polyhexamethylene guanidine laurylsulfonate (PHGLSO) were synthesized to investigate their application in cellulose. The chemical information was verified by element analysis, ^{1}H-NMR and Fourier Transform Infrared Spectroscopy (FTIR). The dissolubility in 1-butyl-3-methylimidazolium chloride ([BMIM]Cl), 4-Methylmorpholine N-oxide monohydrate (NMMO·H_2O) and other solvents was also tested. Furthermore, the properties of the three agents against both bacterial and fungus were measured qualitatively by inhibition zones method. Then, the influence of [BMIM]Cl on antimicrobial effect was discussed. The cellulose membranes with different content of PHGDBS were obtained from PHGDBS/cellulose/[BMIM]Cl solution to determine the antimicrobial minimum dosage. Subsequently, the bacterial reduction of optimum membrane was evaluated by quantitative method. The results showed that the three agents were in line with the expected chemical compositions and structures. They can be dissolved in [BMIM]Cl and NMMO·H_2O under heating while were insoluble in water. It is also found that these three compounds have a resistance against both bacterial (Escherichia coli, Staphylococcus aureus) and fungus (Candida albicans,

Aspergillus niger). Meanwhile, the [BMIM]Cl had no negative influence on the antimicrobial properties of these agents. The cellulose membrane contained only 1.0% dosage of PHGDBS showed excellent killing effect, and at this content, 99.94% and 96.95% bacterial reduction rates were obtained for S. aureus and E. coli respectively. It is shown that the three agents will be suitable for the antimicrobial functionalization of regenerated cellulose.

Keywords: regenerated cellulose, antimicrobial, fungus, non-water soluble, polymeric guanidine

References

[1] KLEMM, D., HEUBLEIN, B., FINK, H., BOHN, A. 2005. Cellulose: fascinating biopolymer and sustainable raw material. *Cheminform*, 36, 3358–3393.

[2] FINK, H. P., WEIGEL, P., PURZ, H., GANSTER, J. 2001. Structure formation of regenerated cellulose materials from NMMO-solutions. *Progress in Polymer Science*, 26,1473-1524.

[3] SWATLOSKI, R. P., SPEAR, SK., HOLBREY, JD., ROGERS, RD. 2002. Dissolution of cellose with ionic liquids. *Journal of the American Chemical Society*, 124, 4974-4975.

[4] ZHANG, Y., JIANG, J., CHEN, Y. 1999. Synthesis and antimicrobial activity of polymeric guanidine and biguanidine salts. *Polymer*, 40, 6189-6198.

[5] TOMŠIČ, B., SIMONČIČ, B., OREL, B., ZERJAV, M., SCHROERS, H. 2009. Antimicrobial activity of AgCl embedded in a silica matrix on cotton fabric. *Carbohydrate Polymers*, 75, 618-626.

[6] KIM, S. S., PARK, J. E., LEE, J. 2011. Properties and antimicrobial efficacy of cellulose fiber coated with silver nanoparticles and 3-mercaptopropyltrimethoxysilane (3-MPTMS). *Journal of Applied Polymer Science*, 119, 2261-2267.

[7] ZEMLJIC, L. F., SAUPERL, O., KREZE, T., STRNAD. S. 2013. Characterization of regenerated cellulose fibers antimicrobial functionalized by chitosan. *Textile Research Journal*, 83, 185-196.

[8] ZHANG, F., ZHANG, D., CHEN, Y., LIN, H.2009. The antimicrobial activity of the cotton fabric grafted with an amino-terminated hyperbranched polymer. *Cellulose*, 16, 281-288.

Preparation of ceria-coated hybrid polymer particles for polishing of quartz wafer

Yoshimi TAKEDA[1], Natsuki UCHIDA[1], Shoji NAGAOKA[2,3], Makoto TAKAFUJI[1],

Zhenghe XU[4], Hirotaka IHARA[3,5]*

[1]Department of Applied Chemistry and Biochemistry, Kumamoto University, Kumamoto, Japan.

[2]Kumamoto Industrial Research Institute, Kumamoto, Japan.

[3]Kumamoto Institute for Photo-electro Organics (PHOENICS), Kumamoto, Japan.

[4]Department of Chemical and Materials Engineering, University of Alberta, Edmonton, Canada.

[5]Department of Nanoscience and Technology, Kumamoto University, Kumamoto, Japan.

ihara@kumamoto-u.ac.jp

Along with the growth of the digital society, the demands for large storage capacity and high-speed access are increasing. To develop high-density devices, the surface of base wafers such as glass wafer and silicon wafer are required to be smooth in nano- to sub-nano scales. In order to polish finely the surface of the base materials, the polishing process and polishing materials have been improving steady progress. Currently, various materials such as silica, alumina and ceria were used for polishing for glass and quartz wafers. Particularly, ceria particles are widely used because caria particles show chemo-mechanical polishing (CMP) performance. However, the supply and the price are unstable in recent years because of rear earth. In this study we demonstrate to fabricate ceria-coated hybrid polymer particles for fine polishing of quartz wafers and evaluate the polishing property of the hybrid microspheres. The advantages of the core-shell microspheres in fine polishing are listed as follows: 1) reduction of ceria usage; 2) reduction of dispersant; 3) no polishing pad and 4) fine polishing. The core-shell hybrid particles with ceria nanoparticles-layered shell on the polymer microsphere (Figure 1) were prepared by the modified O/W suspension polymerization previously reported by us [1,2]. Various core-shell microspheres with different loading amount of ceria and different hardness of core polymer were prepared and used as polishing materials. As a result, we succeed to reduce the usage of ceria nanoparticles in CMP process for quarts wafer by using core-shell microspheres. The detailed results will be discussed.

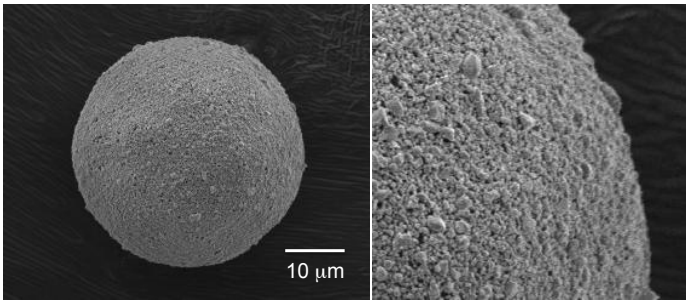

Figure 1 SEM images of ceria-coated hybrid polymer particles.

Keywords: Chemo-mechanical polishing (CMP), Core-shell microsphers, Ceria nanoparticles, Quartz glass wafer

[1] UCHIMURA, A, KUBOTA, S., YAMADA, S., WAKIYA, T., TAKAFUJI, M., SHIROSAKI, T., NAGAOKA, S., IHARA, H. 2011. Facile and versatile method for preparing core-shell microspheres with controlled surface structures based on silica particles-monolayer. *Mater. Chem. Phys.*, 129, 871–880.

[2] IHARA, H., KUBOTA, S., UCHIMURA, A., SAKAI, Y., WAKIYA, T., RAHMAN, M. M., NAGAOKA, S., TaAKAFUJI, M. 2009. A facile preparation method for self-assembled monolayers with silica particles on polystyrene-based microspheres. *Mater. Chem. Phys.*, 114, 1–5.

Preparation of hollow microspheres having nanosilica-layered shell

Makoto Takafuji[1]*, Md. A. Alam[1,2], Zhenghe Xu[3], Hirotaka Ihara[4,5]*

[1]Department of Applied Chemistry and Biochemistry, Kumamoto University, Kumamoto, Japan.

[2]Department of Applied Chemistry and Chemical Engineering,

Noakhali Science and Technology University, Noakhali, Bangladesh

[3]Department of Chemical and Materials Engineering, University of Alberta, Edmonton, Canada.

[4]Department of Nanoscience and Technology, Kumamoto University, Kumamoto, Japan.

[5]Kumamoto Institute for Photo-Electro Organics (PHOENICS), Kumamoto, Japan.

takafuji@kumamoto-u.ac.jp; ihara@kumamoto-u.ac.jp

Recently, we have reported the core-shell microspheres having self-assembled monolayers with inorganic nanoparticles on the polymer core [1,2]. The packing structure of inorganic nanoparticles among the shell could be precisely controlled by the preparation conditions. In this presentation, we demonstrate to fabricate the hollow microspheres having nanosilica-layered shell using previously reported core-shell microspheres (Figure 1). The core-shell microspheres with nanosilica-layerd shell were dispersed in ethanol, and tetraethoxysilane (TEOS), ammonia solution and water were added to the dispersion. After stirring gently of the dispersion at 25 ûC for 6h, the microspheres were collected, washed and dried. SEM images showed that the surface structure of core-shell microspheres was different from their original structure. This is probably due to the sol-gel reaction of TEOS on the surface of core-shell microspheres. The obtained microspheres were calcinated at 600 ûC to burn off the polymer core. No structural change was observed in the surface of microspheres. From the observations of inside of the crushed microspheres, it was clearly defined that the hollow structure was formed. Diffuse reflectance FT-IR spectra indicated that the hollow microspheres were totally composed of silica. The inside and the outside surfaces of hollow microspheres have bumped structure on their surface. Such hollow microspheres have the potential to apply in various fields such as optical materials, carriers and fillers.

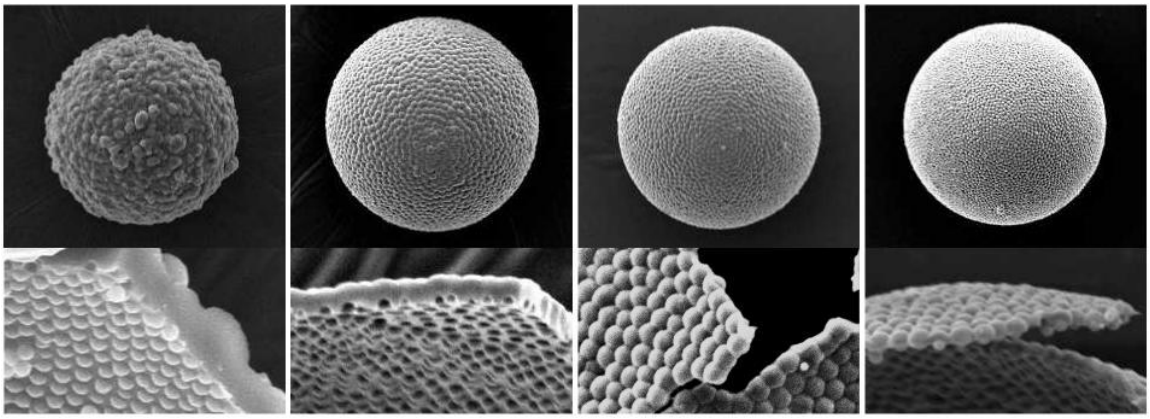

Figure 1 SEM images of hollow microspheres having nanosilica layered shell with various thickness.

Keywords: Core-Shell microspheres, Sol-gel reaction, Suspension polymerization, Inorganic nanoparticles, Composite materials

[1] UCHIMURA, A, KUBOTA, S., YAMADA, S., WAKIYA, T., TAKAFUJI, M., SHIROSAKI, T., NAGAOKA, S., IHARA, H. 2011. Facile and versatile method for preparing core-shell microspheres with controlled surface structures based on silica particles-monolayer. *Mater. Chem. Phys.*, 129, 871–880.

[2] IHARA, H., KUBOTA, S., UCHIMURA, A., SAKAI, Y., WAKIYA, T., RAHMAN, M. M., NAGAOKA, S., TaAKAFUJI, M. 2009. A facile preparation method for self-assembled monolayers with silica particles on polystyrene-based microspheres. *Mater. Chem. Phys.*, 114, 1–5.

Rheological Properties of Waterborne Polyurethane Reinforced with Cellulose Nanocrystals

Eun Joo Shin[1]*, Sun Mi Cho[2], and Soon Mo Choi[2]

[1]Department of Organic Materials and Polymer Engineering, School of Engineering, Dong-a University, Busan 604-714, Republic of Korea

[2]Department of Nano, Medical & Polymer Materials, School of Engineering, Yeung-nam University, Gyeongsan 712-749, Republic of Korea

sejoo6313@dau.ac.kr

Cellulose nanoparticles (CNs) are ideal materials on which to base a new biomass polymer composites industry. Researches about rheological behavior of cellulose suspensions, interaction with water or solvent have been applied with polymeric materials. When investigating the rheological properties of CNs, researchers generally either study the gelation properties through viscometric measurements or seek to discover knowledge about the liquid crystallinity and ordering properties of the CN through rheological characterization. In this study, the interactions of cellulose and waterborne polyurethane were investigated, including mechanical, thermal stability, optical water sorption, and barrier. These studies have been focused on rheological properties of molecular interactions in terms of the various concentration of reinforced CN in polyurethane.

Keywords: cellulose, nanoparticles, polyurethane, waterborne, rheology

[1] Robert J. Moon, Ashlie Martini, John Nairn, John Simonsen and Jeff Youngblood, 2011. Cellulose nanomaterials review: structure, properties and nanocomposites, *Chem. Soc. Rev., 40, 3941–3994*

Synthesis and Characterization of Core-shell type Tb-SiO_2 Particles by Reverse Micelle and Sol-Gel Process

Son HeonJeong[1], and Dong-Sik Bae[1*]
Department of Ceramic Science & Engineering, Changwon National Univ,
Gyeongnam, 641-773 South Korea.
Email: dsbae@chanwon.ac.kr

Abstract

Core shell type Tb-SiO_2 particles have been synthesized using reverse micelle technique combined with metal alkoxide hydrolysis and condensation. The size of the particles and the thickness of the coating can be controlled by manipulating the relative rates of the hydrolysis and condensation reactions of tetraethoxysilane(TEOS) within the microemulsion. The average size of synthesized particles was in the range of 20-30nm. The characterization of synthesized Tb-SiO_2 particles was studied by x-ray diffraction (XRD), transmission electron microscopy (TEM), photoluminence (PL). The properties of Tb-SiO_2 powders were studied as a function of various processing parameters such as kind of precursor and molar ratio of water to surfactant(R). The average size and shape of the Tb doped SiO_2 particles changed by molar ratio of water to surfactant.

Keywords: Tb-SiO_2, Core Shell type, Nanoparticles, Reverse Micelle Process, Sol-Gel Process

Synthesis and characterization of Galic acid-functionalized ZnO nanoparticles and its biomedical application

Kyong-Hoon Choi[1], Jung Hyun Kim[2], Ho-Joong Kim[3,]*, Bong Joo Park[1,2]*

[1]Plasma Bioscience Research Center and [2]Department of Electrical & Biological Physics, Kwangwoon University, 20 Kwangwoongil, Nowon-gu, Seoul, 139-701, Republic of Korea
[3]Department of Chemistry, Chosun University, Gwangju 501-759, Korea

Metal oxide nanoparticles and composite materials are widely applied in the field of research and development and diverse applications in industries including surface coatings, optoelectronics, bioengineering, biodignostics, and agriculture. Among these metal oxide nanoparticles, highly ionic zinc oxide nanoparticles are unique in that they can be produced with high surface area, unusual crystal structures and size. The main advantages of using ZnO nanoparticles have excellent stability or long shelf life with organic antimicrobial agents.

In this study, we report a novel antioxidant ZnO nanoparticle that is newly designed and prepared by simple surface modification process. Antioxidative functionality is provided by the immobilization of antioxidant of 3,4,5-trihydroxybenzoic acid (galic acid, GA) onto the surface of ZnO nanoparticles. Microstructure and physical properties of the ZnO@GA nanoparticles were investigated by field emission scanning electron microscopy (FE-SEM), transmission electron microscopy (TEM), infrared spectroscopy (IR) and steady state spectroscopic methods. The antioxidative activity of ZnO@GA was also evaluated using ABTS (3-ethyl-benzothiazoline-6-sulfonic acid) radical cation decolorization assay. Notably, ZnO@GA showed strong antioxidative activity in spite of the conjugation process of GA on the ZnO surface. These results provide that CA-coating onto ZnO nanoparticles may offer an intriguing potential for biomedical devices as well as nanomaterials.

Synthesis Mechanism and Effect factors of UF/E Microcapsule

Zhang Ming[1,2,3], Xing Feng[4], Ni Zhuo[4], Du Xue-xiao[4]

(1. National Engineering Laboratory for High-Speed Railway Construction, Central South University, Changsha, 410075, China 2. School of Material Science and Engineering, Southeast University, Nanjing, 211189, China; 3. College of Civil Science and Engineering, Yangzhou University, Yangzhou, 225127, China; 4. Guangdong Provincial Key Laboratory of Coastal Civil Engineering Durability, Shenzhen University, Shenzhen, 518060, China)

Abstract: Microcapsule is a novel composite material for storing and protecting core material from outside, this paper analyzed the formation mechanism of urea-formaldehyde resin/epoxy resin microcapsule (UF/E), selection basis of raw material for preparation of shell material and core material, experimental investigated reaction kinetic, effect mechanism of urea-formaldehyde resin, and preparation process of UF/E microcapsule, and studied effect of technological parameters, such as mass ratio of core material/shell material, system pH value, reaction temperature, and stirring rate on synthesis conditions, particle and its distribution, surface morphology and shell thickness. Formation process of microcapsule was observed with biological microscope, and morphology characteristics and chemical structure of shell were characteristic with SEM and FTIR. Meanwhile, the change of microcapsule, shell material and core material under high temperature is tested with TGA and DTA method, and combine the change development of surface morphology under high temperature, made clear the change rule of microcapsule under high temperature, and its limit temperature of heat-resisting.

Keywords: microcapsule; synthesis process; reaction kinetic; chemical structure

Synthesis of Porous Tubular TiN Powders via Ammonia Reduction Nitridation of Nonhydrolytic TiO_2 Gels Using Ethanol as Oxygen Donor

Lifang zhang[1,2,3], Jinglong BU[2*], Hengyong WEI[2], Min CHEN[1*], Huixing LIU[2], Jie NI[2]and Dongfeng LV[2]

[1]School of Metallurgy, Northeastern University, Shenyang, 110819, Liaoning, P.R.China.
[2]Hebei Provincial Key Laboratory of Inorganic Nonmetallic Materials, College of Materials Science and Engineering, North China University of Science and Technology, Tangshan, 063009, Hebei, P.R.China.
[3]Qinggong College, North China University of Science and Technology, Tangshan Key Laboratory of Environment Functional Materials , Tangshan, 063000, P.R.China.

*chzlf131@sina.com; *bjl@heuu.edu.cn; *chenm@smm.neu.edu.cn*

Abstract: Titanium nitride (TiN) materials have the properties of superior hardness, corrosion resistance, excellent electrical / thermal conductivity, chemical / thermal stability, and are widely applied as catalyst and catalyst support materials in dye-sensitized solar cells, fule cells and batteries, and supercapacitors and so on [1]. Especially, porous tubular architectures have been attracting more and more attentions in recent years for their high surface-to-volume ratio, permeability, morphology and charge transport, and shown distinctive physicochemical properties in comparison with conventional nanocrystallites. Therefore, there is a particular interest in controlled synthetic approaches for tubular and porous TiN materials by magnesiothermic reduction of titania replicas of a cellulose substance (filter paper), being pursued to extend the potential applications of TiN materials.[2]

In this study, porous tubular TiN powders were prepared via a novel facile and non-template route for ammonia reduction nitridation of nonhydrolytic TiO_2 gels, with titanium tetrachloride as titanium resource, ethanol as oxygen donor and dichloromethane as solvent. After the as-prepared nonhydrolytic TiO_2 gels were precalcined at 600 ℃ for 0.5 h, the obtained powders were consisted of pure well crystalized anatase TiO_2 phase of porous tubular morphology, with BET specific surface area of 27.717 $m^2 g^{-1}$, an average pore size of 17 nm and pore volume of 0.012 cc g^{-1}. And after the porous tubular TiO_2 powders were calcined at 800 ℃ for 2h at a heating rate of 5 ℃ min^{-1} under NH_3 gas atmosphere in the flowing rate of 800 mL min^{-1}, the TiN powders keeping porous tubular

architecture were obtained, with the BET specific surface area of the resultant TiN powders of 31.06 $m^2 g^{-1}$, its average pore size and pore volume was respectively 12 nm and 0.009 cc g^{-1}, The electrochemical performance of porous tubular TiN powders demonstrated that this material could be used as a promising electrode material.

Keywords: tubular TiN, porous, nonhydrolytic sol-gel, ammonia reduction and nitridation

[1] SENCER, W. R., HIROAKI, S. F., DISALVO, SOLM, G., ULRICH, W. 2014. Monolithic Gyroidal Mesoporous mixed Titanium-Niobium Nitrides. *ACS Nano*, 8, 8217-8223.

[2] XIAO Y. L., YAN, H. Z., TAO, W., JIAN, G. H. 2012. Hierarchical Nanotubular Titanium Nitride Derived From Natural Cellulose Substance and its Electrochemical Properties. *Chem. Commun*., 48, 9992-9994.

Acknowledgments

The authors are grateful to the National Natural Science Foundation of China (51272066) and Natural Science Foundation of Hebei Province (E2013209183) for financial support.

Synthesis, structural and optical characterizations of undoped and Cr-doped SnO_2 nanoparticles using chemical method

Ch.Venkata Reddy[a], Jaesool Shim[a*]

[a]School of Mechanical Engineering, Yeungnam University, Gyeongsan 712-749, South Korea

Presenting author E-mail: cvrphy@gmail.com

Corresponding author E-mail: jshim@ynu.ac.kr

Abstract:

In this present work we report the synthesis and characterizations of undoped and Cr–doped SnO_2 nanoparticles using chemical synthesis method. The as-synthesized nanoparticles were characterized using various measurements such as powder XRD, SEM with EDX, HETEM, Optical absorption, Raman spectra, PL, FT-IR and XPS techniques. From the XRD data the crystal structure is confirmed as a tetragonal rutile phase of SnO_2. EDAX spectra confirmed the presence of Sn, O and Cr in near stoichiometry. The band gap energies were evaluated from the optical absorption spectra, it is observed that the band gap values are increases with increasing the Cr^{3+} concentration and also the band gaps are higher than the bulk band gap value of SnO_2 (3.6 eV). This blue shift may be attributed to strong quantum confinement effects. The PL spectra exhibit the emission in visible region. The X-ray photoelectron spectra confirmed the binding energies of Cr, Sn and O elements. FTIR spectra displays various bands that are due to fundamental over tones of O–Sn–O entities.

Keywords: Nanoparticles, HRTEM, Binding energy, Raman spectra, visible emission.

The Preparation of Cu_2ZnSnS_4/graphene Composites Thin Films on Transparent Conducting Glass Substrates

Zhoujun Pang, Aixiang Wei, Jun Liu, Zhiming Xiao, Yu Zhao

School of Material and Energy, Guangdong University of Technology, Guangzhou 510006, China

zhaoyu@gdut.edu.cn

Recently, the use of CZTS as catalytic materials for counter electrodes (CE) in dye-sensitized solar cells (DSSCs) has attracted lots of attention [1,2]. Even CZTS has electrocatalytic ability comparable to Pt, its low electrical conductivity is still the limitation for high cell efficiency of DSSCs with CZTS CE. The resistivity of CZTS is typical in the range of 0.01 to 10 Ω.cm [3], which is at least three orders of magnitude higher than that of Pt. Therefore, reducing the resistance of CZTS thin film as CE is crucial to the high performance of DSSCs. Graphene has attracted tremendous research interest owing to its exceptional properties. Graphene-based functional materials have been synthesized for various applications [4]. The very low resistivity of graphene sheets (about 10^{-6} Ω.cm) has been utilized to effectively enhance the conductance of graphene-based composites. In this paper, a novel and simple technique was developed to fabricate CZTS/graphene composite thin films directly on transparent conductive fluorine-doped tin oxide (FTO) substrates.

The graphene consists of approximately five layers of carbon sheet was pre-coated onto the FTO substrate using ethanol or ethylene glycol as solvent. A following drying at elevated temperature would lead to the loosenly-attached graphene particle on the FTO substrate. The graphene-textured FTO were used to grow CZTS thin films by a solvothermal method reported by our previous work [5].

Fig. 1 (a) gives the typical SEM images of The CZTS/graphene composite thin films. The film has a smooth and compact surface. As shown in the inset of Fig. 1(a) and TEM Fig. 1 (b), uniform sphere-like nanocrystals with an average diameter of about 10~15 nm are grown on the surface and interspace of graphene sheets. The XRD patterns of

synthesized composite thin films are shown in Fig. 2(a). The major XRD diffraction peaks appeared at 2θ=28.26°, 47.82° and 56.24° can be indexed (112), (220) and (312) of the kesterite crystal structure of CZTS (JCPDS no. 26-0575), while those peaks at 3.3° can be assigned to graphene.

The electrochemical impedance spectroscopy (EIS) and Tafel polarization were also measured. The series resistance and catalytic properties of the CZTS/graphene composite thin films are discussed in detail.

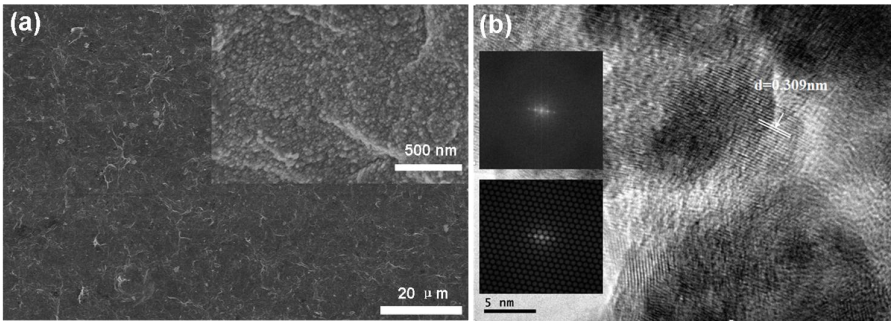

Fig.1 (a) SEM images and (b) HRTEM of CZTS/graphene composite thin films.

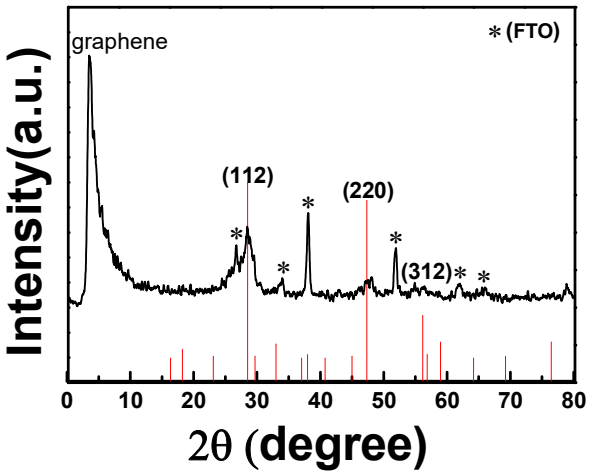

Fig. 2 XRD spectra of CZTS/graphene composite thin films.

Keywords: Cu_2ZnSnS_4, graphene, composites, thin films

[1] FAN, M. S., CHEN, J. H., LI, C. T., CHENG, K. W. & HO, K. C. 2014. Copper zinc tin sulfide as a catalytic material for counter electrodes in dye-sensitized solar cells. *J. Mater. Chem. A*, 3, 562-569.

[2] XIN, X., HE, M., HAN, W., JUNG, J. & LIN, Z. 2011. Low-Cost Copper Zinc Tin Sulfide Counter Electrodes for High-Efficiency Dye-Sensitized Solar Cells. *Angewandte Chemie International Edition*, 50, 11739-11742.

[3] MITZI, D. B., GUNAWAN, O., TODOROV, T. K. & BARKHOUSE, D. A. R. 2013. Prospects and performance limitations for Cu-Zn-Sn-S-Se photovoltaic technology. *Philosophical Transactions of the Royal Society A Mathematical Physical & Engineering Sciences*, 371, 20110432.

[4] HUANG, X., QI, X., BOEY, F. & ZHANG, H. 2012. Graphene-based composites. *Chemical society reviews*, 41, 666-686.

[5] YAN, Z., WEI, A., ZHAO, Y., LIU, J. & CHEN, X. 2013. Growth of Cu_2ZnSnS_4 thin films on transparent conducting glass substrates by the solvothermal method. *Materials Letters,* 111, 120-122.

The Whiskers in Ni-Cr-C System

V.P. Val'chuk[1], D.S. Zmienko[2], V.V. Kolesov[3], T.S. Dolotova[1], D. Golberg[5] and L.A. Chernozatonskii[1]

[1]Emanuel Institute of Biochemical Physics of RAS, Russia, Moscow, 119334

[2]Rosatom State Nuclear Energy Corporation, Russia, Moscow, 119017

[3]Kotel'nikov Institute of Radio Engineering and Electronics of RAS, Russia, Moscow, 125009

[4]Prokhorov Institute of Physics, Russia, Moscow, 117312

[5]National Institute for Materials Science, Japan, Tsukuba, Ibaraki 3050044

kvv@cplire.ru

The hard materials as reinforcements in alloys and composites attract prime attention of both researchers and engineers due to their useful properties. Among these, carbides are becoming most attractive and promising candidates in modern scientific and technological applications. Chromium carbide exhibits an extremely high strength, hardness, anti-erosion and corrosion properties, good surface characteristics, etc. Commonly used alloys are based on chromium carbide with a nickel binder matrix.

In this research, we have successfully prepared for the first time chromium carbide Cr_3C_2 crystalline whiskers, with diameters ~1-10 μm and length >50μm, were produced by sintering a powder mixture Ni-Cr-C at 1200-1300^{o}C followed by rapid cooling as similar procedure for mixture Fe-Ni-C [1]. It was found that the micro-hardness (up to 3300 HV) in densely populated with such whiskers areas is much higher than in previously synthesized alloys of similar compositions.

In the Cr-Ni-C material under study, the whiskers of Cr3C2 were found only in the micropores, similarly to the CNT presence in the pores of the Fe-Ni-C system alloys [1]. We believe that the conditions for the growth of whiskers are realized on the micropore surfaces at temperatures 1100-1300^{o}C, when pores are easily filled with volatile carbon atoms of graphite particles. This growth likely occurs via conventional sol-gel mechanisms21 (similar to the growth of whiskers SiO_2 [2], or CNTs [3]). As heating proceeds, nickel and chromium micrograins start alloying. The carbon present in the system diffuses into both Ni and Cr, however, carbon

dissolves in large quantities specifically in Ni. It is known that upon heating of such metal mixture above 600^{o}C, nickel becomes saturated with carbon, [4] which causes melting of Ni particles. In contrast, with chromium, as stated above, the formation of Cr_3C_2 carbide begins only at 1100-1200^{o}C.

The present chromium carbide whiskers-new sustainable materials are interesting not only as components of the multi-phase alloys, but also for possible future applications in mechanics, optics, electronics, instrumentation, and other industries.

The work was supported by an EU Marie Curie International Research Staff Exchange Scheme Fellowship within the 7th European Community Framework Programme (MC-IRSES proposal 318617 FAEMCAR project).

Keywords: chromium carbide whiskers, Ni-Cr-C system, sol–gel chemistry mechanism

[1] CHERNOZATONSKII, L.A., VAL'CHUK, V.P., KISELEV, N.A., LEBEDEV, O.I., ORMONT, A.B., & ZAKAROV, D.N. 1997. *Carbon*, 35, 749-751.

[2] FAN, J., & CHU, P.K. 2014. SiC Nanowires in Silicon Carbide Nanostructures. *Engineering Materials and Processes*, (Springer), Ch.5.

[3] KUKOVITSKY, E.F., L'VOV, S.G., SAINOV, N.A., SHUSTOV, V.A., & CHERNOZATONSKII, L.A. 2002. *Chem. Phys. Lett.*, 355, 497-503.

[4] SIEGEL, D.J., VAN SCHILFGAARDE, M., & HAMILTON, J.C. 2004. *Phys.Rev.Lett.*, 92, 086101.

ZnO nanowires-Poly(L-lactide) (PLLA) nanofibers composites for Solid Cancer Therapy

Ji Beom Shin[1], Bum Chul Park[1], Min Jun Ko[1], Young Keun Kim[1,*]

[1]Department of Materials Science and Engineering, Korea University, 145 Anam-ro, Seongbuk-gu, Seoul 02841, Korea

advmaterials@korea.ac.kr (Ji Beom Shin), ykim97@korea.ac.kr (Young Keun Kim)

ZnO nanowires (NWs) were used as novel materials for gene delivery and cell separation [1]. Previously, we developed cancer immunotherapy using antigen functionalized Fe_3O_4-ZnO core-shell nanoparticle (NPs) using ZnO Binding Peptide(ZBP) as an antigen carrier [2]. Poly(L-lactide) (PLLA) nanofibers (NFs) with a high surface area to volume ratio take many research's attention because they have great advantages such as bio-compatibility, bio-degradability and little toxicity [3]. In this research we designed and synthesized ZnO NW-PLLA NF composites via electrospinning and hydrothermal methods for solid cancer therapy. These methods have many advantages such as scalability, low-cost, and ease of handling. First of all, we put PLLA polymer 20% (w/v) and ZnO growth solution into solvent based on DMF-THF (v/v=15:85). Subsequently, we synthesized PLLA NF containing ZnO NP via electrospinning method. The curing process was necessary for stabilizing the PLLA NF. Finally, ZnO NW could be grown from the ZnO NP via hydrothermal synthesis. The morphological and structural properties were analyzed by XRD, SEM, and TEM. The diameter of PLLA NF was controlled from 0.6 μm to 1.5 μm, and the length of ZnO NW was controlled from 0.5 μm to 1 μm via the reaction time. The ZnO NW-PLLA NF composites can be used in applications in solid cancer therapy utilizing it as cell separation and DNA transfection platforms.

Keywords: ZnO Nanowires, PLLA nanofibers, Hydrothermal synthesis, Electrospinning, Solid cancer therapy

[1] Nie, L., Gao, L., Feng, P., Zhang, J., Fu, X., Liu, Y., ... & Wang, T. 2006. Three-Dimensional Functionalized Tetrapod-like ZnO Nanostructures for Plasmid DNA Delivery. Small, 2(5), 621-625.

[2] Cho, N. H., Cheong, T. C., Min, J. H., Wu, J. H., Lee, S. J., Kim, D., ... & Seong, S. Y. 2011. A multifunctional core-shell nanoparticle for dendritic cell-based cancer immunotherapy. Nature nanotechnology, 6(10), 675-682.

[3] Yoo, H. S., Kim, T. G., & Park, T. G. 2009. Surface-functionalized electrospun nanofibers for tissue engineering and drug delivery. Advanced drug delivery reviews, 61(12), 1033-1042.

Symposia 2

Advances in Thin Films

- Organic Thin Films
- Superconducting Thin Films
- Metal oxide, carbon, nitrides etc based thins Films
- Innovative Methods for the Structural Characterization of Thin films
- Theory of Structure, Surface and Interface of thin films
- Devices for acoustic wave modulation, sensing and actuating
- Plasma-Surface Interactions for Thin Film Engineering
- Advances in Deposition Techniques for thin films
- Structure Formation in Multi-Component thin films
- Optical, electrical and magnetic properties of thin films
- Synthesis, Characterization and modeling of the atomic processes of bulk and thin-film oxide film formation
- Nanostructured and Architecturally Designed Coatings, Smart Surfaces
- Protective Coatings in Severe Environments
- Thin films for optoelectronics, nanoelectronics and spintronics
- Thin films in Energy Harvesting and Storage
- Thin Films in Biological and environmental Applications
- Applications of Electrochemical and Electroless Depositions
- Advances in Deposition Techniques
- Others

Index Page

Development of Penning magnetron sputtering for thin ferromagnetic film depositions

Phitsanu Poolcharuansin[1], Artit Chingsungnoen[1], Nitisak Pasaja[1], Mati Horprathum[2] And Pongpan Chindaudom[2]

[1] The Technological Plasma Research Unit, Department of Physics, Mahasarakham University, Maha Sarakham, 44150, Thailand

[2] Optical Thin-Film Laboratory, National Electronics and Computer Technology Center, Pathumthani, 12120, Thailand

E Mail/ Contact Details phitsanu.p@msu.ac.th

Magnetron sputtering is a well-established physical vapor deposition technique in which energetic electrons are effectively confined due to the presence of transverse magnetic field lines above a target surface [1]. However, this is not the case for a ferromagnetic target in which most of the magnetic field lines above the target are absent. The conventional magnetron sputtering, therefore, is not suitable for ferromagnetic films.

The objective of the present work is to development of a magnetron based on the planar Penning configuration [2] for ferromagnetic film depositions. Basically, the Penning magnetron consists of an anode covered by a cathode. Permanent magnets embedded in the anode are employed to form the annular transverse magnetic field lines. The cathode consisted of a center nickel plate and a concentric nickel ring was employed as a gap-ferromagnetic target. In this work the anode is biased with a positive voltage while the cathode is grounded.

The voltage-current discharge characteristics show that the magnetron is operated in the abnormal glow mode with a maximum discharge power of 100 W at the argon pressure between 30 mTorr and 1 mTorr. In addition, Langmuir probe measurements have been performed over a range of discharge power and argon pressure. It has been found that the probe floating voltage dramatically increase up to +100 V. This implies that the average ion energy bombarding at the substrate surface is approximately 100 eV which is considerably larger than those in conventional magnetrons. The energetic ions found in configuration could potentially enhance the overall film qualities due to ion bombardment during the film growth.

Keywords: Penning magnetron sputtering, ferromagnetic film deposition, Langmuir probe measurement.

[1] Abolmasov, S. N., Physics and engineering of crossed-field discharge devices. Plasma Sources Sci. Technol. 21, 035006 (2012).

[2] Window, B. and Sharples, F., Magnetron sputtering sources for ferromagnetic material. J. Vac. Sci.

Influences of Elevated Thermal Decomposition of Ammonia Gas on Indium Nitride Grown by Sol-Gel Spin Coating Method

Zhi Yin (Lee)[1,2], Sha Shiong (Ng)[1], Fong Kwong (Yam)[2]

[1]Institute of Nano-Optoelectronics Research and Technology (INOR), Universiti Sains Malaysia, 11800, Minden, Penang, Malaysia.

[2]School of Physics, Universiti Sains Malaysia, 11800, Minden, Penang, Malaysia.

lee_zhiyin2003@yahoo.com

Indium nitride (InN) with unique properties such as small energy band gap of 0.7 eV, high electron affinity and carrier density, is a potential semiconductor material in the applications of optical and electronic devices [1, 2]. Despite, the suitable growth conditions of InN are very stringent due to its low dissociation temperature and volatility of atomic nitrogen [3]. In this study, InN thin films grown on aluminium nitride (AlN) on p-type silicon(111) [AlN/p-type Si(111)] substrates are prepared via sol-gel spin coating method followed by nitridation process. Sol-gel spin coating is a low cost, fast processing and dilute solution based deposition method to produce thin and uniform film on substrate. The spin-coater is programmed to operate in a two-step spin profile; the first spinning speed is slower than the second. In subsequent, two three-zone tube furnaces connected in parallel manner are used for nitriding process; the passage of ammonia gas (NH3) into the first furnace is decomposed to produce reactive nitrogen radicals and brought into the second furnace for crystallization of InN at 600 °C. The effects of thermal decomposition of NH3 gas on structural properties and surface morphologies of the deposited films are explored. X-ray diffraction results reveal that the crystalline quality of InN degrades markedly with increasing thermal decomposition of NH3 gas from 700 to 850 °C; in which, the association of indium oxide in the deposited film is detected. In the meantime, thermal etching effect and formation of indium droplet on the film can be observed at 850 °C; the findings are aligned with the cross-sectional analysis obtained by energy dispersive spectroscopy attached field-emission scanning electron microscopy, where the film thickness is found to be reduced tremendously. This phenomenon is mainly due to the increase of hydrogen partial pressure at elevated thermal decomposition of NH3 gas. On the other hand, the film surface with densely packed InN grains and film thickness of approximately to 620 nm is obtained at 700 °C. The results deduce that this temperature is in favor for the growth of InN thin films.

Keywords: Indium nitride, sol-gel spin coating, characterizations, thermal decomposition

[1] WALTHER, R., LITVINOR, D. FOTOUHI, M., SCHNEIDER, R., GERTHSEN, D., VOHRINGER, R., HU, D. Z. & SCHAADT, D. M. 2012. Microstructure of PAMBE grown InN layers on Si(111). *Journal of Crystal Growth*, 340, 34-40.

[2] XIE, Z. Y., ZHANG, R., XIU, X. -Q., LIU, B., LI, L., HAN, P., GU, S. -L., SHI, Y. & ZHENG, Y. -D.. 2007. Growth and Characterization of InN Thin Films on Sapphire by MOCVD. *Chinese Physics Letters*, 24, 1004-1006.

[3] MCCHESNEY, J. B. BRIDENBAUGH, P. M. & O'CONNOR, P. B. 1970. Thermal Stability of Indium Nitride at Elevated Temperatures and Nitrogen Pressure. *Materials Research Bulletin*, 5, 783-792.

A new approach for forming continuous ultra-thin Ag films with smooth surface

Sun Young Kim[1,3], Jeung-Hyun Jeong[2] , In-Gyu Lee[3], and Won Mok Kim[1]

[1]Center for Electronic Materials, Korea Inst. of Science and Technology, Seoul 02792, Korea

[2]Opto-electronic Hybrid Center, Korea Inst. of Science and Technology, Seoul 02792, Kore

[3]Division of Materials Science and Engineering, Korea Aerospace University, Gyeonggi-do 10540, Korea

Thin metal films made of noble metals such as Ag, Au, Cu and Pt have been widely used in optical and opto-electronic industries, and it is of practical importance and interest to obtain a ultra-thin and smooth metal films. However, it is well known that obtainment of ultra-thin films of noble metals, which cover the surface fully, is extremely difficult due to the fact that they follow the Volmer-Weber (3D) growth mechanism. At the initial growth stage, they grow into the shape of island, resulting in the deteriorated electrical, optical, and morphological properties.

In this study, a new fabrication method of ultra-thin silver films is presented. The concept of this technique is based on the presumption that reactive gas incorporated in the deposition of metal can reduce the surface energy of the growing film, and the fact that the noble metal compound made of oxide, nitride, sulfide or selenide are thermally unstable. It was shown that ultra-thin and smooth Ag films could be formed by depositing Ag-O films by sputtering of Ag target in oxygen-added environment, and by subsequently heat-treating the deposited Ag-O films. Electrical measurement revealed that the percolation threshold of Ag film fabricated by using this method could be obtained even at the nominal thickness of 2 nm, while pure Ag film made by normal sputtering gave percolation threshold thickness of 6 nm. SEM and cross-sectional TEM analyses showed that fully continuous Ag films could be formed at thickness as thin as 4 nm. The 4 nm thick Ag film showed a resistivity of 1.78×10^{-5} □cm which was comparable to that of 8 nm thick Ag film produced by normal sputtering. The film surface was also very smooth, giving the root-mean-squared roughness value of merely 0.35 nm. Oxide-Ag-oxide structure, in which 4 nm thick Ag film is sandwiched between non-conducting oxide films, was successfully fabricated by applying the present method, and the resulting film showed a resistance less than 50 Ω/sq. and transmittance as high as 80% in both visible and near IR region. Since noble metals such as Au, Pt and Cu also known to form thermally unstable compounds with oxygen, nitrogen, sulfur or selenium, the present method may be utilized to fabricate smooth and continuous ultra-thin metal films of such noble metals.

Enzymatic Activity Assay Utilizing Gold Nanoparticles and Reduced Graphene Oxide

Peng Chen [1,2*] Hu Chen,[1,2] Xiaohu Liu,[1,2] Al. Palaniappan, [1,2] Bo Liedberg[1,2*]
[1]Centre for Biomimetic Sensor Science, Nanyang Technological University, 50 Nanyang Drive, Singapore 637553
[2]School of Materials Science and Engineering, Nanyang Technological University, 50 Nanyang Avenue, Singapore 639798

Email: chenp@ntu.edu.sg
Email: bliedberg@ntu.edu.sg

Matrix metalloproteinase (MMP) is a family of zinc dependent enzymes that degrades the collagens in extracellular matrix. Among the 25 types of MMPs, MMP-7 plays a significant role on cell behavior. It has been reported that MMP-7 is up-regulated in many type of cancers, including lung cancer, gastric cancer, colorectal cancer, esophageal cancer and bladder cancer etc.
[2] Furthermore, MMP-7 is involved in numerous pathological conditions, such as metastasis and arthritis etc. [1] Current technologies for diagnosis such as endoscopic imaging could only detect cancer at advanced stages, mitigating effective treatment. Therefore, development of novel MMP-7 assay methodologies for prognosis is critically important for early treatment of cancer.
We have developed a colorimetric assay for MMP-7 based on aggregation of AuNPs with a LOD of ~100 ng/mL.[3] Briefly, we designed a novel synthetic polypeptide substrate for MMP-7 bearing 5 negative charges, with a specific cleavage site for MMP-7. This peptide was immobilized onto AuNPs via cysteine group and the negative charges stabilizes the AuNPs in suspension. Subsequently, it was specifically cleaved by MMP-7, reducing the net negative charges of the peptide on AuNPs from 5 to 1, leading to the aggregation of AuNPs. A red shift of LSPR peak and a red to blue transition in color were observed. This peptide is specific for MMP-7, where MMP 1 and MMP-2 did not give response.

To further improve the LOD to detect other cancers (for instance, colorectal cancer has a very low level of MMP-7 of 13.4 ng/mL), we have developed a rGO FET based sensor.[4]. The same peptide was immobilized onto rGO surface through a pyrene linker. Digestion of the peptide with MMP-7 lead to a decrease in the net negative charges of the peptide, which in turn induce a decrease in the source-drain current of the FET device. With this rGO FET device, we could obtain a LOD of 10 ng/mL in human plasma. This LOD falls below the level of numerous types of cancers, therefore, the proposed methodology has many potential to be further developed into a practical diagnostic tool for cancers.

Keywords: Gold nanoparticles, reduced graphene oxide, MMP-7, botulinum, colorimetric sensor

References

[1] EGEBLAD, M. & WERB, Z. 2002. New functions for the matrix metalloproteinases in cancer progression. *Nature Reviews Cancer,* 2**,** 161-174.
[2] AITKEN, K. J. & BAGLI, D. J. 2009. The bladder extracellular matrix. Part I: architecture, development and disease. *Nat Rev Urol,* 6**,** 596-611.

[3] CHEN, H., CHEN, P., HUANG, J., SELEGÅRD, R., PLATT, M., PALANIAPPAN, A., AILI, D., TOK, A. I. Y. & LIEDBERG, B. 2016. Detection of Matrilysin Activity Using Polypeptide Functionalized Reduced Graphene Oxide Field-Effect Transistor Sensor. *Analytical Chemistry*.

[4] CHEN, P., SELEGÅRD, R., AILI, D. & LIEDBERG, B. 2013. Peptide functionalized gold nanoparticles for colorimetric detection of matrilysin (MMP-7) activity. *Nanoscale,* 5**,** 8973-8976.

[5] LIU, X., WANG, Y., CHEN, P., WANG, Y., ZHANG, J., AILI, D. & LIEDBERG, B. 2014. Biofunctionalized Gold Nanoparticles for Colorimetric Sensing of Botulinum Neurotoxin A Light Chain. *Analytical Chemistry,* 86**,** 2345-2352.

Graphene containing films for chemical acoustoelectronic sensors

I.Kuznetsova[1], V.Anisimkin[1], S. Gubin[2], S.Tkachev[2], V.Kolesov[1], V.Kashin[1], B.Zaitsev[3], A.Shikhabudinov[3]

[1]Institute of Radio Engineering and Electronics of RAS, Moscow, 125009, Russia.

[2]Kurnakov Institute of General and Inorganic Chemistry of RAS, Moscow, 119991, Russia

[3]Institute of Radio Engineering and Electronics of RAS, Saratov Branch, Saratov, 410019,

Russia.

kuziren@yandex.ru

At present time the works over development and producing of chemical acoustoelectronic sensors are actively carried out [1-3]. It should be pointed the questions concerning the increasing of sensitivity, selectivity, working time of such sensors and widening their functional possibilities are very actual. One of the ways that allows solve these tasks is the search of the new gas-sensitive films. The using as the active element graphene and its derivatives will allow to develop whole set of different sensors for analysis of gases and liquids [4]. This possibility is connected with the unique graphene property that allows change the wide of his forbidden zone by the modification of the film surface by using the different ligand groups. The paper proposes to use a film of graphene oxide deposited on a piezoelectric substrate, with the possibility of further reduction to graphene by the heating. The technology of deposition of films from polar and nonpolar solutions of synthesized graphene oxide by an air brush has been developed. This method allowed get homogeneous dense coating from graphene oxide for further reduction to graphene and its modification.

The density, thickness, longitudinal and shear stiffness and viscosity modulus has been defined by the early developed method [5]. This method based on the comparison impedance vs frequency dependences of unloaded and loaded by the film under study acoustic resonators.

For studying the sensing properties of the film surface acoustic wave (SAW) and acoustic plate mode (APMs) delay lines were fabricated. The SAW samples were implemented on strong (128 YX-LiNbO3) and weak (ST, X-SiO2) piezoelectric crystals in order to define the dominant mechanism of the sensing. The APMs lines was integrated on one substrate (ST,X-SiO2) with 2 mutually orthogonal propagation direction along X- and X+90 - axis with joint graphene film between them. It allows studying 2 independent APMs families with 3 (Lamb modes) and one (SH-modes) mechanical displacements. All modes and waves are subjected by humidity adsorption with the value of rh in the range 1 to 90 % at room temperature (22 C).

The measurements showed the changes in electric conductivity and dielectric permittivity of the grapheme film were dominant as compared with relevant elastic variations due to humidity adsorption. The best sensitivity was detected for the Lamb mode at 23 MHz and plate thickness h/ = 1.67 (h – thickness, - wave length). The calibration curve (/ versus rh), the noise level of the phase (/ 1 ppm), and the minimal detectable humidity concentration (rh 0.03 %) were

measured for the mode demonstrating grapheme film and APM prosperity for extra sensitive humidity detection.
The sensitivity of the same film towards oxygen was proved to be negligible. The annealing the film reducing sensitivity and increasing operation times was turn to be not useful.

. This work is supported by Russian Science Foundation Grant #15-19-20046.

Keywords: Oxide graphene film,acoustoelectronic chemical sensor, humidity sensor

[1]. BALANTINE, D.S., WHITE, R.M., MARTIN, S.J., et.al. 1996. Acoustic wave sensors: Theory, design and physico-chemical applications, Academic Press, New York.

[2]. CALIENDO, C., VERONA, E., D'AMICO, A. 1992. Surface acoustic wave gas sensors. In: *Gas Sensors* (Ed. G.Sberveglieri), Kluwer Academic Publishers, Dordrecht, p.28.

[3]. ZUO, C., VAN DER SPIGEL, J., PIAZZA, G. 2010. *IEEE Transactions on Ultrasonics, Ferroelectrics, and Frequency Control*, 57, 82-89.

[4]. ZHU, M. & LI, X. 2015. Photo-induced selective gas detection based on reduced graphene oxide/Si Schottky diode. *Carbon*, 84, 138–145.

[5]. KUZNETSOVA, I.E., ZAITSEV, B.D. & SHIKHABUDINOV, A.M. 2010. Elastic and Viscous Properties of Nanocomposite Films Based on Low- Density Polyethylene. *Trans. on Ultras., Ferroel. and Freq. Contr*ol., 57, 2099-2102.

The Effect of Ferredoxin in Enhancing Sensitivity and Response of Chitosan Based Acetone Sensors

Irwana Nainggolan[1], Tulus Ikhsan Nasution[2,], Devi Shantini[1], Khairel Rafezi Ahmad[1]

[1]School of Materials Engineering, Universiti Malaysia Perlis, Kangar 01000, Perlis, Malaysia

[2]Physics Department, Faculty of Mathematic and Natural Science,University of Sumatera Utara, Medan 20155, Sumatera Utara, Indonesia

irwana@unimap.edu.my

The aim of this study is to investigate the effect of ferredoxin on sensing properties of chitosan based acetone sensor (CBAS). It has been proved [1] that CBASs have good acetone sensing properties including fast response, good stability, complete recovery, good repeatability and good reproducibility. However, the CBAS performance still can be further improved. Some researchers have blended the chitosan with other polymeric compounds however there is no report of using ferredoxin as a mixture of chitosan in order to improve the sensing properties of chitosan films. Ferredoxin appears to be huge promising as a biomixture which contains iron-sulfur proteins and represented as $[2Fe\text{-}2S]^{2+}$. When the ferredoxin is in reduced state, one electron is transferred to the specific iron atom which results in the $[2Fe\text{-}2S]^{2+}$ cluster becomes the reduced $[2Fe\text{-}2S]^{+}$ cluster by releasing one electron. Whereas, in the oxidized state of ferredoxin, one of these two iron atoms accepts an electron and both iron atoms are in a similar chemical state [2-3]. The chitosan-ferredoxin film sensors were prepared using photolithography and electrochemical deposition methods [1]. The ratio of ferredoxin to chitosan solution was varied at 5:95, 10:90, 15:85 and 20:80, respectively.

Chitosan contains two important functional groups, amine (NH_2) and hydroxyl (OH) groups [4]. The existence of amine and hydroxyl groups was evidenced by the absorption peaks of FTIR at 3269.45 cm^{-1} and 2918.08 cm^{-1} for ferredoxin-chitosan film while, the existence of ferredoxin [Fe-S] in 15% ferredoxin-chitosan film was shown by extra peaks appear at 1999 cm^{-1} and 2194 cm^{-1} [5]. The surface analysis of CBAS and Fdx-CBAS were studied using AFM. It was seen that CBAS has rougher surface compared to Fdx-CBAS. The CBAS has root mean square (RMS) of 6.943 nm, mean diameter of 1234 nm and roughness (Ra) of 5.369 nm, respectively, while the Fdx-CBAS has RMS of 3.187 nm and Ra of 1.964 nm. These values indicate that the Fdx-CBAS has smoother surface compared to the surface of CBAS.

For the purpose of exact comparison, the electrical properties of Fdx-CBASs were measured similar to CBAS, in which the sensors were exposed to acetone vapour with the acetone concentrations of 0.1, 1, 2, 5, 10, and 20 ppm respectively. The range was selected based on the medical reports that have expressed the acetone concentration in the breath varies from 0.3 to 0.9 ppm in healthy people to more than 1.8 ppm for diabetics. It was

found that all Fdx-CBASs with various ferredoxin concentrations showed higher sensitivity and response compared to that of CBAS. Among the ferredoxin-CBASs, 15%Fdx-CBAS exhibited the highest response. The comparison between 15% Fdx-CBAS and CBAS for different acetone vapour concentrations showed that the sensitivity and response of 15%Fdx-CBAS is higher 20% than CBAS.

Keywords: Chitosan, Ferredoxin, Acetone vapor, Electrical response, Surface Roughness

References

[1] NASUTION, T.I., NAINGGOLAN, I, HUTAGALUNG, S.D., AHMAD, K.R., AHMAD, Z.A. 2013. The Sensing Mechanism and Detection of Low Concentration Acetone Using Chitosan-Based Sensors. Sensors and Actuators B, 177, 522– 528.

[2] YAGATI, A.K., LEE, V., MIN, J., CHOI, J.W. 2011. Amperometric Sensor for Hydrogen Peroxide Based on Direct Electron Transfer of Spinach Ferredoxin on Au Electrode. Bioelectrochemistry 80, 169–174.

[3] CRISPIN, D.J., STREET, G., VAREY, J.E. 2001. Kinetics of The Decomposition of [2Fe-2S] Ferredoxin from Spinach: Implications for Iron Bioavailability and Nutritional Status. Food Chemistry, 72, 355-362.

[4] BOURTOOM, T., CHINNAN, M.S. 2008. Preparation and Properties of Rice Starch-Chitosan Blend Biodegradable Film. Food Science and Technology, 41, 1633-1641.

[5] CHAVES, M.R.M., VALSARAJ, K.T., DELAUNE, R.D., GAMBRELL, R.P., BUCHLER, P.M. 2011. Modification of mackinawite with L-cysteine: Synthesis, Characterization, and Implications to Mercury Immobilization in Sediment, Department of Chemical Engineering, University of Sao Paulo, Sao Paulo.

Application of molecularly imprinted polymer modified electrodes to detect methyl parathion in soil, water, fruits, and vegetables samples

Fa-Ru Wang[1], Gang-Juan Lee[2], and Jerry J. Wu[3]

Department of Environmental Engineering and Science, Feng Chia University, Taichung 407, Taiwan

jjwu@mail.fcu.edu.tw

Organophosphate (OP) pesticide, such as methyl parathion (MP), has been widely used in agriculture due to its high toxicity to insects and limited persistence in the environment. However, low levels of OP pesticides residual in agricultural products and the natural environment are extremely harmful to human health and zoology. Since methyl parathion can primarily over-stimulate the nervous system, resulting in nausea, dizziness, respiratory paralysis, and death, electrochemical sensors should be developed to rapidly detect MP existence in many environmental media associated with the advantages of low cost, simplicity, mechanical/chemical stability, reliability and a wide choice of templates and functional polymers. In this research, electrochemical sensor was fabricated based on glassy carbon electrode decorated by gold nanoparticles. The molecularly imprinted polymer (MIP) was synthesized on the electrode surface with methyl parathion (MP) as the template molecule and quercetin, resorcinol as functional monomer. The electrochemical behaviors of methyl parathion at the sensor were studied by using cyclic voltammetry (CV). Three important factors, including scanned laps, solution pHs, and immersed time, were evaluated for achieving the optimal condition of preparation and analysis. MP can be determined in the range of 5×10^{-9} to 2×10^{-6} M with a detection limit of 2×10^{-10} M in soil, water, fruit, and vegetable samples.

Keywords: sensors, molecularly imprinted polymer, methyl parathion

[1] Bakas, I., Hayat, A., Piletsky, S., Piletska, E., Chehimi, M.M., Noguer, T., and Rouillon, R. 2014. Electrochemical impedimetric sensor based on molecularly imprinted polymers/sol–gel chemistry for methidathion organophosphorous insecticide recognition. *Talanta*, *130*, 294–298.

[2] Li, H., Wang, Z., Wu, B., Liu, X., Xue, Z., and Lu, X. 2012. Rapid and sensitive detection of methyl-parathion pesticide with an electropolymerized, molecularly imprinted polymer capacitive sensor. *Electrochimica Acta*, *62*, 319–326.

[3] Tan, X., Hu, Q., Wu, J., Li, X., Li, P., Yu, H., and Lei, F. 2015. Electrochemical sensor based on molecularly imprinted polymer reduced graphene oxide and gold nanoparticles modified electrode for detection of carbofuran. *Sensors and Actuators B: Chemical*, *220*, 216–221.

Highly sensitive chitosan based optical fluorescent sensor for gaseous methylamine detection

Mironenko[1], Sergeev[2,3], Nazirov[1,3], Voznesenskiy[2], Bratskaya[1], Mirochnik[1]

[1] Institute of Chemistry Far Eastern Branch of the Russian Academy of Sciences, 159, prosp.100-letiya Vladivostoka, Vladivostok 690022, Russia Vladivostok, Russia.

[2] Institute of Automation and Control Processes Far Eastern Branch of the Russian Academy of Sciences, 5, Radio street, Vladivostok 690041, Russia.

[3] Far Eastern Federal University, 8, Sukhanova St., Vladivostok 690950, Russia.

almironenko@gmail.com

Polymer materials are frequently used matrices for sensitive additives in optical sensors. Due to high availability, relatively low cost and good film-forming properties some of the natural polymers can be considered as an alternative to synthetic polymers for optoelectronic applications. In this paper, we demonstrate new fluorescent methylamine gas sensor based on natural polysaccharide chitosan. Chitosan, natural biocompatible, biodegradable and nontoxic polymer is one of the best candidates for thin film gas sensors fabrication due to its superior film-forming properties [1], vapor permeability and ability to bind cationic and anionic forms of noble and transition metals [2].

An optical fluorescent sensor based on chitosan thin film co-dopped with Eu3+ and bromothymol blue pH indicator has been developed. Near-UV to visible (350-400 nm) excitation of the europium (III) chelate complexes with 1,3-diphenyl-1,3-propanedione exhibits a typical lanthanide emission with maximum at 615 nm. Luminescent spectra of Eu3+ complex were found to be insensitive to presence of methylamine gas. Therefore bromothymol blue, a non-fluorescent pH indicator with absorbance maximum of deprotonated form close to Eu3+ emission band was added to the film to provide non-fluorescent reversible response to different methylamine concentrations which can be detected by measuring of the Eu3+ emission.

Prior to exposure the sensor to methylamine, the absorption of bromothymol blue does not overlap the emission of Eu3+, whereby the coating shows fluorescent properties. In the presence of methylamine, chemochronic shift of bromothymol blue absorption maximum occurs. Overlapping the bromothymol blue absorbance with the europium emission provides the resonant tuning of BTB-Eu3+ system, resulting in reduce of Eu3+ fluorescent intensity and modulating the response signal. It was shown that increase of bromothymol blue content in the system leads to increase of its sensitivity to gaseous methylamine. The detection limit of the developed sensor to gaseous methylamine was found to be 60 ppb, what corresponds to 0.08 MAC. The sensor response is completely reversible and after exposure to methylamine, the luminescence intensity of the sensor coating returns to the original value.

Keywords: luminescence, sensor, chitosan, thin film

[1] RATHKE, T.D., HUDSON, S.M. 1994. Review of Chitin and Chitosan as Fiber and Film Formers. J. Macromol. Sci. Part C, 34, 375–437.

[2] VARMA, A., DESHPANDE, S., KENNEDY, J. 2004. Metal complexation by chitosan and its derivatives: a review. Carbohydr. Polym., 55, 77–93.

Colloidal Co-Crystallisation: A New Route to the Production of Three-Dimensional Metallodielectric Photonic Crystals

S. Kassim[1], M. E. Pemble[2,3]

[1]Universiti Malaysia Terengganu, 21030 Kuala Terengganu, Terengganu, Malaysia.

[2]Department of Chemistry, University College Cork, College Road, Cork, Ireland.

[3]Tyndall National Institute, University College Cork, Dyke Parade, Cork, Ireland.

syara.kassim@umt.edu.my +60169239835

A bottom-up co-crystallisation method is described, which combines polymer particle e.g poly(methyl methacrylate) (PMMA), pre-formed Au nanoparticles and acid-hydrolysed tetraethylorthosilicate (TEOS) solution via self-assembly evaporation process, followed by the removal of the PMMA template is described for the fabrication of 3D metallodielectric photonic crystal (MDPC) inverse opal (IO) structures. This procedure not only overcomes limitations associated with slow, expensive micro-fabrication methods but also results in the formation of relatively large (10s of mm) crack-free areas within these films (below a thickness level of approximately 20 deposition layers) via a single self-assembly step. The results demonstrate that different optical properties can be developed by tuning the concentration of Au NPs, where higher Au loading suppresses the transmission dip and shifts the Bragg peak to higher wavelengths. We produce a robust 3D structure with significant ordering when assembling with the TEOS precursor solution. The role of the silica network in cementing the metal NPs also makes this method versatile since the process is more dependent on the thermodynamics of the particles in suspension rather than on their physiochemical properties, allowing it to be a general strategy for making multifunctional interconnected porous structures. This simple yet effective method for preparing functional complex 3D MDPC structures which facilitates the effective integration of the plasmonic functionalities of the metal inclusion has the potential to be used generically to fabricate a variety of functional porous 3D MDPC structures that could find application not only in new or improved photonic crystal (PC) devices but could also find application in the fabrication of novel/improved surface-enhanced Raman scattering (SERS), sensing, enhanced photovoltaic and energy harvesting modules, catalysis, separation, fuel cells technology, microelectronics and optoelectronics.

Keywords: Photonic crystals, co-crystallisation, metallodielectric, 3-dimensional, inverse opal

RHEED Pole Figure – An "old" Technique for Polycrystalline and Nanostructured Surface Texture Analysis

Gwo-Ching Wang and Toh-Ming Lu

Department of Physics, Applied Physics and Astronomy, and Center for Materials, Devices, and Integrated Systems,

Rensselaer Polytechnic Institute, 110, 8th Street, Troy, New York 12180-3590, USA.
wangg@rpi.edu, http://www.rpi.edu/~wangg

The supply of thin films and nanostructures is driven by the demand of high technology industries for vast applications in electronics, energy, magnetism, catalysts, etc. The reduced dimensions in thin film and nanostructures also contain rich fundamental sciences. In reality most thin films and nanostructures are not single crystalline but polycrystalline with grains and grain boundaries. Often, there exists preferred orientation(s) or texture in polycrystalline thin films and nanostructures. To date the atomistic mechanisms on the texture evolution remains a challenging task due to the lack of experimental techniques that allow one to measure quantitatively the surface texture evolution. Conventional X-ray pole figure analysis with a few micron penetration depth probes an average texture of the entire thin film and nanostructures, and hence the information on the surface texture evolution is lost. I will present a surface pole figure technique using the transmission mode of reflection high energy electron diffraction (RHEED)[1,2]. The 10 keV electron used in RHEED has a few nanometer penetration depth and thus can probe the surface texture evolution of the growth front. Examples of *in situ* and *ex situ* surface texture evolution including the growth of unusual Mg, Mo, W, CaF_2, and CdTe nanostructures will be presented. The instrument response of the RHEED pole figure and the impact of this technique will be discussed.

This work is supported by the US NSF DMR-1305293 and Rensselaer.

Keywords: Electron diffraction, texture, nanostructures, thin films, instrument response

References

[1] TANG, F., WANG, G.-C., & LU, T.-M. 2006. Surface pole figures by reflection high-energy electron diffraction, *Appl. Phys. Lett.* 89, 241903.

[2] WANG, G.-C. & LU, T.-M. 2014. *RHEED transmission and pole figures: Thin film and nanostructure texture analysis*, Springer, NY.

Temperature and concentration dependent crystallization behaviors of Ge2Sb2Te5 phase change films: tungsten doping effects

Shuang Guo[1], Zhigao Hu[1], Liangcai Wu[2], Zhitang Song[2], Junhao Chu[1]

[1] Department of Electronic Engineering, East China Normal University, Shanghai 200241, China.

[2] State Key Laboratory of Functional Materials for Informatics, Shanghai Institute of Microsystem and Information Technology, Chinese Academy of Sciences, Shanghai 200050, China.

Electronic mail: zghu@ee.ecnu.edu.cn

Ge2Sb2Te5 (GST) semiconductor film has been widely investigated due to its rapid crystallization from amorphous to face-centered-cubic (FCC) structure in rewritable optical storages. [1] Additionally, with a small amount of tungsten (W) can improve the phase change characteristics of GST. In the Talk, we focus on the detailed analysis of crystallization mechanism and optical properties for W-doped GST (GSTW*x*%: *x*=0.0, 3.2, 7.1, 10.8) phase change films with the aid of temperature dependent Raman spectra and spectroscopic ellipsometry.

GSTW films were prepared by cosputtering pure GST and elemental W on SiO2/Si (100) substrates at room temperature. The spectra for GSTW have been recorded in the temperature range from 210 to 660 K. The Raman spectra have been fitted using Gaussian oscillator model to quantitatively describe the vibrational modes. The dielectric functions have been evaluated with the aid of Tauc-Lorentz (TL) and Drude dispersion models. The amorphous-FCC phase change can be clarified from temperature evolutions of Raman phonon modes and Tauc gap energy (*Eg*) as shown in Fig. 1. It can be concluded that the dominant phase change mechanism from amorphous to FCC structure is due to the changing of local banding arrangement of Ge atoms. The medium range order increment and chemical bond change from covalent to resonant should be responsible for band gap narrowing and electronic transition enhancement during the phase change process. The crystallization temperature (*Tc*) shifts from 420 K to 520 K with increasing W concentration, which can be related to improved disorder degree by W substitution. Furthermore, it was found that the W doping can lead to a higher crystallization temperature, better thermal stability of amorphous state and higher 10-year data retention ability than pure GST film. The GSTW7.1% film possesses a great potential as phase change materials in the present work. [2, 3]

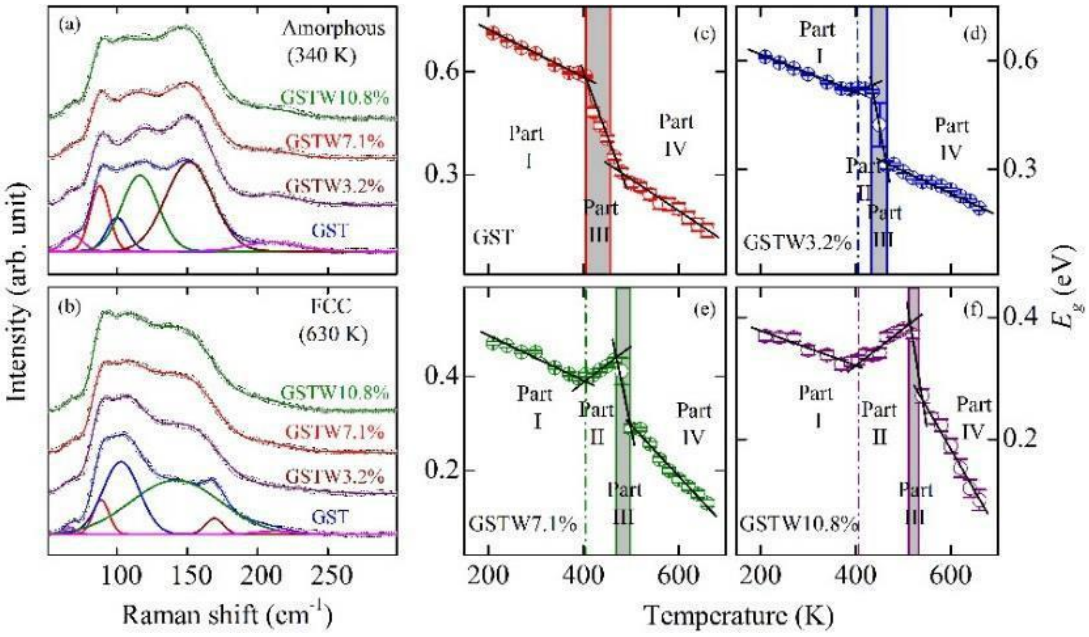

Fig.1 (a), (b) The experimental (dots) and fitted (lines) Raman spectra of GSTW films. (c), (d), (e), (f) Tauc gap energy (*Eg*) evolutions of GSTW films with different W concentration as a function of temperature.

Keywords: phase change films, W-doped, Raman spectra, spectroscopic ellipsometry,

[1] LENCER, D., SALINGA, M., GRABOWSKI, B., HICKEL, T., NEUGEBAUER, J. & WUTTIG, M. 2008. A Map for Phase-Change Materials. *Nat. Mater.*, 7, 972-977.

[2] GUO, S., HU, Z. G., JI, X. L., HUANG, T., ZHANG, X. L., WU, L. C., SONG, Z. T. & CHU, J. H. 2014. Temperature and Concentration Dependent Crystallization Behavior of Ge2Sb2Te5
Phase Change Films: Tungsten Doping Effects. *RSC Adv.*, 4, 57218-57222.

[3] GUO, S., DING, X. J., ZHANG, J. Z., HU, Z. G., JI, X. L., WU, L. C., SONG, Z. T. & CHU, J. H. 2015. Intrinsic Evolutions of Dielectric Function and Electronic Transition in Tungsten Doping Ge2Sb2Te5 Phase Change Films Discovered by Ellipsometry at Elevated Temperatures.
Appl. Phys. Lett., 106, 052105.

A Groove Pattern on Transfer Rollers for Circuit Construction of Digital Screen Surface

P.S. Pa
Department of Digital Content Design, Graduate School of Toy and Game Design
National Taipei University of Education No.134, Sec. 2, Heping E. Rd., Taipei City 106, Taiwan
myhow@seed.net.tw

This project aims to design a system mechanism module having non-polluting, micro elecrtrochemical-etching functions. More particularly, a novel mass-production system will be designed for creating lines on the Indium Tin Oxide film layer of the digital screen surface. The objective of the project is to overcome the problems of high production costs and environmental pollution associated with existing multiple-process etching methods for producing integrated circuit lines in TFT LCDs and touch panel modules. In this project, micro elecrtrochemical-etching is the technical foundation for etching the Indium Tin Oxide film of the digital screens, while the micro-electro mechanical system (MEMS) technique is applied to generate a groove pattern on transfer rollers, so that the conductive Indium Tin Oxide material connected to a DC current is removed during the electrochemical process. This study is focused on establishing a system mechanism module for transfer-based electrolytic etching, producing groove pattern on transfer rollers and creating lines on the Indium Tin Oxide film layer of the digital screens by micro elecrtrochemical-etching. When pattern lines can be defined on the Indium Tin Oxide layer of the digital screens by etching with the groove patterns on transfer rollers, the multiple metal-etching processes (including photoresist application, exposure and developing, etching, photoresist removal, etc.) can be simplified into a single process. Using the appropriate process parameters is able to provide a higher elecrtrochemical-etching removal capability and the Indium Tin Oxide fine line etching speed. The techniques of mask and transfer-based micro elecrtrochemical-etching will be integrated to establish a system mechanism module having high-efficiency elecrtrochemical functions that meet the requirements of commercial designs of the industry. Upon completion of the project, a procedure will be set up for designing and manufacturing the system mechanism module for creating lines on the Indium Tin Oxide layer of the digital screens by electrolytic etching. The results of this project can be further applied to relevant industries as a platform for implementing commercialized designs.

Keywords: Groove Pattern, Transfer Rollers, Digital Screens, MEMS, Indium Tin Oxide, Mass-Production

In-situ monitoring of electro-deposition for iron-nickel thin film by Time-resolved X-ray absorption spectroscopy

W. Limphirat[1], W.Inprasit[2], T. Juagwon[2], P. Prachopchok[2], M. Duriyarattakarn[2], A. Sinsarp[2], K. Tivakornsasithorn[2] and T. Osotchan[2]

[1] Synchrotron Light Research Institute, 111 University Avenue, Muang District, Nakhon Ratchasima, 30000 Thailand

[2] Materials Science and Engineering program, Capabi lity Building Unit of Nanosciences and Nanotechnology, Faculty of Science, Mahidol University, Bangkok, 10400 Thailand

wanwisa@slri.or.th

The crystals structure of iron-nickel thin films depend on the composition of iron and nickel those dissolve with electrolytes. However, it is believed that in electro-deposition the iron and nickel ions are homogenous distribute in the solution and should provide the uniformly homogenous alloy thin film. Due to differences in ion mobility and sticking condition of iron and nickel ions, the real time investigation of electro-deposition of these alloy thin films were investigated by TRXAS during the applying current into the solution. It found that, the intensity of X-ray at Fe dramatically decreases as the Fe ion deposits on the electrode. The slightly shift of Fe edge indicate the metal film forming i.e. Fe(II) ions convert to Fe(0) film. In addition, the signal of Fe(II) in R space also decrease as increasing the deposition time while the component at the nearest neighbor position of Fe metal alloy (at about 2Å) slight increase. However, the scattering signal of alloy at 1st nearest neighbor cannot determine the BCC and FCC crystal structure. These are needed the signal at the third and fourth nearest neighbor which are very weak at this initial deposition.

Keywords: In-situ monitoring, Electrodepositon, Time-resolved X-ray absorption spectroscopy, Fe-Ni alloys.

Diode-like and resistive switching property of diamondoid films

D. Doonyapisut[1], S. Sangphet[1], W. Meevasana[1]

[1]School of Physics, Suranaree University of Technology, 111 University Ave, Muang,

Nakhon Ratchasima, 30000

charting9@gmail.com, *worawat@g.sut.ac.th*

Diamondoids, a series of nano-diamond structures which can be synthesized cheaply or extracted from petroleum waste, have been attracting our attentions due to their unique electronic properties, including negative electron affinity (NEA) [W.L. Yang, et al., Science 316, 1460 (2007)] and ultralow effective work function [K. T. Narasimha, et al., Nat. Nanotech. 11, 267–272 (2015)]. In this work, we have focused on studying the transport properties of the adamantane-thiol films formed on gold substrates (that adamantane is the smallest 1-cage member of the diamondoid series). We have found non-symmetric (diode-like) current–voltage behavior and a signature of resistive switching effect. We also performed spatial mappings of the films using both an AFM microscope (nanometer scale) and also a cat-whisker setup (micron scale). Note that these similar behaviors were also found on CVD-adamantane films which we fabricated. These properties suggest potential applications of diamondoids as electrodes and perhaps resistive random access memory in electronic devices.

Keywords: diamond-like carbon, resistive switching, carbon based thins Films

[1] Narasimha, K., Ge, C., Fabbri, J., Clay, W., Tkachenko, B., Fokin, A., Schreiner, P., Dahl, J., Carlson, R., Shen, Z. and Melosh, N. (2015). Ultralow effective work function surfaces using diamondoid monolayers. Nature Nanotech, 11, 267-272. [2] Yang, W., Fabbri, J., Willey, T., Lee, J., Dahl, J., Carlson, R., Schreiner, P., Fokin, A., Tkachenko, B., Fokina, N., Meevasana, W., Mannella, N., Tanaka, K., Zhou, X., van Buuren, T., Kelly, M., Hussain, Z., Melosh, N. and Shen, Z. (2007). Monochromatic Electron Photoemission from Diamondoid Monolayers. Science, 316, 1460-1462.

Fabrication of large scale functional MoS_2 nanofilms

Xiaoyan Zhang[1], Kan Wu[2], Saifeng Zhang[1], Long Zhang[1] and Jun Wang[1,3*]

1 Key Laboratory of Materials for High-Power Laser, Shanghai Institute of Optics and Fine Mechanics, Chinese Academy of Sciences, Shanghai 201800, China

2 State Key Laboratory of Advanced Optical Communication Systems and Networks, Department of Electronic Engineering, Shanghai Jiao Tong University, Shanghai 200240, China

3 State Key Laboratory of High Field Laser Physics, Shanghai Institute of Optics and Fine Mechanics, Chinese Academy of Sciences, Shanghai 201800, China

Two dimensional (2D) layered transition metal dichalcogenides (TMDs) semiconducting materials, such as MoS_2 and WS_2, have recently triggered worldwide research interest due to their layer-dependent optical and electronic properties, which make them showing potential applications such as flexible and wearable electronics, sensors, photonics and electrochemical energy storage devices. [1] Thus, large-scale and low-cost fabrication of the 2D layered materials will take great roles in promoting the practical applications. Here, we developed two routes to controllably synthesize wafer-scale MoS_2 nanofilms. In the first route, wafer-scale MoS_2 neat films with controllable thicknesses were successfully fabricated by vacuum filtering liquid-exfoliated MoS_2 dispersions. The obtained MoS_2 filtered thin films show a smooth surface and high optical homogeneity verified by AFM and a collimated 532 nm beam, respectively. Ultrafast nonlinear Saturable absorption was observed at both 515 and 1030 nm femtosecond laser pulses, indicating that vacuum filtration is a feasible method for the fabrication of optical thin films, which can be expanded to fabricate other 2D films from the corresponding dispersions. In the second route, functional MoS_2 thin films with controllable infrared absorption were designed using a special solvothermal system containing a small amount of water. Wafer-scale MoS_2 thin films with tunable thickness and morphology are formed on various substrates and excellent passive Q-switching behavior in a fiber laser was demonstrated. The two simple wafer-scale thin film fabrication technologies are expected to greatly enlarge the application of the 2D nanomaterials in photonic devices, especially of MoS_2 as a saturable absorber.

[1] http://www.futuremarketsinc.com/graphene-market/

Influence of Nb Doping Concentration on Bolometric Properties of RF Magnetron Sputtered TiO2-x Films

Y. Ashok Kumar Reddy*, Young Bong Shin, In-Ku Kang, Hee Chul Lee

Department of Electrical Engineering, Korea Advanced Institute of Science and

Technology, Yuseong-gu, Daejeon 305-701, South Korea

E-Mail: akreddy111@gmail.com

Nowadays, considerable attention has been focused on certain semiconducting materials for uncooled microbolometer applications. The present study directly addresses the improved bolometric properties through Nb doping in to TiO2-x films. In order to compare the effect of doping concentration on bolometric properties, low resistivity of the samples such as 0.82 Ω·cm, 0.48 Ω·cm, 0.39 Ω·cm for Nb(0 at%):TiO2-x, Nb(0.5 at%):TiO2-x and Nb(1.0 at%):TiO2-x, respectively were deposited by altering the flow rate of oxygen gas. The X-ray diffraction patterns do not display any obvious diffraction peaks, suggesting that all the films deposited at room temperature had an amorphous structure. The test patterns were fabricated by means of UV-lithography to measure the bolometric properties of resistivity, temperature coefficient of resistance (TCR), and 1/f noise parameters. All the device samples exhibits linear I-V characteristics while changing the voltage from -3 V to +3 V, which attests the formation of good ohmic contact with low contact resistance between the Nb:TiO2-x film and the electrode material. The performance of bolometric material can be evaluated through TCR and the absolute value of TCR was increased from 2.54% to 2.62% with increasing the Nb doping concentration. The voltage spectral density of 1/f noise was measured in a frequency range of 1–100 Hz at a bias voltage of +3 V and it was found to be decrease in Nb doped TiO2-x samples. However, the variation of TCR and 1/f noise values are not too much differ in 0.5 and 1 at% Nb doped TiO2-x samples. Therefore, lower concentration (≤ 0.5 at%) of Nb doping can be sufficient to get better TiO2-x bolometers. Further studies are required in order to conclude the exact doping mechanism of Nb in TiO2-x samples.

Keywords: Thin film, bolometer, crystallinity, resistivity, 1/f noise parameter

The Spectroscopic Investigation of Photoinduced Changes in Water Layers On Hydrated TiO_2 and ZnO Powders.

M.V. Maevskaya, U. Oparicheva, A.V. Rudakova**,** A.V. Emeline, **K.M. Bulanin***,
**kbulanin@mail.ru*

Laboratory "Photoactive nanocomposite materials" St.-Petersburg State University, St.-Petersburg, Russia

Applications to environmental cleanup have been one of the most active areas in heterogeneous photocatalysis for a long time. UV-induced hydrophilicity effect was first reported by Wang et. al. in *Nature* [1].
Titanium dioxide is the most widely used photocatalyst, which provides the most reasonable trade-off between photocatalytic performance, stability in broad variety of chemical environments, low price, and essential low toxisity [2]. Although TiO_2 is considered as the most active photocatalyst, ZnO can also be a suitable alternative to TiO_2 because it is lower in cost and has the similar band gap energy around 3.2 eV [3].
FT-IR spectroscopy is useful technique for study adsorbed species. It is very sensitive to water molecules and superficial OH-groups, though the spectral line broadening due to H-bonding makes the interpretation difficult.
In our experiments powdered samples were pressed into the self-supported pellets with the thickness of about 0.1 mm, and outgassed at elevated temperatures in vacuum followed by the annealing in the presence of oxygen gas for removal of organic impurities. Experiments were carried out at ambient temperature.
In present work the influence of UV-radiation applied to powdered TiO_2 and ZnO samples was investigated spectroscopically under vacuum conditions as well as in the presence of gaseous oxygen for simulation of ambient conditions. Experiments were performed at different stages of surface hydration for simulation of superhydrophylic self-cleaning films at ambient conditions. Surface species formed were detected and analysed. Mechanisms of the hydroxo-hydrated layer reconstruction being under the action of UV-Vis radiation were proposed.

Acknowledgements. The present study was performed within the project "Establishment of the laboratory "Photoactive Nanocomposite Materials" №14.Z50.31.0016 supported by Mega-grant provided by the Government of Russian Federation. MVM thanks RFBR for support by grant № 16-32-00341.

Keywords: Photoinduced processes, hydroxyl-hydrated adsorbed layer, water, multilayer, TiO_2, ZnO.

[1] WANG, R.; HASHIMOTO, K.; FUJISHIMA, A.; CHIKUNI, M.; KOJIMA, E.; KITAMURA, A.; SHIMOHIGOSHI, M.; WATANABE, T. *Nature* **1997**, *388*,431.

[2] LINSEBIGLER, A. L.; LU, G. Q.; YATES, J. T., Jr. Chem. ReV. **1995**, *95*, 735-758.

[3] RUDAKOVA, A.V.; OPARICHEVA, U. G.; GRISHINA, A. E.; MAEVSKAYA, M. V.; EMELINE, A.V.; and BAHNEMANN, D. W.; *J. Phys. Chem.* C **2015**, 119, 9824−9828.

Tungsten-Doped Vanadium Oxide Thin Film Based Tunable Antenna

Eunsung (Shin)[1,2], KuanChang (Pan)[1], Shu (Wang)[1], Weisong (Wang)[1,2], Guru (Subramanyam)[1,2], Kevin (Leedy)[2], Tony (Quach)[2], Vladimir (Vasilyev)[2]

[1]Center of Excellence for Thin-Film Research & Surface Engineering, University of Dayton, Dayton, Ohio, 45469, USA.

[2]Air Force Research Laboratory, Sensors Directorate, Wright Patterson AFB, Ohio,

45433, USA.

E-Mail: eunsung@udayton.edu

Since vanadium dioxide (VO2) is a phase change material that shows a metal to insulator transition behavior at a temperature near 68℃, it has many potential applications in the areas of science and engineering. In this study, tungsten (W) -doped VO2 thin films were synthesized by pulsed laser deposition (PLD) technique with a metallic vanadium target and W-wires which were simply attached on the surface of the vanadium target. Also, bowtie RF antenna structures were fabricated by using the films to check the frequency tunability. The experimental results show a decrease of the transition temperature and a broadening of the transition temperature as the atomic percentage of W in the film structure increases. The results also reveal that the W-doped VO2 thin film based RF antenna was fully functional with the successful frequency tuning capability.

Keywords: Vanadium oxide, thin film, tungsten-doped, phase transition, tunable antenna

A Microporous Crystalline Aluminosilicate Film with Amphiphilic Adsorption Properties

Takuma Nakaoka[1], Takuji Ikeda[2], Ami Irisa[1], Miki Kawano[1], Katsutoshi Yamamoto[1]

[1]Graduate School of Environmental Engineering, The University of Kitakyushu, 1-1 Hibikino, Wakamatsu-ku, Kitakyushu 808-0135, Japan

[2]Research Institute for Chemical Process Technology, National Institute of Advanced Science and Technology, 4-2-1 Nigatake, Miyagino-ku, Sendai 983-8551, Japan

katz@kitakyu-u.ac.jp

Organic-inorganic hybridization has been studied not only to add functions of organic groups to inorganic matrix but also to control surface affinities. In particular, organic-inorganic hybrid porous silicates have been actively synthesized, and a lot of amorphous or crystalline materials have been successfully obtained using various organosilanes. Bellussi et al. employed bridged organosilanes to synthesize a series of microporous crystalline aluminosilicate materials, where layered alminosilicates are pillared with bridging organic groups [1]. Aiming at additional physicochemical properties, we used TEOS together with phenylene-bridged bis(triethoxysilyl)benzene (BTEB) and succeeded in synthesizing a novel organic-inorganic hybrid aluminosilicate material named KCS-2 [2,3]. This material turned out to have a sophisticatedly designed crystal structure that can be called a nanoporous crystallized Langmuir-Blodgett membrane.

Figure 1 illustrates the characteristic crystal structure of KCS-2 determined by the X-ray structure analysis. As clearly observed, two different aluminosilicate layers are piled up alternately. One is a lipophilic layer pillared with phenylene groups derived from the bridging organic group of BTEB. The other is a hydrophilic layer bridged with Q^2 silicon species originating from TEOS. Hexagonally arrayed zeolite-like 12-ring micropores perpendicularly penetrate the stacking layers to form hydrophilic and lipophilic nanospaces in one straight channel.

Owing to the presence of these two different kinds of nanospaces, KCS-2 shows high adsorption capacities for both water and *n*-hexane to indicate its amphiphilic adsorption properties. Their adsorption isotherms are typical Type I, indicating that the adsorption occurs mainly inside the micropores. It is also to be noted that KCS-2 shows little adsorption for bulky 1,3,5-trimethylbenzene molecules, demonstrating that its adsorption behavior was size-selective.

By employing another bridged organosilane or another alkaline source, other crystalline materials have been obtained under similar synthesis conditions. Their adsorption properties will be studied in detail.

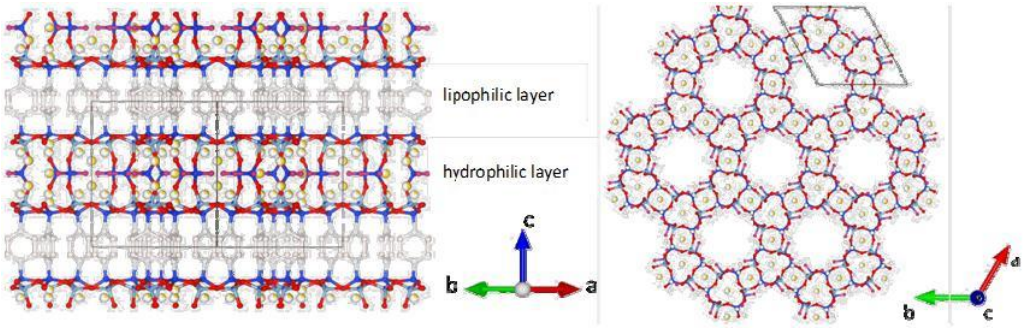

(a) (b)

Figure 1. Crystal structure models of KCS-2 viewed along (a) [110] and (b) [001] directions.

Keywords: organic-inorganic hybrid, Langmuir-Blodgett film, microporous, aluminosilicate

[1] BELLUSSI, G., CARATI, A., PAOLA, E. D., MILLINI, R., PARKER JR., W. O., RIZZO, C. & ZANARDI, S. 2008. Crystalline Hybrid Organic–Inorganic Aluminosilicates. *Micropor. Mesopor. Mater.*, 113(1-3), 252-260.

[2] YAMAMOTO, K., IRISA, A., KAWANO, M. & IKEDA, T. 2014. A Novel Crystalline Organic–Inorganic Hybrid Material Having a Large Adsorption Capacity for Bulky Organic Molecules. *Chem. Lett.*, 43(3), 376-378.

[3] IKEDA, T., HIYOSHI, N., MATSUURA, S., KODAIRA, T., NAKAOKA, T., IRISA, A., KAWANO, M. & YAMAMOTO, K. 2015. Amphiphilic Organic–Inorganic Hybrid Zeotype Aluminosilicate like a Nanoporous Crystallized Langmuir–Blodgett Film. *Angew. Chem. Int. Ed.*, 54(27), 7994-7998.

Antireflective coatings grown as thin films by pulsed laser deposition

M. Filipescu*, V. Ion, F. Stokker-Cheregi, C. Luculescu, M. Dinescu

National Institute for Lasers, Plasma and Radiation Physics, 077125 Magurele, Romania

In this paper we report on the obtaining and characterization of antireflective coatings from dielectric oxides for high power laser optics. The combination of the dielectric materials with low and high refractive index used as thin films and/or heterostructures with antireflection properties were studied. Starting from targets of Ta2O5, Al2O3, SiO2, and HfO2 in a controllable oxygen atmosphere, thin layers were grown at room temperature or high temperatures (700 C) by pulsed laser deposition. The deposition parameters as wavelength, laser fluence, oxygen pressure, substrate temperature were varied in order to obtain antireflection coatings with low roughness, uniform thickness, and high dielectric constant. The obtained HfO2/SiO2, Al2O3/SiO2, Ta2O5/SiO2, HfO2/Al2O3, Ta2O5/Al2O3 heterostructures were investigated by atomic force microscopy, scanning electron microscopy, transmission electron microscopy, Raman spectroscopy, and spectro-ellipsometry.

Growth and Characterization of Gallium Oxide Films With and Without *in-situ* Gallium Nitride Buffer on (0001) Sapphire Substrates

Trong Si (NgO), Duc Duy (Le), Soon-Ku (Hong)

Department of Advanced Materials Science and Engineering, Chungnam National

University, Daejeon 305-764, Republic of Korea

E Mail/ Contact Détails (soonku@cnu.ac.kr)

Gallium oxide (Ga2O3) is a wide-bandgap material with potential applications for high power devices [1], deep-UV photodetectors [2] and transparent electronic devices [3]. Various techniques have been employed to grow Ga2O3 films such as chemical vapor deposition, pulsed laser deposition, plasma assisted molecular beam epitaxy (PAMBE). In this work, we report the growth and characterization of Ga2O3 films on c-plane sapphire with and without *in-situ* GaN buffer layer by MBE technique. The growth processes were monitored by *in-situ* reflection high energy electron diffraction observations. The crystal quality and orientation were characterized by X-ray diffraction. The surface morphology and growth rate were investigated by atomic force microscope and scanning electronic microscope. The growth behavior and structural properties with and without the GaN buffer layer are investigated.

Keywords: Gallium oxide, Gallium nitride, Molecular beam epitaxy

[1] K.Sasaki, M. Higashiwaki, A. Kuramata, T. Masui, and S. Yamakoshi, J. Cryst. Growth Vol. 378 (2013), p. 591

[2] T. Oshima, T. Okuno, and S. Fujita: Jpn. J. Appl. Phys., Vol. 46 (2007), p. 7217

[3] M. Orita, H. Ohta, M. Hirano, and H. Hosono: Appl. Phys. Lett. Vol. 77 (2000), p. 4166

Improved stability and device performances of Si-IZO thin film transistor

Yoo seong Lim[1], Yong jin Im[1], Seung soo Ha[2], Chan hee Park[1] Min-hyung Jang[1], Seung-il Choi[2] Ji-in Park[1] and Moonsuk Yi[1*]

[1] Department of Electronics Engineering, Pusan National University, Busan 46241 , Republic of Korea.

[2] Department of Advanced Integrated Circuit, Pusan National University, Busan 46241, Republic of Korea.

E-mail / Phone: lys9003@pusan.ac.kr / +82-51-510-3970

msyi@pusan.ac.kr / +82-51-510-2381

Indium-zinc-based Amorphous - Oxide Semiconductors (AOSs) materials have received a lot of attention as a potential channel layer for Thin-Film Transistors (TFTs) due to its high mobility at low processing temperatures. This makes the materials well-suited applications for next-generation display devices and for use in flexible transparent devices. The stability and electrical performance plays a major role in TFTs. Usually the stability could be effectively enhanced through control of the defect by adjusting the oxygen content, annealing process, various heavy metal and metal cations. So several metal cations have been applied to control the electrical properties as well as the stability of InZnO-based TFTs, such as silicon (Si^{4+}), gallium (Ga^{3+}), magnesium (Mg^{2+}), hafnium (Hf^{4+}) and zirconium (Zr^{4+}) [1]. It can enhance the stability because of their ionic radii, electron negativity and standard electric potential. In this work, we focused on the improvement of the stability of IZO without affecting it's electrical performance. So SiO_2 was doped in InZnO (SIZO) and used as an active-channel layers for thin-film transistors.

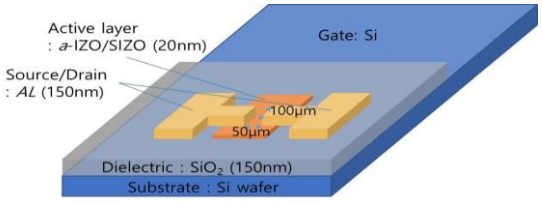

Figure 1:Schematic diagram of a-IZO / SIZO TFTs.

We fabricated amorphous oxide semiconductor thin-film transistors (TFTs) using SiO_2-doped InZnO thin films as active-channel layers (Fig.1). SIZO thin films were deposited at room temperature by radio-frequency (RF) magnetron co-sputtering. There is no change in the RF power (50 W) of the IZO target.

Figure 2 shows the transfer-characteristic curves of the TFTs for IZO and SIZO. It confirm that the electrical performance is better for SIZO compared to IZO. To optimize the stability and electrical performance, we changed two processing parameters such as different oxygen partial pressure (11, 12, 13 %) and different power (0, 5, 10 W) while using only SiO_2 target during sputtering. Among the different parameters of SIZO TFT preparation, the best one is obtained at the oxygen partial pressure of 12% and SiO_2 target power of 5 W while sputtering. The optimized SIZO TFT exhibited the on/off ratio, saturation mobility, threshold voltage and subthreshold swing of 5.2×10^6, 31.2 $cm^2/V\cdot s$, -5 V, 1.5 V/dec, respectively. It is showing best stability and electrical performance because of decreasing oxygen deficiency and defects in Zn-based oxide films.

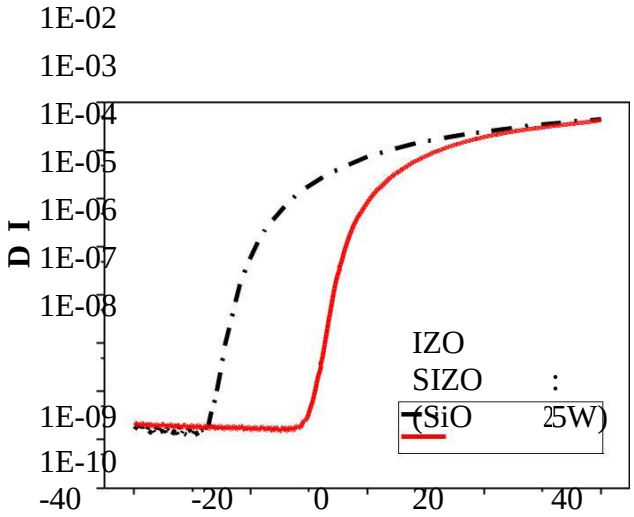

Fig. 2. Comparision of transfer characteristic curves of a-IZO and SIZO TFTs.

Keywords: Metal Oxide, Thin Film Transistor, RF-magnetron sputtering, SIZO

[1] CHONG E. G., KIM S. H., CHO E. A., JANG G. E., LEE S. Y. 2011. The relationship between processing parameters and the performance of novel amorphous silicon–indium–zinc oxide thin film transistors. *Current Applied Physics*, 11, 132-134.

Improved Stability of Indium-Zinc Oxide using Aluminum Oxide by Co-sputtering for Thin-Film Transistor Application

Ji-in Park[1], Yooseong Lim[1], Yongjin Im[1], Chanhee Park[1], Minhyung Jang[1], Seungsoo Ha[2], Seung-il Choi[2], and Moonsuk Yi[1,*]

[1] Department of Electronics Engineering, Pusan National University, Busan 46241, Republic of Korea

[2] Department of Advanced Circuit Interconnection, Pusan National University, Busan 46241, Republic of Korea

E – Mail / Phone : pji0604@pusan.ac.kr / +82-51-510-3970

msyi@pusan.ac.kr / +82-51-510-2381

N-type amorphous indium-gallium-zinc oxide (a-IGZO) is most commonly used material in Thin Film Transistors (TFTs) compared to the other Ionic Amorphous Oxide Semiconductor (IAOSs) materials. The main drawback of this material is that it contains rare earth metal such as Indium (In) and Gallium (Ga). Especially Ga, which is used to control oxygen vacancy, is expensive rare earth metal [1]. Therefore, several researches to find substitute of Ga have been studied. In this work, Al_2O_3 is used instead of Ga in TFTs. Aluminum (Al) has attracted as a substitute of Ga because of its carrier suppressing property, its natural abundance in earth and low cost [2]. The bottom-gated Al_2O_3-IZO (a-AIZO) TFTs were fabricated using n-type silicon wafer which is covered by 150nm thick SiO_2. Al_2O_3 and IZO targets are co-sputtered to deposit amorphous Al_2O_3-IZO (a-AIZO) and different Al_2O_3 target powers (0, 10, 20, 30 W) were used in RF sputtering to find the best composition ratio of Al. The partial pressure of oxygen O_2 / ($Ar+O_2$) was set at 13%. The cross-sectional schematic diagram of a-AIZO TFT is shown in Fig. 1, and the electrical performance of a-AIZO TFT is compared with IZO TFT in Fig. 2.

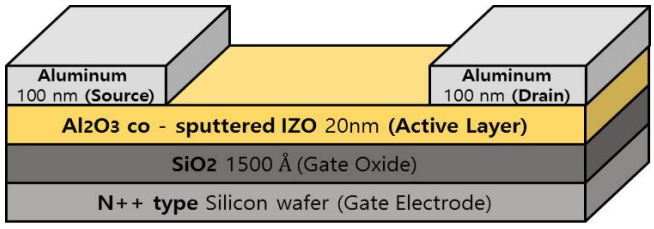

Fig. 1. Cross - sectional schematic diagram of Al_2O_3-IZO TFT

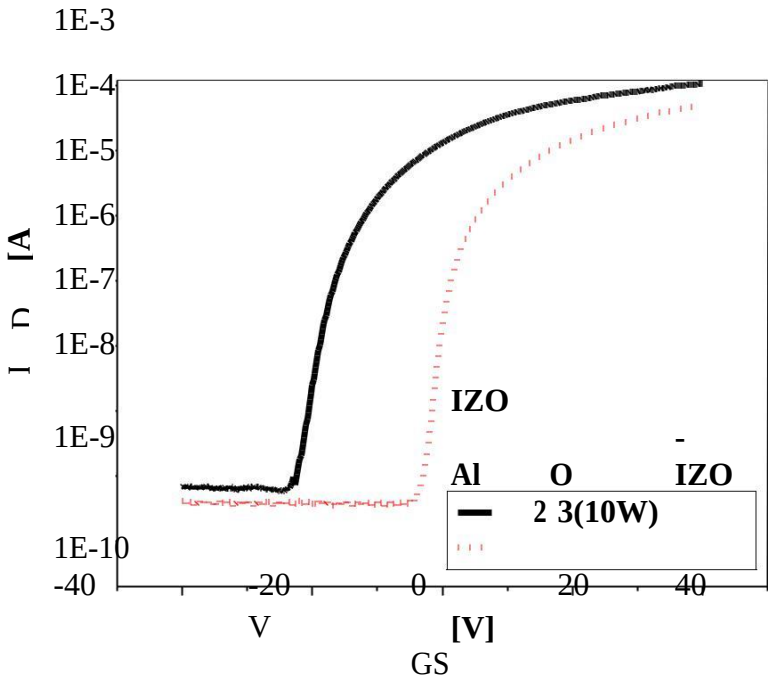

Fig. 2. Transfer characteristic curves of the IZO and Al_2O_3-IZO TFTs

The electrical characteristic parameters of a-AIZO TFTs with different Al_2O_3 RF power are listed in Table 1.

Al_2O_3 Power [W]	μ_{sat} [cm^2/Vs]	V_{th} [V]	I_{on}/I_{off} Ratio	SS [V/dec]
0	25.45	-15.52	2×10^6	1.62
10	**21.70**	**-2.24**	$\mathbf{2 \times 10^6}$	**1.35**
20	16.08	-1.60	1×10^6	1.61
30	11.49	-0.96	6×10^5	1.73

Table 1. Electrical parameters of TFTs while changing the RF power of Al_2O_3 target

In Table 1, threshold voltage (V_{th}) is increased with increasing the Al_2O_3 target power because the Al atoms can suppress the oxygen vacancies with strong oxygen bonding and therefore suppresses the carrier concentration. The best electrical performances were shown in 10 W of Al_2O_3 target power. A mobility of 21.70 $cm^2/V{\cdot}s$, I_{on}/I_{off} ratio of 2 10^6, threshold voltage of - 2.24 V, and subthreshold swing of 1.35 V/dec, were achieved. These results concluded that the performance of a-AIZO TFT is comparable with the standard a-IGZO TFTs.

Keywords: Thin Film Transistor, Al_2O_3 - IZO TFT, RF magnetron co-sputtering.

[1] D. H. Lee, S. M. Park, D. K. Kim, Y. S. Lim, M. S. Yi. 2014. Effects of Ga Composition Ratio and Annealing Temperature on the Electrical Characteristic of Solution processed IGZO Thin-film Transistors, *Journal of Semiconductor Technology and Science*, 14**,** 163-168.

[1] J. SUN, Y. HUANG, H. GONG. 2011. Improved mobility and conductivity of an Al_2O_3 incorporated indium zinc oxide system, *Journal of Applied Physics*, 110**,** 023709.

Low temperature SiO2 growth by wet oxidation of ultra-thin Si films deposited on sapphire substrate

Sinyong Joo[1], Chadrasekhar Loka[1], Kwang Lee[1], Sung Whan Moon[2], Kee-Sun Lee[1,*]

[1]Department of Advanced Materials Engineering, Kongju National University, Cheonan, Chungnam 330−717, South Korea.

[2]Sapphire technology Ltd., Whasung city, Kyunggido, South Korea.

E-Mail:kslee@kongju.ac.kr

We propose wet oxidation process for sputtered silicon thin film on sapphire substrate. The growth kinetics, structural and optical properties of deposited SiO_2 film on sapphire substrate studied at different temperatures. In the oxidation of nano-crystalline silicon films, the activation energy for wet oxidation is observed to be lower than the previous reports due to availability of larger surface area for oxidation reaction. The optical data suggest that, the transmittance of the SiO_2/sapphire can be enhanced when the deposited silicon totally converted in to the SiO_2 which shows refractive index 1.43 and follows the Rayleigh relation for anti-reflecting coatings. When the films oxidized at 1073 K, Si layer was observed to be completely converted in to SiO_2 within 1h and shows the highest value of transmittance 90%, which is the highest transmittance obtained for grown SiO_2 film on sapphire substrate. This SiO_2 films were expected to be useful as antireflection coating for increasing the transparency of sapphire substrate.

Keywords: SiO_2, sputtering, wet oxidation, optical transmittance, refractive index.

[1] ALEXANDROVA, S., SZEKERES, A., HALOVA, E., LISOVSKYY, I., LITOVCHENKO, V., MAZUNOV, D. 2004. Oxide and Interface Charges in Thin SiO_2 Films Thermally Grown on RF Plasma Hydrogenated Silicon. *Vacuum*, 75, 301-305.

Novel and Green Strategy to Highly Porous Anatase TiO2 Nanothin Films Prepared Using NH4TiOF3 Single Crystals

Takumi Fujiwara, Hack-Keun Lee, Takuya Okada, Seung-Woo Lee*

Graduate School of Environmental Eengineering, University of Kitakyushu

Hibikino 1-1, Kitakyushu 808-0135, Japan

*hackkeunlee@gmail.com, *leesw@kitakyu-u.ac.jp*

Crystalline titanium dioxide (TiO2) has attracted considerable attention due to its unique properties and potential applications such as for photocatalysis, photovoltaics, and gas sensing. In particular, TiO2 coatings on glass substrates have been widely used for self-cleaning of the exposed surface [1]. To date, various manufacturing and processing routes of TiO2 coatings have been explored and proposed. In this study, we demonstrate a novel and green process for fabricating TiO2 nanothin films on solid surfaces via hydrolysis of NH4TiOF3 single crystals [2]. To investigate the effect of surface functional groups on TiO2 crystal growth, silicon (Si) substrates modified with different functional groups were tested. Methylen blue was used as a probe to assess the photocatalytic activity of the TiO2 coatings on the Si substrate under ultraviolet irradiation. The size and morphology of the deposited TiO2 crystals served critical roles in understanding their photocatalytic acitivities.

Keywords: TiO2 Nanocoating, Anatase TiO2 thin film, NH4TiOF3 single crystals

[1] DE JESUS, M. A. M. L., DE SILVA NETO, J. T., TIMÒ , G., PAIVA, P, R, P., DANTAS, M, S, S. & DE MELLO FERREIRA, A. 2015. Superhydrophilic self-cleaning surfaces based on TiO2/SiO2 composite films for photovoltaic module cover glass. *Applied Adhesion Science*, 10. 2-9.

[2] LEE, H-. K. & LEE, S-. W. 2015. Surfactant-free NH4TiOF3 Crystals: Self-assembly on Solid Surfaces and Room-temperature Hydrolysis for Hollow TiO2 Structures with High Photocatalytic Activity. *Chemistry Letter*. 44, 604–606.

Structure and transmittance changes of SiON thin films on sapphire annealed at elevated temperatures

Kwang Lee[1], Chadrasekhar Loka[1], Sinyong Joo[1], Sung Whan Moon[2], Kee-Sun Lee[1,*]

[1]Department of Advanced Materials Engineering, Kongju National University, Cheonan, Chungnam 330−717, South Korea.

[2]Sapphire technology, LTD, Whasung city, Kyunggido, South Korea.

E-Mail: kslee@kongju.ac.kr

Silicon oxynitride (SiO_xN_y) and SiO_2 thin films were attracted with considerable attention for various applications such as anti-reflection coatings and surface passivation layers, etc. We present amorphous silicon oxynitride (a-SiO_xN_y) thin films deposition on sapphire by using RF magnetron sputtering at room temperature, and their structural-optical transmittance changes of the films at elevated temperatures (1173 to 1373 K). Topography and surface microstructure of the films were studied by atomic force microscopy and field-emission scanning electron microscopy. The structural changes in films have been analyzed from measurements of refractive index, and x-ray photoelectron spectroscopy (XPS) spectra. XPS spectra revealed that the silicon-nitrogen bonds completely disappeared to form non-stoichiometric silicon oxide (SiO_x), after the direct thermal oxidation of the as-deposited a-SiO_xN_y films in air ambient at 1373 K. Optical transmittance of the films was recorded by UV-Vis-NIR spectrophotometer, it is observed that the transmittance was drastically enhanced after annealing the films at elevated temperatures due to structural changes and change in refractive index of the films.

Keywords: Silicon oxynitride, sputtering, annealing, optical properties, X-ray photoelectron spectroscopy.

[1] ZETENG, Z., YUTA, S., YUKI, K., TAKAHIRO, Y., HIROMASA, O., HIROAKI, K., KIYOSHI, Y. 2013. Interface Properties of SiO_xN_y Layer on Si Prepared by Atmospheric-Pressure Plasma Oxidation-Nitridation. *Nanoscale Research Letters,* 8, 201.

The characteristics of UV frequency selectors fabricated by nanocrystal TCO thin films on GaN

R. X.Wang

Suzhou Institute of Nano-tech and Nano-bionics, Chinese Academy of Sciences, Suzhou 215123, China

E-mail: rxwang2008@sinano.ac.cn

The development of ultraviolet (UV) frequency selectors has been driven by numerous applications in defense, space monitoring, optical communication technique, flames safeguard, fire control areas and so on. UV devices shall have efficient UV opto-electrical responses and their fabrication inquires active materials showing UV photoresponse, for example, some wide band gap semiconductors-gallium nitride [1,2], zinc oxide (ZnO) [3,4] and silicon carbide. For UV frequency selectors, they have been shown to depend on quality of materials as well as fabrication conditions.[5]

One ultraviolet (UV) frequency selectors were fabricated by using TCO thin films on GaN substrates. TCO thin films can be sputtered or e-beam evaporated. Current-voltage (I-V) and opto-electrical characteristics of the devices were characterized. It is found that the optical responsivity of the devices can be significantly influenced by materials and device structures. A narrow frequency selection 8 nm FWHM at 369 nm can be obtained. Such is ascribed to combination effect by TCO materials and GaN substrate.

Keywords: UVdevice, GaN, TCO

[1] S. N. Mohammad, A. A. Salvador, and H. Morkoc, "Emerging Gallium Nitride Based Devices", Proceedings of the IEEE 83,1306-1355 (1995).

[2] A. H. Morkoc, *Nitride Semiconductors and Devices*, (Springer, Berlin, 1999).

[3] T. Saito, T. Hitora, H. Hitora, H. Kawai, I. Saito, and E. Yamaguchi, "UV/VUV photodetectors using group III-nitride semiconductors", Phys. Status Solidi C **6**, pp. S658-S661, 2009.

[4] S.-P. Chang, C.-Y. Lu, S.-J. Chang, Y.-Z. Chiou, T.-J. Hsueh, and C.-L. Hsu, "Electrical and Optical Characteristics of UV Photodetector With Interlaced ZnO Nanowires", IEEE J. Sel. Top. Quant. Electron. **17**, pp.990 ,2011.

[5] R. X. Wang, S. J. Xu, and S. Fung, "GaN Schottky Contacts and Their Applications", in

Gallium Nitride: Structure, Thermal Properties and Applications, Ed. by K.O. Peak, (Nova Science Publisher, New York, 2014), Chap. 5, pp.119-166.

Electroless synthesis of multiscale metal architectures for catalytic applications

Falk Muench[1], Markus Antoni[1], Sandra Schaefer[1], Xin Zhao,[1,2] Wolfgang Ensinger[1]

[1]Technische Universität Darmstadt, Department of Materials Science, Alarich-Weiss-Straße 2, 64287 Darmstadt, Germany.

[2]Northeast Forestry University, College of Material Science and Engineering, No. 26 Hexing Road, Xiangfang District, Harbin 150040, P. R. China.

muench@ma.tu-darmstadt.de

Electroless plating displays a versatile, facile and scalable method for the conformal metallization of arbitrary shaped work pieces.[1,2] From a mechanistic point of view, it is based on the surface-selective, autocatalytic reduction of metal complexes by chemical reducing agents. Modern electroless plating research focuses on nano- and microfabrication, albeit with a strong focus on electronics and smooth metal films.[1]

Several important application fields of nanoscale metals benefit from porous, anisotropic or hierarchic morphologies, which can be created with certain deposition protocols.[3,4] Combined with the ability to deposit a wide range of catalytically active metals or alloys, this renders electroless plating promising for the synthesis of tailored catalysts.[3,5.] In this contribution, we present our recent efforts in the electroless fabrication of well-defined multiscale metal architectures. Two novel strategies will be outlined: (i) The use of ion track etched polymer membranes provides access to anisotropic nanostructures such as nanotubes, which display interesting unsupported catalysts.[3] We show that the purposeful control of the template pore structure allows the deposition of free-standing nanostructure arrays of distinct complexity, such as interconnected metal nanotube networks[6] and hierarchic assemblies of nanorods, nanotubes or nanowires. Such materials combine the benefits of one-dimensional nanoscale building blocks (e.g. large surface area, continuous conduction and diffusion pathways) with those of an ordered superstructure. (ii) While the use of templates provides a high degree of direct morphological control, it also complicates the synthesis. As an alternative approach, we are developing eletroless plating reactions which yield shape-controlled deposits.[4,7] Such reactions allow to exploit intrinsic structuring mechanisms to produce anisotropic nanomaterials. We demonstrate that coating common macroscale supports with such nanostructured metal films represents a general and effective catalyst preparation strategy. The favorable functional properties of the different materials are demonstrated in electroanalytical model applications (amperometric detection of hydrogen peroxide or glucose), in which excellent sensitivity, catalyst utilization and stability are achieved.

Keywords: Electroless plating, template, anisotropic nanoparticles, catalysis, electroanalysis

[1] SHACHAM-DIAMAND, Y.; OSAKA, T.; OKINAKA, Y.; SUGIYAMA, A. & DUBIN, V. 2015. 30 years of electroless plating for semiconductor and polymer micro-systems, *Microelectron. Eng.*, 132, 35-45.

[2] SUDAGAR, J.; LIAN, J. & SHA, W. 2013. Electroless nickel, alloy, composite and nano coatings – a critical review. *J. Alloys Compds.*, 571, 183-204.

[3] MUENCH, F.; NEETZEL, C.; KASERER, S.; BRÖTZ, J.; JAUD, J.-C.; ZHAO-KARGER, Z.; LAUTERBACH, S.; KLEEBE, H.-J.; ROTH, C. & ENSINGER, W. 2012. Fabrication of porous rhodium nanotube catalysts by electroless plating. *J. Mater. Chem.*, 22, 12784-12791.

[4] MUENCH, F., JURETZKA, B., NARAYAN, S., RADETINAC, A., FLEGE, S., SCHAEFER, S., STARK, R. W. & ENSINGERm W. 2015. Nano- and microstructured silver films by halide-assisted electroless plating. *New J. Chem.*, 39, 6803-6812.

[5] DIAO, W.; TENGCO, J. M. M.; REGALBUTO, J. R. & MONNIER, J. R. 2015. Preparation and characterization of Pt-Ru bimetallic catalysts synthesized by electroless deposition methods. *ACS Catal.*, 5, 5123-5134.

[6] MUENCH, F., DE CAROLIS, D., FELIX, E.-M., BRÖTZ, J., KUNZ, U., KLEEBE, H.-J., AYATA, S., TRAUTMANN, C. & ENSINGER, W. 2015. Self-supporting metal nanotube networks obtained by highly conformal electroless plating. *ChemPlusChem*, 80, 1448-1456.

[7] ZHAO, X., MUENCH, F., SCHAEFER, S., BRÖTZ, J., DUERRSCHNABEL, M., MOLINA-LUNA, L., KLEEBE, H.-J., LIU, S., TAN, J. & Ensinger, W. 2016. Electroless decoration of macroscale foam with nickel nano-spikes: A scalable route toward efficient catalyst electrodes. *Electrochem. Commun.*, accepted manuscript, DOI: 10.1016/j.elecom.2016.02.002

Magnetism of Antidot Arrays Fabricated by Different Patterning Methods

M. Marszałek[1], M. Krupiński[1], A. Maximenko[1], M. Perzanowski[1], A. Szkudlarek[2], Y. Zabila[1], A. Zarzycki[1]

[1]Institute of Nuclear Physics Polish Academy of Sciences, PL 31-342 Krakow, Poland

[2]Academic Centre of Materials and Nanotechnology AGH (ACMiN), PL 30-055

Kraków, Poland

*E Mail/ Contact Détails (***Marta.Marszalek@ifj.edu.pl)**

The main driving force behind the development of innovative patterned magnetic materials is the magnetic recording industry. A promising solution is the use of Percolated Pependicular Media (PPM) concept, where one bit of information is stored in an individual magnetically isolated nanostructure. There are many ideas how to produce the media consisted of isolated magnetic nanoislands. Here different methods of magnetic nanoisland fabrication are shown.

The fabrication of FePd and Co/Pd magnetic antidot arrays on porous alumina and titanium oxide templates and on templates prepared by self-assembling nanosphere lithography supplemented by RF-plasma etching will be demonstrated. The use of these patterning methods leads to the creation of arrays of magnetic antidots. Different techniques were used to determine the crystallographic structure, sample surface morphology and the magnetic properties of the nanostructures.

The magnetic properties and magnetization switching exhibited strong dependence on the island and antidot size and separation distance. The easy axis of magnetization for all samples was normal to the sample plane. The perpendicular coercivity increased with the increase of antidot size. The change was more pronounced at low temperatures and it is related to modification of magnetic domain sizes and shapes. For narrow range of nanostructure sizes, the samples have revealed interesting behaviour, in which the antidot array behave magnetically as an array of isolated dots. The presented method of antidot fabrication allows enhancement of PMA for hard magnetic films with in-plane anisotropy and refinement of their magnetic domains into alternating magnetic dots with upward and downward directions for applications.

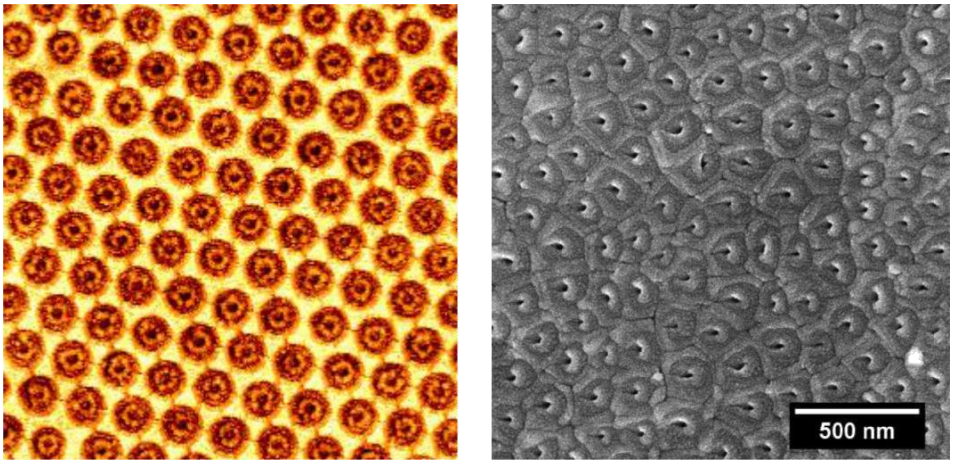

Fig. 1. Images of the Co/Pd antidot array on the template prepared by self-assembling nanosphere lithography (left) and on porous titanium oxide (right).

Keywords: Functional, antidots, magnetic anisotropy, percolated

Biomimetic fabrication of hydroxyapatite/chitosan nanohybrid composite in modified simulated body fluids and its biocompatibility

Kyung Hee Park, Seok-Jae Kim, Woon-Young Lee, Ho-Jun Song, Yeong-Joon Park*

Department of Dental Materials and MRC for Biomineralization Disorders, School of Dentistry, Chonnam National University, Gwangju, Korea

** Corresponding author (yjpark@jnu.ac.kr)*

For the increase of bioactivity and mechanical properties, composites of polymer and bioactive ceramics have been developed for bone tissue engineering [1]. In this study, nucleation of a bone-like hydroxyapatite (HA) mineral was achieved by incubating the chitosan-coated Ti substrate in modified simulated body fluids (mSBF) from 2day to 1 week. Analysis using scanning electron microscopy and energy dispersive x-ray analysis indicated growth of a continuous layer of mineral primarily composed of calcium and phosphorous. The longer the exposure time to the mSBF solution the more crystalline the coating and the lower its adhesion to the substrate. The bioactivity of hydroxyapatite/chitosan nanohybrid composite was examined using an in vitro biomimetic process of cell viability. The resulting composite material, HA/chitosan nanohybrid, has a complicated pop cone-like nanosphere structure that is expected to have high biocompatibility and that may be of use as materials for bone replacement.

Keywords: Mineralization, Simulated body fluid (SBF), Chitosan, Bioactivity, Calcium phosphate

Acknowledgement

This research was supported by the National Research Foundation of Korea (NRF) grant funded by the Korea government (MSIP) (No. 2011-0030121)

[1] RIZZI S. C., HEATH D. J., COOMBES A. G., BOCK N., TEXTOR M. & DOWNES S. 2001. Biodegradable polymer/hydroxyapatite composites: surface analysis and initial attachment of human osteoblasts. *J Biomed Mater Res*, 55(4), 475–486.

Self-assembly of Aligned Carbon Nanotubes in Polypropylene-coated Multi-Walled Carbon Nanotubes Composites

W.H. Li[1], Y.J. ZHU[1], T.Q. ZHAO[1], X.W. JIAN[1]

[1]School of Physics and Optoelectronic Engineering, Guangdong University of Technology, Guangzhou 510006 , P. R. China

E-mail address: liwenhuat@gdut.edu.cn (W.H. Li) Corresponding author. Tel.: +86 2039322265; fax: +86 2039322265.

Orderly assembling as well as interfacial adhesion MWNTs within composites still remains challenging for MWNTs as a reinforcement agent**.** In this case, we overcome these barriers with maleic anhydride(MAH) as a compatibilizer and poly(butyl methacrylate) (PBMA) as a binding, and successfully prepared PP-coated MWNTs composites with MWNTs having exceptional alignment and improved mechanical properties via a simple compounding technique. SEM results showed that MWNTs within composites were aligned without aggregation and the oriented MWNTs were connected by matrix. HRTEM results demonstrated that the nanotubes were densely coated with a PP layer, and the diameter of MWNTs coated by PP was much larger than that of uncoated MWNTs. FTIR results revealed that there was covalently linkage of MWNTs with PP via MAH. The MAH acts as "bridge" function to bond both PP and CNTs by chemical reaction. The interactions between MWNTs-PP and PBMA induced orientation of MWNTs. The formation mechanism was studied in detail.

The tensile strength of the PP-coated MWNTs composites was 35 MPa which was higher than that of net PP (19 MPa) and that of simple PP/CNTs compounding (23 MPa) with the same content of CNTs. The Young`s modulus of the PP-coated MWNTs composites increased by 50% compared with that of net PP. The phenomenon should be owing to the tensile load transmitted from the PP matrix to the MWNTs through the interfacial linkage.

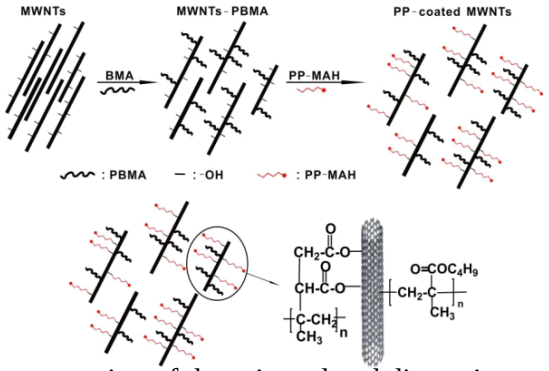

Schematic representation of the oriented and dispersion mechanism of MWNTs in PP-coated MWNTs composite

***Keywords**: Multi-walled carbon nanotubes (MWNTs), Polypropylene (PP)*

ZnO nanorod anchoring of reduced graphene oxide films by electrochemical deposition

A. Pruna[1, 2]*, Q. Shao[2], A. Zapien[2], L.Pilan[1], A. Ruotolo[2]

[1]Polytechnic University of Bucharest, 313 Splaiul Independentei, 060042 Bucharest, Romania

[2]City University of Hong Kong, Tat Chee Av., Kowloon, Hong Kong SAR, China
ai.pruna@gmail.com

Amongst the most promising semiconductor photocatalysts, ZnO has attracted an extensive emphasis due to its physical and chemical stability, high oxidative capacity, low cost, and high availability. The photocatalytic properties of ZnO are highly dependent on its surface morphology, size, crystal structure, aspect ratio, density of crystal and crystallographic orientation[1].

In this work, the residual oxygen functional groups decorating the electrochemically-reduced graphene oxide (ErGO) film surface were exploited for higher specific surface area of ZnO nanostructures as they confer graphene materials with versatile richness of electrochemistry which has been evidently proven to be a fertile field for efficient synthesis of graphene-semiconductor oxide composites[2]. The nucleation and growth of ZnO nanostructures at the surface of ErGO films were studied by electrodeposition method from aqueous $Zn(NO_3)_2$ precursor solution.

The measurements showed the nucleation and properties of ZnO nanostructures are influenced by the content of oxygen functional groups and disorder level in ErGO films. The results indicated electrochemical reduction technique as great alternative for providing ErGO films anchored with ZnO nanostructures with controlled morphology, density and nucleation.

Keywords: graphene oxide, electrochemical reduction, ZnO, nucleation, nanoarchitecture

Acknowledgments. Financial support from the Romanian National Authority for Scientific Research and Innovation, CNCS – UEFISCDI (project number PN-II-RU-TE-2014-4-0806) is gratefully acknowledged.

References

[1] GARCIA S.P., SEMANCIK S. 2007. Controlling the Morphology of Zinc Oxide Nanorods Crystallized from Aqueous Solutions: The Effect of Crystal Growth Modifiers on Aspect Ratio, *Chemistry of Materials*, 19, 4016-4022.

[2] PRUNA A., REYES-TOLOSA M.D., PULLINI D., HERNANDEZ-FENOLLOSA M.A., BUSQUETS-MATAIX D. 2015. Seed-free electrodeposition of ZnO bi-pods on electrophoretically-reduced graphene oxide for optoelectronic applications. *Ceramics International*, 41, 2381-2388.

Influence of Applied Voltage on the Physical and Electrical Properties of Anodic Sm_2O_3 Thin Films on Si

Yew Hoong Wong[1*] and Chit Ying Lee[1]

[1]Department of Mechanical Engineering, Faculty of Engineering, University of Malaya 50603

Kuala Lumpur, Malaysia.

**E-Mail : yhwong@um.edu.my / Tel : +603-79677022 ext. 2654 / Fax : +603-79675317*

Formation of samarium oxide (Sm2O3) thin film by anodization of 100 nm thick sputtered samarium (Sm) metal on silicon (Si) substrate was systematically investigated. Sputtered Sm on Si substrate followed by anodization in 1 M NaOH (pH 14) at various applied voltages (10 V to 25 V) were carried out. All anodization processes were performed for 10 min at room temperature in the bath with constant stirring. The surface root-mean-square roughness of the sample increases as the applied voltage increases. The sample anodized at 20 V demonstrated the highest electrical breakdown field of 8.0 MV cm^{-1} at 10^{-6} A cm^{-2}. This is attributed to the lowest effective oxide charge, interface trap density, and total interface trap density. The Fowler-Nordheim tunneling mechanism has been investigated for all samples and the highest value of barrier height extracted between the conduction band edges of oxide and semiconductor was 1.16 eV.

Keywords: Thin film, oxide, anodization, high-k dielectric

Proton conducting biopolymer membrane electrolytes based on kappa carrageenan doped NH_4Br: structural and ionic conductivity study

N. Yaacob, A.S. Samsudin*

Advanced Materials Research Cluster, Faculty of Industrial Sciences & Technology, Universiti Malaysia Pahang, Lebuhraya Tun Razak, 26300 Kuantan, Pahang, Malaysia.

**E Mail/ Contact Détails : ahmadsalihin@ump.edu.my*

Since the introduction of solid polymer based electrolytes by Fenton and co-workers in 1973, numerous polymers are particularly interesting especially bio-polymer have been investigate. The main interest in developing solid-state polymer electrolyte lies in the hope that such systems will avoid many of the problems encountered when using electrochemical devices with liquid constituents. The costly and rare raw materials that are required, along with expensive materials processing, make for steep barriers to overcome when it comes to power source development. The increasing interest in green energy storage materials for electrochemical devices with the development of biopolymer as electrolytes candidate has attracted great attention which can offer a number of high-value opportunities, provided that lower costs can be obtained besides environmental friendly. In arrears to the fact given, the development of biopolymer membrane electrolytes (BMEs) has been accomplished in this work by incorporating various composition (0 - 35 wt. %) of NH_4Br with kappa carrageenan (KC) via solution casting method. The biopolymer–salt complex structural formation and ionic conduction of the BMEs have been analyzed through infrared spectroscopy, X-Ray Diffraction and impedance measurement. The ionic conductivity at room temperature for the pure KC based BMEs system was achieved at 1.92×10^{-8} S cm^{-1} and was improved to optimum value at 3.89×10^{-4} S cm^{-1} when 20 wt. % NH_4Br was added. It is believed that the conducting elements in this work are predominantly due to proton (H^+) of [NH_4^+] substructure in NH_4Br with the coordination interaction taking place at KC structure as proven from FTIR study. In addition, the amorphousness of the BMEs sample increase with increased wt. % of NH_4Br and the results shown that the conductivity of the KCBMEs system was found to be dependent on the protonation (H^+) and changes in amorphouness behavior.

Keywords: protonation (H^+), solid polymer electrolytes, ionic conductivity, Grotthuss mechanism

[1] FENTON, D. E., PARKER, J. M., & WRIGHT, P. V. (1973). Complexes of alkali metal ions with poly (ethylene oxide). Polymer, 14(11), 589.

[2] AZIZ, N. A., IDRIS, N. K. AND ISA, M. I. N. (2010). Proton conducting polymer electrolytes of methylcellulose doped ammonium fluoride: Conductivity and ionic transport studies. International Journal of the Physical Sciences 5(6): 748-752.

[3] MOBARAK, N. N., RAMLI, N., AHMAD, A., & RAHMAN, M. Y. A. (2012). Chemical interaction and conductivity of carboxymethyl κ-carrageenan based green polymer electrolyte. Solid State Ionics, 224, 51-57.

[4] SOHAIMY, M. I. H., & ISA, M. I. N. (2015). Effect of ammonium carbonate salt concentration on structural and ionic conductivity of cellulose based solid polymer electrolytes. Fibers and Polymers, 16(5), 1031-1034.

Ultrafast Switching and Unique Phase Transition in Vanadium Dioxides Thin Films upon Infrared laser Irradiation and Electric Field

Garam Bae, Hyoung Woo Yang, and Dae Joon Kang*

Department of Physics, Sungkyunkwan University, Suwon 440-746, Republic of Korea.

djkang@skku.edu

Vanadium dioxide (VO2) is one of the fascinating switchable materials due to extremely large change of the resistivity exceeding 10^4, and ultrafast phase transition. The metal-insulator transition induced by an external electric filed or optical power can be exploited for potential applications, in particular high-electric-power switching devices. Here we report that electric field driven and optical triggered MIT phenomena in vanadium dioxide thin film. The single phase monoclinic vanadium dioxide (VO2) films were successfully grown on sapphire (001) substrates by RF sputtering. In x-ray diffraction patterns, we observed reflections originating from monoclinic VO2 with a peak at $2\theta = 39.77°$ corresponding to VO2 (020) for films on sapphire (001) substrates. The VO2 films exhibited metal-insulator transition (MIT) at temperature around 337 K with four orders of change in resistivity upon transition. A simple two-terminal device based on VO2 films on sapphire (001) substrates using gold/titanium electrodes with different channel lengths and widths exhibited abrupt breakover voltage rise according to channel length by an applied voltage at room temperature. The I-V characteristics were found to be dependent on channel length and width. The high on-state current density of 0.25 MA/cm^2, on-state current of 100 mA at 2 V, and high break-over voltage of 96 V were obtained, thus implying that higher device performance can be realized with parallel and series array circuits. The high gating speed of < 50 μs are measured in optical triggered MIT behavior by infrared laser. This work presents a great potential for the high electric power electronics employing multi-array devices of VO2

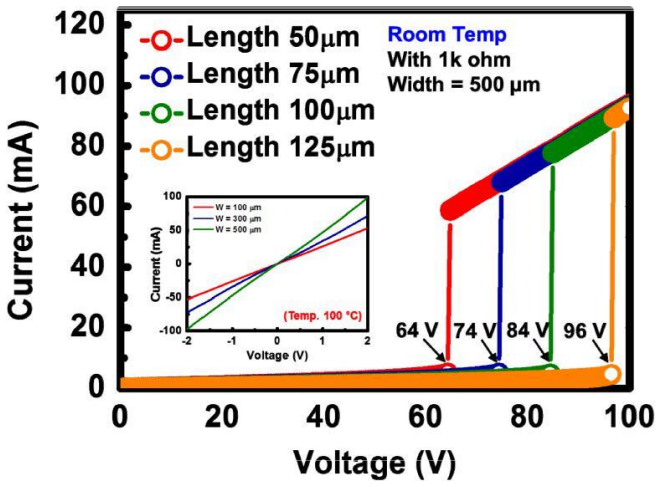

Color appearance of micro-arc oxidized Ti alloys for esthetics in dental implants

Moon-Jin Hwang, Hae-Rim Choi, Young-Hwa Jeong, Ho-Jun Song, Yeong-Joon Park*

Department of Dental Materials and Medical Research Center for Biomineralization Disorders, School of Dentistry, Chonnam National University, Gwangju, Korea

**yjpark@jnu.ac.kr* (corresponding author)

This study aimed to grant bioactivity and esthetic appearance to ash gray colored titanium-based implants. Binary Ti alloys were prepared by arc-melting of titanium and transition metals (Au, Cr, Cu, Mn, Mo, Nb, V and Zr). Ti alloys with 1, 2.5, 5 and 10 wt% alloying elements were micro-arc oxidized in an electrolyte containing Ca and P ions under a constant current using a DC power supply. The crystalline phases and microstructures of the oxide layers were analyzed using X-ray diffractometry and scanning electron microscopy, respectively. Energy dispersive X-ray spectroscopy and X-ray photoelectron spectroscopy were used to analyze the chemical compositions and chemical binding states of the oxide layers. Colors of the oxide layers were expressed in terms of CIE L*a*b* coordinates. UV/Vis/NIR diffuse reflectance spectroscopy was used to analyze the optical properties of the oxide layers. During the micro-arc oxidation (MAO) treatment, the potential vs. time curves were strongly affected by alloying element type and content. The pore size, thickness and crystallinity of oxide layer were increased as the final potential was increased. Colored oxide layers were obtained for the Ti alloys containing 3d (Cr, Cu, Mn and V) and 5d (Au) transition metals. Their colors were dependent to the alloying metal type and content. In the CIE L*a*b* coordinate, the oxide layer of Ti-5Cr alloy exhibited highest average b* value as 19.81 ($p<0.05$). The next was the oxide layer of Ti-2.5Cu, which showed b* value as 16.73. The oxidation state of 3d transition metals contributed to colorization of the micro-arc oxidized Ti alloys. The characteristic colors of MAO-treated Ti alloys were yellow for Cr^{3+}, red for Cu^{+}, yellow for Mn^{4+} and yellow for V^{5+}. The purple color of MAO-treated Ti-Au alloy surfaces was originated from Au nanoparticles. The 4d transition metals (Zr, Nb and Mo) did not affect color revelation of the MAO-treated Ti alloys. From the results of optical absorbance, the band gap energies gradually decreased as the content of 3d transition metals in Ti alloys increased up to 5 wt%. The replacement of Ti in TiO_2 structure by 3d metals creates specific energy level in the band gap of TiO_2, and the reduced band gap energies are responsible for the different color revelation.

Keywords: Binary titanium alloys, Transition metals, Micro-arc oxidation, Oxidation state, Colorization

Acknowledgement

This study was financially supported by Chonnam National University (2015), and by the National Research Foundation of Korea (NRF) grant funded by the Korea government (MSIP) (No. 2011-0030121).

[1] SONG, H. J., KIM, M. K., JUNG, G. C., VANG, M. S. & PARK, Y. J. 2007. The effects of spark anodizing treatment of pure titanium metals and titanium alloys on corrosion characteristics. *Surface and Coatings Technology*, 201, 8738-8745.

[2] ZHU, X., KIM, K. H. & JEONG, Y. 2001. Anodic oxide films containing Ca and P of titanium biomaterials. *Biomaterials* 22, 2199-2206.

Effects of Sputtering Mode on the Microstructure and Ionic Conductivity of Yttria-stabilized Zirconia Films

T.H. Yeh, R.D. Lin, B.R. Chen, J.S. Cherng*

Department of Materials Engineering, Ming Chi University of Technology, Taipei 24301 Taiwan
cherng@mail.mcut.edu.tw

The microstructure and ionic conductivity of reactively sputtered yttria-stabilized zirconia (YSZ) films in various sputtering modes are systematically studied using a closed-loop controlled system with plasma emission monitoring. A transition-mode sputtering corresponding to 45% of target poisoning produces a microstructure with ultrafine crystallites embedded in an amorphous matrix, which undergoes an abnormal grain growth upon annealing at 800°C. At 400°C, its measured ionic conductivity is higher, by about a half order of magnitude, than that of its poisoned-mode counterpart, which is in turn higher than that of the YSZ bulk by about one order of magnitude. The abnormally-grown ultra-large grain size is believed to be responsible for the former comparison due to the suppression of the grain boundary blocking effect, while the latter comparison can be attributed to the interface effect.

Keywords: Sputtering mode, ionic conductivity, zirconia film, grain boundary blocking effect, interface effect

Preparation and luminescence properties of SrAl2O4:Eu^{2+}, Dy^{3+} thin films by pulsed laser deposition

S. W. Kwon, S.H. Kim, Z. J. Zhang, and Woochul Yang*

Department of Physics, Dongguk University, Pildong-ro, Choong-gu, Seoul 04620, Korea * *E-mail address: wyang@dongguk.edu*

$SrAl_2O_4:Eu^{2+}$, Dy^{3+} (SAOED) is a well-known green phosphor with high quantum efficiency, chemical stability and persistent phosphorescence. In addition, it has been found to have a mechano-luminescent property with high intensity to be used for detecting mechanical stress. Thus, it has a high potential to be used in various optical, energy storage, sensing applications. However, most reported research of the SAOED materials has been related to powder type samples. For practical applications, the growth of thin films are preferred due to better thermal stability, less out gassing, and better adhesion to the solid surface. In this study, the SAOED thin films were grown on sapphire (0001) substrates by using pulsed laser deposition (PLD) technique. We investigate the post-annealing, substrates, and thickness on the structural, morphological, and photoluminescence (PL) properties of the films. The as-grown films by PLD have an amorphous structures without any PL emission. However, the films annealed from 950 ^oC to 1100 ^oC under reduction atmosphere using H2/Ar mixture gas (1:2 ratio) showed the single phase crystallity with PL emission. The impurity in the films was reduced and PL intensity increased with annealing temperature. However, the PL emission at 520nm in wavelength was not changed at all annealing temperature. We will discuss the effect of the post-annealing on PL properties in terms of crystallinity of the matrix and charge migration around a luminescent center.

Keywords: $SrAl_2O_4:Eu^{2+}Dy^{3+}$(SEOED), mechano-luminescnce, PL, crystallinity

Synthesis of Transparent $La_4Ti_9O_{24}$ Microspheres via Flame-Spraying Method for High Reflective Film

Xiaoguang Ma[a,b], Xiaoyu Li[a]*, Bingqian Ma[a], Jianqiang Li[a]*

[a] National Engineering Laboratory for Hydrometallurgical Cleaner Production Technology, Key Laboratory of Green Process and Engineering, Institute of Process Engineering, Chinese Academy of Sciences, Beijing 100190, P. R. China

[b] School of Engineering and Technology, China University of Geosciences, Beijing 100083, P. R. China

* Corresponding author. E-mail: jqli@ipe.ac.cn;lixy@ipe.ac.cn.

$La_4Ti_9O_{24}$ (LTO) bulk transparent glasses with high reflective index and good optical property have been fabricated by containerless processing. However, the sizes of glasses are millimeter-scale which limits their applications. Thus, it is urgent to achieve the large scale and controllable synthesis of micrometer-sized LTO spheres. The large-scale transparent $La_4Ti_9O_{24}$ glass microspheres were fabricated by flame-spray method. Their morphologies, structures, components and thermal stabilities were investigated by scanning electron microscope, optical microscope, X-ray powder diffraction apparatus, energy dispersive X-ray diffraction analysis and differential scanning calorimetry measurement. The prepared transparent microspheres are glassy state, and they own high thermal stability and reflective index. We further study the optical application of these glass microspheres with high-reflective-index. The coating of $La_4Ti_9O_{24}$ glass microspheres greatly enhances the reflection of glass slide as substrate, which is very useful for some special surfaces that require illumination by reflection of light rays, such as protective reflective helmet or clothes, and road side signs, etc. In addition, it can be used for heat reflective layer, which saves the urban heat island effect.

Deposition and Characterization of Thin Polymer Films by Initiated Chemical Vapor Deposition

Saibal Mitra and Edgar Kosgey

Department of Physics, Astronomy, and Materials Science, Missouri State University, Springfield, MO 65809. USA.

E Mail/ Contact Détails : saibalmitra@missouristate.edu

Initiated Chemical Vapor Deposition (iCVD), a variation of catalytic CVD, is versatile technique that has been used to deposit thin polymer films. The technique involves the introduction of controlled amounts of monomer and initiator gasses into the reaction chamber and activating them over a hot-filament. Since the filament temperatures are low and the substrates are held at temperatures less the 50 ^{0}C, it is possible to coat polymer films on a variety of substrates that include biological substrates. In addition, conformal coatings of nanostructures have also been achieved. These properties make this deposition technique so attractive.

In this paper, discuss the deposition of polytetrafluoroethylyne (PTFE) films on a variety of substrates. We have used hexafluoropropelyne oxide (HFPO) and perfluorooctane sulfonyl fluoride (PFOS) as the monomer and initiator, respectively. The mixture was heated over an array of heated filaments. Thin PTFE films were deposited on a variety of substrates that included silicon and glass. Once deposited the films were analyzed using IR and electron microscopy. Presence of PTFE films were confirmed from the IR peaks at 1211 cm^{-1} and 1155 cm^{-1}.

Using Monte Carlo simulation we have also modelled the growth of thin films in an iCVD reactor on flat surfaces. The model simulated the growth process where an excited initiator molecule would bind with a monomer molecule on the surface of the substrate. This block would remain stable till the initiator would enable the addition of the next monomer molecule. The initiator would be released in the gas phase where it could bind again with another monomer or polymer molecule leading to a two-dimensional thin film growth. The growth process was simulated for various ratios of the monomer and the initiator and the results will be discussed in detail.

Keywords: polymer films, chemical vapor deposition, MC simulation

Fabrication of Functionally Graded Ti-Gear by Direct Laser Melting Under Variable Shielding Gases

Taewoo. Hwang[1], Sangwook Han[1], Younghoon Moon[1]

[1]A School of Mechanical Engineering, Pusan National University, Busan 609-735, Korea

Corresponding Author: Young Hoon Moon

yhmoon@pusan.ac.kr, +8251-510-2472, FAX : +8251-512-1722

Functionally graded properties are characterized by the variation in composition and structure gradually over volume, resulting in corresponding changes in the properties of the material. Direct laser melting (DLM) process is a kind of prototyping process whereby a 3-D part is built layer-wise by melting the metal powder with laser scanning. DLM can directly build full-density and high-performance complex metal parts from CAD solid model without using any molds and tools. In this study, gear having functionally graded hardness is fabricated by laser melting of titanium powders under variable shielding gases. As the formation of titanium nitride in the laser melted layer has strong potential to increase the hardness of titanium alloy, the hardness of fabricated part has been controlled by changing the flow rates of nitrogen shielding gas. Proposed processing method is attractive because of its flexibility and the possibility of producing functionally graded layers having variable hardness in regions where a minimal effect on the bulk of the part is required. As the local hardness distribution of laser melted titanium part is highly variable, the effect of process parameters was characterized over a wide range of processing variables. From the analysis, functionally graded hardness has been successfully obtained and the proposed method is shown to be feasible with a high degree of reliability.

Keywords: Functionally graded materials, Direct laser melting (DLM), Titanium powder, Nitrogen, Shielding gas

[1] VRANCKEN, B., THIJS, L., KRUTH, J, P., HUMBEECK, J, V. 2012. Heat treatment of Ti6Al4V produced by selective laser melting: Microstructure and mechanical properties. *Alloys and Compounds*, 541, 177-185.

[2] SHISHKOVSKY, I., MISSEMER, F., SMUROV, I. 2012. Direct metal deposition of functional graded structures in Ti-Al system. *Physics Procedia*, 39, 382-391.

[3] MULLER, P., MOGNOL, P., HASCOE, J, Y. 2013. Modeling and control of a direct laser powder deposition process for functionally graded materials (FGM) parts manufacturing. *Materials Processing Technology*, 213, 685-692.

[4] FERRAR, B., MULLEN, L., JONES, E., STAMP, R., SUTCLIFFE, C, J. 2012. Gas flow effects on selective laser melting (SLM) manufacturing performance. *Materials Processing Technology*, 212, 355-364.

[5] VILARO, T., COLIN, C., BARTOUT, J, D., NAZE, L., SENNOUR, M. 2012. Microstructural and mechanical approaches of the selective laser melting process applied to a nickel-base superalloy. *Materials Science and Engineering A*, 534, 446-451.

Growth of small organic molecules on various graphene substrates

C. Teichert[1] , B. Kaufmann[1], J. Genser[1], M. Kratzer[1], J. M. J. Lopes[2], H. Riechert[2], A. Matković[1,3], R. Gajić[3]

[1]*Institute of Physics, Montanuniversitaet Leoben, Franz Josef Str. 18, 8700 Leoben, Austria*
[2]*Paul-Drude-Institut für Festkörperelektronik, Hausvogteiplatz 5-7, 10117 Berlin, Germany*
[3]*Institute of Physics, University of Belgrade, Pregrevica 118, 11080 Belgrade, Serbia*

teichert@unileoben.ac.at

Crystalline films of small semiconducting organic molecules offer attractive potential for organic solar cells and organic light emitting diodes on flexible substrates. However, these applications require a transparent and flexible electrode material; and here the novel two-dimensional (2D) material graphene (Gr) comes into play. Since small conjugated molecules like the rod-like molecule para-hexaphenyl (6P) fit well to the hexagonal structure of graphene, growth of 6P on Gr can be expected in a lying configuration [1,2]. For the applications mentioned above, it is essential to understand organic thin film growth on differently prepared graphene substrates.

On exfoliated, wrinkle-free graphene, we observed by atomic-force microscopy (AFM) the formation of 6P needles (composed of lying molecules) following discrete orientations defined by the Gr lattice [3]. Interestingly, for few-layer exfoliated Gr the needle length decreased significantly with increasing layer number [4].

For chemical vapor deposited Gr which is transferred by polymethylmethacrylate (PMMA) to the support, the 6P needles nucleate preferentially at Gr wrinkles, and the 6P needle growth can be used to sense the cleanliness of the substrate [5]. If 6P is deposited on stepped Gr which has been prepared by Si depletion of SiC(0001) [6], AFM reveals parallel 6P needles nucleating at wrinkles which themselves mainly form at the step edges of the Gr substrate.

[1] G. Hlawacek, F. S. Khokhar, R. van Gastel, B. Poelsema, C. Teichert, Nano Lett. **11**, 333 (2011).

[2] F. S. Khokhar, G. Hlawacek, R. van Gastel, H.J.W. Zandvliet, C. Teichert, B. Poelsema, Surf. Sci. **606**, 475 (2012).
[3] M. Kratzer, S. Klima, C. Teichert, B. Vasić, A. Matković, U. Ravelić, R. Gajić, JVSTB **31**, 04D114 (2013).
[4] M. Kratzer, S. Klima, C. Teichert, B. Vasić, A. Matković, M. Milicević, R. Gajić, e-J. Surf. Sci. Nanotechn. **12**, 015303 (2014).

[5] M. Kratzer, B.C. Bayer, P. R. Kidambi, A. Matković, R. Gajić, A. Cabrero-Vilatela, R. S. Weatherup, S. Hofmann, C. Teichert, Appl. Phys. Lett. **106**, 103101 (2015).

[6] M. H. Oliveira, Jr., T. Schumann, M. Ramsteiner, J. M. J. Lopes, H. Riechert, Appl. Phys. Lett. **99**, 111901 (2011).

Highly Conductive DMSO-Doped PEDOT:PSS Transparent Electrodes at THz Frequency Range

Although indium tin oxide is widely used in electrical devices requiring a transparent electrode, this cannot provide the flexibility and THz-frequency transparency required in many emerging applications. To address this, we used spin coating to produce DMSO-doped PEDOT:PSS electrodes on silicon substrates, which were found to be capable of providing both a high transparency (83.5% transmittance) and high electrical conductivity (5078 S/cm) at 1.22 THz when a single 52 nm layer was used. The transmittance of this electrodes at THz frequencies, as well as its surface morphology and electrical conductivity are subsequently investigated in relation to the thickness of the DMSO-doped PEDOT:PSS films.

Tuning the Ambipolar Charge Transport Properties of N-heteropentacenes for Organic Logic Circuits

Hao-Li Zhang
State Key Laboratory of Applied Organic Chemistry (SKLAOC), College of Chemistry and Chemical Engineering, Lanzhou University, China, 730000

Haoli.zhang@lzu.edu.cn

Ambipolar organic semiconductors, who allow both electron and hole to transport within their OFET devices, have attracted much attention in recent years. Ambipolar materials are potentially useful in constructing COMS-like circuits and organic light-emitting transistors. However, among the reported ambipolar organic semiconductors, few of them showed high and balanced hole and electron mobilities.

We have systematically explored the strategy of design high performance ambipolar organic semiconductors based on azapentacene and oligothiophene frameworks. This presentation will discuss the synthesis and devices applications of these ambipolar organic semiconductors. Individual transistors from substituted azapentacene showed high and balanced performance, with good hole and electron mobilities. In addition, we also studied the effects of side substituent on the properties of the ambipolar materials. By tuning the packing motif of the conjugated cores, unipolar organic semiconductors may be converted into ambipolar materials. Theoretical investigations reveal that the drastic difference in the transport properties of the three materials is due to the difference in their molecular packing and film microstructures. Integrated complementary inverters fabricated using ambipolar materials showed sharp inversions with high gains (>180) and negligible hysteresis.

Keywords: Organic semiconductor, ambipolar, transistor, mobility, circuit

[1] Liu, K.; Song, C. L.; Zhou, Y. C.; Zhou, X. Y.; Pan, X. J.; Cao, L. Y.; Zhang, C.; Liu, Y.; Gong, X.; Zhang, H.-L. J. Mater. Chem. C, 2015,3, 4188-4196

[2] K. Zhou, H. L. Dong, H.-L. Zhang, W. P. Hu, Phys. Chem. Chem. Phys., 2014, 16, 22448 – 22457 (Review)

[3] H. Xu, Y.-C. Zhou, X.-Y. Zhou, K. Liu, L.-Y. Cao, Y. Ai, Z.-P. Fan, H.-L. Zhang, Adv. Funct. Mater. 2014, 24, 2907–2915
[4] Zeng, W. J.; Zhou, X. Y.; Pan X. J.; Song, C. L.; Zhang, H. L., AIP Adv. 2013, 3, 012101
[5] Xu, Z. Z.; Liao, Q.; Shi, Q.; Zhang, H. L.; Yao, J. N.; Fu. H. B.; Adv. Mater. 2012, 24, OP216–OP220
[6] Song, C.-L.; Ma, C.-B.; Yang, F.; Zeng, W.-J.; Zhang, H.-L.; Gong, X., Org. Lett., 2011, 13, 2880-2883
[7] Liu, Y.-Y.; Song, C.-L.; Zeng, W.-J.; Zhou, K.-G.; Shi, Z.-F.; Ma, C.-B.; Yang, F.; Zhang, H.-L.; Gong, X., J. Am. Chem. Soc., 2010, 132, 16349-16351

Magnetic Field-Assisted Alignment of 6,13-Bis(triisopropylsilylethynyl) pentacene Molecules Using Magnetic Nanoparticles

Jin-Hyuk Kwon and Jin-Hyuk Bae

School of Electronics Engineering, Kyungpook National University, Daegu 41566, Korea.

jhbae@ee.knu.ac.kr

Organic electronic materials have attracted considerable attention in nowadays due to the potential for their use as promising semiconductors, insulators and conductors in next-generation electronics. In particular, molecular alignment in organic materials has been studied extensively from various aspects, because the electrical properties of the materials are intimately associated with molecular alignment [1]. Furthermore, the molecular alignment is a critical factor that tremendously influences the electrical performances and characteristics of various electronic devices consisting of organic thin films, such as organic thin-film transistors, organic light-emitting diodes, and organic photovoltaic cells [2]. From this point of view, molecular alignment and physical understanding of its mechanism are one of the most significant assignments for further advancements of organic functional materials. Herein, we suggest a unique and novel method to induce the molecular alignment of 6,13-bis(triisopropylsilylethynyl)pentacene (TIPS-pentacene), which is a solution-processed small-molecule semiconductor. For formation of TIPS-pentacene thin films, a drop-casting method is used with a subsequent thermal treatment for solvent evaporation. In order to induce molecular alignment, magnetic nanoparticles are used and magnetic field is applied to the drop-cast solution during the solvent evaporation process. As a result, thin films of TIPS-pentacene are obtained showing ordered needle-like crystals.

Keywords: Molecular alignment, magnetic field, magnetic nanoparticles, small-molecule semiconductor

[1] KEUM, C.-M., KWON, J.-H., LEE, S.-D. & BAE, J.-H. 2013. Control of the Molecular Order and Cracks of the 6,13-bis(triisopropylsilylethynyl)-pentacene on a Polymeric Insulator by Anisotropic Solvent Drying. *Solid-State Electronics*, 89, 189-193.

[2] ZHENZHONG, S., KAI, X., JONG, K. K., XIANG, Y., KUNLUN, H., JIM, B., ILIA, N. I., JIHUA, C., JOSE, A., DAWEN, L., BOBBY, G. S., EDWARD, A. P., CHRISTOPHER, M. R. & DAVID, B. G. 2011. PS-*b*-P3HT Copolymers as P3HT/PCBM Interfacial Compatibilizers for High Efficiency Photovoltaics. *Advanced Materials*, 23, 5529-5535.

Systematic Investigation of Regiosymmetric Fluoride Atoms on Electron Accepting Unit in Organic Small Molecules for Organic Photovoltaics

Daehee Han[1], Jihoon Lee [2], Mingyu Jeong[1]

, Sung Heum Park[2,*], Changduk Yang[1,*]

[1]Department of Energy Engineering, School of Energy and Chemical Engineering, Ulsan National Institute of Science and Technology(UNIST), Ulsan 689-798, South Korea.

[2]Department of physics, Pukyong National University, Busan 48513, Republic of Korea

daeheehan@unist.ac.kr/ +82 1074202709

** Correspondence to : spark@pknu.ac.kr; yang@unist.ac.kr*

Great advances for high-performance organic photovoltaics (OPVs) are essentially fueled by the molecular engineering of the conjugated backbones as well as the improved experimental techniques for the device fabrication. Notwithstanding the extensive investigations of the conjugated building cores, a fine-tuned regiosymmetric effect on the backbone framework has rarely been investigated (Welch et al., 2013). To address this issue, we have designed and prepared dithienogermole (DTGe)- and dithinosillole (DTSi)-based small molecules, DTGe(BTFTh$_2$), DTGe(BTFBFu)$_2$, DTSi(BTFTh$_2$)$_2$ and DTSi(BTFBFu)$_2$, respectively, wherein the 'fluorine' substitutes are introduced at different positions in the backbone. Through systematic investigation on OPVs, we are able to correlate the different OPV performances in structure–function relationships with the regiosymmetric 'fluorine' positions.

Keywords: Small molecule, regiosymmetric , fluoride atoms, organo photovoltaics.

WELCH, G. C., BAKUS, R. C., TEAT, S. J. & BAZAN, G. C. 2013. Impact of Regiochemistry and Isoelectronic Bridgehead Substitution on the Molecular Shape and Bulk Organization of Narrow Bandgap Chromophores. *Journal of the American Chemical Society*, 135**,** 2298-2305

Thionation Effect on Air-Stability and Electron Mobility of N-Type Organic Field-Effect Transistors

Te- Fang Yang*[1], Sheng-Han Huang[1], Ming-Yu Kuo*[1]

[1] Department of Applied Chemistry, National Chi Nan University, No. 1 University Rd.,

54561 Puli, Nantou, Taiwan.

E-mail: mykuo@ncnu.edu.tw; Fax: +886 49 2917956

The electronic properties of materials targeted for N-type organic field-effect transistors (OFETs), such as pyromellitic diimides (PyDIs), degrade under ambient conditions because of low susceptibility of radical anions. To improve the electronic properties of PyDIs, two pyromellitic dithioimide derivatives (PyDTI-C8 and PyDTI-F) were synthesized by thionated PyDIs with Lawesson's reagent. Thin films of the parent (PyDIs) and derivative compounds (PyDTIs) were then deposited onto Si/SiO_2 substrates as prototype OFETs. Relative to the original diimides, thionation and fluorination increased the electron mobility and on/off ratio by two orders of magnitude and improved the threshold voltage and air-stability. Under ambient conditions, PyDTI-F exhibited an electron mobility as high as 0.62 $cm^2V^{-1}s^{-1}$ along with an on/off ratio of 5.5×10^5 and a low threshold voltage (V_{th} = 16.1 V)

Keywords: Organic field-effect transistor, Thionation, Air-stability, Electron transport.

[1] IE, Y., JINNAI, S., NITANIA, M. & ASO, Y. 2013. Arenedithiocarboxyimide-containing extended □-conjugated systems with high electron affinity. *J. Mater. Chem. C, 1*, 5373-5380.

[2] TILLEY, A. J., GUO, C., MILTENBURG, M. B., SCHON, T. B., YAN, H., LI, Y. & SEFEROS, D. S. 2015. Thionation Enhances the Electron Mobility of Perylene Diimide for High Performance n-Channel Organic Field Effect Transistors. *Adv. Funct. Mater., 25*, 3321-3329.

One-step Microwave-assisted Synthesis of Indium Tin Oxide Nanocrystals with Tunable Surface Plasmon Resonance Frequencies for Plasmonic Electrochromic Window in the Near-IR Region

Xiaodong Li*, Wee Ling Koh, Yanru Lu, Xi Jiang Yin

Advanced Materials Technology Centre, Singapore Polytechnic, 500 Dover Road,

Singapore 139651, Singapore

**li_xiaodong@sp.edu.sg*

Indium Tin Oxide (ITO) Nanocrystals have been successfully synthesized without hot-injection by one-step microwave method with friendly environment. The size and optical properties can be tuned by changing the reaction time, growth temperature, microwave power, and the In/Sn molar ratio. The as-prepared ITO nanocrystals exhibit clear localized surface plasmon resonance (LSPR) properties. ITO nanocrystal thin film was spin-coated on conductive glass and equipped with a counter electrode, a near-infrared selective plasmonic electrochromic window with enhanced NIR optical contrast was obtained. The switching kinetics and cycling durability for ITO thin films were investigated. Compared with the traditional hot-injection approach, ITO nanocrystals synthesized by microwave heating are more efficient and the shortening of the reaction time leads to a high reaction yield. The use of microwave allows for a highly reproducible and effective synthesis protocol that is fully adaptable for mass production and can be easily employed to synthesize a variety of metal oxide nanocrystals.

Keywords: Microwave, surface plasmon, nanocrystal, indium tin oxide, plasmonic electrochromic window

Development of a high temperature oxidation resistance layer on a Ni-base alloy by Al electrodeposition

Andrieanto Nurrochman[1], Ho Jung Lee[1], Sunghoon Hong[1], Sung Hwan Kim[1], Changheui Jang[1]

[1]Korea Advanced Institute of Science and Technology, 34141, Daejeon, Republic of Korea.

Corresponding: chjang@kaist.ac.kr/ Tel.: +82 42 350 3824; fax: +82 42 350 3810

The formation of alumina (Al2O3) layer on the surface is the key to the protection against corrosive environments, especially at high temperature. In this study, an electrodeposition technique [1] was utilized to form a thin Al layer on a Ni-base alloy for the potential applications in high temperature reactors operating in various environments. Ionic liquid of AlCl3/1-ethyl-3-methylimidazolium chloride [EMIm]Cl was utilized for Al electrodeposition at high overpotential to obtain nanoscale grain size of Al layer. After Al electrodeposition, inter-diffusion heat treatment [2] was applied to form the Al-rich layer. Then the specimens were exposed to S-CO2 environment at 550~700 °C and impure He environment at 900 °C up to 1,000 h. Then, the oxide layer was characterized using SEM and TEM. Finally, the performance of the electrodeposition based coating was discussed in terms of corrosion resistance, which was compared with that of other coating methods.

Keywords: Electrodeposition, Aluminum, Corrosion, Surface modification

[1] ASHRAF BAKKAR, VOLKMAR NEUBERT. 2013. Electrodeposition and corrosion characterisation of micro- and nano-crystalline aluminium from AlCl3/1-ethyl-3-methylimidazolium chloride ionic liquid. *Electrochimica Acta,* 103, 211-218.

[2] DONGHOON KIM, INJIN SAH, HO JUNG LEE, SUNGHOON HONG, CHANGHEUI JANG. 2014. Development of an aluminide coating layer on Alloy 617 by Al sputtering and inter-diffusion heat treatments," *Surface and Coating Technology.* 244, 15-22.

Film Formation in Hibiscus Sabdariffa Leaf Extract on Steel to Protect against Corrosion in Hydrochloric Acid Solution

P. V. Hien[1], N. S. H. Vu[2], T. V. Man[2], V. T. H. Thu[2], M. D. Tri[3], N. D. Nam[4]

[1]Department of Chemical Engineering, Ho Chi Minh City University of Technology, 268 Ly Thuong Kiet Street, District 10, Ho Chi Minh City, Vietnam

[2]Faculty of Physics and Engineering Physics, University of Science, 227 Nguyen Van Cu Street, District 5, Ho Chi Minh City, Vietnam

[3]Institute of Chemical Technology, Vietnam Academy of Science and Technology, 01 Mac Dinh Chi Street, District 1, Ho Chi Minh City, Vietnam

[4]Petroleum Department, PetroVietnam University, 762 Cach Mang Thang Tam Street, Long Toan Ward, Ba Ria City, Ba Ria - Vung Tau Province, Vietnam

*Email/Contact Details (*phamvanhien240991@gmail.com and namnd@pvu.edu.vn)

The inhibitive action of ethanol extract of Hibiscus sabdariffa leaves (HSL) on corrosion properties of steel in 0.1 M HCl solution has been investigated using electrochemical techniques including weight loss, potentiodynamic polarization, linear polarization resistance, electrochemical impedance spectroscopy measurements, and surface analysis including attenuated total reflectance Fourier transform infrared spectroscopy, contact angle, X-ray photoelectron spectroscopy, X-ray diffraction, raman and scanning electron microscopic observations. The adsorption of HSL on steel surface follows a film formation mechanism. Electrochemical techniques and surface analysis reveal that the HSL acts as a mixed-type inhibitor. Corrosion resistance of steel was increased with increase of HSL concentration, sugesting an increase of inhibition efficiency. The results of electrochemical techniques and surface analysis were in good agreement.

Keywords: Steel, surface and interface, electrochemistry, green materials

[1] Nam, N.D., Bui, Q.V., Mathesh, M., Tan, M., Forsyth, M. 2013. A study of 4-carboxyphenylboronic acid as a corrosion inhibitor for steel in carbon dioxide containing environments. Corros. Sci. 76, 257-266.

Inhibitor- and Polymer-Containing Protective Coatings on the Magnesium Alloys for Applications in Severe Environments

A.S. Gnedenkov[1], S.L. Sinebryukhov[1], D.V. Mashtalyar[1,2], S.V. Gnedenkov[1]

[1]Institute of Chemistry, Far Eastern Branch, Russian Academy of Sciences, 159, Prosp. 100-letya Vladivostoka, Vladivostok, 690022, Russia

Presenting and corresponding author *(E Mail:* asg17@mail.com /A.S. Gnedenkov)

The results of the corrosion protection of the magnesium alloys on the base of plasma electrolytic oxidation method (PEO) are presented. Corrosion of magnesium alloys with different protective layers are described in details. Protective properties of the composite coatings on the surface of the magnesium alloys in the chloride-containing media were investigated by several independent methods. In order to obtain self-healing coating on the PEO-pretreated Mg alloy surface, the corrosion inhibitor was incorporated into the porous part of the PEO-coatings. Electrochemical parameters of the porous and poreless layers on the surface of the samples have been calculated before and after polarization due to experimental impedance data modeling by means of the equivalent electrical circuits. The results show a significant improvement of the electrochemical properties and corrosion rate values decreasing of the magnesium alloy after inhibitor treatment of the surface (RP = 420 kΩ cm^2; IC = 86 nA/cm ^{2}; $|Z|$f = 0.1 Hz = 170 kΩ cm^2) in comparison with base PEO-coating (RP = 60 kΩ cm^2; IC = 810 nA/cm^2; $|Z|$f = 0.1 Hz = 30 kΩ cm^2) in the corrosion-active media [1]. The influence of the 8-Hydroxyquinoline (8-HQ) on the corrosion rate of PEO-pretreated Mg alloy surface was estimated by modern electrochemical methods (Scanning Vibrating Electrode Technique (SVET) and Scanning Ion-Selective Electrode Technique (SIET)) in combination with volumetry. Special treatment of the PEO-coated magnesium alloys by 8-HQ enables one to increase the inhibitive properties in 30 fold in the corrosion conditions and avert the intensive destruction of the material. Due to the self-healing coating the current density values were decreased by more than 3 orders of magnitude in comparison with bare alloy. The mechanism of the self-healing process has been established by SIET method. Inhibitive effect is based on the activation of the corrosion inhibitor after mechanical damage of the composite coating. It has been ascertained that the inhibitor-containing coating exhibits the enhanced protective properties against influence of the corrosion active chloride-containing media [2]. For severe environments the polymer-containing composite coating can be suggested as well. Such coatings possess the best antifrictional properties that decrease the possibility of the corrosion and mechanical damage during the operation process and therefore increase its reliability [3].

Keywords: Magnesium alloys; composite coatings; corrosion; plasma electrolytic oxidation

[1] GNEDENKOV, A. S., SINEBRYUKHOV, S. L., MASHTALYAR, D. V. & GNEDENKOV, S. V. 2016. Protective properties of inhibitor-containing composite coatings on a Mg alloy. *Corrosion Science*, 102, 348-354.

[2] GNEDENKOV, A. S., SINEBRYUKHOV, S. L., MASHTALYAR, D. V. & GNEDENKOV, S. V. 2016. Localized corrosion of the Mg alloys with inhibitor-containing coatings: SVET and SIET studies. *Corrosion Science*, 102, 269-278.

[3] GNEDENKOV, S. V., SINEBRYUKHOV, S. L., MASHTALYAR, D. V., EGORKIN, V. S., SIDOROVA, M. V. & GNEDENKOV, A. S. 2014. Composite Polymer-Containing Protective Coatings on Magnesium Alloy MA8. *Corrosion Science*, 85, 52-59.

Protective Composite Coatings on Aluminium and Magnesium Alloys for Marine Environment

S.V. Gnedenkov[1], S.L. Sinebryukhov[1], D.V. Mashtalyar[1,2], V.S. Egorkin[1], K.V. Nadaraia[1,2]

[1]Institute of Chemistry, Far Eastern Branch, Russian Academy of Sciences, 159, Prosp. 100-letya Vladivostoka, Vladivostok, 690022, Russia

[2]Far Eastern Federal University, Vladivostok, Primorsky region, Russia

Presenting and corresponding author *(E Mail:* svg21@hotmail.com/S.V. Gnedenkov)

New methods for the formation of the protective composite layers by plasma electrolytic oxidation (PEO) and subsequent treatment with fluoropolymer materials have been developed. The protective multifunctional composite coatings having practically important properties (anticorrosive, antifriction, hydrophobic, superhydrophobic etc.) for severe environment (for marine technique, e.g.) were obtained on the aluminium and magnesium alloys using PEO and fluoropolymer materials (superdispersed polytetrafluoroethylene powder, tetrafluoroethylene telomeric dispersions) and compounds on the base of hydrophobic agent as well. The embedding of nanosized polymer compounds into the coatings compositions allows increasing their stability in corrosion-active media [1]. The obtained polymer-containing coatings decrease the corrosion current density and wear by 6 and 4 orders of magnitude, respectively, as compared to unprotected alloys. Furthermore, the composite coating is characterized by practically important antifriction properties caused by low friction coefficient. Values of the contact angle attain to 171°.The formation methods of hydrophobic (HP) and superhydrophobic (SHP) nanocomposite coatings on the surface of alloys pretreated using PEO were developed also [2]. The layers, formed by the deposition of the hydrophobic agent from its solution in decane onto PEO-coatings, are characterized by high stability and corrosion protection. The impedance modulus value of the coating, pretreated with ethanol, is the maximum among investigated layers and equals to $|Z|_{f= 0,01}$ Hz = $3.4 \cdot 10^{10}$ □·cm^2. The sample with the HP-coating on the PEO-layer treated with ethanol is characterized by the wetting angles (157.7 ± 3.9)º and the rolling angles (22.5 ± 6.4)º. The HP-coating on the PEO-layer treated with ozone plasma showed wetting angles (160.1 ± 6.9)º and rolling angles (17.5 ± 8.8)º.

Keywords: Protective composite coatings; alloys; nanomaterials; plasma electrolytic oxidation

[1] GNEDENKOV, S. V., SINEBRYUKHOV, S. L., MASHTALYAR, D. V., EGORKIN, V. S., SIDOROVA, M. V., GNEDENKOV, A. S. 2014. Composite Polymer-Containing Protective Coatings on Magnesium Alloy MA8. *Corr Sci*, 85, 52–59.

[2] GNEDENKOV, S. V., SINEBRYUKHOV, S. L., EGORKIN, V. S., MASHTALYAR, D. V., EMELYANENKO A. M., BOINOVICH L. B. 2014. Electrochemical Properties of the Superhydrophobic Coatings on Metals and Alloys. Journal of the Taiwan Institute of Chemical Engineers, 45, 6, 3075-3080.

Smart dual thermal insulators and oxidation resistant coatings from aluminum microspheres

F. Pedraza[1], G. Boissonnet[1], B. Grégoire[1], M. Brossard[1], G. Bonnet[1]

[1] LaSIE. Université de La Rochelle UMR-7356-CNRS. Pôle Sciences et Technologie. Avenue Michel Crépeau. 17042 La Rochelle cedex 1. FRANCE

fpedraza@univ-lr.fr

In contrast to most of the works, the synthesis of dual thermal insulators and oxidation resistant coatings in a single step process for severe environments will be described in this work. They are based on slurry compositions containing Al and or Al/Cr microspheres. The shell of the microspheres oxidizes while the metal core simultaneously gets emptied and reacts with the metal substrate to form the aluminide layer [1]. The air contained in the hollow microspheres formed by oxidation of the shells acts a very performing thermal insulator.

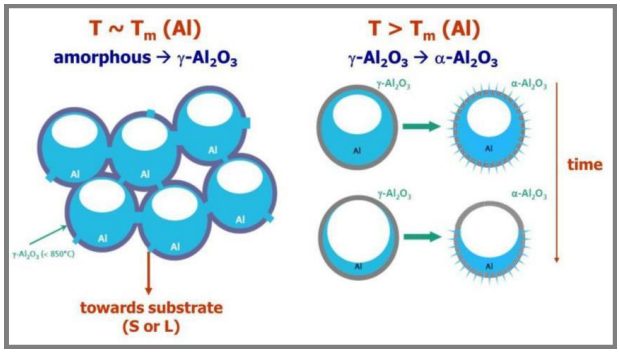

Figure 1: Mechanisms of formation of the hollow spheres.

The performance of these smart and relatively thin dual coatings is studied in terms of thermal conductivity and compared to conventional air plasma sprayed (APS) thick (200 and 400 µm) yttria-stabilized zirconia (YSZ) thick coatings (Figure 2a) and in terms of cyclic (Figure 2b) and isothermal oxidation in air at 1100°C and in water vapour. In agreement with the works from the literature, the thermal conductivity of the alumina-based coatings decreases with increasing temperature. However the differences in overall thermal conductivity values are ascribed to air trapped in the hollow spheres compared to bulk alumina [2]. Protection against oxidation will be demonstrated to be ensured by a thin alumina oxide grown between the thermal insulator and the aluminized coating [3].

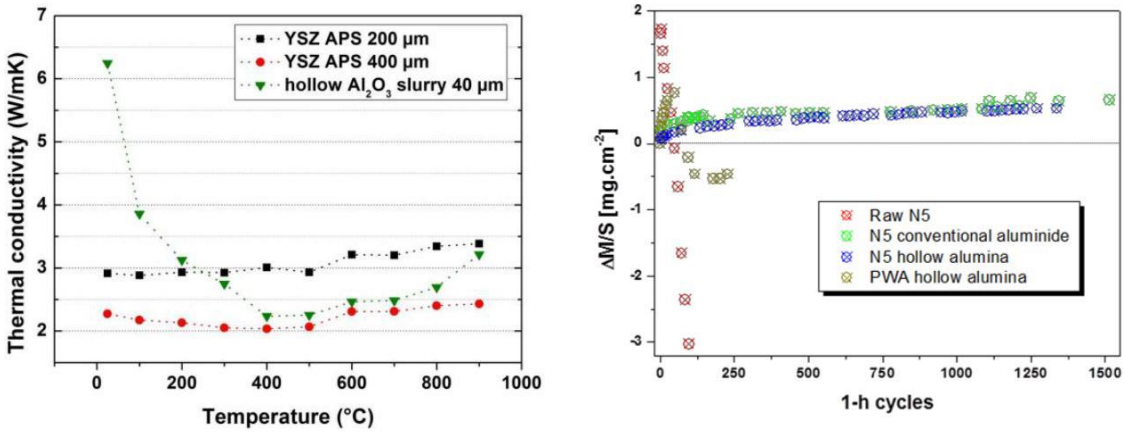

(a) **(b)**

Figure 2.- Thermal conductivity values of the thin hollow alumina slurry with thick YSZ coatings till 900°C and cyclic oxidation resistance in air at 1100°C of uncoated, conventionally aluminized and with slurry coatings containing hollow alumina.

Keywords: Thermal insulator, oxidation resistance, severe environments, alumina, slurry

[1] PEDRAZA, F., MOLLARD, M., RANNOU, R., BALMAIN, J., BOUCHAUD, B., BONNET, G., 2012. Potential thermal barrier coating systems from Al microparticles. Mechanisms of coating formation on pure nickel. *Mater. Chem. Phys. 134, 700-705*.

[2] LIN, C-Y., TUAN, W-H, 2016. Direct Bonding of Aluminum to Alumina for Thermal Dissipation Purposes. *Int. J. Appl. Ceram. Technol., 13 170–176*.

[3] PEDRAZA, F., MOLLARD, M., RANNOU, R., BOUCHAUD, B., BALMAIN, J., BONNET, G., 2016. Oxidation Resistance of Thermal Barrier Coatings Based on Hollow Alumina Particles, Oxid. Met. in press. DOI: 10.1007/s11085-015-9570-3

Protection of Steel Surface in Bio-Ethanol Blended Gasoline Fuel by Film Formation using 4-carboxyphenylboronic Acid Additive

N. S. H. Vu[1], P. V. Hien[2], V. T. H. Thu[1], N. D. Nam[3]

[1]Faculty of Physics and Engineering Physics, University of Science, 227 Nguyen Van Cu Street, District 5, Ho Chi Minh City, Vietnam

[2]Department of Chemical Engineering, Ho Chi Minh City University of Technology, 268 Ly Thuong Kiet Street, District 10, Ho Chi Minh City, Vietnam

[3]Petroleum Department, PetroVietnam University, 762 Cach Mang Thang Tam Street, Long Toan Ward, Ba Ria City, Ba Ria - Vung Tau Province, Vietnam

*Email/Contact Details (*ngsh.vu@gmail.com, phamvanhien240991@gmail.com and namnd@pvu.edu.vn)

Automotive fuel has met the challenges due to reducing the consumption of fossil fuel and improving the efficiency and performance. Bio-ethanol seem to be a promising candidate for alternative energy in automotive applications. Unfortunately, there is controversy regarding the application of bio-ethanol to automotive fuel due to the major concerns regarding the corrosion problems that might occur in metal components of fuel and engine system, particularly steel, magnesium, and aluminum alloys. This study has examined the film formation to protect corrosion of steel in bio-ethanol blended gasoline fuel by 4-carboxyphenylboronic acid using electrochemical techniques and surface analysis. Surface analysis indicated that a thin film has formed on the steel surface due to the adsorption of 4-carboxyphenylboronic acid. In addition, electrochemical results has revealed that the addition of 4-carboxyphenylboronic acid led to the formation of a continuous protective film, which slows down the anodic reactions of steel in bio-ethanol blended gasoline fuel environment.

Keywords: Bio-gasoline, steel, surface and interface, electrochemistry, film formation

[1] Nam, N.D., Bui, Q.V., Mathesh, M., Tan, M., Forsyth, M. 2013. A study of 4-carboxyphenylboronic acid as a corrosion inhibitor for steel in carbon dioxide containing environments. Corros. Sci. 76, 257-266.

Suppression of superconducting transition temperature in bi- and trilayers of NbN and FeN thin films

Tae-Jong Hwang[1], Dong-Ho Kim[1]

[1]Yeungnam University, Gyeongsan, KOREA

E Mail /dhkim@ynu.ac.kr

When a superconducting layer is in contact with a ferromagnetic layer, the superconducting transition temperature (*T*c) would be significantly reduced due to the proximity effect since the superconducting order parameter, which is composed of a single spin configuration of the Cooper pairs in the superconducting layer, is influenced by the electron spin states in the ferromagnetic layer where parallel spin alignment is preferred. In this work, we present a systematic study of *T*c suppression of NbN thin films in NbN/FeN bilayer and FeN/NbN/FeN trilayer structures. Both superconducting NbN and ferromagnetic FeN thin films were prepared on Si substrates by reactive magnetron sputtering. The thickness of FeN films was fixed at 20 nm, while the thickness of NbN films was varied from 3 nm to 100 nm. Suppression of *T*c was larger for thinner NbN films and continued up to NbN thickness of ~34 nm in NbN/FeN bilayers. For FeN/NbN/FeN trilayers, suppression of *T*c was observed up to NbN thickness of ~70 nm, about twice the bilayer case, as expected. This result can be used to design a spin switch whose operation is based on the proximity effect between superconducting and ferromagnetic layers.

Keywords: Proximity effect, NbN /FeN bilayers, FeN/NbN /FeN trilayer,

A SPICE modeling of a-IGZO TFT accompanied by variation of bending strain

Sola Woo, Sinsu Kyoung, Hyungon Oh, Kyoungah Cho, Sangsig Kim*, and Man Young Sung*

Department of Electrical Engineering, Korea University, 145 Anam-ro, Seongbuk-gu, Seoul, 02841, Republic of Korea

wosola@korea.ac.kr/ Tel : +82-10-6627-5598 sangsig@korea.ac.kr/ Tel : +82-2-3290-3909 semicad@korea.ac.kr/ Tel : +82-2-3290-3782

Flexible substrate TFT backplane technology is a critical component for the development of flexible display. Until the recent date, the a-Si:H TFT and LTPS TFT are being considered for future flexible display applications based on their well-established TFT technologies. However, these devices have the fundamental limits such as low performances and poor electrical stability. Recently, amorphous oxide semiconductors have been studied widely due to their suitabilities and high-performances for flexible display. Nevertheless, limited studies about the SPICE modeling of a-IGZO TFT have been reported.

In this study, we conducted the research on the SPICE modeling associated with the bending strain of a-IGZO TFT for the flexible display. We established theoretical models of a-IGZO TFT in response to changes in the voltage-current characteristics under bending strain [1]. Through the TCAD simulation, we found the parameters which can be applied to the SPICE model under bending strain. In the SPICE modeling, the curve fittings were performed with the use of RPI Level 61 TFT model [2], [3]. Here, main parameters are MUBAND and GMIN whose physical meaning is mobility and localized density of states, respectively. From the results of the fitting, the error rate was improved to 2%. Based on this, we presented an optimized SPICE modeling of a-IGZO TFT under bending strain.

Keywords: a-IGZO TFT, Bending strain, Flexible display, SPICE modeling

[1] Minkyung Bae, Analytical Current and Capacitance Models for Amorphous Indium-Gallium-Zinc-Oxide Thin-Film Transistors, *IEEE Transactions on Electron Devices*, Vol.60, No.10, 2013, p.3466-3468

[2] AIM-Spice, circuit simulation program by AIM-software. http://www.aimspice.com

[3] Charlen Chen, AM-OLED Pixel Circuits Based on a-InGaZnO Thin Film Transistors. *SID 09 DIGEST*, 2009, P-14, p.1128-1131

Highly P-doped amorphous SiC thin films prepared by PECVD technology for transmission photocathode

Jozef Huran[1], Nikolay I. Balalykin[2], Alexander A. Feshchenko[2], Pavol Boháček[1],

Štefan Haščík[1], Alexander P. Kobzev[2], Juraj Arbet[1], Mária Sekáčová[1]

[1]Institute of Electrical Engineering, Slovak Academy of Sciences, Dúbravská cesta 9, 4104 Bratislava, Slovakia

[2]Joint Institute for Nuclear Research, Joliot-Curie 6, 141980 Dubna, Moscow Region, Russian Federation

jozef.huran@savba.sk/ Phone: (421 2) 59222778, Fax: (421 2) 54775816

Laser-driven photoelectron sources based on semiconductor photocathodes are widely used in various scientific experiments for the generation of ultracold, short bunched, and spin-polarized high-density electron beams.
Highly P-doped SiC thin film properties on quantum efficiency of prepared transmission photocathode has been investigated.
P doped silicon carbide thin films were deposited on silicon substrate, corning glass and quartz glass by plasma enhanced chemical vapour deposition (PECVD) technology. Concentration of elements in the films was determined by RBS and ERD analytical method simultaneously. The conductivity and Hall measurements on SiC/Corning glass sample was used for galvanomagnetic properties of films investigation at temperature 300 K. The obtained results of resistivity, Hall coefficient, electron Hall mobility, and electron Hall concentration in the sample investigated are analysed and discussed. The quantum efficiency was calculated from the measured laser energy and the measured cathode charge. RBS and ERD analysis indicated that the films contain silicon carbon, hydrogen, phosphorus and small amount of oxygen. Lift off technique was used for Al mesh preparation on SiC/quartz structures. Al mesh was used as mask for dry etching of SiC films in the ICP reactor and as photocathode contact. The prepared transmission photocathode is placed on the hollow cathode assembly of the Pierce structure DC gun to produce photoelectrons. The 15 ns UV laser pulses (quadrupled Nd:YAG laser) with laser spot size 8 mm are used to backside photocathode illumination. To draw the electrons from the photocathode a negative voltage was placed on the cathode. The bunch charge is measured by using Faraday cup (FC). Perspectives for implementation of highly P-doped SiC thin films on quartz glass transmission photocathode in DC gun technology are discussed.
This research has been supported by the Slovak Research and Development Agency under the contracts APVV-0443-12 and has been executed in the framework of the Topical Plan for JINR Research and International Cooperation (Project 02-0-1067-2013/2017).

Keywords: silicon carbide films, plasma deposition, transmission photocathode

Highly transparent and conductive TiO_2/Ag/TiO_2 (TAT) thin films deposited at room temperature on sapphire substrate by sputtering

Chadrasekhar Loka[1], Kwang Lee[1], Sinyong Joo[1], Sung Whan Moon[2], Kee-Sun Lee[1,*]

[1]Department of Advanced Materials Engineering, Kongju National University, Cheonan, Chungnam 330−717, South Korea.

[2]Sapphire technology, LTD, Whasung city, Kyunggido, South Korea.

E-Mail: csloka89@gmail.com, kslee@kongju.ac.kr

Transparent conducting electrodes (TCEs) attract intense interests due to its diverse industrial applications. The three major areas of applications of the TCO thin films are flat panel displays, solar cells, and energy efficient architectural glass coatings [1, 2]. The conventional TCEs require high transmittance (>80%) in the visible wavelength region and low resistivity (~10^{-4} Ω cm). In this study, we report TiO_2/Ag/TiO_2 (TAT) multilayer structure instead of the limited supply Sn-doped indium oxide (ITO) and Ag multilayer structures (such as ITO/Ag/ITO). The TAT thin films were deposited at room temperature on sapphire substrates and a rigorous analysis has been presented on the electrical and optical properties of the films. The deposited films showed high visible transmittance >85% at 550 nm along with noteworthy low electrical resistance ~3.65×10^{-5} Ω cm. The Haacke's figure of merit (FOM) of the TAT thin films is comparable with the conventional ITO/Ag/ITO (IAI) multilayer structures. The carrier concentration of the films has been increased with respect to Ag film thickness. The TAT films were annealed at high temperature >873 K to compare the microstructure and interfaces along with optical-electrical properties of as-deposited and annealed films.

Keywords: TiO_2, silver, multilayer, optical properties, figure of merit.

[1] JUN, H. K., DAE-HYUN, K., TAE-YEON, S. 2015. Realization of Highly Transparent and Low Resistance TiO_2/Ag/TiO_2 Conducting Electrode for Optoelectronic Devices. *Ceramics International*, 41, 3064-3068.

[2] JIN-A, J., HAN-KI, K., HYUN-WOO, K., TAE-WOONG, K. 2013. Transmission Electron Microscopy Study of Degradation in Transparent Indium Tin Oxide/Ag/Indium Tin Oxide Multilayer Films. *Applied Physics Letters*, 103, 011902.

Mechanics of Roll-based Transfer for Interconnection of Thin Film Devices using Anisotropic Conductive Film

Seong-Min Hong[1], Bongkyun Jang[1], Do Hyun Kim[2], Keon Jae Lee[2], Jae-Hyun Kim[1,#]

[1] Department of Nanomechanics, Korea Institute of Machinery & Materials (KIMM), 156 Gajungbuk-ro, Yuseong-gu, Daejeon 34103, South Korea.

[2] Department of Materials Science and Engineering, Korea Advanced Institute of Science and Technology (KAIST), 291 Daehak-ro, Yudeong-gu, Daejeon 34141, South Korea.

Presenting author: Seong-Min Hong (*1aa2bbab@kimm.re.kr*)

[#]*Corresponding author: Jae-Hyun Kim* (*jaehkim@kimm.re.kr*)

Roll-based transfer is an innovative process for integrating inorganic thin film devices on a polymeric substrate with high productivity, but suffers from difficulty in electrical interconnection. In this study, a sophisticated transfer technique is developed to realize both the integration and the electrical interconnection simultaneously based on a roll stamp and anisotropic conductive film (ACF). ACF is mainly composed of epoxy resins and conductive particles, and requires appropriate pressure and heat for making anisotropic electrical connections in a vertical direction. Using finite element analysis, we simulated the contact mechanics during the roll-based transfer process, and found that the simulated distribution of contract pressure on ACF was highly dependent on the mechanical properties of ACF and the roll stamp, and interestingly, the stacking order of stamp/device/ACF/FPCB. The simulated process conditions for electrical interconnection were confirmed by the roll transfer experiments with a capability of measuring pressure distribution. From this understanding of the contact mechanics during transfer, the mechanical integration and electrical interconnection was successfully realized in a highly productive way of roll transfer.

Keywords: Anisotropic Conductive Film (ACF), Roll-based process, Interconnection, Finite element Method(FEM), Pressure sensitive film , Pressure distribution

Application of Zeolite-based Functional Sorbents to Ecological Analysis: Thin-film Microextraction of Volatile Habitat-related Substances in Brackish River Waters

Il-kweun Oh, Tao Wang, Seung-Woo Lee*

Graduate School of Environmental Engineering, the University of Kitakyushu, 1-1 Hibikino, Wakamatsu, Kitakyushu 808-0135, Japan.

*i-o@kitakyu-u.ac.jp, *leesw@kitakyu-u.ac.jp*

Thin-film microextraction (TFME) is a sample preparation technique possessing several advantages over traditional analytical methods such as the convenient integration of extraction, preconcentration, and sample introduction. *Porous materials* and their derivatives have been widely used as adsorbents for analyte preconcentration prior to gas chromatography analysis. In this study, zeolite-based TFME was demonstrated for the GC-MS analysis of habitat-related substances of *Deiratonotus japonicas*. Environmental habitat conditions of *Deiratonotus japonicus* were investigated in the Kita river estuary, Nobeoka, Japan. *Deiratonotus japonicus* is a Japanese endemic species that is specified as a Near Threatened (NT) species in the Red Data Book (RDB) list by the Japanese Ministry of the Environment. *Deiratonotus japonicus* inhabits the isolated locations and upstream brackish water area, and it is affected by variable salinity, sediment and pollutants. To the best of our knowledge, the current approach is the first time for ecological analysis describing the correlation between habitat-related substances and density distribution of *Deiratonotus japonicus*.

Keywords: Porous materials, Thin-film microextraction, Deiratonotus japonicus, Ecological analysis

[1] HIU, Y., OH, IK., KUSUDA, T., HIRATA, M., 2002. Characteristics of distribution, changes of the number of individuals and the conditions on habitation of *Deiratonotus japonicus*. Env. Eng. Res. 39, 467-475.

Controllable Nanoporous Fibril- Like Morphology By Layer-By Layer Self-Assembled Films Of Bioelectronics Poly(Pyrrole-*Co*-Formylpyrrole)/Polystyrene Sulfonate For Tissue Engineering

Prasit Pattananuwat, **Motohiro Tagaya, Takaomi Kobayashi***

Department of Materials Science and Technology, Nagaoka University of Technology, 1603-1 Kamitomioka, Nagaoka, Niigata, 940-2188, Japan

We demonstrate here a new class of nanocoating materials for diverse biomedical applications based on poly (pyrrole-*co*-formyl pyrrole) (P(Py-*co*-Fpy)) multilayers with polystyrene sulfonate (PSS) with self-assembly layer by layer technique. By modulating the number layer of deposition, the unique surface properties of P(Py-*co*-Fpy) were evaluated for bioaffinity. Atomic force microscopy (AFM) demonstrated the controllable morphology of the degree fibril network structure of P(Py-*co*-Fpy)/PSS surface. As suggested by contact angle measurement, P(Py-*co*-Fpy)/PSS surface exhibited the increase of hydrophilicity with number of deposition. The direct adsorption of bovine serum albumin (BSA) onto the top surface of P(Py-*co*-Fpy) by AFM analysis revealed the forming an multilayer with increasing layer deposition of P(Py-*co*-Fpy)/PSS film. The adsorbed fibrinogen (Fgn) revealed the reversible conformation change on surface of P(Py-*co*-Fpy) /PSS. The saturation-adsorption amounts for both proteins were found to be greatest on the LBL film. The effect of degree of fibril network structure of P(Py-*co*-Fpy) surface on primary mouse embryonic fibroblasts (MEF) was investigated. Cell morphology and proliferation on P(Py-*co*-Fpy) /PSS LBL film at different number of layer deposition were evaluated. Obtained results showed that P(Py-*co*-Fpy)/PSS LBL nanocoating surface are non-cytotoxic as morphology-dependent.

Keywords: **Nanoporous, Nanofibril, P(Py-*co*-Fpy), Self-assembly layer by layer, AFM, Protein adsorption, Cell adhesion**

*Corresponding author. Tel.: +81 258 47 9326; fax: +81 258 47 9300 *E-mail address:* pt.pattana@hotmail.com (K.Takaomi)

Electrospun Polycarbonate (PC) Nanofibrous Membrane for High Efficiency PM2.5 Filtration

Yiyang Xu[1], Hanghang Wei[1], Xiaofeng Wang[1*], Yanhong Gao[2], Jing Jiang[2], Qian Li[1*]

[1]National Center for International Research of Micro-Nano Molding Technology, School of Mechanics and Engineering Science, Zhengzhou University, Zhengzhou 450002, China

[2]School of Materials Science & Engineering, Zhengzhou University, Zhengzhou 450002, China

EMail : xiaofengwang@zzu.edu.cn, qianli@zzu.edu.cn

Particulate matter (PM) pollution has gained significant concerns for people's health. Air filtration is an effective way to eliminate the influence of PM pollution. In this study, nanofibers of polycarbonate (PC), a polymer has been widely used as one of theengineering plastics due to its excellent properties, were successfully obtained by electrospinning and applied as PM filters. Hexadecyl trimethyl ammonium Bromide (CTAB) was applied to assist ultrafine PC nanofibers electrospinning. The fiber diameter was around 319 ± 27 nm, which decreased nearly 600% compared to that as reported in other literatures(Sungcheal and Farris, 2008) (Cheal et al., 2014). The ambient PM2.5 was applied for the filtration test. The results revealed that the PM is either intercepted by the fibers or captured by the fiber surface by initea impaction or diffusion(cf. Fig. 1). The filtration efficiency of PC membrane was higher than that of PVA and PS at the similar fibrous morphology suggesting that polarity is predominant in the interaction of particles and fiber surface (cf. Fig. 2) (Liu et al., 2015).

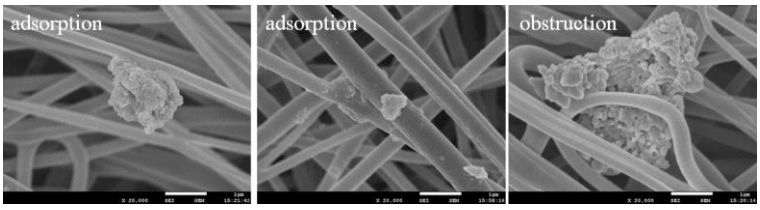

Fig.1 Morphology of the PM2.5 captured by the PC nanofibers. The scale bar is 1 μm

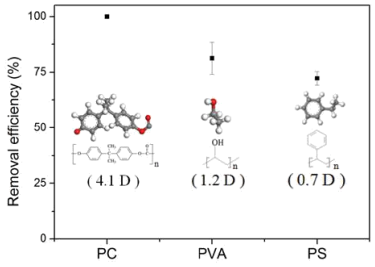

Fig.2 Removal efficiency of different nanofibers.

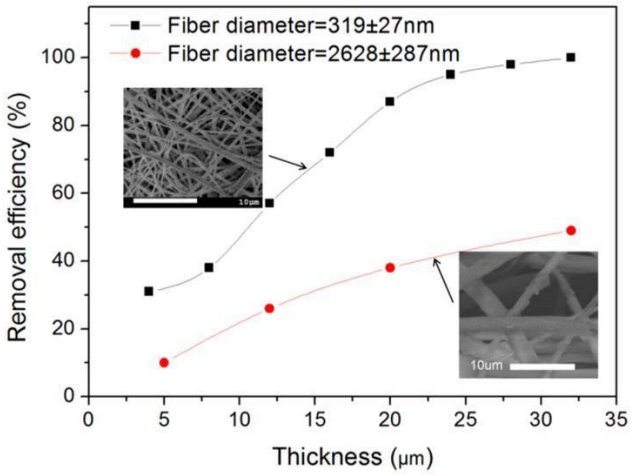

Fig. 3 Removal efficiency of the PC microfibers and nanofibers at different thickness.The scale bar is 10 μm.

The removal efficiency of PC nanofibers with the diameter of about 2.6 μm was smaller than that of ones with the diameter of 320 nm when the membrane thickness kept the same (cf. Fig. 3), indicating the reducing the fiber diameter helps to enhance the filtration efficiency of PC fibrous membrane. The removal efficiency increased with an increase in the thickness of nanofibrous membrane by providing more chances for the particles to meet the fibers when they are travelling through the membrane. The filtration efficiency reached ~100%, when the membrane was 32 μm in thickness. This study showed PC nanofibrous membrane is promising candidate material in air purification and particle filtration.

Keywords: Electrospinning, PC, nanofibers, Filtration, PM2.5

[1] CHEAL, M. S., YEOL, K. J. & TAEK, O. B. 2014. Mechanical and flame resistant properties of polycarbonate-carbon nanotubes-ochre composites. *Polymer Engineering & Science,* 54**,** 1289-1299.

[2] LIU, C., HSU, P. C., LEE, H. W., YE, M., ZHENG, G., LIU, N., LI, W. & CUI, Y. 2015. Transparent air filter for high-efficiency PM2.5 capture. *Nature Communications,* 6.

[3] SUNGCHEAL, M. & FARRIS, R. J. 2008. The morphology, mechanical properties, and flammability of aligned electrospun polycarbonate (PC) nanofibers. *Polymer Engineering & Science,* :48**,** 1848–1854**.**

Hybrid Zeolite Imidazolate Framework Thin Films for Gas Separations

Yang Lo[1], Dun-Yen Kang*[1]

[1]Department of Chemical Engineering, National Taiwan University No. 1, Sec. 4, Roosevelt Road, Taipei 10617, Taiwan

dunyen@ntu.edu.tw

Membranes with a metal organic framework (MOF) and tunable periodic micropores are viewed as promising materials for use in molecular sieving. However, the lack of a rational approach to the synthesis of MOF thin films to enhance separation performance greatly limits further development. In this work, we propose a novel concept referred to as pseudopolymorphic seeding, as an example of rational design in the synthesis of hydrogen-selective MOF thin films. We then employed the pseudopolymorph zeolitic imidazolate framework-8 (ZIF-8) and ZIF-L for the fabrication of hybrid membranes as proof of concept. Layered ZIF-L[1] served as seed crystals in the growth of its pseudopolymorph, ZIF-8, thereby facilitating the creation of ZIF-L@ZIF-8 hybrid membranes with excellent interfacial affinity between the two crystals. Layered ZIF-L with a high degree of hydrogen diffusivity was incorporated within the membranes to increase selectivity for hydrogen. Single gas permeation using H2, N2, CH4, and CO2 indicates that the performance of hybrid membranes in the separation of hydrogen exceeds that of pure ZIF-8 membranes. Simulations of mass transfer at the microscopic level were performed to elucidate the phenomenon of molecular diffusion using ZIF-L@ZIF-8 hybrid membranes. Simulation results indicate that the diffusion of hydrogen through the interlayer spacing of ZIF-L may explain the high separation performance of the hybrid membranes, which was observed in our experiments of single gas permeation. Our proposed methodology based on the rational design of hybrid MOF thin films could greatly facilitate the development of new MOF thin films/membranes for a broad range of applications.

Keywords: Metal Organic Framework, Zeolitic Imidazolate Framework, Thin Film, Gas Separation

[1] LEE, W.-C., CHIEN, H.-T., LO, Y., WANG, T.-P. & KANG, D.-Y. 2015. Synthesis of Zeolitic Imidazolate Framework Core−Shell Nanosheets Using Zinc-Imidazole Pseudopolymorphs. *ACS Applied Materials & Interfaces*, 7, 18353-18361.

TiO_2/SiO_2 film on the modified cellulose surface

R. Buntem, K. Semthaun, R. Maliyam, C. Kaewdang

[1]Department of Chemistry, Faculty of Science, Silpakorn University.

radchadab@yahoo.com

Cellulose, extracted from plant, has been widely used in paper industry. Cellulose is modified by many organic and inorganic substances in order to improve the quality like whiteness and mechanical strength. The causes of cellulose alteration are from biodegradation, photodegradation, acid hydrolysis and oxidation. In this research, filter paper, a representative of cellulose fiber, was coated by thin film of TiO_2 to improve the photostability of the cellulose. The surface of the cellulose was initially modified by various methods as follows:

1. esterification by polycarboxylic acids like tartaric acid (TA) and butanetetra-carboxylic acid (BTCA) to obtain FIL-TA and FIL-BTCA respectively

2. etherification by sodium monochloroacetate to obtain FIL-MCAA

3. coating by carboxymethylcellulose to obtain FIL-CMC

Each of the modified filter papers was subsequently coated by TiO_2/SiO_2. All samples were characterized by SEM/EDS and TGA. The Smoothness (Bekk method), porosity (Gurley method) and bursting test of paper were also performed. The paper modified by esterification and etherification bind to TiO_2/SiO_2 particles more effectively than CMC modifications as evidenced from SEM/EDS and TGA data. The smoothness of the coated paper was reduced as compared to that of original filter paper. The porosity of the paper was greatly reduced when it was coated by inorganic particles.

Keywords: Modified cellulose, TiO_2/SiO_2 film, durability of cellulose

[1] MAHLTIG, B., HAUFE, H., BOTTCHER, H. 2005. Functionalisation of textiles by inorganic sol–gel coatings. *J Mater Chem*, 15, 4385-4398.

[2] DASTJERDI, R.; MONTAZER, M. 2010. A review on the application of inorganic nano-structured materials in the modification of textiles: focus on anti-microbial properties. *Colloids Surface B*, 79, 5–18.

Antimicrobial Ag-doped Al coatings for Air Conditioning System

Y. Jeon[1,2], Y. Lee[2], S. Kim[1], S. Hwangbo[3], J. Kim[4], K. Hwang[1]

[1]Dept. of Biomed. Eng. & Dept. of Mech. Eng., Nambu Univ., South Korea
[2]Dept. of Automobile, Chunnam Techno Univ., South Korea
[3]Dept. of Electronic Eng., Honam Univ., South Korea
[4]Dept. of Photonic Eng., Chosun Univ., South Korea
own-young@hanmail.net and *khwang@nambu.ac.kr*

It is widely known that materials containing silver show antibacterial property [1]. Many metal- and carbon-based materials, such as Ag, Au, Pt, TiO2, ZnO, carbon nano tubes, and grapheme show antimicrobial properties [2-3]. Among the various antibacterial materials, Ag is used in a wide variety of applications including spectrally selective coatings for solar reflectors. It has been reported that the inhibition effect of Ag ions is due to its adsorption to the negatively charged bacterial cell wall, the inactivation of enzymes, the disruption of membrane permeability, and, ultimately, cell death [4]. There is an increasing awareness of serious problems associated with bacteria, molds, fungi, and other destructive microbes in the Heating, Ventilation and Air Conditioning (HVAC) industry. The aim of this work was to verify the capacity of Ag ions to stop the growth of bacteria and molds inside the ducts of HVAC systems when these ducts were coated with Ag-doped Al films. The deposition of Ag-doped Al films on Al foil was carried out by thermal evaporator. High-resolution X-ray diffraction, field emission - scanning electron microscope and energy dispersive X-ray spectrometer were used to analyze crystal structure, surface morphology and composition, respectively. The X-ray diffraction pattern revealed that 3 mol% Ag-doped Al films were single-phased and the doped Ag ion had little influence on the host structure. The surface morphology of the polycrystalline films on Al foils showed fine grains and a good match of EDX peaks from the Ag and Al spectra with a doping mol% was obtained. The number of *Escherichia coli* (*E. Coli*) which remained after each contacting times was counted in order to examine antimicrobial ability of the films. Above 90% reduction of *E. Coli* populations on 3 mol% Ag-doped Al films was observed after being contacted for 240 min, while the reduction rate of *E. Coli* on bare Al foils was under 10%. A duct system with Ag-doped Al thin film has the potential for HVAC and would find wide use in the field of antibacterial.

Keywords: Ag-doped Al film, antimicrobial property, Al foil

[1] HWANG, K., JEON, Y., CHOI, T. & HWANGBO, S. 2013. Combination of Light Emitting Diode at 375 nm and Photo-reactive TiO2 Layer Prepared by Electrostatic Spraying for Sterilization. *J Electro Eng Technol*, 8, 1169-1174.

[2] CUI, Y., ZHAO, Y., TIAN, Y., ZHANG, W., Lu, X. & JIANG, X. 2012. The Molecular Mechanism of Action of Bactericidal Gold Nanoparticles on Escherichia coli. *Biomater*, 33, 2327-2333.

[3] HU, W. B., PENG, C., LUO, W. J., LV, M., LI, X. M., LI, D. et al. 2010. Graphene-based Antibacterial Paper. *ACS Nano*, 4, 4317-4323.

[4] LAND, B. P., PEUMANS, P. & FORREST, S. R. 2004. Long-range Absorption Enhancement in Organic Tandem Thin-film Solar Cells Containing Silver Nanoclusters.
J Appl Phys, 96, 7519.

Core-shell structured chitosan-carbon nanotube membrane as a positively charged drug delivery system: Selective loading and releasing profiles for bovine serum albumin

Han-Sem Kim[a,b], and Ueon Sang Shin[a,b*]

[a]*Department of Nanobiomedical Science & BK21 PLUS NBM Global Research Center for Regenerative Medicine, Dankook University, Chungnam, Cheonan, 330-714, Korea.*
[b]*Institute of Tissue Regeneration Engineering (ITREN), Dankook University, Chungnam, Cheonan, 330-714, Korea.*

*Corresponding author. Tel.: +82 41 550 3691, Fax.: +82 41 559 7911,

E-mail address: drywind010@dankook.ac.kr, and usshin12@dankook.ac.kr.

Here we present carbon nanotube (CNT) bucky-paper with efficient loading and releasing patterns for negatively charged drug. Carbonaceous membrane (Chit-NH2/CNT) with three dimensionally interwoven porous nanostructure and positive surface was prepared by self-assembly of CNT fibers hybridized with chitosan (Chit-NH2) in core-shell structure. Transmission electron microscopy and scanning electron microscopy images clearly showed that core-shell structured Chit-NH2/CNT fibers and countless nano-sized pores at less than 30 nm in length were formed between positively charged Chit-NH2/CNT fibers. Based on Brenauer–Emmett–Teller N2-adsorption method, the surface area, average pore size, and pore volume were approximately 19.7 m^2/g, 9.54 nm, and 0.043 cc/g, respectively. Bovine serum albumin (BSA) loading and releasing profiles of these carbonaceous membrane constructed with positively charged CNT fibers were tested. The maximum entrapment of BSA was at loading capacity of 0.65 mg/mg for 1.0 mg of Chit-NH2/CNT hybrid membrane. The maximum release of BSA was about 65% of the entrapped amount for 1.0 mg of Chit-NH2/CNT hybrid membrane. BSA was almost continuously released over the 11-day period at a rate of about 0.23 g/day. Chit-NH2/CNT hybrid membranes showing impressive drug-loading/-releasing characteristics could be potentially used as transdermal drug delivery system for negatively charged drugs in the medicinal field and tissue regeneration area.

Keywords: CNT bucky-paper, core-shell structure, selective drug-loading and -releasing hybrid membrane, transdermal drug delivery system

Displaceable Biointerface Properties by Using Disulfide-Functionalized Poly-p-xylylene Coatings

Zhen-Yu Guan[1], Hsien-Yeh Chen[1]

[1] Department of Chemical Engineering, National Taiwan University, Taipei 10617,

Taiwan

E Mail/ Contact Détails (f03549004@ntu.edu.tw and hsychen@ntu.edu.tw)

A new class of disulfide functionalized poly-p-xylyene coating has been synthesized to provide switchable and displaceable surface properties for biomaterials. This advanced version of poly-p-xylylene comprises an integrated disulfide moiety within the functional side group, and the switchability is achieved through a thiol-disulfide interchange mechanism for detaching/attaching biomolecules and/or the same mechanism through which the programmed restoration of functions or their displacement by other functions can be carried out. The displacing phenomenon between the immobilized functional molecules is triggered by the redox thiol-disulfide interchange reaction. These dynamically well-defined molecules on the surfaces respond simultaneously to altered biological properties and controlled biointerfacial functions, for example, switching wettability or reversibly altered cell adhesion activity. Poly-p-xylylenes are a key player in controlling surface properties for many important applications, such as medical implants, biosensors, bioMEMS devices, and microfluidics. The introduction of this new facet of poly-p-xylylenes enables the dynamic mimicry of biological functions relevant to the design of new biomaterials.

Keywords: displaceable surface, dynamic biointerface, functionalized poly p xylylene, biomaterials, surface modification

[1] Lahann, J., Mitragotr, S., Tran, T. N., Kaido, H., Sundaram, J., Choi, I. S., Hoffer, S., Somorjai, G. A., Langer, R. 2003. A Reversibly Switching Surface. *Science*, 299, 371-374.

[2] Wu, J. T., Huang, C. H., Liang, W. C., Wu, Y. L., Yu, J., Chen, H. Y. 2012. Reactive Polymer Coatings: A General Route to Thiol-ene and Thiol-yne Click Reactions. *Macromol. Rapid Commun.*, 33, 922-927.

[3] Keire, D. A., Strauss, E., Guo, W., Noszal, B., Rabenstein, D. L. 1992. Kinetics and equilibria of thiol/disulfide interchange reactions of selected biological thiols and related molecules with oxidized glutathione. *The Journal of Organic Chemistry*, 57, 123-127.

[4] Guan, Z. Y., Wu, C. Y., Li, Y. J., Chen, H. Y. 2015. Switching the Biointerface of Displaceable Poly-p-xylylene Coatings. *ACS Applied Materials & Interfaces*, 7, 14431-14438.

Laser processing of microfluidic systems for real-time PCR analysis of DNA

F. Stokker, M. Filipescu, M. Dinescu, A. Palla Papavlu

Lasers Department, National Institute for Lasers, Plasma, and Radiation Physics, Magurele 077125, Romania
Corresponding Author e-mail address: flavian.stokker@inflpr.ro

Our work relates to the evolving need of constructing lab-on-a-chip (LOC) systems for fast and reliable detection of DNA. We address this issue by using different laser-based techniques (PLD, plasma assisted PLD, laser direct-writing) in order to create microfluidic systems based on the polymerase chain reaction (PCR) technique and we analyze their properties.
More specifically, we use ArF and Nd:YAG laser sources, in pulsed laser deposition (PLD) and plasma assisted PLD (RF-PLD) setups, to produce the metallic (conductive) and dielectric (insulating) thin films necessary for the integration of heating elements that are required for the PCR procedure.
Laser direct writing using an ArF source is used to fabricate micro-channels and micro-cavities in different polymers, through which the transport of nutrients and micro-organisms will be operated.
We use optical microscopy, scanning electron microscopy (SEM) and atomic force microscopy (AFM) in order to provide an analysis of how different experimental conditions affect the quality of the obtained micro-devices.

This work was supported by a grant from MEN-UEFISCDI, project PN-PCCA 34/2014.

Tunable Surface Densities of Immobilized Biomolecules for Advanced Biomaterials Design

Chih-Yu Wu[1], Hsien-Yeh Chen[1]

[1] Department of Chemical Engineering, National Taiwan University, No. 1, Sec. 4,

Roosevelt Rd., Taipei 10617, Taiwan (R.O.C.)
picorna.tw@yahoo.com.tw (C-Y W) and hsychen@ntu.edu.tw (H-Y C)

Although the immobilization of functional biomolecules provides the advantage of a significantly low dosage of use, the exhibited biological effectiveness may not be equally extrapolated when used in solution[1] compared with being immobilized on surfaces; and the association of the immobilized biomolecules concentrations to the effectiveness of the induced biological responses yet has only been sporadically discussed[2] or only in a case-by-case manner. The objective of this study was to illustrate the important concept of controlling the coverage of the immobilized biomolecules and the resulting tunable biological activities for advanced biomaterials design. The tunable mechanism was demonstrated by precisely adjusting the density of the underlying anchoring sites, which was achieved by copolymerizing a controlled molar ratio of pentafluorophenol ester-[2.2] paracyclophane and nonsubstituted- [2.2] paracyclophane (1 : 0, 1 : 1, 1 : 20, 1 : 80, 0 : 1, respectively), and resulted in a series of density-varied pentafluorophenol ester-functionalized poly-p-xylylenes during the modification process of chemical vapor deposition (CVD) copolymerization. Pentafluorophenol ester, a chemical motif that provides a bioorthogonal linkage for amine-rich molecules, and forms an amide bond through the amine–pentafluorophenol ester coupling reaction[3], was chosen to realize the idea and was used for the immobilization of biomolecules including polyethylene glycols, aptamers, proteins of bovine serum albumin and fibronectin. The binding efficacy of these molecules and the tunable biological responses with respect to cell adhesion and proliferation as well as protein adsorption were verified. Although the details of the dependencies and mechanism may still require further investigation, the results demonstrate that the biological activities of biomaterial surfaces are tunable and can be tailored by controlling the densities of the underlying chemical motifs or the immobilized biomolecules. The proposed immobilization technique is facile and versatile and may help advance studies and applications that rely on the immobilization of biomolecules on material surfaces, and we foresee the extension of exploiting other functional poly-p-xylylenes for tuning the biointerface with more biomolecules, and/or enabling synergistic and gradient control over multiple functions, as well as the development of industrial products.

Keywords: Surface modification, thin film coatings, controlled coverage, functionalized poly-p-xylylenes, tunable biological responses

[1] LUO, Y. & SHOICHET, M. S. 2004. Light-activated immobilization of biomolecules to agarose hydrogels for controlled cellular response. Biomacromolecules, 5, 2315-2323.

[2] ALVES, D. & OLÍVIA PEREIRA, M. 2014. Mini-review: Antimicrobial peptides and enzymes as promising candidates to functionalize biomaterial surfaces. Biofouling, 30, 483-499.

[3] HERMANSON, G. T. 2008. Bioconjugate techniques, Academic Press, Boston.

Effect of substrate temperature on structural properties of CdTe thin films

P.K.K. Kumarasinghe[1], B.M.K. Pemasiri[1,2], B.S. Dassanayake[1,2]

[1]Postgraduate Institute of Science, University of Peradeniya, Peradeniya, Sri Lanka.

[2]Department of Physics, University of Peradeniya, Peradeniya, Sri Lanka.

E-Mail: kumarasinghe.p3k@gmail.com

Cadmium Telluride (CdTe) is a well investigated II-VI group compound semiconductor especially due to its potential applications in photovoltaics. CdTe thin films have a polycrystalline nature with a cubic zinc-blende structure [1]. The properties of CdTe thin films are strongly dependent upon the fabrication technique, annealing treatment, film thickness, $CdCl_2$ treatment, doping and substrate temperature [2]. In this study, the correlation between the substrate temperature and the CdTe structural properties are discussed.

CdTe thin films were deposited under a chamber pressure of 10^{-5} Torr using thermal evaporation technique. Samples of thickness 5 µm were deposited at different substrate temperatures from 125 to 300 ^{o}C and annealed at 400 ^{o}C for 20 min. The structural properties of the thin films were analyzed employing an X-ray diffractometer using CuKα radiation (λ=1.5418 Å) and 2θ in the range of 10-100°. X-ray diffraction analysis suggests that all CdTe thin films are polycrystalline and have a cubic zinc-blende structure with reflections corresponding to (111), (220), (311), (400), (331), (422), (511), (440), (531) and (620) plane orientations (JCPDS data file: 15-0770). No phase change was observed with changing substrate temperature and the intensity of the reflection (111) was observed to increase with increasing substrate temperature. Furthermore, the analysis also revealed the presence of Te, TeO_2 and CdO on the fabricated thin films.

The crystallite size of the CdTe thin films was evaluated by using the Debye-Scherrer's formula. Crystallite size was found to increase with increasing substrate temperature from 125 to 250 ^{o}C. Highest crystallite size of 27.2 nm and lowest dislocation density value of 1.35×10^{15} were recorded for samples deposited under a substrate temperature of 250 ^{o}C.

In addition, films fabricated under a substrate temperature of 250 °C showed the lowest micro strain (3.57×10^{-3}) while it was highest at 300 ^{o}C.

Financial assistance from National Science Foundation of Sri Lanka (NSF, RG/12/BS/03) and Prof. S. Sivananthanthan of University of Illinois at Chicago (USA) are gratefully acknowledged. Support from Prof. M.A.K.L. Dissanayake of National Institute of Fundamental Studies, Sri Lanka and Dr. A.C.K. Dissanayake of Western Michigan University, Kalamazoo, USA are also appreciated.

Keywords: Thermal evaporation, cadmium telluride, substrate temperature, structure, XRD

[1] ENRIQUE, J. P. & MATHEW, X. 2003. The effect of annealing on the structure of CdTe films electro-deposited on metallic substrates. *J. Cryst. Growth*, 259, 215–222.

[2] CHANDER, S. & DHAKA, M. S. 2015. Optimization of physical properties of vacuum evaporated CdTe thin films with the application of thermal treatment for solarcells. *Mat. Sci. Semicon. Proc.*, 40, 708-712.

Energy Storage Performance of PZT/BZT/PZT Sandwich Structure Thin Films

Xiangqun Chen[1], Yilun Tang[1], Qiu Sun[2*], Teizhu Xin[1]

[1] Department of Materials Physics and Chemistry, School of Materials Science and Engineering, Harbin Institute of Technology, Harbin 150001, PR China

[2] School of Chemical Engineering and Technology, Harbin Institute of Technology,

Harbin 150001, PR China

Presenting author sunqiu@hit.edu.cn

corresponging author sunqiu@hit.edu.cn

$Pb(Zr_x,Ti_{1-x})O_3/Ba(Zr_x,Ti_{1-x})O_3/Pb(Zr_x,Ti_{1-x})O_3$ (PZT/BZT/PZT) sandwich structure thin films were grown on the $Pt(111)/Ti/SiO_2/Si$ substrate by a sol-gel method. All the thin films had a pure perovskite phase structure. The effects of Zr/Ti ratio on dielectric properties and energy storage performance of PZT/BZT/PZT sandwich structure thin films were investigated in detail. The dielectric constant increased and the dielectric loss decreased with increase of the Zr/Ti ratio. Dielectric loss remained quite low (less than 0.028) in the whole frequency or voltage ranges. An improvement on the energy storage performance was found. The maximum energy storage density was 16.41 J/cm^3 at the electric field of 1000kV/cm in the PZT/BZT/BZT sandwich structure thin film with Zr/Ti of 2:8. The electrical properties and energy storage performance of BZT thin films can be optimized by Zr/Ti and sandwich structure. Therefore, PZT/BZT/PZT sandwich structure thin films are capable of enhancing energy storage properties and have the potential for their application in high-energy storage capacitors.

Keywords: PZT/BZT/PZT sandwich structure thin films, sol−gel, dielectric properties, energy-storage properties

[1] YANG, J., MENG, X. J., SHEN, M. R., SUN, J. L. & CHU, J. H. 2009. Effects of Mn Doping on Dielectric and Ferroelectric Properties of $(Pb,Sr)TiO_3$ Films on $(111)Pt/Ti/SiO_2/Si$ Substrates. *J. Appl. Phys.*, 106, 094108.

[2] ZHAO, Y., HAO, X. & ZHANG, Q. 2014. Energy-Storage Properties and Electrocaloric Effect of $Pb_{(1-3x/2)}La_xZr_{0.85}Ti_{0.15}O_3$ Antiferroelectric Thick Films. *ACS Appl. Mater. Interfaces*, 6, 11633-11639.

[3] TONG, S., MA, B., NARAYANAN, M., LIU, S., KORITALA, R., BALACHANRAN, U. & SHI, D. 2013. Lead Lanthanum Zirconate Titanate Ceramic Thin Films for Energy Storage. *ACS Appl. Mater. Interfaces*, 5, 1474-1480.

Influence of substrate temperature on optical, electrical and compositional properties of thermal evaporated CdTe thin films

P.K.K. Kumarasinghe[1], B.M.K. Pemasiri[1,2], B.S. Dassanayake[1,2]

[1]Postgraduate Institute of Science, University of Peradeniya, Peradeniya, Sri Lanka.

[2]Department of Physics, University of Peradeniya, Peradeniya, Sri Lanka.

E-Mail: buddhid@gmail.com

Cadmium Telluride (CdTe) is one of the most promising photovoltaic materials due to its low fabrication cost, nearly optimum band gap (1.5 eV) for efficient photo conversion, high optical absorption coefficient (>10^4 cm^{-1}) at band edge and variety of techniques available for its deposition [1]. In this work, CdTe thin films were fabricated using thermal evaporation technique to investigate the effect of substrate temperature on its optical, electrical, morphological and compositional characteristics.

Thermal evaporation of CdTe was done using Edward's Vacuum Coating Unit using commercially available CdTe powder (Sigma-Aldrich, 99.99%). The samples were deposited under a chamber pressure of 10^{-5} Torr. Films of CdTe of thickness 5 µm were deposited at different substrate temperatures from 125 to 300 ^oC.

Optical characterization revealed that the thin films annealed at 400 ^oC for 30 min have a lower band gap compared to as-deposited ones, potentially due to increment of particle size with annealing. However, no significant variation of band gap was observed with respect to substrate temperature, within the experimental uncertainties and yielded a value of 1.50 eV.

Resistivity measurements were conducted using Van der Pauw method, and the lowest resistivity was recorded for samples deposited at a substrate temperature of 200 ^oC. This can be due to the higher sticking coefficient of Te compared to Cd around 200 ^oC, making the material more Te rich and p-type [2]. EDX measurements were conducted using a 10 keV electron beam along the cross-section of a film. Measurements revealed that the atomic composition is non-uniform with existence of Cd rich and Te rich regions along the cross-section.

Financial assistance from National Science Foundation of Sri Lanka (NSF, RG/12/BS/03) and Prof. S. Sivananthanthan of University of Illinois at Chicago (USA) are gratefully acknowledged.

Keywords: Thermal evaporation, substrate temperature, CdTe, thin films

[1] ENRIQUES, P.J., MATHEWS, N.R., HERNANDEZ, G.P. & MATHEW, X. 2013. Influence of the film thickness on structural and optical properties of CdTe thin films electrodeposited on stainless steel substrates. *Mater. Chem. Phys*., 142, 432-437.

[2] NASEEM, S., NAZIR, D., MUMTAZ, R. & HUSSAIN K. 1996. Evaporated thin films of CdS and CdTe: Optimization for photovoltaic applications. *J. Mater. Sci*. Technol., 12, 89-94.

Triboelectric-potential-regulated charge transport through p-n junctions for area-scalable conversion of mechanical energy

Harvesting ambient mechanical energy is a promising approach to sustainable and maintenance-free power source for electronics that are wireless, stand-alone and autonomous. The sources of mechanical energy cover a wide spectrum of amplitude and frequency. Typical mechanical motions that are usually utilized include vibrations, body movement, and motions in nature such as wind and water waves. Conventional methods of converting mechanical energy mainly rely on piezoelectric effect, electromagnetic effect, and electrostatic induction. Recently developed triboelectric generators (TEGs) have shown prominent advantages in power density due to the use of thin-film polymeric materials. However, they require either two separate electrodes or a grounded electrode so that net induced charge can be created by charge redistribution. Besides, it lacks a general structure that works for multiple types of mechanical motions. More importantly, all the aforementioned energy-harvesting techniques including the TEG generate ac output; then phase mismatch among separate devices brings a major problem for constructive and area-scalable integration of a number of devices.

Herein we report the regulation of charge transport direction by the coupling of three effects among triboelectrification, electrostatic induction, and semiconducting properties for converting mechanical energy in an area-scalable way. The change of electric potential induced by a moving triboelectric-charged object alters the Fermi level of a working electrode. For two series-connected p-n junctions that are bridged by the working electrode in between, such an alternation of the Fermi level essentially introduces transient bias voltages of opposite polarities across the two p-n junctions, making one forward-biased while the other reverse-biased. The asymmetric rectifying property of the junctions makes them act as unidirectional “gates” that regulate the direction of charge transport. As a result, the induced electrons can only flow in a single direction. Theoretical analysis of the electricity-generating process is conducted by analytical calculation and numerical simulation. Based on the above principle, a new class of integrated direct-current triboelectric generators (dc-TEGs) is developed. They can effectively harvest energy from air flow, rotation, and feet motions. The generated electricity can be either stored in batteries or used for applications such as lighting and wireless sensing. Compared to other energy-harvesting techniques including the previously reported TEGs, the integrated dc-TEG possesses several significant advantages. First, it has a planar structure with only one layer of electrode that has extremely small thickness. Second, electricity can be generated regardless of how the external object interacts with the integrated dc-TEG, i.e. either intermittent contacts or continuous sliding. Most importantly, the output current from different units can always constructively add up even though they are not synchronized, which proposes a practical route to scaling up TEGs and other energy-harvesting techniques.

Reference

[1] Z. L. Wang, J. Song, *Science* **2006**, *312*, 242.

[2] G. Zhu, J. Chen, T. Zhang, Q. Jing, Z. L. Wang, *Nat. Commun.* **2014**, *5*. 3426.

[3] T. Thundat, *Nat. Nanotechnol.* **2008**, *3*, 133.

[4] A. Varpula, S. J. Laakso, T. Havia, J. Kyynäräinen, M. Prunnila, *Sci. Rep.* **2014**, *4*. 6799.

[5] J. Bae, J. Lee, S. Kim, J. Ha, B.-S. Lee, Y. Park, C. Choong, J.-B. Kim, Z. L. Wang, H.-Y. Kim, *Nat. commun.* **2014**, *5*. 4929.

[6] B. Y. Lee, J. Zhang, C. Zueger, W.-J. Chung, S. Y. Yoo, E. Wang, J. Meyer, R. Ramesh, S.-W. Lee, *Nat. Nanotechnol.* **2012**, *7*, 351.

[7] R. Vullers, R. van Schaijk, I. Doms, C. Van Hoof, R. Mertens, *Solid-State Electron.* **2009**, *53*, 684.

[8] J. Briscoe, M. Stewart, M. Vopson, M. Cain, P. M. Weaver, S. Dunn, *Adv. Energy Mater.* **2012**, *2*, 1261.

Copper-based ink for conductive printed layers

S. Koutcheiko, B. Griffith

National Research Council Canada, National Institute for Nanotechnology, Edmonton , T6G 2M9 Alberta

Ink-jet printing of copper is an attractive method for patterning conductive layers due to low waste and low cost. A copper compound based ink which can be used for material printing on flexible substrate such as paper has been developed. A new ink was formulated by mixing copper organic precursor with pure copper nanoparticles of a size below 100 nm. The viscosity and surface tension of the ink was properly adjusted for ink-jet printing. Printed material decomposes into conductive copper layer at the temperature below 260 ^{o}C in flowing forming gas (1-5% of hydrogen balanced with nitrogen).

Deposition and electrochemical properties of magnetite thin film prepared by electron beam evaporation

Mansoo Choi[1], Jei-Kwon Moon[1], Wang-Kyu Choi[1*]

[1] *Decontamination and Decommissioning Research Division, Korea Atomic Energy Research Institute, Daejeon 305-353 Korea*

*Corresponding author e-mail: nwkchoi@kaeri.re.kr

Iron-based oxide materials have been regarded as great importance for technologies and applications. Among them, magnetite (Fe3O4) has been thoroughly investigated as lithium intercalation electrodes because of its low cost, eco-friendliness, natural abundance, and high theoretical capacity. However, the poor rate capability and rapid capacity fading upon the cycling caused by agglomeration and volume expansion during the charge-discharging process prevent its practical application for anode electrode. In this study, the Fe3O4 thin film as anode material for energy storage device was prepared by electron beam evaporator system. The as-fabricated Fe3O4 thin film readily used as anode electrode and investigated the electrochemical performance of anode electrode versus Li.

Keywords: Magnetite, thin film, anode, energy storage device

[1] H. CHENG, Z. LU, R. MA, Y. DONG, H. E. WANG, L. XI, L. ZHENG, C. K. TSANG, H. LI, C. Y. CHUNG, J. A. ZAPIEN Y. Y. LI, 2012. : Rugated porous Fe3O4 thin films as stable binder free anode materials for Li ion batteries. J. Mater. Chem., 22, 22692-22698.

N-type Bi-Te and p-type Sb-Te thin films in application for thermoelectric energy harvesting

Seoungwoo Han*, Su Hyun Lee, Chang-Soo Woo

Korea Institute of Machinery & Materials, Department of Nano Mechanics

171 Jang-dong, Yuseong-gu, Daejeon, 305-343, Korea

*swhan@kimm.re.kr

Thermoelectric thin films are usually applicable for energy harvesting smaller amounts waste heat in the order of micro watts to a few watts. Thermal energy harvesting using thin film thermoelectric generators is a promising approach to alleviate the power supply challenge in low power systems

In this study, thermoelectric n-type Bi-Te and p-type Sb-Te thin films were deposited on various substrates temperature by co-evaporation. Bi-Te and Sb-Te thin films were analyzed using X-ray diffraction, field emission–scanning electron microscopy and energy dispersive X-ray spectroscopy. The thin films were measured electrical properties and Seebeck coefficient. Thermal conductivity was measured by 3-omega method and TDTR (Time-domain thermoreflectance).

The Bi-Te film deposited on 200℃ substrate had Seebeck coefficient of -198.92 μV/K, power factor of 1.51 $mW/K^2 \cdot m$ and ZT of 0.46. The Sb-Te film deposited on 250℃ substrate had Seebeck coefficients of 232.25 μV/K, power factor of above 2.18 $mW/K^2 \cdot m$ and ZT of 0.41.

Keywords: Thermoelectric thin film, substrate temperature, Seebeck coefficient, thermal* c*onductivity, figure of merit

Symposia 3

Advances in Polymers and Ceramics

- Progress in the synthesis of polymers and ceramics
- Advances in the characterization techniques for polymer and ceramics
- Theoretical Studies and Modeling of polymer and ceramics
- Biomedical and Cosmetic Applications of polymers
- Optoelectronics, sensing, energy and electronic Applications of polymers
- Polymer materials from renewable resources
- Nanofabrication and Nanopatterning of polymers: Challenges and Innovation
- Porous Polymers and ceramics
- Electroactive polymers (ionic and electronic), shape memory polymers, and ionic gels
- Advanced Ceramic Materials and Processing for Photonics and Energy
- Next Generation Bioceramics and Biocomposites
- Modelling of processes and properties of polymers and ceramics
- Others

Index Page

Effect of sintering temperature and micro structural analysis on sol-gel derived silver bismuth titanate ceramics

S. Supriya[a,b,*], Chaoyu You[a], F. Fernández-Martinez[a]

[a]Mechanical Engineering, Chemistry and Industrial Design Department, E.T.S.I.D.I, Technical University of Madrid (UPM), Madrid-28012, Spain.

[b]Department of Physics, Velammal Institute of Technology, Panchetti, Thiruvallur Dist- 601 204, Tamilnadu, India.
*Corresponding author Tel.: +34 91 336 7682 Fax: +34 91 530 9244
E-mail: sciencepriya@gmail.com (S. Supriya)

The silver bismuth titanate electroceramics with various grain sizes were synthesized by strearic acid gel method. The density measurement was calculated based on pycnometric method. The relative density of silver bismuth titanate pellet was calculated as 64.91 %. The microstructure analysis establishes the relationship between the sintering temperature and grain size. Moreover, the micrographs show the pores and oriented particles of nano meter to micrometer size. The effect of sintering temperature on grain growth behavior of sol-gel derived porous silver bismuth titanate sample was discussed in detail.

Effects of Flux on the Phase Formation and the Luminescence of $MgGa_2O_4:Mn^{2+}$ Green-emitting Phosphors

Wonsik Ahn, Minhyuk Im, Young Jin Kim*

Department of Advanced Materials Engineering, Kyonggi University, Suwon 443-760, Korea

**Corresponding author: yjkim@kgu.ac.kr*
Presenting author: wonsik0223@naver.com

Mn^{2+}-doped XGa2O4 (X = Mg^{2+}, Zn^{2+}) spinels are green-emitting phosphors and have been developed for use in plasma display panels, field emission displays, and white light emitting diodes because of their high luminescence efficiencies under UV excitation. In this work, MgGa2O4:Mn^{2+} powders were synthesized by a flux method using boric acid, and the effects of flux on the phase formation and the photoluminescence (PL) were investigated. Rietveld refinement was performed to determine the crystal structure, confirming that the MgGa2O4 single phase was formed, and that the Mn^{2+} ions were completely substituted for the Mg^{2+} ions. The PL excitation spectra consisted of a broad peak (295 nm) and sharp peaks (380 nm, 425 nm, and 440 nm), which were assigned to the charge transfer band of Mn^{2+}–O^{2-} and forbidden d–d transitions of the Mn^{2+} ions [(^{6}A1 → ^{4}T2 (^{4}D), ^{6}A1 → ^{4}A1 (^{4}G)/^{4}E (^{4}G), ^{6}A1 → ^{4}T2 (^{4}G)].The PL spectra exhibited the strong green emission, which originated from the ^{4}T1 → ^{6}A1 transition of the Mn^{2+} ions. The crystallinity and particle morphologies were strongly affected by the amount of flux, leading to the change in the PL spectra. These behaviors were explained and discussed, considering the change in the structure and the crystal field surrounding the Mn^{2+} ions.

Keywords: Magnesium gallate, manganese, phosphors, luminescence

[1] SONG, E. H., WANG, J. L., YU, D. C., YE, S. & ZHANG, Q. Y. 2014. Anomalous tunable visible to near infrared emission in the Mn^{2+}-doped spinel MgGa2O4 and room-temperature upconversion in the Mn^{2+} and Yb^{3+}-codoped spinel. *J. Mater. Chem. C*, 2, 8811–8816.

Preparation and characterization of （xCe,yEu）:$Y_{3-x-y}Al_5O_{12}$ phosphor by high-temperature solid-state reaction

Gui-sheng GAN[1,2,] , Yiping Wu[1], Chen Bida[1], Donghua Yang[2]

1.College of Materials Science and Engineering, Huazhong University of Science and Technology, Wuhan 430074, China

2.Chongqing Municipal Engineering Research Center of Institutions of Higher Education for Special Welding Materials and Technology (Chongqing University of Technology), Chongqing 400054, China
ggs@cqut.edu.cn

White light emitting diodes, the so-called next generation solid-state lighting sources, were gaining lots of attentions because of their numerous advantages over the existing incandescent and fluorescent lamps in energy saving, reliability, lifetime and environment-amity. Although the white radiation can be generated from many methods, the combination of a GaN-based blue LED and a cerium-activated yttrium aluminum garnet (YAG:Ce3+) phosphor was the most popular and sophisticated method at present. However, this strategy suffered from low color-rendering index (CRI) and high color-temperature due to the weak emission intensity in red spectral region. An efficient way to improve the temperature stability of YAG:Ce3+ phosphor was absent in this paper. Ce:$Y_{3-x}Al_5O_{12}$ (x=0.01~0.15) and （xCe,yEu）:$Y_{3-x-y}Al_5O_{12}$ phosphor were synthesized by high-temperature solid-state reaction respectively at first, then the structural properties were studied by using their XRD measurements and the luminescent properties of these phosphors were investigated by the measurement of their excitation and emission spectra. The experimental results have shown that Ce:$Y_{3-x}Al_5O_{12}$ phosphor had a strong excitation peak at 460nm, the light emitting intensity maximum with 347lm in Ce:$Y_{3-x}Al_5O_{12}$ phosphor can be measured at x=0.075. The emission intensity increased at first and then decreased from 0.01 to 0.15 with the Ce^{3+} ion concentration increases, but the color temperature decreased and the size of Ce:$Y_{3-x}Al_5O_{12}$ phosphor increased respectively. With the Eu^{2+} ion concentration increases at the same concentrations of Ce^{3+}, the size of xCe,yEu ）:$Y_{3-x-y}Al_5O_{12}$ phosphor increased at first and then decreased, but the color temperature was just the opposite, however the emission intensity decreased. At the same concentrations of Eu^{2+}, the size of （xCe,yEu）:$Y_{3-x-y}Al_5O_{12}$ phosphor decreased at first and then increased with the increasing of Ce^{3+} ion concentration, but the emission intensity increased and the emission intensity decreased. The xCe,yEu :$Y_{3-x-y}Al_5O_{12}$ phosphor with x=0.075 and y=0.005 had the the best optical properties, the emission intensity and the color temperature were 268.94 lm and 3966 K respectively.

Keywords: white LED; YAG phosphor; high-temperature solid-state; doping element

Upconversion luminescence of (Lu,M)NbO_4:Yb^{3+}/Er^{3+} (M: Al^{3+}, Ga^{3+})

Jieun Park, Young Jin Kim*

Department of Advanced Materials Engineering, Kyonggi University, Suwon 443-760, Korea

**Corresponding Author: yjkim@kgu.ac.kr*
Presenting Author: jieun5550@naver.com

(Lu,M)NbO_4:Yb^{3+}/Er^{3+} (M: Al^{3+}, Ga^{3+}) powders were prepared by a flux method and their upconversion (UC) luminescent properties were investigated. The XRD patterns of the synthesized powders corresponded to those of LuNbO4, demonstrating that a LuNbO4 single phase was formed, and that the Yb^{3+}, Er^{3+}, Al^{3+}, and Ga^{3+} ions were completely incorporated into the host lattices. The synthesized powders were activated by infrared (980 nm) radiation, and their photoluminescence (PL) UC spectra were composed of the strong green and weak red emission bands, which were assigned to the transition of the ^{2}H11/2/^{4}S3/2 levels and ^{4}F9/2 to the ground state (^{4}I15/2) of the Er^{3+} ions, respectively, through an energy transfer process from Yb^{3+} to Er^{3+}. The emission ratio of green to red depended on the ratio of Yb^{3+}/Er^{3+}. The substitution of the Al^{3+} and Ga^{3+} ions caused the modification of the host structure, resulting in the change in the UC spectra.

Keywords: $LuNbO_4$, upconversion, luminescence, energy transfer

[1] KWON, S. H., KIM, Y. J. 2013. Enhancement of Up-Conversion Emission of Na(Y,Al)F4:Yb^{3+}/Er^{3+} Prepared by a Solvothermal Method. *ECS J. Solid State Sci. Technol.* 2, R223–R236.

Variation in thermoelectric characteristics of ZnO nanofibers by thermal treatment

Yoonbeom Park, Kyoungah Cho*, Donghoon Lee and Sangsig Kim**

Department of Electrical Engineering, Korea University, Anam-ro 145, Sungbuk-gu, Seoul 136-701, Korea

E-Mail: lancerevo@korea.ac.kr, chochem@korea.ac.kr, sangaig@korea.ac.kr

Recently, oxide nanofibers (NFs) have attracted much attention as environmentally friendly thermoelectric materials that are distinct from conventional thermoelectric materials including bismuth telluride compounds [1, 2]. Over the years, adjustments to heating temperature and cooling rate have been attempted to achieve oxide NFs with high thermoelectric efficiency [3, 4]. Nevertheless, there are few studies on the effect of heating time on thermoelectric characteristics. Hence, we investigate in this study the effect of thermal annealing time on the thermoelectric characteristics for *n*-type ZnO NFs prepared by electrospinning. NFs prepared by electrospinning are transformed into *n*-type ZnO NFs after thermal heating for 30 min at 550 ºC. For the ZnO NFs, the Seebeck coefficient decreases from -132.1 μV/K to -44.6 μV/K with a heating time from 30 to 120 min, while the electrical conductivity increases from 2.07×10^{-3} to 0.18 S/m. The inverse variation in the Seebeck coefficient and the electrical conductivity originates from a contraction in the diameters of the NFs with heating time because there is a relationship between the diameter of the NFs and the charge carrier concentration. The ZnO NFs heated thermally for 60 min have a maximum power factor of 0.46 nW/K^2m. Our study demonstrates that sintering time has an influence on the thermoelectric characteristics of ZnO NFs through the thermal contraction of the diameters.

Keywords: ZnO, nanofiber, thermal treatment, thermoelectric

[1] MA, F., OU, Y., YANG, Y., LIU, Y., XIE, S., LI, J., CAO, G., PROKSCH, R. & LI, J. 2010. Nanocrystalline Structure and Thermoelectric Properties of Electrospun $NaCo_2O_4$ Nanofibers. *J. Phys. Chem. C*, 114, 22038-22043.
[2] XU, W., SHI, Y. & HADIM, H. 2010. The fabrication of thermoelectric $La_{0.95}Sr_{0.05}CoO_3$ nanofibers and Seebeck coefficient measurement. *Nanotechnology*, 21, 395303-395308.

[3] ZHANG, M., PARK, H., KIM, J., PARK, H., WU, T., KIM, S., PARK, S., CHOA, Y. & MYUNG, N. V. 2015. Thermoelectric Properties of Ultralong Silver Telluride Hollow Nanofibers. *Chem. Mater*., 27, 5189-5197.

[4] MAENSIRI, S. & NUANSING, W. 2006. Thermoelectric oxide $NaCo_2O_4$ nanofibers fabricated by electrospinning. *Mater. Chem. Phys*., 99, 104-108.

Formulation and estimating the fire behavior of thin film intumescent coatings using flame retardant bio-filler

This paper analyzes the fire protection performance, char formation and heat release characteristics of the thin film intumescent coatings that incorporate eggshell (ES) as a bio-filler. In this study, the Bunsen burner and the fire propagation (BS 476: Part 6) tests of coatings were measured. Experiments on the samples were also tested to evaluate their fire behavior using a cone calorimeter according to ISO 5660-1 specifications. On exposure, the samples B, C and D had been certified to be Class 0 because their fire propagation indexes were less than 12. Samples B and D showed a significant reduction in total heat rate (B=11.6 MJ/m^2 and D=12.0 MJ/m^2) and uniform char structures with the addition of 3.30 wt.% and 2.75 wt.% ES bio-filler, respectively. As a result, ES bio-filler composition good to slow down the fire expanding due to its positive synergistic effect with flame retardant ingredients on physical and chemical reactions in fire protection.

Structure Investigation of $La_{1-x}Sr_x(Na, K, Ba)MnO_3$ Nanoparticles by X-ray Absorption Spectroscopy (XAS) Technique

S. Daengsakul[2], P. Kidkhunthod[1], N. Tookokkruad[2], and S. Maensiri[3]

[1]Synchrotron Light Research Institute (Public Organization), 111 University Avenue, Muang District, Nakhon Ratchasima 30000, Thailand

[2] Physics Department, Faculty of Science, Khon Kaen University, Muang District, Khon Kaen, 40002, Thailand

[3]School of Physics, Institute of Science, Suranaree University of Technology, Nakhon Ratchasima, 30000, Thailand

Email: pinit@slri.or.th

This work presents the structural study of $La_{1-x}Sr_x(Na, K, Ba)MnO_3$ or LSAM nanoparticles synthesized using thermal-hydro decomposition method where A denotes Na, K and Ba, respectively. The effect of A dopants and the size mismatch of A-site cations, from the substitution of A for La and Sr on the MnO_6 octrahedral structure is focused. The LSAM nanoparticles are carefully studied and analized using X-ray diffraction (XRD) including Rietveld refinement and X-ray Absorption Spectroscopy (XAS) including X-ray Absorption Near edge Structure (XANES) and X-ray Absorption Fine Structure (EXAFS). The XRD-Rietveld refinement results show that all nano-powder samples have rhombohedral structure. From the XANES technique we found that the effect of A substitutions at A-site causes a slight change of mean oxidation state of Mn between 3.4 and 3.6. Furthermore, the results of MnO_6 octrahedral analysis obtained from EXAFS technique show that the local structure around Mn atoms for all LSAM samples can be explained by 4(s) +2(l) model and by 6 model [1].

Keywords: *LSAM nanoparticles, X-ray Absorption Spectroscopy, Rietveld refinement*

[1] Cherif, K., Dhahri, J., Vincent, H., Zemni, S., Dhahri, E. and Oumezzine, M., *Physica B* vol. 321, 48-53 (2002)

The properties of color mortar using inorganic pigment and redispersible polymer

Uihyeon Jeon[1], Dohyeong Kim[2], Minu Park[2], Pilyong Youn[2],

Jinhyeok Kim[2], Hongseok Jang[2]

[1]Seo-Do Construction, Jeonju, Republic of Korea, 54966, Republic of Korea

[2]Department of Architectural Engineering, Chonbuk National University, Research Center Industrial Technology, 561-756, Republic of Korea

rcit@jbnu.ac.kr *Tel: +82-10-2613-5170*

Polymer provides a dual effect for mortar: In the fresh, wet paste (within the first ~ 60 min), polymer solely acts as a water retention agent while later, when the water has been consumed by hydration and desiccation, polymer modifies the mechanical properties of mortar through polymer film formation in the cementitious matrix [1] and physical plugging of pore spaces existing in the cement mortar by associated 3D polymer networks [2,3]. This polymer films prevent the transport of soluble calcium towards the surface, and decreases efflorescence. This is due to the reduction of overall amount of micro pore. This study was to investigate the color expression characteristics and physical properties of colored mortar using acrylic polymer, and the basic data for the manufacture of economical color concrete using redispersible polymer was provided.

Following are results of a study on the “Leaders Industry university Cooperation” Project, supported by the Ministry of Education, Science & Technology (MEST).

Keywords: redispersible polymer, inorganic pigment, color mortar

[1] D. Bülichen, J. Kainz and J. Plank, *Cement Concrete Res.* 42 (**2012**)

[2] A. Jenni, L. Holzer, R. Zurbriggen and M. Herwegh, *Cement Concrete Res. 35* (**2005**)

[3] A. Jenni, R. Zurbriggen, M. Herwegh, L. Holzer, *Cement Concrete Res.* 36 (**2006**)

Bacterial cellulose/gelatin/alginate composite films and their properties for biomedical application

Chiaoprakobkij[1], Phisalaphong[1], Seetabhawang[1], Sanchavanakit[2]

[1]Chemical Engineering Research Unit for Value Adding of Bioresources,
Department of Chemical Engineering, Faculty of Engineering, Chulalongkorn University,
Phayathai Rd.,Patumwan, Bangkok, 10330, Thailand.

[2]Department of Anatomy, Faculty of Dentistry, Chulalongkorn University, Bangkok 10330, Thailand

E Mail/ Contact Details: muenduen.p@chula.ac.th

Biocomposite films of bacterial cellulose (BC), alginate (A) and gelatin (G) were developed for biomedical application. Glycerol as a plasticizer was added to improve plasticity and to prevent shrinkage of the films during drying process. The films were fabricated by air-dried casting method. Effects of each component on film characteristics were investigated. The modified films were characterized for physical, chemical, mechanical and biological properties. Based on physical and mechanical properties, the optimal composition of the composite films was at the ratio of BC/A/G equal to 60/20/20 (by weight). Fourier transform infrared (FT-IR) spectroscopy showed the existence of some physical interactions in intermolecular level of the composite films [1]. X-Ray diffraction patterns showed no new peak, but the addition of glycerol would lead to a slight increase in BC crystallinity [2]. The water absorption capacity of the composite films increased when compared to that of BC film. The water vapor permeability (WVTR) of the plasticized films was slightly higher than that of the non-plasticized ones. The improvement of WVTR of the films could be caused by the modified fiber morphology, resulting in a larger free volume [3]. The composite BC/A/G films showed considerably improved mechanical properties, with increases in the Young's modulus and tensile strength. The results indicated the good interfacial, adhesion, interaction and well-dispersion in the blends. The BC/A/G film showed no cytotoxicity against Vero cells and could also promote cell spreading and cell adhesion. Tear resistance testing by suturing the BC/A/G film to pig skin with a monofilament nylon thread showed that the film was able to be sutured, since it resisted to the surgical needle and thread including force during the procedure and it was well attached to the pig skin. The novel BC/A/G film has several potential advantages to be applied as a biomaterial for biomedical engineering.

Keywords: bacterial cellulose, gelatin, alginate, biomaterials, membrane

[1] VANIN, F., SOBRAL, P. MENEGALLI, C., CARVALHO, A. & HABITANTE, M. 2005. Effects of plastizicers and their concentration on thermal and functional properties of gelatin-based films. *Food Hydrocolloids*, 19, 899-907.
[2] BERGO, P & SOBRAL, A. 2007. Effects of plasticizer on physical properties of pig skin gelatin films. *Food Hydrocolloids*, 21, 1285-1289.
[3] DONG, Z. WANG, Q & DU, Y. 2006. Alginate/Gelatin blend films and theirs properties for drug controlled released. *Journal of membrane science*, 280, 37-44.

Binary Blends of Poly(3-hydroxybutyrate)/Poly(β-alanine) and Its Derivatives: New Tissue Scaffold Materials

Efkan (Çatıker)[1], Elvan (Konuk)[2], Tuğçe (Gültan)[3], Menemşe (Gümüşderelioğlu)[3]

[1]Faculty of Art&Science, Department of Chemistry, Ordu University, 52200, Ordu, Turkey

[2]Inst. of Graduate Studies in Science, Nanotechnology and Nanomedicine, Hacettepe University

[3]Faculty of Engineering, Chemical Engineering Department, Hacettepe University, 06800, Ankara, Turkey
ecatiker@gmail.com/mobile:+905335623764

Poly(3-hydroxybutyrate) (P3HB), is a typical natural polyester, produced by many microorganisms as intracellular carbon and energy storage. P3HB has some undesirable properties such as processing difficulty and brittleness due to its high crystallinity, high hydrophobicity and low biodegradation rate comparing to the polylactides besides its positive properties such as biodegradability and biocompatibilty that enable it to be used as a tissue scaffold. The study aims to either suppress the properties of P3HB limiting its use as a biomaterial (to decrease crystallinity and hydrophobicity of P3HB, ease of processability) or bring P3HB in some desirable properties (to improve the rate of biodegradation, cell adhesion and proliferation). For this purpose, poly-β-alanine (PBA), poly(α-methyl-β-alanine) (mPBA) and poly(N-(3-methoxypropyl)-β-alanine) (PNMPBA) were synthesized by hydrogen transfer polymerization (HTP) [1] using corresponding monomers. Characterization of the prepared polymers was done by using FTIR, ^{1}H-NMR and MALDI analyses. In order to fabricate 3D scaffolds P3HB/PBA, P3HB/mPBA and P3HB/PNMPBA blends' with different compositions (polyamide content: 2%-5%-10% by mass) were prepared. Briefly, 5% (w/v) P3HB solution with different polyamide contents was dissolved in chloroform at 60-65□C and then, it was mixed with (1:1) acetic acid to obtain emulsion solution. Pre-frozen emulsion was freeze-dried at -80□C for 5 days and acetic acid droplets were removed from structure to produce porous scaffold. Characterization of matrices was done by optical (SEM), spectroscopic methods (FTIR, XRD), thermal analysis (DSC), mechanical durability test (compression test), swelling test, and porosity and wettability measurement. Thus, we had information about both characterization of tissue scaffolds and miscibility of the components in the binary blends. SEM results represent the morphology of scaffolds varies with composition of blends. According to the results, the scaffolds with desired porous structure (pore size and interconnectivity) were obtained by blending P3HB with 2% PBA.

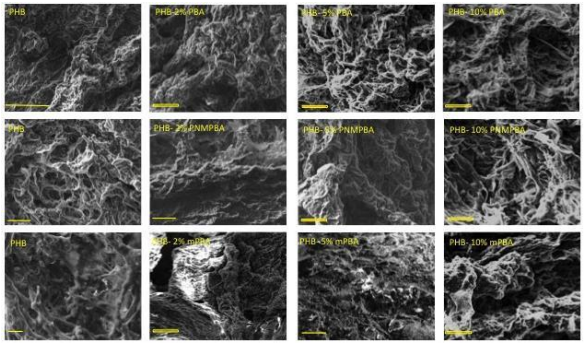

Figure 1: *A morphological feature of P3HB scaffolds and PBA blends (Scale bars represent 100µm at 500x, 20µm at 1 Kx and 10µm at 1,5 KX magnification for P3HB, respectively. Other bars represent 20µm at 1 Kx magnification).*

Compression test results indicate the compression strength and elastic modulus of scaffolds decrease with increasing blending ratio. While compression strength and elastic modulus are 14.0 kPa and 27.4 kPa, respectively, for P3HB scaffolds, they are 5.7 kPa and 12.1 kPa for P3HB-2%PBA scaffolds. The cytotoxicity test (MEM-extract test, MTT test for 72 h incubation) was performed with respect to the ISO 10993/EN 30993 standard. Briefly, 150 g scaffolds were extracted at 37ºC for 24 h in 30 ml of 10% fetal bovine serum containing Dulbecco's modified Eagle's medium. L929 mouse fibroblasts were incubated at an inoculation density of $6x10^4$ cells/ml with various dilutions of extract (0%, 25%, 50%, 100%). The MTT analysis was conducted for 3 days and results demonstrate that neither P3HB nor PBA derivatives have cytotoxic effect for cells even if blending ratio is applied 10%. These preliminary results indicated that P3HB-PBA blends can be considered suitable candidate material for the fabrication of freeze-dried issue scaffolds.

Keywords: Tissue scaffold, polymer blends, poly(3-hydroxy butyrate), poly-β-alanine

[1] **GUR'EVA**, L. L., TKACHUK, A. I., DZHAVADYAN, E. A., ESTRINA, G. A., SURKOV, N. F., SULIMENKOV, I. V., ROZENBERG, B. A. 2007. Kinetics and Mechanism of the Anionic Polymerization of Acrylamide Monomers, Polymer Science Series A, 49(9), 987-999.

Optimization of Design Parameters for Biodegradable Stent Manufacturing with 3d Printer

Osman Iyibilgin[1,2,C] , Muhammet Baran Çikili[1] , Fehim Findik[2,3]

[1] Sakarya University, Eng. Faculty, Mechanical Eng. Dept. Sakarya/Turkey

[2] Sakarya University, BIMAS-RC, Sakarya/Turkey

[3] Sakarya University, Technology Faculty, Metallurgy & Materials Eng. Dept. Sakarya/Turkey

[C] Corresponding Author: Tel: **+90 5332417860**, e-mail: **ibilgin@sakarya.edu.tr**

Stents are elements used for opening the blocked veins in the body. They are designed to open the blocked region and resist the inner compressive forces. In the present study, various stents in diverse pattern structure will be designed in a virtual environment. In the next step, the optimal stent geometry will be determined. Finally, a detailed analysis will be performed on the dimensions and cross sections of different design prototypes. The purpose of the current study is to perform the required design changes to minimize the stresses forming in the stent geometry generated from the biocompatible photopolymer. Then selecting the most suitable pattern structure, the stresses on the stent will be determined for different materials. Later, an infrastructure will be formed for the biocompatible metallic stent planned for the production. As a result of the obtained knowledge, the most suitable pattern structure will be determined. It will then be used in the metallic stent production. After apprehending the stent model production achieved the design, the analysis results will be correlated with the experimental data.
As a result, forming the stent geometry and when determining the pattern structure repeating itself, the following conclusions will be reached as required:

- Avoiding sharp corners,

- Designing the stent geometry to allow for growth in the diameter, thus minimizing the stresses in the section

- Occurring length shortening and ensuring the shrinking area remain large enough to fully support depending on the growth in stent diameter.

Keywords: Stent, Biocompatible, Stress Distribution, Finite Element (FE) Analysis

Poly(methyl methacrylate) supported TiO_2 nanostructures for stereolithographic dentures

Eftimie Totu E.[1], Cristache C.M.[2]

[1]Department of Analytical Chemistry and Environment Engineering, Faculty of Applied Chemistry and Materials Science, University Politehnica of Bucharest, 1-7 Polizu St., sector 1, 011901, Bucharest, Romania

[2] Department of Dental Techniques, Faculty of Midwifery and Medical Assisting, "Carol Davila" University of Medicine and Pharmacy, Bucharest, 8 Eroii Sanitari Blvd., sector 5, 050474, Bucharest, Romania,

eugenia_totu@yahoo.com, corinacrstache@gmail.com

Nowadays there are important challenges to overcome in the area of dentistry. Different laboratories developed various materials based on nanomaterials for tissue regeneration, alveolar bone applications as well as for dental implant surgery. Actually, the most popular denture material, poly(methyl-methacrylate) (PMMA) which is used for its optical properties, biocompatibility and aesthetics, presents few important drawbacks, namely: limited mechanical strength and ductility, water sorption, limited resistance to bacterial attacks and also lack of radio-opacity [1, 2]. Lately, there are important efforts directed towards synthesis of new improved biocompatible polymer for dental applications [3]. Through our work, we propose PMMA supported titania nanostructures as an improved alternative for a composite biomaterial. The TiO_2 nanoparticles used as additive improve physicochemical, optical and electrical properties of materials and enhance the mechanical resistance, transforming the polymer-nanoTiO_2 based composite an attractive material for dental usage, being known that TiO_2 nanoparticles are useful tools in nanotherapeutics [4]. Considering the antimicrobial properties of TiO_2 nanoparticles - following an induced photocatalytic production of oxygen radicals, it is expected to obtain a denture characterized by a low adherence of microbial agents. Our material, based on PMMA and titania nanoparticles presenting specific UV photo-reticulation properties allows the manufacturing of dental prosthesis applying CAD/CAM modeling and a subsequent stereolithographic technique. In this way, it is possible to obtain a complete denture available for any dental laboratory adequately equipped. In our work, we assured a corresponding bonding between additive and polymeric matrix for improving the mechanical and anti-bactericidal properties of dental composites. Thus, the TiO_2 nanoparticles are functionalized with glycidil methylmethacrylate using a coupling agent and afterwards blended with methacrylate monomers to produce a precursor of UV-cured nanocomposite material. The applied preparation method of TiO_2 nanoparticles was the sol-gel synthesis [5], presenting important advantages: low working temperatures, versatility of performance, and the product homogeneity at molecular level. The new composite material fully physicochemical characterized (SEM, TEM, X-rays, FT-IR, thermal analysis) allows to design personalized 3D printed complete dental prosthesis. The effectiveness and quality of the 3D printed complete dental prosthesis is assessed through clinical follow-up at

various periods (1 and 6 months) of a patients' task group to whom such dental devices were inserted. The performed clinical evaluation creates the premises for optimizing the composite material and the execution technique for the 3D printed dental prosthesis according to the results of the clinical studies.

Keywords: Stereolithography, PMMA, TiO_2 nanoparticles, denture, CAD/CAM

[1] AKIN H., TUGUT F., GUNEY U. & AKAR T. 2014. Shear Bond Strength of Denture Teeth to Two Chemically Different Denture Base Resins After Various Surface Treatments. *J Prosthodont*., 23(2),152-156.

[2] AKIN H., TUGUT F. & POLAT Z.A. 2015. In Vitro Comparison of the Cytotoxicity and Water Sorption of Two Different Denture Base Systems. *J Prosthodont*., 24(2), 152-155.

[3] ARIOLI FILHO J.N., BUTIGNON L.E., PEREIRA R.de P., LUCAS M.G. & MOLLO F. de A., Jr. 2011. Flexural Strength of Acrylic Resin Repairs Processed by Different Methods: Water Bath, Microwave Energy and Chemical Polymerization. *J Appl Oral Sci*., 19(3), 249-253.

[4] CHIDAMBARAM M. & KRISHNASAMY K. 2012. Nanotoxicology: Toxicity of Engineered Nanoparticles and Approaches to Produce Safer Nanotherapeutics. *International Journal of Pharma Sciences*, 2 (4), 117-122.

[5] BAGHERI S., MOHD HIR Z.A., YOUSEFI A.T., & ABDUL HAMID S.B. 2015. Progress on Mesoporous Titanium Dioxide: Synthesis, Modification and Applications. *Microporous and Mesoporous Materials*, 218, 206-222.

Redox-responsive poly(amido amine)s from trifunctional amines for bioapplications

Ye Liu

Institute of Materials Research and Engineering, A*STAR (Agency for Science, Technology and Research), 2 Fusionopolis Way, Innovis #08-03, Singapore 138634.
Email: ye-liu@imre.a-star.edu.sg

Through exploring the large difference in redox potential between intramolecular compartments and extracellular matrix, redox-responsive disulfide containing polymers, which will be stable in intracellular spaces but be degraded in extracellular spaces, are promising for many bio-applications[1, 2]. On the basis of our previous fundamental understanding of Michael addition polymerization of trifunctional amines and acrylic monomers [3-5], we have developed redox-responsive linear and hyperbranched poly(amido amine)s via Michael addition polymerization of trifunctional amines and disulfide-containing bisacrylamide for drugs delivery,[6-9] gene delivery,[10] bioimaging,[11] and MRI[12].

Keywords: Michael addition polymerization; trifunctional amines; redox-responsive; drug delivery; gene delivery.

References:

1. Bauhuber, S., Hozsa, C., Breunig, M., & Gopferich, A. Advanced Materials, 2009, 21, 3286-3306.
2. Meng, F.H., Hennink, W. E., Zhong, Z.. Biomaterials, 2009, 30, 2180-2198.
3. Liu, Y. Wu, D. C., Ma, Y. X. Tang G. P., Wang S., He, C. B., Chung, T. S., Goh, S. T. Chemical Communications, 2003, 2630-2631.
4. Wu, D. C., Liu, Y., He, C. B., Chung, T. S., Goh, S. T. Macromolecules, 2004, 37, 6763-6770.
5. Wu, D. C. Liu Y., Chen, L., He, C. B., Chung, T. S., Goh, S. T. Macromolecules 2005, 38, 5519-5525.
6. Wu, D. C., Loh, X. J., Wu, Y. L., Lay, C. L., Liu, Y. Journal of the American Chemical Society, 2010, 132, 15140-15143.
7. Cheng W. R., Wang G., Pan X. Y., Zhang Y., Tang B. Z., Liu Y. Macromolecular Bioscience, 2014, 14, 14, 347.
8. Weiren Cheng, Guan Wang, Jatin Nitin Kumar, Ye Liu. *Macromolecular Rapid Communications,* 2015, 36 (23), 2102–2106
9. Weiren Cheng; Jatin N. Kumar; Yong Zhang; Ye Liu, pH- and redox-responsive self-assembly of amphiphilic hyperbranched poly(amido amine)s for controlled doxorubicin delivery, *Biomaterials Sci.,* 2015, 3, 597-607.
10. Ping Y., Wu, D. C. Kumar N. J., Cheng W. R., Lay C. L., Liu Y., Biomacromolecules, 2013, 14, 2083-2094.
11. Cheng W. R., Kumar N. J., Zhang Y., Liu Y. Macromolecular Bioscience, 2014, 14, 347.
12. Cheng W. R., Rajendran R., Gu L. Q., Ren W., Zhang Y., Chuang K. H., Liu Y. J. Mater. Chem. B., 2014, 2, 5295-5301.

Surfactant-Free Emulsion-Based Preparation of Redox-Responsive Nanogels

Weiren Cheng[1], Ye Liu[1]

[1]Institute of Materials Research and Engineering, A*STAR (Agency for Science, Technology and Research), 2 Fusionopolis Way, Innovis, #08-03, 138634, Singapore.

chengwr@imre.a-star.edu.sg / (65) 6501 1835

Nanogels are ideal drug carriers as they possess favorable properties of both hydrogels and nanoparticles like hydrophilicity, good drug protection, and improved targeting capability. However, strategies to prepare these nanogels are often very complex and require the usage of potentially cytotoxic surfactant, crosslinkers, initiators, catalysts and monomers. As a result, exhaustive purification has to be performed to remove residual compounds and by-products before pure nanogels which are necessary for biomedical applications can be obtained. Furthermore, loading of active compounds into the nanogels are usually done via physical entrapment, or electrostatic/hydrophobic interaction, thus, the choice of payload is limited and often with poor efficiency, especially for neutral charged carbohydrate-based drugs.

Recently, we have developed a surfactant-free emulsion-based preparation technique for redox-responsive nanogels which does not require purification process and can ensure efficient loading of neutral charged compounds. A mixture of water and PEGylated hyperbranched poly(amido amine)s, poly(BAC2-AMPD1)-PEG in chloroform can spontaneously and feasibly form a water-in-oil emulsion without any energy input. In the emulsion, the dispersed water droplets are stablized and filled with the poly(BAC2-AMPD1)-PEG, and via intermolecular disulfide exchange reaction of these polymers, nanogels are obtained. Water soluble active compounds can be loaded into the nanogels easily by simply dissolving the compounds in water before emulsification.

Keywords: Redox-Responsive, Nanogels, Surfactant-Free Emulsion, Drug Delivery

[1] CHENG, W., KUMAR, J. N., ZHANG, Y. & LIU, Y. 2015. pH- and redox-responsive self-assembly of amphiphilic hyperbranched poly(amido amine)s for controlled doxorubicin delivery. *Biomaterials Science*, 3, 597-607.

[2] CHENG, W., WANG, G., KUMAR, J. N. & LIU, Y. 2015. Surfactant-Free Emulsion-Based Preparation of Redox-Responsive Nanogels. *Macromolecular Rapid Communications*, 36, 2102-6.

Temperature-sensitive silver nanocomposites hydrogels for inactivation of bacterial growth

Tippabattini Jayaramudu[1, 2], Gownalla Malegowd Raghavendra[3], Kokkarachedu Varaprasad[4], Emmanuel Rotimi Sadiku[2], Li Yaguang[1], Jaehwan Kim[1*]

[1] Center for NanoCellulose Future Composite, Dept. of Mechanical Engineering, Inha University, 253 Yonghyun-Dong, Nam-Ku, Incheon 22212, South Korea.
[2] Department of Polymer Technology, Tshwane University of Technology, CSIR-Campus, Building 14D, Private Bag X025, Lynwood Ridge 0040, Pretoria, South Africa
[3] Department of Packaging, Yonsei University, 1Yonseidae-gil, wonju, Gangwon-do220-710, South Korea
[4] Centre de Investigacion de Polimeros Avanzados, CIPA, Beltran Mathieu 224, Piso 2, Concepcion, Chile.

Presenting author: Tippabattini Jayaramudu Email: mr.jayaramudu@gmail.com

* **Corresponding Author:** Prof. Jaehwan KIm
Center for EAPap Actuator, Dept. of Mechanical Engineering, Inha University, 253 Yonghyun-Dong, Nam-Ku, Incheon 402-751, South Korea
E-mail: Jaehwan@inha.ac.kr

The present work reports the temperature-sensitive green tea-based silver nanocomposite hydrogels for the bacterial growth inactivation. The temperature-sensitive silver nanocomposite hydrogels were prepared via free-radical polymerization, using N-isopropyl acrylamide with green tea as the hydrogel matrix. Silver nanoparticles were prepared via bioprocess. The formation of the temperature-sensitive silver nanocomposite hydrogels and the conformation of silver nanoparticles were analyzed by using Fourier transformed spectroscopy, ultraviolet–visible spectroscopy, thermo gravimetric analysis, X-ray diffractometer, scanning electron microscopy-energy dispersive spectroscopy and transmission electron microscopy studies. The temperature-sensitive silver nanoparticles composites prepared were tested for the bacterial growth inactivation. The inactivation of bacteria of the silver nanocomposites hydrogels was studied by inhibition zone method, against gram negative (*Escherichia coli)* and gram positive *(Staphylococcus aureus)*, which suggested that the temperature-sensitive silver nanocomposites hydrogels prepared were helpful for the inactivation of these bacteria's. Therefore, the temperature-sensitive silver nanoparticles generated hydrogels can be used effectively in biomedical (inactivation of bacteria) applications.

Key words: Silver nanoparticles, hydrogel, neem leaves, green process.

[1]. RUEL-GARIEPY, E., & LEROUX, J.C. 2004. In situ-forming hydrogels - Review of temperature-sensitive systems. *European Journal of Pharmaceutics and Biopharmaceutics*. 58(2),409-426, 2004.

[2]. WEI, H., CHENG, S.-X., ZHANG X.-Z., & ZHUO, R.-X. 2009. Thermo-sensitive polymeric micelles based on poly(N-isopropylacrylamide) as drug carriers. *Progress in Polymer Science. 34(9), 893-910.*

[3]. JAFARI, B., RAFIE. F., & DAVARAN, S.2011. Preparation and characterization of a novel smart polymeric hydrogel for drug delivery of insulin. *BioImpacts, 1(2),135-143.*

Volumetric change and remineralizing of dental composites with calcium phosphate silicate

Xiaorong Wu[a,*], Tom Troczynski[b], Weili Xie[c]

[a] Department of Astronautic Science and Mechanics, Harbin Institute of Technology, China

[b] Department of Materials Engineering, University of British Columbia, Canada

[c] Department of Stomatology, Harbin Medical University, China

Dental composite resins are the main direct tooth restorative materials. The more recent research and development efforts on dental composite resins focused on developing adequate strength, high wear resistance and low shrinkage. However, polymerization shrinkage and its accompanying stress may destroy the composite/tooth interfacial bond and lead to recurrent caries. In this paper, dental composite resins with tricalcium silicate (C_3S) and calcium phosphate monobasic (CPM) were synthesized. C_3S hydrates to produce calcium silicate hydrate (C–S–H) gel and calcium hydroxide (CH) which accompanied volume expansion. Polymerization shrinkage of dental composite resins with C_3S fillers were compensated and improved. CPM reacts with the CH to precipitate hydroxyapatite (HAP) in situ within C–S–H which can largely remove CH to enhances its biocompatibility and bioactivity. As the main component of bone and tooth, the precipitate HAP has the potential to remineralize tooth and inhibit caries. FTIR, SEM, WXRD, DSC were used to characterize the microstructures of dental composite resins. Comprehensive properties were assessed include mass and volume change, polymerization shrinkage, mechanical properties, water adsorption, ion release and remineralization properties. The results showed that the experimental dental composite resins incorporated with calcium phosphate silicate had volumetric expansion to compensate shrinkage, antibacterial and remineralizing components and competitive mechanical properties.

A new estimation of the bioactive components in the sericin layer of silkworm cocoon as a stock of functional biomaterials

Jin-Ge Zhao and Yu-Qing Zhang*

Silk Biotechnology Laboratory, School of Biology and Basic Medical Sciences, Soochow University; RM702-2303, No. 199, Renai Road, Dushuhu Higher Edu. Town, Suzhou 215123; P R China
*Corresponding author: 086-0512-65880181(Tel/Fax); E-mail: sericult@suda.edu.cn

The cocoon shell of the silkworm *Bombyx mori* is mainly composed of ~70% silk fibroin fibers, ~25% sericin, and ~5% non-sericin components, with the sericin and non-sericin components concentrated in a layer surrounding the silk fibroin**.** The fibroin and the sericin all are the medical biomaterials, and the most of the non-sericin components belongs some alcohol-soluble flavonoid glycosides involving quercetin and kaempferol. The amount of the total flavonoids was estimated conventionally by a colorimetric method using rutin as a standard. Recently, there are some doubt about its accuracy. Here, an efficient procedure of hydrolysis-assisted extraction (HAE) was first established to estimate the level of the total flavonoids through the determination of their aglycones, quercetin and kaempferol. These aglycones were released from flavonol glycosides by HAE and then detected quantitatively by HPLC-DAD. The average contents of quercetin and kaempferol were 1.98 mg/g and 0.42 mg/g in Daizo cocoon, their recoveries were 99.56% and 99.17%. The total sum of quercetin and kaempferol was detected to be 2.40 ±0.07 mg/g by HAE-HPLC, while the total flavonoids (2.59 ±0.48 mg/g) estimated by the traditional colorimetric method were only equivalent to 1.28 ±0.04 mg/g of quercetin. These results show that the HAE-HPLC method is suitable to the estimation of bioactive components in silkworm cocoon and far superior to the colorimetric method. It is possible that the HAE-HPLC method are used to the estimation of total flavonoids in other functional biomaterials.

Key Words: silkworm cocoon, total flavonoids, aglycones, quercetin, kaempferol, hydrolysis, extraction, HPLC-DAD, biomaterial

Efficacy Study of Carrageenan As An Alternative Infused Material In Poly(3-Hydroxybutyrate-co-3-Hydroxyvalerate) (PHBV) Porous 3-D Scaffold

Nor Syamimi Che Johari, Syazwan Aizad & Saiful Irwan Zubairi*

School of Chemical Sciences and Food Technology, Faculty of Science and Technology, Universiti Kebangsaan Malaysia, 43600 UKM Bangi, Selangor, Malaysia.

*Corresponding author: saiful-z@ukm.edu.my

Polymeric porous 3-D scaffold plays an important role in culturing cells as *ex vivo* model. However, the scaffold used is ineffective due to its weaknesses on the physical and biological structure. Therefore, this research attempts to overcome the weaknesses by using carrageenan from red seaweed *Kappaphycus alvarezii* as an alternative infused material of polymeric porous 3-D scaffold. The 3-D PHBV porous scaffold was fabricated using the solvent-casting particulate-leaching (SCPL) method. Karrageenan was later infused into 3-D porous scaffold by means of freeze drying process. Five carrageenan concentrations were prepared and its physico-chemical properties such as pH, water holding capacity and viscosity were carried out on each concentration to identify the best solution to produce a new composite 3-D structure. The preliminary result shows that carrageenan concentrations of 2, 4 and 6% (w/v) were considered the best selection for the infusion process due to its stable rheology properties. The pH, water holding capacity (WHC) (at 25 °C and -18 °C) and viscosity of carrageenan solution exhibited in the range of 9.00-9.20, 99.74-100% (w/w), 76.13-83.09% (w/w) and 0.047-1.144 Pa.s respectively. Moreover, the carrageenan gel incorporated fraction was around 9-21% (w/w) which was determined by gravimetric analysis and dye staining method. The well infused carrageenan 3-D scaffold was further analyzed based on its morphological and degradability performance. The vertical cross sectional of the scaffolds showed homogeneous dried gelatinous carrageenan covered throughout porous wall. The degradation rate (K) of the carrageenan infused 3-D scaffold was in between 0.01 ± 1.66 (mg/day) to 0.03 ± 3.23 (mg/day). However, it depends on the concentration of carrageenan used. The higher the concentration of carrageenan, the faster the degradation rate occurred. The 3-D infused scaffold of 4% (w/v) carrageenan concentration (S2) produced a moderate degradation rate of 0.02 ± 1.55 (mg/day) with a sustained structural integrity up to 28 days. The carrageenan infused scaffold with 4% (w/v) was demonstrated to be the best 3-D structure for long term cell culture (>2 weeks). In conclusion, the usage of carrageenan as a composite material exhibit its great potential to be used in tissue engineering application and 3-D cell culture model.

Fabrication of highly interconnected porous poly(lactic acid) scaffold by combining vacuum-assisted resin transfer moulding (VARTM), thermally-induced phase separation and particle leaching

Zhixiang Cui[1,2] Junhui Si[1,2] Qiu Liu[1,2] Qianting Wang[1,2] Wenzhe Chen[1,2,3]

(1 School of Materials Science and Engineering, Fujian University of Technology, Fujian, Fuzhou 350118;

2 Fujian Provincial Key Laboratory of Advanced Materials Processing and Application, Fujian, 350118;

3 School of Materials Science and Engineering, Xiamen University of Technology, Fujian, Xiamen 361024)

In this study, vacuum-assisted resin transfer moulding ， thermally-induced phase separation and particle leaching approach was developed to fabricate three-dimensional porous poly(lactic acid) (PLA) and CS-coated PLA scaffolds. To control the porous morphology and porosity, different processing parameters, such as NaCl particle size and PLA concentrations were studied. The porous structures of PLA and CS-coated PLA scaffolds were characterized by SEM. Other properties of PLA and CS-coated PLA scaffolds, including porosity, water absorption, compression modulus, and compression strength were also investigated. The results showed that three-dimensional PLA and CS-coated PLA scaffolds with high porosity and interconnectivity had been fabricated successfully. The porosity and water absorption of PLA scaffolds decrease with increasing of the size of NaCl particles. It was also found that the lower the concentration of the PLA solution, the higher the porosity of PLA scaffolds. In addition, the hydrophellolic and mechanical properties of CS-coated PLA scaffolds were improved compared to those of PLA scaffolds by using CS coating treatment.

Sustainedly Releasing Antibiotic-Loaded Alginate Hydrogel for the Treatment of Otitis Media

H. R. Lee[1], T. H. Kim[1], Y. T. Kim[2], I. S. Lee[2], S. H. Oh[3], J. H. Lee[1,*]

[1]Dept. of Advanced Materials, Hannam University, Daejeon, Republic of Korea
[2]Dept. of Biotechnology, Hannam University, Daejeon, Republic of Korea

[3]Dept. of Nanobiomedical Science, Dankook University, Cheonan, Republic of Korea

**E Mail : jhlee@hnu.kr*

Otitis media is defined as an inflammatory disease occurring to middle ear. Common otitis media therapies are oral and injection administrations of antibiotics. However, those therapies have a possibility of systemic toxicity, various side effects, and low antibacterial effects. In this study, we prepared an injectable antibiotic (ofloxacin)-loaded alginate hydrogels with sustained release of the drug, which can be a desirable system for the treatment of otitis media. The drug was incorporated in the alginate hydrogel using alginate/CaSO4 mixture with controllable gelation rate. The *in vitro* drug release behavior, cytotoxicity, and antibacterial effect of the antibiotic-loaded hydrogel were investigated. It was observed that the ofloxacin loaded in the hydrogel shows a sustained release behavior for up to 14 days. The ofloxacin-loaded hydrogel showed high cell viability and effective antibacterial effect compared to the free drug *(This research was supported by the National Research Foundation of Korea (NRF- 2014R1A2A2A04003979).*

Keywords: Alginate hydrogel, antibiotic, sustained release, otitis media

[1] OH, S. H., NAM, B. R., LEE, I. S. & LEE, J. H. 2016. Prolonged Anti-bacterial Activity of Ion-complexed Doxycycline for the Treatment of Osteomyelitis. *Eur. J. Pharm. Biopharm.*, 98, 67-75.

The processing of a novel chitosan hydrogel membrane derived from the chitin of silkworm pupa and its characteristics in vitro

Hai-Yan Wang, Jin-Ge Zhao and Yu-Qing Zhang*

Silk Biotechnology Laboratory, School of Biology and Basic Medical Sciences, Soochow University; RM702-2303, No. 199, Renai Road, Dushuhu Higher Edu. Town, Suzhou 215123; P. R. China
*Corresponding author: 086-0512-65880181(Tel/Fax); E-mail: sericult@suda.edu.cn

In our research, pupa chitosan were prepared using silkworm pupa as a raw material via a freezing-thawing cycle process. The chitosan had good solubility in dilute acetic acid, although the degree of deacetylation of the pupa chitosan was only approximately 50%. The experimental results showed that the freezing-thawing can obviously reduce the crystallinity of chitin and destroy the original order of the hydrogen bonding interactions. Here, a novel chitosan hydrogel membrane (CHM) was prepared using the chitosan derived from silkworm pupa by an improved electrophoretic deposition. The CHM was formed on a nanoporous film as a barrier using a homemade electrophoretic device at a high DC voltage (60 VDC). The CHM maximum recovery of 81.7% could be achieved after 1 h of electrophoretic deposition. The transparent CHM with an elongation of 42.46% was a mixture of type I and type II crystal structures. SEM revealed that the CHM had an irregular net structure. The CHM was sufficient for L-929 mouse fibroblast cell adhesion and growth. Thus, the CHM is a promising medical biomaterial candidate for loading appropriate cells for use as artificial skin or in transplantation.

Keywords: Silkworm pupa; chitosan; electrophoretic deposition; hydrogel membrane; medical biomaterials

Rigidity Tunable Multifunctional Composites for Soft Robotics

Wanliang Shan

Department of Mechanical Engineering, University of Nevada, Reno, NV 89557, USA

The design of soft robotics taking human machine interactions into consideration requires invention of new multifunctional materials that can adapt their physical properties, geometries and functionalities according to the environment they encounter. Among these tunable rigidity is one of the most desirable traits. The past approaches for rigidity tuning typically demanded unwieldy supporting hardware such as pheumatics, magnetic fields or external heating facilities, which are not suitable for soft robotics intended for human use. We have recently worked on approaches of rigidity tuning for soft robotics based on onboard heating mechanisms. We designed and fabricated a conductive thermoplastic with low glass transition temperature that can be easily reached through joule heating of the thermoplastic. Using this thermoplastic and embedding elastomers we achieved rigidity tuning within seconds. The potential applications of these smart composites were demonstrated by design and fabrication of a soft gripper that would otherwise be very complicated to fabricate and control. Perspectives into future research in this area will also be discussed.

Enhanced long-term stability of electrochromic P3HT modified by graphene oxide protective layer

Tae-Ho Kim[1], Ki In Choi[2], Hyeri Kim[2], Seong Hyeon Oh[1] Jaseung Koo[2], and Yoon-Chae Nah[1*]

[1]School of Energy, Materials, and Chemical Engineering, Korea University of Technology And Education, Cheonan 31253, Republic of Korea

[2]Division of Neutron Science, Korea Atomic Energy Research Institute (KAERI), 989-111 Daedeok-daero, Yuseong-gu, Daejeon, 34057, Republic of Korea

In general, organic electrochromic materials have shown a poor long-term stability during the electrochemical reactions, which is mainly due to the weak mechanical properties of the materials in organic electrolytes. There have been several approaches to enhance the stability of electrochromic polymers. As one of the effective methods, incorporation of graphene oxide (GO) into the polymers has been introduced to solve the stability issue because GO has known to significantly improve the physical properties of polymers having a good compatibility with them. A poly (3-hexyl thiophene) (P3HT) is one of the important electrochromic polymers showing color changes between red and pale blue during electrochemical reactions. However, a poor life time of P3HT is deemed a main obstacle to utilize it as an active layer in commercial applications such as displays or smart windows. In this study, we prepare the electrochromic P3HT layer modified with GO and discuss the electrochromic properties of the composites. In order to construct the composites, the GO protective layer which has been modified by octadecylamine (ODA) is transferred on spin-coated P3HT layer by using Langmuir-Schaefer technique. The GO-ODA protective layer shows a high coverage with closed packed molecules and a good compatibility with P3HT layer. Furthermore, it is observed that the P3HT modified by GO-ODA protective layer shows a superior long-term stability compared to pristine P3HT layer during electrochromic reactions.

Long-term cyclability of electrochromic P3HT by the control of applied voltages

Tae-Ho Kim, Seok Hyun Song, Seong Hyeon Oh, Hyo Jae Kim, and Yoon-Chae Nah*

School of Energy, Materials, and Chemical Engineering, Korea University of Technology and Education, Cheonan 31253, Republic of Korea

An Electrochromic (EC) phenomenon refers to a reversible optical change of a specific material during the electrochemical reactions. Since the EC properties of tungsten oxides were reported by S. K. Deb in 1969, EC devices have been studied extensively because they exhibit high color contrast and low voltage consumption. These features provide the basis for their applications in smart window, rear-view mirrors, information displays, and optical shutters. There are several parameters to evaluate the EC properties of materials and devices such as coloration efficiency, response time, life time, and memory effect. Among them, the memory effect is designated as color retention time under voltage-off condition, which can be utilized as an index of energy saving in the field of smart windows. On the other hand, it can be generally accepted that the memory effect influences the life time of EC materials because the voltage application can cause the degradation of materials during the electrochemical reactions. In general, organic EC materials have a fast coloration speed under a low voltage condition, but a short cycle time during EC reactions. In this study, therefore, we investigate the EC long-term cyclicality of P3HT [poly (3-hexyl thiophene)] by controlling voltage retention time. Furthermore, we obtain the optimal retention time during the oxidation and reduction reactions by using the memory effect of P3HT. This method using the memory effect suggests an easy way to maximize the long-term cyclicality of EC materials.

Optimization of Polyolefinic Compound Recipes Utilised for Foam Production Based on Polymer Melt Rheological Characterization

Aneta Sklenarova, Vera Canova, Pavlina Plskova, Tomas Sedlacek

Centre of Polymer Systems, Tomas Bata University in Zlin, Trida T. Bati 5678, 76001 Zlin, Czech Republic.

sklenarova@cps.utb.cz

Development of polyolefinic compounds composed of commercially available polyethylenes with various molecular structures suitable for polymeric foam production was the main aim of the presented study. Low density polyethylene was taken as the primary component, while linear low density polyethylenes with defined diverse length of branches as well as their density were selected as the compound counterparts. Polymer compounds prepared via thorough mixing of selected ingredients by the help of the twin screw extruder were characterised from rheological point of view in order to describe susceptibility of chosen materials to be successfully foamed. Since extensional capability of an employed polymer melt is the crucial parameter for the foam manufacturing process the routine description of shear viscosity carried out using oscillatory and capillary rheometers was completed with the definition of elongational viscosity and the evaluation of polymer melt strength. Careful rheological characterisation of selected tested materials revealed essential influence of polyolefinic molecular structure on processed compound foamability.

Keywords: elongational viscosity, shear viscosity, polymer melt strength, low density polyethylene, linear low density polyethylene

Measurement of Fiber Orientation using Intersection Aggregate Method in GFRP

Jung-Hoon (Lee)[1], Jin-Woo (Kim)[2]

[1]Department of Mechanical System Engineering, Chosun University Graduate School, 375 Seosuk-Dong, Dong-Gu, Gwang-ju, Korea

[2]Department of Mechanical System Engineering, Chosun University, 375 Seosuk-Dong, Gwangju, Korea

jinu763@chosun.ac.kr/ Tel: +82-62-230-7014 fax: +82-62-230-6596

The fiber oriented condition inside glass fiber reinforced composite material is basic factor of mechanical properties of composite materials. It is very important to measure the fiber orientation angle for the determination of molding conditions, mechanical characteristics, and the design of composite materials. In the study, to examine effect of fiber states on accuracy of fiber orientation measurement using image processing, fiber orientation function is derived by drawing simulation figures for the fiber orientation as varying fiber aspect ratio and fiber orientation state, respectively. The values of fiber orientation function measured by intersection aggregate method are compared with the calculated values of fiber orientation function.

Keywords: Intersection aggregate method, Fiber orientation angle, Fiber aspect ratio, Fiber orientation function

[1] JIN-WOO, K. & DONG-GI, L. 2008. M Measurement of fiber orientation angle in FRP by intensity method. *J. of Mat. Processing Tech.*, 120, 3650-3654.

Use of artificial neural network for the simulation of color expression of color mortar using acrylic polymer

Hongseok Jang[1], Youngteak Lim[1], Uihyeon Jeon[2], Seungyoung So[1]

[1]Department of Architectural Engineering, Chonbuk National University, Research Center Industrial Technology, 561-756, Republic of Korea
[2]Seo-Do Construction, Jeonju, Republic of Korea, 560-800, Republic of Korea

Jadolli@naver.com/ Tel: +82-63-270-3572, Fax: +82-63-270-3573

In this study, an artificial neural networks study was carried out to predict the color evaluation of color mortar using inorganic pigment and acrylic polymer. A data set of a laboratory work, in which a total of 4 type mortars were produced, was utilized in the Artificial Neural Networks (ANNs) study. Each mortar was measured at ten locations on the surface and averaged. Color can be evaluated by measurements of tristimulus values L*, a* and b*, represented in the chromatic space CIELAB. ANN model is constructed, trained and tested using these data. The data used in the ANN model are arranged in a format of two input parameters that cover the pigment and polymer of samples and, an output parameter which is the color parameters of the colored mortar. The results showed that ANN can be an alternative approach for the predicting the color parameters using mortar ingredients as input parameters.
This research was supported by a grant (14CTAP-C078857-01) from infrastructure and transportation technology promotion research Program funded by Ministry of Land, Infrastructure and Transport of Korean government.

Keywords: Color concrete, Acrylic polymer, Artificial neural networks

[1] LEE, H. S., LEE, J. Y., YU, M. Y., 2005. Influence of inorganic pigments on the fluidity of cement mortars. Cement and Concrete research 35, 703-710.

Diacetylene monolayers and aggregates self-assembled on atomically flat surfaces

Ververiotis[1], Okawa[1], Makarova[1,2], Koide[3], Liu[3], Šmíd[3], Watanabe[3], Taniguchi[3], Komatsu[3], Joachim[1,4],Aono[1]
[1]International Center for Materials Nanoarchitectonics (WPI-MANA), National Institute for Materials Science (NIMS), 1-1 Namiki, Tsukuba, Ibaraki 305-0044, Japan
[2]Institute of Physics, Czech Academy of Sciences, Na Slovance, 2, Prague 8, 18221, Czech Republic
[3]National Institute for Materials Science (NIMS), 1-1 Namiki, Tsukuba, Ibaraki 305-0044, Japan
[4]Centre d'Elaboration de Matériaux et d'Études Structurales (CEMES), Centre National de la Recherche Scientifique (CNRS), 29 rue J. Marvig, 31055 Toulouse Cedex, France
Contact Email: Ververiotis.Elisseos@nims.go.jp

Conductive polymers are expected to be integral parts in molecular electronic devices. They can play the role of on-surface fabricated molecular wires [1], which will aid the miniaturization of future electronics. We have already demonstrated that the end of a poly-diacetylene (PDA) chain can hybridize with different functional molecules forming a molecular-resonant-tunneling diode [2].
Progress in the field is plagued by the lack of flat substrates on which the PDA precursors form planar, self-assembled monolayers (SAM), something necessary for in-plane electronic device fabrication. Up to date, formation of such SAMs has been demonstrated only on metallic [3] and semiconductive [4] substrates. This is problematic for electronic devices due to the inherent substrate-based current leakage.
In this work we tackle the problem by testing atomically flat, insulating substrates: highly polished oxidized monocrystalline diamond, sapphire, and hexagonal Boron Nitride (h-BN). Using atomic force microscopy, we show that only on h-BN we obtain a flat-lying SAM of the PDA precursors, while on the other two substrates the molecules are standing up. The assembly mechanism is elucidated by subsequent deposition of diacetylene on hydrogenated monocrystalline diamond, where the molecules do assemble in a flat-lying manner. We show that the mechanism is dominated by the nature of the surface dipole and hydrophilicity / hydrophobicity of the substrate. We present a model and demonstrate polymerization on h-BN surfaces.

Keywords: Self-assembly, atomic flatness, diamond, h-BN, diacetylene

[1]OKAWA, Y. & AONO, M. 2001. Materials Science: Nanoscale Control of Chain Polymerization. *Nature*, 409, 683-684

[2] OKAWA, Y., AKAI-KASAYA, M., KUWAHARA, Y., MANDAL, S. K. & AONO, M. 2012. Controlled Chain Polymerisation and Chemical Soldering for Single-Molecule Electronics. *Nanoscale*, 4, 3013-3028.

[3] ENDO, O., FURUTA, T., OZAKI, H., SONOYAMA, M. & MAZAKI, Y. 2006. Structures of 17, 19-Hexatriacontadiyne Monolayers on Au(111) Studied by Infrared Reflection Absorption Spectroscopy and Scanning Tunneling Microscopy. *J. Phys. Chem. B*, 110, 13100-13106.

[4] MANDAL, S. K., OKAWA, Y., HASEGAWA & T., AONO, M. 2011. Rate-Determining Factors in the Chain Polymerization of Molecules Initiated by Local Single-Molecule Excitation. *ACS Nano*, 5, 2779–2786.

Mesoscale Simulation of Line-Edge Roughness Based on Polymer Chain in Extreme Ultra Violet Lithography

Sang-Kon Kim[1,2]

[1]Department of Applied Physics, Hanyang University, Ansan, Gyeonggi-do 426-791, Korea. [2]Department of Science, Hongik University, Seoul 121-791, Korea.

sangkona@hanyang.ac.kr

Extreme Ultra Violet (EUV) Lithography is expected as a potential candidate for next-generation lithography. When the pattern size becomes smaller several nanometers in the lithography, molecular dynamics (MD) can play an important role to understand and determine the pattern profile in terms of the molecular behaviors of the resist polymer. In this study, we investigate MD simulation of the chemically amplified resist processes in the below sub-10-nm-half-pitch node, assuming the use of extreme ultraviolet (EUV) lithography. Resist materials in lithography convert an optical image to a resist image for device manufacturing. For EUV exposure, the breaking positions in the polymer chain are randomly selected and the rate of chain scission in the resist is proportional to the exposure intensity distribution preliminarily calculated by the Monte Carlo simulation of photoelectron scattering. For this exposure, post-exposure-bake, and development processes, the efficiency of conversion processes is determined mainly by resist material properties. For chemically amplified resist processes, below sub-10-nm-half-pitch pattern can form in based on resist material significant improvement.

Keywords: Optical lithography, Mesoscale simulation, Line edge roughness, Extreme ultra violet, EUVL

[1] S.-K. Kim, 2014. Modeling and Simulation of Line Edge Roughness for EUV Resists, J. Semiconductor technology and science, 14, 61-69.

[2] S.-K. Kim, 2013. Stochastic Simulation Studies of Line-Edge Roughness in Block Copolymer Lithography: J. Nanosci. Nanotechnol.14, 6143-6145.

Preparation and Characteristics of HA/TCP Cancellous Bone-like Scaffold with Pore-orientational Structure

Jin Wen[1,2], Hongquan Zhang[1,2,*], Chunpeng Zhao[2] and Xiaoyan Li [2]

[1] State Key Laboratory of Silicate Materials for Architectures, Wuhan 430070, China.
[2]School of Materials Science and Engineering, Wuhan University of Technology, Wuhan 430070, China.

* corresponding author , *email :zhhquan@whut.edu.cn*

Calcium phosphate based porous scaffolds provide an effective route to repair bone defects, but conventional such materials have low porosity and connectivity, showing inferior flexural strength and low reliability. Usually, *in vivo* behavior of the scaffolds depends on their chemical composition and pore structure characteristics. Scaffolds with unidirectional pore structure can not only enhance the mechanical properties required for bone defect repair or substitution, but also can induce new bone formation and the regeneration of nerve tissue as well as the formation of blood vessels. Therefore, the preparation technology and structure characteristics of the hydroxyapatite/tricalcium phosphate (HA/TCP) cancellous bone-like scaffolds were studied here.

HA whiskers and HA powders were used as raw materials. Their sully was evenly mixed with bioglass binder, coagulation aid and dispersing agent in accordance with a certain proportion. The green body was then prepared by a freeze drying method, and the porous HA/TCP scaffolds were finally sintered at a high temperature.

The pore structure of the scaffolds was mainly affected by the frozen drying system and sully characteristics. The freezing temperature and velocity had a great impact on the formation of ice crystals in the HA paste. Although freezing speed slower ice crystal diameter is larger, but low temperature easily leads to the appearance of branches of ice crystals. Thus, the freezing temperature was appropriately controlled at from -12 ^{o}C to -45 ^{o}C. In addition, the sully characteristics were correlated with the solid content, diserpersibility of HA whiskers and the suspension stability, which would affect the nucleation and growth of ice crystals, giving rise to the change of the mechanical properties, porosity and pore structure. The optimum solid content should be controlled within 30-40%.

HA whisker showed a good dispersibility in the sully. The addition of whiskers did not seriously affect the pore orientation in the scaffolds. Adding bioglass powder favored the materials sintering and the phase transformation of Ca-deficient HA to β-TCP. Calcium phosphate based scaffolds with composition from HA to HA/β-TCP complex could be obtained by controlling the freezing molding system and slurry composition. The scaffold had a porosity of 70-80%, compressive strength 0.5~1.0MPa and the pore size range of 50~160μm.

Acknowledgements: This work was supported by National Nature Science Foundation of China (No.51372182)

Keywords: Hydroxyapatite, freeze drying, pore-orientation, structure characteristics

[1] AOKI, H. 1991. Science and Medical Applications of Hydroxyapatite, Japanese Association of Apatite Science.

[2] ZHANG, H. & DARVELL, B.W. 2011. Morphology and Structural Characteristics of Hydroxyapatite Whiskers: Effect of the Initial Ca Concentration, Ca/P Ratio and pH. Acta Biomater, 7, 2960-2968.

[3] ZHANG, H. & DARVELL, B.W. 2010. Synthesis and Characterization of Hydroxyapatite Whiskers by Hydrothermal Homogeneous Precipitation Using Acetamide. Acta Biomater, 6, 3216-3222.

[4] MONMATURAPOJ, N.，SOODSAWANG, W. & THEPSUWAN W. 2012. Porous Hydroxyapatite Scaffolds Produced by the Combination of the Gel-casting and Freeze Drying Techniques. Journal of Porous Materials. 19, 441-447.

[5] LI, Y. & YANG, S.T. 2001. Effects of Three-dimensional Scaffolds on Cell Organization and Tissue Development. Biotechnology and Bioprocess Engineering. 6, 311-325.

Preparation and Characterization of Biodegradable nanocomposite from Green - polymers and Cellulose Nanowhiskers

P. Phanwiroj[1,2,a], S.Tanpichai[3,b], P. Potiyaraj[1,2,c*]

[1]Center of Excellence in Textiles, Department of Materials Science, Faculty of Science, Chulalongkorn University, Bangkok 10330, Thailand.

[2]National Center of Excellence for Petroleum, Petrochemicals and Advanced Materials, Chulalongkorn University, Bangkok 10330, Thailand

[3]Learning institute, King Mongkut's University of Technology Thonburi, Bangkok 10140,

[a]p.prompoom@gmail.com, [b]supachok.tan@kmutt.ac.th, [c]pranut.p@chula.ac.th

Due to the environment pollution, natural polymer and fillers using from regenerate biomass extracted has continuously gained much attractive in many application, films, sheets, filters and reinforcements. Cellulose is a most biopolymers play a crucial role in versatile functions due to its biodegradability, biocompatibility and sustainability. Two biodegradable polyesters, poly(butylene adipate-co-terephthalate) (PBAT) and poly(butylene succinate) (PBS) were solution casted to fabricate a PBS, PBAT PBS/PBAT blend and its composite. The first target of this research was to study the parameters on the properties of cellulose nanowhiskers. The effect of preparation conditions on the morphology of cellulose nanowhiskers was investigated. Cellulose nanowhiskers were characterized using scanning electron microscopy and transmission electron microscopy. The results showed that 9 nm. diameter cellulose nanowhiskers can be prepared. A possible correlation between the preparation conditions and cellulose particle sizes could not be observed, but the titration process used to neutralize cellulose can shorten the length of the preparation time from 168 h to only 50 h. The second point of this study resulted the success of this CNWs to use as reinforcing agent for all bio-based polymer and blend composites. CNWs from filter paper source show the results that improved in decomposition temperature, increased in thermal stability in PBS and PBS/PBAT composites but slightly decrease in PBAT, and improved in tensile properties of composites. The third point of this study showed the compatibility of the blend was attributed to the trans esterification reaction that was confirmed by Fourier transform. Flexibility of blends was improved when adding PBAT into PBS but no significant change in thermal properties.

Keywords: Biodegradable polymer. Biodegradable composites, Cellulose nanowhisker, poly(butylene adipate-co-terephthalate, polybutylene succinate

[1] SIQUERA G, BRAS J, DUFRESNE A. 2009. Cellulose whiskers versus microfibrils: Influence of the nature of the nanoparticle and its surface functionalization on the thermal and mechanical properties of nanocomposites. Biomacromolecules 10, 2, 425-432.

[2] KVIEN I, TANEM BS, OKSMAN K. 2005. Characterization of cellulose whiskers and their nanocomposites by atomic force and electron microscopy. Biomacromolecules 6, 6, 3160-3165.

Synthesis and Structural Characteristics of Magnesium and Zinc Doped Hydroxyapatite Whiskers

Hongquan Zhang[1,2,*], Jin Wen[1,2], Luwei Fu[2] and Ying Guo[2]

[1] State Key Laboratory of Silicate Materials for Architectures, Wuhan 430070, China.
[2]School of Materials Science and Engineering, Wuhan University of Technology, Wuhan 430070, China.
* corresponding author , *email :zhhquan@whut.edu.cn*

Applications of hydroxyapatite (Ca10(PO4)6(OH)2, HA) based biomaterials are limited to small and unloaded implants due to the poor flexural strength and low reliability. Reinforcement by whiskers or fibers is an effective way to improve the mechanical strength and durability of biomaterials. In our previous work, long HA whiskers with high aspect ratio have been successfully developed, and the whiskers reinforced biomaterials conferred a significant increase in fracture toughness and slight improvement in flexural strength.

Zn and Mg, which are essential trace elements required for bone and connective tissues, have specific osteogenic effects on bone formation and selective inhibitory effect. Although both Mg and Zn doped HA powders have been successful developed from an aqueous solution, but no more literature reports were found about the synthesis of Zn or Mg ions doped HA whiskers. Thus, the aim here was to prepare Zn or Mg doped HA whiskers and study the effects of the ions substitution on the constitution and microstructure as well as their thermal stability of HA whiskers.

Metal ions doped HA whiskers were prepared by a hydrothermal homogeneous precipitation. The aqueous solution containing 2-40 mol% Mg or Zn ions was hydrothermally treated at 170~190 C for 10h. After processing, they were dried at 80 ºC for 3-4 h for use. The morphology and structure of the products before and after heat-treatment at 800-1000 ºC were characterized using SEM, XRD, and FTIR. The lattice parameters were determined by Rietveld refinements.

Mg or Zn doped HA whiskers were successfully prepared using amide additives, they had a length of 60 - 110 m and aspect ratio 30 – 50 when the doping proportion were less than 5 mol%. Substitution of Mg and Zn ions in HA impaired the crystallization of whiskers and led to changes in the morphology, crystallinity, lattice parameters and their thermal stability. The phase composition, morphology, crystallinity and thermal stability of the whiskers would be impaired by increasing the initial concentration of Mg and Zn ions. To obtain a product with single HA phase, Mg or Zn doping concentration should be <10 mol%, otherwise Ca19.68Mg0.12H1.8(PO4)13.80 or CaZn2(PO4)2·2H2O would appear in the products. The morphology and thermal stability of ions doped HA whiskers was obviously affected by the species of doping ions and their content.

Acknowledgements: This work was supported by National Nature Science Foundation of China (No.51372182)

Keywords: Mg and Zn ions, ions doped hydroxyapatite, morphology, crystal structure

[1] AOKI, H. 1991. Science and Medical Applications of Hydroxyapatite, Japanese Association of Apatite Science.

Carbon Nanotube-gelatin-hydroxyapatite Nanohybrids with Multilayer Core–shell Structure for Mimicking Natural Bone

Ji Hye (Kang) [1,2], Ueon Sang (Shin) [1,2],

[1] Department of Nanobiomedical Science & BK21 PLUS NBM Global Research Center for Regenerative Medicine, Dankook University, Cheonan, Chungnam 330-714, Korea

[2]Institute of Tissue Regeneration Engineering (ITREN), Dankook University, Cheonan, Chungnam 330-714, Korea

E Mail : addio9187@dankook.ac.kr and usshin12@dankook.ac.kr

We attempted to mimic collagen fibrils bearing apatite crystals in natural bone, using gelatin, carboxylic acid functionalized carbon nanotubes (f-CNTs), and hydroxyapatite (HA). Gelatin molecules were covalently grafted on the surface of f-CNTs by the formation of amide linkages. HA crystals were then assembled onto the gelatin-grafted f-CNTs in a highly concentrated CaP solution, resulting a multilayered core–shell structure, consisting of a f-CNT core and gelatin-HA shells (as a fibrous multilayered f-CNT/Gel/HA nanohybrid), and in a similar formation to the collagen fibers of natural bone. The tensile strength, elastic modulus, and elongation rate of the new hybrid material were significantly improved compared to both pure (f-CNT free) gelatin and a mixture of f-CNT and gelatin, by 4.6–8.8, 9–10, and 28–42 times, respectively. Cell viability studies of the f-CNT/Gel/HA nanohybrid also suggest a higher degree of biocompatibility compared to pure gelatin.

Keywords: core–shell structure, Carbon nanotube, hydroxyapatite, bio mimicking, gelatin

[1] THULA, T. T., SVEDLUND, F., RODRIDUEZ, D. E., PODSCHUN, J., PENDI, L. & GOWER, L. B. 2011. Mimicking the nanostructure of bone: comparison of polymeric process-directing agents. *Polymers*, 3, 10–35.

[2] OLIVEIRA, A. L., MANO, J. F. & REIS, R. L. 2013. Nature-inspired calcium phosphate coating: present status and novel advances in the science of mimicry. *Current Opinion in Solid State and Materials Science*, *7*, 309–318.

[3] ROSS-MURPHY, S. B. 1992. Structure and rheology of gelatin gels: recent progress. *Polymer*, 33, 2622–2627.

[4] KUIJPERS, A. J., VAN WACHEM, P. B., VAN LUYN, M. J. A., PLANTINGA, J., ENGBERS, G. H. M., KRIJGSVELD, J., ZAAT, S. A. J., DANKERT, J. & FEIJEN, J. 2000. In vivo compatibility and degradation of crosslinked gelatin gels incorporated in knitted Dacron. *J Biomed Mater Res*, 51, 136–145.

[5] YANG, W., THORDARSON, P., GOODING, J. J., RINGER, S. P. & BRAET, F. 2007. Carbon nanotubes for biological and biomedical applications. *Nanotechnology*, 18, 412001–412012.

Achieving High External Quantum Efficiency in Solution-Processed Green Phosphorescent Organic Light-Emitting Devices by Thermal Annealing of Hole Transporting Polymer Layer

Jae-Hoon Jung, Dae-Gyu Moon

Department of Materials Engineering, Soonchunhyang University, Asan-so,

Chungcheongnam-do, Republic of Korea.

dgmoon@sch.ac.kr/ Tel :+82-41-530-1312

Solution-processed phosphorescent organic light-emitting devices (OLEDs) have drawn great interest since they can provide low cost displays and lighting applications on the large area substrates [1,2]. We developed highly efficient solution-processed green phosphorescent OLEDs by thermal annealing of hole transporting polymer layer. Poly[N,N'-bis(4-butylphenyl)-N,N'-bis(phenyl)benzidine] (Poly-TPD) was used as a hole transporting polymer and *fac*-tris(2-phenylpyridine) iridium [Ir(ppy)3] doped N,N'-dicarbazolyl-3,5-benzene (mCP) was used as a solution-processed emission layer. The annealing temperature was critical to realize the well-defined interface between the hole transporting poly-TPD and solution-processed mCP:Ir(ppy)3 emission layers. In addition, the charge balance factor can be significantly improved by annealing of poly-TPD layer. An external quantum efficiency of 17.3% and a current efficiency of 61 cd/A was achieved by optimizing an annealing temperature and the thickness of poly-TPD layer.

Keywords: hole transporting polymer, poly-TPD, annealing, organic light-emitting devices

[1] MULLER, C. D., FALCOU, A., RECKEFUSS, N., ROJAHN, M., WLEDERHLRN, V., RUDATI, P., FROHNE, H., NUYKEN, O., BECKER, H. & MEERHOIZ, K. 2003. Multi-color organic light-emitting displays by solution processing. *Nature,* 421, 829-833.

[2] WU, H., YING, L., YANG, W. & CAO, Y. 2009. Progress and perspective of polymer white light-emitting devices and materials. Chem. Soc. Rev., 38, 3391-3400.

Carbon Nanotubes -Polydimethyl Siloxane-3D Graphene Flexible Electrochemical Electrodes for Heavy Metal Ion Detections

Thitima M. Daniels[1], Ditsayut Phokharatkul[1], Kata Jaruwongrungsee[1], Adisorn Tuantranont[1], Anurat Wisitsoraat[1]

[1]National Electronics and Computer Technology Center (NECTEC), 112 Thailand Science Park, Phahon Yothin Rd., Klong 1, Klong Luang, Pathumthani, Thailand.
E Mail: anurat.wisitsoraat@nectec.or.th

3D graphene foam structure is a highly promising platform for advanced electrochemical sensing applications due to its large effective specific surface area, high electron transfer rate and high electrical conductivity [1]. However, its structural stability must be improved and its sensing performances may enhanced by properly combining with other effective materials. In this work, 3D graphene-PDMS-CNTs electrodes were fabricated and applied for determination of cadmium and lead by differential pulse anodic stripping voltammetry (DPASV). Graphene foam was fabricated by chemical vapor deposition (CVD) on Ni foam using acetylene carbon source (3 sccm) and hydrogen gas carrier (24 sccm) at 700°C for 3 minutes followed by fast cooling. Next, graphene/PDMS/CNTs composite was then formed by dip coating the graphene foam into PDMS solution with CNTs dispersion and dried in an oven at 70°C for 12 hour. The nickel foam template was then removed by chemical etching in a hot hydrochloric acid at 80°C for 12 hour. The electrochemical performances of the electrode were systematically studied with different CNTs contents. The optimal CNTs content for detection of cadmium and lead was found to be 1 mg/ml. The graphene-PDMS-CNTs electrode showed good analytical performances for cadmium and lead detections over linear ranges from 1 mg/L to 5 mg/L and 500 µg/L to 5 mg/L, respectively. Moreover, cadmium and lead can be simultaneously detected at different working potentials of electrode. Therefore, the graphene-PDMS-CNTs electrode is a promising candidate for detection of heavy metal pollution in the natural or tap water.

Keywords: Carbon nanotubes, 3D graphene, Polydimethy siloxane, Heavy metal ion detections.

[1] Wu S., Huang X., Wu Y., Luo L., Jin Y., Li Q., Differential Pulse Anodic Stripping Voltammetry Detection of Cadmium with Nafion-Graphene Modified Bismuth Film Electrode. 2015. International Journal of Electrochemical Science, 10, 8255 – 8262.

Contact resistance dependence on alkyl-chain length in Poly(3-alkylthiophene) based organic field-effect transistors

Kshitij Bhargava[1] and Vipul Singh[1*]

[1]Molecular and Nanoelectronics Research Group (MNRG), Discipline of Electrical Engineering, Indian Institute of Technology Indore, Indore-453446, India.

[*]E-mail: vipul@iiti.ac.in

Contact resistance is one of the performance limiting issues in organic field-effect transistors (OFETs). Large contact resistance in OFETs limits charge carrier injection and extraction efficiency resulting in lower drive current and switching speed of these devices [1]. Therefore, contact resistance minimization is essential for achieving the improved performance of OFETs. Poly(3-alkylthiophene)s (P3ATs) which are generally used as active layer in OFETs consists of alkyl side chain responsible for making it soluble in organic solvents. These side chains have been reported in past to affect the morphology of solution processed thin films and the field-effect mobility in OFETs [2]. However, the influence of alkyl-chain length on contact resistance in OFETs is still not well understood. Thus, we report the contact resistance dependence on alkyl-chain length in OFETs using two different P3ATs viz. regioregular Poly(3-hexylthiophene) (rr-P3HT) and Poly(3-otylthiophene) (rr-P3OT) used as obtained from Sigma Aldrich. For this purpose we prepared OFET devices in bottom gate bottom contact configuration with P3AT films as active layer prepared by spin coating method from 1wt% solution in anhydrous chloroform, on a Si(n+)/SiO2 substrate, having a 200nm thick oxide layer. Measured rr-P3HT and rr-P3OT film thicknesses were 48 nm and 45 nm respectively.
Typical p-type OFET, output characteristics were observed from the OFETs fabricated using rr-P3HT and rr-P3OT as is shown in Fig. 1 (a & b) respectively. From these characteristics a clear difference in the values of drain current (*IDS*) was observed in the two cases. Figure 2 shows the comparison between the transfer characteristics of two devices. The rr-P3HT OFET showed higher ON-state current and field-effect mobility over rr-P3OT OFET. The contact resistance values were estimated from devices of several channel lengths using transmission line method. It was observed that contact resistance of rr-P3OT OFET (2×10^9 Ω) was an order higher than that of rr-P3HT OFET (9×10^7 Ω) as shown in Fig. 3. These observations have been attributed to the presence of longer alkyl-chain in rr-P3OT affecting the morphology of thin film and contact resistance in based devices. The observations were further confirmed through comparison of absorption spectra as shown in Fig. 4, where lesser extent of π-conjugation was evident in rr-P3OT films over rr-P3HT films leading to higher contact resistance in rr-P3OT OFETs. We conclude that contact resistance is dependent on alkyl-chain length and a trade-off between the length of alkyl-chain and solubility is required for achieving the improved performance of P3AT based OFET devices. Moreover, the influence of alkyl-chain length over the photoresponse of these devices will be discussed in detail during the conference.

Keywords: OFET, P3ATs, contact resistance.

[1] BHARGAVA, K., & SINGH, V., 2014. Electrical characterization and parameter extraction of organic thin film transistors using 2-D numerical simulations. J. Comp. Electron.,13, 585.

[2] PARK, Y.D. et al., 2006. Effect of side chain length on molecular ordering and field-effect mobility in poly (3-alkylthiophene) transistors. Org. Electron., 7, 514.

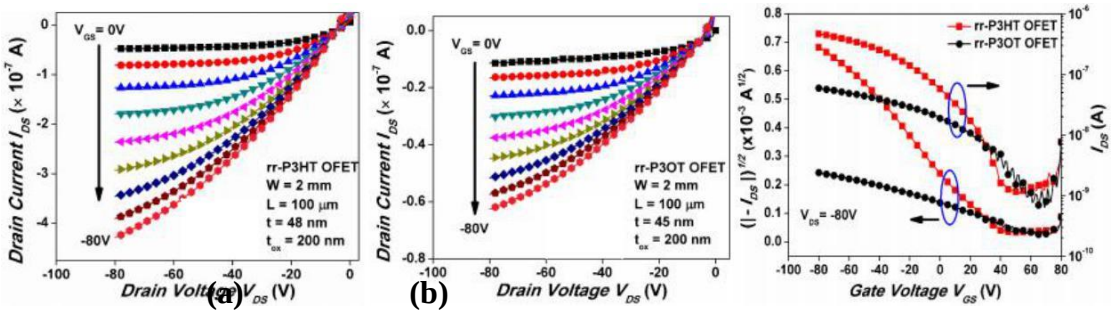

Fig. 1 Output characteristicsrr-P3HT OFET, (b) of (a) rr-P3OT

Fig. 2 Transfer characteristics of rr-P3HT and rr-P3OT OFETs.

[3]

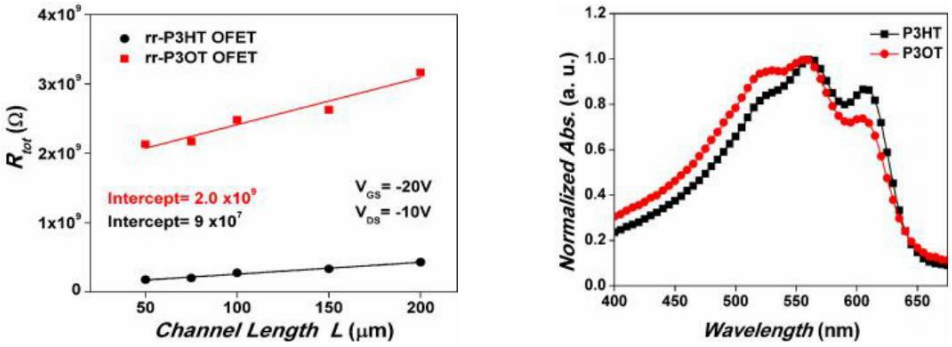

Fig. 3 Contact resistance estimation in P3AT OFETs.

Fig. 4 Normalized absorption spectra of P3AT thin films.

Effects of Carbon Nanotubes Doping and Mechanical Strain on the Optoelectronic Properties of P3HT-based Sensing Thin Films

Donghyeon Ryu[1*]

[1]Department of Mechanical Engineering, New Mexico Tech, 801 Leroy Place, Socorro, NM 87801

[*]*Email: donghyeon.ryu@nmt.edu*

Regioregular poly(3-hexylthiophene) (P3HT) conjugated polymers have drawn researchers' attention due to its extraordinary optoelectronic properties. In particular, it has been known that the optoelectronic properties of the P3HT-based thin films are greatly influenced by the degree of crystalline structures ordering of the P3HT [1, 2]. Ryu and Loh [4] suggested P3HT-based thin film strain sensors by utilizing the P3HT's unique optoelectronic properties and crystallinity. It was shown that the direct current (DC) generated from the P3HT-based sensing thin films under broadband light varied with the tensile strain up to ~0.5%. It was hypothesized that the photocurrent-based strain sensing resulted from the tensile strain-induced ordering of P3HT molecules and thus the enhanced light absorption, as shown in ultraviolet visible (UV-Vis) light absorption results (Fig. 1) [3]. Preliminary study was conducted to test the hypothesis using X-ray diffractometer (XRD) for the pristine and stretched P3HT-baserd thin films. In Fig. 2, it can be seen that both pristine and stretched P3HT-based thin films show two peaks at ~5° and ~12°, which indicate existence of P3HT lamellae and ordered P3HT in (100) and (200), respectively. The higher peaks in the stretched films indicate larger number of the ordered P3HTs in each direction. So, it can be regarded that the mechanical strain enhanced crystallinity of P3HT. In addition, it was shown that multi-walled carbon nanotubes (MWNTs) doping could help alignment of P3HT molecules based on the enhanced strain sensitivity [4]. It was theoretically known that the P3HT molecules tend to non-covalently functionalize MWNTs and end up being elongated along the longitudinal axis of MWNTs [5, 6].

The research objective is to investigate doping effect of MWNTs and mechanical strain to the optoelectronic properties of P3HT-based sensing thin films. First, the P3HT-based sensing thin films with and without MWNTs will be fabricated using the spin-coating technique on flexible substrates. The P3HT-based sensing thin films will be interrogated using the UV-Vis spectrophotometer to investigate the strain effects on the light absorptivity. Second, the crystallinity and surface morphologies of the sensing thin films will be characterized using XRD, scanning electron microscope, and atomic force microscope at various tensile strain levels. Last, the electrical properties of the P3HT-based thin films will be studied at various strain levels.

Keywords: P3HT, single-walled carbon nanotubes, crystallinity, strain effect, optoelectronics

[1] O'CONNOR, B. T., REID, O. G., ZHANG, X., KLINE, R. J., RICHTER, L. J., GUNDLACH, D. J., DELONGCHAMP, D. M., TONEY, M. F., KOPIDAKIS, N. & RUMBLES, G. 2014. Morphological Origin of Charge Transport Anisotropy in Aligned Polythiophene Thin Films. *Adv. Funct. Mater.*, 24(22), 3422-3431.

[2] SALIM, T., LEE, H.-W., WONG, L. H., OH, J. H., BAO, Z. & LAM, Y. M. 2016. Semiconducting Carbon Nanotubes for Improved Efficiency and Thermal Stability of Polymer–Fullerene Solar Cells. *Adv. Funct. Mater.*, 26(1), 51-65.

[3] RYU, D. & LOH, K. J. 2014. Multi-Modal Sensing Using Photoactive Thin Films. *Smart Mater. & Struct.*, 23(8), 085011.

[4] RYU, D. & LOH, K. J. 2012. Strain Sensing Using Photocurrent Generated by Photoactive P3HT-Based Nanocomposites. *Smart Mater. & Struct.*, 21(6), 065016.

[5] BERNARDI, M., GIULIANINI, M. & GROSSMAN, J. C. 2010. Self-Assembly and Its Impact on Interfacial Charge Transfer in Carbon Nanotube/P3HT Solar Cells. *ACS Nano*, 4(11), 6599-6606.

[6] GIULIANINI, M., WACLAWIK, E. R., BELL, J. M., CRESCENZI, M. D., CASTRUCCI, P., SCARSELLI, M., DIOCIAUTI, M., CASCIARDI, S. & MOTTA, N. 2011. Evidence of Multiwall Carbon Nanotube Deformation Caused by Poly(3-Hexylthiophene) Adhesion. *The Journal of Physical Chemistry C*, 115(14), 6324-6330.

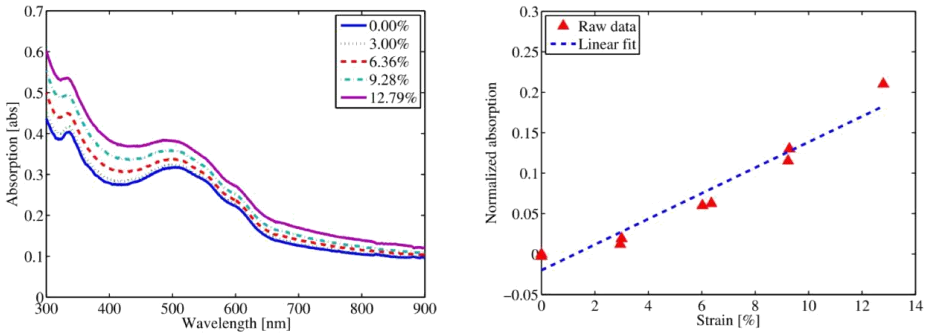

(a) (b)

Fig. 1. Light absorption of P3HT-based thin film increases with applied tensile strain [3]. (a) Up to ~13%, overall light absorption increases as applied tensile strain increases. (b) It shows linear relationship between the normalized absorption (by the absorption at ~0% strain) and the applied strain during loading and unloading.

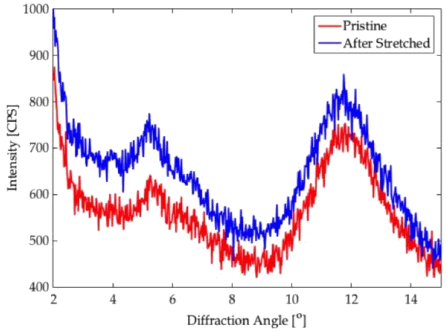

Fig. 2. XRD shows increased peak intensities at ~5° and ~12° when the P3HT-based thin films are stretched. This indicates possible alignment of P3HT molecules due to mechanical strains applied to the thin films.

Improved Performance of Water Vapour to Electric Convertion Based on Chitosan by Adding Carboxymethyl Cellulose

Tulus Ikhsan Nasution[1,2]*, Muhammad Balyan[1], Irwana Nainggolan[3]

[1]Physics Department, Faculty of Mathematics and Natural Science, University of Sumatera Utara, Medan 20155, Sumatera Utara, Indonesia
[2]Laboratory of Fisika Terpadu, University of Sumatera Utara, Medan 20155, Sumatera Utara, Indonesia
[3]School of Materials Engineering, Universiti Malaysia Perlis, Jejawi 02600, Perlis, Malaysia

*Corresponding author's: ikhsan_05@yahoo.com
Presenting author's: muhammad_balyan@yahoo.com

A water vapour cell based on chitosan has been successfully fabricated in thin film form to convert water-vapour to electricity [1]. This device is named water vapour cell because the cell works based on direct chemical interactions between the chitosan layer surface and water-vapour to generate electrical power. The cell manufactured in a single chip form with size of 1 cm x 1 cm consists of chitosan film on the top layer, patterned gold layer in the middle and isolator substrate in the bottom layer. This configuration has provided the positive polarity on the gold surface and negative polarity on chitosan film, so that the potential difference between them has existed. When the water vapour was exposed onto chitosan film surface, the chitosan film resistance changed and as a consequence, the output electrical power could be measured. In the previous work, water vapour cell generated electrical power at 230 nW and twenty weeks for lifetime [1]. As a raw material, chitosan has been used in many applications such as energy storage [2-4], photovoltaic cells [5,6], supercapasitors [7-10] lithium-ion batteries [11-13] and polymer electrolyte membrane (PEM) in the fuel cell [14-18]. The application of chitosan has evidences some advantages including: (1) chitosan is low-cost and eco-friendly; (2) the hydrophilicity of chitosan is a desirable property for use in high temperature and low relative humidity environment; (3) the backbone of chitosan has certain functional groups which allow chemical modification to tailor its properties [19,20]. However, chitosan has weakness in swelling properties [20]. In order to improve that, Carboxymethyl Cellulose (CMC) choosed as plasticizer. In this case, CMC is preferred to use because has properties such as, high viscosity, non-toxic, low cost and relatively similar structure with chitosan[21]. This allows CMC to improve the characteristics of chitosan itself. Then, CMC dissolved into chitosan 2% solution within concentration variations of 0 g, 0.01 g, 0.05 g, 0.1 g and 0.5 g. The cell was fabricated in a thin film form using an electrochemical deposition method. In electrical measurement, each cell exposed to water vapor and placed into a chamber. As a contact, the camber equipped with positive and negative electrodes. The result showed that the lifetime increased to twenty seven weeks by adding 0.5 g concentration of CMC but decreasing electrical power to 163 nW. Therefore, the best performance of lifetime and electrical power exhibited at 0.1 g is twenty four weeks and 226 nW, respectively. Based on FITR characterization, it was found CMC addition until 0.1 didn't change structure chitosan. However, chitosan

structure changed at 0.5 g. Bands at 2349 cm^{-1} and 1974 cm^{-1} could be founded with the increase in CMC content. This caused water vapour cell electrical power degenerated. Therefore, chitosan based water vapour cell added by 0.1 g CMC has best lifetime and electrical power.

Keywords: Water Vapour, Electrical Conductivity, Chitosan, Carboxymethyl Cellulose, Film.

[1] NASUTION, T.I., BALYAN, M., NAINGGOLAN, I., IQBAL, M. 2015. A Small Hydroelectric Cell Based on Chitosan. 5th International Conference on Fuel Cell & Hydrogen Technology, Kuala Lumpur, Malaysia, 1-3 September 2015.

[2] CHUPP, J., SHELLIKERI. A., PALUI. G., CHATTERJEE, J. 2015. Chitosan-based gel film electrolytes containing ionic liquid and lithium salt for energy storage applications. *Journal of Applied Polymer Science*, 132.

[3] HASSAN, S., SUZUKI, M., EL-MONEIM, A. A. 2014. Synthesis of MnO2-chitosan nanocomposite by one-step electrodeposition for electrochemical energy storage application. *Journal Power Sources*, 246, 68-73.

[4] RAMKUMAR, R., MINAKSHI, M. 2015. Fabrication of ultrathin CoMoO4 nanosheets modified with chitosan and their improved performance in energy storage device. *Dalton Transactions*, 44, 6158-68.

[5] AROF, A. K., BURAIDAH, M. H., TEO, L. P., MAJID, S. R., YAHYA, R., TAHA, R. M. 2010. Characterizations of chitosan-based polymer electrolyte photovoltaic cells. *International Journal Photoenergy*. 2010.

[6] MOHAMAD, S. A., YAHYA, R., IBRAHIM, Z. A., AROF, A. K. 2007. Photovoltaic activity in a ZnTe/PEO-chitosan blend electrolyte junction. *Solar Energy Material Solar Cells*, 91, 1194-8.

[7] HAO, P., ZHAO, Z., LENG, Y., TIAN, J., SANG, Y., BOUGHTON, R. I. 2015. Graphene-based nitrogen self-doped hierarchical porous carbon aerogels derived from chitosan for high performance supercapacitors. *Nano Energy,*15, 9-23.

[8] SUN, G., LI, B., RAN, J., SHEN, X., TONG, H. 2015. Three-dimensional hierarchical porous carbon/graphene composites derived from graphene oxide-chitosan hydrogels for high performance supercapacitors. *Electrochim Acta*, 171, 13-22.

[9] YAMAGATA, M., SOEDA, K., IKEBE, S., YAMAZAKI, S., ISHIKAWA, M. 2013. Chitosan-based gel electrolyte containing an ionic liquid for high-performance nonaqueous supercapacitors. *Electrochimica Acta*, 100, 275-80.

[10] SUDHAKAR, Y. N., SELVAKUMAR, M. 2012. Lithium perchlorate doped plasticized chitosan and starch blend as biodegradable polymer electrolyte for supercapacitors. *Electrochimica Acta*, 78, 398-405.

[11] MA, L., ZHOU, X., XU, L., XU, X., ZHANG, L., CHEN, W. 2015. Chitosan-assisted fabrication of ultrathin MoS2/graphene heterostructures for Li-ion battery with excellent electrochemical performance. *Electrochimica Acta*, 167, 39-47.

[12] ALI, A. M. M., YAHYA, M. Z. A., MUSTAFFA, M., AHMAD, A. H., SUBBAN, R. H. Y, HARUN, M. K. 2005. Electrical properties of plasticized chitosan-lithium imide with oleic acid-based polymer electrolytes for lithium rechargeable batteries. *Ionics*, 11, 460-3.

[13] KIM, K. W., KIM, J. S., LEE, S.W., LEE, J. K. 2015. Employment of chitosan-linked iron oxides as mesoporous anode materials for improved lithium-ion batteries. *Electrochim Acta*, 170, 146-53.

[14] XIANG, Y., YANG, M., GUO, Z., CUI, Z. 2009. Alternatively chitosan sulfate blending membrane as methanol-blocking polymer electrolyte membrane for direct methanol fuel cell. *Journal Membrane Science*, 337, 318-23.

[15] SHAARI, N., KAMARUDIN, S. K. 2015. Chitosan and alginate types of bio-membrane in fuel cell application: An overview. *Journal Power Sources*, 289, 71-80.

[16] MA, J., SAHAI, Y. 2013. Chitosan biopolymer for fuel cell applications. Carbohydrat Polymer, 92, 955-75.

[17] NOROOZIFAR, M., KHORASANI-MOTLAGH, M., EKRAMI-KAKHKI, M. S., KHALEGHIAN-MOGHADAM, R. 2014. Enhanced electrocatalytic properties of Pt-chitosan nanocomposite for direct methanol fuel cell by LaFeO3 and carbon nanotube. *Journal Power Sources*, 248, 130-9.

[18] MA, J., CHOUDHURY, NA., SAHAI, Y., BUCHHEIT, RG. 2011. A high performance direct borohydride fuel cell employing cross-linked chitosan membrane. Journal Power Sources, 196, 8257-64.

[19] RINAUDO, M. 2006. Chitin and chitosan: Properties and applications. *Progress Polymer Science*, 31, 603-32.

[20] DUTTA, P. K., DUTA, J., TRIPATHI, V. S. 2004. Chitin and Chitosan: Chemistry, properties and applications. *Journal Science Industrial Research*, 63, 20-31

[21] FATEH., PEDRAM,. 2011. Synergi of Carboxymethyl Celluosa (CMC) and Modified Chitosan on Strength Properties of Cellulosic Fiber Network. *Carbohydrate Polymers*, 80, 208-214.

Painless Diabetes Detection Using a Chitosan Based Breath Acetone Sensor

TulusIkhsan Nasution[1,2*], Rica Asrosa[1], Yetty Machrina[3], Irwana Nainggolan[4], Muhammad Balyan[1], Ridho Rumansyah[2]

[1]*Physics Department, Faculty of Mathematics and Natural Science, University of Sumatera Utara, Medan 20155, Sumatera Utara, Indonesia*
[2]*Laboratory of FisikaTerpadu, University of Sumatera Utara, Medan 20155, Sumatera Utara, Indonesia*
[3]*Medical Faculty, University of Sumatera Utara, Medan 20155, Sumatera Utara, Indonesia*
[4]*School of Materials Engineering, Universiti Malaysia Perlis, Jejawi 02600, Perlis, Malaysia*

*Corresponding author's and Presenting author's:ikhsan_05@yahoo.com

In this work, a painless method for diabetes detection using a practical, reliable and cheap breath acetone sensor from chitosan has been successfully fabricated. It has been well known that the expired breath of diabetics often smells with fruity scent. This fruity scent, or the smell of decayed apples, is a direct result of acetone presence in the breath [1]. Generally, the exhaled acetone level of healthy people is 0.3–0.9 ppm, while the concentration in diabetes patients exceeds 1.8 ppm [2,3]. This makes acetone to be a potential biomarker for painless detection of diabetes. In our previous report, chitosan based sensor has been well studied and proven to be able to detect very low concentrations of acetone vapour [4]. Chitosan solution was prepared by dissolving chitosan powder in 2% acetic acid using a magnetic stirrer with the rotation speed of 300 rpm for 24 h at room temperature. The chitosan based sensor was fabricated in a thin film form using an electrochemical deposition method. In the operation, each sensor tested was placed into a chamber, equipped with positive and negative electrodes. In order to obtain a practical detection, the data were recorded in a mobile phone via a bluetooth communication. The chitosan sensors were tested to 30 volunteers for both non-diabetic and diabetic patients in some Community Health Centers. The measurement results using chitosan sensor system showed that there was a significant difference of sensor readings, indicating different acetone concentrations in the breath of diabetics and non-diabetics. The sensor readings in term of resolution were below 30 for diabetics and above 40 for non-diabetics. Gaseous acetone concentration in exhaled breath has been recognized to possess tight and quantitative connection with blood glucose level [5-7]. Taking this into consideration, the sensor reading of the chitosan sensors and blood glucose values are compared. It was found that the blood glucose values of diabetics were above 114 mg/dl and non-diabetics were below 114 mg/dl using glucometer. The characterization result of SEM micrograph on the chitosan film showed the existence of very close distance among the chitosan particles which caused the chitosan surface layer to be smooth. The smooth surface has been believed to possess tight and influence with fast sensor response. Then, the AFM 3D image of the chitosan film exhibited even surface with the value of RMS and Ra of 0.1025 and

0,0759, respectively. The even surface has been believed could enhance the conductive pathways for electron transfer. Meanwhile, the FTIR spectra of chitosan indicated the presence of amino groups as the active sites in chitosan film structure which allowed the drastic improvements in sensitivity and selectivity. Therefore, the proposed breath sensor has provided a promising capability to be used as a new biomarker for diabetes detection.

Keywords: Chitosan, Painless Detection, Sensor, Breath Acetone, Diabetes

[1] S.S. LIKHODII, K. MUSA, S.C. CUNNAE. 2002. Breath acetone as a measure of systemic ketosis assessed in a rat model of the ketogenic die. *Clinical Chemistry*, 48, 115–120.

[2] A.M. DISKIN, P. SPANEL, D. SMITH. 2003. Time variation of ammonia, acetone, isoprene and ethanol in breath: a quantitative SIFT-MS study over 30 days. *Physiological Measurement*, 24, 107–119.

[3] C.H. DENG, J. ZHANG, X.F. YU, W. ZHANG, X.M. ZHANG. 2004. Determination of acetone in human breath by gas chromatography–mass spectrometry and solid-phase microextraction with on-fiber derivatization. *Journal of Chromatography B*, 810, 269–275.

[4] NASUTION, T.I., NAINGGOLAN, I, HUTAGALUNG, S.D., AHMAD, K.R., AHMAD, Z.A. 2013. The sensing mechanism and detection of low concentration acetone using chitosan-based sensors. *Sensors and Actuators B*, 177, 522-528.

[5] RIGHETTONI, M., SCHMID, A., AMANN, A., PRATSINIS, S.E., 2013. Correlations between blood glucose and breath components from portable gas sensors and PTR-TOF-MS. *Journal of Breath Research*. 7, 3.

[6] C. TURNER, C. WALTON, S. HOASHI, M. EVANS. 2009. Breath acetone concentration decreases with blood glucose concentration in type I diabetes mellitus patients during hypoglycaemic clamps. *Journal of Breath Research*. 3 .

[7] P.R. GALASSETTI, B. NOVAK, D. NEMET, C. ROSE-GOTTRON, D.M. COOPER, S. MEINARDI,et al. 2005. Breath ethanol and acetone as indicators of serum glucose levels: an initial report. *Diabetes Technology Therapeutics*. 7, 115–123.

Effect of alkyl side chain and electron-withdrawing group on BT–thiophene-based molecules in OPVs

Eunhee Lim (Lim)

Department of Chemistry, Kyonggi University, San 94-6, Iui-dong, Yeongtong-gu,

Suwon-si, Gyeonggi 443-760, Republic of Korea.

ehlim@kyonggi.ac.kr

A series of BT–thiophene-based small molecules, 2F-DH5TBs and DH5TPys, were synthesized to compare their physical and photovoltaic properties to those of DH5TBs and F-DH5TBs. The optical and electrochemical properties of the small molecules were systematically controlled by introducing electron-withdrawing substituents or modifying the alkyl pattern. In a series of small molecules containing thiophene and benzo[1,2,5]thiadiazole (BT), the electron-accepting units of BT were modified with fluorine and pyridyl nitrogen to enhance their electron-withdrawing abilities, which resulted in DH5TPys, F-DH5TBs, and 2F-DH5TBs. The solubilizing hexyl groups were introduced at two different β-positions on both ends of the thiophene rings. The highest occupied molecular orbital (HOMO) energy levels were decreased by the increasing number of fluorine substituents; 4-substitution resulted in deeper HOMO energy levels than 3-substitution. Among various BT–thiophene-based small molecules, 2F-DH5TB-4 yielded the best PCE of up to 1.27% in solution-processed OPVs.

Keywords: Photovoltaic, solar cell, materials, thin films

[1] CHO, A, KIM, Y., SONG, C. E., MOON, S.-J. & LIM, E. 2014. Synthesis and Characterization of Fluorinated Benzothiadiazole-Based Small Molecules for Organic Solar Cells. *Science of Advanced Materials*, 6, 2411-2415.

White Light Emitting Diodes by Casting Wavelength- converting Polymer on InGaN Devies

Chi-Jung Chang[1,*], Chun-Feng Lai[2], Yun-Yi Leong[1], Min-Ju Su[1], Wei-Yung Chiou[1]

[1]Department of Chemical Engineering, [2] Department of Photonics, Feng Chia University, 100, Wenhwa Road, Seatwen, Taichung 40724, Taiwan, ROC

*E Mail : purpleshinnystar@hotmail.com (*Yun-Yi Leong, **presenting author)**

E Mail : changcj@fcu.edu.tw (*Chi-Jung Chang, **corresponding author)

Transparent UV-curable polysiloxane encapsulants were prepared by a hydrosilylation reaction of tris(dimethylsiloxy)phenylsilane monomers, dimethoxymethylvinylsilane, and methacryl polyhedral oligomeric silsesquioxane. Thermal curing takes longer than UV curing [1]. Researchers found that encapsulating the blue LED with organic polymer blend encapsulant can produce efficient white light emitting diodes (WLEDs). In this study, transparent UV-curable polysiloxane encapsulants were blended with the red fluorescent polymer and green fluorescent polymer to make the wavelength-converting polymer (WCP). WCP were casted on blue light emitting InGaN diodes and UV cured to fabricate WLEDs. The encapsulants exhibit good thermal and mechanical properties, together with good compatibility with fluorescent polymers. We try to produce WLEDs with appreciable performances, such as color rendering index (CRI), the Commission Internationale de l'Éclairage (CIE) coordinates, and correlated color temperature (CCT). Increasing the content of red fluorescent polymer lead to an increase in CRI and shift towards warm white light. However, the efficacy decreased with increasing red fluorescent polymer content.

Keywords: White light emitting diodes, UV curable, polysiloxane, fluorescent polymer, wavelength conversion.

[1] BASIN, G., WEST, R.S., MARTIN, P.S., HARBERS, G., SMITS, W.H., HENDRIKS, R.F., & KONIJN, F.H. 2008. Overmolded lens over LED die. *U.S. Patent* 7,344,902.

White Light Emitting Diodes by Encapsulating InGaN with Thermally Curable Polysiloxane/Inorganic Phosphor Composites

Chi-Jung Chang[1,*], Chun-Feng Lai[2], Wei-Yung Chiou[1], Min-Ju Su[1]

[1]Department of Chemical Engineering, [2] Department of Photonics, Feng Chia University,

100, Wenhwa Road, Seatwen, Taichung 40724, Taiwan, ROC

*E Mail : dres6118@gmail.com (*Min-Ju Su, **presenting author)**

*E Mail : changcj@fcu.edu.tw (*Chi-Jung Chang, **corresponding author)**

Thermally curable polysiloxane-based encapsulants were prepared by hydrosilylation reaction of phenyltris(dimethylsiloxy)silane (PTDMSS) monomers and aromatic diallyl or dimethacrylate monomers. Blue light emitting diodes (LEDs) were used with phosphors [1,2], quantum dots [3] to produce white light emitting devices. In this study, a blue light emitting InGaN diode was disposed in a reflective cup and surrounded by thermally curable polysiloxane encapsulants/inorganic phosphor hybrid to fabricate white light emitting diodes (WLEDs). The thermal resistance, optical, and mechanical properties of the encapsulants were tuned by changing the chemical structure of diallyl or dimethacrylate monomers. We try to produce WLEDs with appreciable performances by wavelength conversion mechanism, such as color rendering index (CRI), the Commission Internationale de l'Éclairage (CIE) coordinates, and correlated color temperature (CCT). The Ra, CRI and CCT of WLEDs were tuned by incomplete energy transfer of inorganic phosphors.

Keywords: White light emitting diodes, thermally curable, polysiloxane, inorganic phosphor, organic/inorganic hybrid.

[1] SRIVASTAVA, A. M., COMANZO, H. A., & MCNULTY, T. F. 2003. White light emitting phosphor blends for LED devices. *U.S. Patent 6,621,211*.

[2] SHIN, M. H., HONG, H. G., KIM, H. J., & KIM, Y. J. 2014. Enhancement of Optical Extraction Efficiency in White LED Package with Quantum Dot Phosphors and Air-gap Structure. *Applied Physics Express*, *7*, 052101.

A study of chiral nematic behavior of self-assembled cellulose nanocrystal films

Bumbudsanpharoke Nattinee, Seonghyuk Ko
Department of Packaging, Yonsei University,Yonseidaegil, Wonju-si, Gangwon-do, 220-710 Korea
Corresponding author: s.ko@yonsei.ac.kr

Cellulose nanocrystals (CNCs), a high crystalline rod-like particle derived from renewable resources, have recently been attracting large interest due to their unique optical properties. Concentrated colloidal suspension of CNCs forms self-assembled structure in a stable chiral nematic liquid crystalline phase. In the fluid state, the periodically ordered helical CNCs are usually in the range of tens of micrometers, but upon drying, the periodicity could be reduced to submicrometer. This value of dried films is small enough in Bragg reflection of visible light, consequently, striking iridescent color. The alteration in periodically repeat distance, called pitch, by expanding or contracting the helix leads to distinct color reflectance. In this study, we have prepared the CNCs suspension by the sulfuric acid hydrolysis of pure cotton microcrystals. The extracted crystal was characterized by X-ray powder Diffraction (XRD). The morphology and thermal properties were analyzed with Field Emission Scanning Electron Microscope (FESEM), Atomic-Force Microscopy (AFM), Thermogravimetric Analysis (TGA), and Differential Scanning Calorimetry (DSC). An attempt is made to qualitatively interpret the observed liquid crystal behavior in terms of the chiral nematic orientation of the CNCs via the freestanding films. The gradual evaporation of CNCs suspensions at the critical concentration yielded an iridescent film with reflection colors at visible wavelengths. The effect of concentration of CNCs suspension on chiral nematic behavior as well as the factors that control a periodicity or helical pitch affecting to the diversity in reflection colors of CNCs film are investigated. The chiral nematic structure and helical pitch lengths of dry films will be presented with FE-SEM and AFM micrograph. The change in color reflectance from helical pitch may find potential application for the color indicator system.

Keywords: cellulose nanocrystal, chiral nematic structure, reflection colors, indicator

[1] LAGERWALL, J. P. F., SCHUTZ, C., SALAJKOVA, M., NOH, J., PARK, J. H., SCALIA, G. & BERGSTROM, L. 2014. Cellulose nanocrystal-based materials: from liquid crystal self-assembly and glass formation to multifunctional thin films. Npg Asia Materials, 6, e80.
[2] MAJOINEN, J., KONTTURI, E., IKKALA, O. & GRAY, D. G. 2012. SEM imaging of chiral nematic films cast from cellulose nanocrystal suspensions. Cellulose, 19, 1599-1605.
[3] ZHANG, Y. P., CHODAVARAPU, V. P., KIRK, A. G. & ANDREWS, M. P. 2012. Nanocrystalline cellulose for covert optical encryption. Journal of Nanophotonics, 6, 063516-1-063516-9.
[4] PAN, J. H., HAMAD, W. & STRAUS, S. K. 2010. Parameters Affecting the Chiral Nematic Phase of Nanocrystalline Cellulose Films. Macromolecules, 43, 3851-3858.
[5] ZHANG, Y. P., CHODAVARAPU, V. P., KIRK, A. G. & ANDREWS, M. P. 2013. Structured color humidity indicator from reversible pitch tuning in self-assembled nanocrystalline cellulose films. Sensors and Actuators B-Chemical, 176, 692-697.

Acknowledgment
This research was supported by Basic Science Research Program through the National Research Foundation of Korea (NRF) funded by the Ministry of Education (Grant No. 2013R1A1A2060023).

Flame retardant fibers prepared by aromatic polysulfonamide and cellulose co-dissolved in ionic liquid

Kaijian Wu[1], Yongbo Yao[1], Xinyang Liu[1], Shenhui Chen[2], Xiaofeng Wang[2], Yumei Zhang[1], Huaping Wang[1]

[1] State Key Laboratory for Modification of Chemical Fibers and Polymer Materials, College of Materials Science and Engineering, Donghua University, Shanghai, 201620, China; 2 Shanghai Tanlon Fiber Co., Ltd, Shanghai, 201419, China

Presenting author: email: 1142029@mail.dhu.edu.cn;

Corresponding author email: zhangym@dhu.edu.cn.

1-Butyl-3-methylimidazolium chloride ([BMIM]Cl) was selected as co-solvent to dissolve cellulose and aromatic polysulfonamide fiber (PSA) and the cellulose/PSA blend fibers were first fabricated with dry-jet wet spinning technology. It is shown that PSA and cellulose can be dissolved in [BMIM]Cl, The complex viscosity of the blend solution decreased with increasing ratio of PSA. The structure, mechanical properties, flame retardant behavior of the blend fibers were also investigated, it is found that the blend fibers have excellent mechanical properties, and the Limited Oxygen Index(LOI) increases with the addition of PSA, when the contend of PSA reached 70%, the LOI of blend fiber is 26.2, which shows good flame retardant behavior.

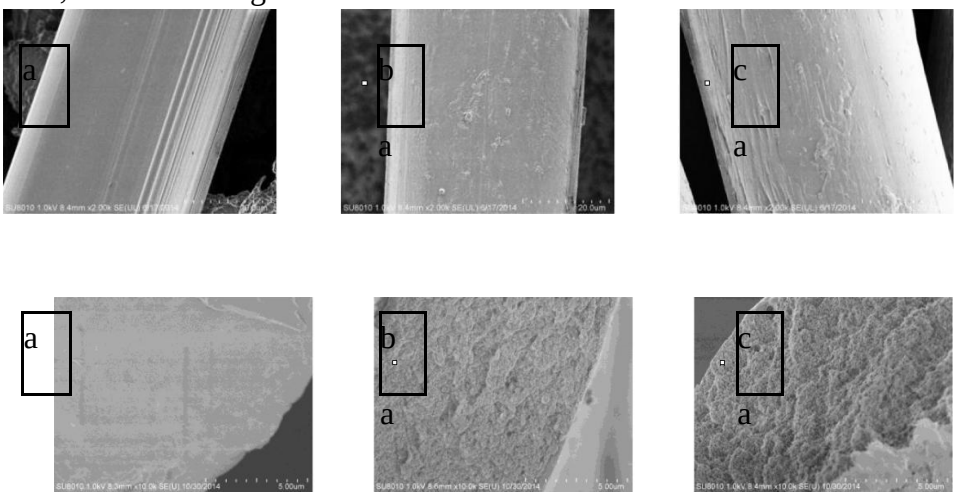

Figure 1: SEM of cellulose/PSA blend fibers: a cellulose fiber, b CP73 fiber, c CP37 fiber**.**

Keywords: cellulose; aromatic polysulfonamide; blend fiber; co-dissolution; flame retardant behavior.

[1] KOCER H B., CERKEZ I., WORLEY S D. 2011. Cellulose/starch/HALS composite fibers extruded from an Ionic liquid. Carbohydrate Polymers, 86, 922-927.

[2] BOMOU M., ZHANG M., CHUNJU H. 2012. New binary Ionic liquid system for the preparation of chitosan/cellulose composite fibers. Carbohydrate Polymers, 88, 347-351.

[3] SALIHU G., GOSWAMI P., RUSSELL S. 2012. Hybrid electrospun nonwovens from chitosan/cellulose acetate. Cellulose, 19, 739-749.

[4] ZHUANG X P., LIU X F., LI S Y. 2008. Preparation and properties of 2-(2- aminoethoxy) ethyl chitosan/cellulose fiber using N-methylmorpholine-N-oxide process. Fibers and Polymers, 9, 400-404.

[5] XINGWEI S., YANLI H., FEIYA F., JINPING Z., YIXIANG W., LINGYUN C., HONGMING Z., JI L., XIANHONG W., LINA Z. 2014. Construction of PANI–cellulose composite fibers with good antistatic properties. Journal of Materials Chemistry a, 2, 7669-7673.

Nonadherent drug delivery nanofabrics developed from assembled prolamin proteins

Yixiang Wang, Zhigang Tian, Lingyun Chen*

*Corresponding author: Lingyun Chen, Dept. of Agricultural, Food and Nutritional Science, University of Alberta, Edmonton, Canada T6G 2P5
Tel.: 1-780-492-0038; Fax: 1-780-492-4265; Email: lingyun.chen@ualberta.ca

Development of value-added functional materials from the co-products of industrial processing of cereal crops has attracted more and more attentions. Zein and hordein are the major storage proteins in corn and barley, respectively. We presented an assembled nanofabric prepared by incorporating compact zein nanoparticles in electrospun hordein networks. Zein particles in one aspect acted as the plasticizer to decrease the strong hydrogen bonding interactions among extended hordein molecules, leading to the accelerated continuous electrospinning and narrowed diameter distribution of composite fibers. In another, they also played as the reinforcing filler in the flexible hordein matrix. The assembled fibers exhibited significantly improved tensile strength and wet stability in both water and ethanol. The alignment of electrospun fibers further strengthened the nanofabrics in both tangential and normal directions to 17.26 ± 1.41 and 14.02 ± 0.74 MPa, respectively, stronger than that of cancellous bones (5-10 MPa), by not only altering the piling up pattern, but also promoting phase separation and improved interactions. It has also been discovered that, by simply altering the applied voltage, the resultant hordein/zein nanofabrics can rapidly (within 30 s) form either flat sheets or self-rolled tubes when they were immersed in water. Particularly, the fibers fabricated at relatively lower voltage were stabilized by the pre-aggregated nanoscale hydrophobic domains, exhibiting restricted swelling, while maintaining a flat sheet shape with minimal changes to secondary structure when immersed in water. By applying a higher voltage, a greater bending instability was triggered during the electrospinning process, and the generated hordein/zein network structure could rapidly relax in an aqueous environment. This increased mobility of molecular chains allowed the uneven aggregation of hydrophobic dopants which catalyzed the self-rolling of the aligned fibers. All the fibers demonstrated low toxicity in human primary dermal fibroblast cell culture. Moreover, the electrospun fabrics exhibited a strong resistance to protein adsorption and cell attachment, and the release experiment indicated that they could serve as a carrier for controlled-release of incorporated bioactive compounds into phosphate-buffered saline. Therefore, these electrospun prolamin protein fabrics represent an ideal and novel platform to develop nonadherent drug delivery systems for wound dressing and other biomedical applications.

Preparation and Properties of Natural Rubber Grafted with Poly(Butyl Acrylate-*co*-Fluorinated Acrylate)

KotchamonYimmut[1], NapidaHinchiranan[2]

[1]Program in Petrochemistry and Polymer Science, Faculty of Science, Chulalongkorn University, Bangkok 10330, Thailand.
[2]Department of Chemical Technology, Faculty of Science, Chulalongkorn University, Bangkok 10330, Thailand.

**E Mail/ Contact Details:kotchamon_nam@hotmail.com[1], napida.h@chula.ac.th[2].*

Fluorinated polymers have attractive properties in terms of thermal stability, high electronegativity and low surface energy resulting in high contact angles for water and oil. However, they are expensive and have poor mechanical properties such as low flexibility and high brittleness. This problem can be solved by copolymerization with other monomers such as acrylate monomers. According to the excellent properties of the fluorinated polymers, they are expected to be used for improving the properties of natural rubber (NR), which has poor resistance to heat, hydrocarbon solvents and weather resulting from its low polarity and high surface energy. However, thedirect blending of NR and fluorinated polymers is limited since they have large properties difference. Thus, the graft copolymerization is applied for enhancing the phase compatibility in the blends. In this research, 2,2,2-trifluoroethyl methacrylate (3FMA), one of the fluorinated monomers, was selected to be grafted onto the NR backbone. The butyl acrylate (BA) was used as a co-monomers for this system since it could be copolymerized with 3FMA and also grafted with NR. The graft copolymerization of poly(BA-*co*-3FMA) onto NR was carried out in the emulsion polymerization using potassium persulfate as an initiator. The effects of initiator concentration, wt ratio of BA/3FMA, reaction temperature and reaction time ongrafting properties, thermal properties, morphology and water contact angle of the graft NR were investigated. The chemical structure of NR before and after modification was detected by using attenuated total reflectance Fourier transform infrared spectroscopy (ATR-FTIR) and nuclear magnetic resonance spectroscopy (^{1}H NMR and ^{19}F NMR). The thermal properties were evaluated by using thermogravimetric analysis (TGA) and differential scanning calorimetry (DSC). From the initial study, it was observed that the graft product was consisted of 20wt% free NR, 12wt% free copolymer and 70wt% graft copolymer (NR-*g*-(BA-*co*-3FMA)) when the reaction was performed at 60 ^{o}C for 8 h. It was noticed that the contact angle of the graft product was gradually increased from 60^{o} to 111.6^{o} with increasing the 3FMA content from 0 to 70 phr.

Keywords: Natural rubber, graft copolymerization, butyl acrylate, 2,2,2-trifluoroethyl methacrylate

[1]CHUMSAMRONG, P., MONPRASIT, O. 2007. Preparation, Adhesive performance and stability of natural rubber latex grafted with n-butyl acrylate (BA) and methyl methacrylate (MMA). *Suranaree Journal* of *Science* and *Technology*, 14.

[2] ZHANG, C., MAN, C., PAN, Y., WANG, W., JIANG, L., DAN, Y. 2011. Toughening of polylactide with natural rubber grafted with poly(butyl acrylate). *Polymer International*, 60, 1548–1555.

Biocatalytic Self-Cleaning Polymer Membranes

Agnes Schulze (Schulze), Isabell Thomas (Thomas), Andrea Prager (Prager)

Leibniz Institute of Surface Modification, Permoserstr. 15, D-04318 Leipzig, Germany

E-Mail: Agnes.Schulze@iom-leipzig.de / Tel.: +49-341-235-2400

Porous polymer membranes are of increasing importance regarding modern separation technologies such as waste water treatment, sterilization filtration, hemodialysis, dairy industry, etc. To comply with required process conditions these polymer membranes are predominantly fabricated from synthetic materials such as polyethersulfone, polysulfone, or polyvinylidene fluoride. However, membranes made from these polymers are prone to *fouling* which is caused by hydrophobic interactions of the membrane surface with biomolecules or colloids in the mixture to be filtered and results in irreversible adsorption, aggregation, and finally, in a reduced filtration performance.

To improve the antifouling properties of polymer membranes, many approaches for surface modification have been reported. However, commonly used hydrophilization methods are characterized by serious disadvantages as they risk the contamination of the eluent by non-permanently immobilized compounds or by applied initiators/catalysts. Furthermore, they require a substantial number of process steps (e.g. activation of the scaffold polymer for subsequent grafting reaction and additional purification steps), and additionally, harmful or even toxic compounds are used.

We have reported that electron beam (EB) technology can be efficiently used for the hydrophilization of polymer membranes by directed grafting of hydrophilic small molecules/polymers to the membrane surface [1-2]. This approach combines surface activation of the membrane polymer and simultaneous immobilization of the hydrophilic compounds by application of low-energy EB in an aqueous system. The procedure neither requires any preceding surface functionalization nor the use of catalysts or other toxic reagents.

In this presentation, the covalent immobilization of the digestive enzyme trypsin on polymer membranes by EB induced grafting is described [3-4]. Trypsin is a well-studied proteolytic enzyme that catalyzes the hydrolysis of peptide bonds at an optimum pH value of 7.5–8.5. Since free trypsin is stable within a pH range of 3–11 this enzyme can be used in common membrane-based water treatment applications, even when pH changes occur in the process.

The resulting membranes showed significantly improved antifouling properties as demonstrated by repeated filtration of protein solutions. Furthermore, by changing pH the biocatalytic membrane can be simply “switched on” to actively degrade a fouling layer on the membrane surface and regain the initial permeability. It was demonstrated that the resulting membranes showed a significantly higher catalytic activity as compared to enzyme immobilization per adsorption on the membrane surface. Additionally, the enzyme immobilization itself didn’t negatively impact the membrane surface as demonstrated by pure water flux experiments, scanning electron microscopy, and mercury porosimetry measurements.

Keywords: polymer membrane, enzyme immobilization, fouling, self-cleaning, electron beam

[1] SCHULZE, A., MARQUARDT, B., KACZMAREK, S., SCHUBERT, R., PRAGER, A. & BUCHMEISER, M. R. 2010. Electron Beam-Based Functionalization of Poly(ethersulfone) Membranes. *Macromol. Rapid Comm.*, 31, 467-472.

[2] SCHULZE, A., MAITZ, M. F., ZIMMERMANN, R., MARQUARDT, B., FISCHER, M., WERNER, C., WENT, M. & THOMAS, I. 2013. Permanent Surface Modification by Electron-Beam-Induced Grafting of Hydrophilic Polymers to PVDF Membranes. *RSC Adv.*, 3, 22518-22526.

[3] JAHANGIRI, E., REICHELT, S., THOMAS, I., HAUSMANN, K., SCHLOSSER, D. & SCHULZE, A. 2014. Electron Beam-Induced Immobilization of Laccase on Porous Supports for Waste Water Treatment Applications. *Molecules*, 19, 11860-11882.

[4] SCHULZE, A., STOELZER, A., STRIEGLER, K., STARKE, S. & PRAGER, A. 2015. Biocatalytic Self-Cleaning Polymer Membranes. *Polymers*, 7, 1837-1849.

On Influence of Processing Conditions on Characteristics of Thermally Bonded Polypropylene Meltblown Fabrics

Tomas Sedlacek, Pavel Bazant, Patrik Rohrer

Centre of Polymer Systems, Tomas Bata University in Zlin, Trida T. Bati 5678, 76001

Zlin, Czech Republic.

sedlacek@cps.utb.cz

Polypropylene melt was processed using a laboratory meltblown line into the form of nonwoven fabrics made of bicomponent core-sheath staple fibres. Processing conditions as temperature of extruded polymer melts and blowing air entering the spinneret, distance between the spinneret and the web forming device, and temperature of the compacting calendar were altered in order to change created fibres diameters as well as pores sizes distribution and density of prepared fabric structures. In this way the variety in softness, surface feeling, absorption ability and mechanical properties of the final web were achieved. For evaluation of changes in pursued properties the scanning electron microscope, the gas pycnometer, the mechanical universal testing machine, and the developed software predicting filtration ability were employed. The thorough analysis of processing conditions and nonwovens characteristics relation defined feasibility to purposefully affect and determine air filtration efficiency as well as mechanical performance of prepared meltblown fabrics.

Keywords: meltblown process, bicomponent fibres, nonwoven fabric, polypropylene

PCDTBT Nanotubes: Template Replication via Polymer Melts of Above Melting Point

Nor Asmaliza (Bakar)[1], Azzuliani (Supangat)[2], Khaulah (Sulaiman)[2]

[1]Department of Physics, Faculty of Science, University of Malaya, 50603 Kuala Lumpur, Malaysia.

[2] Low Dimensional Materials Research Centre, Department of Physics, Faculty of Science, University of Malaya, 50603 Kuala Lumpur, Malaysia.

azzuliani@um.edu.my

Poly [N-9'-heptadecanyl-2,7-carbazole-alt-5,5-(4,7-di-2-thienyl-2',1',3'benzothiadiazole] (PCDTBT) nanotubes have recently received much more interest and have become a promising *p*-type material in the nanotechnology field. Generally, PCDTBT nanotubes can be easily synthesized and controlled by nanoporous alumina templating method. In this work, replication of template by PCDTBT nanotubes has been realized by applying temperature above its melting point. The process has undergone the template wetting of polymer melts [1]. This research will present the effective ways to enhance replication of nanochannels, which typically focused on the effect of wetting time, melting temperature and solution concentration. Aligned PCDTBT nanotubes with the rounded openings have been obtained at the elevated temperature. Optical properties of aligned nanotubes have shown the red-shifted and quenching properties. PCDTBT nanotubes are potential to be integrated as sensors and in organic electronics devices.

Keywords: PCDTBT, nanotubes, template, polymer melt, optical properties

[1] SARMAD ALI, WEI TIAN, NISAR ALI, LINGXIAO SHI, JIE KONG, NAZAKAT ALI. 2015. Polymer Melts Flow through Nanochannels: from Theory, Fabrication to Application. *RSC Advances*, 5, 7160-7172.

Preparation and Characterisation of Foams with Optimized Polyolefinic Molecular Structure

Pavlina Plskova, Vera Canova, Aneta Sklenarova, Tomas Sedlacek

Centre of Polymer Systems, Tomas Bata University in Zlin, Trida T. Bati 5678, 76001

Zlin, Czech Republic.

plskova@cps.utb.cz

Preparation and characterisation of polymeric foams made of polyolefinic compounds composed of commercially available polyethylenes with various molecular structure using chemical foaming process was the main aim of the presented study. Polymer compounds utilised for foam preparation were obtained via thorough mixing of selected materials utilizing twin screw extruder. While low density polyethylene was taken as the primary component, linear low density polyethylenes with defined diverse length of branches as well as their density were chosen as the suitable counterparts. In this way was modified melt strength of processed polymers as the main factor affecting growth and collapse of pores during foaming procedure. Foaming of prepared compounds was carried out by the help of the manual heated/cooled presses under optimized process conditions. Achieved foamed structures, namely foam densities, pores size distributions and ratio of open/close pores, were evaluated employing computer tomography and pycnometer. The careful comparison of foams characterisations revealed the crucial influence of the molecular arrangement of utilised compounds on the final structure of prepared polyethylene foams.

Keywords: polymer foam, foam density, pores size distribution, low density polyethylene, linear low density polyethylene

Effect of heat treatment on porous geopolymer using spent materials

Seongyeol Kim[1], Yooteak Kim[1]

[1]Kyonggi university, Department of Materials Engineering, Suwon, Republic of Korea 16227

E-mail : ytkim@kyonggi.ac.kr, Contact Details : +82-70-4024-9765

Porous geopolymer has many application fields like thermal insulation and fire resistant materials because it possesses excellent properties such as low bulk density, high permeability, low thermal conductivity, and high surface area. In this study, porous geopolymer was fabricated by using spent materials (waste catalyst slag with spent silicon sludge as bloating agent for making numerous pore). Spent silicon sludge which was produced in the silicon wafer polishing processing for producing substrate of solar cell was used as bloating material for porous geopolymer. Waste catalyst slag which was obtained after metals recovery of spent catalyst was used as raw material for porous geopolymer in order to recycle useful spent materials and to treat hazardous material in safe way. The density and compressive strength of porous geopolymers decreased with an increase in silicon sludge addition because silicon sludge reaction discharges H2 gas and forms many pores. Compressive strength of geopolymers increased up to 7MPa after calcination at 500℃ because of combination of geopolymerization and formation of networks by heat treatment. Density of geopolymers decreased to less than 1.5g/cm^3 with an increase in temperature due to activated silicon sludge reaction. In conclusion, spent silicon sludge acts effectively as a bloating agent and low density porous geopolymers having relatively high compressive strength was obtained using waste catalyst slag. The typical porous geopolymers usually have density less than 1.5g/cm^3 and compressive strength less than 2MPa. Therefore, it is concluded that the heat treatment of geopolymer has a good effect on the mechanical strength of porous geopolymers and the optimum temperature of heat treatment was 500℃.

Keywords: geopolymer, silicon sludge, waste catalyst slag, porous ceramic

Fabrication of three dimensional graded macroporous biodegradable scaffold by vacuum assisted resin transfer molding

Qiu Liu[1,2] Qianting Wang[1,2] Zhixiang Cui[1,2] Junhui Si[1,2] Wenzhe Chen[1,2,3]

[1] School of Materials Science and Engineering, Fujian University of Technology, Fujian, Fuzhou 350118;

[2] Fujian Provincial Key Laboratory of Advanced Materials Processing and Application, Fujian, 350118;

[3] School of Materials Science and Engineering, Xiamen University of Technology, Fujian, Xiamen 361024

In this study, elastic polydimethylsiloxane (PDMS) and CS-coated PDMS scaffolds with graded microporous were fabricated by vacuum-assisted resin transfer moulding (VARTM) and particle leaching technologies. To control the porous morphology and porosity, different processing parameters, such as compression load, compression time, and NaCl particle size for preparing NaCl preform, were studied. The porous structures of PDMS cell scaffolds were characterized by scanning electron microscopy (SEM). The properties of PDMS cell scaffolds, including porosity, water absorption, interconnectivity, compression modulus, and compression strength were also investigated. The results showed that the interconnectivity of PDMS cell scaffolds increases with an increase in the size of NaCl particles. It was also found that the smaller the size of the NaCl particles, the higher the porosity and water absorption of PDMS cell scaffolds. In addition, the hydrophellolic and mechanical properties of CS-coated PDMS scaffolds were improved compared to those of PDMS scaffolds by using CS coating treatment.

Template synthesis of macroporous calcium monosilicates and based on them new bioceramic composites using Spark Plasma Sintering

Papynov E.K.[1,2], Shichalin O.O.[1,2], Modin E.B.[2], Mayorov V.Yu[1], Portnyagin A.S.[1,2], Gridasova E.A.[2], Tananaev I.G.[1,2], Avramenko V.A.[1,2]

[1]Institute of Chemistry, Far Eastern Branch of Russian Academy of Sciences, 159, Prosp. 100-letiya Vladivostoka, Vladivostok 690022, Russia

[2]Far Eastern Federal University, 8, Suhanova St., Vladivostok 690091, Russia

Papynov@mail.ru

Here we suggest a new method of template sol-gel synthesis of porous calcium monosilicates and show that the ordered macroporous structures can be obtained for silicate materials (average pore size 160 nm) using siloxane-acrylate latexes as a template. Effect of thermal conditions during template destruction on morphological properties of nanostructured silicates have been elucidated. The novel method of fabrication of macroporous wollastonite with immobilized gold nanoparticles (average size 5-30 nm) have been developed using pre-functionalized siloxane-acrylate latex template. The new porous ceramic composites based on nanostructured wollastonite, also with Au nanoparticles, have been successfully synthesized by Spark Plasma Sintering (SPS) technology. Peculiarities of structural parameters variation of studied materials under SPS conditions within the temperature interval 800 – 1000 °C are described also the optimal parameters of synthesis are determined. The very useful procedure of porous structure control of wollastonite ceramic that allows obtaining of hierarchically porous silica framework from nano- to microsized pores through a poreforming agent (carbonaceous template) is suggested. The nanostructured silicate materials that were obtained by template synthesis and wollastonite ceramic consolidated via SPS technique are characterized by a number of unique features: chemical composition stability, appropriate for various bioactive media, developed porous structure similar to that of bone tissue, and mechanical strength (Young's modulus more than 100MPa), which is responsible for durability. These ceramic composites can be classified as a bioceramic which are prospective for medical practice.

Keywords: Nanostructured materials, macroporous silicates, bioceramic, template synthesis, Spark Plasma Sintering.

Effect of Constitutional Variations on Glass-Forming Ability of $Y_3Al_5O_{12}$ Melts

Xiaoguang Ma[a,b], Xiaoyu Li[a], Bingqian Ma[a], Jianqiang Li[a]*

[a] National Engineering Laboratory for Hydrometallurgical Cleaner Production Technology, Key Laboratory of Green Process and Engineering, Institute of Process Engineering, Chinese Academy of Sciences, Beijing 100190, P. R. China

[b] School of Engineering and Technology, China University of Geosciences, Beijing 100083, P. R. China
* Corresponding author. E-mail: jqli@ipe.ac.cn

The $Y_3Al_5O_{12}$ (YAG) composition glass material has great potential application in the fields of optical information communication, and luminescence. The formation of hexagonal $YAlO_3$ (YAH) and YAG crystalline phases cannot be avoided in the preparation of $Y_3Al_5O_{12}$ glass using the containerlessly rapid solidification method owing to its fragile glass-forming ability. However, for many optical applications, it is desirable to obtain pure amorphous glass with uniform optical properties. In this work, $Y_3Al_5O_{12}$-based transparent glasses were successfully fabricated by adding excess Al_2O_3, or substitute Nd_2O_3 in place of Y_2O_3 to stoichiometric YAG composition. And their effects on the glass-forming ability of $Y_3Al_5O_{12}$-based composite were studied. Differential scanning calorimetry results show that the substituting of Al_2O_3 and Nd_2O_3 is beneficial for improving its glass-forming ability, while the glass-forming ability would decrease with the substituting of Y_2O_3. Interestingly, X-Ray Diffraction patterns indicate that the gradual increasing of the Al_2O_3 and Nd_2O_3 resulted different trends of inhibition of crystal formation. YAG and YAH in $Y_3Al_5O_{12}$-based glass both disappeared when the content of Nd_2O_3 increased to 15 at%.

Polyethyleneimine Templated Biomimetic mineralization forNanostructured Chiral and Photoluminescent ceramics/carbon

Ren-Hua JIN
(Department of Material and Life Chemistry, Kanagawa University, 3-27-1 Rokkakubashi, Yokohama 221-8686, Japan)
Tel: 045-481-5661 (3845), E-mail: rhjin@kanagawa-u.ac.jp

Chiral ceramic materials have recently attracted significant interest because of their unique structures and properties as well as potential applications in many fields, such as chiral catalysis, optical separation, and drug delivery. Especially chiral silica has been extensively investigated due to its excellent thermal stability, good chemical inertness, carrier capability and easy solubility in specific media. We have established a universal process of constructing shaped and/or chiral silica nanomaterials by means of polyethyleneimine (PEI) templated silicification approach, from which we can extensively design photoluminescent, chiral, catalytic ceramics and carbons. Here, we report our recent achievements in the synthesis and application of nanostructured/chiral silica for developing chiral ceramics with photoluminescence, catalysis and for developing nanocarbon.

1) Chiral ceramics Scheme 1 shows one typical example of synthesis of Ag/silica composite with chirality and catalysis.

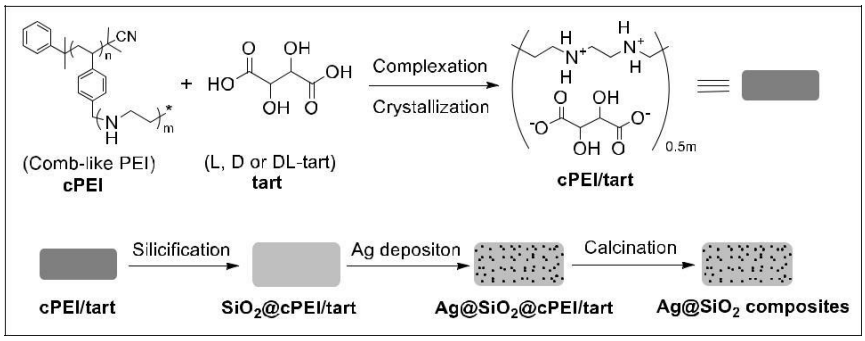

Scheme 1

2) Nanocarbons As shown in the Scheme 2, silica nanofiber obtained via PEI-templating can self-promote polycondensation of aldehydes and resorcinol and resulted in polyphenol coat along the silica surface. Subsequent carbonization and remove of silica produced carbon nanotube.

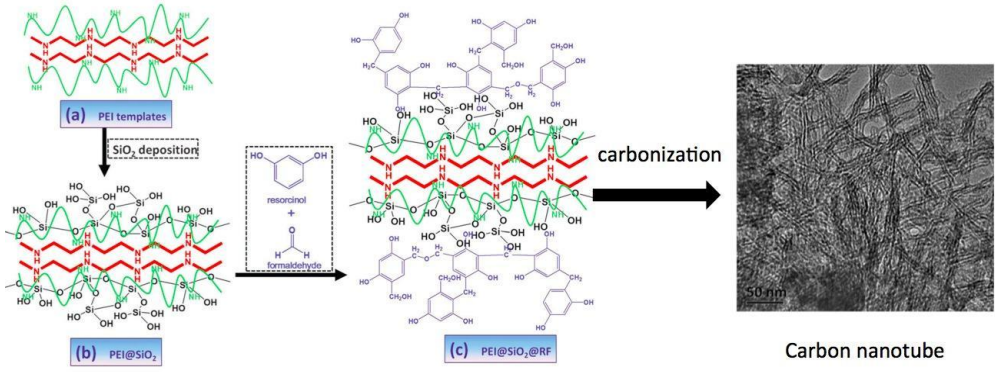

Scheme 2

Properties analysis of partially-stabilized zirconia doped Na^+-beta-alumina prepared by calcining-cum-sintering process

Dae-Han Lee, Sung-Tae Lee, Jin-Sik Kim and Sung-Ki Lim*

Department of Materials Chemistry and Engineering, Konkuk University, 1 Hwayang-dong, Kwangjin-gu, Seoul 143-701, South Korea

Corresponding Author: Sung-Ki Lim
E-mail: sklim@konkuk.ac.kr

In order to overcome the demerit of conventional process including complex steps, Na^+-beta-aluminas as a Na^+ solid electrolyte were prepared by calcining-cum-sintering process. Na^+-beta-aluminas were sintered at once from the mixture of α-alumina, sodium carbonate and magnesium hydroxide without separate calcination process. In granulation step, partially CaO/Y_2O_3-stabilized zirconia (CSZ or YSZ) was added as a sintering additive to improve the sintering properties. The properties of Na^+-beta-aluminas have been investigated with respect to the microstructure, the phase fraction, the relative density and the ionic conductivity. The addition of zirconia could contribute to an improvement in the degree of densification. Ionic conductivity of specimens was measured by AC-impedance spectroscopy between 25 ^oC and 350 ^oC and the total (grain and grain-boundary) specific resistivity was observed to be ~ 7.6 **Ω** cm at 350 ^oC.

Keywords: Na^+-beta-alumina, Na^+ solid electrolyte, Na-based battery, stabilized zirconia

Rheological Properties of Self-Healing Thermoplastic Polyurethanes Containing Reversible Covalent Bonds

Dae Woo Lee, Hanna Kim, and Dai Soo Lee

Department of Chemical Engineering, Chonbuk National University,
Jeonju 54596, South Korea

dslee@jbnu.ac.kr

Polyurethane is one of versatile polymers for foams, coatings, adhesives, and elastomers. Polyurethane elastomers are generally thermoplastic and can be processed by injection molding and extrusion process due to the linear nature of polymer chains. Such thermoplastic polyurethane (TPU) elastomers show the microphase separation of soft segments and hard segments which are composed of polyols and isocyanates used for the preparation of TPU respectively. The microphase separation of TPU is affected by the hydrogen bonds between the urethane groups of TPU as well as the miscibility of soft segments and hard segments. Strong hydrogen bonds of TPU play the role of physical crosslinks and impart excellent elastomeric mechanical properties to TPU. However, due to the strong hydrogen bonds of TPU, TPU melts are very viscous and heating of TPU near the degradation temperatures is frequently necessary for melt processing.

Recently, we found TPU featuring self-healing properties by reversible nature of urethane groups which are obtained by reactions between phenolic hydroxyl groups of polyols and aromatic isocyanates of 4,4' diphenyl methane diisocyanate [1]. As the specific urethane groups become reversible above the glass transition temperatures of TPU, TPU showed self-healing properties. Furthermore, viscosities of TPU in melts can be lowered by the chain splits and the decrease of molecular weights due to the reversible nature of the urethane groups and the processing of TPUs becomes easy in the melts. We have investigated rheological properties of TPU with reversible covalent bonds in melts and reported in this paper. With increasing the melt temperatures, large decrease of viscosities was observed in the TPUs with reversible covalent bonds in comparison with the TPUs without reversible covalent bonds in the range of temperatures. Thus, TPUs with reversible covalent bonds can be processed at relatively lower temperatures in melts without disadvantages of sacrificing the physical properties in solid states where the covalent bonds of urethane groups are not reversible. It is postulated that the TPUs with the reversible covalent bonds can be very useful for hot melt adhesives and powder coating due to the relatively low processing temperatures. By introducing the reversible covalent bonds into polyurethanes, even the network polyurethanes can be processed like TPUs and the physical recycling of such network polyurethanes became possible, maintaining the advantages of network polymers.

Keywords: rheology, reversible covalent bond, thermoplastic polyurethane, self-healing

[1] LEE, D., KIM H., & Lee D., 2015. Characteristics of Polyurethane Elastomers Having Reversible Urethane Linkages. *Proceeding of Annual Conference of Korea Polymer Society in Fall, 10,* 104.

Synthesis And Characterizations Of Hydrophilic Phema And Poly(Hema-Nvp) Copolymer Nanoparticles *Via* Inverse Miniemulsion Polymerization Techniques

Zalikha (Ismail)[1], Noor Aniza (Harun)[2]

School of Fundamental Science, Universiti Malaysia Terengganu, 21030, Kuala Terengganu, Terengganu[1,2]

E-mail:nooraniza@umt.edu.my

This study highlights on the development of polymer nanoparticles with improved hydrophilicity prepared *via* inverse miniemulsion polymerization, a convenient and robust technique to prepare hydrophilic and aqueous-soluble polymeric nanoparticles. 2-hydroxyethyl methacrylate (HEMA) and N-vinylpyrrolidone (NVP) are excellent candidates for homo-polymerization and co-polymerization due to its biocompatibility and biodegradability characteristic with high hydrophilicity properties. Several parameters including the effects of sonication time and amplitude towards the particles size and morphology of homo-polymerization and co-polymerization of HEMA and NVP were investigated. The formation of homopolymer PHEMA and copolymer of poly(HEMA-NVP) nanoparticles were confirmed by Fourier transform infrared (FTIR).The morphology of the polymer nanoparticles have been determined using scanning electron microscope (SEM) and transmission electron microscopy (TEM). Dynamic light scattering (DLS) indicates the mean diameters of homopolymer PHEMA and copolymer of poly(HEMA-NVP) nanoparticles were in a range of 100 – 200 nm. It is speculated that the hydrophilic polymer nanoparticles obtained can be further utilized in the fabrication of polymer composite nanoparticles especially in medical and biological applications.

Keywords: 2-hydroxyethyl methacrylate, N-vinylpyrolidone, inverse miniemulsion polymerization, hydrophilic polymer nanoparticles.

[1] CAO, Z., YANG, L., YAN. Y., SHANG, Y., YE, Q., QI, D., ZIENER, U., SHAN, G., & LANDFESTER, K. 2013. Fabrication of Nanogel Core-Silica Shell and Hollow Silica Nanoparticles *via* an Interfacial Sol-Gel Process Triggered By Transition-Metal Salt In Inverse System. *Journal of Colloid and Interface Science*, 406, 139-147.

[2] CAPEK, I. 2010. On Inverse Miniemulsion Polymerization of Conventional Water-Soluble Monomers. *Advance in Colloid and Interface Science*, 156(1-2), 35-61.

[3] GULSEN, D., & CHAUHAN, A. 2005. Dispersion Of Microemulsion Drops In HEMA Hydrogel: A Potential Ophthalmic Drug Delivery Vehicle. *International Journal of Pharmaceutics*, 292, 95-117.

[4] LANDFESTER, K., MUSYANOVYCH, A., MAILANDER, V., 2010. From Polymeric Particles to Multifunctional Nanocapsule for Biomedical Applications Using The Miniemulsion Process. *Journal of Polymer Science Part A-Polymer Chemistry*, 48, 493-515.

[5] OH, J. K., BENCHERIF, S. A., & MATYJASZEWSKI, K. 2009. Atom Transfer Radical Polymerization in Inverse Miniemulsion: A Versatile Route Towards Preparation and Functionalization of Microgels/Nanogels For Targeted Drug Delivery Application. *Polymer*, 50, 4407-4423.

Predicting the compressive strength of desulfurization gypsum using artificial neural network

Hongseok Jang[1], Juhee Kim[1], Seonghwan Jeon[2], Sehwan Jeon[2]

[1]Department of Architectural Engineering, Chonbuk National University, Research Center of Industrial Technology, 561-756, Republic of Korea
[2]Daewonbathech cooperation, 573-882, Republic of Korea

jadolli@naver.com *Tel: +82-63-270-3572, Fax: +82-63-270-3573*

In this study, an artificial neural networks study was carried out to predict the compressive strength of desulfurization gypsum mortar. The mortar mixture parameters were five different water–cement ratios (0.4, 0.45, 0.5, 0.55 and 0.6) and five partial slag replacement ratios (2%, 4%, 6%, 8% and 10%). Compressive strengths of moist cured specimens were measured at 3, 7, 28, 90, and 360 days. ANN model is constructed, trained and tested using these data. The data used in the ANN model are arranged in a format of three input parameters that cover the cement, water and age of samples and, an output parameter which is compressive strength of mortar. The results showed that ANN can be an alternative approach for the predicting the compressive strength of desulfurization gypsum mortar using concrete ingredients as input parameters.

Keywords: Desulfurization gypsum, artificial neural networks, Compressive strength

This research was supported by Basic Science Research Program through the National Research Foundation of Korea (NRF) funded by the Ministry of Science, ICT & Future Planning (NRF-2015R1C1A1A01055046) and the improvement of development project of Eco-Industrial Park (EIP)

[1] CAHIT, B., CENGIZ, D. A., HARUN, T., OKAN, K., 2009. Predicting the compressive strength of ground granulated blast furnace slag concrete using artificial neural network. Advances in Engineering software 40, 334-340.

Symposia 4

Advances in Energy Storage and Conversion Devices

- Lithium, Sodium, Magnesium and potassium Ion Batteries
- Electrochemical Supercapacitors
- Fuel Cells
- Solar Cells
- Photocatalytic and electrochemical water splitting
- Artificial photosynthesis
- Advances in electrolyte and electrolyte additives for energy storage devices
- Computational modeling and simulation for energy storage and conversion devices
- Others

Index Page

Charge Carrier Concentration and Mobility of Polymer Electrolytes Using Impedance and FTIR Spectroscopy

Asheila (Jamal), F.H. (Muhammad), Tan (Winie)*

Faculty of Applied Sciences, Universiti Teknologi MARA, 40450 Shah Alam, Malaysia

* *tanwinie@salam.uitm.edu.my*

The ionic conductivity of a polymer electrolyte is described by $\sigma = en\mu$. In this work, we evaluate the charge carrier concentration (n) and mobility (μ) using impedance and Fourier transform infrared (FTIR) spectroscopy. Nyquist plots of electrolytes based on hexanoyl chitosan/ epoxidized natural rubber (ENR) blends incorporated with lithium bis-trifluoromethanesulfonylimide ($LiN(CF_3SO_2)_2$) have been generated from impedance measurements. An equivalent circuit comprising a parallel combination of a resistor and a constant phase element (CPE) that are connected in series with another CPE is employed to represent the obtained Nyquist plot. Relevant impedance equations are derived based on this equivalent circuit[1,2]. Parameters required in the equations are obtained by trial and error until the Nyquist plots are fitted. The n and μ are then calculated and validated using FTIR spectroscopy. Enhancement of conductivity for hexanoyl chitosan/ENR blends as compared to neat hexanoyl chitosan is observed. The conductivity enhancement is achieved by controlled percolation of Li salt in one of the polymer phases.

Keywords: Impedance, FTIR, controlled percolation, hexanoyl chitosan, ENR

[1] TAN, W. & AROF, A. K. 2014. 'Impedance Spectroscopy: Basic Concepts and Application for Electrical Evaluation of Polymer Electrolytes' in *Physical Chemistry of Macromolecules*, eds C. H. Chan, C. H. Chua & S. Thomas, Apple Academic Press, USA, pp. 333 – 363.

[2] AROF, A. K., AMIRUDIN, S., YUSOF, S. Z. & NOOR, I. M. 2014. A Method based on Impedance Spectroscopy to Determine Transport Properties of Polymer Electrolytes. Phys. Chem. Chem. Phys., 16(5), 1856-1867

Film-forming electrolyte additives to improve the electrochemical performances of high voltage lithium ion batteries

Lidan Xing[1,2]*, Jianhui Li[1], Zaisheng Wang[1], Kang Wang[1], Xiongwen Zheng[1], Huozhen Zhi[1], Weishan Li[1,2]*

[1] School of Chemistry and Environment, South China Normal University, Guangzhou 510006, China

[2] Engineering Research Center of MTEES (Ministry of Education), Research Center of BMET (Guangdong Province), Engineering Lab. of OFMHEB (Guangdong Province), Key Lab. of ETESPG (GHEI), and Innovative Platform for ITBMD (Guangzhou Municipality), South China Normal University, Guangzhou 510006, China.

E Mail : xingld@scnu.edu.cn

High power and energy density lithium ion batteries (LIBs) have received great attention as potential power sources for electric vehicles (EVs) and hybrid EVs, which can be achieved by using high specific capacity and high operating voltage cathode materials [1]. However, the common used carbonate-based electrolytes tend to decompose under high voltage (>4.3 V vs. Li/Li^+), resulting in poor cyclic stability and safety of LIBs, which severely limit the application of high energy density LIBs [2]. One of the most economic and effective methods to solve this issue is to use electrolyte additives to create a protective film on the surface of high voltage cathode electrode/electrolyte [3-6]. By using a combined theoretical and experimental approach, several novel film-forming electrolyte additives were investigated to improve the cyclic stability and rate capability of high voltage cathode, at room and elevated temperature. The mechanism of these additives improving the electrochemical performances of high voltage cathode will be discussed in this presentation.

Keywords: High energy density, lithium ion batteries, film-forming electrolyte additives, high voltage cathode

[1] GOOGENOUGH J.B. 2014. Electrochemical energy storage in a sustainable modern society. *Energy Environ. Sci.*, 7, 14-18.

[2] XU K., 2014, Electrolytes and Interphases in Li-Ion Batteries and Beyond, *Chem. Rev.*, 114, 11503–11618.

[3] WANG Z.S., XING L.D*. LI J.H., XU M.Q., LI W.S., 2015, Triethylborate as an electrolyte additive for high voltage layered lithium nickel cobalt manganese oxide cathode of lithium ion battery, *J. Power Sources,* In presses.

[4] LI J.H., XING L.D.*, ZHANG R.Q., CHEN M., WANG Z.S., XU M.Q., LI W.S., 2015, Tris(trimethylsilyl)borate as an electrolyte additive for improving interfacial stability of high voltage layered lithium-rich oxide cathode/ carbonate- based electrolyte, *J. Power Sources*, 285:360-366.

[5] HUANG W.N., XING L.D.*, ZHANG R.Q., WANG X.S., LI W.S., 2015, A novel electrolyte additive for improving the interfacial stability of high voltage lithium nickel manganese oxide cathode, *J. Power Sources*, 293:71-77.

[6] HUANG W.N., XING L.D.*, WANG Y.T., XU M.Q., LI W.S. XIE F.C., XIA S.G., 2014, 4-(Trifluoromethyl)-Benzonitrile: A Novel Electrolyte Additive for Lithium Nickel Manganese Oxide Cathode of High Voltage Lithium Ion Battery, *J. Power Sources*, 267:560-565.

Effect of $Ni^{2+}/Cu^{2+}/Co^{2+}$ ratio on the structural stability and electrochemical performance of $Ni(OH)_2$

W.H. Li[1], Y.J. ZHU[1], T.Q. ZHAO[1], X.W. JIAN[1]

[1]School of Physics and Optoelectronic Engineering, Guangdong University of Technology, Guangzhou 510006 , P. R. China

E-mail address: zhuyj@gdut.edu.cn (Y.J. ZHU)
Corresponding author. Tel.: +86 2039322265; fax: +86 2039322265.

Abstract: Nano-nickel hydroxide doped with different ratio of Cu/Co was synthesized by means of ultrasonic-assisted precipitation. The crystal structure, particle size distribution and doped elements of all samples were inverstigated by X-ray diffraction (XRD), Fourier Transform Infrared Spectroscopy(FTIR), Laser Particle Analyzer (LPA) and Energy Dispersive Spectrometry (EDS). The effect of the Cu/Co doped ratio on the crystal phase and structural stability was investigated. The results showed that the samples were nano-$Ni(OH)_2$. With the increasing of Cu doped content, the α-$Ni(OH)_2$ ratio of samples was increasing, and the average particle size was also increasing. With the same doped radio, Cu was more effective than Co on the formation of α-$Ni(OH)_2$, but which was not beneficial to the stability of crystal structure. The crystal structure stability of samples doped with more Cu were better, the sample doped 15% Cu and 5% Co have the highest crystal structure stability. The cyclic voltammetry (CV) and charge/discharge test were also carried out. It was found that the sample doped with 15% Cu and 5% Co exhibits better electrochemical reversibility and cyclic stability, higher charge efficient and discharge potential, large proton diffusion coefficent and discharge capacity than the simple doped with Cu or Co. This result indicates that all doped elements can produce the synergic effect and further improve the electrochemical properties of α-$Ni(OH)_2$. Furthermore, the synergistic effect mechanism was also discussed.

Keyword: *Cu/Co doped; Nickel hydroxide crystal; Structure stability*

[1] BAO J., ZHU Y.J., ZHANG Z.J., XU Q.S., ZHAO T.Q., ZHAO W.R., CHEN J., ZHANG W. & HAN Q.Y. 2013. Structure and electrochemical properties of nanometer Cu substitude

alpha-nickel hydroxide. *Materials Research Bulletin*, 48(2), 422-428.

[2] HE F., HU Z.B., LIU K.Y., GUO H.J., ZHANG S.R., LIU H.T.& XIE Q.L. 2015. Facile fabrication of GNS/NiCoAl-LDH sonposite as an advanced electrode material for high-performance supercapacitors. *Journal of Solid State Electrochemistry*, 19, 607-617.

[3] WANG M.M., XUE J.Y., ZHANG F.M. &MA W.L. 2015. H.T.Cu. Growth of aluminum-substituted nickel hydroxide nanoflakes on nickel foam with ultrahigh specific capacitance at high current density. *J. Mater. Sci,* 50, 2422-2428.

Diffusion Processes in Proton Conducting Materials

Manfred Martin, Fabian Draber, Andreas Falkenstein
Institute of Physical Chemistry
RWTH Aachen University and JARA-Energy, Aachen, Germany

Interest in materials exhibiting proton conduction has increased during the last years owing to their great importance for energy and environmental applications, such as solid oxide fuel cells for converting chemical to electrical energy, solid oxide electrolyzer cells for high-temperature electrolysis of water, or hydrogen permeation membranes for separating hydrogen.

$BaZrO_3$-based oxides are proto-type proton conductors. Using density-functional theory (DFT), we have investigated proton migration energies in Y-doped $BaZrO_3$. The macroscopic proton conductivity was then investigated by means of Kinetic Monte Carlo (KMC) simulations. We analyze the resulting proton conductivities concerning special percolation pathways for protons.

Lanthanum tungstate, $LaWO_{54}$, is a mixed conductor where oxygen ions, protons and electron holes are mobile. Using the conductivity relaxation technique, we find during hydration a two-fold relaxation kinetics. From the formal analysis of the relaxation curves, we obtain different chemical diffusion coefficients for oxygen and hydrogen. These results show that during incorporation of H_2O both hydrogen and oxygen move independently.

.

Investigation of piezoelectric array energy harvester excited by vortex-induced pressure

Tinghai Cheng[1, 2*], Yingting Wang[1], Xianpeng Fu[1], Hongwei Zhao[2],

Gang Bao[3], Haibo Gao[4*]

[1]School of Mechatronic Engineering, Changchun University of Technology, Changchun, Jilin, 130012, China

[2] School of Mechanical Science and Engineering, Jilin University, Changchun, Jilin, 130025, China

[3]School of Mechatronic Engineering, Harbin Institute of Technology, Harbin, Heilongjiang, 150080, China

[4]State Key Laboratory of Robotics and System, Harbin Institute of Technology, Harbin, Heilongjiang, 150001, China

*(*E-mail: chengtinghai@163.com, gaohaibo@hit.edu.cn)*

Mechanical energy sources are abundant in our living environment, such as breezy wind, mechanical vibration[1]. This part of energy has always been underestimated in many cases before a long time. Nowadays, as the power shrink of electronic equipment, harvesting mechanical energy to power electronic devices is a feasible way[2]. Smart materials are played the important roles for energy transformation. Piezoelectric material is one of the smart materials and is has higher energy density and smaller size[3]. Piezoelectric materials could convert various minute energy, such as vibration energy and air pressure energy, into electric energy directly. The air pressure energy harvesting has been researched clearly by previous researchers [4].

The aim of this paper is research the performance of piezoelectric array energy harvester which is placed under vortex-induced pressure. The PZT patches have the different dynamic resistance when they bear the different pressure. This paper explores the relationships between the hyperbaric air and connection relation of piezoelectric array.

Figure 1 shows a schematic of the piezoelectric array energy harvester. Fig. 1(a) shows the energy harvesting method using the direct piezoelectric effect. The pressure difference between the power chamber and the micro-chamber causes the deformation of the PZT patch to be produced. When the deformation is generated, the current is driven through the load. Fig.1 (b) shows the structure of the harvester. The harvester is composed of two parts and they are named as power chamber and storage chamber.

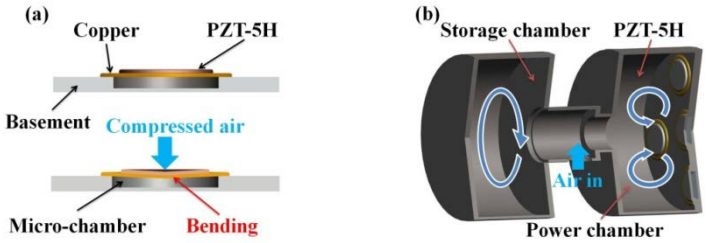

FIG.1 Schematic of the piezoelectric array energy harvester

Figure 2 shows the peak voltage and output power under different loads. In Fig. 2, the parallel of A and B is represented by A//B. In Fig. 2(a), the maximal peak voltage is 42.27 V at 8 MΩ. In Fig. 2(b) the maximal output power is about 0.65 mW.

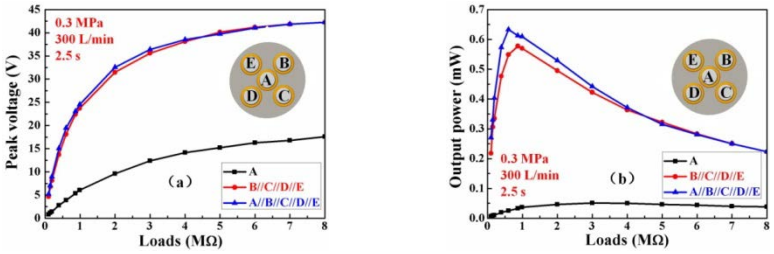

FIG. 2 The peak voltage and output power under different loads

Figure 2 (a) shows that the peak voltages are increased with resistance increased. Due to the influence of parallel relation, the voltage of B//C//D//E is similar as A//B//C//D//E. In Fig.2 (b), the output power is largest for parallel of five resistances. The optimal matching resistor becomes smaller with number of parallel PZT patch increased.

Keywords: hyperbaric air, piezoelectric array, vortex-induced pressure

[1] JUNG, S. J., KANG, M. G., MOON, H. G., BAEK, S. H., YOON, S. J., WANG, Z. L., KIM, S. W. & KANG, C. Y., 2015. High Output Piezo/Triboelectric Hybrid Generator. Scientific Reports, 5, 9309.

[2] COOK, K. A., THAMBI, N. & SASTRY, A. M., 2008. Powering MEMS Portable Devices-a Review of Non-regenerative and Regenerative Power Supply Systems. Smart Materials and Structures, 17(4), 043001.

[3] TOPRAK, A. & TIDLI, O., 2014. Piezoelectric Energy Harvesting State-of-the-art and Challenges. Applied Physics Review, 1(3), 031104.

[4] WANG, Y. T., WANG, L., CHENG, T. H., SONG, Z. Y. & QIN, F., 2016. Sealed Piezoelectric Energy Harvester Driven by Hyperbaric Air Load. Applied Physics Letters, 108(3), 033902.

Band offsets between the perovskite $CsSnCl_3$, $CsSnBr_3$ and $CsSnI_3$

Jaroenjittichai, A. P.[1]

[1]Department of Physics and Materials Science, Faculty of Science, Chiang Mai University, Chiang Mai 50200, Thailand

E Mail : AtcharaPunya@gmail.com

The perovskite $CsSnCl_3$, $CsSnBr_3$ and $CsSnI_3$ are of interest because of their potentials to shape the progress of the third generation photovoltaic cell [1]. Band offsets between their interfaces are vital parameters to investigate the electronic transport properties in the heterostructure devices [2]. In this work, the band offsets between $CsSnCl_3$, $CsSnBr_3$ and $CsSnI_3$ are determined from full potential linear muffin-tin orbital (FP-LMTO) within the local density approximation (LDA). The dipole potential formed at the interface was determined from self-consistent supercell calculations including the difference between the bulk band-edges energy levels. Furthermore, the bulk band edges relative to the LDA edges were corrected by the advanced technique called Quasiparticle self-consistent GW (QSGW) [3]. A staggered type-II alignment was found, suggesting that hole and electrons would separate in different regions.

Keywords: band offset, DFT, QSGW, perovskite, solar cell

[1] HUANG, L. & LAMBRECHT, W.R. L. 2014. Lattice dynamics in perovskite halides $CsSnX_3$ with X = I, Br, Cl. *Phys. Rev. B* 90, 195201.

[2] LANG, L., ZHANG, Y., PENG, X., CHEN, S., XIANG, H. J. & GONG, X. G. 2015. Three-step approach for computing band offsets and tis application to inorganic ABX_3 halide perovskites. *Phys. Rev. B* 92, 075102.

[3] KOTANI, T., SCHILFGAARDE, M. & FALEEV, S. V. 2007. Quasiparticle self-consistent *GW* method : A basis for the independent-particle approximation. *Phys. Rev. B* 76, 165106.

Enhancing $CH_3NH_3PbI_3$ Perovskity Solar Cell Efficiency with Band Gap Tuning and Structural Surface Stabilizing by Cl and Br Doping : First Principles Study

S. Pramchu[1], Y. Laosiritaworn[1,*]

[1]Department of Physics and Materials Science, Faculty of Science,

Chiang Mai University, Chiang Mai 50200, Thailand

** Corresponding author: Email: yongyut_laosiritaworn@yahoo.com; Tel.: +66 (0)53943367; Fax: +66 (0) 53943445; Postal address: Department of Physics and Materials Science, Faculty of Science, Chiang Mai University, Chiang Mai 50200, Thailand***)**

$CH_3NH_3PbI_3$ perovskite has recently gained much attention as being an efficient sensitizer for emerging photovoltaic technologies. One of the most important factors that directly affects the solar cell efficiency is the quality of perovskite interfaces. To acquire high interface quality, the perovskite should firstly have stable flat surfaces. However, based on the density functional theory (DFT) results by Haruyama et al. [1], it has been indicated that a surface with PbI_2-vacancy is more stable than flat surface, under thermodynamic equilibrium conditions of bulk $CH_3NH_3PbI_3$. Therefore, there is high possibility to have defects resulting in the low interface quality for a stable surface. On the other hand, recent experiments have found that mixing Cl [2] and Br [3] into $CH_3NH_3PbI_3$ greatly improved compound/structural stability. Consequently, in this work, we hypothesize that Cl and Br doping on $CH_3NH_3PbI_3$ surface may help stabilizing the desirable flat surface. For this aspect, we used DFT based on plane wave pseudopotential method to analyze the surface stability and its corresponding optical properties of Cl/Br-incorporated $CH_3NH_3PbI_3$ under the surface doping environment. To analyze surface stability, a chemical potential diagram of bulk $CH_3NH_3PbI_3$ was constructed by considering CH_3NH_3I and PbI_2 as competitive secondary phases. The surface structures of pure $CH_3NH_3PbI_3$ were modeled in (001) texture as a prototype study. In this (001) directional growth condition, $CH_3NH_3PbI_3$ surface structures consist of CH_3NH_3I and PbI_2 alternating sublayers. The band gaps were then calculated using generalized gradient approximation(GGA) because it can reproduce the experimental value. From the results, the bulk results of $CH_3NH_3PbI_3$ is consistent with both theoretical and experimental reported in literature [4], which confirms the reliability of this work.

For the undoped surface calculations, the formation energies indicate PbI_2-vacant surface is the most stable surfaces being consistent with the previous work [1]. However, the introduction of Cl/Br on surface significantly reduces the formation energy, indicating the ability of Cl/Br to stabilize the perovskite flat surface. The chemical potential diagram of bulk $CH_3NH_3PbCl_3$ and $CH_3NH_3PbBr_3$ were also constructed. The narrow stability region of $CH_3NH_3PbI_3$ in its chemical potentials diagram (compared with those from $CH_3NH_3PbCl_3$ and $CH_3NH_3PbBr_3$) shows that $CH_3NH_3PbI_3$ compound has high tendency to decompose into PbI_2 and CH_3NH_3I. This may be a reason why PbI_2-vacant surface (releasing PbI_2) is stable. The wider stability region of $CH_3NH_3PbCl_3$ and $CH_3NH_3PbBr_3$ provides a low possibility to decompose, which indicate their structural stability/tolerance under small stoichiometric variation. This characteristic implies that the occurrence of $PbCl_2$ or $PbBr_2$, instead of PbI_2, help stabilizing the flat perovskite surface. In addition, we found that surface doping is more energetically preferable than bulk doping, indicating Cl/Br has high tendency to segregate to surface (resulting in $PbCl_2$ or $PbBr_2$ surfaces). This fruitful information then open window of opportunity for the production of perovskite solar cell substance in mass scale as small variation penetration depth of the dopant is not significant. The tunability of band gap due to Cl/Br doping positions (e.g., surface and bulk doping) was also found. Namely, surface doping yields smaller band gap than that of bulk doping. However, we found that both Cl and Br doping enhances band gap compared with pure $CH_3NH_3PbI_3$ value. Consequently, with the further clarification of the role of Cl/Br doping on flat surface stabilization and the tunability of the band gap, it is expected that this work may lead to an improvement of the interface quality and optical properties of the perovskite solar cell towards real applicable production.

Keywords: DFT, surface doping, mixed halide perovskites solar cell, flat surface stabilization

[1] Haruyama, J., Sodeyama, K., Han, L., & Tateyama, Y. 2014. Termination Dependence of Tetragonal $CH_3NH_3PbI_3$ Surfaces for Perovskite Solar Cells. J. Phys. Chem. Lett., 5, 2903-2909.

[2] Lee, M. M., Teuscher, J., Miyasaka, T., Murakami, T. N., & Snaith, H. J. 2012. Efficient Hybrid Solar Cells Based on Meso-Superstructured Organometal Halide Perovskites. Science, 338, 643–647.

[3] Noh, J. H., Im, S. H., Heo, J. H., Mandal, T. N., & Seok, S. I. 2013. Chemical Management for Colorful, Efficient, and Stable Inorganic–Organic Hybrid Nanostructured Solar Cells. Nano Lett., 13, 1764-1769.

[4] Umari, P., Mosconi, E., & Angelis, F.D. 2014. Relativistic GW calculations on $CH_3NH_3PbI_3$ and $CH_3NH_3SnI_3$ Perovskites for Solar Cell Applications. Sci. Rep., 4, 4467.

Carbon nanotubes-3D graphene foam-Polyaniline Composite for High-performance Supercapacitor Applications

Ditsayut Phokharatkul[1], Kata Jaruwongrungsee[1], Thitima M. Daniels[1], Adisorn Tuantranont[1], Anurat Wisitsoraat[1]

[1]National Electronics and Computer Technology Center (NECTEC), 112 Thailand Science Park, Phahon Yothin Rd., Klong 1, Klong Luang, Pathumthani, Thailand.

E Mail: anurat.wisitsoraat@nectec.or.th

3D graphene foam structure is a highly promising platform for advanced supercapacitors (SCs) applications due to its large effective specific surface area, high theoretical electric double layer capacitance (EDLC) and structural suitability as support for material hybridization [1]. However, its performances may still be further improved by properly combining with other effective materials. In this work, we present a novel supercapacitor (SC) material based on Carbon nanotubes (CNTs)-3D graphene foam-polyaniline (Pani) composite prepared by chemical vapor deposition and electropolymerization processes and characterize its supercapacitor performances compared. CNTs-Graphene foam were simultaneously grown by chemical vapor deposition (CVD) on Ni foam decorated with $FeCl_3$ particles using acetylene (C_2H_2) carbon source and hydrogen gas carrier at 700^oC at the atmospheric pressure for 5 minutes. Next, the foam was then etched in 3M HCl for an hour to partially remove Ni support. Electropolymerization in 0.2 M aniline monomer solution was then conducted on the prepared GP-foam at working electrode potential of 0.55 V vs. Ag/AgCl. Characterizations by SEM confirmed the deposition of Pani on CNTs-GP foam network with a number of nanowire features appeared on GP foam surface. SC performances were then tested by cyclic voltammetry (CV) and galvanostatic charge-discharge (GCD) measurements in 2M H_2SO_4 electrolyte. CV results showed that PANI's redox peaks were broadened due to the presence of Pani and CNTs, indicating enhanced pseudocapacitance. From GCD measurements, it is found that CNTs-Pani-GP foam exhibits a high specific capacitance of more than 1050 Fg^{-1} at a specific current of 1 Ag^{-1}, which is more than twice higher than that of Pani-GP foam. Therefore, CNTs- GP foam-Pani composite prepared by electropolymerization is highly promising for advanced SC applications.

Keywords: Carbon nanotubes, 3D graphene, Polyaniline, Supercapitor.

[1] Gómez H., Ram M.K., Alvi F., Villalba P., Stefanakos L., Kumar A. 2011. Graphene-conducting polymer nanocomposite as novel electrode for supercapacitors, J. Power Sources. 196, 4102-4108.

Synthesis and Testing of a Composite Membrane Based on Sulfonated Polyphenylene Oxide and Silica Compounds as Proton Exchange Membrane for PEM Fuel Cells

Irina Petreanu, Adriana Marinoiu, Claudia Sisu, Mihai Varlam, Radu Fierascu, Paul Stanescu, Mircea Teodorescu

The present work is an attempt to improve the usseful properties of sulfonated polyphenylene oxide in order to obtain a proton exchange membrane (PEM) for PEM fuel cells. The formation of siloxane compounds inside the polymer matrix through an in situ sol-gel process improves the water retention, the tensile strength and the dimensional stability of the membrane. The presence of the silicone atoms inside the polymer matrix is highlited in the X-ray fluorescence spectra. Some properties related to water absorbtion and proton transport inside the membrane such as: water uptake, hydration number (λ), expansion of the area by hydration, ion exchange capacity and sulfonation degree show an optimization of the composite membrane compared to the polymeric one. Furthermore, the tensile strength of the composite membranes is improved in the hydrated state compared to hydrated polymeric membrane.

Dear Ms. Petreanu, Your Abstract has been successfully submitted. Please use Reference # AFM-16-2BD0E-1137500129: for future correspondence. Thanks

Glucose: A medium for green synthesis of supported nanoparticles

Injoon Jang[1,2], Hee-Young Park[1], In Young Cha[1],
Yung-Eun Sung[2] and Sung Jong Yoo[1,*]

[1]Fuel Cell Research Center, Korea Institute of Science and Technology,
39-1 Hawolgok-dong, Seoul 136-791, Republic of Korea
[2]School of Chemical and Biological Engineering, Seoul National University (SNU),
Seoul 151-742, Republic of Korea

Recently, there has been a high interest on the topic of eco-friendly chemistry and chemical processes. But carbon-supported Pt nanoparticles (Pt/C), which used primarily as PEMFC catalyst, have synthesized by complex and chemical methods such as impregnation and polyol. In this study, we present a novel, facile and totally green approach toward the synthesis of Pt/C catalyst for PEMFC by using the α-D-glucose. The Pt/C was successfully prepared in only two main steps: A platinum NPs was sputter-deposited on α-D-glucose particles in continuous mixer chamber. This Pt deposited glucoses (Pt/Glucose) was adopted as a new type of precursor to synthesize the Pt/C catalyst. Then, Pt/Glucose was dissolved in carbon (Vulcan XC-72)-dispersed water and boiled on raised temperature. The synthesized Pt/C was evaluated physically via XRD, XPS, TGA and TEM. Also, electrochemical properties were examined in order to assess the suitability for PEMFC catalyst. As a result, Pt/C, synthesized in completely new way, exhibited high activity to oxygen reduction reaction.

Drastically Increased Surface Area and Supercapacitive Properties of Carbothermally Reduced Cotton Textile

Do Van Lam[1,2], ChangHyun Kim[1,2], Jae-Hyun Kim[1,2], Seung-Mo Lee[1,2,*]

[1] Nano Mechatronics, Korea University of Science and Technology (UST), 217 Gajeong-ro, Yuseong-gu, Daejeon 34113, South Korea

[2] Department of Nanomechanics, Korea Institute of Machinery & Materials (KIMM), 156 Gajeongbuk-ro, Yuseong-gu, Daejeon 34103, South Korea

Presenting author: Do Van Lam (hlamdo@yahoo.com)

[*]Corresponding author: Seung-Mo Lee (sm.lee@kimm.re.kr)

Carbothermal reduction of various ores using carbon as a reducing agent, which is sacrificed in the process, has been long used since ancient times in order to smelt metal. Here, in order to greatly increase the surface area of general carbon based materials, we used carbothermal reduction in a different way. Namely, we employed metal oxide as a sacrificed agent for nanostructuring of carbonaceous materials. We conformally coated ZnO on bare cotton textile using atomic layer deposition (ALD). Subsequently, by simple thermal annealing, Zn element was completely evaporated and finally we obtained nanostructured activated carbon textile (aCT) with greatly increased surface area. As compared to carbonized cotton textile prepared by thermal annealing only (bare aCT), the surface area was measured to increase over 7 times. Furthermore, the electrochemical supercapacitors made of the nanostructured aCT electrodes showed excellent cycling stability and over 10 times improvement in energy density without losing power density as compared to the bare aCT. It is expected that our method could open a novel pathway for nanostructuring of other innumerable carbon-based materials for energy applications.

Keywords: Carbothermal reduction, Atomic layer deposition (ALD), Energy storage, Carbon based materials, Supercapacitor

High Performance Activated Carbon Supercapacitor with current collectors of 3D Porous Silver Nonwoven Mats

Yunseok Jang and Kwang-Young Kim

Department of Printed Electronics, Korea Institute of Machinery & Materials

171 Jang-Dong, Yuseong-Gu, Daejeon, 305-343, Republic of Korea

*E Mail :***yjang@kimm.re.kr**

In recent years, supercapacitors have attracted considerable attention for their higher power density compared to batteries and their higher energy density compared to common capacitors.(1) These particular properties make them suitable for numerous applications in such diverse fields as power electronics, military equipment, and hybrid electric vehicles (HEVs).(2-3) Supercapacitors have four major components: current collectors, electrodes, electrolytes and separators. Among these components, electrodes have been the most actively studied but relatively little attention has been given to current collectors. Previously, we demonstrated the usefulness of a solution processed Ag current collector in supercapacitors through a study of a 2-dimensional (2D) Ag plated polymer film as a current collector. In the present study, we sought to enhance the efficiency of such solution processed Ag current collectors by fabricating a 3-dimensional (3D) porous Ag nonwoven mat current collector from a cellulosic template. This method was chosen in order to maximize the contact area between the electrode and electrolyte.(4) We developed a simple method for fabricating a 3D porous Ag nonwoven mat for use as the current collector in supercapacitors, and investigated the supercapacitive properties of this mat using cyclic voltammetry. The specific capacitance of an activated carbon electrode on the 3D porous Ag nonwoven mat was 1.24 times greater than that observed for an activated carbon electrode on a conventional 2D Ag plate.(4)

Keywords: supercapacitor, activated carbon, porous Ag nonwoven mat

[1] X. Dong, W. Shen, J. Gu, L. Xiong, Y. Zhu, H. Li, J. Shi, J. Phys. Chem. B 110, 6015 (2006).
[2] C. Portet, P. L. Taberna, P. Simon, E. Elahaut, C. Laberty-Robert, Electrochim. Acta 50, 4174 (2005).
[3] G. Wang, L. Zhang, J. Zhang, Chem. Soc. Rev. 41, 797 (2012).
[4] Y. Jang, J. Jo, Y. –M. Cho, S. Kwon, K. –Y, Kim, Energy 93, 1303 (2015).

Nanoporous Carbon from Coffee Bean Waste by Chemical Activation with KOH and K_2CO_3: A Comparative Study

Chang-Hyun Kim[1,2], Do Van Lam[1,2], Hyung Cheoul Shim[1], Sung-Min Hong[1], Jae-Hyun Kim[1,2], Seung-Mo Lee[1,2,#]

[1] Department of Nanomechanics, Korea Institute of Machinery & Materials (KIMM), 156 Gajungbuk-ro, Yuseong-gu, Daejeon 34103, South Korea.

[2] Nano Mechatronics, University of Science and Technology (UST), 217 Gajung-ro, Yuseong-gu, Daejeon 34113, South Korea.

Presenting author: Chang-Hyun Kim (*kch1250@kimm.re.kr*)

[#]*Corresponding author: Seung-Mo Lee* (*sm.lee@kimm.re.kr*)

We produced nanoporous carbon from coffee bean waste (CBW) by pyrolysis at 800 ^oC and subsequent chemical activation with K_2CO_3 and KOH. For the comparative study, the effects of mixing ratio of activation agents to CBW on the porosity and the electrochemical properties were systematically investigated. We observed that the specific capacitance is highly dependent on the volumetric mixing ratio of KOH/K_2CO_3 to CBW. The nanoporous carbons activated by KOH/K_2CO_3 with a mixing ratio of 4:1 (KOH:CBW)/1:1 (K_2CO_3:CBW) showed the best specific capacitance. Parametric studies revealed that the activation by both KOH and K_2CO_3 generated micropores (less than 2 nm) rather than meso- and macropores. In particular, increase in volume of pores with size between 1 nm and 2 nm leaded to noticeable increase in specific capacitance, while increase in volume of pores with the size of less than 1 nm is detrimental to specific capacitance. These results indicated that both KOH and K_2CO_3 could be promising agents for activating CBW into nanoporous carbon with good electrochemical performance.

Keywords: Coffee bean waste, Chemical activation, Nanoporous carbon

ADVANCE FUNCTIONAL MATERIALS-2016

Synthesis of Reduced Graphene Oxide Supported Flower-like Bismuth Subcarbonate Microsphere ($BI_2O_2CO_3$-rGO) for Supercapacitor Application

L. Gurusamy and Jerry .J. Wu*

Department of Environmental Engineering and Science, Feng Chia University, Taichung,

Taiwan 407

jjwu@mail.fcu.edu.tw

The reduced graphene oxide (rGO) nanosheets have attracted rapidly increasing attention in the energy storage field since their excellent conductivity will enhance the electrically conducting as charge transfer channel. Herein we report novel bismuth subcarbonate microsphere with different weight (%) of rGO. The physical and chemical characterization of as prepared nanocomposites material were investigated by using XRD, FE-SEM, HR-TEM, EDX, FT-IR, CV, GCD, and EIS. A remarkable specific capacitance of 250 F/g at a scan rate 20 mV/s was obtained for the optimal 33% of RGO with $Bi_2O_2CO_3$ electrode. The electrode also delivers exceptional rate performance (with capacitive retention of 91.2% at 20mV/s) and outstanding cycling stability. Comparison with the capacitance behavior of pure bismuth subcarbonate and $Bi_2O_2CO_3$ hydrothermally mixed with rGO display the importance of the self-assembly of the nanosheets in making wide range of graphene based composite materials for application in electrochemical energy storage.

Keywords: bismuth subcarbonate, hydrothermal, energy storage, specific capacitance

[1] Jinfeng Sun, Jinqing Wang, Zhangpeng Li, Zhigang Yang, and Shengrong Yang. 2015. Controllable synthesis of 3D hierarchical bismuth compounds with good electrochemical performance for advanced energy storage devices. *RSC Adv.* 5, 51773-51778.

[2] Jun Zhang, Pengliang Liu, Yupeng Zhang, Guolong Xu, Zhengda Lu, Xiyu Wang, Yan Wang, Lingxia Yang, Xi Tao, Hongbo Wang, Erpan Zhang, Junhua Xi, and Zhenguo Ji.

2015. Enhanced Performance of nano-Bi2WO6-Graphene as Pseudocapacitor Electrodes by Charge Transfer Channel. SCIENTIFIC REPORTS 5: 8624.

[3] Biplab Sarma, Abraham L. Jurovitzki, York R. Smith, Swomitra K. Mohanty, and Mano Misra. 2013. Redox-Induced Enhancement in Interfacial Capacitance of the Titania Nanotube/Bismuth Oxide Composite Electrode ACS Appl. Mater. Interfaces 5, 1688−1697.

[4] Huan-Wen Wang, Zhong-Ai Hu, Yan-Qin Chang, Yan-Li Chen, Zi-Qiang Lei, Zi-Yu Zhang, and Yu-Ying Yang. 2010. Facile solvothermal synthesis of a graphene nanosheet–bismuth oxide composite and its electrochemical characteristics. Electrochimica Acta 55, 8974–8980.

[5] S.T. Senthilkumar, R. Kalai Selvan, M. Ulaganathan, and J.S. Melo. 2014. Fabrication of Bi2O3||AC asymmetric supercapacitor with redox additive aqueous electrolyte and its improved electrochemical performances Electrochemical Acta 115, 518– 524.

[6] S.X. Wang, C.C. Jin, and W.J. Qian. 2014. Bi_2O_3 with activated carbon composite as a supercapacitor electrode. Journal of Alloys and Compounds 615, 12–17.

Film-forming electrolyte additives to improve the electrochemical performances of high voltage lithium ion batteries

Lidan Xing[1,2]*, Jianhui Li[1], Zaisheng Wang[1], Kang Wang[1], Xiongwen Zheng[1], Huozhen Zhi[1], Weishan Li[1,2]*

[1] School of Chemistry and Environment, South China Normal University, Guangzhou 510006, China

[2] Engineering Research Center of MTEES (Ministry of Education), Research Center of BMET (Guangdong Province), Engineering Lab. of OFMHEB (Guangdong Province), Key Lab. of ETESPG (GHEI), and Innovative Platform for ITBMD (Guangzhou Municipality), South China Normal University, Guangzhou 510006, China.

E Mail : xingld@scnu.edu.cn

High power and energy density lithium ion batteries (LIBs) have received great attention as potential power sources for electric vehicles (EVs) and hybrid EVs, which can be achieved by using high specific capacity and high operating voltage cathode materials [1]. However, the common used carbonate-based electrolytes tend to decompose under high voltage (>4.3 V vs. Li/Li^+), resulting in poor cyclic stability and safety of LIBs, which severely limit the application of high energy density LIBs [2]. One of the most economic and effective methods to solve this issue is to use electrolyte additives to create a protective film on the surface of high voltage cathode electrode/electrolyte [3-6]. By using a combined theoretical and experimental approach, several novel film-forming electrolyte additives were investigated to improve the cyclic stability and rate capability of high voltage cathode, at room and elevated temperature. The mechanism of these additives improving the electrochemical performances of high voltage cathode will be discussed in this presentation.

Keywords: High energy density, lithium ion batteries, film-forming electrolyte additives, high voltage cathode

[1] GOOGENOUGH J.B. 2014. Electrochemical energy storage in a sustainable modern society. *Energy Environ. Sci.*, 7, 14-18.

[2] XU K., 2014, Electrolytes and Interphases in Li-Ion Batteries and Beyond, *Chem. Rev.*, 114, 11503–11618.

[3] WANG Z.S., XING L.D*. LI J.H., XU M.Q., LI W.S., 2015, Triethylborate as an electrolyte additive for high voltage layered lithium nickel cobalt manganese oxide cathode of lithium ion battery, *J. Power Sources,* In presses.

[4] LI J.H., XING L.D.*, ZHANG R.Q., CHEN M., WANG Z.S., XU M.Q., LI W.S., 2015, Tris(trimethylsilyl)borate as an electrolyte additive for improving interfacial stability of high voltage layered lithium-rich oxide cathode/ carbonate- based electrolyte, *J. Power Sources*, 285:360-366.

[5] HUANG W.N., XING L.D.*, ZHANG R.Q., WANG X.S., LI W.S., 2015, A novel electrolyte additive for improving the interfacial stability of high voltage lithium nickel manganese oxide cathode, *J. Power Sources*, 293:71-77.

[6] HUANG W.N., XING L.D.*, WANG Y.T., XU M.Q., LI W.S. XIE F.C., XIA S.G., 2014, 4-(Trifluoromethyl)-Benzonitrile: A Novel Electrolyte Additive for Lithium Nickel Manganese Oxide Cathode of High Voltage Lithium Ion Battery, *J. Power Sources*, 267:560-565.

High capacitance properties of porous polyaniline on a carbon fiber cloth substrate by electrochemical deposition

Jun Ma[a,b], Shaochun Tang [a], and Xiangkang Meng[a,*]

[a] Institute of Materials Engineering, National Laboratory of Solid State Microstructures, and College of Engineering and Applied Sciences, Nanjing University, Jiangsu, P. R. China

[b] Electrical and Mechanical Department, Nantong Science and Technology College, Jiangsu, P. R. China

Fax: (+86)-25-83595535 E-mail: mengxk@nju.edu.cn

Abstract

Electrochemical deposition of polyaniline (PANI) is carried out on a porous carbon fiber cloth substrate for supercapacitor studies. The effect of substrate is studied by comparing the results obtained using stainless steel and porous carbon fiber cloth substrates. Experimental variables, namely, concentrations of aniline monomer are varied and arrived at the optimum concentration to obtain a maximum capacitance of PANI. PANI deposited at 0.15M aniline and 0.1M H_2SO_4 by cyclic voltammetry on carbon fiber cloth is found to possess superior capacitance properties. Low concentrations of both aniline and H_2SO_4 produce low ratio of PANI. The PANI deposits prepared under these conditions possess network morphology of nanofibrils. Capacitance values as high as 1600 F/g are obtained and porous PANI coated carbon electrodes facilitate charge–discharge current densities as high as 30 $mAcm^{-2}$. Electrodes are found to be fairly stable over a long cycle-life, although there is some capacitance loss during the initial stages of cycling.

Keywords:

Electro polymerization; Porous polyaniline; Supercapacitor

Anthraquinone derivative Schiff base copper (II) complexes as mediators including laccase for cathode of biofuel cells

Yuto YAKEUCHI[1], Nobumitsu SUNAGA[1], Takashiro AKITSU[1]

[1]Department of Chemistry, Faculty of Science, Tokyo University of Science,

1-3 Kagurazaka, Shinjuku-ku, Tokyo 162-8601, Japan

akitsu@rs.kagu.tus.ac.jp

The cathode of biofuel cells requires appropriate mediators to improve efficiency of electron transfer between electrode and laccase for four electron reduction from oxygen to water. Since laccase acts specific one-electron oxidation of phenolic-related compounds as substrate, anthraquinone derivative Schiff base copper (II) complexes containing quinine moiety is expected to be a good mediator. Herein, we have synthesized and characterized new Schiff copper(II) complexes using several L-amino acids (alanine, valine, leucine, and isoleucine). TD-DFT calculation assigned MLCT band at 528 nm to be HOMO-2 to LUMO+1 transition. The inclusion of copper(II) complexes into laccase was detected by spectral changes during titration of laccase into solution of copper(II) complexes. Based on crystal structures and docking simulation, hydrophobic region near T1 copper site of laccase can include a mediator copper(II) complex incorporating hydrophobic L-amino acid moiety. Reduction potentials of water were successfully lowered to be 0.93 V, 0.59 V, [2] and 0.51 V for original water, catalyzed by laccase, and catalyzed by laccase including the mediator, respectively.

Keywords: Biofuel cell, Chiral Cu(II) complexes, Anthraquinone, Laccase, Redox potentials

[1]Y. Kurosawa, Y. Takeuchi, T. Akitsu *et al.*, Threonine: Food Sources, Functions and Health Benefits, 73 (2015). .

[2] Yun Chen, Panpan Gai, J. Mater. Chem. A, 3, 11511 (2015).

Chiral salen type Mn (II), Co (II), Ni (II), Cu (II), Zn (II) complexes having azo groups in laccase toward application to biofuel cell

Yuya MITSUMOTO[1], Nobumitsu SUNAGA[1], Takashiro AKITSU[1]

[1] Department of Chemistry, Faculty of Science, Tokyo University of Science,

1-3 Kagurazaka, Shinjuku-ku, Tokyo 162-8601, Japan

akitsu@rs.kagu.tus.ac.jp

Laccase (an enzyme reducing oxygen to water) has been used as cathode of biofuel cells. To enhance the performance, electron transfer to laccase from cathode should be improved by using metal complexes mediators. Recently, we tried to overcome the spatial disadvantage of these complex mediators by the inclusion and photo-induced control molecular orientation.[1] After linearly polarized UV light irradiation to complex, Weigert effect enhanced optical anisotropy of the complexes.[2,3] Herein, we have investigated polarized UV light induced molecular orientation of new chiral Schiff base Mn(II), Co(II), Nil(II), Cu(II), and Zn(II) complexes containing azo-compounds in laccase matrix. Interestingly, simulated spectra of complexes by TD-DFT supported that supramolecular chiral arrangement was induced in chiral laccase matrix by irradiation of linearly polarized UV light. Electronic transitions (419 nm, HOMO-1(189) to LUMO+3(191)) of the light absorption is associated with the increase in the current density of the Mn(II) complex.

Keywords: Chiral metal complexes, Azo-compounds, Molecular orientation, Redox potentials

[1] C. Kominato, T. Akitsu, *Lett. Appl. NanoBioSci.*, **2**, 264(2015).

[2] Y. Aritake, T. Takanashi, A. Yamazaki, T Akitsu, *Polyhedron*, **30**, 886 (2011).

[3] A. Yamazaki, T. Akitsu, *RSC Advances,* **2**, 2975 (2012) and references therein.

Synthesis and Testing of a Composite Membrane Based on Sulfonated Polyphenylene Oxide and Silica Compounds as Proton Exchange Membrane for PEM Fuel Cells

Irina Petreanu, Adriana Marinoiu, Claudia Sisu, Mihai Varlam, Radu Fierascu, Paul Stanescu, Mircea Teodorescu

The present work is an attempt to improve the usseful properties of sulfonated polyphenylene oxide in order to obtain a proton exchange membrane (PEM) for PEM fuel cells. The formation of siloxane compounds inside the polymer matrix through an in situ sol-gel process improves the water retention, the tensile strength and the dimensional stability of the membrane. The presence of the silicone atoms inside the polymer matrix is highlited in the X-ray fluorescence spectra. Some properties related to water absorbtion and proton transport inside the membrane such as: water uptake, hydration number (λ), expansion of the area by hydration, ion exchange capacity and sulfonation degree show an optimization of the composite membrane compared to the polymeric one. Furthermore, the tensile strength of the composite membranes is improved in the hydrated state compared to hydrated polymeric membrane.

Dear Ms. Petreanu, Your Abstract has been successfully submitted. Please use Reference # AFM-16-2BD0E-1137500129: for future correspondence. Thanks

Three-dimensional porous architectures of Graphene/CNT composites in polymer electrolyte membrane fuel cells

E. –J. Oh[1], V. Nica[1,2], H. Natter[1], R. Hempelmann[1]

[1]Physical Chemistry, Saarland University, Campus Geb. B2 2, D-66123 Saarbrücken, Germany.

[2]Faculty of Physics, Department of Physics, Alexandru Ioan Cuza University of Iasi, Carol I nr.11, 700506, Iasi, Romania.

eunjin.oh@uni-saarland.de/ Saarland University, Saarland University, Campus B2 2, 66123 Saarbrücken

The polymer electrolyte membrane fuel cells (PEM-FC), as a clean and high-efficiency device, have drawn a great deal of attention in terms of both fundamentals and applications. Among the various materials, platinum (Pt) display rapid response times, high power densities and enhanced energy efficiency. However, the high cost and scarcity of the requisite platinum (Pt) catalyst has become the greatest barrier to large-scale industrial application of PEM-FC.

In present work, we investigated a unique combination of three-dimensional (3D) porous carbon structure, such as mixtures of two-D (2D) nanosheet and one-D (1D) carbon nanotubes (CNT), with well-defined morphology and small size by controlling of the Pt catalyst loading. Moreover, with increasing CNT contents the mixtures of graphene/CNT-supported Pt (Pt/G:CNT) catalysts lead to the formation of higher catalyst loading efficiency, catalytic activity, and stability.[1-4] Electrochemical evaluation showed that Pt/G-CNT is a good catalyst with a higher electrochemical surface area (ECSA) of Pt than pure graphene supports, which can be attributed to the uniform dispersion of Pt particles on the 3D structures and good accessibility of these sites for hydrogen adsorption and desorption reactions. For structural characterization, the prepared electrodes are demonstrated by powder X-ray diffraction, electron microscopy and ICP-OES. Polarization curves in PEM-FC are also performed on the hybrid catalysts at

different temperatures and at different relative humidities. The anode coated with self-made graphene and CNT 1:2 / 0.4 mg cm^{-1} Pt leads to enhanced power density P(650mV) = 0.70 W cm^{-2} in the fuel cell.

Keywords: 3D structure, porous carbon, ECSA, PEM-FC

[1] Girishkumar, G., Hall, Timothy D., Vinodgopal, K. & Kamat, Prashant V. 2006. Single Wall Carbon Nanotube Supports for Portable Direct Methanol Fuel Cells. *J. Phys. Chem. B*, 110, 107-114.

[2] Brian, S. & Kamat, Prashant V. 2009. Electrocatalytically Active Graphene-Platinum Nanocomposites. Role of 2-D Carbon Support in PEM Fuel Cells. *J. Phys. Chem. C*, 113, 7990-7995.

[3] Si, Y. C. & Samulski, Edward T. 2008. Exfoliated Graphene Separated by Platinum Nanoparticles. *Chem. Mater.*, 20, 6792-6797.

[4] K. K. Anusorn, Vinodgopal, K. Kuwabata, S., Kamat & Prashant V. 2006. Highly Dispersed Pt Catalysts on Single-Walled Carbon Nanotubes and Their Role in Methanol Oxidation. *J. Phys. Chem. B*, 110, 16185-16188.

Characterization of Polypyrrole-Modified Carbon Nanotube Anode in Microbial Fuel Cells

Ho-Young Jung[1], Sung-Hee Roh[2]

[1]Department of Environment & Energy Engineering, Chonnam National University, Gwangju, Korea
[2] College of General Education, Chosun University, Gwangju, Korea

rohsh@chosun.ac.kr

Microbial fuel cells (MFCs) are a hybrid bio-electrochemical system, which converts bio-convertible substrate directly into electricity by the oxidation of organic matter in the presence of bacteria under ambient temperature/pressure condition. The MFCs have become an interesting alternative to produce electrical energy and provide wastewater treatment simultaneously. The anodic material, which contains a matrix for the attachment of the microorganisms, is usually a limiting factor in power production in an MFC.

Carbon nanotubes-based networks architectures are not only mechanically strong and electrically conductive, but they also contribute considerably to the adhesion and growth of bacterial cells. Polypyrrole is an important conducting polymer due to its relatively facile processability, electrical conductivity, and environmental safety. Thus, the enhanced conductive polypyrrole-modified carbon nanotube anode could possibly be used in MFCs to improve performance.

In this study, we investigated the characterization of the polypyrrole-modified carbon nanotube anode for MFCs and discussed the influence of the anodic composition on the discharge behaviors on acetate oxidation via electrochemical catalyst of bacteria. The polypyrrole-modified carbon nanotube anode exhibited an enhanced power output due to the presence of a thin and uniform conducting polymer layer, and their performance was strongly dependent on the loading amount of the composite. The polypyrrole-modified carbon nanotube anode therefore offers good prospects for application in MFCs.

Keywords: Carbon nanotube, polypyrrole, anode, microbial fuel cell

[1] LOGAN, B. E. & RABEY, K. 2012. Conversion of Wastes into Bioelectricity and Chemicals by Using Microbial Electrochemical Technologies. *Science*, 337, 686-690.

[2] HOU, J., LIU, Z., YANG, S. & ZHOU, Y. 2014. Three-Dimensional Macroporous Anodes Based on Stainless Steel Fiber Felt for High-Performance Microbial Fuel Cells. *J Power Sources*, 258, 204-209.

[3] PANT, D., BOGAERT, G. V., DIELS, L. & VANBROEKHOVEN, K. 2010. A Review of the Substrates Used in Microbial Fuel Cells (MFCs) for Sustainable Energy Production. *Bioresources Technol*., 101, 1533-1543.

[4] MODIN, O. & GUSTAVSSON, D. J. 2014. Opportunities for Microbial Electrochemistry in Municipal Wastewater Treatment an Overview. *Water Science Technol*., 69, 1359-1372.

Effect of Microstructure on the Performance of Micro-tubular Solid Oxide Fuel Cells Made by Aqueous Electrophoretic Deposition

L. Chen, R.J. Liu, F.A. Yu, J.S. Cherng*

Department of Materials Engineering, Ming Chi University of Technology, Taipei 24301 Taiwan

cherng@mail.mcut.edu.tw

A series of anode-supported micro-tubular solid oxide fuel cells (mSOFCs) are manufactured by sequential aqueous electrophoretic deposition (EPD). The process of these mSOFCs includes sequential aqueous EPDs of an anode layer, an electrolyte layer, and a cathode layer onto a thin wire electrode, followed by stripping, drying, and a single-step co-sintering. The effects of the anode/cathode microstructure on the cell resistance and electrochemical performance of such mSOFCs are investigated and discussed based on the microstructural, AC-impedance and voltage–current–power analyses. It is found that finer microstructure gives improved cell performance by increasing the area of three phase boundary.

Keywords: Electrophoretic deposition, micro-tubular solid oxide fuel cells, anode/cathode microstructure, AC-impedance

Electrochemical properties of Co@C nanocatalysts for oxygen reduction reaction in anion exchange membrane fuel cell

Jue-hyuk Jang[1,2], Namgee Jung[3] and Sung Jong Yoo[1,*]

[1]Fuel Cell Research Center, Korea Institute of Science and Technology, Hwarang-ro 14-gil, Seongbuk-gu, Seoul 02792, Republic of Korea

[2]Graduate school of Energy Enviroment Policy & Technology, Korea Univ., Anam-ro 145-gil, Seongbuk-gu, Seoul 02841, Republic of Korea

[3]Graduate school of Energy Science Technology, Chungnam National Univ., Dahak-ro, Yuseong-gu, Daejeon 34134, Republic of Korea

Fuel cells are direct energy conversion device that the chemical energy of a fuel converts into electricity by electrochemical reactions for zero-emission energy sources. However, the Pt/C catalysts for oxygen reduction reaction (ORR) are much expensive than the non-platinum group metal (non-PGM) and the transition metal catalysts show comparable performance and stability in alkaline media for ORR to Pt/C catalyst. Therefore, non-PGM catalysts have been applied to replace commercial catalysts with the transition metal groups such as Ni, Co, and Fe. In this study, the nano-scaled cobalt-carbon core-shell catalysts (Co@C) were prepared by a ligand stabilization method and thermal treatment. The structural and physical properties were characterized by TEM, XRD, XAFS, and XPS. The Co@C catalysts exhibited uniform spheres structures with an average particle size of 5nm with carbon-shell on the cobalt nano particles surface after thermal treatment. The electrochemical properties are measured by cyclic voltammetry for ORR activity of the Co@C catalysts and polarization curves for single cell performance. Consequently, the Co@C catalysts exhibited similar ORR activity compared to the Pt/C catalysts and it will be good chance for low-cost catalysts with the Co@C catalysts for the replacement of the Pt/C catalysts.

Glucose: A medium for green synthesis of supported nanoparticles

Injoon Jang[1,2], Hee-Young Park[1], In Young Cha[1],
Yung-Eun Sung[2] and Sung Jong Yoo[1,*]

[1]Fuel Cell Research Center, Korea Institute of Science and Technology,
39-1 Hawolgok-dong, Seoul 136-791, Republic of Korea
[2]School of Chemical and Biological Engineering, Seoul National University (SNU),
Seoul 151-742, Republic of Korea

Recently, there has been a high interest on the topic of eco-friendly chemistry and chemical processes. But carbon-supported Pt nanoparticles (Pt/C), which used primarily as PEMFC catalyst, have synthesized by complex and chemical methods such as impregnation and polyol. In this study, we present a novel, facile and totally green approach toward the synthesis of Pt/C catalyst for PEMFC by using the α-D-glucose. The Pt/C was successfully prepared in only two main steps: A platinum NPs was sputter-deposited on α-D-glucose particles in continuous mixer chamber. This Pt deposited glucoses (Pt/Glucose) was adopted as a new type of precursor to synthesize the Pt/C catalyst. Then, Pt/Glucose was dissolved in carbon (Vulcan XC-72)-dispersed water and boiled on raised temperature. The synthesized Pt/C was evaluated physically via XRD, XPS, TGA and TEM. Also, electrochemical properties were examined in order to assess the suitability for PEMFC catalyst. As a result, Pt/C, synthesized in completely new way, exhibited high activity to oxygen reduction reaction.

Material Life Cycle Assessment (MLCA) on BZY-Ni Hydrogen seperation Membrane by sol-gel process

Jung-Il Lee, Young-Geun Lee, Ho-Jun Lee, Soon-Chul Ur, Soon-Yong Kweon, Jung-Ho Ryu, Kyoung-Won Cho, Eun-Hye Park, Tae-Whan Hong*

Department of Material Science and Engineering/Research Center of Sustainable Eco-Device and Materials (ReSEM), Korea National University of Transportation, Daehak-ro 50, Chungju, Chungbuk, 380-702, Korea

* **Email :** twhong@ut.ac.kr

Recently, various studies to try clean energy from fossil fuel because of the environment pollution and resource depletion [1]. To seperate high purity hydrogen from hydrogen that is typical clean energy, we produced cermet membrane combined metal and ceramic materials for hydrogen separation from syngas [2]. A Material Life Cycle Assessment (MLCA) should be conducted for prospective products to solve real or potential environmental problems. MLCA is also a process of identifying opportunities to improve the environment by evaluating the environmental impact of energy and material resources. In the study, we prepared BZY-Ni composite membrane using ball-milling and Hot Press Sintering process (HPS). BZY powder prepared by the sol-gel method and calcination treatment. After Material Life Cycle Assessment using GaBi6, 3 impact catagories most affected on environment. First is Marine Aquatic Ecotoxcity Potential (MAETP), 4.29×10^{-13}, second is Human Toxicity Potential (HTP), 2.44×10^{-14}, third is Acidification Potential (AP), 1.25×10^{-14}.

Keywords: Material Life Cycle Assessment (MLCA), Sol-gel, Hydrogen separation, BZY($\mathrm{Ba}Zr_{0.8}Y_{0.2}$ ***), Cermet membrane***

[1] Wang Qidong, Wu Jing, Chen Changpin, Luo Weifang. 1986. THE SEPERATION AND RECOVERY OF HYDROGEN FROM THE RECYCLING GAS IN AMMONIA PRODUCTION BY MEANS OF LANTHANUM-RICH MISCHMETAL NICKEL HYDRIDE BEDS, *Hydrogen Systems, 2, 319-326.*

[2] T.H. Lee, C.Y. Park, J.E. Emerson, J.J. Picciolo, S.E. Dorris. 2014. Dense cermet membranes for hydrogen separation, *Seperation and Purification Technology, 54-59.*

Nanocarbon materials for biofuel elements

Kolesov V.V [1,3], Kitova A.E.[2], Krupenin S.V.[1], Reshetilov A.N.[2,3]

[1] Kotel'nikov Institute of Radio Engineering and Electronics of RAS, Russia, Moscow

[2] Scryabin Institute of Biochemistry and Physiology of microorganisms of RAS, Russia, Moscow

[3] NRC "Kurchatov Institute", Russia, Moscow

kvv@cplire.ru

Systems, in which used a biological material, oxidizing organic materials and the generation of electric potential is produced, are called biofuel elements (BFE). The biofuel element transforms energy of biochemical oxidation of organic substrata to electric energy, allowing use electrochemical passive substances as fuel [1]. In such electrochemical devices the chemical energy converts to electric by means of biocatalysts. Enzymes or organellas and the whole cells that energy is transformed due to metabolic activity of microorganisms can be used as aforesaid biocatalysts [2]. The electrodes for BFC have to provide good electrical conductivity, chemical resistance, biocompatibility, a high specific surface, and also possibility of technological processing. In this regard, the nanocarbon graphene materials, for example, thermoexpanded graphite (TEG), are rather perspective [3]. Technologies of thermal expansion of intercalated graphite particles and receiving of highly conductive materials with a well-developed surface belong to nanotechnological processes. In the work was also realized the bianode option on the basis of TEG with immobilized intact cells of *G. oxydans*. In the preliminary experiments, it was shown that in the absence of a mediator after adding of ethanol to the electrolyte solution there was no any changes of stationary potential of the bioanode [4]. This was due to the absence of a non-mediated electron transport from a donor-substrate (ethanol) on the electrode with immobilized intact cells. So, for enhancing of bioelectrochemical reaction of oxidation of ethanol, a redox mediator DCPIP was injected into the reaction system. After adding of redox mediator and ethanol into the reaction electrolyte, the change of the electrode potential was 160 mV from a reference value.

Thus, the basic possibility formation of the bioanode of a fuel element on the basis of thermoexpanded graphite with the immobilized membrane fractions of bacteria of *G. oxydans* which are bioelectrocatalysts was shown. The ethyl alcohol was used as fuel. Nature of potential

change of a working electrode indicates the direct transfer of a charge. The membrane fractions deposited on an electrode with inclusion in gel of a chitosan allow carry out direct bioelectrocatalytic oxidation of ethanol on an electrode. The obtained results allow estimate correctly further ways of development of biofuel elements, including production of small-sized BTE which can be effectively used in a biorobotics, and also in medical equipment as the implanted elements.

Work is performed with partial support of the RFBR- grants 15-29-01292, 16-07-00933.

Keywords: biofuel elements, bioanode, membrane fractions, nanocarbon materials

[1]. LOGAN, B. E. 2008. Microbial fuel cells. John Wiley & Sons, New Jersey, 200.

[2] KOLESOV, V.V., KRUPENIN, S.V., SOLDATOV, E.S., RESHETILOV, A.N. 2013. Biosensor on the Basis of Planar Nanostructure with built-in Enzymatic molecular Complexes. *International Journal of Materials, Mechanics and Manufacturing,* 1, 117-120.

[3] FILIP, J., TKAC, J. 2014. Is graphene worth using in biofuel cells? *Electrochimica Acta*, 136, 340–354.

[4] INDZHGIYA, E., PONAMOREVA, O., ALFEROV, V., RESHETILOV, A., GORTON, L. 2012. Interaction of ferrocene mediators with Gluconobacter oxydans immobilized whole cells and membrane fractions in oxidation of ethanol. *Electroanalysis*. 24, 924 -930.

Hafnium Doped Nanostructured Anatase as Efficient Anode Material for Lithium Ion Battery

S.L. Sinebryukhov[1], D.P. Opra[1], S.V. Gnedenkov[1], A.A. Sokolov[1,2], E.I. Voit[1], Yu.V. Sushkov[1], V.V. Zheleznov[1]

[1]Institute of Chemistry, Far Eastern Branch, Russian Academy of Sciences, 159, Prosp. 100-letya Vladivostoka, Vladivostok, 690022, Russia
[2]Far Eastern Federal University, Vladivostok, Primorsky region, Russia

E Mail/ Contact Détails sls@ich.dvo.ru/Sergey Sinebryukhov

Li-ion batteries (LIB) have successfully used as a power sources for different high-tech applications, e.g., portable electronics, medical devices, hybrid and electric vehicles, unmanned underwater vehicles, etc. due to their high energy density, long cycle life, low self discharge and environmental friendliness [1]. Technological progress requires the high LIB performances, including the capacity, power, reliability, storage life, and safety. It should be noted that the safety of modern LIBs is quite insufficient (because of the high reactivity of lithiated carbon) for using them as power supply modules consisting of a large number of cells [2, 3]. However, the extremely strong reactivity of lithiated graphite anode causes an irreversible unfavourable reactions with electrolyte. TiO_2(anatase) is a more suitable anode material for safe LIB as compared to graphite due to its higher Li^+ intercalation–deintercalation potential. However the slow Li^+ diffusion as well as poor conductivity limits the TiO_2(anatase) use as alternative anode. In the present work, the promising way of TiO_2(anatase) modification by Hf^{4+} doping are suggested in order to improve its Li^+ storage properties.

Original nanostructured Hf-doped TiO_2(anatase) was synthesized by template sol-gel method on a carbon fiber and investigated as Li-ion battery anode. It was found that the as-synthesized material consists of microtubes (length of 10–100 μm, outer diameter of 1–5 μm). Microtubes composed of nanoparticles with a size of 15–30 nm. 15-fold discharge–charge cycling shows that the reversible capacity for Hf-doped TiO_2 (Hf/Ti = 0.05) significantly higher (155 mAh g^{-1}) than one (65 mAh g^{-1}) for the undoped (Hf/Ti = 0) titania. It has been shown that the deviation from Hf/Ti = 0.05 decreases a cycle

performance of the TiO_2(anatase). The reversibility of the electrochemical process associated with the more open structure due to changing of the unit cell parameters.

Keywords: Li-ion battery, nanostructured material, anatase, doping, transition metal.

[1] LI, S., CHEN, C., FU, K., XUE, L., ZHAO, C., ZHANG, S., HU, Y., ZHOU, L., & ZHANG, X. 2014. Comparison of Si/C, Ge/C and Sn/C Composite Nanofiber Anodes Used in Advanced Lithium-Ion Batteries. *Solid State Ionics*, 254, 17–26.
[2] GNEDENKOV, S.V., OPRA, D.P., SINEBRYUKHOV, S.L., KURYAVYI, V.G., USTINOV A.Yu., & SERGIENKO V.I. 2015. Structural and Electrochemical Investigation of Nanostructured C:TiO_2–$TiOF_2$ Composite Synthesized in Plasma by an Original Method of Pulsed High-Voltage Discharge, *J Alloy Compd*, 621, 364–370.
[3] MAROM, R., AMALRAJ, S.F., LEIFER, N., JACOB, D., & AURBACH, D. 2011. A Review of Advanced and Practical Lithium Battery Material, *J Mater Chem*, 21, 9938–9954.

Hollow CuO/Cu_2O/C composite derived from a metal-organic framework via an in-situ process for Li- and Na-ion batteries

A-Young Kim[1,2], Joong Kee Lee[1]

[1]Center for Energy Convergence Research, Green City Research Institute, Korea Institute of Science and Technology, Hwarang-ro 14-gil 5, Seongbuk-gu, Seoul 02792, Republic of Korea

[2]Department of Material Science and Engineering, Korea University, Anam dong 5 ga, Seongbuk-gu, Seoul 02841, Republic of Korea

*aykim@kist.re.kr (***presenting author)**

leejk@kist.re.kr **(corresponding author)**

In light of the increasing energy demand of various portable electronic devices and electric vehicles, Li-ion batteries have attracted considerable attention as important energy storage devices [1]. However, Li resources are limited and are unevenly distributed globally, which may increase the cost of Li in the near future [2]. Na-ion batteries have attracted significant attention as alternatives to Li-ion batteries because of their relatively low cost, high natural abundance of Na, and similarities in the chemistry of Li and Na [3].

The hybrid composite electrode comprising CuO and Cu_2O nanoparticles in hollow carbon structures with porous morphologies has a rational design and is a promising strategy for the development of transition metal oxides as highly stable electrode materials for both Li- and Na-ion batteries. The hollow CuO/Cu_2O/C composites are synthesized by pyrolizing a Cu-based metal–organic framework template via an in-situ thermal transformation process. The electrochemical performances of the hollow CuO/Cu_2O/C composite anodes in Li- and Na-ion batteries are systematically investigated, and exhibit excellent discharge capacities of 880.7 mAh/g at 60 mA/g and 244.6 mAh/g at 50 mA/g after 100 cycles in Li-ion batteries and Na-ion batteries, respectively. The enhanced electrochemical performances were obtained via the rational strategy, mainly owing to the synergistic effect of the CuO

and Cu_2O nanoparticles and a conductive hollow carbon matrix with porous shells. Due to the simple in-situ thermal transformation process and the resultant high electrochemical performance, the hollow $CuO/Cu_2O/C$ composites are prospective anode materials for rechargeable Li- and Na-ion batteries.

Keywords: Copper oxide-based anode, metal-organic framework, in-situ process, lithium-ion battery, sodium-ion battery

[1] B. Dunn, H. Kamath, J. M. Tarascon, 2011. Electrical Energy Storage for the Grid: A Battery of Choices. *Science*, 334, 928-935.

[2] A. Yaksic, J. E. Tilton, 2009. Using the Cumulative Availability Curve to Assess the Threat of Mineral Depletion: The Case of Lithium. *Resources Policy*, 34, 185-194.

[3] K. Sakaushi, E. Hosono, G. Nickerl, T. Gemming, H. S. Zhou, S. Kaskel, J. Eckert, 2013. Aromatic Porous-Honeycomb Electrodes for a Sodium-Organic Energy Storage Device. *Nat. Commun.*, 4, 1485.

Parasitic Reactions for $LiNi_{0.6}Mn_{0.2}Co_{0.2}O_2$: a Mechanistic Study and Material Development

Zonghai Chen[1], Xiaoqiao Zeng[1], and Khalil Amine[1]

[1]Chemical Sciences and Engineering Division, Argonne National Laboratory,

9700 South Cass Avenue, Argonne, IL 60439, USA.

E-mail: zonghai.chen@anl.gov

The side reactions between the change electrode materials, delithiated cathodes or lithiated anodes, significantly contributes to the continuous and irreversible consumption of accessible lithium during the normal charge/discharge cycling, leading to a degradation on electrochemical performance of lithium-ion batteries. Understanding these side reactions, parasitic reactions, is crucial for the development of robust algorithm for predicting the remaining life of a specific battery and for the development of functional materials for long-life lithium-ion batteries.

Figure 1a shows a home-built high precision electrochemical testing system used to study the kinetics of parasitic reactions on $LiNi_{0.6}Mn_{0.2}Co_{0.2}O_2$. Figure 1b schematically shows the principle of the measurement. The working electrode was held at a specific potential using the source meter, maintaining a constant state-of-the-charge (SOC) for the working electrode. During this process, the electron obtained from the environment by the oxidation of the solvent, will be electrochemically collected by the external circuit. The measured leakage current is proportional to the reaction rate of parasitic (side) reactions between the working electrode and the electrolyte. Hence, the static leakage current can be used as a quantitative indicator for the reaction rate of the side reactions. Figure 1c shows a typical current relaxation curve collected, an exponential decay function was used to extract the static current (y_0 in Figure 1C), and to (1) minimize the impact of the high frequency noise, and (2) to get rid of the potential impact of slow intercalation/deintercalation reaction.

In this talk, the reaction mechanisms between delithiated $LiNi_{0.6}Mn_{0.2}Co_{0.2}O_2$ and the non-aqueous electrolyte will be discussed. In addition, development of function coating layers to suppress the parasitic reactions will also be presented.

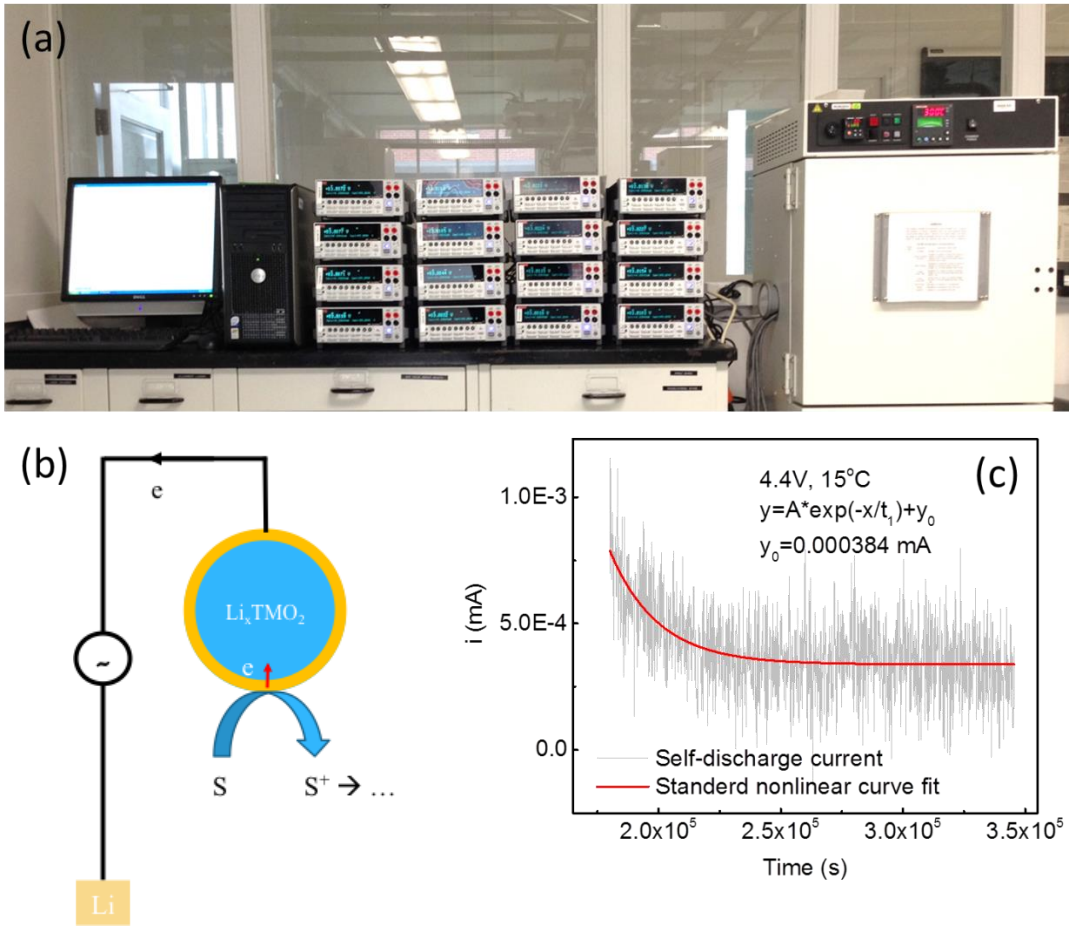

Figure 1 (a) Picture of a 16-channel high precision leakage current measuring system; (b) schematics showing the connection between the leakage current and the rate of parasitic reactions; (c) a typical current relaxation curve collected to extract the static leakage current.

Keywords: Lithium-ion battery, parasitic reaction, cathode, coating, kinetics

Preparation and electrochemical analysis of high-voltage Lithium-Iron-Manganese spinel cathodes for Lithium-ion batteries

Hans Kungl, Svitlana Eurich, Anja Hoffmann, Peter Jakes, Desiree van Holt, Roland Schierholz, L.G.J. de Haart, and Rüdiger-A. Eichel

Forschungszentrum Juelich, Institute of Energy and Climate Research (IEK-9), Fundamental Electrochemistry, Ostring 10, 52425 Juelich, Germany

h.kungl@fz-juelich.

In order to enhance volumetric and gravimetric energy density of Li-ion battery cathodes, two lines of development are in the focus of research. Both, materials with higher capacities and materials with higher voltages are under investigation. Among the high voltage cathode materials, the material class based on Lithium-Manganese spinels, in which part of the Manganese is substituted by a transition metal, is subject of current research and development activities [1]. Most attention within this material class has been paid to the $LiNi_xMn_{2-x}O_4$ spinels, in which the 2-electron process of the Ni^{2+}/Ni^{4+} redox couple provides a voltage of 4.7 V on discharge and specific capacities close to the theoretical capacities of 148 mAh/g can be realized.

Alternatively, substitution of part of the manganese by iron has been shown to provide even higher potentials than those obtained for the Ni-substituted compositions [2]. However, the high-voltage capacities of the $LiFe_xMn_{2-x}O_4$ spinels realized so far are considerably lower than those obtained with the corresponding Ni-substituted materials. In the present work Lithium-iron-manganese spinels $LiFe_xMn_{2-x}O_4$ with compositions ranging from x=0.1 to 1.0 have been prepared by a solid state synthesis route. Powder characteristics and structure of the materials are characterized by particle size measurements, scanning electron (SEM) and X-ray diffraction. X-ray diffraction results show an inversion of the spinel along with high iron contents. The Magnetic properties of the materials are investigated by means of electron paramagnetic resonance (EPR). Depending on the iron content enhanced ferrimagnetic activity is detected. Electrochemical analysis was performed in half cells with Li-anode. Charge-discharge behavior and current-voltage characteristics are analyzed with respect to capacities and voltage depending on composition and cutoff voltages. Perspectives and limits of the

Lithium-iron-manganese spinel cathodes with respect to applications in Li-ion batteries are discussed.

Keywords: Energy Storage, Lithium Ion Batteries, Cathode materials, High-Voltage Spinel

[1] KRAYTSBERG, A. and EIN-ELI, Y. 2012. Higher, stronger, better… A review of 5 Volt cathode materials for advanced lithium ion batteries. *Advanced Energy Materials,* 2 922-939.

[2] AMINE, K., TUKAMOTO, H., YASUDA, H. and FUJITA, Y. 1997. Preparation and electrochemical investigation of $LiMn_{2-x}Me_xO_4$ (Me: Ni and Fe, and x = 0.5, 1) cathode materials for secondary lithium batteries. *Journal of Power Sources,* 68, 604-608.

$(Si\text{-}Fe)_{85}C_{15}$ nanocomposite anode materials prepared by high energy mechanical milling for high capacity Li-ion secondary batteries

Yun Mo Yang, Chadrasekhar Loka, Dong-Pil Kim, Kee-Sun Lee*

Department of Advanced Materials Engineering, Kongju National University, Cheonan, Chungnam 330−717, South Korea.

E-mail: csloka89@gmail.com, kslee@kongju.ac.kr

Silicon-based anode materials have received much attention due to the high theoretical capacity (~4200 mAh g^{-1}). However, the capacity fading was very serious due to the large volume expansion and contraction during lithiation and delithiation. In this study, $(Si\text{-}Fe)_{85}C_{15}$ nanocomposite anode materials comprised of outer layer carbon and an inner core Si-Fe has been prepared by high-energy mechanical milling (HEMM) process for lithium-ion rechargeable batteries. The crystal structure, microstructure, and electrochemical performance of the nanocomposite materials have been studied. Raman spectra revealed the existence of D- and G-bands indicating glassy carbon. The transmission electron microscopy results showed that the thickness of carbon layer was about 10 nm. The impregnation of carbon was effective to enhance the capacity retention (low capacity fading) and coulombic efficiency (99.4%) at prolonged cycles. The electrochemical capacities of 1^{st}, 3^{rd}, and 30^{th} cycle for the composite anode are 1312, 1117, and 997 mAh g^{-1}, respectively. The electrochemical Li-alloying reactions of the nanocomposite anode have been identified by the differential capacity plots (DCPs) which indicate the phase change of Si from crystalline to amorphous after the initial cycle. The $(Si\text{-}Fe)_{85}C_{15}$ nanocomposite could be a promising candidate as an anode material because of its stable Li-storage performance and also the HEMM was an effective synthesizing tool for large-scale production.

Keywords: Silicon anode, carbon coating, nanocomposite, lithium-ion battery, mechanical milling.

[1] ARMAND, M., TARASCON, J. M. 2008. Building Better Batteries. *Nature*, 451, 652-657.

[2] HYOUNG, K. H., CHADRASEKHAR, L., YUN, M. Y., JAE, H. K., SUNG, W. M., JONG, S. C., Lee, K. S. 2015. High Capacity Retention Si/Silicide Nanocomposite Anode Materials Fabricated by High-Energy Mechanical Milling for Lithium-Ion Rechargeable Batteries. *Journal of Power Sources*, 281, 293-300

Effects of Electrolyte Concentration on Surface Film Formation on Graphite in Ethylene Carbonate-Based solutions

Soon-Ki Jeong

Department of Chemical Engineering, Soonchunhyang University, Asan, 336-745, Republic of Korea.

hamin611@sch.ac.kr/ +82-41-530-1313

Graphite is widely used as a negatively charged electrode material in commercially available lithium-ion batteries. When a graphite electrode is polarized to a negative potential in ethylene carbonate (EC)-based electrolytes, electrolyte decomposition creates a film on the graphite surface. This surface film, often called the solid electrolyte interface, allows lithium ions to pass through, while blocking the transfer of electrons [1,2]. This surface film suppresses electrolyte decomposition caused by electron transfer between electrode and electrolyte, and allows for selective intercalation and de-intercalation of lithium ions. Surface films significantly influence battery performance, so identifying their physicochemical characteristics is crucial. Even though surface films have been studied in detail, many issues still need to be investigated. This study aims to clarify the effects of electrolyte concentration on surface film formation in some EC-based solutions.

The electrolyte solutions were prepared by dissolving $LiN(SO_2C_2F_5)_2$ in a 1:1 (by volume) mixture of EC and diethyl carbonate. The test electrode was prepared by coating a mixture of the graphite powder and the polymeric binder on copper micro grids (Veco Co., 100 meshes). After the cycling tests, the copper electrodes were removed from the test cells and mounted in a sealed sample holder to examine by transmission electron microscopy (TEM, Hitachi, H-800). This procedure was performed in an argon-filled glove-box which enables the electrodes to avoid air exposure throughout the TEM measurements. TEM observations were performed at an accelerating voltage of 300 kV. Raman spectra were recorded using a triple monocromator (Jobin-Yvon, T-64000). Excitation of all samples was carried out with 514.5 nm radiation (200 mW) from an argon ion laser (NEC, GLG3260).

TEM observation revealed that the film formed on graphite surface was highly reactive and unstable in the air. The formation of a surface film in EC-based solutions was an electrochemical reaction that strongly depends on the electrolyte concentration. In concentrated EC-based solutions, relatively thick film with high resistivity was formed on graphite surface. Raman spectroscopic analysis suggested that the thermodynamic stability of the solvated

lithium ions was an important factor that determined the surface film formation in EC-based solutions.

Keywords: graphite, surface film, ethylene carbonate, electrolyte

This research was supported by Basic Science Research Program through the National Research Foundation of Korea (NRF) funded by the Ministry of Education (2015R1D1A1A02062148). This work was supported by the Human Resource Training Program for Regional Innovation and Creativity through the Ministry of Education and National Research Foundation of Korea (NRF-2014H1C1A1060729).

[1] YAZAMI, R., GUERARD, D., 1993. Some Aspects on The Preparation, Structure and Physical and Electrochemical Properties of Li_xC_6. *J. Power Sources*, 43, 39-46.

[2] PELED, E., 1979. The Electrochemical Behavior of Alkali and Alkaline Earth Metals in Nonaqueous Battery Systems? The Solid Electrolyte Interphase Model. *J. Electrochem. Soc.*, 126, 2047-2051.

Electrochemical Characteristic of Reduced Graphene Oxide/Nitrogen-doped Carbon form/Sulfur Nanocomposite as a Cathode for Lithium-sulfur Batteries

Jeongyeon Lee[1], Seung-Keun Park[1], Yuanzhe Piao[1,2]

[1]Program in Nano Science and Technology, Graduate School of Convergence Science and Technology, Seoul National University, 145 Gwanggyo-ro, Yeongtong-gu, Suwon-si, Gyeonggi-do 443-270, Republic of Korea

[2] Advanced Institutes of Convergence Technology, 145 Gwanggyo-ro, Yeongtong-gu, Suwon-si, Gyeonggi-do 443-270, Republic of Korea

httpower@snu.ac.kr / parkat9@snu.ac.kr

Hetero-atom doping processing with carbon materials is a significant tool for high electrochemical performance in lithium-sulfur batteries due to capping effect by strong interaction between hetero-atom doped carbon materials and polysulfides. However, general hetero-atom doping processing has the challenges for toxicity and complexity at doping process. In this study, we used commercial melamine foams with a quantity of N-functional group. Therefore, without additional steps, we fabricated the N-doped carbon framework easily and used with graphene for reservoirs of sulfur cathode. The electrode shows an initial capacity of about 1360 mA h g^{-1} at 0.1 C, and retains a specific capacity of about 630 mA h g^{-1} for 150 cycles (0.5 C). The enhanced cycling stability and high efficiency (~100%) are attributed to the capping effect of polysulfides by N-doping and fast electron and ion diffusion pathway of carbon framework and graphene.

Keywords: Carbon framework, nitrogen doping, graphene, lithium-sulfur batteries

Enhanced electrochemical performance of Ni-rich cathode by Li_2ZrO_3 surface coating

Jun Won (Lee), Yong Joon (Park)

Department of Advanced Materials Engineering, Kyonggi University, Iui-dong, Yeongtong-gu, Suwon-si, Gyeonggi-do, 443-760, Republic of Korea

E-mail : yjpark2006@kyonggi.ac.kr ***(Yong Joon Park)***

The Ni-rich materials (such as $Li[Ni_{0.8}Co_{0.15}Al_{0.05}]O_2$) are promising cathode materials with high specific discharge capacity. However, they have several disadvantages such as insufficient cyclic performance, rate capability and thermal stability. One of the approaches to address these issues, surface modification with stable material has been applied various cathode materials. The stable coating layer can suppress the unwanted side reaction between cathode and electrolyte, and improve the electrochemical performance of cathode. In this study, the surface of the $Li[Ni_{0.8}Co_{0.15}Al_{0.05}]O_2$ was coated by Li_2ZrO_3. Li_2ZrO_3 is stable oxide and has ionic conductivity, which can facilitate the ionic exchange during charge-discharge process as well as protecting effect against the reactive electrolyte during cycling. So, the Li_2ZrO_3 coated $Li[Ni_{0.8}Co_{0.15}Al_{0.05}]O_2$ is expected to show enhanced electrochemical performance.

Keywords: cathode material, lithium secondary batteries, coating

Fabrication and Electrochemical Performances of Carbon-coated Silicon Anodes Using Recycled Poly-vinyl Butyral Sheets

Sung-Woo Park, Mingu Choi, Jae-Chan Kim, Dong-Wan Kim

School of Civil, Environmental and Architectural Engineering, Korea University, Seoul 136-713, Korea

E-mail: 2015010567@korea.ac.kr, dwkim1@korea.ac.kr

Lithium ion batteries (LIBs) have been commonly used as power sources for portable electronics because of its higher energy density than previous energy storage devices. To respond future needs of the large scale energy storage markets such as hybrid electric vehicles and energy storage systems, advanced LIBs having large reversible capacities should be developed. Silicon (Si) is one of attractive candidate anode materials for LIBs to replace commercial carbon-based anodes due to its high theoretical capacity (4200 mAh/g for $Li_{22}Si_5$), low discharge potential (0.37 mV vs. Li/Li^+), and abundant reserves. However, Si anodes are accompanied by large volume expansion up to ~400%, which cause cracking and destruction of Si anodes by mechanical stress upon cycling. Carbon coating is one of the methods that solve these drawbacks [1].

Poly-vinyl Butyral (PVB) is mainly used as an adhesive for safety glass but its recycled products are rated low value in the industry. So, majority of the PVB sheets have been buried in landfill [2]. In this study, we prepared Si/pyrolytic carbon (Si/PC) composites via simple pyrolysis process at a low-temperature using commercial Si nanopowders and recycled PVB as carbon sources. The recycled PVB sheets were dissolved in ethyl alcohol and then Si nanopowders were dispersed in prepared PVB solution. The mixtures were prepared in various Si/PVB weight ratio (1/10, 1/20, 1/30, 1/40, 1/60, 1/100). The dried Si/PVB films were subsequently pyrolyzed at 500ºC for 4 h in Ar atmosphere. The uniform carbon-coating on Si nanoparticles was confirmed using a field-emission scanning electron microscopy and transmission electron microscopy. The electrochemical characterizations demonstrated that the optimized Si/PC composite electrodes exhibited an excellent capacity retention even after 100 cycles, compared with commercial Si powders. This facile, cost-effective, and scalable carbon-coating process using recycled PVB

could provide an efficient electronic conductivity and volume relaxation in Si anodes during cycling.

Keywords: Li ion batteries, Si/C composites, recycling, Poly –Vinyl Butyral, wind shield glass

[1] NG S. H., WANG J. Z., WEXLER D., KONSTANTINOV K., GUO Z. P. & LIU H. K. 2006. Highly Reversible Lithium Storage in Spheroidal Carbon-Coated Silicon Nanocomposites as Anodes for Lithium-Ion Batteries. *Angew. Chem. Int. Ed.*, 45, 6896-6899.

[2] TUPY M., MOKREJS P., MERINSKA D., SVOBODA P. & ZVONICEK J. 2013. Windshield Recycling Focused on Effective Separation of PVB Sheet. *J. Appl. Polym. Sci*., 131, 39879.

Investigating the local degradations of $LiNi_{0.8}Co_{0.15}Al_{0.05}O_2$ Cathode Materials during Initial charge/discharge with Rate effect

Eunmi (Jo) [1,2], Sooyeon (Hwang)[1], Seung Min (Kim)[3], and Wonyoung (Chang)[1,*]

[1] Center for Energy Convergence, Korea Institute of Science and Technology, Seoul 136-791, Republic of Korea.
[2] Energy Conversion Technology, Korea University of Science and Technology, 217 Gajeong-ro Yuseong-gu, Daejeon 305-333, Republic of Korea.
[3] Carbon Composite Materials Research Centre, Institute of Advanced Composite Materials, KIST, Wanju-gun 565-905, Republic of Korea

Presented by *H15507@kist.re.kr (E. Jo)*

Corresponded to **cwy@kist.re.kr (W. Chang)*

Lithium ion batteries have been widely used in portable devices such as laptops and cellular phones and have attracted interests for large-scale applications, representatively electric vehicles (EV), which require high capacity, high power and good cycle performance. $LiNi_{0.8}Co_{0.15}Al_{0.05}O_2$ (NCA) is considered as a promising cathode material for EV applications due to its high discharge capacity (200 mAh g^{-1}). However, NCA cathode materials have a disadvantage of structural instability, which results in a drastic capacity fade and impedance rise with cycling. Thus it is important to understand the degradation mechanisms of NCA cathode materials under various electrochemical conditions.

Our previous study delineated the structural evolution of NCA as a function of the extent of first charge. It was found that the crystallographic structures are modified from the layered structure (space group $R\bar{3}m$) to the disordered spinel structure ($Fd\bar{3}m$), and eventually to the rock-salt structure ($Fm\bar{3}m$). Changes in crystal structures are accompanied by significant changes in the electronic structures, which are reflected in oxygen K-edge electron energy-loss spectra (EELS). [1]

In this work, we further investigate the structural changes that occur in NCA cathode materials during the initial charge/discharge under the various conditions of C-rates and the state of charge. As the structural changes initiate at the nanoscale, we take advantage of transmission electron microscopy (TEM), which is an ideal tool to investigate incipient structural changes with a high spatial resolution. Modifications in crystallographic and electronic structures at the subsurface are investigated with selected-area electron diffraction (SAED) patterns and oxygen K-

edge EELS. Additionally, structural changes occurred at the edge of NCA particles are examined with a high-resolution electron microscopy (HREM) images and fast Fourier transformations. This study demonstrates that local structural degradation can occur at the subsurface or surface of NCA cathode materials and electrochemical testing conditions have a great impact on the structural stability of NCA even during the initial charge/discharge. All the details will be available at the meeting.

Keywords: Lithium ion battery, cathode materials, $LiNi_{0.8}Co_{0.15}Al_{0.05}O_2$ (NCA), transmission electron microscopy, electron energy-loss spectroscopy

[1] SOOYEON, H., WONYOUNG, C., SEUNG MIN, K., DONG, S., DONG HYUN, K., JEONG YONG, L., KYUNG YOON, C., & ERIC, A. S. 2014. Investigation of Changes in the Surface Structure of $LiNi_{0.8}Co_{0.15}Al_{0.05}O_2$ Cathode Materials Induced by the Initial Charge. Chem. Mater., 26, 1084−1092

Li_2ZrO_3 -coated $Li_{1.2}Ni_{0.2}Mn_{0.8}O_2$ for the High Performance Cathode Material in Lithium Ion Batteries

Hana Noh[1,2], Yonguk Kwon[1], Hyeongwoo Kim [1,3], Yongho Lee[1,4], Wonchang Choi[1,2*]

[1] Center of Energy Convergence Research, Korea Institute of Science and Technology, Republic of Korea

[2] Department of Energy and Environmental Engineering, Korea University of Science and Technology, Republic of Korea

[3] Department of Materials science and Engineering, Korea University

[4] Department of Chemical and Biological Engineering, Korea University

Presenting author : yonguk04@naver.com

Corresponding author : wonchangchoi@kist.re.kr

Recently, high energy density lithium ion batteries (LIBs) play an important role in the field of portable and electronic devices and electrical vehicles. Current $LiCoO_2$ is around 160 $mAhg^{-1}$ with lithium utilization in the structure less than 50%. Moreover, their cost and safety requirement are still problems for the adoption of lithium ion technology for these large-battery application. To overcome this problem, Over-lithiated Layered Oxide (OLO) materials have been considered one of the promising cathode materials for the next generation of cathode materials. Among them, $0.5Li_2MnO_3 \cdot 0.5LiNi_{0.5}Mn_{0.5}O_2$ which is known as high capability (250 $mAhg^{-1}$) has excellent electrochemical performance and stability at higher cut-off voltage beyond 4.8 V. However, its severe capacity fading during high current rates is generally related to the unstable structure and the side reaction with electrolytes. Herein, we reports Li_2ZrO_3 -coated $Li_{1.2}Ni_{0.2}Mn_{0.8}O_2$ for high performance cathode material in lithium ion batteries. The concept is both to decrease the interface resistance by crystallization of the surface layer and cover the particles with Li_2ZrO_3 that would suppress the particles against side reactions with the electrolyte.

Keywords: surface modification, lithium zirconate, lithium-rich layered oxide, cathode, lithium-ion battery

Magnetic and structural properties of $Na_2FeP_2O_7$ as Pyrophosphate cathode material

Hyunkyung (Choi)[1], Eun Joo (Hahn)[2], Sam Jin (Kim)[1], and Chul Sung (Kim)[1]

[1] Department of Physics, Kookmin University, Seoul, Republic of Korea

[2] Department of Physics, Suwon University, Suwon, Republic of Korea

newton@kookmin.ac.kr / presenting author

cskim@kookmin.ac.kr / corresponding author

The $Na_2FeP_2O_7$ of Na-based pyrophosphate show outstanding thermal stability, reversible capacity, which can be suitable as for a cathode material. $Na_2FeP_2O_7$ compounds were prepared by solid-state reaction under Ar. In this study, the crystal and magnetic structure of $Na_2FeP_2O_7$ has been investigated by using XRD, VSM, and Mössbauer spectroscopy. Based on the Rietveld refinement, the crystal structure was analyzed to be a Triclinic with space group of *P*-1. The lattice constants of $Na_2FeP_2O_7$ were determined to be a_0 = 6.43, b_0 = 9.41, c_0 = 11.00 Å , α = 64.387 °, β = 85.279 °, γ = 72.748 °. The magnetic properties of $Na_2FeP_2O_7$ pyrophosphate was measured from the zero-field-cooled magnetization curves under 1000 Oe between 4.2 and 295 K. The results, Nèel temperature (T_N) were confirmed to be 11 K. Based on this, temperature dependent Mössbauer spectrum recorded at various temperatures ranging from 4.2 to 295 K. The Mössbauer spectrum of the $Na_2FeP_2O_7$ at 295 K consists of three-sets of Fe^{2+}. Mössbauer spectra of $Na_2FeP_2O_7$ at 4.2 K were analyzed with one-set of Fe^{2+} eight Lorentzian (A-site) and two-sets of Fe^{2+} sextets (B_1, B_2-site) subspectra. With increasing temperature, spectrum changes with decrease of magnetic hyperfine field (H_{hf}), and then it shows double phase at 11 K. These results lead to the reduction of strong electric quadrupole interaction.

Keywords: Mössbauer, $Na_2FeP_2O_7$, Na-battery, cathode material

[1] KIM, H., SHAKOOR, R. A., PARK, C., LIM, S. Y., KIM, J. -S., JO, Y. N., CHO, W., MIYASAKA, K., KAHRAMAN, R., JUNG, Y., AND CHOI, J. W. 2013. $Na_2FeP_2O_7$ as a Promising Iron-Based Pyrophosphate Cathode for Sodium Rechargeable Batteries: A Combined Experimental and Theoretical Study. *Adv. Funct. Mater.*, 23, 1147.

Magnetic properties of Na substituted $Li_{0.9}Na_{0.1}FePO_4$ by Mössbauer Spectroscopy

Byung Ug Ko[1], Young Bae Lee[2], Sung Baek Kim[3], Chul Sung Kim[1]

[1] Department of Physics, Kookmin University, Seoul, 02707, South Korea.

[2] Department of Liberal Arts, Hanzhong University, Donghae, 25800, South Korea

[3] The College of General Education, Konyang University, Chungnam 35365, South Korea

kobo428@kookmin.ac.kr / presenting author

cskim@kookmin.ac.kr / corresponding author

The olivine type cathode materials lithium iron phosphate ($LiFePO_4$) has been investigated about substitution. The starting materials of $FeC_2O_4{\cdot}2H_2O$, $NH_4H_2PO_4$, $Na(CH_3COO)$ and Li_2CO_3 were grinded for 1 hour and calcined at 300℃ for 4 hours under argon atmosphere. Then this mixture was pelletized sintered at 700℃ for 10 hours under argon atmosphere. The XRD patterns of $Li_{0.9}Na_{0.1}FePO_4$ were analyzed by Rietveld refinement method. This crystal structure determined to be orthorhombic and the lattice constants were a_0 = 10.332, b_0 = 6.012 and c_0 = 4.710 Å . The zero-field-cooled (ZFC) and field-cooled (FC) curves were mesured VSM (vibrating sample magnetometer) from 4.2 to 300 K. The Néel temperature (T_N) and spin reorientation temperature (T_S) were T_N = 49.5 K and T_S = 20 K, respectively. We measured Mössbauer spectra from 4.2 to 295 K and analyzed 8-line absorption spectra. The magnetic hyperfine field (H_{hf}), electric quadrupole splitting (ΔE_Q) and isomer shift (δ) values was obtained to be H_{hf} = 124.53 kOe, ΔE_Q = 2.74 mm/s, δ = 1.24 mm/s. θ = 15.0°, φ = 0.0°, η = 0.79 and R = 3.21 at 4.2 K. The isomer shift (δ) was 1.11 mm/s at room temperature and the Fe ion state was ferrous (Fe^{2+}).

Keywords: Mössbauer spectroscopy, $LiFePO_4$, Na substitution

[1] WANG, J., SUN, X., 2015. Olivine $LiFePO_4$: the remaining challenges for future energy storage. *Energy Environ*, 8, 1110-1138.

Melamine resin-based nonwoven membrane to improve cycle life of $LiMn_2O_4$/graphite battery

Qingfu Wang[1], Jun Ma[1], Zhihong Liu[1], Guanglei Cui[1*]

[1] Qingdao Institute of Bioenergy and Bioprocess Technology, Chinese Academy of Sciences, Qingdao 266101, P. R. China

E-Mail : wangqf@qibebt.ac.cn, cuigl@qibebt.ac.cn

In LIBs, the separator performs crucial functions of physically separating the anode and cathode while permitting free flow of lithium ions. Thus, separator is paramount importance for battery safety and reliability.[1-6] A flame retardant and thermally dimensional stable membrane with high permeability and electrolyte wettability can overcome the safety issues of lithium ion batteries (LIBs) at elevated temperatures. In this work, a multifunctional thermoset nonwoven membrane composed of melamine formaldehyde resin (MFR) nano-fibers was prepared by a reactive electro-spinning method. The resultant porous nonwoven membrane possesses superior permeability, electrolyte wettability and thermally dimensional stability. Using the electrospun MFR membrane, the $LiFePO_4$/Li battery exhibits high safety and stable cycling performance at the elevated temperature of 120 ℃. Most importantly, the MFR membrane contains lone pair electron in the nitrogen element, which can chelate with Mn^{2+} ions and suppress their transfer across the separator. Therefore, the $LiMn_2O_4$/graphite cells with the electrospun MFR multifunctional membranes reveal an improved cycle performance even at high temperature. This work demonstrated that electrospun MFR is a promising candidate material for high-safety separator of LIBs with stable cycling performance at elevated temperatures.

Keywords: thermal-stability. flame-retardant. melamine formaldehyde resin. separators. lithium ion battery.

[1] TARASCON, J. M., ARMAND, M. 2001. Issues and challenges facing rechargeable lithium batteries. *Nature*, 414, 359-367.

[2] GOODENOUGH, J. B., KIM, Y. 2010. Challenges for Rechargeable Li Batteries. *Chem. Mater.*, 22, 587-603.

[3] THACKERAY, M. M.,WOLVERTON, C., ISAACS, E. D. 2012. Electrical energy storage for transportation-approaching the limits of, and going beyond, lithium-ion batteries. *Energy Environ. Sci.*, 5, 7854-7863.

[4] ORENDORFF, C. J., LAMBERT, T. N., CHAVEZ, C. A., BENCOMO, M., FENTON, K. R. 2013. Polyester Separators for Lithium-Ion Cells: Improving Thermal Stability and Abuse Tolerance. *Adv. Funct. Mater.*, 3, 314-320.

[5] KRITZER, P., COOK, J. A. 2007. Nonwovens as separators for alkaline batteries - An overview. *J. Electrochem. Soc.*, 154, A481-A494.

[6] WHITTINGHAM, M. S. 2004. Lithium batteries and cathode materials. *Chem. Rev.* 104, 4271-4302.

One-pot Low-temperature Fabrication of CuO/Graphene Nanosheet Composites for High-capacity Li Ion Battery Anodes

Da-Sol Kim, Jae-Chan Kim, Dong-Wan Kim

School of Civil, Environmental and Architectural Engineering, Korea University, Seoul 136-713, Korea

E-mail: solggangi@korea.ac.kr, dwkim1@korea.ac.kr

Nanosized transition metal oxides have extensively studied as promising anode materials for Li ion batteries due to their high theoretical capacities by conversion reactions. The copper oxide (CuO) also undergoes a reversible conversion reaction with two lithium ions per mole, providing the large specific capacity of 674 mAh/g. However, CuO has critical drawbacks such as low electronic conductivity as well as high volume change during conversion reaction [1]. Thus, the huge efforts, which could be the preparation of carbon-based composites and design of novel nanostructures, have been devoted to overcome these problem [2]. One dimensional CuO nanowires/carbon composites are the potential candidate anodes because of their advantages such as buffer spaces to accommodate large volume change, superior electrical conductivity, and efficient Li-ion transport pathways. Especially, graphene nanosheets, one of advanced carbonaceous materials can provide large surface area, superior electronic conductivity, high porosity, and other fascinating properties.

In this study, CuO nanowire/graphene nanosheet (CuO/G) composites were successfully prepared via the ultrasound-assisted process at low temperatures. Firstly, the starting materials of $Cu(Ac)_2 \cdot H_2O$ and NaOH were dissolved in ethanol and deionized water. Then, this solution was ultrasonically reacted with the output power of 49% of 20 kHz ultrasound irradiation at 283 K for 2h. The crystal structure, particle size, and morphology of CuO/G composites and pure CuO nanowires were confirmed by X-ray diffraction, field-emission scanning electron microscopy, and transmission electron microscopy. The Li-electroactivities were also evaluated by galvanostatic cycling and cyclic voltammetry. The CuO/G composites exhibited an enhanced cycle stability and better rate capability, compared with the pure CuO nanowires, which can be attributed to the beneficial incorporation of graphene nanosheets offering large active surface areas and efficient electron conduction pathways.

Keywords: Copper oxide, nanowires, graphene, ultrasound, Li ion batteries

[1] CHEN H., FENG F., HU Z. L., LIU F. S., GONG W. Q. & XIANG K. X. 2012. Preparation of Uniform Flower-like CuO and Flower-like CuO/graphene Composite and Their Application in Lithium Ion Batteries. *Trans. Nonferrous Met. Soc. China*, 22, 2523-2528.

[2] Zhou J., Ma L., Song H., Wu B. & Chen X. 2011. Durable High-rate Performance of CuO Hollow Nanoparticles/graphene-nanosheet Composite Anode Material for Lithium-ion Batteries. Electrochem. Commun., 13, 1357-1360.

Phase transition properties of the Lithium cathode materials $Li_{1-x}Fe_{1/3}Co_{1/3}Ni_{1/3}PO_4$

Hyunkyung (Choi), In-Bo (Shim), In Kyu (Lee), and Chul Sung (Kim)

Department of Physics, Kookmin University, Seoul, Republic of Korea

newton@kookmin.ac.kr / presenting author

cskim@kookmin.ac.kr / corresponding author

Mixed Olivine phosphate, Li*M*PO_4 (*M* = Fe, Co, Ni) have been reported as a new candidate high energy battery [1]. $Li_xFe_{1/3}Co_{1/3}Ni_{1/3}PO_4$ (x = 0,1) samples were prepared by the solid state reaction method, and chemical-oxidation process with reaction of $LiFe_{1/3}Co_{1/3}Ni_{1/3}PO_4$ and NO_2BF_4 in acetonitrile. In this study, the crystal and magnetic structure of $Li_xFe_{1/3}Co_{1/3}Ni_{1/3}PO_4$ has been investigated by usnig x-ray diffraction, vibrating sample magnetometer, and Mössbauer spectroscopy. $Li_xFe_{1/3}Co_{1/3}Ni_{1/3}PO_4$ (x = 0,1) samples crystallized in orthorhombic with the *P*nma space group. The Mössbauer spectra at room temperature shows the valence transition with the $LiFe_{1/3}Co_{1/3}Ni_{1/3}PO_4$ exhibits one ferrous doublet whereas fully deintercalated $Fe_{1/3}Co_{1/3}Ni_{1/3}PO_4$ show the One ferric doublet. The temperature dependence of the isomer shifts of the both samples reveals that the different $Fe^{2+/3+}$ valence states existed ni all temperature range. The temperature dependent of the magnetic susceptibility and Curie-Weiss fitted inverse magnetic susceptibility cruves for the $Li_{1-x}Fe_{1/3}Co_{1/3}Ni_{1/3}PO_4$ samples. The magnetic ordering of the both samples were reveals that the typical antiferromagnetic structure enhanced by two valence state. The Néel Temperature (T_N) from 51 K (x= 0) and 35 K (x= 1). We have analyzed that the changes of phase transition and valence state by lithium deintercalation.

Keywords: magnetic measurements, Li-ion battery, cathode material, Mössbauer spectroscopy

[1] PARK, Y.-U., KIM. J., GWON. H., SEO. D.-H., KIM, S.-W., AND KANG, K., 2010. Synthesis of Multicomponent Olivine by a Novel Mixed Transition Metal Oxalate Coprecipitation Method and Electrochemical Characterization. *Chem. Mater.* 22, 2573-2581.

Pitch-coated Hard Carbon/Sn Composite Synthesized by High Energy Ball Milling as an Anode Material for Sodium Ion Batteries

Hyeongwoo Kim[1,3], Yongho Lee[1,4], Hana Noh[1,2], Yonguk Kwon[1], Wonchang Choi[1,2]

[1] Center of Energy Convergence Research, Korea Institute of Science and Technology, Republic of Korea

[2] Department of Energy and Environmental Engineering, Korea University of Science and Technology, Republic of Korea

[3] Department of Materials science and Engineering, Korea University

[4] Department of Chemical and Biological Engineering, Korea University

Presenting author : 115508@kist.re.kr

Corresponding author : wonchangchoi@kist.re.kr

Energy storage technology has been on the rise in recent years with the development of Li-ion batteries (LIBs). Na-ion batteries (NIBs) are recognized as the promising next generation battery system alternative to the LIBs. However, the NIB system suffers from the disadvantage of low energy density. To overcome this problem, hard carbon was introduced which shows 200~300 $mAhg^{-1}$ of initial reversible capacity at a low current density and excellent cycle performance. However, its capacity was still low in comparison with alloy-based anode materials. Meanwhile, Tin, alloy-based anode material ($Na_{15}Sn_4$), can realize the 847 $mAhg^{-1}$ of high theoretical capacity. However, it also has lower cycle performance with respect to the 420 % of huge volume expansion. We suggested that hard carbon/Sn composite that synthesized by using the high energy mechanical milling can make up for both of two materials' limitations and make the best use of their advantages. However, it still had a degradation due to the volume expansion of Sn. Moreover, Sn shows limited cycle performance on its operating voltage range because of the electrolyte decomposition of at >0.8 V vs. Na/Na^+.[1] Hence, we coated HC/Sn composite particles with pitch which can prevent reactions with electrolyte at the operating potential and enhance the conductivity of the HC/Sn composite anode material.

Keywords: Composite, hard carbon, tin, anode, sodium-ion battery

[1] Y. Kim, Y. Kim, Y. Park, Y.N. Jo, Y.J. Kim, N.S. Choi, K.T. Lee, SnSe alloy as a promising anode material for Na-ion batteries, Chemical Communications 51(2015) 50–53

Role of Crystal Defects in the Unit Cell Breathing Mechanism and Electrochemical Performance of Li_2MoO_3

Jun Ma, Guanglei Cui

Qingdao Industrial Energy Storage Research Institute, Qingdao Institute of Bioenergy and Bioprocess Technology, Chinese Academy of Sciences, Qingdao 266101, China.

Presenting author. E-mail address: majun@qibebt.ac.cn.

Corresponding author. E-mail address: cuigl@qibebt.ac.cn.

Layer-structured Li_2MoO_3 with high theoretical capacity (339 mAh/g), high conductivity, reversible structure transition, and absence of oxygen evolution has been considered as an ideal replacement of Li_2MnO_3 in constructing novel Li_2MoO_3-based Li-rich cathode materials.[1-3] Furthermore, Li_2MoO_3 has a unit cell breathing mechanism during Li ions deintercalation and intercalation, which will be beneficial to suppress the structure degradation and enhance the cycling performance of commercial layered cathode materials $LiMO_2$ (M = Ni, Co, Mn).[4] The unit cell breathing mechanism in Li_2MoO_3 is closely related with its metal-metal bond (Mo-Mo). For Li_2MoO_3, the lattice parameters, *a*(*b*), expand during charge due to the extended Mo-Mo bond, which is different from the lattice contraction in $LiMO_2$ caused by the shrinking metal-oxygen bond. However, the Mo-Mo bond can be influenced by the crystal defects, such as Li^+ ion vacancies, O^{2-} ion vacancies, and metal ions arrangement. Here, we propose to investigate the role of crystal defects in the unit cell breathing mechanism and electrochemical performance of Li_2MoO_3 synthesized at different conditions. Comprehensive studies by X-ray diffraction (XRD), X-ray absorption spectroscopy (XAS), and spherical-aberration-corrected scanning transmission electron microscopy (STEM) demonstrate the crystal defects in Li_2MoO_3, as well as the crystal structure transition and oxidation state variation of Mo ions during charge and discharge. The electrochemical measurements show that Li_2MoO_3 with different defects has different voltage platform, capacity, cycling life and rate capability. This work will give new understanding on the relation between crystal structure and electrochemical performance of Li_2MoO_3 and shed light on the performance optimization of Li_2MoO_3-based Li-rich cathode materials.

Keywords: Li-rich cathode materials, layer structure, structure degradation, defects, lithium ion batteries

[1] MA, J., ZHOU, Y. N., GAO, Y. R., YU, X. Q., KONG, Q. Y., GU, L., WANG, Z. X., YANG, X. Q., CHEN, L. Q. 2014. Feasibility of using Li_2MoO_3 in constructing Li-rich high energy density cathode materials. *Chemistry of materials*, 26, 3256-3262.

[2] MA, J., ZHOU, Y. N., GAO, Y. R., KONG, Q. Y., WANG, Z. X., YANG, X. Q., CHEN, L. Q. 2014. Molybdenum substitution for improving the charge compensation and activity of Li_2MnO_3. *Chemistry-A European Journal*, 20, 8723-8730.

[3] MA, J., GAO, Y. R., WANG, Z. X., CHEN, L. Q. 2014. Structural and electrochemical stability of Li-rich layer structured Li_2MoO_3 in air. *Journal of Power Sources*, 258, 314-320.

[4] ZHOU, Y. N., MA, J., HU, E., YU, X. Q., GU, L., NAM, K. W., CHEN, L. Q., WANG, Z. X., YANG, X. Q. 2014. Tuning charge-discharge induced unit cell breathing in layer-structured cathode materials for lithium-ion batteries. *Nature Communications.*, 5, 5381.

Sulfur-impregnated Uniform Hollow Carbon Nanospheres/Graphene Hybrids as Cathode for Lithium-Sulfur Batteries

Seung-Keun Park[1], Jeongyeon Lee[1], Yuanzhe Piao[1,2]

[1]Program in Nano Science and Technology, Graduate School of Convergence Science and Technology, Seoul National University, 145 Gwanggyo-ro, Yeongtong-gu, Suwon-si, Gyeonggi-do 443-270, Republic of Korea

[2] Advanced Institutes of Convergence Technology, 145 Gwanggyo-ro, Yeongtong-gu, Suwon-si, Gyeonggi-do 443-270, Republic of Korea

agape09@snu.ac.kr / parkat9@snu.ac.kr

Among next-generation battery systems, lithium-sulfur (Li-S) batteries have attracted great attention due to their high specific energy density (2600 W h kg^{-1}), environmentally benign and natural abundance of sulfur. In spite of these considerable advantages, there are two major issues of using sulfur: its electronic insulating character and a rapid capacity fading caused by the high solubility of Li_2S_x ($2 < x \leq 8$, intermediate products) in electrolyte solutions. A promising strategy to overcome these problems is to combine conductive carbon materials as effective hosts, such as, graphene, carbon nanotubes, porous carbon and hollow carbon spheres to enhance the electrical conductivity of electrode materials and minimize the dissolution of Li_2S_x into the electrolyte.

Herein, we propose a simple strategy to synthesize uniform hollow carbon nanospheres/graphene nanosheets (UHCN/G) hybrids as promising host materials to confine sulfur for Li-S batteries. After impregnating elemental melted sulfur in the pore structure of UHCN/G, the UHCN/G-sulfur (UHCN/G-S) composite shows significantly improved electrochemical properties compared to that of bare graphene nanosheets.

Keywords: Li-S batteries, graphene, hollow carbon, cathode

The Preparation of Nitrogen Doped Graphene and Electrochemical Performance for High Performance Lithium- Sulfur Battery

Yong Huang, Mengyu Ren, Mingming Che, Rong Yang

Xi'an University of Technology, Xi'an 710048, China

Huangy01@xaut.edu.cn *yangrong@xaut.edu.cn*

Lithium-sulfur battery is attracted the attention of the researchers due to a high theoretical capacity of 1675 mA ħ/g and high energy density of 2600 Wh/kg while it is still seriously hindered by low utilization of sulfur and the dissolution of the discharge intermediates polysulfides. Considering the excellent performances of graphene, a series of graphene/sulfur composites would be synthesized and studied in lithium-sulfur batteries.

Graphene oxide has been synthesized by Hummer's method. Graphene has been synthesized from graphene oxide by pyrolysis method. And then graphene/sulfur composite (RE-RGO/S) has been synthesized by chemical method. The size of sulfur is about 50nm distributed uniformly on the graphene and the morphology of graphene was distorted the film layer with the surface appears fold through the observation of SEM and TEM. The discharge specific capacity of RE-RGO/S is delivered at 1558 mA ħ/g after 1st cycle, which is closing to the theoretical specific capacity of sulfur, and it remains at 536.9 mA ħ/g after 45 cycles at 0.1C. The discharge specific capacity of RE-RGO/S composite is 405 mA ħ/g at 0.2 C and 300 mA ħ/g at 1 C, respectively. It is obvious that the RE-RGO/S composite has showed good rate stability.

Nitrogen doped graphene (RE-NRGO) has been synthesized by pyrolysis method with urea as nitrogen source. Nitrogen content is 7.63 wt% in the nitrogen doped grapheme. To probe the chemical composition and the bonding types of carbon, and nitrogen in, XPS measurements were carried out. It reveals that there are three types of N species in RE-NRGO, corresponding to graphitic-N (401.0 eV), pyrrolic-N (399.8 eV), and pyridinic-N (398.2 eV). The atomic percentages for the three N species show that pyridinic-N is the major part. As the electrochemical performance tests showed, the RE-

NRGO/S composite has displayed the initial discharge capacity and Columbic efficiency are 1464 mA ħ/g and 98.0%, respectively, and then the discharge capacity remains at 582 mA ħ/g after 70 cycles at 0.1 C. Here, RE-NRGO/S presents a high reversible capacity comparing to RE-RGO/S composite. This may be due to the pyridinic nitrogen which can act as good adsorption sites for sulfur or polysulfides and help to confine the diffusion of soluble polysulfides and improve the cyclability of lithium–sulfur batteries.

Key words: Lithium-sulfur batteries, graphene, nitrogen doping, sulfur

Acknowledgment: *This work was supported by International Science Technology Cooperation Program of China）（2015DFR50350）*

[1] YAND Y, YU GH, CHA JJ, WU H, VOSGUEROTCHIAN M, YAO Y, et al. 2011. Improving the Performance of Lithium–sulfur Batteries by Conductive Polymer Coating. *ACS Nano*, 5, 9187–9193.

[2] EVERS S, NAZAR LF. 2012. Graphene-enveloped Sulfur in A One Pot Reaction: A Cathode with Good Coulombic Efficiency and High Practical Sulfur Content. *Chem Commun*. 48. 1233–1235.

[3] SUN F, WANG J, CHEN H, LI W, QIAO W, LONG D, et al. 2013.High Efficiency Immobilization of Sulfur on Nitrogen-enriched Mesoporous Carbons for Li–S Batteries. *ACS Appl Mater Interfaces*, 5. 5630–5638.

[4] WEI DC, LIU YQ,WANG Y, ZHANG HL, HUANG LP, YU G. 2009.Synthesis of N-doped Graphene by Chemical Vapor Deposition and Its Electrical Properties. *Nano Lett*. 9. 1752–1758.

Application of ANOVA Method to Study Solar Renewable Energy for Hydrogen Production

M.S. Hossain[a*], N. A. Rahim[a,c], M.M. Aman[b], Jeyraj Selvaraj[a], A K Pandey[b], Abdul Faheem Khan[a]

a Centre of Research UMPEDAC, Level 4, Wisma R&D, University of Malaya, 59990 Kuala Lumpur, Malaysia

b Department of Electrical Engineering, NED university of engineering and technology, 75270, Karachi Pakistan.

c Faculty of Engineering, King Abdulaziz University, Jeddah 21589, (Saudi Arabia)

Abstract

Outline exact methodology speaks to a novel approach to focus the effect of any given data parameter on the aggregate conduct for any arrangement of trial results. At that point the choices concerning which parameters impact on the framework's conduct. This study is directed to clarify the data's effect parameters on the hydrogen creation utilizing sun based vitality fueling water electrolysis. The ANOVA technique is used to see other factual demonstrative devices with respect to real and anticipated qualities, the reaction in the middle of residuals and anticipated, 3-D surface and shape plot investigation. The database of the created model was acquired in view of a down to earth study. Factual model was produced and exploratory acceptance for the investigation of polynomial was set up applying Response Surface Methodology (RSM). The factual investigation of info parameters and the relating reaction demonstrated that the proposed model and the analysis results will be set under a predominant fit.

Keywords: statistical model, ANOVA method, hydrogen production, solar energy

* Corresponding Author: Md. Shouquat Hossain
Email: shouquat64@gmail.com / engi.shouquat@siswa.um.edu.my

Macroporous heteroatom-doped g-C_3N_4 beads with superior visible-light-induced photocatalytic performances

Yudong Li[1], Kaifeng Lin[2], Yanqiu Jiang[3]

[1,2,3] College of Chemistry and Chemical Engineering, Harbin Institute of Technology, No.2 Yikuang Street, Nangang District, Harbin.

[1]499392289@qq.com [2]linkaifeng@hit.edu.cn

Polymeric semiconductors on the basis of graphitic carbon nitride (g-C_3N_4) and heteroatom-doped g-C_3N_4 have been widely investigated as a metal-free visible-light-induced photo-catalyst that fulfills the basic requirements for photo-degradation of organic pollutants and H_2-generation. Particularly, porous g-C_3N_4 with relatively higher specific surface area is favorable for enhancing the mass transfer of the pollutant molecules, leading the photocatalytic efficiency to a higher level. Up to now, most of samples focus on synthesis of mesoporous g-C_3N_4 with tunable pore sizes and less attention has been paid to prepare macroporous g-C_3N_4 with defined morphology. More importantly, it has been noticed that in the limited reports on macroporous g-C_3N_4, macropores in them are particularly large defect cavities, which are normally not connected to construct a continuous pore channel. From the view of mass transport in porous materials, continuous and open macropore channels are considered to be more promising for diffusion of reactants on the inner surface of g-C_3N_4. Herein, we applied macroporous silica beads as a solid sacrificial template to fabricate macroporous heteroatom-doped g-C_3N_4 beads containing continuous and open macropore channels. Our protocol allows for the simultaneous optimization of both macropore architecture and surface functionalities of g-C_3N_4. Compared with the pristine g-C_3N_4, the obtained macroporous heteroatom-doped g-C_3N_4 beads proved to be more active in the visible-light-induced photodegradation of organic pollutants and H_2 evolution, thanks to the combined advantages of the improved mass transport stemming from the continuous and open macropore channels and doping of heteroatoms (such as P, S, B and F) in the matrix. We believe that the current solid-template-based strategy to control macropore architecture and composition can be extended to dope other heteroatoms by changing the sources.

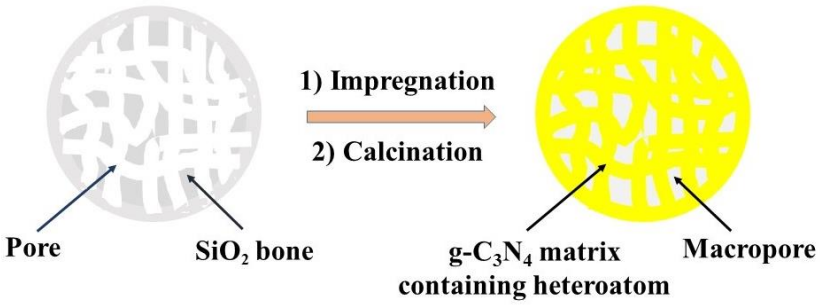

Scheme 1 Synthesis of heteroatom-doped macroporous g-C_3N_4 by solid sacrificial template approach

Keywords: Heteroatom-doped, Macroporous g-C_3N_4, H_2 evolution

[1] Yan, S. C., Li, Z. S., Zou, Z. G., 2010. Photodegradation of Rhodamine B and Methyl Orange over Boron-Doped g-C_3N_4 under Visible Light Irradiation. Langmuir, 26(6), 3894-3901.

[2] Wang, Y., Zhang, J., Wang, X., Antonietti, M., Li, H., 2010. Boron- and Fluorine-Containing Mesoporous Carbon Nitride Polymers: Metal-Free Catalysts for Cyclohexane Oxidation. Angew. Chem. Int. Ed., 49, 3356-3359.

[3] Zhang, J., Zhang, M., Zhang, G., Wang, X., 2012. Synthesis of Carbon Nitride Semiconductors in Sulfur Flux for Water Photoredox Catalysis. ACS Catal., 2, 940-948.

Effects of Electrochemical Deposition Parameters on Performance of MoS_2 Electrocatalyst for Hydrogen Evolution Reaction

Sungjoon Kim, Sunyoung Lee, Zhenyu Jin, Seokhee Shin, Ranjith Bose, Yo-Sep Min

Department of Chemical Engineering, Konkuk University, 120 Neungdong-Ro,

Gwangjin-Gu, Seoul 143-701, Korea

E Mail/ golite@naver.com, young085119@naver.com and ysmin@konkuk.ac.kr

Molybdenum sulfide (MoS_x) has been rising as a promising catalyst material for hydrogen evolution reaction (HER) due to its high activity and stability. Among various methods for the synthesis of amorphous MoS_x, electrochemical deposition is a competitive method due to its inexpensive equipment and the ability to make compact depositions. The films deposited with this method have rough and uneven surfaces, which is advantageous in increasing the number of catalytic active sites.[1] Here, we have used the solution of sodium molybdate (Na_2MoO_4) and sodium sulfide (Na_2S) as molybdenum and sulfer precursors, respectively. The precursor solution was used to deposit catalyst films by the reduction of tetrathiomolybdate ions on carbon fiber paper (CFP) substrate.[2] In order to investigate the effects of deposition parameters of electrochemical deposition process, we have modified the deposition time, precursor concentration, and deposition potential to obtain high HER performance of the catalyst in acidic media. The MoS_x catalyst prepared with the optimized deposition parameters exhibits excellent cathodic current density of 10 mA/cm^2 at an overpotential of 130 mV.

Keywords: MoS_2, deposition parameter, electrochemical deposition, hydrogen evolution reaction

[1] E.A. PONOMAREV, M. NEUMANN-SPALLART, G. HODES, C. LEVY-CLEMENT. 1996. Electrochemical Deposition of MoS_2 Thin Films by Reduction of Tetrathiomolybdate. *Thin Solid Films* 280, 86.

[2] RANJITH BOSE, SURESH KANNAN BALASINGAM, SEOKHEE SHIN, ZHENYU JIN, DO HYUN KWON, YONGSEOK JUN, YO-SEP MIN. 2015. Importance of Hydrophilic Pretreatment in Hydrothermal Growth of Amorphous Molybdenum Sulfide for Hydrogen Evolution Catalysis. *Langmuir*, 31, 5220.

Highly active perovskite-based catalysts for oxygen evolution and reduction reactions

Nam-In Kim, Jun-Young Park*

HMC & Green Energy Research Institute, Department of Nanotechnology and Advanced Materials Engineering, Sejong University, Seoul, 143-747, Korea

Abstract

Unitized regenerative fuel cells (combined fuel cells and electrolyzers such as photo/electrochemical water-splitting cells) have received many attentions because of their renewable and clean methodology to produce electricity and hydrogen. However, noble metals such as Ir, Ru, and Pt, have still used as catalysts for oxygen evolution and reduction reactions (OER & ORR) of unitized regenerative fuel cells. This prohibits various applications of the electrochemical cells due to high cost and limited long-term stability of noble metal catalysts.

In this work, hence, various perovskite-based catalysts have developed for the bifunctional OER (in the anode of photoelectrochemical water-splitting cells) and ORR catalysts (in the cathode of fuel cells) as alternative of noble metal-based catalysts, because the current electrocatalysts show sluggish kinetics with the high polarization loss and limited durability. Single perovskite materials (e.g. $Ba_{0.5}Sr_{0.5}Co_{0.8}Fe_{0.2}O_{3-\delta}$, BSCF, $La_{0.5}Sr_{0.5}Co_{0.8}Fe_{0.2}O_{3-\delta}$, LSCF) and double perovskite materials (e.g. $Nd(Ba_{0.5}Sr_{0.5})Co_{1.5}Fe_{0.5}O_{5+\delta}$, NBSCF) are synthesized by the glycerin-nitrate method to obtain the nanostructured powders.

Physicochemical properties of these perovskite materials are characterized by using various analytic techniques such as SEM, TEM, BET, and XRD. For electrochemical characterizations, samples are tested by the rotating disk electrode (RDE) system in 0.1 M KOH electrolyte with a Pt counter electrode and an Ag/AgCl reference electrode. The electrocactivity of perovskite materials is measured by linear sweep voltammetry (LSV) from 1.2 to 1.7 V, cyclic voltammetry (CV), and polarization curve in alkaline solution.

Keywords: Water-splitting cells, fuel cells, oxygen evolution reaction, oxygen reduction reaction, perovskite materials, electrocatalysts.

References

1. J. Suntivich, K. J. May, H. A. Gasteiger, J. B. Goodenough, Y. Shao-Horn, *Science*, **334**, 1383 (2011).
2. J. Suntivich, H. A. Gasteiger, N. Yabuuchi, Y. Shao-Horn, *Nature Chemistry* , **3**, 546 (2011).
3. I. C. Man, H. Y. Su, F. C. Vallejo, H. A. Hansen, J. I. Martínez, N. G. Inoglu, J. Kitchin, T. F. Jaramillo, J. K. Nørskov, J. Rossmeisl, *ChemCatChem*, **3**, 1159 (2011)
4. T. Reier, M. Oezaslan, P.Strasser, *ACS Catal.*, **2**, 1765 (2012).
5. J. Y. Cheon, C. Ahn, D. J. You, C. Pak, S. H. Hur, J. Kim, S. H. Joo*, J. Mater. Chem. A*, **1**, 1270 (2013).
6. C. A. Wang, S. Li, L. An*, Chem. Comm.*, **49**, 7427 (2013).

***** Corresponding authors: jyoung@sejong.ac.kr (J.-Y. Park)

MoS_2 Electrocatalyst Prepared by Chemical Bath Deposition for Hydrogen Evolution Reaction

Seokhee Shin[1], Zhenyu Jin[1], Ranjith Bose[1], Do Hyun Kwon[1], Yo-Sep Min[1*]

[1]Department of Chemical Engineering, Konkuk University, 120 Neungdong-Ro, Gwangjin-Gu, Seoul 143-701, Korea

E Mail/ ssh0105b@gmail.com and ysmin@konkuk.ac.kr

Recently MoS_2 has attracted great attention as an electrochemical catalyst for hydrogen evolution reaction (HER). Here we report MoS_2 catalysts prepared in liquid phase via chemical bath deposition for HER.[1] The MoS_2 catalyst is deposited at 90 ℃ on carbon fiber papers (CFP) in an aqueous solution of ammonium molybdate and thioacetamide as molybdeunm and sulfur precursors, repectively. Sodium dithionite is added to the solution as a reducing agent of molybdate ions. The MoS_2 catalysts are synthesized with various concentrations of each precursor. The representative catalyst exhibits an excellent cathodic current density of 10 mA/cm^2 at 162 mV vs. RHE. The Tafel slope and the exchange current density are 45.95 mV/dec and 3.04 $\mu A/cm^2$, respectively.

Keywords: MoS_2, electrocatalyst, chemical bath deposition, hydrogen evolution reaction

[1] P. Pramanik and S. Bhattacharya, 1990, Deposition of Molybdenum Chalcogenide Thin Films by The Chemical Deposition Technique and the Effect of Bath Parameters on these Thin Films, Mat. Res. Bull, **1990**, 25, 15-23.

Surface Coverage Effect of Molybdenum Sulfide on Electrochemical Hydrogen Evolution

Ranjith Bose[1], Zhenyu Jin[1], Seokhee Shin[1], Yo-Sep Min[1*]

[1]Department of Chemical Engineering, Konkuk University, 120 Neungdong-Ro, Gwangjin-Gu, Seoul 143-701, Korea

Email : ranjithsaga@gmail.com and ysmin@konkuk.ac.kr

The electrochemical water splitting is one of the most important pathways to produce hydrogen gas on a large scale through hydrogen evolution reaction (HER) for the renewable and sustainable energy society.[1] In this work, we present a comprehensive study on the performance of amorphous molybdenum sulfide (MoS_x) which is grown on Au or Pt substrates by cyclic voltammetric (CV) deposition. It is well known that the activity of MoS_x is higher than that of Au but much lower than that of Pt. By changing the number of CV cycles in the deposition process, the surface coverage of MoS_x is controlled to investigate its effect on the HER performance of MoS_x on each substrate. We discuss the influence of the surface coverage on the figures of merit such as Tafel slope and exchange current density of the HER considering the electrochemical mechanism.

Keywords: MoS_x, electrocatalyst, surface coverage, hydrogen evolution reaction

[1] JARAMILLO, T.F., JORGENSEN, K.P., BONDE, J., NIELSEN, J.H., HORCH, S., & CHORKENDORFF, IB. 2007. Identification of active edge sites for electrochemical hydrogen evolution from MoS_2 nanocatalysts. *Science*, 317, 100-102.

A hole-conductor-free perovskite solar cell based on a low-temperature carbon counter electrode

Zhiyong Liu[a], Tielin Shi[a,b], Zirong Tang[a,b], and Guanglan Liao[a,b]*

a State Key Laboratory of Digital Manufacturing Equipment and Technology, Huazhong University of Science and Technology, Wuhan 430074, China

b Flexible Electronics Research Center, Huazhong University of Science and Technology, Wuhan 430074, China

corresponding author, tel: +86-27-87793103, fax: +86-27-87793103,

e-mail: guanglan.liao@hust.edu.cn

We demonstrate the application of low-temperature carbon counter electrode in fabricating hole-conductor-free perovskite solar cell. A mesoscopic TiO_2 film was deposited on a transparent conductive fluorine-doped tin oxide substrate by screen printing method. Then commercial conductive carbon slurry was used to prepare the counter electrode at a temperature of 130℃. The light absorber, $CH_3NH_3PbI_3$, was formed instantly inside the pores of the entire TiO_2/carbon layer upon single-step deposition of $CH_3NH_3PbI_3$ precursor. The devices were characterized with XRD, SEM, and UV-vis absorption spectroscopy.

As presented in Fig. 1, the carbon CE we used is composed of flaky graphite, and the large size of the graphite flakes has guaranteed the good conductivity of the carbon layer. Fig. 1a and c show the different morphology of the carbon CE solar cells after and before infiltrated by $CH_3NH_3PbI_3$ precursor. It's evident that the $CH_3NH_3PbI_3$ precursor passed through the carbon layer and finally filled the pores in the TiO_2 mesoscopic films. To confirm it, amplified SEM images of the cross section of TiO_2 films have been obtained. Comparing to the bare TiO_2 films (Fig. 1d), we can conclude that the TiO_2 films are in indeed coated by the $CH_3NH_3PbI_3$ perovskite nanocrystalline [1].

Fig 2 display that the sensitized film give strong diffraction peaks at 14.01, 28.16, 28.45, 31.84, 34.997, 40.46, 43.08, which can be assigned to the (110), (004), (220), (310), (312), (224)

and (314) planes of the tetragonal perovskite structure with a = 8.872 Å and c = 12.637 Å, suggesting a complete transformation to $CH_3NH_3PbI_3$ [2,3]. Except for some peaks introduced by FTO and TiO_2, the final perovskite absorber was well crystallized and the phase was pure.

As a result, an energy conversion efficiency of 8.64% was got under AM1.5G condition and there was no obvious decay during a testing period of 624 h. This carbon counter electrode has the features of low-cost and low-temperature preparation, making it potential for the application in large-scale flexible fabrication of perovskite solar cells in the future.

Keywords: Low-temperature, Carbon Counter electrode, Perovskite, Solar Cell.

[1] Z. Ku, Y. Rong, M. Xu, T. Liu and H. Han, Scientific reports 3, (2013)
[2] J. Qiu, Y. Qiu, K. Yan, M. Zhong, C. Mu, H. Yan and S. Yang, Nanoscale 5 (8), 3245 (2013)
[3] X. Gao, J. Li, J. Baker, Y. Hou, D. Guan, J. Chen and C. Yuan, Chemical Communications 50 (48), 6368 (2014)

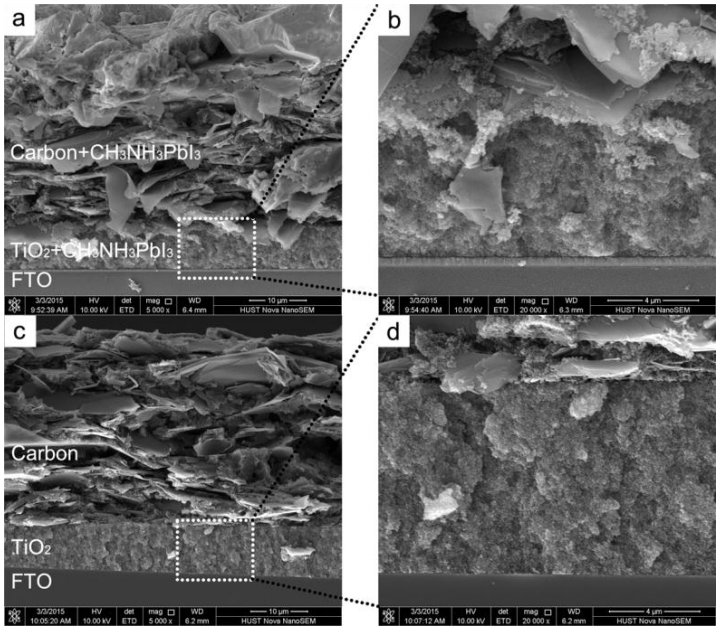

Fig. 1 cross-sectional structure of the devices. a) Carbon CE perovskite solar cell infiltrated by $CH_3NH_3PbI_3$. b) un-infiltrated Carbon CE perovskite solar cell. c) the magnified image of $CH_3NH_3PbI_3$ coated TiO_2 film. d) bare TiO_2 film.

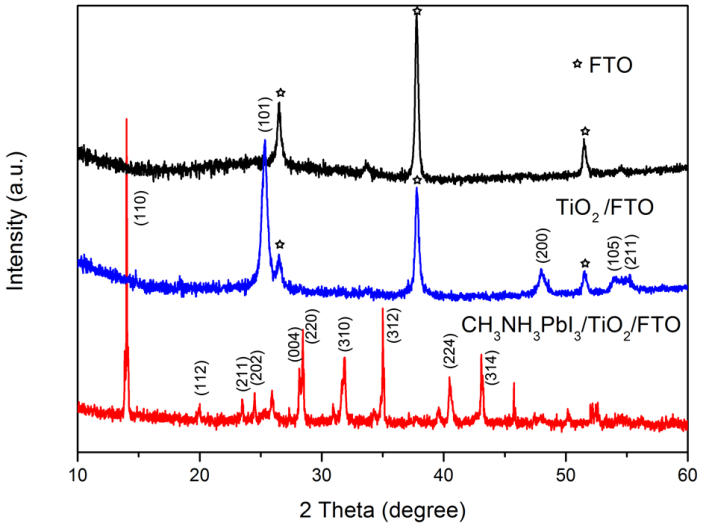

Fig. 2 XRD patterns of the perovskite sensitizers dip-coated on mesoscopic TiO_2 layer and FTO (black line), the mesoscopic TiO_2 layer on FTO (blue line) and the bare FTO glass (red line).

A Quercetin and Fe-Quercetin Complex Dye Based Solar Cell Application

Soner ÇAKAR[1], Mahmut ÖZACAR[1,2]

[1]Department of Chemistry, Science&Arts Faculty, Sakarya University, Sakarya 54187, Turkey.

[2]Biomedical, Magnetic and Semiconductor Materials Research Center (BIMAS-RC), Sakarya University, Sakarya 54187, Turkey.

E Mail: mozacar@hotmail.com

Dye sensitized solar cells (DSSCs) have approve attention as an encouraging low cost solar energy into electricity [1]. Recently, several groups have developed natural dye sensitizers have been obtain with anthocyanin, carotene, chlorophyll and tannin [2]. Flavonoids are a natural compounds found in many fruits, vegetables, leaves and grains. Quercetin is a flavonoid and it's almost found in many food and plants [3].

In this study, we have synthesis TiO_2 nanoparticles using rapidly, relatively low temperatures and without any organic surfactants via microwave assistant hydrothermal synthesis and characterized via XRD, FE-SEM and DRS. The TiO_2paste was prepared to 500 mg TiO_2 nanoparticle and 50 mg ethyl cellulose was added 5 mL methanol mixed a magnetic stirrer.The TiO_2 slurry was pasted on FTO substrate using a doctor blade. After drying the air, the film was sintered for 30 min 450^{o}C. The quercetin and Fe-quercetin complex dye prepared with 0.01 M quercetin and 0.01 M $FeCl_3.9H_2O$ (2:1) and stirring magnetic stirrer for 30 min. The quercetin and Fe-quercetin complex dyes were characterized with UV-vis, FTIR and CV. The resulting films were immersed in quercetin and Fe-quercetin complexes in acetonitrile for 24h. The dye coated TiO_2 photoanode were rinsed acetonitrile to remove excess dye from the surface and dried room temperature. In order to prepare counter electrode a 5 mM $H_2PtCl_6.6H_2O$ solution in 2-propanol was spread onto FTO substrate and heated at 450^{o}C for 1h.The electrolyte was content of 0.1 M LiI, 0.05 M I_2 and 0.5 M 4-tert butyl pyridine in acetonitrile. The current densities versus voltage (J−V) characteristics and impedance spectra of the cells were measured using a solar simulator (Oriel) and CHI 660C electrochemical workstation. The quercetin and Fe-quercetin dye based solar cells efficiency are

approximately 1% and 3% of TiO_2 nanoparticles, respectively. The Fe-quercetin complexes have higher light absorption, and then resulting in the efficiency of quercetin solar cell improving from 1% to 3% after the Fe complexes. Our results strongly supported the prospects for successfully application of DSSCs based on natural dye system and indicate the importance of molecular complexation design for natural dye system to produce highly efficient DSSCs.

Keywords: dye sensitized solar cell, quercetin, Fe-quercetin, TiO_2

[1] SHANG, H., LUO, Y., GUO, X., HUANG, X., ZHAN, X., JIANG, K., MENG, Q. 2010. The Effect of Anchoring Group Number on the Performance of Dye-Sensitized Solar Cells*DYES PIGMENTS*, 87, 249-256.

[2]HUG, H., BADER, M., MAIR, P., GLATZEL, T., 2014. Biophotovoltaics: Natural Pigments in Dye-Sensitized Solar Cells *APPL. ENERGY*, 115, 216-225.

[3] VAN ACKER, S.A.B.E., VAN BALEN, G.P., VAN DEN BERG, D.-J., BAST, A., VAN DER VIJGH, W.J.F. 1998. Influence of iron chelation on the antioxidant activity of flavonoids *BIOCHEM. PHARMACOL.*, 56, 935-943.

High efficient and stable 2D perovskite materials for PSC

Haiying Zheng,[ab] Jiajiu Ye,[ab] Xuhui Zhang,[ab] Liangzheng Zhu,[ab] Zhipeng Shao,[a] Xu Pan[*a] and Songyan Dai[*c]

a. Key Laboratory of Novel Thin-Film Solar Cells, Institute of Applied Technology, Hefei Institutes of Physic Science, Chinese Academy of Sciences, Hefei 230031

b. University of Science and Technology of China, Hefei 230026, China

c. State Key Laboratory of Alternate Electrical Power System with Renewable Energy Sources, North China Electric Power University, Beijing 102206, China

Perovskite solar cells(PSC) have drawn increasing attention because of their recent rapid increase in power conversion efficiency (PCE).However, its problems of stability and easy degradation in humidity environment hindered its commercial application. In this study, we reported a new two-dimensional hybrid perovskites and used as absorber in solar cells. Compared to 3D perovskites, 2D perovskites are more stable, have higher moisture resistant, stronger photoluminescence and light absorption in infrared area. The decive based on 2D perovskite shows a good performance with the efficiency of 13.8%. These results demonstrate that 2D perovskite can replace the traditional 3D perovskite materials with long-term-stability and high efficient, which give us great prospects to its commercialization.

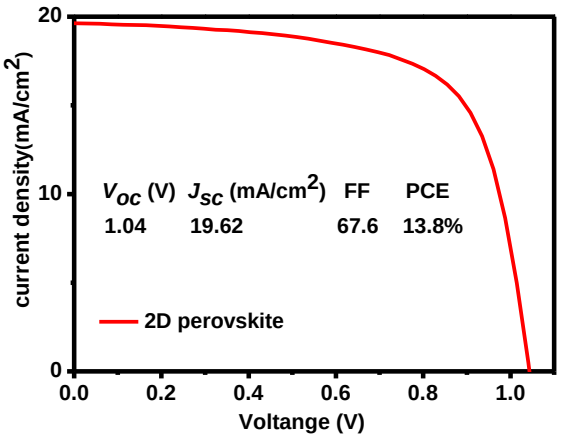

Figure 1. *J*− *V* curves of 2D perovskite-based devices

Notes and references

1. Cao, D. H.; Stoumpos, C. C.; Farha, O. K.; Hupp, J. T.; Kanatzidis, M. G., 2D Homologous Perovskites as Light-Absorbing Materials for Solar Cell Applications. *Journal of the American Chemical Society* **2015,** *137* (24), 7843-50.

2. Koh, T. M.; Shanmugam, V.; Schlipf, J.; Oesinghaus, L.; Müller-Buschbaum, P.; Ramakrishnan, N.; Swamy, V.; Mathews, N.; Boix, P. P.; Mhaisalkar, S. G., Nanostructuring Mixed-Dimensional Perovskites: A Route Toward Tunable, Efficient Photovoltaics. *Advanced materials* **2016**.

3.Smith, I. C.; Hoke, E. T.; Solis-Ibarra, D.; McGehee, M. D.;Karunadasa, H. I. A Layered Hybrid Perovskite Solar-Cell Absorber with Enhanced Moisture Stability.Angew. Chem., Int. Ed. **2014**, 53, 11232 – 11235.

Morphology Studies of Ternary Organic Bulk Heterojunction Solar Cells

Jiangquan Mai, Tsz Ki Lau, Xinhui Lu*
Department of Physics, The Chinese University of Hong Kong, Hong Kong, Hong Kong

Ternary organic solar cells are emerging as a promising strategy to enhance organic photovoltaic device efficiency by broadening light absorption range. However, how to find compatible donor materials which allow comparable loadings of each component remains a challenge. In this article, we focus on studying the donor polymer compatibilities in ternary systems. Four typical donor polymers with quite different chemical structures and absorption ranges were combined mutually to form six distinct ternary systems with fullerene derivative acceptor. We find that morphology compatibility in terms of molecular packing and phase separation is the key to donor material selection which greatly extends the donor candidate pool for ternary organic solar cell research.

A novel chemistry for Atomic Layer Deposition of Zn(O,S)

Donghyun Ko[1], Zhenyu Jin[1], Seokhee Shin[1], Sungjoon Kim[1], Yo-Sep Min[1*]

[1]Department of Chemical Engineering, Konkuk University, 120 Neungdong-Ro, Gwangjin-Gu, Seoul 143-701, Korea

E Mail/ cmdkdh@gmail.com and ysmin@konkuk.ac.kr

Zinc oxysulfide, Zn(O,S), is a promising buffer layer for Copper Indium Gallium di-Selenide (CIGS) solar cells. It is well known that Zn(O,S) has a variable bandgap depending on the sulfur content. Atomic layer deposition (ALD) has the advantage of easily modifying composition by controlling the ratio of precursor exposure times and its sequence. In the previous reports, Zn(O,S) thin films grown by ALD require H_2S gas as a sulfur precursor.[1] However, this is a toxic and inconvenient process due to the high reactivity of H_2S. This results in difficulty to tailor the sulfur content precisely. There has been no previous work for ALD of Zn(O,S) without hydrogen sulfide. Here we report a new approach to ALD of Zn(O,S) without hydrogen sulfide by using diethylzinc, water and a sulfur compound. Zn(O,S) can be grown at 200 ^{o}C on SiO_2/Si substrate by using the novel chemistry.

Keywords: Zn(O,S), buffer layer, atomic layer deposition, solar cell

[1] JEON, S., BANG, S., LEE, S., KWON, S., JEONG, W. & JEON, H. 2008. Characteristics of Zinc-Oxide-Sulfide-Mixed Films Deposited by Using Atomic Layer Deposition. *J. Korean Phys. Soc.*, 53, 3287-3295

Enhancement of Electrical Conductivity and UV Stability of Poly(methyl methacrylate) for Dye-Sensitized Solar Cells Application

Godchaporn Bunmee[1*], Nuttapol Pootrakulchote[2], Napida Hinchiranan[2]

[1]Program of Petrochemisty and Polymer Science, Faculty of Science, Chulalongkorn University, Bangkok, Thailand 10330

[2]Department of Chemical Technology, Faculty of Science, Chulalongkorn University, Bangkok, Thailand 10330

[*]*E Mail/Contact Detail: dava-hunnypooh@hotmail.com[1], napida.h@chula.ac.th[2]*

Dye-sensitized solar cells (DSSC) are normally consisted of transparent electrodes, semiconductors, coordination compounds, inorganic salts and metallic catalysts. However, transparent electrodes made from the conductive glass have some inherent problems such as brittleness, heavy weight and high cost. To solve these drawbacks of glass electrode, this research selected poly(methyl methacrylate) (PMMA) to replace the conductive glass since PMMA sheet has excellent optical transparency, low cost and light weight. Although PMMA has high transparency as well as glass, it is deteriorated by ultraviolet (UV) resulting in the limitation for DSSC application. Moreover, the electrical resistance of PMMA (10^{14}-10^{16} Ω/cm^2) is higher than that of the conductive glass containing fluorine-doped tin oxide (FTO) layer (13 Ω/cm^2). Thus, this work aimed to improve the electrical conductivity and UV stability of PMMA sheet for expectedly using as a working electrode for DSSC. The one side of PMMA sheet was coated by poly(3,4-ethylenedioxythiophene) (PEDOT) via spin coating technique to increase the electrical conductivity of PMMA, which were detected by using a four-point probe technique. The results indicated that the PMMA coated with PEDOT (PMMA-PEDOT) had the effective electrical resistivity approximately 30-40 $m\Omega/cm^2$ depended on the number of the spin coating cycle. This value was higher than that of the conductive glass covered by FTO layer. Another side of PMMA sheet was coated by zinc oxide quantum dots (ZnOQDs) synthesized via a sol-gel method (PMMA- ZnOQDs) for acting as the transparent UV-protective layer or UV-shielding windows. The UV stability of the PMMA-ZnOQDs sheet was measured by using a UV simulator at 60^oC for 168h. Moreover, the physical

properties in terms of yellowness index and refractive index including mechanical properties (impact strength and flexible strength) of the modified PMMA sheet were also evaluated.

Keywords: Poly(3,4-ethylenedioxythiophene), UV stability, electrical conductivity, poly(methyl methacrylate), zinc oxide quantum dots

[1] FOROUTANI, K., POURABBAS, B., SHARIF, M., FALLAHIAN, M., KHADEMI, S., MOHAMMADIZADEH, M. 2014. In situ deposition of polythiophene nanoparticles on flexible transparent films: Effect of the process condition. *Mater. Sci*, 19, 57-65.

[2] HANSEN, T.S., WEST, K., HASSAGER, O., LARSEN, N.B. 2006. Integration of conducting polymer network in non-conductive polymer substrates. *Syn. Mater*, 156, 1203-1207.

[3] PYSHKINA, O., KUBARKOV, A., SERGEYEV, V. 2010. Poly(3,4-ethylenedioxythiophene): Synthesis and Properties. *Mater. Sci*, 21, 51-54.

[4] SIERROS, K.A., MORRIS, N.J., KUKUREKA, S.N., CAIRNS, D.R. 2009. Dry and wet sliding wear of ITO-coated PET components used in flexible optoelectronic applications. *Wear.*, 267, 625-631.

[5] ZHANG, Y., ZHUANG, S., XU, X., HU, J. 2013. Transparent and UV-shielding ZnO@PMMA nanocomposite films. *Opti. Mater*, 36, 169-172.

Synthesis and Application in Dye-Sensitize Solar Cells of Ho^{3+}-Yb^{3+}-F^{-} Tridoped TiO_2 Upconverting Nanoparticles

Aixiang Wei*, Lili Song, Yu Zhao, Jun Liu, Zhiming Xiao

School of Material and Energy, Guangdong University of Technology, Guangzhou 510006, China

Abstract:

The efficiency of most photovoltaic devices is severely limited by near-infrared (NIR) transmission losses. To overcome this limitation, nanoscale upconversion materials, which can transform NIR photons to UV and vis photons, have been considered as one of the most promising solutions and already been applied in the fields of solar cells and photocatalysis. In this work, upconversion nanoparticles of Ho^{3+}-Yb^{3+}-F^{-} tridoped TiO_2 were fabricated by hydrosol−hydrothermal method. The dye-sensitized solar cells (DSSCs) with Ho^{3+}-Yb^{3+}-F^{-} tridoped TiO_2 nanoparticles photoanode are studied.

In the solvothermal fabrication process, precursor of 25ml tetrabutyl titanate，2.5ml HNO_3, 0.4ml HF and 60 ml deionized water were heated with vigorous stirring at 95 ℃ for 2 h to fabricate a transparent hydrosol. $Ho(NO_3)_3$ and $Yb(NO_3)_3$ as dopants were added slowly into the hydrosol under high-intense stirring, the obtained product was transferred into a Teflon-lined stainless steel autoclave and hydrothermally treated at 200℃ for 24h. The Ho^{3+}-Yb^{3+}-F^{-} tridoped TiO_2 nanoparticles were obtained. The analyses of phase structure and the optical properties including XRD, TEM and upconversion photoluminescence spectra of Ho^{3+}-Yb^{3+}-F^{-} tridoped TiO_2 nanoparticles have been performed in detail to reveal the complex energy transfer and change mechanism. The DSSCs were assembled with Ho^{3+}-Yb^{3+}-F^{-} tridoped TiO_2 anode, Pt counter electrode and I^{-}/I_3^{+} electrolyte, the photovoltaic performance of DSSCs were studied. The XRD pattern, TEM image , HRTEM image and Up-conversion fluorescence spectra of the Ho^{3+}-Yb^{3+}-F^{-} tridoped TiO_2 nanoparticles were shown in Figs. (a)-(d). The results indicated that the

Ho^{3+}-Yb^{3+}-F^{-} tridoped TiO_2 nanoparticles were mixtures of anatase and rutile phases. The ratio of anatase/rutile decrease with increasing of doped Yb^{3+} ions. The average sizes of the Ho^{3+}-Yb^{3+}-F^{-} tridoped TiO_2 nanoparticles is estimated to be 20 nm. The HRTEM shows clear lattice fringes with spacing of 3.50 Å , which is ascribed to the d spacing of (101) facets in anatase TiO_2. Under the excitation of 980 nm NIR light, the Ho^{3+}-Yb^{3+}-F^{-} tridoped TiO_2 nanoparticles emitted strong green upconversion fluorescence with three emission bands at 543, 650, and 751 nm. The XPS analysis indicated that the content of Ti, O, F, Yb and Ho element is 28.42, 65.68, 5.59, 0.24 and 0.07 at.%, respectively for sample A4. The conversion efficiency of DSSC assembled with Ho^{3+}-Yb^{3+}-F^{-} tridoped TiO_2 nanoparticles photoanode has a 20% enhancement compared to DSSCs with pure TiO_2 photoanode.

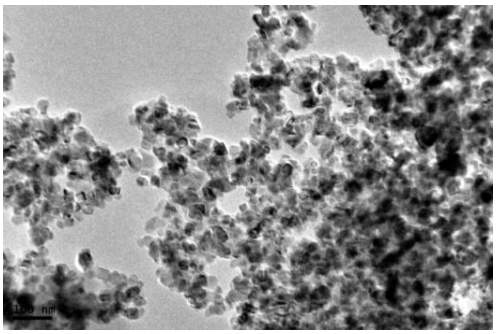

(a) TEM image

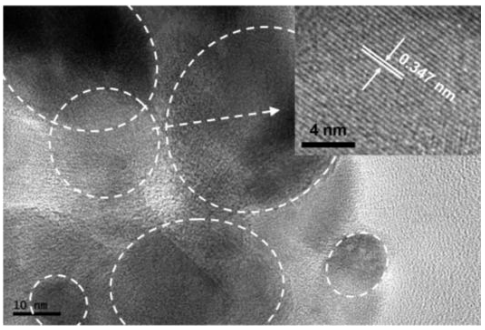

(b)HRTEM image

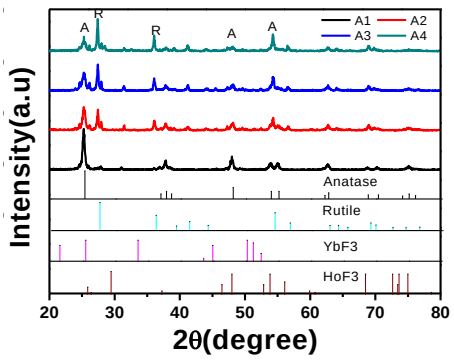

(c) X-ray diffraction pattern

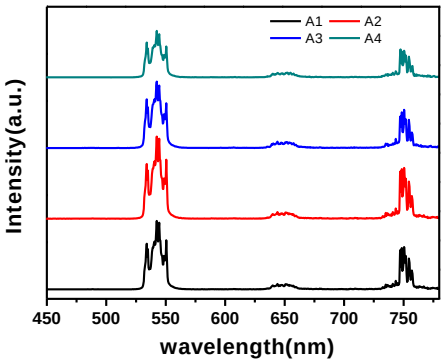

(d) Upconversion fluorescence spectra

Weight-percent control at the DMSO assisted perovskite deposition with dipping method

Ki-Hwan Hwang, Yong-Min Lee, Dong-In Kim, Hyeon-Jin Seo, Sang-Hun Nam and Jin-Hyo Boo*

Department of Chemistry and Institute of Basic Science, Sungkyunkwatn University, Suwon 440-746, Korea

Organic-inorganic hybrid perovskite solar cell is getting a lot of attention as next-generation solar cells. It is important that improvement of the active-layer electrical and optical properties for high power conversion efficiency (PCE) of solar cells. In this work, we study on the morphology and electrical properties of methylammonium lead iodide ($MAPbI_3$) thin films. $MAPbI_3$ was deposited with various weight-percent in dimethylformamide (DMF) and dimethyl sulfoxide (DMSO) solution. we fabricated solar cells which is consisted with ITO/PEDOT:PSS/$MAPbI_3$/PCBM/Ag. To comparatively study the weight-percent control effects on the resulted electrical and optical properties. The solar cell performance and impedance were investigated with solar-simulator. At the same time, morphology, optical properties and crystalline variations were investigated by field emission scanning electron microscopy (FE-SEM), UV-Vis spectroscopy and XRD respectively.

Symposia 5

Advances in Biosensors and Biomaterials

- Advances in Enzymatic and Non-Enzymatic Biosensors
- Functional biomaterials for drug delivery
- Advances in Bioelectronics and Commercial biosensors,
- DNA chips and nucleic acid sensors
- Biomaterials for Cardiovascular Applications
- Environmental biosensors
- Biosensors for Imaging
- Application of Biosensors in Drug Delivery and Clinical Chemistry
- Lab-on-a-chip
- Printed biosensors and microfabrication
- Applications of Biopolymer for Drug Delivery
- Computational modeling and simulation of Biosensors
- Others

Index Page

Multifunctional graphene for biotechnology and drug delivery

Yaqing Liu[a]*, Shuo Wang

Key Laboratory of Food Nutrition and Safety (Tianjin University of Science and Technology), Ministry of Education, Tianjin, 300457, P. R. China.

Email: yaqingliu@tust.edu.cn

Graphene and graphene oxide (GO), as novel polyaromatic molecule, have attracted tremendous interest in the fields of materials science and biotechnology due to their fascinating properties with ultrathin structural feature [1]. GO is water-soluble and has been demonstrated to be promising platform for the construction of bioelectronic devices. Herein, multiple logic gates were integrated on a universal GO/DNA platform for the first time to implement both arithmetic functions of half adder (HA) and half subtractor (HS). Different from GO, pristine graphene is highly hydrophobic, which has limited its applications in biological systems [2]. In our investigations, graphene was chemically modified with phospholipid DMPG (1,2-dimyristoyl-sn-glycero-3-phospho-(1-rac-glycerol) sodium salt). The resultant lipid monolayer functionalized graphene nanomaterials (DMPG-G) exhibited high stability in aqueous solution and excellent performance as carrier for loading anticancer drug, doxorubicin, with a high loading capacity of 70%, Figure 1. The loaded drug can be released under pH control. As known that lipid films can provide an excellent biological microenvironment to maintain the activity of the bound proteins. A DMPG-G functionalized electrode was further developed as biosensor for high sensitive determination of H_2O_2 and enzyme direct electrochemistry.

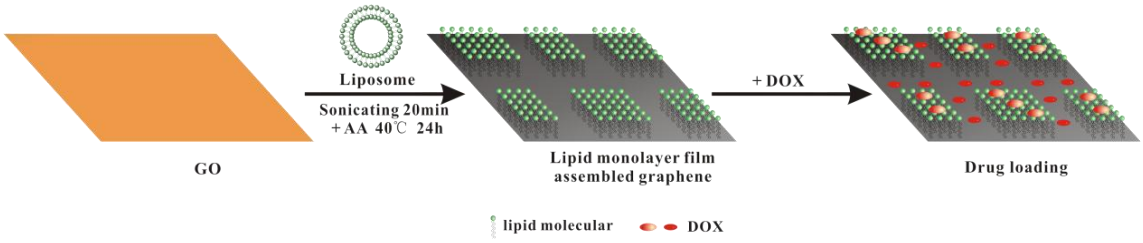

Fig.1 Schematic illustration of DMPG–G and DMPG–G–DOX preparation.

Acknowledgements

This work was supported by the National Natural Science Foundation of China (grant no. 21190040 and 21105095) and State Key Instrument Developing Special Project of Ministry of Science and Technology of China (2012YQ170003).

References

1. S. Stankovich, D. A. Dikin, G. H. B. Dommett, K. M. Kohlhaas, E. J. Zimney, E. A. Stach, R. Piner, S. Nguyen and R. Ruo, *Nature* 2006, 442, 282.
2. J. Liu, S. Guo, L. Han, T. Wang, W. Hong, Y. Liu, E. Wang, *J. Mater. Chem.* 2012, 22, 20634.

Graphene Foam/β-Cyclodextrin-PDMS Nanocomposite as a Recognition of Dopamine Detection

S. Pakapongpan[1], T. Maturos[2], D. Phokharatkul[2], A. Tuantranont[1]

[1]Thailand Organic and Printed Electronics Innovation Center, National Electronics and Computer Technology Center, NSTDA, Pathumthani, Thailand.

[2]Nanoelectronics and MEMs Laboratory, National Electronics and Computer Technology Center, NSTDA, Pathumthani, Thailand.

E Mail: saithip.pakapongpan@nectec.or.th

In the present work, a flexible and sensitive electrochemical sensor for detection of dopamine was fabricated using a nanocomposite structure of graphene foam (GF) incorporated poly(dimethylsiloxane) (PDMS) and β-cyclodextrin as an electrode with a simple procedure, 3D graphene foam grown by chemical vapor deposition. The graphene foam/β-cyclodextrin-PDMS composite provides a very high electrical conductive working electrode and excellent electron transfer property thereby suggesting that the graphene foam structure enhances the electrochemical response capability not only by increasing the surface area, but the porous structure also improve the electron transfer and β-cyclodextrin exhibits high supramolecular recognition capability of dopamine and improve hydrophilicity of PDMS. In addition, this sensor showed excellent analytical performances including low detection limit, wide dynamic range with a high sensitive quantification in the presence of interferences. From the results, this flexible electrode can provide a promising platform to develop electrochemical sensors as well as other applications, such as energy storage and conversion.

Keywords: Dopamine, graphene foam, flexible sensor, PDMS

[1] ABBASPOUR, A., NOORI, A. 2011. A cyclodextrin host–guest recognition approach to an electrochemical sensor for simultaneous quantification of serotonin and dopamine. *Biosensors and Bioelectronics*, 26, 4674-4680.

Immobilization of Glucose Oxidase on Tannic Acid Modified-Reduced Graphene Oxide Surface for Biosensing Applications

Bekir ÇAKIROĞLU[1], Mahmut ÖZACAR[1,2],

[1] Sakarya University, Biomedical, Magnetic and Semiconductor Materials Research Center (BIMAS-RC), Sakarya 54187, Turkey

[2]Sakarya University, Department of Chemistry, Sakarya 54187, Turkey

bekircakiroglu@sakarya.edu.tr

Today, a large number of studies upon biosensing of important analytes have been conducted by many researchers. However, there are still drawbacks for the mass production of biosensors called third generation biosensors, which is based on the direct electron transfer between redox center of the enzymes and electrode surface. To overcome the poor conductivity in biosensors, graphene oxide(1), carbon nanotubes(2), conducting polymers such as polyaniline(3), polypyrroleare widely used, and to enhance the catalytic activity, conductivity, enzyme loading, stability, reproducibility; various modifications, element doping(4), introducing metal nanoparticles have been carried out and reported in the literature.

In this study we aimed to design an appreciable electrode coating material for a biosensor fabrication, which significantly enhances abovementioned essentials and overcomes the problem of poor conductivity. Graphene oxide (GO) was prepared according to the modified Hummer method and used as the main conducting material. Tannic acid (TA) was used as a modifying agent for substantial glucose oxidase (GOx) loading, and as a reducing agent for synthesizing of gold nanoparticles (Au), and for the reduction of graphene oxide, which is rich in oxygen containing functional groups, to obtain reduced

grapheme oxide (rGO). Thus, one-pot synthesis of rGO- Au-TA-GOx was achieved and the successively obtained samples were characterized. We confirmed the formation of rGO from graphite by comparing the Raman spectra of the graphite derivatives. The modification of TA and immobilization of GOx were confirmed by using Attenuated total reflectance Fourier transform infrared spectroscopy. Further characterization of the samples was performed using a thermogravimetric analyzer under an inert atmosphere. Enzyme kinetic parameters were determined by obtaining Lineweaver-Burk plot. To investigate the surface morphologies of samples, scanning electron microscopy was performed at high magnifications. Cyclic voltammetry experiments were carried out for the investigation of biosensing properties. Amperometric glucose sensing studies are in progress by using rotating disc electrode system.

Keywords: Enzyme immobilization, glucose oxidase, tannic acid, graphene oxide, biosensing

[1] ZHOU, M., ZHAI, Y. & DONG S. 2009. Electrochemical Sensing and Biosensing Platform Based on Chemically Reduced Graphene Oxide. *Analytical Chemistry*, 81, 5603–5613.

[2] CAI, C. & CHEN, J. 2004. Direct electron transfer of glucose oxidase promoted by carbon nanotubes. *Analytical Biochemistry*, 332, 75–83.

[3] ZHONG, H., YUAN, R., CHAI, Y., LI, W., ZHONG, X. & ZHANG, Y. 2011. In situ chemo-synthesized multi-wall carbon nanotube-conductive polyaniline nanocomposites: Characterization and application for a glucose amperometric biosensor, *Talanta,* 85, 104–111

[4] DENG, C., CHEN, J., CHEN, X., XIAO, C., NIE, L. & YAO, S. 2008. Direct electrochemistry of glucose oxidase and biosensing for glucose based on boron-doped carbon nanotubes modified electrode, *Biosensors and Bioelectronics*, 23 , 1272–1277.

Laser desorption/ionization (LDI) mass spectrometry based on nanomaterials for biomedical applications

Jae-Chul Pyun*, Jo-Il Kim, and Jong-Min Park
Yonsei University, Department of materials science & engineering
Seoul, 120-749, Korea
*jcpyun@yonsei.ac.kr

Keywords: mass spectrometry, laser desorption/ionization, solid matrix, MALDI

In conventional MALDI-TOF mass spectrometry, analyte molecules are known to be ionized by mixing with organic matrix molecules. As the organic matrix molecules are ionized, they generate unreproducible mass peaks such that MALDI-TOF mass spectrometry is nearly impossible in the low mass-to-charge (*m/z*) range (< 1000). In this work, we present laser desorption/ionization (LDI) mass spectrometry based on solid-matrices for the detection of small biomolecules in the low *m/z* range by using MALDI-TOF mass spectrometry: (1) Top-down synthesized TiO_2nanowires were synthesized as arrays using a modified hydrothermal process directly on the surface of a Ti plate; (2) The nylon nanoweb with TiO_2 particles was prepared by the simultaneously electrospinning a nylon nanoweb and electrospraying TiO_2nanoparticles; (3) The parylene-matrix chip was fabricated by the deposition of a partially porous parylene-N thin film on a dried organic matrix array. The mass spectrometry of multiple analytes was demonstrated in the low molecular weight range using eight amino acids. Additionally, model were used as model analytes to test the feasibility of solid-matrix chips for MALDI-TOF mass spectrometry. The biomedical application of LDI mass spectrometry was demonstrated for (1) the detection of chemical and biological warfare agents, (2) the newborn metabolite analysis and (3) the antibiotics-resistant bacteria screening.

References:

[1] J.I. Kim, et al. Analytica Chimica Acta, 836 (2014) 53-60.
[2] J.I. Kim, et al. Rapid communications in mass spectrometry, 28 (2014) 2301-2306.
[3] J.M. Park, et al. Biosensors and Bioelectronics 71 (2015) 306-312.
[4] J.I. Kim, et al. Chemosphere, 143 (2016) 64-70.

Silk nanoparticles for potential controlled drug release

Shenzhou Lu, Xiang Xue, Juan Wang, Zhuping Yin, Hua Fu, Teiling Xing

National Engineering Laboratory for Modern Silk, College of Textile and Clothing Engineering, Soochow University, Suzhou 215123, China

Corresponding author E-mail: lushenzhou@suda.edu.cn

Natural silk protein nanoparticles are a promising biomaterial for drug delivery due to their pleiotropic properties, including biocompatibility, high bioavailability, and biodegradability. In this paper, Chinese oak tasar Antheraea pernyi silk fibroin nanoparticles were prepared for drug deliver. Doxorubicin hydrochloride, Ibuprofen, and Ibuprofen-Na were selected as positively charged, uncharged, and negatively charged model drugs. The results indicate that the drug release rate depends on charge-charge interactions between the drugs and the nanoparticles. The release rate can be controlled by different charges. The positively charged molecules are released in a more prolonged and sustained manner.

The biodegradable behavior, cell viability and growth suggest that the fibroin nanoparticles of this underutilized can be exploited as an alternative matrix for drug carrying and controlled release in diverse biomedical applications. We hope these new nanoparticles from the non-mulberry silkworm *Antheraea pernyi* can be considered a very good alternative as fibroin based biomaterials for controlled drug release.

Keywords: silk fibroin, nanoparticles, controlled drug release, cell culture

Silk nanoparticles for potential controlled drug release

Shenzhou Lu, Xiang Xue, Juan Wang, Zhuping Yin, Hua Fu, Teiling Xing

National Engineering Laboratory for Modern Silk, College of Textile and Clothing Engineering, Soochow University, Suzhou 215123, China

Corresponding author E-mail: lushenzhou@suda.edu.cn

Natural silk protein nanoparticles are a promising biomaterial for drug delivery due to their pleiotropic properties, including biocompatibility, high bioavailability, and biodegradability. In this paper, Chinese oak tasar Antheraea pernyi silk fibroin nanoparticles were prepared for drug deliver. Doxorubicin hydrochloride, Ibuprofen, and Ibuprofen-Na were selected as positively charged, uncharged, and negatively charged model drugs. The results indicate that the drug release rate depends on charge-charge interactions between the drugs and the nanoparticles. The release rate can be controlled by different charges. The positively charged molecules are released in a more prolonged and sustained manner.

The biodegradable behavior, cell viability and growth suggest that the fibroin nanoparticles of this underutilized can be exploited as an alternative matrix for drug carrying and controlled release in diverse biomedical applications. We hope these new nanoparticles from the non-mulberry silkworm *Antheraea pernyi* can be considered a very good alternative as fibroin based biomaterials for controlled drug release.

Keywords: silk fibroin, nanoparticles, controlled drug release, cell culture

Production of Biomedical Ti-(16-22)Nb-(0-4)Sn (wt.%) Alloys by Powder Injection Molding and Characterization

Eren Yılmaz[1], Azim Gökçe[1,2], Fehim Fındık [1,2,c]

1: Sakarya University, Biomedical, Magnetic and Semiconductor Research Center (BIMAS-RC), Esentepe Campus, 54187 Sakarya, Turkey

2: Sakarya University, Faculty of Technology, Metallurgy and Materials Dept, Esentepe Campus, 54187 Sakarya, Turkey

C: Communication author: Tel: +90-264-295 64 87, Fax: +90-264-295 64 24, e-mail: findik@sakarya.edu.tr

The most commonly used alloy is Ti-6Al-4V within first generation from α + β phased biomedical alloys. Via emerging of toxic effects of V and Al elements, those elements are substituted with the Nb and Mo non-toxic elements effecting β phase stabilized elements, thus the second generation implant materials have been created. Ti-Nb based alloys have low elastic modulus close to the elastic modulus of the bone, therefore they decrease the "stress shielding" effect between bones and implant. Also, these alloys exhibit shape memory and super elastic property. This feature can be increased by alloying. Sn addition prevents the formation of brittle athermal ω-phase and increases the recovered strain. Combination of Nb and Sn elements gives better mechanical properties results for titanium alloy.

These alloys are produced by melting or powder metallurgy methods. For biomedical applications of titanium alloys, compared to traditional methods, Powder Injection Molding (PIM) is a growing interest method due to the advantages of a large number of complex shaped parts that lower costs of production, better surface quality and superior mechanical properties and giving a near net shape product.

In this study, Ti- (16-22) NB (0-4) Sn alloy has been produced successfully with PIM. In the production of this alloy, the optimum parameters are determined for PIM process. Specimens are characterized by melt extraction, optical microscopy, XRD, SEM, EDS, hardness and tensile test. An amount of precipitation of TiC was observed originating from the process steps and binder within the sintered alloy. Porosity and amount of precipitate increased with the increment of Nb content. Sintered samples contain a combination of high tensile strength and a low elastic modulus. The resulting elastic modulus is very lower than α + β phase of the titanium alloy.

Keywords: Biomedical β-titanium alloys, powder injection molding, elastic modulus, super elasticity

Development of Ln3+-based Core/Shell Nanoparticles for Magnetic Resonance Imaging of Cancer

Boguslaw Tomanek[1,2,3], Anurag Gautam[4], Barbara Blasiak[1,2], Frank C. J. M. van Veggel[4]

[1]Experimental Imaging Center, University of Calgary, Calgary, Alberta, Canada T2N 4N1

[2]Institute of Nuclear Physics, Polish Academy of Sciences, Krakow, Poland

[3]Department of Oncology, University of Alberta, Alberta, Canada T6G 2T4

[4]Department of Chemistry, University of Victoria, Victoria, British Columbia V8W 3V6, Canada

E Mail: ***tomanek@ualberta.ca***

Introduction: Magnetic Resonance Imaging (MRI) has been used for early cancer detection and treatment monitoring. This imaging technique has excellent spatial resolution but low specificity. Standard contrast enhanced MR images, including application of Gd-based T_1 contrast agents or iron-oxide based T_2 contrast agents do not provide sufficiently high contrast for tumor diagnosis [1-2].

Objectives: To provide an improved MRI contrast of cancer we have developed and tested *in vivo* core/shell $NaDyF_4/NaGdF_4$ nanoparticles [2-4] with tunable core and shell dimensions.

Methods: The relaxation times (T_1 and T_2) of water solutions of nanoparticles with various score/shell sizes and concentrations were measured at 9.4T and 3T to find the optimum T_1/T_2 ratio for MRI. The water proton relaxivity results showed that $NaDyF_4$ (20 nm)/$NaGdF_4$ (~ 0.5 nm) core/shell NPs have the highest r_1- and r_2-relaxivity at both 3 T (clinical field) and 9.4 T (pre-clinical field). T_1-, T_2-weighted images of phantoms and animals models of brain, breast and prostate cancers were collected and post-processed. The combined T_1 and T_2-weighted MR images were also obtained. Investigations of $NaDyF_4/NaGdF_4$ core/shell NPs basic cytotoxicity, bio-distribution, and in-vivo imaging were performed *in vivo*.

Results: The stable and non-toxic contrast agents based on Ln^{3+} nanoparticles with the optimal core and shell sizes were developed. They provided improved tumor contrast when the synergetic T_1/T_2 MR technique was applied.

The basic cytotoxicity study showed no adverse effects in Balb/C mice even at the highest dose over a period of one week after intravenous injection. The bio-distribution studies in Balb/C

mice and CD 11 nude mice showed that the liver and spleen were the most dominant organs where the NPs accumulated after injection. Our study showed a high performance of the $NaDyF_4$ /$NaGdF_4$ core/shell NPs in magnetic resonance imaging of brain and breast tumor in CD 11 nude mice and prostate tumor in Wistar rats.

The results may improve early detection of cancer due to the increased efficacy of the new contrast agents. Further studies using targeted NPs are planned.

Keywords: core/shell nanoparticles, Magnetic Resonance Imaging, cancer imaging

References:

[1] BLASIAK, B., TOMANEK, B., ABULROB, A., IQBAL, U., STANIMIROVIC, D., ALBAGHDADI, H., FONIOK, T., LUN, X., FORSYTH, P., SUTHERLAND G. R. 2010. Detection of T_2 changes in an early mouse brain tumor. *Mag Res Imag* 28:784-9.

[2] TOMANEK, B., IQBAL, U., BLASIAK, B., ABULROB, A., ALBAGHDADI, H., MATYAS, J. R., PONJEVIC, D., SUTHERLAND, G. R. 2012, Evaluation of Brain Tumor Vessels Specific Contrast Agents for Glioblastoma Imaging. *Neuro-Oncology*, 14(1), 53-63.

[3] DAS, G. K., JOHNSON, N. J. J., CRAMEN, J., BLASIAK, B., LATTA, P., TOMANEK, B., VAN VEGGEL, F. C. J. M. 2012. $NaDyF_4$ Nanoparticle as T_2 Contrast Agent for Ultra-High Field Magnetic Resonance Imaging. *J. Phys. Chem. Lett*. 3, 524-529.

[4] DONG, C., KORINEK, A., BLASIAK, B., TOMANEK, B., VAN VEGGEL, F. C. J. M. 2012. Cation exchange: a facile method to make NaYF4:Yb,Tm-NaGdF4 core-shell nanoparticles with a thin, tunable, and uniform shell. *Chemistry of Materials*. 24(7), 1297–1305.

Feasibility Study for Photoacoustic Brain-Machine Interface Sensors

Jae-Ho (Han)[1], Yeong-Mun (Cha)[1], Lua (Ngo)[1], Geown (Yih)[1]

[1]Dept. Brain and Cognitive Engineering, Korea University, 145 Anam Rd. Seongbuk-gu, Seoul, Republic of Korea 02841

hanjaeho@korea.ac.kr

Technologies for brain-machine interface (BMI) sensors are gaining momentum and emerging as the latest disruptive innovation in the information technology field. Various modalities of BMI are promising; however, research for more sophisticated technology remains in demand for practical application. In this work, we introduce a feasibility study of a new BMI sensor system based on a photoacoustic effect as a potential discovery. By adapting the effect to BMI, we expect that the system will provide characterized performances with high depth transmittance and temporal/spatial resolution differing from the existing BMI systems. In addition, the photoacoustic effect is non-invasive for bio-tissues and able to equip portability and real-time processing. We believe that this research represents a significant improvement over the existing BMI sensor technologies via characterized performances for brain activity measurement.

The system uses a photoacoustic effect, which is a phenomenon of converted energy of light absorption inducing an acoustic emission in the form of an ultrasound wave arising in the matter [1]. The principle of this effect can be explained as follows: first, tissues (matter) absorb the incident light (lasers) according to their wavelength absorption coefficient, and the absorbed energy is manifested as a temperature rise [2]. This temperature rise leads to a reaction in terms of a thermoelastic expansion effect, and it is finally converted to an acoustic emission, which is detectable by an ultrasonic transducer. As a prime advantage, the photoacoustic effect overcomes the optical diffusion limit. The signal generation depends not only on ballistic photons, but also on the diffused photons that contribute equally to the signal, leading to a centimeter-scale imaging depth [3]. Thus, it enables input signals to penetrate the deeper intra-tissues non-invasively and allows for multi-scale imaging by scaling depth and resolution.

Previous studies of BMI technologies have proven that, in real applications, the photoacoustic effect can induce the centimeter scale depth transmittance [4]. As a further prime advantage, the effect allows for a micrometer scale of temporal/spatial resolution [5]. Since the effect arises through diffused photons, widely spreading light sources throughout the tissues are available, and this is related to a high spatial resolution. The emitted ultrasound wave can be measured at different wavelengths to enable the identification of the absorbing components of the sample. Similar to the NIRS principle, the system is established by noninvasively measuring the blood flow and monitoring the blood oxygenation by using the absorption coefficients of oxyhemoglobin and deoxyhemoglobin quantitatively, depending on the cognition and action states.

Acknowledgement: This work was supported in part by the Basic Science Research Program through the National Research Foundation of Korea (NRF-2013R1A1A2062448).

Keywords: Biological sensors, Brain-computer interfaces, photoacoustic effects.

[1] WANG, L. V. & HU, S. 2012. Photoacoustic tomography: in vivo imaging from organelles to organs. *Science*, 335, 1458-1462.

[2] BURTON, N. C., PATEL, M., MORSCHER, S., DRIESSEN, W. H. P., CLAUSSEN, J., BEZIERE, N., JETZFELLNER, T., TARUTTIS, A., RAZANSKY, D., BEDNAR, B. & NTZIACHRISTOS, V. 2013. Multispectral opto-acoustic tomography (MSOT) of the brain and glioblastoma characterization. *Neuroimage*, 65, 522-528.

[3] SUBOCHEV, P., KATICHEV, A., MOROZOV, A., ORLOVA, A., KAMENSKY, V. & TURCHIN, I. 2012. Simultaneous photoacoustic and optically mediated ultrasound microscopy: phantom study. *Opt. Lett.*, 37, 4606-4608.

[4] WANG, S. TAO, C., WANG X. & LIU, X. 2013. Quantitative detection of stochastic microstructure in turbid media by photoacoustic spectral matching. *Appl. Phys. Lett.,* 102, 114102.

[5] YANG, J.-M., FAVAZZA, C., CHEN, R., YAO, J., CAI, X., MASLOV, K. ZHOU, Q. SHUNG, K. K. & WANG, L. V. 2012. Simultaneous functional photoacoustic and ultrasonic endoscopy of internal organs in vivo. *Nat. Med.*, 18, 1297-1302.

Investigation on the interaction between Single Strand Deoxyribonucleic Acid and Cancer Molecule by Molecular Simulation

Shin-Pon Ju[1,2,a],Hong-Wei Yang[3,b], Che-Hao Cheng[4,c]

[1]Department of Mechanical and Electro-Mechanical Engineering, National Sun Yat-sen University, Kaohsiung 804, Taiwan.

[2]Department of Medicinal and Applied Chemistry, Kaohsiung Medical University, Kaohsiung 807, Taiwan

[3]Department of institute of medical science and technologe, National Sun Yat-sen University, Kaohsiung 804, Taiwan.

[4]Department of Mechanical and Electro-Mechanical Engineering, National Sun Yat-sen University, Tainan 741, Taiwan

[a]jushin-pon@mail.nsysu.edu.tw,

[b]howardyang@mail.nsysu.edu.tw,[c]hogeso81324@gmail.com.tw

The limitation of current clinical diagnostic screening technology has still made impossible to quickly and accurately detect the cancer molecules at a very low concentration. Therefore, the development of novel probe for cancer molecule detection is the most demanding issue in the bio-technology field. We have developed a procedure to predict the interaction between the single strand deoxyribonucleic acid (ssDNA) and the cancer molecule (PSA,PDB code 1PFA) at different distances by molecular dynamics (MD) simulation and simulated annealing basin-hopping method (SABH) with the AMBER force field [1]. This procedure will be further used to design the DNA sequence of rapid screening cancer cells for medical treatment in the further.

Keywords: deoxyribonucleic acid, cancer molecules, nucleic acid aptamer

[1] Scott J. Weiner, Peter A. Kollman, "A New Force Field for Molecular Mechanical Simulation of Nucleic Acids and Proteins, "*Chem.* 1984, *106,* 765-784

Chemical Vapor Deposition Grown graphene based DNA Field Effect Transistor Biosensor with Gold Nanoparticles Signal Amplification

Chunyu Chan[1], Feng Yan[2], Mo Yang[1]

[1]Interdisciplinary Division of Biomedical Engineering, the Hong Kong Polytechnic University, Hong Kong

[2]Department of Applied Physics, the Hong Kong Polytechnic University, Hong Kong

E Mail: Mo.Yang@polyu.edu.hk

Avian influenza A H7N9 is a virus with extremely high mortality rate that infect human from poultry or contaminated environments [1,2] The H7N9 posts a great threat to human creating an urgent need for developing a reliable and low-cost biosensor for screening H7N9. To detect viral oligonucleotide genes, bioFET is a very promising candidate. BioFET provides a label free, sensitive, quickly responding, and point-of-care detection platform for analyzing biomolecules. Combining bioFET with the two dimensional nanomaterial, graphene, the bioFET could molecular target in a very sensitive manner. Here, we propose a chemical vapor deposition (CVD) graphene based bioFET for the detection of H7 gene with a signal amplification scheme using reporter probe conjugated gold nanoparticles (AuNPs). Firstly, a long capture probe was used as recognition element in this bioFET. The long capture probe consists of two portions: (a) a complementary sequence for capturing target H7 DNA target and (b) an extended single-stranded sequence for π-π stacking immobilization. Secondly, a reporter probe-AuNPs composite was applied to co-hybridize with H7 target. The reporter probe-AuNPs composite brought extra negative charges to the proximity of graphene amplifying the sensing signal. The bioFET was measured. Both 15 nm AuNPs and 30 nm AuNPs were used for signal amplification. The results demonstrated that 30 nm reporter probe-AuNPs provided a better signal amplification affect due to the increased number of reporter loading loaded on a single 30 nm AuNPs. This proposed platform is very sensitive in detecting H7 target gene with detection limit down to 64 fM. Also, it is specific to H7 target and able to differentiate single nucleotide polymorphism.

Keywords: Graphene, field effect transistor, gold nanoparticle, biosensor, avian influenza

References

[1] GAO, R., CAO, B., HU, Y., FENG, Z., WANG, D., HU, W., CHEN, J., JIE, Z, QIU, H., XU, K., 2013. Human Infection with A Novel Avian-Origin Influenza A (H7N9) Virus, *N. Engl. J. Med.* 368, 1888-1897.

[2] HVISTENDAHLl, M., NORMILE, D., COHEN, J., 2013. Despite Large Research Effort, H7N9 Continues to Baffle, *Science* 340, 414-415.

DNA Detection by Unconventional Optical Response of Coupled System of Heterogeneous Metal Nanoparticles

Shiho Tokonami,[1] Keisuke Nishida,[1] Shimpei Hidaka,[1] Yojiro Yamamoto,[2] Hidenobu Nakao,[3] Takuya Iida[4]

[1]Graduate School of Engineering, Osaka Prefecture University.

[2] Nano-Architecture Group, National Institute for Materials Science.

[3]GreenChem Inc.

[4]Graduate School of Science, Osaka Prefecture University.

E Mail/ Contact Détails: tokonami@chem.osakafu-u.ac.jp

Detection methods of DNA play crucial roles for the gene analysis. A strong optical response is promising for the detection of biological materials, and densely assembled metallic nanoparticles (NPs) on a plastic bead exhibits strong broadband light scattering [1]. In this contribution, paying attention to such a property, the optical response in the coupled system of a Ag NP-fixed beads (AgNP-FB) and Au nanorods (AuNRs) via DNA hybridization has been investigated [2]. Before and after adding complementary DNA or mismatched DNA, the modulation of white light scattering of a single AgNP-FB was observed by the dark-field optical microscope. The scattering spectrum of a AgNP-MS coupled with many AuNRs via complementary DNA was enhanced in the visible region but significantly suppressed in the ultraviolet region. This mechanism would be used for zmol-level DNA detection, which will lead to a simple and sensitive gene analysis.

Keywords: DNA, Metallic nanoparticle, nanophotonics, biosensor, analytical chemistry

[1] Tokonami, S., Hidaka, S., Nishida, K., Yamamoto, Y., Nakao, H., Iida, T., 2013. Multipole Superradiance from Densely Assembled Metallic Nanoparticles, *The Journal of Physical Chemistry C*, 117, 15247-15252.

[2] Tokonami, S., Nishida, K., Hidaka, S., Yamamoto, Y., Hidenobu Nakao, H., Iida, T. 2014. DNA-mediated Anomalous Optical Coupling of Heterogeneous Metallic Nanostructures", *The Journal of Physical Chemistry C*, 118, 7235-7241.

Air Pollution Sensor for Prediction of Area Source using Smart Electronics Nose System

T.Pogfay, N.Watthanawisuth, A.Wisitsoraat and A.Tuantranont

Thailand Organic & Printed Electronics Innovation Center, National Electronics and Computer Technology Center (NECTEC)

Adisorn.Tuantranont@nectec.or.th

Atmospheric odor pollution from industries and environment should be regularly monitored for human health safety. In this work, smart electronic nose system has been developed by employing the commercial electrochemical gas sensors array, wind vane sensor and anemometer. The gas sensor array includes gas sensors for oxygen, sulfur dioxide, hydrogen chloride, hydrogen sulfide, ammonia, carbon monoxide, nitrogen monoxide and nitrogen dioxide. The system is applied for environmental classification to define air pollution and predict source of pollution. The electronics nose system consists of Raspberry pi main wireless controller unit, a signal conversion board and sensor module. The data of the electronic nose including eight gas sensing response, wind vane signal and wind speed will be sent to a database via wireless network every 50 seconds. The data is analysed by PCA technique to obtain odor dispersion and environment classification. The classification is identified based on the plot between (PC1 and PC2). The data stored in a database is also displayed in real time together with the PCA analysis results on a website for remote monitoring. The system has been used to measure ambient quality at Thai Red Cross Hospital. The results show that the data of air from different areas can be better separated in the domain of the first and second principal components (PC1-PC2). Moreover, the wind direction and speed of air pollution are displayed on the wind rose plot, allowing the prediction of pollution source or location. Therefore, the smart electronic nose system is potential for automatic environmental monitoring applications.

Keywords: electronics nose, air pollution, principal component analysis

Biomimetic apatite hybrid biomaterials for protein controlled delivery

Jinli Qin[1], Jun Ma[1, 2]

[1]Advanced Biomaterials and Tissue Engineering Center, Huazhong University of Science and Technology, Wuhan 430074, P.R.China.

[2] Department of Biomedical Engineering, School of Life Science and Technology, Huazhong University of Science and Technology, Wuhan 430074, P.R.China.

E-Mail : caltary@gmail.com

Bone tissues show unique mechanical properties because of the assembly of collagen and hydroxyapatite. Biomimetic self-assembling is a facile method to fabricate apatite hybrid biomaterials for bone tissue engineering, which show similar structures to bone mineral [1]. In this study, biomimetic apatite materials by using silk fibroin [2] and chitosan nanogel as templates were investigated as potential carriers for protein, respectively. The structure and morphology of the hydroxyapatite nanoparticles could be regulated by the template applied in the synthesis. Sheet-like crystals in microscales were obtained by using silk fibroin, while hedge-like assembly for chitosan nanogel. The loading and release of protein from the apatite hybrid biomaterials were studied and sustained release behaviors were found for the apatite hybrid biomaterials. The controlled release of protein could be mediated by both hydroxyapatite crystals and template molecules. The release rate of protein from the hybrid materials differed due to the template, ionic substitution, and release medium pH value.

Keywords: biomimetic, hybrid materials, biomaterials, hydroxyapatite

[1] Ma, J.; Wang, J.; Ai, X.; Zhang, S. 2014. Biomimetic self-assembly of apatite hybrid materials: From a single molecular template to bi-/multi-molecular templates. *Biotechnol. Adv.*, 32 (4), 744–760.

[2] Ma, J.; Qin, J. 2015. Graphene-like zinc substituted hydroxyapatite. Cryst. Growth Des., 15 (3), 1273-1279.

Eucalytus ash: a Natural Functional Resource for Potential Hair Treatment

Aroonsri (Priprem)*, Kedsarin (Saodaeng), Suppachai (Tiyaworanant)

Faculty of Pharmaceutical Science, Khon Kaen University, Khon Kaen, 40002 Thailand.

apriprem@gmail.com, dek_bondoy@hotmail.com*

An effect of wood or charcoal ashes, traditionally used for hair treatment in some cultures, was tested as a natural functional resource for potential use in the treatment of hair using the human hair. Eucalyptus ashes from 2 processes, A1 being spray-dried powder of eucalyptus extracts and A2 being industrial waste, were obtained by slow aerobic combustion. Calcium oxide and potassium are the majority of the contents identified in chemical analysis of A1 and A2. Semi-log plots between pH and concentrations of A1 or A2 in water were found to be positively correlated ($r \geq 0.97$), indicating that the pH of > 9 would be expected with the presence of eucalyptus ashes in water. At the same dilution, A1 gave lower pH elevation than A2, while NaOH and KOH induced higher pH elevation than A1 and A2. A2 gave higher pH elevation than NH4OH. Treatments of A1 and A2 on excised grey hair samples, observed by SEM, AFM and dyeing, indicate that hair cuticles were altered by the alkaline pH. Stress-strain curves exhibit changes in yield stress of the hair samples treated with water for 10 h and ash extract for half an hour, indicating that alkalinity of the ash accelerated mechanical changes of the hair. Therefore, eucalyptus ashes, particularly A2, were mild- to moderate alkalinizing agent which altered orientation of hair proteins, potentially useful for pretreatment of hair dye or perm products.

Keywords: eucalyptus ash, hair, pH, SEM, AFM

[1] BHUSHAN, B. 2008. Nanoscale characterization of human hair and hair conditioners. *Prog Mater Sci,* 53, 585-710.

[2] KUZUHARA, A. 2013. Analysis of internal structure changes in black human keratin fibers resulting from bleaching treatments using Raman spectroscopy; *J Mol Struct*, 1047, 186-193.

[3] BLUME, U., FERRACIN, J., VERSCHOORE, M., CZERNIELEWSKI, J. M. & SCHAEFER, H. 1991. Physiology of vellus hair follicle: hair growth and sebum excretion. *Brit J Dermatol*, 124, 21-28.

[4] HARKEY, M. R. 1993. Anatomy and physiology of hair. *Forensic Sci Int*, 63, 9-18.

[5] VANKAR, P., TIWARI, V. & SRIVASTAVA, J. 2006. Extracts of stem bark of Eucalyptus Globulus as food dye with high antioxidant properties. *Electron J Environ Agri Food Chem*, 5, 1664-1669.

Liver tumor cell selectivity by paclitaxel-conjugated gold nanoparticles

Yuan-Yue Gao[1], Huan Chen[2], Ying-Ying Zhou[1], Jia-Jia Shen[1], Ya Ding[1,a,*]

[1]Key Laboratory of Drug Quality Control and Pharmacovigilance, China Pharmaceutical University, Ministry of Education, Nanjing 210009, China

[2]Department of Biochemistry, School of Life Science and Technology, China Pharmaceutical University, Nanjing 210009, China

[a]ayanju@163.com

*Corresponding authors

Keywords: liver tumor selectivity, gold nanoparticles, paclitaxel, galactose, treatment efficacy

Abstract:

Paclitaxel (PTX) is one of the most commonly used antineoplastic agents. However, its clinical application confronts with several difficulties [1,2], including poor water solubility, broad biodistribution, and serious side effects. To improve the overall performance of PTX, we synthesized a series of PTX-PEG-SH ligands and attached them on the surface of gold nanoparticles (GNPs) to construct a series of PTX-conjugated GNPs. These gold conjugates showed enhanced water solubility, tumor cell killing ability, and therapeutic efficacy of liver tumor *in vivo* [3,4]. To further increase selectivity of the liver tumor cells, an easily synthesized ligands with different galactose (Gal)-modified polyethylene glycol (PEG) molecules were employed to achieve target to the asialoglycoprotein receptor in the membrane of liver cells. In the Heps-xenograft tumor model on mice, the drug concentrations in liver and tumor were comparable. While in the orthotopic liver tumor model on mice, the optimized PTX-conjugated GNPs bearing Gal moiety showed higher inhibition and apoptosis in tumor and less toxicity in normal liver tissue. These results indicated that this gold conjugate showed greatly potential in liver tumor selectivity and practical application of liver tumor therapy.

References:

[1] *Biomaterials* **2012**, 33, 856-866.

[2] *Molecular Pharmaceutics* **2014**, 11, 4164-4178.

[3] *Biomaterials* **2013**, 34, 10217–10227.

[4] *Biomaterials* **2016**, 74, 280-291.

Nanomaterials modified with self-assembled aptamers as anticoagulants

San-Shan Huang and Chih-Ching Huang

Department of Bioscience and Biotechnology, National Taiwan Ocean University, Keelung 20224, Taiwan

e-mail: huanging@ntou.edu.tw

We demonstrated that thrombin-binding aptamer-conjugated gold nanoparticles (TBA–Au NPs), prepared from a self-assembled hybrid monolayer (SAHM) of triblock aptamers on Au NPs (13 nm), can effectively inhibit thrombin activity toward fibrinogen. The first block poly(adenine) at the end of the triblock TBA was used for the self-assembly on Au NP surface. The second block, in the middle of TBA, was composed of oligonucleotides that could hybridize with each other. The third block, containing TBA_{15} (15-base, binding to the exosite I of thrombin) and TBA_{29} (29-base, binding to the exosite II of thrombin) provided bivalent interaction with thrombin. The SAHM triblock aptamers have optimal distances between TBA_{15} and TBA_{29}, aptamer density, and orientation on the Au NP surfaces. These properties strengthen the interactions with thrombin ($K_d = 1.5 \times 10^{-11}$ M), resulting in an extremely high anticoagulant potency. The thrombin clotting time mediated by SAHM TBA_{15}/TBA_{29}–Au NPs was >10 times longer than that of four commercially available drugs (heparin, argatroban, hirudin, or warfarin). In addition, the rat-tail bleeding assay time further demonstrated the SAHM TBA_{15}/TBA_{29}–Au NPs were superior to heparin. The SAHM TBA_{15}/TBA_{29}–Au NPs exhibited excellent stability in the human plasma (half-life >14 days) and good biocompatibility (low cytotoxicity and hemolysis). Most interestingly, the inhibition by SAHM TBA_{15}/TBA_{29}–Au NPs was controllable by the irradiation of green laser, *via* heat transfer-induced TBA release from Au NPs. Our study opens up the possibility of regulation of molecule binding, protein recognition, and enzyme activity using SAHM aptamer-functionalized nanomaterials.

Keywords: Aptamers; Self-assemble; Gold nanoparticles; Thrombin; Anticoagulants

Nanostructured Particles Functionalized Acrylic Bone Cements with Enhanced Antibiotic Release

Shou-Cang Shen[1], Wai Kiong Ng[1], Leonard Chia[1], Kumaran Letchmanan[1], Reginald B. H. Tan[1,2]

[1] Institute of Chemical and Engineering Sciences, 1 Pesek Road, Jurong Island, Singapore 627833.

[2] Department of Chemical and Biomolecular Engineering, The National University of Singapore, 4 Engineering Drive 4, Singapore 117576

E-mail: shen_shoucang@ices.a-star.edu.sg

A sustained release of antibiotic acrylate-based bone cement is designed to prevent prosthesis-related infections. The current antibiotic-loaded bone cements showed very limited drug release and typically less than 10% of total drug load. To enhance the drug delivery efficiency for poly(methyl methacrylate (PMMA)-based bone cement, three types of nanostructured particles (mesoporous silica nanoparticles, carbon nanotubes, and hydroxyapatite nano-rods) have been used in our study to functionalize bone cement. The results showed that the non-porous rod-like hydroxyapatite nanoparticles only slightly improved drug delivery efficiency. With 11.5% (w/w) of hydroxyapatite nanorods in Simples® bone cement, about 13% of gentamicin could be released in two months during an in-vitro study. As comparison, the hollow nanostructured particles modified bone cements could achieve sustained drug release. With the presence of 5.3%(w/w) of carbon nanotubes in bone cement, a more sustained release of antibiotic could be achieved with more than 60% of gentamicin in 60 days. While 8% of mesoporous silica nanoparticles formulated bone cement exhibited a sustained release of gentamicin in 80 days and achieved about 60% of total drug release too. The hollow nanostructured nanomaterials are believed to form a nano-network path for gentamicin diffusion from the composite to the surface and released to the medium. This kind of nano diffusion network could not be created by the non-porous nanoparticles as filler, as gentamicin particles formulated in bone cement are embedded inside the PMMA matrix during polymerization and cannot diffuse to the surface of the bone cement for drug release. The mechanical properties (such as compression and three-point bending) of mesoporous silica nanoparticles functional bone cement were measured and were close to that of regular bone cement without antibiotics, and within permissible ranges. However, the presence of carbon nanotubes in the bone cement matrix significantly affected the mechanical properties. Due to the sustained release of antibiotics, the mesoporous silica nanoparticles functionalized antibiotic bone cements exhibited extended antibacterial activity.

Keywords: Nanostructured particles; acrylic bone cement; drug delivery; diffusion network

[1] Shen Shou-Cang, NgWai Kiong, Leonard Chia, Reginald Tan, Nanostructured material formulated with bone cement for effective antibiotic delivery US 9155814 B2 (2015).

Near-infrared optical applications of nanoparticles: nonlinear optical, surface-enhanced Raman scattering, and photothermal/photodynamic therapy

Chih-Chia Huang[1]

[1] Department of Photonics, National Cheng Kung University, Tainan City, Taiwan.

E Mail: c2huang@mail.ncku.edu.tw; huang.chihchia@gmail.com

Extensive efforts have been devoted to the development of a new biophotonic system using near infrared (NIR) nano-agents for non-invasive cancer diagnosis and therapy. Here, we developed a simple carboxylate ligand-assisted and one-pot synthesis method for the preparation of optical Fe_3O_4, Au@polymer, Cu@polymer, and Ag@polymer nanomaterials. Based on the inverse spinel-structured magnetite (Fe_3O_4) material, Fe(II) and Fe(III) in the octahedral sites of the Fe_3O_4 nanocrystal were found to produce an intervalence charge transfer (IVCT) that gives rise to the second near infrared (NIR-II) region over 1000 nm. We present the first example of magnetomotive optical coherence tomography cellular imaging combined with enhanced photothermal therapy using Fe_3O_4 nanocrystal and applying a magnetic field. Among these nanocomposites, the Au@polymer nanoparticle with good biocompatibility exhibited shell-dependent signal enhancement in the surface plasmon resonance shift, nonlinear fluorescence, and surface-enhanced Raman scattering properties. The Au@polymer/methylene blue (MB) nanoparticle was prepared and produced a high quantum yield of singlet oxygen molecules, over 50% as much as that of free MB, when they were excited by a dark red light source at 660 nm, but without significant dark toxicity. After conjugating transferrin (Tf), the Au@polymer/MB-Tf NPs showed a two-fold enhancement of photodynamic therapeutic efficiency toward HeLa cells over the use of free MB at 4 times

Keywords: photodynamic therapy, photothermal therapy, SERS, Au, magnetic nanoparticles,

[1]. HUANG, C.-C., CHANG, P.-Y., LIU, C.-L., WU, S.-P., KUO, W.-C. 2015. *Nanoscale*, 7, 12689–12697.

[2]. YU, J., HSU, C.-H., HUANG, C.-C., CHANG, P.-Y. 2015. *ACS Appl. Mater. Interfaces,* 7, 432−441.

Sequential Drug Release by pH/Redox Dual Responsive Non-covalent Polymer Gatekeepers in Hollow Mesoporous Silica Nanoparticle for synergistic cancer therapy

Ja-Hyoung Ryu*

Department of Chemistry, Ulsan National Institute of Science and Technology, Ulsan, South Korea

Abstract

Nanoscopic delivery vehicles capable of encapsulating drug molecules and releasing them in response to external stimuli are of great interest due to implications in therapeutic applications. Sequential drug delivery with dual stimulus responsive nanotherapeutics is highly desirable for disease specific treatment in cancer therapy with minimized adverse effects. In addition to this, on-demand therapy received considerable attention among the treatment techniques. Herein, we present the design of robust, new and simple pH dependent charge conversional non-covalent polymer gatekeepers technique by preparing the hydrophilic and hydrophobic drug loading at high capacity and improved encapsulation stability in hollow mesoporous container for target specific cellular uptake for cancer treatment. The di-isopropyl methacrylate functionalized monomer facilitates the fast cellular uptake at acidic environment of cancer cells and allows the on-demand release of hydrophillic drug at acidic pH of endosomes upon protonation. Pyridine disulfide facilitates the strong encapsulation of loaded cargo upon crosslinking by thiol-disulfide exchange and releases the cargo upon exposure with increased intracellular glutathione concentration. The co-delivery of the multi-drugs in single carrier enables a synergistic chemotherapeutic effect. Based on this new design, a wide range of sequential and synergistic therapy can be achieved to satisfy varied clinical requirements.

Smart Nanoparticle Composite Platform for Drug Delivery Systems

Myoung-Hwan Park

Department of Chemistry at Sahmyook University
1st Science Building room #203, Hwarangro-815 Nowon-gu, Seoul, South Korea
Email: pmhdream@gamil.com & mpark@syu.ac.kr

Lots of drug delivery technologies have been developed for a real patient need for more efficient release of newer drugs using effective delivery platforms. In our research, we utilized composites composed of dendrimers and gold nanoparticles for an efficient drug delivery platform. Chemically directed dithiocarbamate binding of amine groups of dendrimers to NPs in the presence of CS_2 that enables to enhance the robustness of NP assembles, used to generate a biocompatible, highly flexible platform capable of providing sustained release of small organic molecules and biologics. The hybrid membrane was integrated with a fluidic delivery device and a refillable drug reservoir for providing continuous sustained release. With a gold nanorod contained composite membrane, a smart on-demand pulsatile release from a drug reservoir was further demonstrated. These versatile nanoparticle platforms with more appropriate drug plasma profiles able to improve therapeutic efficacy and reduce side effects will provide potential utilities in the future design of implantable medical devices combined with microscale and macroscale technologies.

The Penetrated Delivery of Drug and Energy to Tumors by Bio-inspired Nano-materials

Shang-Hsiu Hu

Department of Biomedical Engineering and Environmental Sciences, National Tsing Hua University, Hsinchu, Taiwan

Email:shhu@mx.nthu.edu.tw

A magneto-responsive energy/drug carrier that enhances deep tumor penetration with a porous nano-composite is constructed by using a tumor-targeted lactoferrin (Lf) bio-gate as a cap on mesoporous iron oxide nanoparticles (MIONs). With a large payload of a gas-generated molecule, perfluorohexane (PFH), and a hydrophobic anti-cancer drug, paclitaxel (PTX), Lf-MIONs can simultaneously perform bursting gas generation and on-demand drug release upon high-frequency magnetic field (MF) exposure. Biocompatible PFH was chosen and encapsulated in MIONs due to its favorable phase transition temperature (56 ℃) and its hydrophobicity. After a short-duration MF treatment induces heat generation, the local pressure increase via the gasifying of the PFH embedded in MION can substantially rupture the three-dimensional tumor spheroids *in vitro* as well as enhance drug and carrier penetration. As the MF treatment duration increases, Lf-MIONs entering the tumor spheroids provide an intense heat and burst-like drug release, leading to superior drug delivery and deep tumor thermo-chemo-therapy. With their high efficiency for targeting tumors, Lf-MIONs/PTX-PFH suppressed subcutaneous tumors in 16 days after a single MF exposure. This work presents the first study of using MF-induced PFH gasification as a deep tumor-penetrating agent for drug delivery.

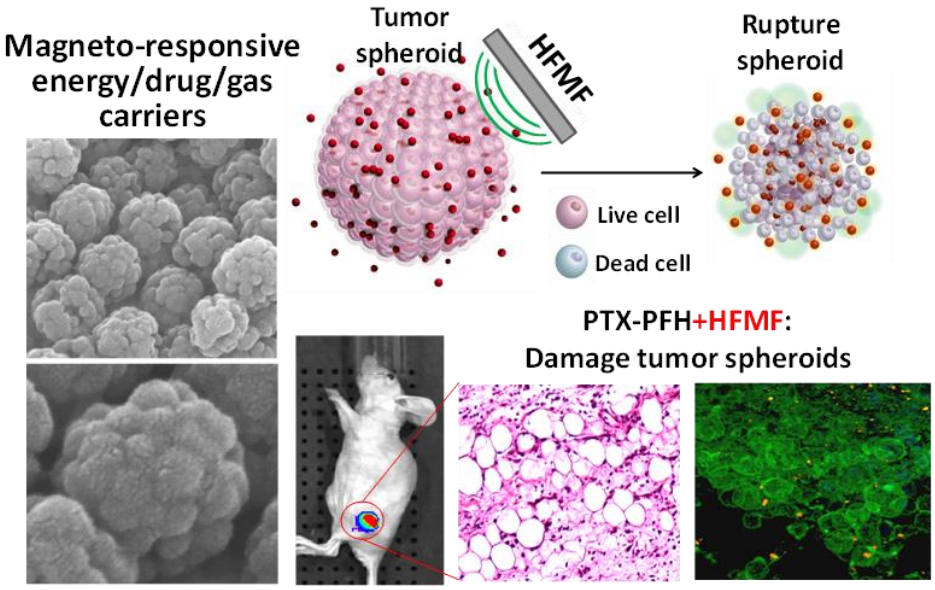

Fig1. Schematic illustration of the lactoferrin-capped mesoporous iron oxide nanoparticle (Lf-MION). The hydrophobic pores of Lf-MION carry both paclitaxel (PTX) and perfluorohexane (PFH), and these cargos can be triggered when treated with a high-frequency magnetic field (MF).

1. Y. L. Su, J. H. Fang, C. Y. Liao, C. T. Lin, Y. T. Li, S. H. Hu*, Theranostics **5,** 1233 (2015).
2. J. H. Fang, Y. T. Li, W. H. Chiang, S. H. Hu, Small **11,** 2417 (2015).

Barley protein nanoparticles as an oral delivery system for bioactive compounds

Zhigang Tian, Jingqi Yang, Lingyun Chen*

Barley is ranked fourth among world cereals in total production and second major crop in Canada. However, most of barley is used as livestock feed. Current research on value-added applications of barley mainly focuses on barley carbohydrate and oil components. Barley proteins are lack of research effort. Due to their hydrophobic characteristic and good barrier properties at medium relative humidity, barley protein may be a good candidate as biomaterials to entrap bioactive compounds, antioxidants, *etc.*.

Barley protein nanoparticles have been successfully prepared by high pressure homogenization as a potential delivery system to improve the bioavailability of hydrophobic bioactive compounds. This nanoparticle preparation process is green and economic without addition of organic solvents, synthetic surfactants and cross-linking reagents. The influence of formula and processing conditions (pressure and number of circulation) on the particle size and size distribution are systematically investigated. It is found that smaller size nanoparticles with narrower size distribution can be obtained by increase the homogenization pressure and circulation (up to 20kpsi and 6 passes). Mass production (up to 5% w/w protein) can be achieved when the oil/protein ratio is maintained between 1 and 1.5. Optimal nanoparticles have a sphere shape, small particle size (90-150nm), homogenous size distribution (PDI < 0.3) and high payload (51-55%). The high zeta-potential (~-35mV) keeps barley protein nanoparticles stable in aqueous solution without surfactants. The encapsulated hydrophobic bioactive compounds are protected by barley protein coating in the gastric environment and released completely in the simulated intestinal fluids. The barley protein nanoparticles are relatively safe and can be internalized by Caco-2 cells. Furthermore, since barley protein shows excellent surface activities, its interfacial behaviors are investigated. The degradation of the protein coating is also further studies. This barley protein nanoparticle can be potentially utilized in many industries, such as food, cosmetics and pharmaceutical. Also, the knowledge gained from this study can help us tailor the properties of barley protein nanoparticles for different specific applications.

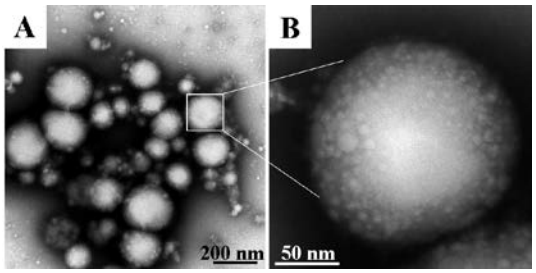

Figure 1(A) Transmission electron microscope image of barley protein nanoparticle (2 wt% protein and 2.5% v/v oil) prepared at 16kpsi with 14kx magnification; (B) same sample observed with 10kx.

*Corresponding author: Lingyun Chen, Dept. of Agricultural, Food and Nutritional Science, University of Alberta, Edmonton, Canada T6G 2P5
Tel.: 1-780-492-0038; Fax: 1-780-492-4265; Email: lingyun.chen@ualberta.ca

Barley protein nanoparticles as an oral delivery system for bioactive compounds

Zhigang Tian, Jingqi Yang, Lingyun Chen*

Barley is ranked fourth among world cereals in total production and second major crop in Canada. However, most of barley is used as livestock feed. Current research on value-added applications of barley mainly focuses on barley carbohydrate and oil components. Barley proteins are lack of research effort. Due to their hydrophobic characteristic and good barrier properties at medium relative humidity, barley protein may be a good candidate as biomaterials to entrap bioactive compounds, antioxidants, *etc.*.

Barley protein nanoparticles have been successfully prepared by high pressure homogenization as a potential delivery system to improve the bioavailability of hydrophobic bioactive compounds. This nanoparticle preparation process is green and economic without addition of organic solvents, synthetic surfactants and cross-linking reagents. The influence of formula and processing conditions (pressure and number of circulation) on the particle size and size distribution are systematically investigated. It is found that smaller size nanoparticles with narrower size distribution can be obtained by increase the homogenization pressure and circulation (up to 20kpsi and 6 passes). Mass production (up to 5% w/w protein) can be achieved when the oil/protein ratio is maintained between 1 and 1.5. Optimal nanoparticles have a sphere shape, small particle size (90-150nm), homogenous size distribution (PDI < 0.3) and high payload (51-55%). The high zeta-potential (~-35mV) keeps barley protein nanoparticles stable in aqueous solution without surfactants. The encapsulated hydrophobic bioactive compounds are protected by barley protein coating in the gastric environment and released completely in the simulated intestinal fluids. The barley protein nanoparticles are relatively safe and can be internalized by Caco-2 cells. Furthermore, since barley protein shows excellent surface activities, its interfacial behaviors are investigated. The degradation of the protein coating is also further studies. This barley protein nanoparticle can be potentially utilized in many industries, such as food, cosmetics and pharmaceutical. Also, the knowledge gained from this study can help us tailor the properties of barley protein nanoparticles for different specific applications.

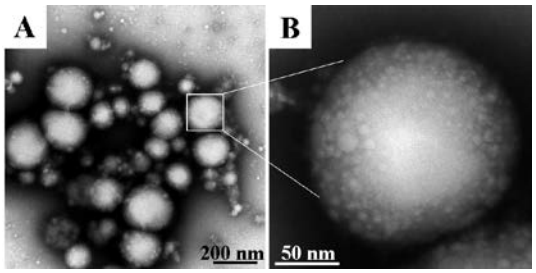

Figure 1(A) Transmission electron microscope image of barley protein nanoparticle (2 wt% protein and 2.5% v/v oil) prepared at 16kpsi with 14kx magnification; (B) same sample observed with 10kx.

*Corresponding author: Lingyun Chen, Dept. of Agricultural, Food and Nutritional Science, University of Alberta, Edmonton, Canada T6G 2P5
Tel.: 1-780-492-0038; Fax: 1-780-492-4265; Email: lingyun.chen@ualberta.ca

Development of ROS-Responsive polymeric Micelle in Cytosolic Drug Delivery System application in cancer therapy

Lu-Yi Yu[1], Geng-Min Su[1], Chun- Liang Lo[1*]

[1]Department of Biomedical Engineering, National Yang-Ming University, Taipei, Taiwan 112, ROC.

* cllo@ym.edu.tw

Abstract:

Cytosolic delivery system places important in recent development in drug therapeutic technologies. Since biomacromolecules, including genes, oligonucleotides, and proteins, the development of technologies for improving the efficiency of the delivery of these therapeutic molecules into cells, more specifically into the cytosol and nucleus, is significantly required. [1-7] Furthermore, in many researches had proved the level of ROS in tumor is higher than normal tissue. [8-10] Therefore, we designed a strategy of cytosolic drug delivery system using by ROS sensitive polymer for cancer therapy, showed in figure 1. This ROS sensitive polymer is compose of polysulfide which will be oxidation into sulfoxide. And, the sulfoxide group of this polymer will make micelle swelling to release the cytosolic drug before endosome becoming secondary endosome. This effect will help drug to escape from endosome and increase drug efficiency.

First, in the Elemental Analyzer data incubated the oxygen composition of copolymer after treated high concentration H_2O_2 was high than treated low concentration H_2O_2, showed in figure 2a. And then, the size of this polymeric micelle was about 225 nm and the size of this polymeric micelle after treated H_2O_2 was significantly swelling to 500-fold, showed in figure 2b. Therefore, we found the drug release of this micelle was been about 100 % after treated H_2O_2 3 days, showed in figure 2c. In figure 2d, the MTT assay showed that the cell toxicity of this micelle would be same as free drug. Moreover,

in the image of confocal microscopy that we found this micelle in the high concentration ROS environment of cancer cell would escape from endosome, showed in figure 2e. These results all indicate that this strategy of drug delivery system has great potential for future application for cytosolic drug delivery.

Key word: polymeric micelle, cytosolic drug delivery, cancer therapy.

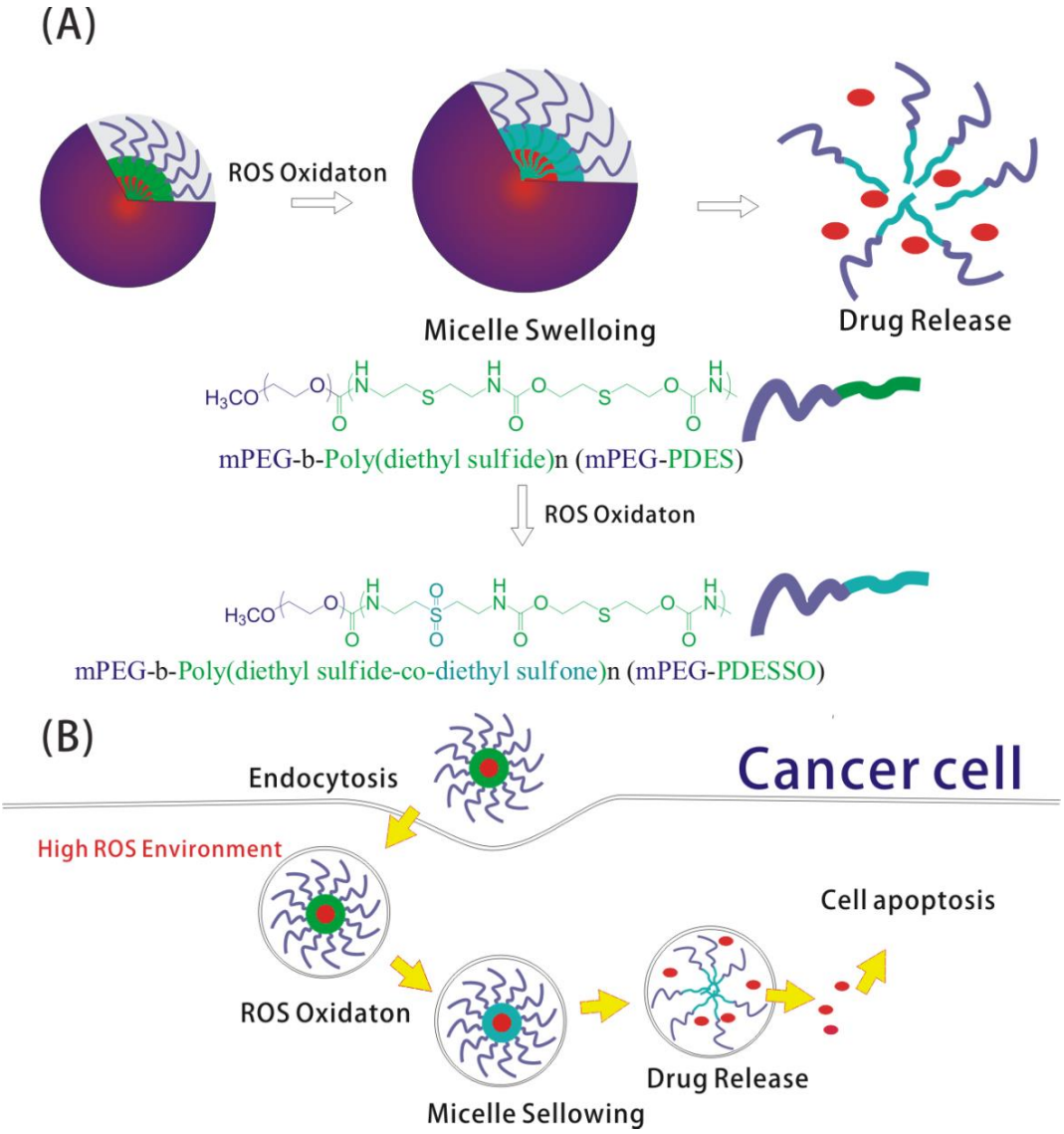

Figure 1. The concept of this research. (A) This polymer would be oxidation by ROS and then the sulfide- group became the sulfone- group. (B) This polymeric micelle

uptake into cancer would be oxidation and swelling and then release the cytosolic drug.

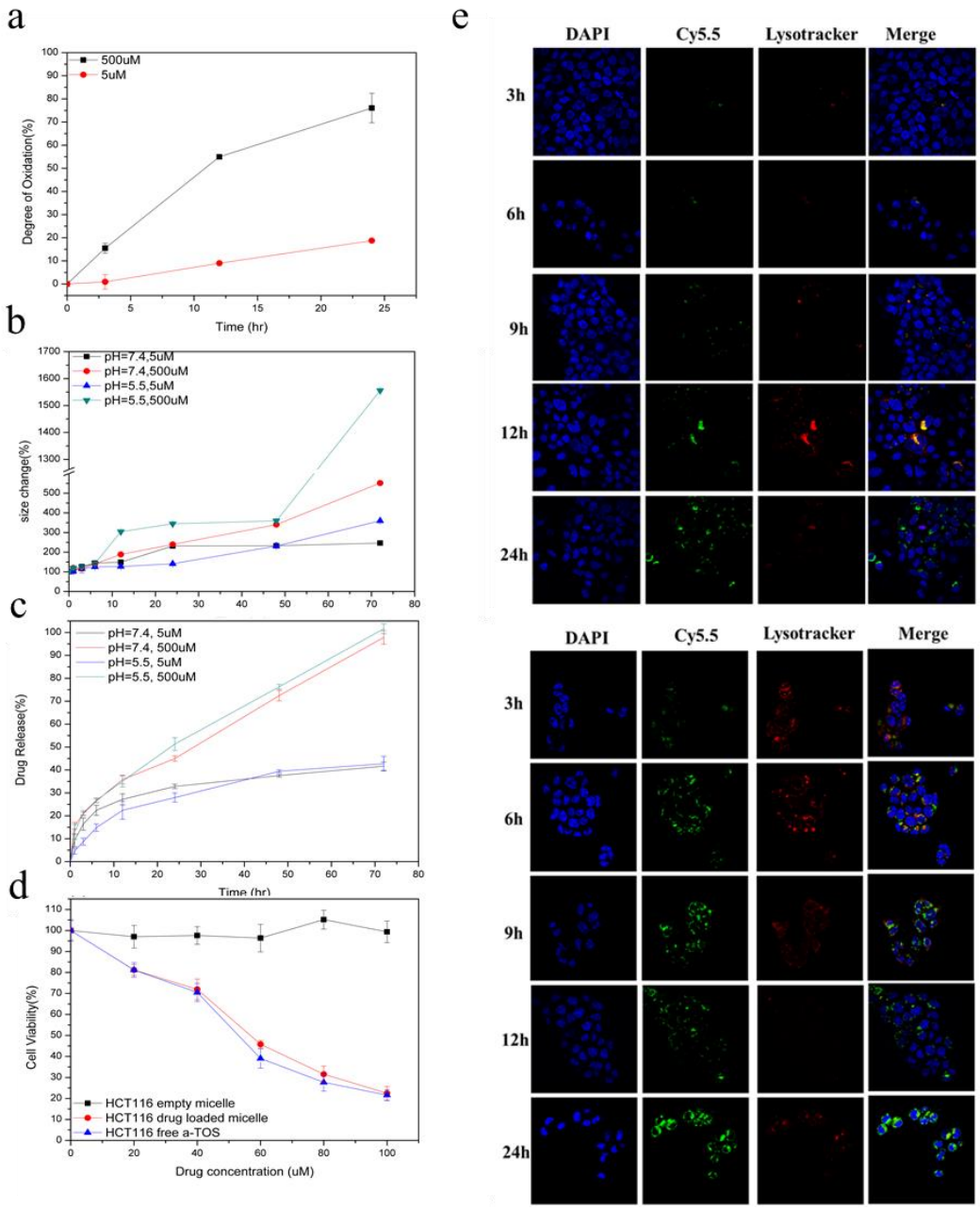

Figure 2. The characteristic of this micelle. a.) the oxidation of the copolymers after treated different concentration H_2O_2 was determined by Elemental Analyzer. b.) The particle size exchange of the micelles after treated different concentration H_2O_2 were measured by dynamic laser scanning. c.) The drug release of the micelles after treated

different concentration H_2O_2 were measured by UV spectrometry. d.) In vitro cytotoxicity of the micelles were measured by MTT assay. e.) the confocal microscopy image of the micelle treated L929 cell line and HCT116 colon cancer cell line, upper is L929 and blow is HCT116.

Reference:

1. Allen M. Theresa, and Pieter R. Cullis. "Drug delivery systems: entering the mainstream." Science 303.5665 (2004): 1818-1822.
2. Kristina Riehemann, Stefan W. Schneider, Thomas A. Luger et al. "Nanomedicine—challenge and perspectives." Angewandte Chemie International Edition 48.5 (2009): 872-897.
3. Whitehead A. Kathryn, Robert Langer, and Daniel G. Anderson. "Knocking down barriers: advances in siRNA delivery." Nature reviews Drug discovery 8.2 (2009): 129-138.
4. Mark E. Davis, Zhuo Chen and Dong M. Shin "Nanoparticle therapeutics: an emerging treatment modality for cancer." Nature reviews Drug discovery 7.9 (2008): 771-782.
5. Jayanth Panyam and Vinod Labhasetwar. "Targeting intracellular targets." Current drug delivery 1.3 (2004): 235-247.
6. Gwyn W. Gould and Jennifer Lippincott-Schwartz. "New roles for endosomes: from vesicular carriers to multi-purpose platforms." Nature Reviews Molecular Cell Biology 10.4 (2009): 287-292.
7. Jason Mercer and Ari Helenius “Virus entry by micropinocytosis”. Nature cell biology, 11.5 (2009): 510-520.
8. Sue Hyun Lee, Mukesh K. Gupta, Jae Beum Bang et al. "Current Progress in Reactive Oxygen Species (ROS) Responsive Materials for Biomedical

Applications." Advanced healthcare materials 2.6 (2013): 908-915.

9. Lallana Enrique, Nicola Tirelli. "Oxidation-Responsive Polymers: Which Groups to Use, How to Make Them, What to Expect From Them (Biomedical Applications)" Macromolecular Chemistry and Physics 214 (2013): 143−158
10. L Zhang, FX Gu, JM Chan et al. "Nanoparticles in medicine: therapeutic applications and developments." Clinical pharmacology & therapeutics 83.5 (2008): 761-769.

Fabrication of double layered scaffolds for drug delivery

Soonmo Choi[1], Eunjoo Shin[2], Sungsoo Han[1]

[1]Department of Nano, Medical & Polymer Materials, School of Engineering, Yeung-nam University, Gyeongsan 712-749, Republic of Korea

[2]Department of Organic Materials and Polymer Engineering, School of Engineering, Dong-a University, Busan 604-714, Republic of Korea

sshan@yu.ac.kr

The scaffolds which are consisted of two structural part were fabricated in aqueous solution by the fusion technique of freeze-drying and thermal inducing with the formation of gelatin-based aggregation. The fabricated scaffold is consisted of gelatin dense layer and gelatin porous layer caused from working as foaming agent of an anionic surfactant sodium dodecyl sulfate (SDS). It was expected that the interaction between gelatin and SDS induced structural difference, which characterized by scanning electron microscopy (SEM) yielding different behavior in degradation. It was demonstrated a potential for efficient drug delivery in terms of sustained release patterns with considering initial burst and simple fabrication method.

Keywords: Functional, scaffold, drug delivery, tissue engineering, structure

[1] CHOI, S. M., SINGH, D., SINGH, D. & HAN, S. S. 2013. Surfactant role in modifying architecture of functional polymeric gelatin scaffolds. *International Journal of Polymeric Materials and Polymeric Biomaterials*, 63, 951-956

On-Command Multifunctional Bimagnetic Core-Shell Nanoparticles for Biomedical Applications

V. Nica[1,2], M. Hammad[2], M.L. Garcia Martin[3], R. Hempelmann[2]

[1]"Alexandru Ioan Cuza" University of Iasi, Department of Physics, Iasi, Romania.

[2]Saarland University, Department of Physical-Chemistry, Saarbrücken, Germany.

[3] Andalusian Centre for Nanomedicine and Biotechnology, Malaga, Spain.

E Mail/ Contact Détails: nicaval@gmail.com, Valentin Nica.

Our syntheses of magnetic nanoparticles aimed at tuning the magnetic properties and surface modification of particles [1-4]. Previously, we described the possibility to confine highly toxic low-molecular 5-Fluorouracil antineoplastic agent into biocompatible, core-shell (CS) magnetic mesoporous silica nanoparticles with high efficiency [5]. More recently, we reported the preparation of imino-chitosan biopolymer films by acid condensation of the amino groups of chitosan with a higher biocompatibility as compared to the chitosan parent [6].

The goal of this study was to achieve both hyperthermia and release-on-command of drug-like molecule from new CS bimagnetic carriers with improved specific absorbtion rate (SAR). For controlled drug release induced by an external magnetic field we used a mechanism of reversible splitting of a C=C bond as thermoresponsive switch. The bimagnetic nanoparticles (MNPs) are functionalized with a thermo-liable linker that on-demand controls the drug release by switching an external oscillating magnetic field. We synthesized hexagonal shape nanoparticles of $Co_{0.6}Fe_{2.4}O_4$@$MnFe_2O_4$ using the thermal decomposition of metallic oleate complexes. The dark field transmission electron microscopy (DF-TEM) showed the formation of nanoparticles with a mean radius of 8 nm and the shell thickness of 2 nm. The Bragg reflections of X-ray diffraction patterns match with the reported values of face-centered cubic (fcc) unit cell of $CoFe_2O_4$. The magnetization curve at room temperature of CS MNPs showed a superparamagnetic behavior with a specific saturation magnetization (M_s) of 90 emu/g. The SAR values of CS MNPs range from 280 W/g to 440 W/g and those are higher than the core

nanoparticles (140-250 W/g). This indicates the spin exchange coupling through the interfacial interactions of the bimagnetic CS structure. The magnetic nanoparticles are further functionalized with furyl-isothiocyanate and maleimide trifluoracetate in order to achieve the reversible Diels-Adler reaction (rDA). The fluorescein was used as drug-like molecule. Thermogravimetric analysis (TG) and infrared spectroscopy (FTIR) have demonstrated the binding of the coupling agents to the surface of bimagnetic nanoparticles. The release of drug from magnetic nanocarriers was determined by fluorescence spectrometry. Upon alternating magnetic field (AMF), the loaded fluoresceine is released rapidly (>60% in first 10 minutes) due to partial rDA reaction as effect of local heating. The cytotoxicity tests have been achieved using HeLa cells via MTT assay. The cell viability is maintaining more than 90% over 24 h of treatment.

Acknowledgements: This work was supported by Andalucía Talent Hub Program, co-funded by the European Union FP7 Program, Marie Skłodowska-Curie actions (COFUND-Grant Agreement n° 291780) and the Ministry of Economy, Innovation, Science and Employment of the Junta de Andalucía.

Keywords: core-shell nanoparticles, Diels-Adler reaction, hyperthermia, drug release

[1] NICA, V., BRINZA, F., CALTUN, O.F. & HEMPELMANN, R. 2012. Synthesis and Characterization of Co-Ni and Fe_3O_4-Pd Nanocomposites. *IEEE Trans. Magn.*48 (4), 1356-1359.

[2] NICA, V., GHERCA, D., URSU, C., TUDORACHE, F., BRINZA, F. & PUI, A. 2013. Synthesis and Characterization of Co-Substituted Ferrite Nanocomposites" *IEEE Trans. Magn.*49 (1), 26-29.

[3] GHERCA, D., PUI, A., CORNEI, N., COJOCARU, A. NICA, V. & CALTUN, O.F. 2012. Synthesis, Characterization and Magnetic Properties of MFe_2O_4 (M = Co, Mg, Mn, Ni) Nanoparticles Using Ricin Oil as Capping Agent. *J. Magn. Magn. Mater.* 324 (22), 3906-3911.

[4] DUMITRESCU, A.M., SAMOILA, P.M., NICA, V., DOROFTEI, F., IORDAN, A.R. & PALAMARU, M.N. 2013. Study of The Chelating/Fuel Agents Influence on $NiFe_2O_4$ Samples with Potential Catalytic Properties. *Powder. Technol.* 243, 9-17.

[5] TOMOIAGA, A.M., CIOROIU, B.I., NICA, V. & VASILE A, 2013. Investigations on Nanoconfinement of Low-Molecular Antineoplastic Agents into Biocompatible Magnetic Matrices for Drug Targeting" *Colloid. Surface B*, 111, 52-59.

[6] MARIN, L., AILINCAI, D., MARES, M., PASLARU, E., CRISTEA, M., NICA, V. & SIMIONESCU, B.C. 2015. Imino-Chitosan Biopolymeric Films. Obtaining, Self-Assembling, Surface and Antimicrobial Properties. *Carbohyd. Polym.* 117, 762-770.

Polysaccharides Conjugated Micelles Possessing CD44 Targeting Potential for Gene Delivery

Wen Jen Lin, Wei-Chi Lee

School of Pharmacy, National Taiwan University, Taipei, Taiwan.

wjlin@ntu.edu.tw

The aim of this study was to develop polysaccharide-conjugated PLGA-PEG micelles possessing CD44 receptor targeting ability for gene delivery. The CD44 receptor was selected as the target binding receptor which is overexpressed in many kinds of tumors including human breast cancer cells and glioblastoma cells etc. [1]. Two linear polysaccharides, hyaluronic acid (HA) and chondroitin sulfate (CD) were included in this study as CD44 receptor targeting moieties. Hyaluronic acid and chondroitin sulfate are endogenous polysaccharides existed in the extracellular matrix. It was proved that both polysaccharides possess specific binding ability to CD44 receptor [2]. In this study, the synthesized polysaccharide-conjugated copolymers were applied as nanocarriers for DNA delivery. The size and zeta potential of DNA loaded micelles were measured by Zetasizer. The DNA encapsulation efficiency was quantified by using PicoGreen reagent. The effect of polysaccharide on biocompatibility, stability, *in vitro* release, cytotoxicity and cellular transfection of DNA loaded micelles were investigated. The results showed that the DNA loaded micelles possessed negative-charged character which prevented erythrocytes from agglutination. All micelles exhibited sustained release behavior. Both polysaccharide-conjugated micelles possessed high selectivity between CD44-positive U87 cell and CD44-negative HepG2 cell. The cellular transfection of DNA loaded CD-b-PEG-PLGA micelles was higher than HA-b-PEG-PLGA micelles in CD44-positive cancer cell. The high selectivity to cancer cell and low cytotoxicity in normal cell assured the potential of polysaccharide-conjugated micelles as gene delivery nano-carriers.

Keywords: Polysaccharide, poly(lactide-co-glycolide), gene delivery, CD44 receptor

[1] WILLIAMS, K., MOTIANI, K., GIRIDHAR, P. V. & KASPER, S. 2013. CD44 Integrates Signaling in Normal Stem Cell, Cancer Stem Cell and (Pre)Metastatic Niches. *Exp Biol Med*, 238, 324-338.

[2] MURAI, T., SOUGAWA, N., KAWASHIMA, H., YAMAGUCHI, K. & MIYASAKA, M. 2004. CD44-Chondroitin Sulfate Interactions Mediate Leukocyte Rolling Under Physiological Flow Conditions. *Immunol Lett*, 93, 163-170.

Preparation and Characterization of Cyclic oligosaccharide cross-linked carboxymethylcellulose hydrogel

Daham (Jeong)[1], Ben El (Lee)[1], Sang-Woo (Joo)[1], Eunae (Cho)[2], Seunho (Jung)[1*]

[1]Department of Bioscience and Biotechnology, Microbial Carbohydrate Resource Bank (MCRB) & Center for Biotechnology Research in UBITA (CBRU), Konkuk University, Seoul 143-701, South Kore).

[2]Institute for Ubiquitous Information Technology and Applications (UBITA) & Center for Biotechnology Research in UBITA (CBRU), Konkuk University, 120 Neungdong-ro, Gwangjin-gu, Seoul 05029, Korea

amir@konkuk.ac.kr / shjung@konkuk.ac.kr

Cyclic oligosaccharide cross-linked hydrogels were prepared from varying amount of carboxymethylcellulose sodium salt (CMC), β-cyclodextrin (βCD) and cyclosophoraose using epichlorohydrin (ECH). The structure and morphology of the resulting hydrogels were characterized using Fourier transform infrared (FT-IR) spectroscopy, solid-state nuclear magnetic resonance (NMR) spectroscopy, field-emission scanning electron microscopy (FE-SEM). The swelling propertis of hydrogels were evaluated against aqueouse solution containig various salts. The results revealed that the cyclic oligosaccharide contributed to the change of pore sizes and the adsorption ability for target drugs with its strong complexation ability in the hydrogel. The cyclic oligosacchride cross-linked CMC hydrogel are promising for the application in the biomaterial field.

Keywords: Hydrogel, Carboxymethylcellulose, Cyclosophoraose, β-cyclodextrin, Swelling

Preparation and Characterization of Cyclic oligosaccharide cross-linked carboxymethylcellulose hydrogel

Daham (Jeong)[1], Ben El (Lee)[1], Sang-Woo (Joo)[1], Eunae (Cho)[2], Seunho (Jung)[1*]

[1]Department of Bioscience and Biotechnology, Microbial Carbohydrate Resource Bank (MCRB) & Center for Biotechnology Research in UBITA (CBRU), Konkuk University, Seoul 143-701, South Kore).

[2]Institute for Ubiquitous Information Technology and Applications (UBITA) & Center for Biotechnology Research in UBITA (CBRU), Konkuk University, 120 Neungdong-ro, Gwangjin-gu, Seoul 05029, Korea

amir@konkuk.ac.kr / shjung@konkuk.ac.kr

Cyclic oligosaccharide cross-linked hydrogels were prepared from varying amount of carboxymethylcellulose sodium salt (CMC), β-cyclodextrin (βCD) and cyclosophoraose using epichlorohydrin (ECH). The structure and morphology of the resulting hydrogels were characterized using Fourier transform infrared (FT-IR) spectroscopy, solid-state nuclear magnetic resonance (NMR) spectroscopy, field-emission scanning electron microscopy (FE-SEM). The swelling propertis of hydrogels were evaluated against aqueouse solution containig various salts. The results revealed that the cyclic oligosaccharide contributed to the change of pore sizes and the adsorption ability for target drugs with its strong complexation ability in the hydrogel. The cyclic oligosacchride cross-linked CMC hydrogel are promising for the application in the biomaterial field.

Keywords: Hydrogel, Carboxymethylcellulose, Cyclosophoraose, β-cyclodextrin, Swelling

Preparation and Characterization of Cyclic oligosaccharide cross-linked carboxymethylcellulose hydrogel

Daham (Jeong)[1], Ben El (Lee)[1], Sang-Woo (Joo)[1], Eunae (Cho)[2], Seunho (Jung)[1*]

[1]Department of Bioscience and Biotechnology, Microbial Carbohydrate Resource Bank (MCRB) & Center for Biotechnology Research in UBITA (CBRU), Konkuk University, Seoul 143-701, South Kore).

[2]Institute for Ubiquitous Information Technology and Applications (UBITA) & Center for Biotechnology Research in UBITA (CBRU), Konkuk University, 120 Neungdong-ro, Gwangjin-gu, Seoul 05029, Korea

amir@konkuk.ac.kr / shjung@konkuk.ac.kr

Cyclic oligosaccharide cross-linked hydrogels were prepared from varying amount of carboxymethylcellulose sodium salt (CMC), β-cyclodextrin (βCD) and cyclosophoraose using epichlorohydrin (ECH). The structure and morphology of the resulting hydrogels were characterized using Fourier transform infrared (FT-IR) spectroscopy, solid-state nuclear magnetic resonance (NMR) spectroscopy, field-emission scanning electron microscopy (FE-SEM). The swelling propertis of hydrogels were evaluated against aqueouse solution containig various salts. The results revealed that the cyclic oligosaccharide contributed to the change of pore sizes and the adsorption ability for target drugs with its strong complexation ability in the hydrogel. The cyclic oligosacchride cross-linked CMC hydrogel are promising for the application in the biomaterial field.

Keywords: Hydrogel, Carboxymethylcellulose, Cyclosophoraose, β-cyclodextrin, Swelling

Preparation and Characterization of Cyclic oligosaccharide cross-linked carboxymethylcellulose hydrogel

Daham (Jeong)[1], Ben El (Lee)[1], Sang-Woo (Joo)[1], Eunae (Cho)[2], Seunho (Jung)[1*]

[1]Department of Bioscience and Biotechnology, Microbial Carbohydrate Resource Bank (MCRB) & Center for Biotechnology Research in UBITA (CBRU), Konkuk University, Seoul 143-701, South Kore).

[2]Institute for Ubiquitous Information Technology and Applications (UBITA) & Center for Biotechnology Research in UBITA (CBRU), Konkuk University, 120 Neungdong-ro, Gwangjin-gu, Seoul 05029, Korea

amir@konkuk.ac.kr / shjung@konkuk.ac.kr

Cyclic oligosaccharide cross-linked hydrogels were prepared from varying amount of carboxymethylcellulose sodium salt (CMC), β-cyclodextrin (βCD) and cyclosophoraose using epichlorohydrin (ECH). The structure and morphology of the resulting hydrogels were characterized using Fourier transform infrared (FT-IR) spectroscopy, solid-state nuclear magnetic resonance (NMR) spectroscopy, field-emission scanning electron microscopy (FE-SEM). The swelling propertis of hydrogels were evaluated against aqueouse solution containig various salts. The results revealed that the cyclic oligosaccharide contributed to the change of pore sizes and the adsorption ability for target drugs with its strong complexation ability in the hydrogel. The cyclic oligosacchride cross-linked CMC hydrogel are promising for the application in the biomaterial field.

Keywords: Hydrogel, Carboxymethylcellulose, Cyclosophoraose, β-cyclodextrin, Swelling

Preparation and Characterization of Hydroxypropyl Cyclosophoraose-Pullulan Microspheres and Their Application in Naproxen Release

Jae Min (Choi)[1], Kyeong Hui (Park)[2], Jae-pil (Jeong)[2], Eunae (Cho)[1], Seunho (Jung)[2]*

[1]Institute for Ubiquitous Information Technology and Applications (UBITA) & Center for Biotechnology Research in UBITA (CBRU), Konkuk University, 120 Neungdong-ro, Gwangjin-gu, Seoul 05029, Korea

[2]Department of Bioscience and Biotechnology,, Microbial Carbohydrate Resource Bank (MBRC) & Center for Biotechnology Research in UBITA (CBRU), Konkuk University, 120 Neungdong-ro, Gwangjin-gu, Seoul 05029, Korea

jm.choi.25@gmail.com/ shjung@konkuk.ac.kr

The key feature of a drug delivery system is to transfer the proper amount of drug to a target site and then maintain the desired drug concentration over a period of time. There are various approaches to overcome the drawbacks of a conventional drug delivery system using biomaterials which are constantly being developed. For example, liposomes, hydrogels, polymer-based discs, rods, pellets, or microparticles have been used in controlled release systems [1]. In this study, we prepared hydroxyprolyl cyclosophoraose-pullulan (HPCys-pullan) microspheres for the first time as an efficient drug delivery system in which non-toxic pullulan was combined with the advantages of HPCys as a complexation host against the guest drug. The HPCys-pullan microspheres were made using pullulan crosslinked by epichlorohydrin with HPCys, and cyclosophoroase was isolated from *Rhizobium leguminosarum*. The physico-chemical properties of the microspheres were characterized with various instrumental analyses. Naproxen loading and release with the microspheres were investigated by UV-vis spectroscopy. The HPCys-pullulan microspheres were able to capture 759 μg/g (naproxen/microspheres, μg/g) of naproxen, which is 4.2 folds higher than that of the pullulan microspheres. Naproxen release from the HPCys-pullulan microspheres was controlled by pH difference, where the release of 630 μg/g of NPX at pH 7.2 decreased to 362 μg/g at pH

1.2. These results suggest that the HPCys-pullulan microspheres could be used as an efficient biomaterial for the controlled drug delivery.

Keywords: Pullulan, Hydroxypropyl Cyclosphoraose, Microspheres, Drug delivery, Naproxen

[1] CORY, B., Kyekyoon, K., & DANIEL, W. P. 2004. Precision Polymer Microparticles for Controlled-Release Drug Delivery. *Carrier-Based Drug Delivery*, 879, 197-213.

Preparation and Characterization of Hydroxypropyl Cyclosophoraose-Pullulan Microspheres and Their Application in Naproxen Release

Jae Min (Choi)[1], Kyeong Hui (Park)[2], Jae-pil (Jeong)[2], Eunae (Cho)[1], Seunho (Jung)[2]*

[1]Institute for Ubiquitous Information Technology and Applications (UBITA) & Center for Biotechnology Research in UBITA (CBRU), Konkuk University, 120 Neungdong-ro, Gwangjin-gu, Seoul 05029, Korea

[2]Department of Bioscience and Biotechnology,, Microbial Carbohydrate Resource Bank (MBRC) & Center for Biotechnology Research in UBITA (CBRU), Konkuk University, 120 Neungdong-ro, Gwangjin-gu, Seoul 05029, Korea

jm.choi.25@gmail.com/ shjung@konkuk.ac.kr

The key feature of a drug delivery system is to transfer the proper amount of drug to a target site and then maintain the desired drug concentration over a period of time. There are various approaches to overcome the drawbacks of a conventional drug delivery system using biomaterials which are constantly being developed. For example, liposomes, hydrogels, polymer-based discs, rods, pellets, or microparticles have been used in controlled release systems [1]. In this study, we prepared hydroxyprolyl cyclosophoraose-pullulan (HPCys-pullan) microspheres for the first time as an efficient drug delivery system in which non-toxic pullulan was combined with the advantages of HPCys as a complexation host against the guest drug. The HPCys-pullan microspheres were made using pullulan crosslinked by epichlorohydrin with HPCys, and cyclosophoroase was isolated from *Rhizobium leguminosarum*. The physico-chemical properties of the microspheres were characterized with various instrumental analyses. Naproxen loading and release with the microspheres were investigated by UV-vis spectroscopy. The HPCys-pullulan microspheres were able to capture 759 μg/g (naproxen/microspheres, μg/g) of naproxen, which is 4.2 folds higher than that of the pullulan microspheres. Naproxen release from the HPCys-pullulan microspheres was controlled by pH difference, where the release of 630 μg/g of NPX at pH 7.2 decreased to 362 μg/g at pH

1.2. These results suggest that the HPCys-pullulan microspheres could be used as an efficient biomaterial for the controlled drug delivery.

Keywords: Pullulan, Hydroxypropyl Cyclosphoraose, Microspheres, Drug delivery, Naproxen

[1] CORY, B., Kyekyoon, K., & DANIEL, W. P. 2004. Precision Polymer Microparticles for Controlled-Release Drug Delivery. *Carrier-Based Drug Delivery*, 879, 197-213.

Preparation and Characterization of Hydroxypropyl Cyclosophoraose-Pullulan Microspheres and Their Application in Naproxen Release

Jae Min (Choi)[1], Kyeong Hui (Park)[2], Jae-pil (Jeong)[2], Eunae (Cho)[1], Seunho (Jung)[2]*

[1]Institute for Ubiquitous Information Technology and Applications (UBITA) & Center for Biotechnology Research in UBITA (CBRU), Konkuk University, 120 Neungdong-ro, Gwangjin-gu, Seoul 05029, Korea

[2]Department of Bioscience and Biotechnology,, Microbial Carbohydrate Resource Bank (MBRC) & Center for Biotechnology Research in UBITA (CBRU), Konkuk University, 120 Neungdong-ro, Gwangjin-gu, Seoul 05029, Korea

jm.choi.25@gmail.com/ shjung@konkuk.ac.kr

The key feature of a drug delivery system is to transfer the proper amount of drug to a target site and then maintain the desired drug concentration over a period of time. There are various approaches to overcome the drawbacks of a conventional drug delivery system using biomaterials which are constantly being developed. For example, liposomes, hydrogels, polymer-based discs, rods, pellets, or microparticles have been used in controlled release systems [1]. In this study, we prepared hydroxyprolyl cyclosophoraose-pullulan (HPCys-pullan) microspheres for the first time as an efficient drug delivery system in which non-toxic pullulan was combined with the advantages of HPCys as a complexation host against the guest drug. The HPCys-pullan microspheres were made using pullulan crosslinked by epichlorohydrin with HPCys, and cyclosophoroase was isolated from *Rhizobium leguminosarum*. The physico-chemical properties of the microspheres were characterized with various instrumental analyses. Naproxen loading and release with the microspheres were investigated by UV-vis spectroscopy. The HPCys-pullulan microspheres were able to capture 759 μg/g (naproxen/microspheres, μg/g) of naproxen, which is 4.2 folds higher than that of the pullulan microspheres. Naproxen release from the HPCys-pullulan microspheres was controlled by pH difference, where the release of 630 μg/g of NPX at pH 7.2 decreased to 362 μg/g at pH

1.2. These results suggest that the HPCys-pullulan microspheres could be used as an efficient biomaterial for the controlled drug delivery.

Keywords: Pullulan, Hydroxypropyl Cyclosphoraose, Microspheres, Drug delivery, Naproxen

[1] CORY, B., Kyekyoon, K., & DANIEL, W. P. 2004. Precision Polymer Microparticles for Controlled-Release Drug Delivery. *Carrier-Based Drug Delivery*, 879, 197-213.

Size-changeable Graphene Quantum Dot Nano-aircrafts for Penetrated Drug Delivery and Photothermal Therapy

Yu-Lin Su, Yun-Ting Lee, Shuo-Yuan Song, Shang-Hsiu Hu*

Department of Biomedical Engineering and Environmental Sciences,

National Tsing Hua University, Hsinchu, 300, Taiwan

yuhlinsu@hotmail.com.tw

Delivery within carriers that effectively accumulate at tumor promotes improving the tumor therapeutic efficacy. Due to heterogeneity, however, these carriers which usually display low accumulation and are piled up at the tumor's periphery blood veesels must address the issues for effective therapy. Here, a size-changeable graphene quantum dot (GQD) nano-aircraft is developed to solve these problems. GQD (5 nm) functionalized by pH-sensitive N-acetyl histidine-conjugated D-α-tocopherol polyethylene glycol 1000 succinate (HTPGS) that changes its size and aggregates at tumor through pH-sensitivity exhibits a double increase in accumulation than it without modification. Furthermore, this nano-aircraft carries high payload of doxorubicin (DOX) on GQD and possesses long half-life in circulation with PEG on HTPGS. A size conversion was actuated by NIR which disassembles 450 nm of nano-aircraft clusters into 5 nm of DOX/GQD like bombs-loaded jets, facilitating the penetration far from tumor blood vessels, achieved by atomic-thin structures of GQD and hyperthermia. Followed by sequentially releasing DOX near the nucleus, GQD nano-aircraft integrates a penetrated photothermal-chemo therapy.

Keywords: Graphene quantum dot, pH-sensitive, tumor penetration, photothermal-chemo therapy

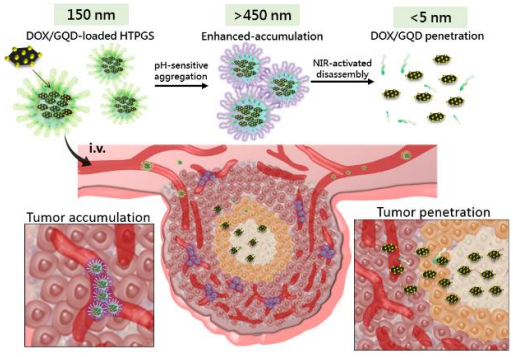

[1] H. Kobayashi, R. Watanabe, P.L. Choyke, Improving conventional enhanced permeability and retention (EPR) effects; what is the appropriate target?, *Theranostics*, 4 (2013) 81-89.

[2] H. Yu, Z. Cui, P. Yu, C. Guo, B. Feng, T. Jiang, S. Wang, Q. Yin, D. Zhong, X. Yang, Z. Zhang, Y. Li, pH- and NIR Light-Responsive Micelles with Hyperthermia-Triggered Tumor Penetration and Cytoplasm Drug Release to Reverse Doxorubicin Resistance in Breast Cancer, *Adv. Funct. Mater.*, 25 (2015) 2489-2500.

Combined sensing and concentrating in one-chip by an microelectrode array for biological applications

Hye Jin Kim[1, 2], Jinsik Kim[1], Yong Kyoung Yoo[1], Myung-Sic Chae[1], Gangeun Kim[1], Jung Ho Park[2] and Kyo Seon Hwang[1]

[1]Center for BioMicrosystems, Korea Institute of Science and Technology, Seoul 136-791, Korea

[2]Department of Electrical Engineering, Korea University, Seoul 136-713, Korea

kshwang@kist.re.kr/ Kyo Seon Hwang

One of the focus points in sensor research field is improving the sensing performance of sensor to detect biomolecule in lower concentration range. Enhancing of the K_d value (dissociation constant) of antibody-antigen pairs is important to promote the performance of the sensor. For it, many methods to improve the K_d value with longer incubation (binding time) and with high concentration of antigen are attempted such as a concentration using many materials [1-3]. But the concentration using many materials, almost methods to improve the K_d, use the different materials for sensing and concentrating of targets; concentration using polymer layer and sensing using conductive material [2], concentration and sensing using different conductive materials [4, 5].

Here, we suggest a simple concept based on interdigitated microelectrodes to detect and concentrate in one-chip with improved performance. By applying the AC voltage to the arrays of conductive and dielectric materials to be used as sensor, the sensing and concentrating is occurred in same conductive materials of one-chip. Also, a concentration by AC voltage increases the K_d value of antibody-antigen and consequently the performance of sensor, such as sensitivity and the limit of detection, is promoted.

To proof of the concept, the resistance change (ΔR) of the sensor by reaction of the antibody-antigen is compare in reference condition (without AC voltage for immune reaction) and AC condition (with AC voltage for immune reaction). The sensor consisted of a 30 pairs of platinum (Pt) with 5 μm interval and width is fabricated on SiO_2 surface and is filled with a PBS buffer. For immunoassay, the antibody is immobilized on SiO_2.

Applied frequency is fixed at 50 MHz [6]. Applied voltage (V_a) to trap the 4.5 kDa antigen (Amyloid beta 42 protein, Aβ42) on reaction region is calculated by COMSOL and the V_a is computed 5 V. Actually, ΔR by 10 pg mL^{-1} Aβ42 has a maximum value in V_a = 0.5 V and decrease under and over the condition.

Also, ΔR by Aβ42 in range 0.01 pg mL^{-1} to 100 pg mL^{-1} is measure in reference and AC condition. The ΔR change about 1.36 to 4.08% and 2.95 to 6.07% in reference and AC condition respectively by concentration of Aβ42 and the sensitivity enhances about 2.11-fold. Also, the LOD improves under the 0.01 pg mL^{-1} by concentrating considering that the background noise by non-specific binding is about 2%. The improvement of sensor`s performance is also observed using fluorescent image and the intensity by fluorescent is higher about 2-fold in AC condition.

Moreover, the expandability of the concept is verified using other molecules, a 34 kDa PSA protein. The V_a to trap the PSA protein is computed 0.02 V, and in the condition ΔR by 1 pg mL^{-1} PSA protein is biggest. Also, the sensitivity improves about 2.35-fold and the LOD enhances (ΔR is changed about 1.93 to 2.84% and 2.94 to 5.08% in reference and AC condition respectively in PSA range 1 pg mL^{-1} to 1000 pg mL^{-1}).

Consequently, we verify that the detection and concentration is able to be occurred in one-chip followed by the enhancement of the sensor`s performance.

Keywords: Enhancement of sensitivity, Lab on a chip, conductive material array, bio-sensor

[1] A. E. Herr, A. V. Hatch, D. J. Throckmorton, H. M. Tran, J. S. Brenna, W. V. Giannobile and A. K. Singh, 2007, PNAS, 104, 5268-5273.

[2] H. Song, Y. Wang, C. Garson, K. Pant, 2014, Microfluid Nanofluid, 17, 693-699.

[3] L. F. Cheow, S. H. Ko, S. J. Kim, K. H. Kang and J. Han, 2010, Anal. Chem, 82, 3383-3388.

[4] Y.-H. Choi, D. –H. Kang, S. –I, Yoon, M. –g. Kim, J. Sim, J. Kim and Y. –J. Kim, 2011, MEMS 2001, Cancun, MEXICO, 23-27.

[5] Y. –C. Wang and J. Han, 2008, Lab Chip, 8, 392-394.

[6] S. I. Han, S. M. Lee, Y. D. Joo and K. H. Han, 2011, Lab Chip, 11, 3864-3872.

Inkjet Printed Ag-Nanoparticle Light Filters - Light Emitting Diode Irradiation Control of Optical Properties of PEI/Ag layers

Falk Kemper (Kemper)[1,2], Erik Beckert (Beckert)[1], Ramona Eberhardt (Eberhardt)[1], Andreas Tünnermann (Tünnermann)[1,2]

[1]Fraunhofer Institute for Applied Optics and Precision Engineering (IOF), Albert-Einstein-Str. 7, D-07745 Jena, Germany

[2]Institute of Applied Physics, Abbe Center of Photonics, Friedrich Schiller University Jena, Max-Wien-Platz 1, D-07743 Jena, Germany

falk.kemper@iof.fraunhofer.de
erik.beckert@iof.fraunhofer.de
ramona.eberhardt@iof.fraunhofer.de
andreas.tuennermann@iof.fraunhofer.de

Microfluidic lab-on-a-chip systems (LoCs) integrate chemical or biological micro-reactions on compact chips. Polymer replication techniques ensure that the production of these chips having low manufacturing costs and are therefore disposable and suitable for single-use. When further on-chip functionalities are integrated to replace expensive external lab equipment, low-cost manufacturing will be essential. Inkjet printing provides the possibility of depositing different functional materials in a non-contact and mask-less manner. This flexibility enables the integration of many functionalities such as pumping, heating or optical detection onto those LoCs [1].

For investigation of analytes with LoCs fluorescent light detection is widely used because it is a very sensitive measurement technique with the possibility of detecting very low concentrations of the substance of interest. To perform fluorescent light detection, a light filter must be combined with a sensitive photodetector in order to exclude measurement error from excitation light. The surface plasmon resonance (SPR) of nanoparticles can be used to absorb light of a certain wavelength. Depending on the size and shape of these nanoparticles, the absorption band changes [2]. In this contribution we demonstrate the integration of silver nanoparticles into polyethylene imine (PEI) layers by inkjet printing those layers, using either a PEI/Ag-NP/I2959 dispersion or a PEI/$AgNO_3$/I2959 solution.

Once the layer is dried, spherical Ag-nanoparticles can be formed by UV-light exposure. As it was shown in water before [2], the I2959 photo inhibitor reduces the Ag ions inside the layers to Ag atoms leading to an initial nanoparticle formation. In case of the PEI/Ag-NP printing this was done in solution before printing it. An absorption peak at ≈ 400 nm occurs; this is related to the SPR of very small, spherical Ag-nanoparticles. By exposing the resulting seed layers to intense visible LED light, the absorption properties of the nanoparticles can be changed by affecting their shape and size. Ag atoms are expected to adsorb at energetically preferable positions at the nanoparticles, depending on the forced oscillation of the plasmons. Therefore, the absorption band of the filter layers can be varied depending on the emission wavelength of the LEDs. With this method, the whole visual light spectrum can be addressed, showing a very flexible way to adapt a light filter to any wavelength for fluorescent light detection.

In this contribution, the shaping of silver nanoparticles by LED irradiation inside a solid polymer layer is presented for the first time. The resulting colored layers can be used for light filtration purposes. The spectra of the different shaped Ag-nanoparticles can be adapted to different absorption bands within the whole visible spectrum. The optical layer properties mainly depend on the post treatment. Therefore, the possibility of printing only one ink for many different applications makes the process simple and cost effective.

Keywords: inkjet, printing, light filter, surface plasmon resonance, nanoparticles

[1] BECKERT, E., EBERHARDT, R., PABST, O., KEMPER, F., SHU, Z., TÜNNERMANN, A., PERELAER, J., SCHUBERT, U. & BECKER, H. 2013. Inkjet printed structures for smart lab-on-chip systems. *Proc. SPIE 8615*, 86150E.

[2] MOCK, J. J., BARBIC, M., SMITH, D. R., SCHULTZ, D. A. & SCHULTZ, S. 2002. Shape effects in plasmon resonance of individual colloidal silver nanoparticles. Journal of Chemical Physics 116, 6755-6759

[3] STAMPLECOSKIE, K. G. & SCAIANO, J. C. 2010. Light Emitting Diode Irradiation Can Control the Morphology and Optical Properties of Silver Nanoparticles. Journal of the American Chemical Society, 132, 1825–1827.

Monitoring of amyloid-beta fibrillogenesis with reduced graphene oxide based biosensor

Dahye Jeong[1,2], Jinsik Kim[1], Myung-Sic Chae[1], Yong Kyoung Yoo[1], Hye Jin Kim[1], Gangeun Kim[1], Jungkyu Choi[2] and Kyo Seon Hwang[1]

[1]Center for BioMicrosystems, Korea Institute of Science and Technology, Seoul, Korea

[2]Department of Chemical and Biological Engineering, Korea University, Seoul, Korea

- *Presenter : dahye303@gmail.com / Dahye Jeong*
- *Contact Author : kshwang@kist.re.kr/ Kyo Seon Hwang*

Alzheimer's disease (AD) is one of the worldwide issues in aging society. Efforts to diagnose with human body fluid in early stage of AD have been performed by various methods. In human body fluid-based AD diagnosis, monitoring the ratio of amyloid-beta (Aβ) type is essential information to know the status of AD. The Aβ is a peptide of 39-43 amino acid residues strongly associated with AD and Aβ monomers are prone to cleave an insoluble Aβ aggregates such as oligomers and fibrils and these pathogenic progress is commonly called Aβ fibrillogenesis [1]. The Aβ aggregates have toxicity leading to cell death and progression of neurodegenerative diseases, monitoring Aβ fibrillogenesis plays important role in study of AD [2].

For the exact monitoring of Aβ fibrillogenesis, electrical measurement with reduced graphene oxide (rGO) was utilized. The rGO has both remarkable electrical properties and surface functionalities as graphene, so that researchers have studied to develop as graphene-based biosensing applications. The rGO has more uniformity and reproducibility in fabrication process than the process with graphene into a single-device level [3].

Here we utilized rGO films as sensing interfaces of biomolecule interactions fabricated with conventional microelectromechanical system (MEMS) process to detection of Aβ monomer and its pathogenesis. In order to fabricate rGO-based sensor, GO films were deposited on 300 nm SiO_2 substrate by meniscus-dragging deposition which is simple and inexpensive method rather than conventional manner [3]. The GO films were chemically reduced by acetic acid and hydriodic acid vapor to form rGO. Then rGO films were patterned by dimension of $100\times50\ \mu m^2$ with photolithography and oxygen plasma assisted etching process. The Cr/Au (500/2000 nm)

electrodes were patterned as contact pads for rGO patterns by lift-off technique. The conductivity change of rGO patterns from biomolecular interaction were measured by I-V meter.

In order to monitor Aβ fibrillogenesis, rGO sensor was functionalized with 10 μg/mL monoclonal Aβ antibody which has binding specificity to 1-16 amino acid residues of Aβ monomers on rGO surface. The antibody was covalently immobilized on rGO surface with coupling agents. The samples of Aβ aggregates were prepared by incubation of 100 pg/mL Aβ peptides in 10 mM phosphate-buffered saline (PBS) at 37 ℃ for several hours to lead fibrillization. When the samples were introduced, the conductivity changes by molecular interaction between antibody and Aβ monomers decreased over fibrillization time. The results implied that the concentration of Aβ monomers lowered by forming Aβ aggregates over the time. The formation of Aβ aggregates in pathogenic progress were also observed by atomic force microscopy (AFM) to cross-check. With theses results, the rGO sensor is sufficient to monitor an important pathogenic progress of AD by detection of Aβ monomers and has feasibilities toward biological sensing application.

Keywords: Reduced graphene oxide, fibrillogenesis, amyloid-beta, Alzheimer's disease

[1] WALSH, D., LOMAKIN, A., BENEDEK, G., CONDRON, M. AND TEPLOW, D. 1997. Amyloid β-Protein Fibrillogenesis: DETECTION OF A PROTOFIBRILLAR INTERMEDIATE. *Journal of Biological Chemistry*, 272(35), 22364-22372.

[2] KIM, H., KIM, H., JO, S., LEE, C., CHOI, S., KIM, D. AND KIM, Y. 2015. EPPS rescues hippocampus-dependent cognitive deficits in APP/PS1 mice by disaggregation of amyloid-β oligomers and plaques. *Nature Communications*, 6(8997), 1-12.

[3] KO, Y., KIM, N., LEE, N. AND CHANG, S. 2014. Meniscus-dragging deposition of single-walled carbon nanotubes for highly uniform, large-area, transparent conductors. *Carbon*, 77, 964-972.

A polymeric microfluidic device integrated with functionalized nanoporous alumina membranes for electrochemical detection of multiple foodborne pathogens

Yu Zhang[1], Tian Feng[2], Mo Yang[2]

[1]Mechanical Engineering, the Hong Kong Polytechnic University, Hong Kong

[2]Interdisciplinary Division of Biomedical Engineering, the Hong Kong Polytechnic University, Hong Kong

E Mail: fiona.yu.zhang@polyu.edu.hk

Conventional biochemical methods for foodborne pathogen detection are time-consuming, labor-intensive and can only be used for single type bacteria detection with one sample.[1,2] There is always an urgent need for fast, accurate and easy to handle devices for identification and monitoring of multiple foodborne pathogens at the same time. Recently, nanoporous membrane based electrochemical sensor has been used in biosensing areas due to its enhanced sensitivity and easy fabrication process. Especially, alumina nanoporous membrane has aroused much interest due to its high surface to volume ratio, established fabrication process and good biocompatibility. Herein, we present a non-biofouling polyethylene glycol (PEG) based microfluidic chip integrated with functionalized nanoporous alumina membrane for simultaneous electrochemical detection of two types of bacteria *Escherichia coli O157:H7* and *Staphylococcus aureus* from the mixed samples. The sensing mechanism is based on the nanopore blocking effect by captured pathogens on the nanoporous membrane through antigen-antibody interaction. The experimental results demonstrated the specificity for target bacteria detection and the low cross-binding of non-target bacteria. The simultaneous detection of mixed bacteria sample of *E. coli O157:H7* and *S. aureus* was also demonstrated. This sensor has a linear detection range from 10^2 CFU/mL to 105 CFU/mL with the limit of detection (LOD) around 10^2 CFU/mL.

Keywords: Nanopoous membrane, electrochemical sensor, microfluidic device, food-borne pathogens

References

[1] SANDSTROM, G.E., WOLF-WALTZ, H., TARNVIK, A. 1986, Duct ELISA for detection of bacteria in fluid samples *J. Microbiol. Methods*, 5, 41–47.

[2] CIERVO A., PETRUCCA, A., VISCA, P., CASSONE, A., Evaluation and optimization of ELISA for detection of anti-Chlamydophila pneumoniae IgG and IgA in patients with coronary heart diseases, 2004, *J. Microbiol. Methods*, 59, 135–140

Femto-molar sensitive Amyloid β detection and quantification with ion concentration polarization integrated sensor

Yong Kyoung Yoo[1,2], Sung Il Han[1], Junwoo Lee[1], Cheonjung Kim[1], Kyoungjae Lee[1], Kyo Seon Hwang[2], Jeong Hoon Lee[1]

[1]Kwangwoon Universitiy, Korea.

[2]Korea Institute of Science and Technology (KIST), Korea.

yongkyoung0108@gmail.com / jhlee@kw.ac.kr

Sensitivity and detection limit in low concentration of the dissociation constant below between recognition and target materials are the most important criteria that aim to analysis of molecular interaction for biochemistry: genomics, proteomics and pathogenesis. To enhance sensitivity and detection limit and overcome low affinity from low concentration and high dissociation constant, various study have been reported with new materials and scale down and hybridization between each other technique. There are still few report for the realistic example although many research group have been investigated on various type sensor. Recently, due to high preconcentrator factor and simple method, the interest of ion concentration polarization (ICP) for sensor has been increasingly recognized. [1]

Here, we report ion concentration polarization based preconcentrator with ion perm-selective material integrated electrical biosensor system to overcome low affinity of low concentration. Furthermore, we have been detect Amyloid β sample (Aβ; as known as the strongest biomarker of Alzheimer's disease) of femto-molar with high dissociation constant (K_D = 22.3 nM) between Aβ and antibody. For Aβ detection, we have developed optimized interdigitated microelectrodes (IMEs) sensor. And also, we achieve approximately 25-fold concentrated sample on IMEs sensor with ICP preconcentrator. Utilizing ICP preconcentrator integrated IMEs sensor, we are able to detect below 22.15 fM Aβ with 3.2-fold higher sensitivity of impedance change. Moreover, detection limit of Aβ has also improved under concentration of 2.215 fM with ICP preconcentrator integrated IMEs sensor. From these results show our newly proposed ICP preconcentrator integrated IMEs sensor was better than conventional method for detection and quantification of low Aβ level and affinity. Also, a unifying technique between preconcentration and sensor

platform is provide new opportunities with analytical sensitivity and detection limit within a few minutes.

Keywords: ICP, low affinity, Amyloid ß, dissociation constant

[1] Y. Wang, J. Han 2008. Pre-binding dynamic range and sensitivity enhancement for immuno-sensors using nanofluidic preconcentrator. *Lab on a Chip*, 8, 392-394.

Biocompatibility of screen printed graphene-carbon paste electrode for MDA-MB-231 breast cancer cells-based electrochemical detection

U. Waiwijit[1], S. Pakapongpan[1], D. Phokharatkul[2], A. Wisitsoraat[2], A. Tuantranon[1]

[1]Thai Organic and Printed Electronics Innovation Center, [2]Nanoelectronics and MEMS Laboratory, National Electronics and Computer Technology Center (NECTEC), Nationual Science and Technology Development Agency (NSTDA), 112 Thailand Science Park, Thanon Phahonyothin, Tambon Khlong Neung, Amphoe Khlong Luang, Pathum Thani 12120, Thailand.

Uraiwan.waiwijit@nectec.or.th

Graphene-based electrochemical electrodes have been recently employed for cell-based biosensing. Cell–substrate interactions play crucial roles in proliferation, differentiation and apoptosis. However, it has not been well studied on graphene-based electrodes. In this work, biocompatibility of screen printed graphene–carbon paste electrode (SPGE) with MDA-MB-231 breast cancer cells is determined by electrochemical measurements. SPGE was prepared by mixing 2.5 wt. % of graphene powder into carbon paste and screen printed with a 0.5 cm^2 circular pattern on glass substrate using semi-automatic screen printer. The characterizations by scanning electron microscope (SEM) and Raman spectroscopy confirmed that multi-layer of graphene dispersed on carbon paste electrode. Electrochemical measurement was performed in a cylindrical PDMS chamber that could compactly contain three electrochemical electrodes. SPGE, a platinum wire, and Ag/AgCl electrode were used as working (WE), counter (CE) and reference (RE) electrode, respectively. The cancer cells were immobilized on SPGE surface for 24 hrs and cyclic voltammetric (CV) experiments were performed in a potential range from +0.1 to +1.0 V at a scan rate of 50 mV/s. The CV curve indicates an irreversible

electrochemical reaction with an anodic peak at +0.8 V. The anodic peak may be attributed to the oxidation of H_2O_2 generated from the cells. The relationship between the peak current and the cell number was determined. It shows a linear plot of oxidation peak current as a function of cell number and the peak current is found to increase linearly with the increasing cell number. Trypan Blue and nucleus fluorescence staining were performed and confirmed the cell viability in accordance with the CV results. Therefore, SPGE is useful not only as a biocompatibility substrate for the culture of cancer cells but also as an electrode for measurement of cellular electrochemical properties and assessment of cell viability.

Keywords: graphene–carbon paste electrode, screen printed, biocompatibility, cyclic voltammetry, cell-based electrochemical sensor

[1] W. A. El-SAID, C. H. YEA, H. Kim, B. K. OH, and J. W. CHOI, 2009. Cell-based chip for the detection of anticancer effect on HeLa cells using cyclic voltammetry. *Biosens Bioelectron*, 24, 1259-1265.

Symposia 6

Advances in Catalysis

- Homogeneous and Heterogeneous Catalysis
- Nano and Environmental catalysis
- New concepts in catalyst design and preparation
- Industrial and green catalysis
- Theoretical modeling of catalytic reactions
- Catalyst preparation & characterization
- Organo-metallic catalyst
- Catalysis for chemical energy transformation and storage
- Catalysis for clean energy, Transportation, industrial and domestic fuels
- Catalytic transformation of CO2
- Others

Index Page

Design, Synthesis and Structure-Performance Relationship of High Performance Cathode Catalysts for Li-air Batteries

Rui Gao, Xiuling Zhang, Zhongbo Hu, Xiangfeng Liu*

（*College of Materials Science and Opto-Electronic Technology, University of Chinese Academy of Sciences, Beijing,100049*）

E-mail: liuxf@ucas.ac.cn

Recently, rechargeable Li-air batteries have attracted extensive attention due to their high energy density. However, the poor cycling stability, low rate capability, low coulombic efficiency, high charge-discharge voltage gap and some other problems hinder the practical application of Li-air battery. The sluggish kinetics of the oxygen reduction reaction (ORR) and oxygen evolution reaction (OER) on the cathode is one of the biggest challenges for Li-air batteries. One effective way to solve this issue is to develop efficient cathode catalysts. Some noble metals or alloys, metal oxides and nanostructured carbon materials have been extensively studied as cathode catalysts to facilitate ORR/OER and enhance the electrochemical performances of Li-O_2 battery. Herein, the study on the structure-performance relationship of some transition metal oxides based cathode catalysts with different surface or interface structures (exposed crystal planes, electron structures, atom arrangements, oxygen vacancies, and so on.) in our group will be presented.

Experimental Studies of Gas Adsorption on Alkali Promoted $Cu/ZnO/Al_2O_3$ Catalyst for Higher Alcohol Synthesis

Ji In Park[1,3], Jae-Sun Jung[1,2], Gi Hoon Hong[1,2], Kwan Young Lee[3], and Dong Ju Moon[1,2]

[1]Clean Energy Research Center, Korea Institute of Science and Technology, Seoul, Korea

[2]Clean Energy & Chemical Engineering, University of Science and Technology, Daejeon, Korea

[3]Chemical and Biological Engineering, Korea University, Seoul, Korea

Corresponding author. Email: djmoon@kist.re.kr

Presenting author. Email: parkjiin@naver.com

Higher alcohols have been interesting research subject as alternative resources for clean fuels, as well as fuel additives. Increasing concerns over global climate crisis, Higher alcohol can be used for fuel additives to substitute petroleum energies.

Alkali promoted $Cu/ZnO/Al_2O_3$ catalysts was used for studies of gas adsorption based on our previous study which suggested that alkali promoted $Cu/ZnO/Al_2O_3$ catalysts have more basic site on the surface because of high basicity of alkali metal.

In this experiment, Adsorption of CO was identified with in-situ DRIFT to show which sites adsorb the carbon monoxide over $Cu/ZnO/Al_2O_3$ and alkali promoted $Cu/ZnO/Al_2O_3$ catalysts. Temperature-programmed desorption of CO_2, Methanol and Ethanol was carried out to know how much gases adsorbed on each catalysts and correlation between the adsorption of these gases and higher alcohol synthesis.

Keywords: Higher Alcohol Synthesis, Gas Adsorption, Promoter, Basicity

[1] J. H. Lee, K. H. Reddy, J. S. Jung, E. H. Yang, and D. J. Moon, *Appl. Catal. A Gen.* 480, 128 (**2014**).

The Effect of Nickel Loading on Production of SNG over Silicon Carbide Support

Jae Sun Jung[1,2], Eun-hyeok Yang[1,2], Ga-yeong Joo[1], Young-su Noh[1], and Dong Ju Moon*[1,2]

[1] Clean Energy Research Center, KIST, Seoul, Korea
[2] Clean Energy & Chemical Engineering, UST, Daejeon, Korea

**djmoon@kist.re.kr*

In recent years, production of synthetic or substitute natural gas(SNG) from coal or biomass has attracted much interest due to the increasing demand for natural gas, the wish for enhancing domestic energy security, the opportunity of reducing CO_2 emission, and the high energetic conversion efficiency.[1-2]

Silicon carbide (SiC) have many physical properties such as excellent mechanical strength, superior thermal stability, high heat conductivity, and chemical inertness. It is important catalyst support instead of the traditional insulated supports in highly endothermic or exothermic reactions such as methanation reaction and Fischer Tropsch Synthesis.[2]

A series of Ni (5-30 wt %) based SiC supported catalysts were prepared by impregnation method and investigated for methanation reaction. The methanation reaction was carried out in a fixed bed reactor system with the H_2/CO molar ratio of 3, GHSV of 10,000h^{-1}, reaction temperature of 350℃ and reaction pressure of 20 bar for 40 h. All catalysts have been characterized by N_2 physisorption, XRD, TPR, TGA, SEM and TEM techniques. The aim of this research is to find out the effect of nickel loading on production of SNG over silicon carbide support.

Keywords: nickel, silicon carbide, Methanation, synthetic or substitute natural gas (SNG)

[1] GUOQUAN Z., TIANJUN S., JIAXI P., SHENG W., SHUDONG W., 2013. A comparison of Ni/SiC and Ni/Al2O3 catalyzed total methanation for production of synthetic natural gas, Applied Catalysis A: General 462– 463, 75– 81.

[2] JAE SUK L., JAE SUN J., DONG JU M., 2015. The Effect of Cobalt Loading on Fischer Tropsch Synthesis Over Silicon Carbide Supported Catalyst. Journal of Nanoscience Nanotechnology 15, 396–399.

Catalytic Convsersion of Syngas to Higher Alcohols over Mesoporous Perovskite Catalytsts

Tae-Wan Kim[1,*], Freddy Kleitz[2], Mahesh Muraleedharan Mair[2], and Chul-Ung Kim[1]

[1] Center for Convergent Chemical Process, Korea Research Institute of Chemical Technology, 141, Gajeong-ro, Yuseong-gu, Daejeon 305-600, South Korea.

[2] Department of Chemistry and Centre de recherche sur les matériaux avancés (CERMA), Universite Laval, Quebec, G1V0A6, QC, Canada.

twkim@krict.re.kr/tel: +82-42-860-7257, fax: +82-42-860-7508

C_{2+} alcohols (higher alcohols) have been attracted interest as a use of alternative fuels, fuel additives, energy carriers, and basic materials or intermediates for chemical feedstocks [1–3]. Conventionaly ethanol is produced by fermentation of edible resoures, and propanol and butanol are obtained from petroleum derived light olefins. Under present circumstances such as high oil price, oil depletion, and readuction of greenhouse gas have pushed up the request of developing alternative routes for production of higher alcohols from renewable, non-edible, and non-petroluem resources such as biomass, natural gas, and coal. In addition, newly accessibility of nonconventional natural gas (shale gas) has brought about an increase interest in the catalytically thermo-chemical conversion of syngas-to-higher alcohols (STA) coupled with reforming of natural gas to syngas. Perovskite-type oxide (PTOs) have attracted their wide applications in catalysts due to high catalytic activity, thermal stability and low cost [4]. Particulary, PTOs have been used as FT and STA catalysts for conversion of syngas to many useful chemcials and liquid fuels due to uniformly distributed the active metal ion species at the atomic level in the spinel structure [5–8]. However, perovskites prepared by conventional synthetic methods still have low specific surface areas (<10 m^2/g) and poor porosity, which limit their efficiency in potential applications. Two types of pervoskite-type mixed oxide materials (PTOs), $LaCo_{0.7}Cu_{0.3}O_3$ and $LaFe_{0.7}Cu_{0.3}O_3$, were synthesized by combining a template-synthetic route and a citrate complex method. The PTOs possess mesoporosity, high surface area and large pore volume comparing with a typical perovskite material. The mesoporous PTOs (Meso-PTOs) were introduced as catalysts for the catalytic conversion of syngas-to-

higher alcohol. The characteristics of the catalysts were analyzed through a series of different techniques, including transmission electron microscopy (TEM), powder X-ray diffraction (XRD), N_2 sorption analysis, and temperature programing reduction (TPR) analysis. The catalytic performances of syngas-to-higher alcohol using the Meso-PTO were tested in a fixed-bed reactor with various reaction conditions such as temperature, pressure, and space velocity. Meso-PTO catalysts exhibited superior catalytic activity compared with bulk-PTO catalyst, which could be attributed to the increase of active sites by the high surface of Meso-PTO materials. Among the two types of Meso-PTO catalysts, it was found that the mesoporous $LaFe_{0.7}Cu_{0.3}O_3$ catalyst show better higher alcohol selectivity and lower methane selectivity than the mesoporous $LaCo_{0.7}Cu_{0.3}O_3$ catalyst. The maximum space-time-yield of total higher alcohols and C_{2+} oxygenates using the Meso-$LaFe_{0.7}Cu_{0.3}O_3$ catalyst was 448 and 1003 mg/(g_{-cat} h), respectively.

Keywords: Mesoporous material, Mixed Alcohols, Syngas to alcohols, Mesoporous perovskite, Perovskite catalyst

[1] SURISETTY, V. R., DALAI, A. K. & KOZINSKI, J. 2011. Alcohols as alternative fuels: An overview. *Applied Catalysis A: General,* 404**,** 1-11.

[2] GUPTA, M., SMITH, M. L. & SPIVEY, J. J. 2011. Heterogeneous Catalytic Conversion of Dry Syngas to Ethanol and Higher Alcohols on Cu-Based Catalysts. *ACS Catalysis,* 1**,** 641-656.

[3] FANG, K., LI, D., LIN, M., XIANG, M., WEI, W. & SUN, Y. 2009. A short review of heterogeneous catalytic process for mixed alcohols synthesis via syngas. *Catalysis Today,* 147**,** 133-138.

[4] PE A, M. A. & FIERRO, J. L. G. 2001. Chemical Structures and Performance of Perovskite Oxides. *Chemical Reviews,* 101**,** 1981-2018

[5] ESCALONA, N., FUENTEALBA, S. & PECCHI, G. 2010. Fischer–Tropsch synthesis over LaFe1−xCoxO3 perovskites from a simulated biosyngas feed. *Applied Catalysis A: General,* 381**,** 253-260.

[6] BEDEL, L., ROGER, A. C., ESTOURNES, C. & KIENNEMANN, A. 2003. Co0 from partial reduction of La(Co,Fe)O3 perovskites for Fischer–Tropsch synthesis. *Catalysis Today,* 85**,** 207-218.

[7] SOUZA, J. R., MELO, M. A. F., MELO, D. M. A., ROJAS, L. O. A., SILVA, C. F. & OLIVEIRA, F. S. 2011. LayCu0.4Fe0.6O3 PEROVSKITE OXIDES: SYNTHESIS, CHARACTERIZATION AND CATALYTIC REACTIVITY IN THE FISCHER-TROPSCH SYNTHESIS. *Brazilian Journal of Petroleum and Gas,* 5**,** 1-9.

[8] TIEN-THAO, N., ALAMDARI, H., ZAHEDI-NIAKI, M. H. & KALIAGUINE, S. 2006. LaCo1−xCuxO3−δ perovskite catalysts for higher alcohol synthesis. *Applied Catalysis A: General,* 311**,** 204-212.

Catalytic Fast Pyrolysis of Wood Polymer Composite over Mesoporous Y Zeolite

Hyung Won (Lee)[1], Young-Min (Kim)[1,2], Young-Kwon (Park)[1]

[1]School of Environmental Engineering.

catalica@uos.ac.kr/Tel+82-2-6490-2870

Wood plastic composite (WPC), a composite materials made of wood and thermoplastics, is being widely used as consumable furniture due to its advantages, i.e. high durability, improved hardness, and good workability. Due to the increased market for WPC, the amount of waste WPC is also increasing, calling for environmentally friendly methods for waste WPC treatment. Some researchers are considering pyrolysis as a desirable treatment technique of WPC.

In this study meosporous Y zeolites with different Si/Al ratio were applied to the catalytic pyrolysis of wood polymer composite (WPC) for the first time using ex-siut k. By the catalytic pyrolysis over mesoporous Y zeolites, the content of aromatics, furans, and hydrocarbons in bio-oil were increased while the content of oxygenates and phenols were reduced. The detailed reaction mechanism will be suggested.

Keywords: Wood polymer composite, mesoporus Y, catalytic fast pyrolysis, Py-GC/MS

This work was supported by the National Research Foundation of Korea(NRF) grant funded by the Korea government(MSIP) (No. 2015R1A2A2A11001193).

In-situ Upgrading of Omani Heavy oil with Amphiphilic Bimetallic NiMo Catalyst

A study on the upgrading of Omani heavy oil under aquathermolysis conditions was carried out. The objective was to determine optimum conditions for upgrading to allow for greatest viscosity reduction and hence improved recovery of heavy oil. A high temperature high pressure reactor was used for all upgrading experiments, and a design of experiment with 3 factors and 10 levels was used with a quasi ransom sampling sequence to develop the response surface for optimization of viscosity reduction. In addition to the design of experiment, one-factor experiments were conducted to isolate the effects of the responses observed in the multi-factor experiments. For the design of experiment, the temperature was varied between 260°C to 300°C, water concentration varied between 0 to 30%, with the catalyst concentration varied between 0 to 0.6% NiMo metal content. Analysis of the design of experiment results show that the higher reaction temperatures experimented at, the higher the viscosity reduction, in addition, the water content used for upgrading causes an increase in viscosity as observed in 1 factor experiments. The optimized settings for viscosity upgrading was at 300°C, 0.3% NiMo metal content and 5% water content – resulting in an 94% reduction in viscosity, and a 12% reduction in sulfur content. FT-IR and ^{1}H NMR confirm the occurrence of hydrodealkylation reaction in upgrading of the heavy oil. GC-FID spectrum showed a 55% decrease in >C21 component of the heavy oil and an increase in <C21 components.

The upgrading of heavy oil in-situ would allow for the recovery of higher value hydrocarbons and a reduction in decline rates of reservoirs owing to the increased production that would be associated with the less viscous oil.

Keywords – Aquathermolysis, Amphiphilic, In-situ upgrading

Enhanced photocatalytic activity of *g*-C_3N_4 via Li intercalation

Z. J. Zhang, W.B. Zhang, S.W. Kwon, S. L. Zhang, Woochul Yang*
Department of Physics, Dongguk University, Pildong-ro, Choong-gu, seoul 04620, Korea
* *E-mail address: wyang@dongguk.edu*

Photocatalysts for organic pollutants degradation and hydrogen generation from water splitting utilizing solar light energy have attracted tremendous attention due to growing energy demand and environment concerns [1]. Graphic carbon nitride (*g*-C_3N_4) as a metal-free photocatalyst, has received wide attention in the past years, due to the suitable bandgap (2.7 eV), proper conduction band and valence band potion straddling water splitting potentials, as well as high hardness [2]. However, *g*-C_3N_4 would suffer limited dislocalized conductivity, high recombination rate and low specific surface area, leading to the overall low photocatalytic efficiency [3], even though numerous strategies have been employed to engineer the textures and photoelectrical structures of *g*-C_3N_4 for optimal photocatalysis [4, 5].

Herein, the *g*-C_3N_4 with Li^+ intercalation was prepared by mild-solution method using *n*-butyllithium for the first time. The photo-activity evaluation, via the photocatalytic degradation of Rhodamine B under visible light, demonstrated that *g*-C_3N_4 with Li^+ intercalation exhibits much enhanced photocatalytic activity than bare *g*-C_3N_4. In addition, the mechanism of enhanced photocatalytic activity for g-C_3N_4 with Li^+ intercalation has been investigated in detail on the basis of simulation using density functional theory (DFT), and the energy band positions obtained from experiment.

Keywords: g-C_3N_4, photocatalysis, DFT, Li intercalation

[1] ASAHI, R.; MORIKAWA, T.; OHWAKI, T.; AOKI, K.; TAGA, Y. 2001. Visible-Light Photocatalysis in Nitrogen-Doped Titanium Oxides. *Science*, 293, 269-271.

[2] WANG, X.; MAEDE, K.; THOMAS, A.; TAKANABE, K.; XIN, G.; CARLSSON, J. M.; DOMEN, K.; ANTONIETTI, M. A Metal-Free Polymeric, Photocatalyst for Hydrogen Production from Water under VisibleLight. *Nat. Mater*, 2009, 8, 76-80.

[3] ZHANG, Y.; LIU, J.; WU, G.; CHEN, W. 2012. Porous Graphitic Carbon Nitride Synthesized Via Direct Polymerization of Urea for Efficient Sunlight-Driven Photocatalytic Hydrogen Production. *Nanoscale*, 4, 5300-5303.

[4] LIN, Z.; WANG, X. 2013. Nanostructure Engineering and Doping of Conjugated Carbon Nitride Semiconductors for Hydrogen Photosynthesis. *Angew. Chem., Int. Ed*, 52, 1735-1738.

[5] ZHANG, G.; WANG, X. 2013. A Facile Synthesis of Covalent Carbon Nitride Photocatalysts by Co-Polymerization of Urea and Phenylurea for Hydrogen Evolution. *J. Catal*, 307, 246-253.

Synthesis of ZnO/TiO_2 Nanocomposite and Photocatalytic Activity for Methyl Orange Degradation

Wichuda Lachom[1], Santi Maensiri[2], Paveena Laokul[1*]

[1] Department of Physics, Faculty of Science, Mahasarakham University, Kantarawichai, Mahasarakham 44150, Thailand.
[2] School of Physics, Institute of Science, Suranaree University of Technology, Nakhon Ratchasima 30000, Thailand.

[*] Corresponding author: Tel.: +66845170205; Fax: +6643754379
E-mail address: paveena@msu.ac.th; paveena.kku@gmail.com

Abstract

The purposes of this work were synthesis nanoparticles of TiO_2 ZnO and nanocomposite ZnO/TiO_2 via coprecipitation method and study on their photocatalytic activity in methyl orange aqueous solution (MO). To obtain nanometer crystallite size, the precursor powders were calcined in air at 400 and 500 ^oC for 2h. From XRD technique, the formation of tetragonal structure of anatase TiO_2 and hexagonal wurtzite structure of ZnO was observed in the samples calcine at above 400 ^oC. Crystallite sizes of the obtained samples were in the range of 11-36 nm. The X-ray diffraction patterns of nanocomposite ZnO/TiO_2 showed the combination of anatase and wurtzite phases corresponding to TiO_2 and ZnO, repectively whit out the present of impurity phase of $ZnTiO_3$. The result from transmission electron microscopy technique reveals that there were 3 types of particles observed in ZnO/TiO_2 calcined samples: fine particle of TiO_2 and submicron ellipsoid and rod-like particles of ZnO. Energy band gap (E_g) of ZnO and nanocomposite ZnO/TiO_2 powders could be evaluated by using UV-vis absorption spectra and it found to be in the range of 3.15-3.18 eV. These E_g values seem to be lower in comparable to the theoretical value of 3.20 and 3.37 eV corresponding to anatase TiO_2 and ZnO, respectively. The efficiencies of photodegradation of ZnO and nanocomposite ZnO/TiO_2 in MO solution were investigated under the irradiation of UVA light. The result showed that nanocomposite ZnO/TiO_2 calcined at 400 ^oC exhibited the highest value of rate constant, k of 0.0186 min^{-1} which is corresponding to the higher removal ability for MO in comparable to those of TiO_2 and ZnO particles. The knowledge from this work can be developed to obtain higher photocatilytic activity nanocomposite ZnO/TiO_2 powder for wastewater treatment application.

Keywords: ZnO/TiO_2 nanocomposite, copricipitation method, photocatalysis, methyl orange, wastewater treatment

Atmospheric CO_2 utilization via methanation process

Pavel Parunin[1, 2, 3], Janna Veselovskaya [1,2,3], Olga Netskina[1], Vladimir Derevshikov[1,2,3], Anton Lysikov[1, 2 ,3], Aleksey Okunev[1,2]

[1] Boreskov Institute of catalysis SB RAS, pr. Lavrentieva street 5, Novosibirsk, Russia, 630090.

[2] Novosibirsk State University, Pirogova street 2, Novosibirsk, Russia, 630090.

[3] Scientific research centre "Energy efficient catalysis", Novosibirsk State University, Pirogova street 2, Novosibirsk, Russia, 630090.

e-mail : parunin@catalysis.ru

Nowadays due to rapid depletion of fossil fuels alternative energy sources become more attractive in energy field – the part of renewable energy will rise up to 60% of all generated energy in 2035. However, there are still some unresolved problems that prevent these technologies from being economically viable. For instance, large scale integration of wind and solar energy into the electrical grid requires a storage and distribution technology for the excess renewable electricity produced by these fluctuating sources. One of the promising and safe methods is converting renewable electricity in methane (power to gas concept) via two steps:

1. Water electrolysis: $2H_2O = 2H_2 + O_2$;
2. Sabatier process: $CO_2 + 4H_2 = CH_4 + 2H_2O$.

Renewable methane production by Sabatier process requires a sustainable source of carbon dioxide. Direct CO_2 capture from ambient air (a.k.a. "direct air capture", DAC) offers more flexibility compared to conventional carbon capture from large point sources. Incorporation of the DAC unit with the renewable energy storage system offers an opportunity to use anthropogenic carbon dioxide as a valuable feedstock for the production of renewable methane which can be utilized in the heating market or as a fuel for transportation.

The objective of the work is to investigate the methanation process of atmospheric CO_2. For this purpose, we developed lab-scale reactor (Fig. 1) that provides desired experimental conditions: temperature up to 400°C, controllable gas inlet, humidity control and recirculation. The reactor has compartments for catalyst and CO_2 sorbent, which allows carrying out CO_2 desorption and methanation processes simultaneously. However, in this work we studied methanation and CO_2

sorption/desorption processes separately in order to identify the main factors affecting each individual process.

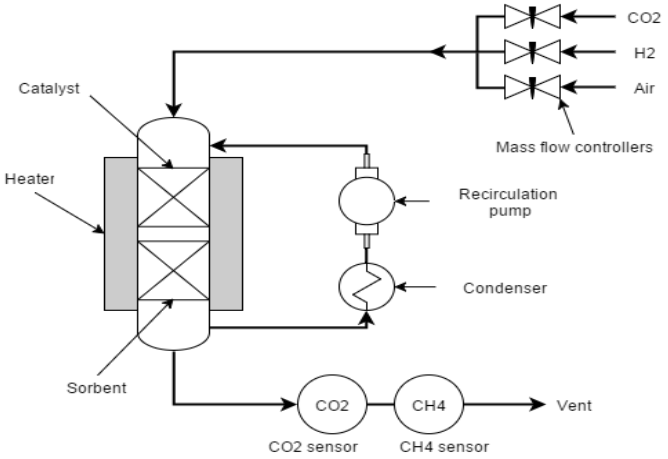

Figure 1. Scheme of the lab-scale reactor

Kinetics of Sabatier process was studied using several heterogeneous catalysts. We tested commercial nickel catalyst of methanation NKM, as well as ruthenium catalysts synthesized using activated carbon and alumina as porous supports. The kinetic experiments were performed in the temperature range from 200 to 400°C. The gaseous mixture of CO_2 and H_2 was fed to the reactor. Concentrations of CO_2 and CH_4, as well as the total flow rate, were measured at the output of the reactor.

$K_2CO_3/\gamma\text{-}Al_2O_3$ composite sorbent was synthesized as described in [1] and then tested in a following cycle: CO_2 absorption from ambient air, heating the reactor up to 300°C, hydrogen purging at 300°C. The CO_2 absorption capacity of the sorbent was calculated for each cycle.

It was demonstrated that the most active methanation catalyst was Ru/Al_2O_3. Nevertheless, nickel catalyst NKM should also be considered for large-scale application due its lower price. The $K_2CO_3/\gamma\text{-}Al_2O_3$ composite sorbent showed a good stability in CO_2 sorption/desorption cycles and will be implemented in the combined DAC/methanation system.

Acknowledgements

The reported study was supported by RFBR, research project No. 16-33-00198 mol_a..

Keywords: carbon dioxide, absorption, methanation, composite sorbent, heterogeneous catalyst

[1] VESELOVSKAYA, J. V., DEREVSCHIKOV, V. S., KARDASH, T. Yu., STONKUS, O. A., TRUBITSINA, T. A., OKUNEV, A. G. 2013. Direct CO_2 capture from ambient air using K_2CO_3/Al_2O_3 composite sorbent. *Int. J. Greenhouse Gas Control*, 17, 322-340.

Functional Layered Double Hydroxides and Their Catalytic Activity for 1,4-Addition of n-Octanol to 2-Propenonitrile

Zavoianu[1], Pavel[1], Cruceanu[1], Florea[1], Birjega[2]

[1]*University of Bucharest, Faculty of Chemistry, Dept. Organic Chemistry, Biochemistry & Catalysis, Blv. Regina Elisabeta, Nº 4-12, S3, Bucharest, 030018, ROMANIA*

[2]*National Institute for Lasers, Plasma and Radiation Physics, 409 Atomistilor Str., 77125 Bucharest-Magurele, ROMANIA*

rodica.zavoianu@chimie.unibuc.ro

Aims and scope This contribution concerns the catalytic activity of hybrid layered double hydroxides (LDHs) solids for 1,4-addition of n-octanol to 2-propenonitrile aiming to investigate the influence of the organic interlayer anion nature on their physico-chemical and catalytic performances.

Experimental Two series of hybrid LDHs e.g $Mg_{2.5}Al$, and $Zn_{2.5}Al$ respectively were synthesized by direct precipitation at pH 9.5 [1] using a metal nitrates $M^{2+}(NO_3)_2 \bullet 6H_2O$ (M^{2+} = Mg, Zn), $Al(NO_3)_3 \bullet 9H_2O$ solution, an organic acid sodium salt (e.g. sodium dodecyl sulfate (NaDS), sodium laurate (NaL), or sodium stearate (NaS)) as sources of organic anions (DS, L or S) and NaOH solution for pH adjustment. The resulting gel was aged 18h at 50°C under He. The solids recovered by filtration were washed until the conductivity of the wastewater was <100 μS/cm and dried at 60°C for 72 h. The resulting 6 powders were labeled $M^{2+}_{2.5}$Al-DS, $M^{2+}_{2.5}$Al-L, and $M^{2+}_{2.5}$Al-S respectively. All solids were fully characterized by chemical and elemental analyses, XRD, DRIFTS, DR-UV-Vis NIR, TG-DTA, textural analyses by N_2 adsorption–desorption isotherms, base sites determination [2]. The catalytic activity tests were performed during 4 h at reflux temperature in a thermostatic glass reactor provided with water cooled condenser using 0.03 moles *n*-octanol, 0.01 moles 2-propenonitrile and an amount of catalysts equal to 3% wt. of the reaction mixture. The composition of the reaction mixture was analyzed by GC, and the reaction products were identified also by GC-MS, and by 1H-NMR.

Results and discussion XRD, DRIFTS and DR-UV-Vis-NIR characterizations indicated a better intercalation of DS in the interlayer region compared to L or S. $M^{2+}_{2.5}$Al-DS had also larger S_{sp} and higher basicity. For each series of hybrid materials, the catalytic

activity followed the order: $M^{2+}_{2.5}$Al-DS > $M^{2+}_{2.5}$Al-L > $M^{2+}_{2.5}$Al-S. The catalytic activity of these solids was both due to their organophilic character and to their basicity, ($Mg_{2.5}$Al-DS samples, which were more basic, showed a higher activity than the corresponding $Zn_{2.5}$Al-DS).

Conclusions $M^{2+}_{2.5}$Al-DS are promising catalysts for 1,4-addition of n-octanol to 2-propenonitrile yielding solely β-octoxy-propanenitrile as reaction product.

Authors acknowledge financial support by UEFISCDI – PCCA1 project 137/2012.

Keywords: hybrid LDH, 1,4-addition, 2-propenonitrile

[1] DU, B., GUO, Z. & FANG, Z. 2009. Effects of organo-clay and sodium dodecyl sulfonate intercalated layered double hydroxide on thermal and flame behaviour of intumescent flame retarded polypropylene. *Polym. Degrad. Stab.*, 94, 1979–1985.

[2] ZAVOIANU, R., IONESCU, R., PAVEL, O.D., BIRJEGA, R. & ANGELESCU, E. 2011. MeIIMg/Al hydrotalcites and hydrotalcite-supported Me(II) acetylacetonates (Me(II)=Co, Cu or Ni) catalysts for the epoxidation of cyclohexene with molecular oxygen. *Appl. Clay Sci.*, 52, 1 – 10.

Photocatalytic Effect of $ZnWO_4$ (Sanmartinite) Powders Synthesised by Mechanochemical Method

Altinsoy, I.[1,2], Guy, N.[1,3], Ozacar, M.[1,3], Bindal, C.[*1,2]

[1]Sakarya University, Biomedical, Magnetic and Semiconductor Materials Research Center (BIMAS-RC), Sakarya 54187, Turkey.

[2]Sakarya University, Engineering Faculty, Department of Metallurgy and Materials Engineering, Sakarya 54187, Turkey.

[3] Sakarya University, Art-Science Faculty, Department of Chemistry, Sakarya 54187, Turkey.

E Mail : ialtinsoy@sakarya.edu.tr, [*]bindal@sakarya.edu.tr

In this study, it was aimed to produce $ZnWO_4$(sanmartinite) powders by mechanochemical synthesis (MCS) using 1:1 ratio of ZnO and WO_3 as starting powders at 700 rpm for 25 and 100 minutes. The change in physical properties such as particulesize,sanmartinite purity of as synthesized samples and effect of the variation of this physical properties on photocatalytic efficiency of the samples were investigated. SEM observations indicated that ratio of sub-micron sized $ZnWO_4$ particles in the microstructure were raised and particle size distribution was homogenized by increasing of process time. XRD analysis revealed that only sanmartinite phase was detected in the powder samples at higher process time. Raman Spectroscopy confirmed the XRD results except detection of few amounts of WO_3 and ZnO phases were still remained in the samples.According to particle surface area measurements, the surface area of the samples were ranged between 3,65-4,05 m^2/g. Absorbance and reflectance spectrum of the as synthesed powder samples indicated that powder samples have low absorbance and mean reflectance across the light spectrum. Optical band gap energies of the samples increased from 2,67eV to 2,82 eV by raising process time. It was found that under thevisible light, nearest photocatalytic efficieny to ZnO powders (for reference known as strong photocatalyst [1]) for degregading malachite-green dyes were observed in MCS7-25sample as a result of photocatalytic oxidation experiments. On the other hand, MCS7-100 samples have lower photocatalytic activity compared to MCS7-25. The efficiency of

photocatalytical activities changed from 45% to 83%, approximately after 120 min. photocatalysis process for the test materials. Although photocatalytic activity of the higher milled sample (MCS7-100) have a low degree, its efficieny is close to similar powders synthesized by same method for degregadition of Malachite-Green dye reported by Mancheva et al. [2] It is possible to claim that $ZnWO_4$ powders synthesized by mechanochemical route is promising photocatalyst and can be used in visible light region.

Keywords:$ZnWO_4$, Mechanochemical synthesis, particle surface area (BET), optical band gap, photocatalytic efficieny

[1] Johansson, M. B., Baldissera, G., Valyukh, I., Persson, C., Arwin, H., Niklasson, G.A., Osterlund, L.2013. Electronic and optical properties ofnanocrystalline WO3 thin films studied byoptical spectroscopy and density functional calculations. *J. Phys.: Condens. Matter*, 25, 1-10.

[2] Mancheva, M., Iordanova, R., Dimitriev, Y. 2011.Mechanochemical synthesis of nanocrystalline ZnWO4 at room temperature. *J. Alloys Compd.*, 509, 15–20.

Synthesis of Novel Magnetically Separable Ag_3PO_4/ZnO/Fe_3O_4 Nanocomposites with Highly Enhanced Photocatalytic Activities under Visible-Light Irradiation

Nuray Guy[1,2], Mahmut Ozacar[1,2]

[1]Department of Chemistry, Science&Arts Faculty, Sakarya University, Sakarya 54187, Turkey.

[2]Biomedical, Magnetic and Semiconductor Materials Research Center (BIMAS-RC), Sakarya University, Sakarya 54187, Turkey.

E Mail : nurayg@sakarya.edu.tr, mozacar@sakarya.edu.tr

Semiconductor photocatalysts have attracted increasing attention during the past decades due to their high efficiency for degrading/mineralizing a wide range of bacteria, pesticides, dyes, and volatile organic compounds into carbon dioxide, water and mineral acids under light [1-2]. Among numerous semiconductor photocatalysts, ZnO as one of excellent photocatalysts has been extensively studied owing to its high photosensitivity, non-toxic nature, low cost and adjustable morphologies [3]. However, because of its wide band gap (Eg≈ 3.2−3.3 eV), ZnO is particularly suitable for applications based on UV-light irradiation. Additionally, the practical application of ZnO is also limited by its insufficient electron−hole separation, which leads to a lower energy conversion. Usually semiconductors with narrow band gaps (2.36−2.43 eV) such as Ag_3PO_4, are ideal visible light photocatalyst to improve photocatalytic activity in the Ag_3PO_4/ZnO system [2-3]. The magnetically separable visible-light-driven photocatalysts could be prepared by immobilization of a proper magnetic material, with photocatalysts having considerable absorption under visible-light irradiation. In this study, we have proposed a simple way to prepared ZnO, Ag_3PO_4/ZnO, ZnO/Fe_3O_4, Ag_3PO_4/ZnO/Fe_3O_4 photocatalysts. The as-

prepared products are characterized by X-ray diffraction (XRD), field emission scanning electron microscope (FESEM), diffuse reflectance spectra (DRS) and vibrating sample magnetometer (VSM). Detailed investigations of the photocatalytic activity of samples were carried out under visible light irradiation. Furthermore, the as-obtained products not only have high photocatalytic activity under visible-light irradiation, but are also easily retrievable by magnet for recycling.

Keywords:Ag_3PO_4/ZnO/Fe_3O_4, visible light, magnetically separable, photocatalytic activity

[1] Ahmad, M., Ahmed, E., Hong, Z.L., Khalid, N.R., Ahmed, W., Elhissi, A. 2013, Graphene–Ag/ZnO nanocomposites as high performance photocatalysts under visible light irradiation. *Journal of Alloys and Compounds, 577, 717–727.*

[2] Xu, J.W., Gao, Z.D., Han, K., Liu, Y., Song, Y.Y. 2014, Synthesis of magnetically separable $Ag_3PO_4/TiO_2/Fe_3O_4$ heterostructure with enhanced photocatalytic performance under visible light for photoinactivation of bacteria. *ACS Appl. Mater. Interfaces, 6, 15122−15131.*

[3] Cai, A., Sun, Y., Dua, L., Wang, X. 2015, Hierarchical Ag_2O–ZnO–Fe_3O_4 composites with enhanced visible-light photocatalytic activity. *Journal of Alloys and Compounds 644, 334–340.*

An improvement of biodiesel production from waste cooking oil by applying thought Multi-Response Surface Methodology using Desirability Functions

Marina Corral Bobadilla[1], Ruben Escribano Garcia [2], Ruben Lostado Lorza[1], Fatima Somovilla Gomez[1], Roberto Fernandez Martinez[3], Eliseo P. Vergara Gonzalez[1]

[1]Mechanical Engineering Department, University of La Rioja, Spain

[2]Mechanical Engineering Department, University of Leeds, UK

[3]Department of Electrical Engineering, University of The Basque Country UPV/EHU, Spain

marina.corral@unirioja.es, roberto.fernandezm@ehu.es

The exhaustion of natural resources, increased petroleum price and the negative of environmental impacts of crude oil has stimulated the search of an alternative source of energy like biodiesel. Biodiesel is synthesized from direct transesterification of vegetable oils, where the corresponding triglycerides react with a short-chain alcohol in the presence of a catalyst. The catalyst improves the solubility and accelerates the reaction [1]. Waste cooking oil is a potential substitution of vegetable oils for the production of biodiesel due to the low cost of raw material and for solving their disposal problem. This paper used Multi-Response Surface Methodology (MRS) with desirability functions [2] in order to find the combination of parameters necessary in the catalyzed transesterification reactions with methanol and sodium hydroxyde for improve the production of biodiesel. In this case, the input parameters studied were: the dosage of catalyst, process temperature, mix speed, mix time, humidity and impurities of waste cooking oil, while the biodiesel yield was maximized and the viscosity of the biofuel obtained was minimized. A Design of Experiments (DoE) based on Box-Behnken [3] was developed with the purpose of covering the entire space of possibilities so that the regression models developed had the greatest possible generalization ability. The results obtained demonstrated that although waste cooking oil was collected from different sources, the dosage of catalyst is one of the most important parameters in the yield of biodiesel production while the viscosity obtained was similar in all samples of biodiesel studied.

Keywords: Biodiesel, Waste Cooking Oil, Catalysis, Multi-Response Surface Methodology.

[1] BALAKRISHNAN, K., OLUTOYE, M. A., & HAMEED, B. H. 2013. Synthesis of methyl esters from waste cooking oil using construction waste material as solid base catalyst. *Bioresource technology, 128, 788-791.*

[2] HARRINGTON, E. C. 1965. The desirability function. *Industrial quality control, 21(10), 494-498.*

[3] FISHER, R. A. 1935. The design of experiments.

Selective Ring Opening of Phenanthrene over Tungsten-based Catalyst Supported on Mesoporous Y Zeolite

Jeong-Rang (Kim)*, Eun-Sang (Kim), You-Jin (Lee), Hyung-Ju (Kim), Tae-Wan (Kim), Ho-Jeong (Chae), Chul-Ung (Kim), Soon-Yong (Jeong)

Korea Research Institute of Chemical Technology, 141, Gajeong-ro, Yuseong-gu, Daejeon 34114, South Korea

jrkim@krict.re.kr / Tel. +82-42-860-7324

Heavy oil, produced from oil refineries and petrochemical plants, has been used as low-value fuel. The heavy oil includes heavy molecules with high sulfur content such as multi-ring aromatics and asphaltenes. Due to the oil depletion and the strict environmental regulations for the use as fuel, heavy oil upgrading to high-value middle distillates with low aromatics has attracted interest to many researchers [1]. Multi-ring aromatics are the major components of the heavy oil and their selective ring opening (SRO) should be a potential route for the production of valuable middle distillates from the heavy oil. Bifunctional catalyst (metallic and acidic functions) is required in the SRO of multi-ring aromatics [2]. In this study, phenanthrene was selected as a model compound for multi-ring aromatics in heavy oil. Mesoporous Y zeolite (Meso-Y) was synthesized via pseudomorphic synthesis and the bifunctional catalysts were prepared by the impregnation method using the zeolites. The SRO of phenanthrene has been investigated using the bifunctional zeolite catalysts with the mesopore in batch reaction system. The Meso-Y catalyst had higher product yield for alkyl-benzenes than those of the Y zeolite catalyst. These results suggest that the mesoporosity of the Meso-Y catalyst has more advantages for the SRO of multi-ring aromatics due to the easier access of the large molecules to catalytic active sites compared to the Y zeolite catalyst.

Keywords: heavy oil upgrading, selective ring opening, phenanthrene, HY zeolite, mesopore

[1] RANA, M. S., SÁMANO, V., ANCHEYTA, J. & DIAZ, J. A. I. 2007. A review of recent advances on process technologies for upgrading of heavy oils and residua. *Fuel*, 86, 1216-1231.

[2] MCVICKER, G. B., DAAGE, M., TOUVELLE, M. S., HUDSON, C. W., KLEIN, D. P., BAIRD, W. C. Jr., COOK, B. R., CHEN, J. G., HANTZER, S., VAUGHAN, D. E.W., ELLIS, E. S. & FEELEY, O. C. 2002. Selective Ring Opening of Naphthenic Molecules. *Journal of Catalysis*, 210, 137-148.

Title:
A new strategy to synthesize TiO2 mesocrystals with superior photocatalytic activity

Speakers: Jin Chen; Lei Zhou*

Abstract:
Mesocrystals are a new class of solid materials, which is built of crystallographically oriented nanocrystals. Usually, mesocrystals are formed by a bottom-up self-assembly process. Recently, we developed a new top-down strategy to prepare TiO2 mesocrystals using topotactic transformation reactions of ammonium oxofluorotitanates. The morphologies and building structures of the TiO2 mesocrystals can by adjusted by the precursors. Due to the presence of F-, most products are built of TiO2 nanocrystals with dominantly exposed {001} facets. The unique structures lead to superior photocatalytic activities, which is close to 3 times of that of P25. Because of their large sizes (3um ~ 100 um), it is very easy to remove these TiO2 mesocrystals from the reaction system via centrifugation or filtration. This is very good for their applications in practice.

Abatement of Phenolic Compounds by Microwave-Enhanced Catalytic Degradation Method over High Valenced Nickel Oxide

Teh-Long Lai[1], Chih-Wei Tang[2], Youn-Yuen Shu[3], **Chen-Bin Wang**[4]

[1]Chung-Shan Institute of Science and Technology System Manufacturing Center, Taipei 23742 Taiwan, ROC

[2]Department of General Education, Army Academy ROC, Chungli, Taoyuan, 32092, Taiwan, ROC

[3]Environmental Analysis Laboratory, Department of Chemistry, National Kaohsiung Normal University, Kaohsiung, 802, Taiwan, ROC

[4]Department of Chemical and Materials Engineering, Chung Cheng Institute of Technology, National Defense University, Tahsi, Taoyuan 33509, Taiwan, ROC

E-mail address: chenbinwang@gmail.com **(Chen-Bin Wang)**

In this work, an environmental friendly process via the microwave-enhanced catalytic degradation (MECD) method for the abatement of phenolic compounds (phenol, 2, 3, 4-chlorophenol and 4-nitrophenol) has been successfully developed. A high valenced nickel oxide was prepared from nickel nitrate aqueous solution through a precipitation with sodium hydroxide and an oxidation by sodium hypochlorite with/without microwave-assisted heating. The MECD experiments were carried out in a thermostated static microwave apparatus (CEM. Discover, USA, 2450 MHz, 300 W, temperature was controlled with IR sensor) upon continuous stirring, likewise providing an equal level of all parameters describing the state of the system (catalyst, temperature, pH, initial concentration and dosage of catalyst). The results showed that all the phenolic compounds were completely degraded using the high efficiency MECD method within 15 min under different conditions for treatment the concentration of 200 ppm organic pollutants over our fabricated high-valenced nickel oxide, i.e. pH 7 and 40 °C within 8 min for phenol, pH 4 and 40 °C within 10 min for 2, 3-chlorophenol, pH 4 and 70 °C within 5 min for 4-chlorophenol, pH 0 and 40 °C within 15 min for 4-nitrophenol, respectively.

Keywords: Microwave-enhance catalytic degradation, Nickel oxide, Phenolic compounds

[1] LAI, T. L., YONG, K. F., YU, J. W., CHEN, J. H., SHU, Y. Y. & WANG, C. B. 2011. High efficiency degradation of 4-nitrophenol by microwave-enhanced catalytic method. *Journal of Hazardous Materials,* 185, 366-372.

[2] HUANG, Q., CAO, M., AI, Z. & ZHANG L. 2015. Reactive oxygen species dependent degradation pathway of 4-chlorophenol with Fe@Fe_2O_3 core–shell nanowires. *Applied Catalysis*, B162, 319-326.

Effective photocatalytic degradation of paracetamol using La-doped ZnO photocatalyst under visible light irradiation

Viet Ha-Tran Thi, Byeong-Kyu Lee*
Department of Civil and Environmental Engineering, University of Ulsan, Nam-gu, Daehak-ro 93, Ulsan 680-749, Republic of Korea
* Corresponding author. Tel: 82-52-259-2864, Fax: 82-52-259-2629,
E-mail: bklee@ulsan.ac.kr

Abstract

Visible light-driven photocatalysts of lanthanum (La) doped ZnO nanoparticles were successfully prepared by a facile precipitation method using various La doping concentrations (0.5, 1.0 and 1.5 wt%). La doping did not modify the crystallinity of ZnO significantly, but enhanced the optical absorption of visible light due to the reduction in particle size and band gap energy. La-doped ZnO photocatalysts were applied to treat 100 mg/L paracetamol in aqueous solution under visible light irradiation after 3 h. 1.0 wt% La-doped ZnO photocatalyst showed the highest photocatalytic activity for the degradation of paracetamol with a degradation efficiency of 99 % and TOC removal of 85 %. Based on the chemical analysis of photocatalytic products detected, proposed mechanism for paracetamol removal by La-doped ZnO nanoparticles under visible light illumination including radical generation with use of photocatalytic degradation and subsequent reaction pathways was proposed.

Keywords: photocatalytic activity, doped ZnO, lanthanum, paracetamol, reaction pathways

Functional Materials Obtained from Red Mud Waste and Their Catalytic Activity for Sulfide Oxidation in Wastewater

Cruceanu[1], Zavoianu[1], Pavel[1], Florea[1]

[1]*University of Bucharest, Faculty of Chemistry, Dept. Organic Chemistry, Biochemistry & Catalysis, Blv. Regina Elisabeta, Nº 4-12, S3, Bucharest, 030018, ROMANIA*

anca.cruceanu@chimie.unibuc.ro rodica.zavoianu@chimie.unibuc.ro

Aims and scope This contribution aims the obtaining of functional materials from red mud (RM), and their use as catalysts for oxidative removal of S^{2-} from wastewaters. The preparation method involves chemical and thermal activation of RM and functionalization of Fe(III) sites with polycarboxylic acids. Disodium ethylenediamminotetraacetic acid (E) and trisodium citrate (*C*) were selected as functionalization agents considering that Fe(III) coordination in the ligands field should be strong enough to avoid its precipitation as sulfide or hydroxide while maintaining its ability to change the oxidation state during the redox cycle [1-4].

Experimental Before functionalization, red mud from Tulcea-Romania alumina plant (39.2 % Fe_2O_3) [5] was activated in a 3-step sequence: (i) neutralization with 35% NaCl solution yielding RMN, (ii) treatment of RMN with 20% HCl at 50^{o}C yielding RMNHCl, and (iii) treatment of RMNHCl with 25% NH_3 yielding activated red mud (**RMA)** [6]. Functional materials were obtained by submitting **RMA** to 3 different treatments: (i) with (E) solution, molar ratio E/Fe=1-1.5 yielding **RMA-E**, (ii) with (*C*) solution, molar ratio *C*/Fe=1-2 yielding **RMA-C** and (iii) with a combined E+C solution, molar ratio E/Fe/C=1/1/1 yielding **RMA-E-C** [5]. Catalysts were characterized by DRIFT, DR-UV-Vis, XRD, surface area and porous structure determinations. Catalytic tests for S^{2-} oxidation by O_2 from air were performed during 2 h at 25^{o}C, 1 atm, under 4L/h air flow using 1 g of catalyst and 75 mL wastewater (1 g S^{2-}/L).

Results and discussion XRD, DRIFTS and DR-UV-Vis-NIR characterizations indicated the organic ligands presence in all functional materials. Catalytic tests results showed that functional RMA catalysts increased by 60% the removal of S^{2-} from wastewaters.

Functional solids had an enhanced stability towards deactivation by FeS precipitation. For the most stable (RMA-E-C), the decrease of activity after 4 reaction cycles is < 2%.

Conclusions The functional RMA-derived materials are active catalysts for S^{2-} oxidation under mild reaction conditions and reduce the formation of FeS in treated wastewater. The proposed preparation method is simple and not expensive. The formation of Fe(III) complexes on the surface of the red mud leads to a surface area increase of the functional catalysts.

Authors acknowledge financial support by UEFISCDI - PCCA2 project 78/2014.

Keywords: functional materials, red mud, sulfide oxidation

[1] TERORDE, R. J. A. M., VAN DEN BRINK, P. J., VISSER, L. M., VAN DILLEN, A. J. & GEUS, J. W. 1993. Selective Oxidation of Hydrogen Sulfide to Elemental Sulfur Using Iron Oxide Catalysts on Various Supports. *Catal. Today,* 17, 217-225.

[2] JUNG, K.D., JOO, O.S., CHO, S.H. & HAN, S.H. 2011. Catalytic wet oxidation of H_2S to sulfur on Fe/MgO catalyst. *Appl. Catal. A: General* 240, 235-241.

[3] SAHU, R.C., PATEL, R. & RAY, B.C. 2011. Removal of hydrogen sulfide using red mud at ambient conditions. *Fuel Process Technol.,* 92, 587-1592.

[4] CRUCEANU, A., ZAVOIANU, R. & ANGELESCU, E. 2001. Catalytic desulphurisation of gaseous streams containing H_2S in the presence of Fe, Co and Cr chelates catalysts. *Prog. Catal.,* 10 (1-2), 27-39.

[5] ZAVOIANU, R., CRUCEANU, A., PAVEL, O. D., MARA, L., VELEA, T. & BIRJEGA, R. 2015. Alternative valorisation of red mud waste as catalyst for sulphide oxidation in wastewater. *Proceedings of Bauxite Residue Valorisation and Best Practices, Leuven,* 219-230.

[6] GENÇ-FUHRMAN, TJELL, H., J. C. & McCONCHIE, D. 2004. Increasing the arsenate adsorption capacity of neutralized red mud (Bauxsol). *J. Colloid Interface Sci.,* 271, 313-320.

Mixed metal (oxy)nitride materials for clean energy applications

Minghui Yang*, Mingming Zou and Yutong Jiao
Dalian National Laboratory for Clean Energy, 457 Zhongshan Road, Dalian, Liaoning 116023, P.R. China

A simple process for preparing mesoporous transition metal nitrides (MTMN) by the ammonolysis of bulk ternary oxide powders that contain K, Zn and Cd will be presented. Mesoporous VN, TiN, CrN, Ta_3N_5, TaN, NbN, WN, MoN and Mo_2N powder have been obtained, as well as mesoporous nitrides containing more than one transition metal as shown in [Figure 1].[1] Chemical analysis shows some residual oxygen (~5 mol%) remains in the products, as has been observed previously in the preparation of nitrides by ammonolysis of oxides. The products were characterized by Rietveld refinement of powder X-ray diffraction (PXRD) patterns and by scanning electron microscopy (SEM). Pore sizes ranging from 10 to 50 nm were commonly observed. Under compression at a low pressure of 35 bar, powder conductivities of 76 S/cm (VN), 464 S/cm (TiN) and 1.8 S/cm (WN) were obtained. The conductivities of metal nitrides are much higher than carbon black at a similar pressure, for instance. Pt/MTMNs catalysts exhibit a higher catalytic activity than Pt/C catalysts.[2]

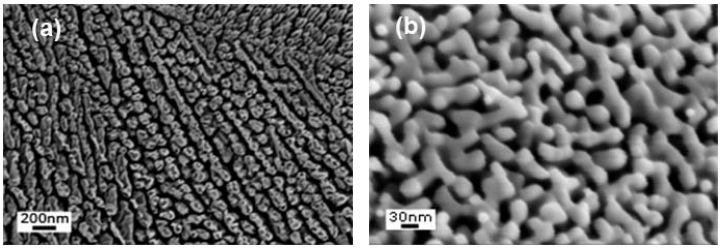

[Figure 1]. SEM images of ammonolysis products of (a) Zn_2TiO_4 and (b) $Zn_2V_2O_7$. obtained after heating at 800 °C for 8 hours.

Reference:

1. Yang, M. H.; Guarecuco, R.; DiSalvo, F. J., Mesoporous Chromium Nitride as High Performance Catalyst Support for Methanol Electrooxidation. *Chem Mater* **2013,** *25* (9), 1783-1787.
2. Cui, Z. M.; Yang, M. H.; DiSalvo, F. J., Mesoporous Ti0.5Cr0.5N Supported PdAg Nanoalloy as Highly Active and Stable Catalysts for the Electrooxidation of Formic Acid and Methanol. *Acs Nano* **2014,** *8* (6), 6106-6113.

Practical Design of Green Nano-catalysts for Polyester Recycling

Arvin Sangalang(Sangalang)[1], Yunsu Kim(Kim)[1], Seunghwan Seok (Seok)[1], Jae-Min Jeong (Jeong)[1], Do Hyun Kim(Kim)[1]

[1]Department of Chemical and Biomolecular Engineering, KAIST, Daejeon, Republic of Korea

*E Mail/ Contact Détails (***DoHyun.Kim@kaist.ac.kr)**

The recycling of chemicals and generation of alternative energy are central topics in the efforts toward sustainable development. Among these, research on plastics recycling has received significant attention [1], with the aim of designing novel catalysts to improve yield and efficiency. We highlight our work on these areas focusing on the chemical depolymerization of polyethylene terephthalate (PET) to recover its constituent monomer. We demonstrate various flexible yet practical synthesis strategies (e.g. ultrasound-assisted deposition and biomimicking structure for various substrate) [2] that were used to obtain catalytic properties optimized for these applications. The effectiveness and simplicity of these methods render the catalysts to be truly green — from synthesis up to process application.

Keywords: PET glycolysis, ultrasound, polydopamine, nanocomposites

[1] BARTOLOME L, IMRAN M, CHO BG, AL-MASRY WA, KIM DH. Recent developments in the chemical recycling of PET. 2012, In: ACHILIAS D, editor. Material Recycling — Trends and Perspectives. INTECH,. p. 65–84. DOI: 10.5772/33800.

[2] PARK G, BARTOLOME L, LEE KG, LEE SJ, KIM DH, PARK TJ. 2012, One-step sonochemical synthesis of a graphene oxide-manganese oxide nanocomposite for catalytic glycolysis of poly(ethylene terephthalate). Nanoscale.;4, 3879–3885.

Renewable Aromatics from the Degradation of Polystyrene at Mild Conditions

Nouf Aljabri, Kuo-Wei Huang*

KAUST Catalysis Centre and Division of Physical Science and Engineering, King Abdullah University of Science and Technology, Thuwal 23955-6900, Saudi Arabia

hkw@kaust.edu.sa

Plastic products play a crucial role in many aspects of the modern life. At the same time, they become one of the biggest issues facing humanity in the 21st century. There has been increasing attention to identifying new energy resources to reduce the cost and energy associated with the conventional oil production. Considering the fact that waste plastics have high calorific contents to be recovered, heterogeneous catalysts are being developed for converting waste plastics into valuable and renewable chemicals. In this contribution, we demonstrate the catalytic activity of a series of bi and tri-metallic catalysts to degrade polystyrene into useful products at mildest possible reaction conditions with high oil yields.

Activity and Surface Characteristics of manganese oxide catalysts supported on TiO_2

Kim. M.S[1,2], Park. E.S [1], Jung. H.D[1,2], Jurng. J.S[1,2,*]

[1]Center for environment, Health and Welfare research, Korea Institute of Science and Technology, Seongbuk-gu, 136-791, Seoul, Republic of Korea.

[2]GREEN SCHOOL(Graduate School of Energy and Environment), Korea University, Seongbuk-gu, 136-701, Seoul, Republic of Korea

*E Mail kms1482@kist.re.kr, * : Jongsoo@kist.re.kr*

Manganese oxides are reported to be among the most efficient transition-metal compounds in catalytic oxidation [1] and they are considered environment-friendly materials. Manganese oxides such as Mn_3O_4, Mn_2O_3 and MnO_2 are known for exhibiting high activity in the oxidation of hydrocarbons. The Mn-based catalysts impregnated on TiO_2 with two different crystalline phases, chemical vapor condensation (CVC) and P25. The catalysts were characterized by X-ray photoelectron spectroscopy(XPS), H_2-Temperature Programmed Reduction(TPR).

Figure 1 shows the Mn 2p XPS spectra of the surface of the MnOx/TiO_2 catalysts. It can be deduced from the asymmetry of the Mn $2p_{3/2}$ and Mn $2p_{1/2}$ profiles that MnOx existed in three states, MnO_2, Mn_2O_3 and Mn_3O_4. The peak at lower binding energy (639~641 eV) was attributed to Mn^{3+}, and the peak high binding energy (642~644 eV) was attributed to Mn^{4+}. The Mn atomic concentration and Mn^{3+}/Mn ratio measured by XPS are shown in Table 1. The ratio of Mn^{3+}/Mn is a measurement of the dispersion of MnOx on the surface of TiO_2. Although the nominal Mn loading in all the catalysts were the same, their Mn^{3+}/Mn ratios on the catalysts surface were different. MnOx/CVC has a higher Mn^{3+}/Mn ratio better than MnOx/P25. This revealed again that MnOx on the last catalyst existed in a highly dispersed phase and was intercalated with TiO_2 lattice. The high Mn^{3+}/Mn ratio on CVC surface may be due to two reasons: one is the low specific surface area and pore volume of CVC[2], and the other is the weak interaction between CVC and MnOx, which only allowed MnOx to cover the CVC surface as isolated species that do not interact with the support. Its performance is significantly affected by the

presence of other phases Mn_2O_3 and Mn_3O_4. Mn_3O_4 improves the catalytic activity due to the increase of the reactivity and mobility of lattice oxygen, while Mn_2O_3 has the opposite effect. As shown in the TPR result, MnOx/CVC has higher reduction ability than MnOx/P25. This means that MnOx/CVC has higher lattice oxygen mobility, leading to higher activity for the oxidation, as mentioned earlier, the order of catalytic activity for VOCs oxidation of Mn oxides was reported to be Mn_3O_4 > Mn_2O_3 > MnO_2.[3] In MnOx/CVC, the high activity Mn_3O_4 was dispersed well. Compared to CVC, P25 gave better dispersion of MnOx on the support surface, suppressed the agglomeration of catalyst particle, and also produced more Mn_3O_4, which was more active for the oxidation of VOCs.

The catalytic oxidation of VOCs was carried out over manganese oxide catalysts (Mn_3O_4, Mn_2O_3 and MnO_2). The BET, XPS and TPR results indicated that MnOx/CVC catalyst with high oxygen mobility and high surface area exhibits high catalytic activity.

▪ ***Keywords : Manganese Oxide, TiO_2, XPS, TPR***

[1] Morales, M.R., Barbero, B. P. & Cadus, L. E. 2006. Total oxidation of ethanol and propane over Mn-Cu mixed oxide catalysts. *Applied catalysis B : Environmental*, 67, 229-236.

[2] Park, E.S., Chin, S. M., Kim, J. S., Bae, G. N. & Jurng, J. S. 2011. Preparation of MnOx/TiO_2 ultrafine nonocomposite with large surface area and its enhanced toluene oxidation at low temperature. *Powder Technology*, 208, 740-743.

[3] Kim, S. C. & Shim, W. G., 2010. Catalytic combustion of VOCs over a series of manganese oxide catalysts. *Applied catalysis B : Environmental*, 98, 180-185.

Table. 1 XPS results of the MnOx/TiO_2 catalysts

Catalysts	Atomic concentration		
	Mn2p content (at%)	Mn/Ti Atomic ratio	Mn3+/Mn atomic ratio
Mn / CVC	4.06	18.00	53.1%
Mn / P25	2.53	15.43	42.5%

Fig. 1 Mn $2p_{1/2}$ and Mn $2p_{3/2}$ XPS spectra of the MnOx/TiO_2 catalysts (a) Mn/CVC-TiO_2, (b) Mn/P25-TiO_2

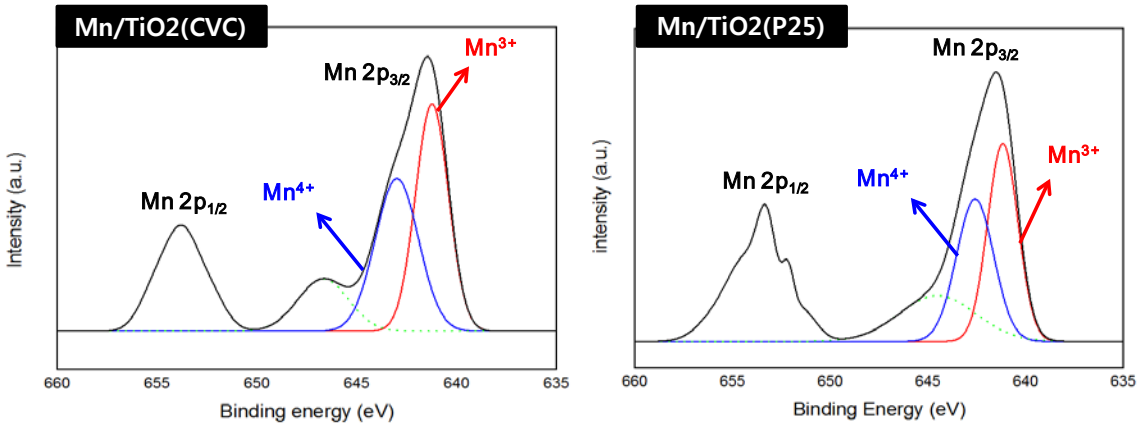

Fig.2 H_2-TPR profiles of the MnOx/TiO_2 catalysts. Heating rate : 10℃/min

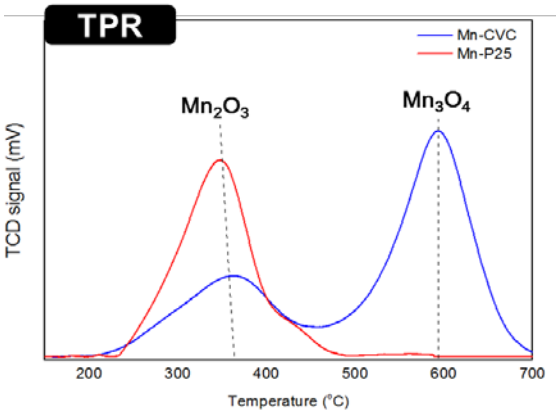

Activity of dimensional converged MnO_2-CeO_2 prepared by electrodeposition for selective catalytic reduction of NO_x gases

Su Hyo Kim[1], Yoo Sang Jeon[1], Jin Sun Cha[2], Min Chul Shin[2] and Young Keun Kim[1*]

[1]Department of Materials Science and Engineering, Korea University, 145 Anam-ro, Seongbuk-gu, Seoul 02841, Korea

[2] Material Testing Center, Basic Industry Division, Korea Testing Laboratory, Seoul 08389, Republic of Korea

slash80@korea.ac.kr (Su Hyo Kim), ykim97@korea.ac.kr (Young Keun Kim),

Nitrogen oxide (NO_x) gases including NO and NO_2 resulting from automobile exhaust and industrial combustion of fossil fuels have been major pollutants for air pollution. Selective catalytic reduction (SCR) with ammonia (NH_3) in the presence of oxygen is the most widely employed technology for NO_x control. In the previous studies, various metal oxide catalysts have been prepared by impregnation [1], co-precipitation [2], and sol-gel [3] methods for the SCR. These days, MnO_2 and CeO_2 have brought out much interest for the researchers in the field of SCR. Because, MnO_2 showed high reactivity to NO_x gases at low temperature and CeO_2 has unique oxygen storage capacity, which results in high reactivity properties especially at high temperature [4]. Therefore, we report the facile synthesis of nanostructured MnO_2-CeO_2 catalysts grown inside a cordierite disc filter which have high efficiency in the large ranges of temperature. The MnO_2 and CeO_2 catalysts were prepared in one bath using an electrodeposition method by pulsed current density without heat treatment. The mixture of MnO_2 and CeO_2 ratio was 3:7, 5:5, 7:3 wt.%.The microstructural and surface properties were studied by SEM, TEM, XRD, XPS and BET, whereas the de-NO_x efficiency was characterized using a NOx analyzer. As a results of SEM and TEM, we could observed dimensionally converged nano-catalysts. CeO_2 nanocrystals, which were spherical in shape and have a tight size distribution with an average particle size of ~5 nm. MnO_2 were wire shape an average size of 150 nm. Moreover, we observed the increase of Mn^{4+}/Mn^{3+} ratio which is efficient to removal of NO_x. These catalysts activity showed broad operating temperature range from 150 to 400^{o}C for the SCR of NO_x with NH_3 at the space velocity of 15,000 h^{-1}.

Keywords: MnO_2-CeO_2 catalysts, Environmental catalysis, Electrodeposition, De-NO_x efficiency, Diesel exhaust

[1] Jemal, J., Tounsi, H., Djemel, S., Pettito, C., Delahay, G. 2013. Characterization and deNO_x activity of copper-hydroxyapatite catalysts prepared by wet impregnation. Reac. Kinet. Mech. Cat., 109, 159-165

[2] Chang, H., Li, J., Chen, X., Ma, L., Yang, S., Schwank, J., W., Hao, J., 2012. Effect of Sn on MnO_x-CeO_2 catalyst for SCR of NO_x by ammonia: Enhancement of activity and remarkable resistance to SO_2, Catal. Commun., 27, 54-57

[3] Rodella, C., B., Mastelaro, V., R., 2003. Structural characterization of the V_2O_5/TiO_2 system obtained by the sol-gel method. J. Phys. Chem. Solids, 64, 833-839

[4] Jo, S., -H., Lee, H., 2015. Local structure and short-range ordering of MnO_2-$Ce_{(1-x)}ZrxO_2/TiO_2$, Mater. Charact., 110, 102-108

From NH_4TiOF_3 Single Crystals to N-Doped Titania Microcages: Enhanced Visible Light Photodegradation of Water Pollutants

Takuya Okada, Hack-Keun Lee, Takumi Fujiwara, Seung-Woo Lee*

Graduate School of Environmental Engineering, the University of Kitakyushu, Fukuoka 808-0135, Japan

*t2511007@eng.kitakyu-u.ac.jp, *leesw@kitakyu-u.ac.jp*

Titanium dioxide (TiO_2) with an anatase or rutile crystal structure has attracted considerable attention as a potential photocatalyst for environmental and industrial applications such as air or water purification and solar energy conversion. However, such photocatalytic reactions of TiO_2 are performed under the ultraviolet light region and the development of TiO_2 materials with photocatalytic activity under visible light are strongly required [1]. In our previous study, we reported a novel synthesis of hollow-structured TiO_2 microcages via room-temperature hydrolysis of NH_4TiOF_3 microsingle crystals [2]. Inside light scattering of the hollow structure played a beneficial role in improving the efficiency of photocatalytic reaction. To fabricate N-doped TiO_2 hollow structures, we used a dye compound of tetrakis(1-methylpyridinium-4-yl)porphyrin *p*-toluenesulfonate (TMPyP) as a nitrogen resource during the hydrolysis of NH_4TiOF_3 and the TMPyP-loaded TiO_2 composites were calcined at different temperatures in the range from 400 °C to 600 °C. The nitrogen content of the calcined products significantly affected the photocatalytic activity of TiO_2 under visible light.

Keywords: N-doped anatase TiO_2, NH_4TiOF_3 \single crystals, Microcage structure,

[1] Maeda, K., Lee, B., Lu, D. & Domen K. 2009. Physicochemical Effects on Photocatalytic Water Oxidation by Titanium Fluorooxynitride Powder under Visible Light. *ACS Chem. Mater*. 2009, 21, 2286–2291

[2] LEE, H.-K. & LEE, S.-W. 2015. Surfactant-free NH_4TiOF_3 Crystals: Self-assembly on Solid Surfaces and Room-temperature Hydrolysis for Hollow TiO_2 Structures with High Photocatalytic Activity. *Chemistry Letter*. 44, 604–606.

NiO/TiO_2 films for photocatalytic degradation of acid orange 7 with and without UV illumination: Effects of storage time and NiO calcination temperature

Chanagun (Wongburapachart)[1], Pramoch (Rangsunvigit)[1,2], Pailin (Ngaotrakanwiwat)[3]

[1] The Petroleum and Petrochemical College, Chulalongkorn University.

[2] Center of Excellence on Petrochemical and Materials Technology.

[3] Department of Chemical Engineering, Burapha University.

E-Mail : pramoch.r@chula.ac.th

TiO_2 photocatalyst has been widely used for the decomposition of environmental pollutants because of its strong oxidizing ability for the decomposition of organic pollutants. However, the photocatalysts need light as excitation source because the above reduction and oxidation reactions are driven by photos. To maintain the functions of the photocatalytic in the absence of light, the photocatalysts with energy storage ability have been developed by coupling a redox-active semiconductor with TiO_2. In this research, NiO/TiO_2 film was prepared by spin coating method on a glass slide plate. Photocatalytic degradation and energy storage ability were evaluated by decomposition of acid orange 7 (AO7). The effects of storage time and NiO calcination temperature were also studied. Concentration of AO7 was detected by UV-vis spectrometer, and properties of NiO/TiO_2 were characterized by field emission scanning electron microscopy (FE-SEM) and X-ray diffractometer (XRD). The result showed that 2 hours for storage energy and NiO calcined 300 ºC are suitable for both photocatalytic activity and energy storage. After light irradiation, the maximum degradation efficiency without UV illumination can reach 22.0%.

Keywords: Energy storage, Photocatalytic degradation, Acid orange 7

[1] Takahashi, Y., and Tatsuma, T. (2005). Oxidative energy storage ability of a TiO_2-$Ni(OH)_2$ bilayer photocatalyst. Langmuir, 21(26), 12357-12361.

Reduced $Cu_3(BTC)_2$ MOF Materials for [3+2] Cycloaddition Reaction

Hyuntae Kang, Soohee Kim, Cho Hye Yoon and Kang Hyun Park*

Department of Chemistry and Chemistry Institute for Functional Materials, Pusan National University, Busan 609-735, Korea

chemistry@pusan.ac.kr

Cu(II) MOF ($Cu_3(BTC)_2$ MOF) porous metal-organic framework consisting of copper was synthesized, and additionally $Cu@Cu_2O$ nanoparticles were prepared by using 10 equivalents $NaBH_4$ as precursor. Cu(II) MOFs were changed into nanoparticles through the chemical reduction. And throughout XPS and XRD data, it was identified that Cu(II) MOFs consisted of Cu^{2+} and that $Cu@Cu_2O$ nanoparticles were mixed with Cu^0 and Cu^+. Copper oxidation state determined the catalytic reactivity in [3+2] cycloaddition reaction. We also found that $Cu@Cu_2O$ exhibited the high activity followed by Cu(II) MOF, Cu/MOF, $CuO+Cu_2O$, Cu/[$CuO+Cu_2O$] and calcined Cu(II) MOF. As a result, we demonstrated that $Cu@Cu_2O$ nanocatalysts showed high activity for a wide range of substrates for [3+2] cycloaddition reaction.

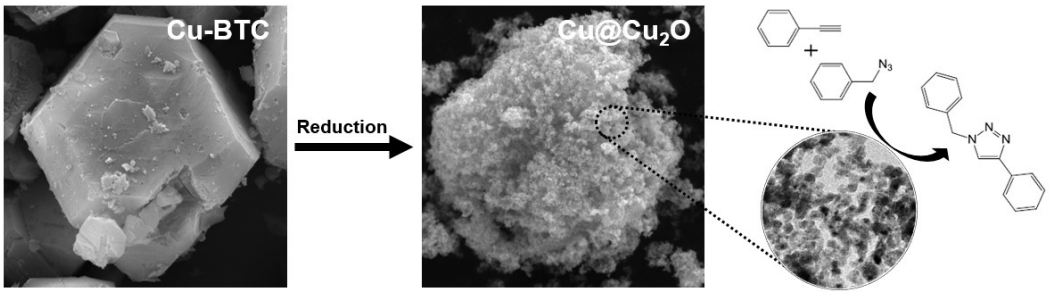

Keywords: Nanoparticles; Heterogeneous; Copper; Catalyst; Click reaction

Dear Organizers of the AFM 2016:

As you requested, the following information about the submitted abstract are provided for your reference.

The contact details of the presenting author:

Professor Chiu-Hsun Lin
Department of Chemistry, National Changhua University of Education, Changhua, 500 Taiwan, ROC
-mail: *chlin@cc.ncue.edu.tw* Tel: *886-4-7232105 ext. 3541* Fax: *886-4-7292361*

The preferred mode of presentation: Poster

The topic of my abstract to be considered for presentation: Nano and Environmental Catalysis

Sulfated and Phosphated H-type Niobate Nanotubes as Solid Acid Catalysts

Y.-M. Huang, C.-H. Lin

Department of Chemistry, National Changhua University of Education, Changhua, 500 Taiwan, ROC

E-mail: *chlin@cc.ncue.edu.tw* ***Tel:*** *886-4-7232105 ext. 3541* ***Fax:*** *886-4-7292361*

Liquid acid catalysts or acidic halides such as H_2SO_4 and $AlCl_3$ are used in many acid-catalyzed reactions, including Friedel-Craft reactions, esterification, hydration and hydrolysis. These conventional acid catalysts are hazardous and corrosive, and are difficult to separate and regenerate. Solid acid catalysts are stable and safe; readily separable from reaction mixtures, and reusable; they pose little environmental hazard and are convenient to use. Therefore, many solid acids such as pillar clay, heteropoly acids, ion-exchange resins, sulfonated carbon materials, sulfated metal oxides and zeolites have been studied. Microporous solid acid catalysts, such as zeolite, have a high surface area, but their small pores limit the rate of diffusion of bulky reactants through them and reduce product yields. Accordingly, large quantities of such catalysts are required when they are used in solid acid catalysis. One-dimensional mesoporous nanotubes have large interior voids, which confine reactants, improving their catalytic performance; they high surface areas, which provide many active sites where the catalytic reaction can proceed. Additionally, these materials typically have a hierarchical pore structure, comprising spaces in the voids of the hollow tubes and those between the nanotubular particles. This pore structure increases the efficiency of diffusion of the reactants and products and, thereby, the efficiency of the catalyst.

Highly pure sodium niobate nanotubes (NaNbNTs) were prepared by treating nonporous Nb_2O_5 powder with 1.0 M NaOH solution at 423 K. SEM revealed that these NaNbNTs formed nanotube-bundles with diameters of 50-250 nm and lengths of several microns. TEM indicated that these nanotubes had outer diameters of 15-20 nm and inner pore diameters of 3-4 nm. BET surface area and pore volume of NaNbNTs were 65 $m^2 g^{-1}$ and 0.17 mL g^{-1}, respectively. Treatment with diluted phosphoric or sulfuric solutions

transformed NaNbNTs into phosphate- or sulfate-promoted protonated niobate nanotubes (PO_4^{-3}/HNbNTs and SO_4^{-2}/HNbNTs), which had a surface area of ~ 80 m^2 g^{-1} , a pore volume ~ 0.26 mL g^{-1} and a surface that was densely covered with acid sites (1.0 ~ 1.5 mmol g^{-1}). Owing to the high density of its acid sites, SO_4^{-2}/HNbNTs outperformed the superacidic SO_4^{-2}/HfO_2 in catalyzing the formation of cyclic acetals from carbonyl compounds and ethylene glycol. TPD/NH_3 indicated that the acid site density in PO_4^{-3}/HNbNTs was even higher than in SO_4^{-2}/HNbNTs, but its activity in catalyzing the formation of cyclic acetals was an order of magnitude lower. These results reveal that acid sites in PO_4^{-3}/HNbNTs had a severe steric effect owing to the thick surface phosphate layer, permitting only the adsorption of small molecules. Large molecules, like heptanal, may not be easily adsorbed on a surface that is densely populated with PO_4^{-3} groups, causing PO_4^{-3}/HNbNTs to have a lower activity than SO_4^{-2}/HNbNTs, which had a lower surface population of equally bulky SO_4^{-2} groups.

Keywords: Niobate, Nanotubes, Acid site density, Acid treatment, Acetal

[1] BUSCA, G., 2007. Acid Catalysts in Industrial Hydrocarbon Chemistry. *Chem. Rev.*, 107, 5366-5410.

[2] CLARK, J. H., 2002. Solid Acids for Green Chemistry. *Acc. Chem. Res.*, 35, 791-797.

Carbon Monoxide Promoted Deposition of Ordered Pt Adlayer on Au(111) and Its Electrocatalytic Properties

Shuehlin Yau*

Department of Chemistry, National Central University, Jhongli, Taiwan 320
yau6017@gmail.com

Abstract

In situ scanning tunneling microscopy (STM) was used to examine the microstructures of platinum (Pt) deposited on ordered Au(111) substrate in aqueous Na_2PtCl_6 solution saturated with carbon monoxide (CO) with and without potential control at room temperature. $PtCl_6^{2-}$ complexes were reduced to Pt atoms by CO molecules and deposited on Au(111) in a hexagonal array without potential control. The adsorption of CO molecules first mobilized and rearranged Pt adatoms on Au(111) from disordered Pt aggregates to 0.9 nm wide tortuous stripes, and then to patches of ordered atomic arrays at 0.1 V (versus reversible hydrogen electrode).

Electrodeposition of Pt in the presence of CO ceased with a monatomic Pt film capped with CO molecules arranged in a (2 × 2) array at 0.1 V. The CO monolayer adsorbed on Pt/Au(111) was stripped off at 0.96 V in 0.1 M H_2SO_4, as compared with 0.83 V observed with Pt(111). The $E_{1/2}$ potential for oxygen reduction reaction (ORR) observed with the Pt-modified Au(111) electrode was 0.81 V in sulfuric acid, which is 0.16 V more positive than that of Pt(111). The microstructures of the as-prepared Pt monolayer on Au(111) changed with potential cycling between 0.05 and 1.0 V.

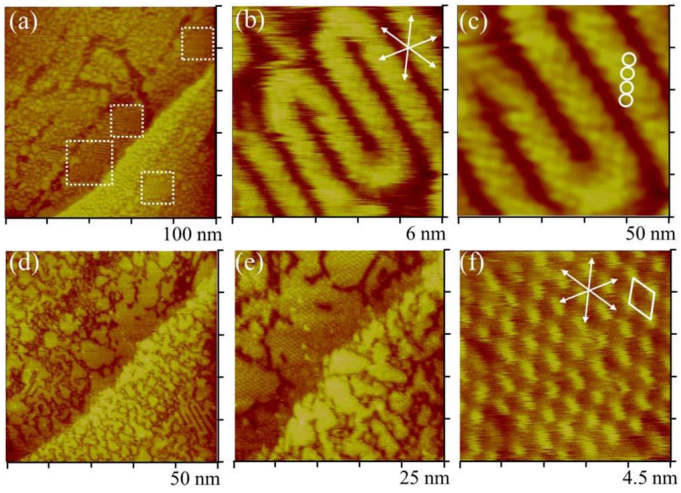

Figure 1. In situ STM images obtained with Pt/Au(111) electrode at 0.1 V in CO-saturated 0.1 M H_2SO_4. Panel (a) was obtained 20 min after CO was added. Torturous chains are highlighted with the dotted squares in panels (b) and (c). Panel (d) shows that the second stage of CO-induced structures imaged as hexagonal arrays ~30 nm (e). The molecular structure of the CO adlayer is revealed in panel (f). The bias voltage and setpoint current were 150 mV and 1 nA.

References

[1] Liao W., Liao W., Yau S. *J. Electrochem. Soc.*162 (2015) H767-773.

Design and Growth of MoS_2 Electrocatalyst by Atomic Layer Deposition for Hydrogen Evolution Reaction

Zhenyu Jin[1], Seokhee Shin[1], Do Hyun Kwon[1] Yo-Sep Min[1*]

[1]Department of Chemical Engineering, Konkuk University, 120 Neungdong-Ro, Gwangjin-Gu, Seoul 143-701, Korea

E Mail/ jwkim1227@gmail.com and ysmin@konkuk.ac.kr

Atomic layer deposition (ALD) has emerged as a useful tool for design and synthesis of catalysts with atomic scale precision. Here, we report ALD of MoS_2 which has attracted great attention as an electrocatalyst for hydrogen evolution reaction (HER). MoS_2 catalysts are grown at 100 ^oC using molybdenum hexacarbonyl and dimethyldisulfide as precursors of Mo and S, respectively.[1] The crystallographic phases of the catalysts grown at 100 ^oC by ALD depend on the selection of a supporting substrate. The ALD-MoS_2 is amorphous on Au but a mixture of amorphous and nano-crystalline phases on carbon fiber paper (CFP). The most important advantage of the ALD-MoS_2 is its high turnover frequency for the HER,[2] and the electrocatalytic performance of the ALD-MoS_2 can be improved by choosing a porous supporting substrate of CFP with a large specific surface area. To unveil the inherent activity of the ALD-MoS_2, we discuss the effects of fractional surface coverage of MoS_2 on the CFP and the crystallographic phases on the electrocatalytic activity.

Keywords: MoS_2, electrocatalyst, atomic layer deposition, hydrogen evolution reaction

[1] JIN, Z., SHIN, S., KWON, D. H., HAN, S. J. & MIN, Y. S. 2014. Novel Chemical Route for Atomic Layer Deposition of MoS_2 Thin Film on SiO_2/Si substrate. *Nanoscale,* 6, 14453-14458.

[2] SHIN, S., JIN, Z., KWON, D. H., BOSE, R., & MIN, Y. S. 2015. High Turnover Frequency of Hydrogen Evolution Reaction on Amorphous MoS_2 Thin Film Directly Grown by Atomic Layer Deposition. *Langmuir,* 31, 1196-1202.

Symposia 7

Low dimensional, Nano and 2D materials

- Structural, electrical, mechanical and optical of low dimensional, nano and 2D-layered oxides, nitrides and sulfides
- Advances in the Synthesis and Characterization of low dimensional, nano and 2D materials
- Large Scale Growth & Characterization of 2D-layered oxides, nitrides, carbides and sulfides
- Spectroscopy studies of low dimensional, nano and 2D materials Carbon Based materials
- Advanced Nuclear Materials
- Magnetic Materials
- Applications of low dimensional, nano and 2D materials
- Nano-optics, Nano-optoelectronics, Nano-Photonics and Nano-photonics
- Computational modeling and simulation of low dimensional, nano and 2D materials
- Low dimensional, nano and 2D materials for optical devices, Flexible Electronics Sensors & Composites
- Nanomedicine, Nanobiotechnology, Environment and Nanotoxicology
- Photonic and optoelectronic device applications of low dimensional, nano and 2D materials
- Exfoliation and unzipping 2D materials
- Others

Index Page

Clusterization of rubber blends by means of its carbon black particles used as reinforcing agent using softcomputing techniques

Roberto Fernandez Martinez[1], Pello Jimbert[1], Maider Iturrondobeitia[1], Julen Ibarretxe[1]

[1]eMERG, University of the Basque Country UPV/EHU, Bilbao, Spain

roberto.fernandezm@ehu.es / ETSI. University of the Basque Country, UPV/EHU, Alameda Urquijo s/n. 48013 Bilbao, Spain.

The process of clustering rubber blends through their reinforcing agent, which define the structure of the material, according to their shape using Automated (TEM) Image Analysis (AIA) is a complicated task, but the results of this clusterization can predict an approximation of the final mechanical properties of the material. This clusterization can be performed using variables that identify the reinforcing agent object by its 2D shape. There are many features that define the 2D shape of an aggregate, but in this work, 21 features are defined and measured from 7714 fillers obtained through TEM images. Defined in ASTM Standard D3849-07: aggregate area (A), aggregate perimeter (P), diameter of a circle with the same area (D), aggregation factor (α), average particle size for an aggregate (d_p), aggregate volume (V_A), particle volume (V_p) and number of particles in the aggregate (n). Based on the boundary: roughness (R_o), signature (SSD), number of Fourier descriptors (FD), number of segments that intercept the boundary (CC_{seg}) and total number of interceptions (CC_{cu}). And based on the region: circularity (C), solidity (S_o), extent (E_x), eccentricity (E_c), mean and standard deviation of extent (Ex_{Mean}, Ex_{SD}) and mean and standard deviation of the solidity (So_{Mean}, So_{SD}) [1]. Once a dataset with all these features are automatically calculated, neural networks techniques are used to cluster rubber blends using a methodology that tune parameters within the algorithm to improve the models performance. Also, and like the number of parameters

can be high to get accurate results, genetic algorithms are applied to make a feature selection in order to get robust and accurate models. Using feed-forward neural networks with a single hidden layer without feature selection, it is obtained an accurate 74.80% of positive classification, and using genetic algorithm to optimize the models the results are improved, obtaining a total accuracy of 75.75%. Also the number of features used during the process turned out to be reduced from 21 to 16 significant features. It is demonstrated that the combination of genetic algorithms with neural networks improves the results and cluster rubber blends by means of its carbon black particles used as reinforcing agent accurately.

Keywords: Clusterization, softcomputing techniques, rubber blends, carbon black particles

[1] FERNANDEZ MARTINEZ, R., OKARIZ, A., IBARRETXE, J., ITURRONDOBEITIA, M. & GURAYA, T. 2014. Use of decision tree models based on evolutionary algorithms for the morphological classification of reinforcing nano-particle aggregates. *Computational Materials Science*, 92, 102–113.

Dual Nature of Asymmetry in Raman line shapes of heavily doped silicon nanowires

Shailendra K. Saxena*, Hari Mohan Rai, Priyanka yogi Suryakant Mishra, Vikash Mishra, Rajesh Kumar and Pankaj R. Sagdeo

Material Research Laboratory, Discipline of Physics, Indian Institute of Technology Indore Simrol, Indore (M.P.) – 452020, India

Corresponding Author phd12115112@iiti.ac.in*

Well aligned Silicon nanowires (SiNWs) have been successfully fabricated from heavily doped n-type and p-type Si wafers by metal induced etching (MIE). Raman spectra of heavily doped SiNWs have been analyzed. The asymmetry of Raman line shape shows the different nature from as usual phonon confined systems. Asymmetry in the lower energy side of Raman peak for n-type SiNWs whereas the asymmetry turns from lower energy side to the higher energy side of the Raman peak as compared to c-Si in p-type SiNWs. The origin of flipping of asymmetry is investigated as attributed from the presence of electron phonon interaction[1–3] in addition to phonon confinement in the SiNWs which plays the role in flipping the asymmetry. The presence of electron phonon interaction was confirmed from the Raman spectra of their bulk counterpart and observed antiresonance in Raman spectra which are the pronounced signature of electron phonon interaction. This study is very much important for the researchers who used phonon confinement model for quantum confined systems.

[1] Bar-Ad S, Kner P, Marquezini MV, Mukamel S, Chemla DS. Quantum Confined Fano Interference. Phys Rev Lett 1997;78:1363–6. doi:10.1103/PhysRevLett.78.1363.

[2] Sagar DM, Atkin JM, Palomaki PKB, Neale NR, Blackburn JL, Johnson JC, et al. Quantum confined electron-phonon interaction in silicon nanocrystals. Nano Lett 2015;15:1511–6. doi:10.1021/nl503671n.

[3] Saxena SK, Borah R, Kumar V, Rai HM, Late R, Sathe V g., et al. Raman spectroscopy for study of interplay between phonon confinement and Fano effect in silicon nanowires. J Raman Spectrosc 2015:n/a – n/a. doi:10.1002/jrs.4820.

Enhanced Long-term Stability of Graphene-Cu Nanowires Hybrid Film

Liangjing Shi, Ranran Wang, Jing Sun

State Key Laboratory of High Performance Ceramics and Superfine Microstructure,

Shanghai Institute of Ceramics, Chinese Academy of Sciences, 1295 Dingxi Road,

Shanghai 200050, People's Republic of China.

slj198804@mail.sic.ac.cn, jingsun@mail.sic.ac.cn

Recently, there has been a quest of new materials to replace ITO because of the rising cost and its brittleness, which limit its usage in flexible electronic devices. Metal nanowires, such copper nanowires (Cu NWs), have been demonstrated a promising material for transparent electrodes, considering their low cost and high optical-conductive performance which is comparable to or even better than ITO [1]. However, several disadvantages of the copper nanowire films, such as poor adhesion to substrates, typically high junction resistance, high contact resistance between the network (because of the non-contacted, open space in the network) and especially material instability in a severe environment, have limited their applications into commercial devices [2]. On the other hand, Graphene owns extremely high electron mobility, but low optical absorption throughout the visible range, which makes it a valuable material in electronic area. Moreover, passivation properties of graphene on protecting metal foil from oxidation have been demonstrated [3]. While, whether graphene can provide specifically effective protection to the Cu NW network needs to be investigated systematically because Cu NWs have different surface morphologies and properties with copper foil.

In this work, we fabricated graphene covered Cu NW films and demonstrated the long term oxidation resistant effect of graphene on the underlying Cu NW network. The graphene covered Cu NW film exhibited much more great resistance stability than pristine film. The ratio of R/R_0 was only 1.27 after being stored in an ambient atmosphere for 45 days, and that ratio was maintained below 2 (1.91) even after 6 months. Besides, we proposed the two-step oxidation kinetics of Cu NWs by using Raman spectra and X-ray photoelectron spectroscopy and discovered the anti-oxidation mechanism of graphene on Cu NWs particularly. Cu NWs have high surface energy and are more easily oxidized than copper foil, which resulted in a

significant increase in the sheet resistance in an ambient atmosphere. the main function of graphene is preventing the permeation of O_2 and H_2O, decelerating the oxidation from Cu to Cu_2O and hindering the oxidation Cu_2O to CuO. The results obtained in this work are of referring significance to make metal nanowire based transparent electrodes with both high optical-electrical performance and excellent stability.

Keywords: copper nanowires film, graphene, anti-oxidation

[1] ZHANG, D. Q., WANG, R. R., WEN, M. C., WENG, D., CUI, X., SUN, J., LI, H. X. & LU, Y. F. 2012. Synthesis of ultralong copper nanowires for high-performance transparent electrodes. *J. Am. Chem. Soc.*, 134, 14283-14286.

[2] WU, Y., XIANG, J., YANG, C., LU, W. & LIEBER, C. M. 2004. Single-crystal metallic nanowires and metal/semiconductor nanowire heterostructures. *Nature*, 430, 61-65.

[3] PRASAI, D., TUBERQUIA, J. C., HARL, R. R., JENNINGS, G. K. & BOLOTIN, K. I. 2012. Graphene: Corrosion-Inhibiting Coating. *ACS Nano*, 6, 1102-1108.

Growth and Properties of Ribbons from layered $GaSe_xTe_{1-x}$ Alloys

Fonseca, Jose J.[1,2,*], Jaquez, Maribel[1,2], Walukiewicz, Wladek[2], Dubon, Oscar D.[1,2]

[1] Department of Materials Science and Engineering, University of California, Berkeley, California 94720, USA

[2]Materials Sciences Division, Lawrence Berkeley National Laboratory, Berkeley, California 94720, USA

E-Mail: jose.j.fonseca@berkeley.edu (presenting and corresponding author)

The growth of one-dimensional (1D) structures of layered semiconductors has allowed for the further exploration and control of already exciting properties observed in these materials. In contrast to the layered semiconductors grown by bulk-growth methods, e.g. Bridgman growth, mesoscopic structures offer some advantages such as different geometries and dimensionalities, high-quality as-grown surfaces, and a reduced density of stacking faults, generally formed during crystal-pulling from melt or sample cleaving. Growth of 1D structures of III-VI, monochalcogenide, layered semiconductors like GaS, GaSe and GaTe has been previously shown [1–3]. Here, we demonstrate the growth of layered ribbons, typically less than 100 nm in thickness and less than 500 nm in width, across the $GaSe_xTe_{1-x}$ compositional range and compare their structural and optical properties to the same alloys grown by a bulk method. Consistent with previous studies [4], we observed a discontinuity in the crystal structure of ribbons from monoclinic on the Te-rich side to hexagonal on the Se-rich side. However, while a single-phase product within the composition range of $0.35 < x < 0.7$ has not been obtained via bulk crystal growth, monoclinic structures for $x \leq 0.45$ and hexagonal structures for $x \geq 0.6$ were grown in the form of ribbon. On the Se-rich (hexagonal) side of the composition range, ribbons show a strong, room-temperature photoluminescence peak ranging from 2.0 eV for GaSe (x=1) to 1.4 eV for x=0.6, the latter being well below the excitonic emission from either GaTe or GaSe, respectively. The source of this photoluminescence as well as other structural and optical properties will be discussed. This research project is part of the Electronic Materials Program at the Lawrence Berkeley National Laboratory, supported by the Director, Office of Science, Office of Basic Energy Sciences, Materials Sciences and Engineering Division, of the U.S. Department of Energy under Contract No. DE-AC02-05CH11231. In addition, the presenting author

acknowledges the support from the National Science Foundation Graduate Research Fellowships Program (Grant No. DGE-1106400).

Keywords: layered semiconductor, nanostructure growth, semiconductor alloy, GaSe, GaTe

[1] SHEN, G., CHEN, D., CHEN, P., & ZHOU, C. 2009. Vapor-Solid Growth of One-Dimensional Layer-Structured Gallium Sulfide Nanostructures. *ACS Nano*, 3, 1115–1120.

[2] PENG, H., Meister, S., CHAN, C. K., ZHANG, X. F., & CUI, Y. 2007. Morphology control of layer-structured gallium selenide nanowires. *Nano Lett.*, 7, 199–203.

[3] YU, G., LIU, Z., XIE, X., OUYANG, X., & SHEN, G. 2014. Flexible photodetectors with single-crystalline GaTe nanowires. *J. Mater. Chem. C*, 2, 6104–6110.

[4] CAMASSEL, J., MERLE, P., MATHIEU, H. & GOUSKOV, A. 1979. Near-band-edge optical properties of $GaSe_xTe_{1-x}$ mixed crystals. *Phys. Rev. B*, 19, 1060–1068 .

Highly Luminescent Gold Nanoclusters: the Design Strategies

Dongil Lee

Department of Chemistry, Yonsei University, Korea

Ultrabright luminescent nanomaterials have received tremendous research attention for their applications in light emitting diode displays, luminescent sensors and biological imaging. Atomically precise gold clusters with well-defined core-shell structures present bright pros pects to achieve high photoluminescence efficiencies. In this study, gold clusters with luminescence quantum yield higher than 60% were synthesized based on $Au_{22}(SG)_{18}$ c luster, where SG is glutathione, by rigidifying its shell-gold with tetraoctylammonium (TOA) cations. Time-resolved and temperature-dependent optical measurements on $Au_{22}(SG)_{18}$ have shown the presence of high quantum yield visible luminescence below fr eezing indicating that shell rigidity enhances the luminescence quantum efficiency. To achieve high rigidity of shell-gold, $Au_{22}(SG)_{18}$ was bound to bulky TOA that resulted in greater than 60% quantum yield luminescence at room temperature. Optical measu rements have confirmed that the rigidity of shell-gold was responsible for the lumines cence enhancement. This work presents an effective strategy to enhance the photolumines cence efficiencies of gold clusters by rigidifying the Au(I)-thiolate shell.

In-situ X-ray diffraction study on crystal growth of iron sulfide minerals

Y. H. Chen[1], M. Y. Lin[1], S. H. Li[1], J. J. Lee[2], and H. S. Sheu[2]
[1]Department of Earth Sciences, National Cheng Kung University, Tainan
[2]National Synchrotron Radiation Research Center, Hsinchu

Pyrite (FeS_2) is a very common mineral in nature and the variations in chemical compositions result in different iron sulfide minerals, such as mackinawite (FeS), pyrrhotite (Fe_7S_8), and greigite (Fe_3S_4). However, the formation mechanisms of different types of iron sulfide minerals in sediments and the chemical conditions for their stable existence remain unclear [1-3]. Therefore, in this study, in-situ X-ray diffraction is used to explore novel crystal growth paths, and instant investigations on the crystal growth of iron sulfide minerals.

The iron sulfide minerals were synthesized via a simple co-precipitation method, and the precipitates were separated using deionized water without oxygen and freeze-dried to obtain mackinawites (Fig. 1). The possible reaction was as follows. $FeSO_4+Na_2S \rightarrow FeS+Na_2SO_4$. This indicated that the precursor for this synthetic process was the mackinawite phase. The iron sulfide minerals were also fabricated at pH 3, 7, and 11. It was found the mackinawite phase existed at pH 3 (Fig. 2) When the reaction time was increased from 1 h to 24, 48, and 72 hr, the major phase showed the following transformation: mackinawite $\rightarrow$ greigite + S $\rightarrow$ greigite + pyrite + S $\rightarrow$ greigite + pyrite + S (Fig. 3). This suggested that the precursor would transform to other mineral phases within 24 hr.

The "in-situ" crystal growth of iron sulfide minerals was carried out via the synchrotron radiation experiment on beamline beamline 17A1 and 01C2 at the National Synchrotron Radiation Research Center, Hsin-Chu, Taiwan. During the temperature process from 25 to 250°C, the (220) diffraction peak of greigite and the (311) peak of pyrite disappeared at 120°C; a different diffraction pattern was observed at 200°C. Furthermore, the amorphous mackinawite phase was transformed into greigite and pyrite kept at 150°C lasting for 0.5 hr. This observation suggested that the reaction time and temperature indeed influenced the Fe-S formation pathway and the possible reaction was as follows. $FeS+2H^+=Fe^{2+}+H_2S \Rightarrow 3FeS+H_2S=Fe_3S_4+H_2 \Rightarrow Fe_3S_4+2H_2S=3FeS_2+2H_2$.

Keywords: iron sulfide mineral, crystal growth, in-situ and ex-situ, co-precipitation method, simulation, synchrotron radiation.

Luminescent carbon dots and their applications for DNA detection and cell imaging

Ying Li, Chun Chun Luo and Hui Peng

Key Laboratory of Polar Materials and Devices, Ministry of Education, East China Normal University, P. R. China

E Mail: hpeng@ee.ecnu.edu.cn

Over the past two decades quantum dots (QDs) have been the subject of intense research due to a unique combination of properties, particularly their high chemical stability, resistance to photodegradation and easily tuned optical properties.[1; 2] QDs may give rise to very promising applications in biosensing[3] and bioimaging[4] if obstacles such as strict synthesis conditions, high prices and known toxicity (e.g. with CdSe and CdTe QDs) can be addressed.[4] Thus, significant efforts have been devoted to synthesizing QDs based on alternative materials with lower toxicity while retaining advantageous optical properties.

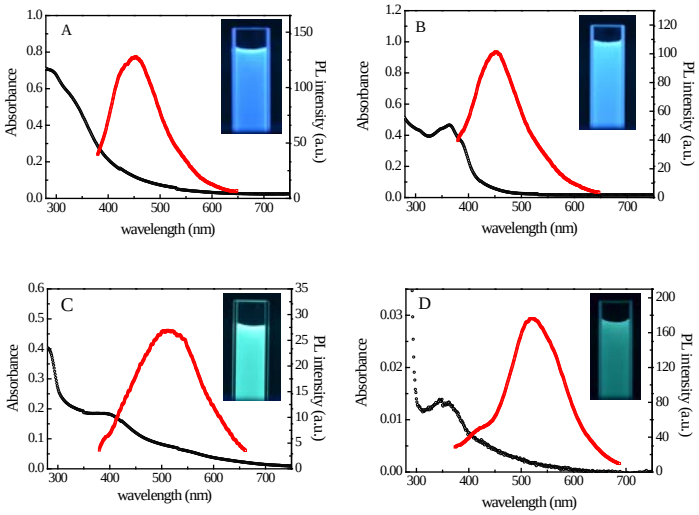

Figure 1 Absorption spectra and emission spectra of (A) *GT*-C-dots, (B) *CT*-C-dots, (C) *GD*-C-dots and (D) *CD*-C-dots. The emission spectra were recorded at an excitation wavelength of 340 nm. Insets: the optical images of prepared C-dots under UV lamp (324 nm).

Carbon dots (C-dots) are an alternative type of materials to QDs, firstly isolated from carbon nanotubes (CNTs) and yielding interesting photoluminescence properties. [5] Here

we reported how to tune the properties of nitrogen-doped C-dots by reaction precursors. Four types of luminescent nitrogen-doped C-dots are prepared by using glucose (G) or citric acid (C) as carbon source, and dopamine (D) or 4,7,10-trioxa-1,13-tridecanediamine (T) as nitrogen source, named GD-C-dots, GT-C-dots, CD-C-dots and CT-C-dots. The investigation on the optical, pH-sensitivity and photovoltaic properties of these C-dots illustrates that nitrogen source plays a key role in the properties of obtained C-dots. GD-C-dots and CD-C-dots show interesting electrochemical activities, which can provide fluorescent and electrochemical dual signals for practical applications. We demonstrate that not only the optical properties but also other physicochemical properties can be tuned by appropriate choice of the reaction precursors. At last, the application of C-dots to the DNA detection based on the fluorescence resonance energy transfer and the cell imaging will be discussed.

Keywords: Nitrogen-doped carbon dots, pH-sensitivity

Reference

[1]. BRUCHEZ, M., JR., MORONNE, M., GIN, P., WEISS, S., ALIVISATOS, A.P., 1998. Semiconductor nanocrystals as fluorescent biological labels. *Science* 281(5385), 2013-2016.

[2]. PENG, Z.A., PENG, X., 2001. Formation of high-quality CdTe, CdSe, and CdS nanocrystals using CdO as precursor. *J. Am. Chem. Soc.* 123(1), 183-184.

[3]. PENG, H., ZHANG, L., KJAELLMAN, T.H.M., SOELLER, C., TRAVAS-SEJDIC, J., 2007. DNA Hybridization Detection with Blue Luminescent Quantum Dots and Dye-Labeled Single-Stranded DNA. *J. Am. Chem. Soc.* 129(11), 3048-3049.

[4]. MICHALET, X., PINAUD, F.F., BENTOLILA, L.A., TSAY, J.M., DOOSE, S., LI, J.J., SUNDARESAN, G., WU, A.M., GAMBHIR, S.S., WEISS, S., 2005. Quantum Dots for Live Cells, in Vivo Imaging, and Diagnostics. *Science* 307(5709), 538-544.

[5]. RAO, C.N.R., SATISHKUMAR, B.C., GOVINDARAJ, A., NATH, M., 2001. Nanotubes. *ChemPhysChem* 2(2), 78-105.

One-step Preparation of Reduced Graphene Oxide Thin Films by Bipolar Electrochemistry in Deionized Water

Allagui, A.[1,2], Alawadhi. H.[1,3], Abdelkareem, M.A.[2], Elwakil, A.S.[4]

[1] Center for Advanced Materials Research, [2] Dept. of Sustainable and Renewable Energy Engineering, [3] Dept. of Applied Physics, [4] Dept. of Electrical Engineering, University of Sharjah, PO Box 27272, Sharjah, United Arab Emirates

aallagui@sharjah.ac.ae / Tel: +971-5-69500184

Most of today's preparation techniques for graphene and graphene-related materials, such as chemical oxidation-exfoliation-reduction [1], sonication [2], chemical vapor deposition [3], and epitaxial growth on SiC wafer [4], either suffer from a low production yield and/or require expensive setups and make use of complex and toxic chemical and physical processes, thus making them unattractive for widespread use. Furthermore, the subsequent transfer of the graphene layers onto a substrate, makes the overall process even more intricate and time-consuming. Here we present a single-step, single-pot direct preparation of metal-supported reduced graphene oxide (rGO) using the principle of bipolar electrochemistry of a wireless graphite in deionized water [5]. Under a 15 V cm^{-1} electric field between two stainless steel feeder electrodes (see figure below), a maximum surface potential difference of 9 V was induced between the two ends of the floating graphite substrate (0.6 cm diameter) which is sufficient enough (> 1.5V) to promote coupled redox reactions at its anodic and cathodic poles. Graphene layers at the anodic pole of the wireless graphite were oxidized into colloidal dispersion of GO, which migrated electrophoretically towards the anodic side of the cell, and deposited in the form of rGO by van der Waals forces (d(002) = 0.395 nm). The deposits were characterized by scanning electron microscopy, X-ray diffraction, micro-Raman spectroscopy, and UV-Vis spectroscopy. This method is shown to be straightforward, inexpensive, environmentally-friendly, and could be easily scaled up for high yield large area production of rGO thin films on flat or complex three-dimensional surfaces.

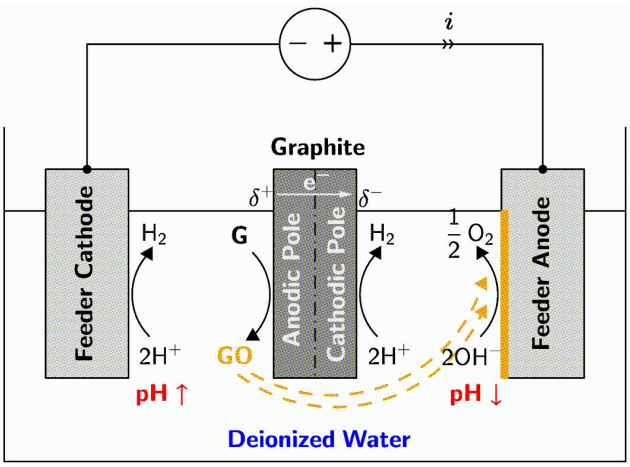

Fig. 1: Schematic diagram of bipolar electrochemical setup used for the preparation of stainless steel-supported rGO [5]. In a typical synthesis process, a voltage difference is applied between two stainless steel feeding electrodes inducing a polarization of the wireless graphite. On the cathodic pole, water reduction reaction takes place, whereas GO, resulting from the oxidation of the anodic side of the graphite rod, migrates eletrophoretically towards the positive stainless steel to be deposited in the form a uniform light yellow thin film of rGO.

Keywords: Graphene, Graphene oxide, Bipolar electrochemistry, Redox reactions

[1] HUMMERS, W. S. & OFFEMAN, R. E. 1958. Preparation of graphitic oxide. *J. Am. Chem. Soc.*, 80, 1339–1339.

[2] HERNANDEZ, Y. et al. 2008. High-yield production of graphene by liquid-phase exfoliation of graphite. *Nat. Nano.*, 3, 563–568.

[3] BAE, S. et al. 2010. Roll-to-roll production of 30-inch graphene films for transparent electrodes. *Nat. Nano.*, 5, 574–578.

[4] BERGER, C. et al. 2004. Ultrathin epitaxial graphite: 2d electron gas properties and a route toward graphene-based nanoelectronics. *J. Phys. Chem. B*, 108, 19912–19916.

[5] ALLAGUI, A., ABDELKAREEM, M. A., ALAWADHI, H. & Elwakil, A. S. 2016. Reduced graphene oxide thin film on conductive substrates by bipolar electrochemistry. *Sci. Rep.*, Accepted for Publication.

Opportunities for sp^2-hybridized Carbon Nitride

P.O.Å. Persson[1], J. Palisaitis[1], and A. Kakanakova-Georgieva[1]

[1]Department of Physics, Chemistry and Biology, IFM, Linköping University, SE-58183 Linköping Sweden

anelia@ifm.liu.se

A widespread interest is currently emerging in graphitic carbon nitride, which consists of covalently-linked, sp^2 hybridized carbon and nitrogen atoms in an alternating fashion [1]. It is suggested to be 2D material of inherent semiconductivity with band gap of between 1.6 and 2.0 eV [1]. Therefore, it will enable the development of bang gap engineered device applications at the 2D limit.

We present here evidences of sp^2 hybridized carbon nitride resulting from metalorganic chemical vapour deposition (MOCVD) experiments at various temperatures, which were originally designed to tailor the surface treatment of the SiC substrate before the deposition of AlN epitaxial layers [2, 3]. The overall heteroepitaxial stack is accomplished in a continuous process under characteristic MOCVD process implementing the principal precursors ammonia and trimethylaluminum [4]. The low process pressure of 50 mbar is prompted to promote a low supersaturation of the SiC vapor over the heated substrate surface. Further control of the appearance of the substrate surface relates to the implementation of high process temperature of 1250^{o}C, and up to 1450^{o}C, coupled together with the etching effect of the hydrogen carrier gas, and furnished further by the exposition of the SiC substrate surface to ammonia. Ammonia is introduced at the end of the temperature ramping step and ahead of the TMAl introduction. It is known to give rise to surface effects including nitrogen chemisorption.

Topographic and phase AFM [5] analysis shows step-bunched wide terraces with characteristic domains interspersed along the steps and of apparently different material. The domains with lateral size of tens-of-nanometers originate from the intervening SiC substrate treatment. The heteroepitaxial stack is analyzed by high resolution scanning

TEM (HR- STEM) and local electron energy loss spectroscopy (EELS). The domains were identified as sp^2 hybridized carbon nitride.

Looked upon from a different perspective, our findings may also have implications for managing significantly better any successful epitaxial growth of AlN (group III-Nitrides) on SiC supported graphene templates for electronic devices, including in the context of managing significantly better the heat dissipation in the devices operating under high currents, i.e. the group III-Nitrides based LEDs [6].

Keywords: MOCVD, layered materials, CN, semiconductors, templates

[1] A. I. Cooper, and M. J. Bojdys, Materials Today 17 (2014) 468.

[2] A. Kakanakova-Georgieva, D. Nilsson, and E. Janzén, J. Cryst. Growth 338 (2012) 52.

[3] D. Nilsson, E. Janzén, and A. Kakanakova-Georgieva, paper no.7 in Linköpings Studies in Science and Technology Dissertation No. 1597 (2014), ISBN 978-91-7519-332-8.

[4] A. Kakanakova-Georgieva, et al., Cryst. Growth & Design 9 (2009) 880.

[5] S. Jhou, LITH-IFM-A-EX—13/2815—SE.

[6] N. Han, T.V. Cuong, M. Han, et al., Nature Communications 4 (2013) 1452.

[7] This research was supported by the Swedish Governmental Agency for Innovation Systems (VINNOVA) and the Swedish Research Council (VR).

Photoluminescent Gold Nanoparticles – Synthesis and Applications

Sheng-Feng Lai[1,2], Yeukuang Hwu[*1,2,3]

[1] Department of Engineering Science, National Cheng Kung University, Tainan 701, Taiwan

[2] Institute of Physics, Academia Sinica, Taipei 115, Taiwan

[3] Advanced Optoelectronic Technology Center, National Cheng Kung University, Tainan 701, Taiwan

Corresponding author's email: phhwu@sinica.edu.tw;

presenting author's email: samuellai@gate.sinica.edu.tw

A simple and effective method based on reduction by intense X-ray irradiation successfully produces high quality colloidal surface-functionalized gold nanoparticles (Au NPs) with tunable sizes. Specifically, controlling particle size by surface thiolation with alkanethiolate coatings of different carbon chain lengths yields strong visible photoluminescence as the chain length increases. Multimodality imaging using visible light fluorescence and X-ray microscopy is demonstrated by tracing the nanoparticle-loaded tumor cells. We further demonstrate that the excellent imaging characteristics and the very high accumulation in cancer cells possessed by very small Au NPs (< 2 nm) synthesized in the presence of carboxyl-terminated *n*-alkanethiolate are particularly favorable to the biomedical applications.

Keywords: gold nanoparticles, radiation synthesis, photoluminescence

[1] LAI, S. F., CHEN W. C., WANG, C. L., CHEN, H. H., CHEN, H. T., CHIEN, C. C., CHEN, Y. Y., HUNG, W. T., CAI, X., LI, E., KEMPSON, I. M., HWU, Y., YANG, C. S., TOK, E. S., TAN, H. R., LIN, M., MARGARITONDO, G. 2011. One-Pot Tuning of Au Nucleation and Growth: From Nanoclusters to Nanoparticles. *Langmuir*, 27, 8424-8429.

[2] LAI, S. F., CHIEN, C. C., CHEN W. C., CHEN, H. H., CHEN, Y. Y., WANG, C. L., HWU, Y., YANG, C. S., CHEN, C. Y., LIANG, K. S., PETIBOIS, C., TAN, H. R., TOK,

E. S., MARGARITONDO, G. 2013. Very Small Photoluminescent Gold Nanoparticles for Multimodality Biomedical Imaging. *Biotechnol. Adv.*, 31, 362-368.

[3] LAI, S. F., TAN, H. R., TOK, E. S., CHEN, Y. H., ONG, E. B. L., LI, M. T., CHEN, Y. Y., CHIEN, F. C., CHEN, P., MARGARITONDO, G., HWU, Y. 2015. Optimization of Gold Nanoparticle Photoluminescence by Alkanethiolation. *Chem. Commun.*, 51, 7954.

Synthesis of Silver Triangular Nanoplates: Control the over Size and Thickness

B. Ajitha, Hwan-Jin Jeon, Chi Won Ahn*

Division of Nano-Structure Materials, National NanoFab Center, Daejeon 305-338, Republic of Korea.

E-Mail: ajithabondu@gmail.com, cwahn@nnfc.re.kr

Silver nanotriangles (AgNTs) show more LSPR bands through their reduced symmetry and the in-plane dipole resonance can be simply tailored with their edge length comparing to the spherical or quasi-spherical nanoparticles. In the present study, AgNTs were synthesized through seed-mediated growth process. The size of the nanotriangles can be tuned within a wide range by simply changing the experimental parameters such as volume of seed solution, concentration of poly vinyl pyrrolidone (PVP), reaction time and among others. The volume of seed solution in the growth solution and the time interval between multiple steps of growth were key factors which determine the improvement of uniform triangular Ag nanoplates. Herein, we synthesized the AgNTs with different volumes of seed solution and studied the morphology change. Moreover, by further isotropic overgrowth, the edge length and the thickness of triangular Ag nanoplates can be finely tuned. The edge length was found to be varied from 300 nm to 2 μm and the thickness was increased by 2 nm for each overgrowth step. It has been confirmed that the Ag seeds can be governed to grow into nanocrystals enclosed by {111} or {100} facets by the addition of citrate ions or PVP, which makes them more stable with respect to the other facets [1]. Finally, the synthesized nanotriangles have a high yield of anisotropy with improved uniformity, which will ultimately facilitate the SERS-based applications.

Keywords: Silver nanotriangles, morphology, edge length, thickness, anisotropy

[1] ZENG, J., ZHENG, Y., RYCENGA, M., TAO, J., LI, Z. Y., ZHANG, Q., ZHU, Y. & XIA, Y. 2010. Controlling the Shapes of Silver Nanocrystals with Different Capping Agents. *J. Am. Chem. Soc*, 132, 8552-8553.

Investigating the growth of single-crystal-like Ag films on mica

Dah-An Luh[1,2], Chen-Wei Liu[1], Chia-Hsin Wang[2], Yaw-Wen Yang[2]

[1]Department of Physics, National Central University, Taoyuan, Taiwan

[2]National Synchrotron Radiation Research Center, Hsinchu, Taiwan

E Mail: luh.dah.an@gmail.com

The surfaces of metallic single crystals have been utilized to grow and study highly ordered 2D overlayers. However, the applications of constructing devices on them are limited severely because of their high cost and conducting nature. One way to address these issues is to grow 2D overlayers over the single-crystal-like metallic thin films on insulating substrates: The high quality of the 2D overlayers is ensured because of the single-crystal-like substrates as the platform, and the metallic thin films may be etched away, leaving the 2D overlayer on the insulating substrates for further processes. In this study, we investigated the Ag/mica system, in which Ag is deposited on cleaved mica surface. Our results showed that, after sputtering and annealing, the Ag/mica film formed a highly ordered surface without disorientated domains. A clear (1×1) LEED pattern was observed, indicating that the surface of the Ag/mica film resembles a clean Ag(111) surface. Furthermore, we deposited Si on this Ag/mica film, and produced successfully the surface reconstructions of silicence. This result is the same as the growth of Si on Ag(111), demonstrating that the surface of the Ag/mica thin film indeed possesses the surface characteristics of the Ag(111) single crystal.

Keywords: metallic thin films, silicence, mica, LEED

Microstructure and magnetic properties of Co-V nanotubes

Yoo Sang Jeon[1], Su Hyo Kim[1], Da Yeon Nam[1], and Young Keun Kim[1]

Presenting author should be underline

[1]Department of Materials Science and Engineering, Korea University, 145 Anam-ro, Seongbuk-gu, Seoul 02841, Korea

chunyoosang@korea.ac.kr (Yoo Sang Jeon), ykim97@korea.ac.kr (Young Keun Kim)

Magnetic 1-D nanomaterials have aroused attention for potential applications in electronic and biomedical sensors because they have shape anisotropy and their surfaces can be utilized, for example, by binding various chemical and biological molecules. The Ni nanowire arrays have been applied for a highly sensitive diagnosis platform for acute myocardial infarction [1]. Nanotubes have an advantage over nanowires because of their larger specific surface areas including interior and exterior ones. In this study, we present the one-bath synthesis of Co-V nanotube arrays using nanoporous anodic alumina oxide (AAO) membranes with pore diameters of about 200 nm. The fabrication was followed by electrodeposition under constant current densities. It was reported that VO^{2+} ions preferred to adhere to the wall to form nanotubes owing to the electrostatic attraction [2]. We added a small amount of strong acid and vanadyl sulfate hydrate expecting VO^{2+} ions to assist Co to form nanotubes instead of nanowires. Fig. 1 shows the microstructure and elemental distribution of Co nanotubes observed by SEM, and TEM. Nanotubes have an average inner diameter of 80 nm. Elemental mapping suggests that a small amount of V is distributed in the Co matrix uniformly. The result is well matched with our hypothesis that the vanadyl ions would attract Co ions to the nanotube walls during the electrochemical reactions. Fig. 2 represents the magnetic properties of nanotube arrays measured by VSM

at RT. As expected, the easy direction of magnetization lies parallel to nanotube axis due to strong shape anisotropy.

Keywords: Co-V nanotube, magnetic properties, microstructure, electrodeposition

[1] PARK, J. -S., CHO, M. K., LEE, E. J., AHN, K. –Y., JUNG, J. H., CHO, Y., HAN, S. –S., KIM. Y. K., & LEE, J. 2009. A highly sensitive and selective diagnostic assay based on virus nanoparticles. *Nature Nanotechnol.*, 4, 259-264

[2] WANG, Y., TAKAHASHI, K., SHANG, H., & CAO, G. 2005. Synthesis and electrochemical properties of vanadium pentoxide nanotube arrays. *J. Phys. Chem. B*, 109, 3085-3088

Preparation and Properties of Amino Functionalized Mesoporous Silica/PVA Fibers

Jianfang Wang*, Sida Zhang, Hui Zhu, Cheng-an Tao, Yujiao Li, Jian Huang

College of Science, National University of Defense Technology, Changsha 410073, China

wangjianfang@nudt.edu.cn

In this paper, the amino functionalization of mesoporous silica/PVA nanofibers was prepared by the co-synthesis surface modification vis electrospinning, and the loading of the electrochemical active materials on the fibers and their electrochemical sensing properties were studied. The results showed that the morphology and the structure of the mesoporous silica fibers were affected by CTAB content, PVA content and aging time. The amino functionalized mesoporous silica/PVA nanofibers with a diameter of 200-650 nm, a uniform pore size of 2.89 nm, and a specific surface area of 656 m^2g^{-1} were obtained. The amino functionalized mesoporous silica/PVA fibers membrane electrode can load phosphomolybdic acid to be a sensor and keep its electrochemical activity, which has a linear current response to different concentrations of BrO_3^-. The mesoporous silica nanofibers have the advantages of stable structure, large specific surface area, adjustable pore size, easy to carry out functional modification, more importantly, the gaps among the self supporting membrane fibers are beneficial to material and signal transmission, and is easy to be assembled into functional device.

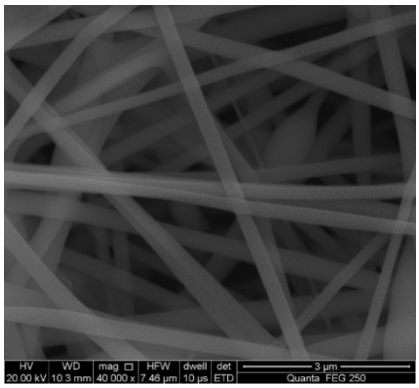

Figure 1. SEM of the mesoporous silica fibers

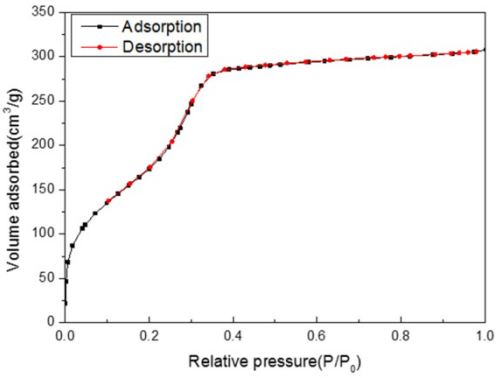

Figure 2. Nitrogen adsorption/desorption curve of the mesoporous silica fibers

Keywords: Mesoporous, amino functionalized, silica /PVA nanofibers

[1] KRESGE, C. T., LEONOWICZ, M. E., ROTH, W. J., VARTULI, J. C. & BECK, J. S. 1992. Ordered Mesoporous Molecular Sieves Synthesized by A Liquid-Crystal Template Mechanism. *Nature*, 359, 710-712.

[2] ZHANG, X. A., WU, W. J., WANG, J. F., & LIU, C. L. 2007. Evaporation-Induced Self-Assembly of Amino-Functionalized Mesoporous Silica Thin Films by Sol-Gel Process. *J Am Ceram Soc*, 90, 965-968.

[3] TAHA, A. A., QIAO, J., LI, F. & ZHANG, B. 2012. Preparation and Application of Amino Functionalized Mesoporous Nanofiber Membrane via Electrospinning for Adsorption of Cr^{3+} from Aqueous Solution. *Journal of Environmental Sciences*, 24, 610-616.

Preparation of Metal Foils with Close Lattice Match to Graphene and Their Use

Sunghwan Jin[1], Youngwoo Kwon[1], Sangjun Oh[2], Bao-Wen Li[1], Ming Huang[1,3], Mandakini Biswal[1], Da Luo[1], Rodney S. Ruoff[1, 2, 3,*]

[1]Center for Multidimensional Carbon Materials, Institute for Basic Science (IBS), Ulsan 44919, Republic of Korea

[2]Department of Chemistry and [3]School of Materials Science and Engineering, Ulsan National Institute of Science and Technology (UNIST),Ulsan 44919, Republic of Korea

E Mail/ sunghwanjin00@gmail.com (presenting author), ruofflab@gmail.com (corresponding author)

Transition metals have been widely used as substrates for graphene growth by chemical vapor deposition method. Among them, single crystal metals such as Cu (111), Ni (111), and Co (0001) have a small lattice mismatch with graphene, and graphene has been grown on such single crystal metals. However, the growth to date has typically been on expensive and relatively small single crystals grown by bulk crystal growth methods or from deposition of thin films onto single crystal substrates (such as sapphire with a particular orientation). We have targeted and found methods to prepare Cu (111), Ni (111), and Co (0001) with very large grain size starting with large, commercially available, polycrystalline metal foils. We will present and discuss our methods to obtain and to analyze such metal foils. We suggest, and will show some examples, that these foils afford new directions for growth of large area graphene and multilayer graphene. We further note that they are also of interest for hexagonal boron nitride thin film growth, as well as perhaps other thin film materials including diamond.

Keywords: Metal foil, graphene, chemical vapor deposition, lattice match

Acknowledgements

This work was supported by IBS-R019-D1.

Study on Defect Modulations of ZnO Nanowires Using Oxygen Plasma Treatments

Xiao-Yen Dai[1,2], Chieh-Wei Chen[1,2], Ming-Pei Lu[3], Ming-Yen Lu[1,2]

[1] Graduate Institute of Opto-Mechatronics, National Chung Cheng University, Chia-Yi 62102, Taiwan.

[2] Advanced Institute of Manufacturing with High-tech Innovations, National Chung Cheng University, Chia-Yi 62102, Taiwan

[3] National Nano Device Laboratories, Hsinchu 300, Taiwan

E-Mail : cnd0917@gmail.com *(presenting author)*

mylu@ccu.edu.tw *(corresponding author)*

ZnO nanostructures have been demonstrated to exhibit the excellent performances for diverse applications. However, defects in ZnO play an important role in influencing the deice performances. In present study, we implemented the modification of defect states of ZnO NW devices using oxygen plasma treatments. The ZnO nanowires grown by vapor-liquid-solid (VLS) method in vacuum furnace possessed the large amount of oxygen defects, which is confirmed with the X-ray photoelectron spectroscopy (XPS). After the oxygen plasma treatments, the defect density decreased accordingly, meanwhile, the conductivity of ZnO NW devices decreased. Moreover, the defect density of ZnO NW device was investigated by using the low-frequency noise analysis, the defect densities were estimated to be 3.6 x10^{21} cm^{-3} eV^{-1}、2.85x10^{21} cm^{-3} eV^{-1}、1.36 x10^{21} cm^{-3} eV^{-1} and 1.09 x10^{20} cm^{-3} eV^{-1} for as-grown, 10 s, 20 s, and 30 s oxygen plasma treatments, respectively. The results showed that the defect density of ZnO NW was decreased with the oxygen plasma treatments. Furthermore, the recovery time and the responsivity of ZnO NW devices to the UV light illumination became shorter and smaller as the oxygen plasma treatment time increased.

Keywords: ZnO, Oxygen plasma, Defect.

Synthesis of Quantum Dots using Continuous Micro-reactor Method

Dongyoon Shin[1], Duk-Hee Lee[1*], Myung-Hwan Hong[1], Lee-Seung Kang[1], Chan-Gi Lee[1]

[1] *Advanced Materials & Processing Center, Institute for Advanced Engineering (IAE), 449-863, Yongin-si, Korea*

Great interest has been given to quantum dots (QDs) over the last decades due to their unique optical properties and wide applications. Furthermore, many methods for the synthesis of QDs such as solvothermal, hydrothermal, hot-injection etc. are been developed. Especially, the continuous micro-reaction systems has attracted approach for QDs synthesis due to the enable rapid mass and control thermal transfer for nanoparticles synthesis. In this work, we utilized a capillary micro-reactor to prepare Cd, Non-Cd based QDs and effects of various operating conditions (temperature, flow rate, precursor concentration etc.) on optical properties also investigated. For characterize the synthesized nanoparticles, X-ray diffraction, UV-vis, photoluminescence, TEM were used and the produced QDs showed that the color with UV irradiation changed in accordance with reaction temperature and flow rate. From now on, it is anticipated that these QDs can be used in many field.

* Address all correspondence to this author.
TEL: +82-31-330-7501; E-mail: shin@iae.re.kr

Template-free self-assembly of bismuth oxide nanobelts assisted by oleylamine

Chunli Jiang[1], Zhi Wang[1,2], Hui Peng[1,*]

[1] Key Laboratory of Polarized Materials and Devices, Ministry of Education, East China Normal University, Shanghai 200241, P. R. China

[2] School of Physics and Electrical Engineering, Anyang Normal University, Anyang 455000, P. R. China

Email: 616531906@qq.com; hpeng@ee.ecnu.edu.cn

Self-assembly which can design structures and patterns at the nanoscopic length scale with purposeful function has been attracting more and more attention over the past two-decades, because it greatly benefits nanofabrication in biology, microelectronics and optics.[1-3] Bismuth oxide shows great potential applications in many fileds due to its unique features of large band gap, high dielectric permittivity, as well as marked photoluminescence and photoconductivity. Nanoscale bismuth oxide with various morphologies, such as nanowires[4], nanotubes[5], nanofibers[6] and nanoplates[7] has been fabricated due to its size and structure related properties. However, to the best of our knowledge, efforts were almost limited to the microsized architecture of Bi_2O_3 materials, it remains a significant challenge to develop facile, solution-based and shape controlled self-assembly routes for the formation of nanosized and tailored hierarchical architectures of Bi_2O_3-based materials.

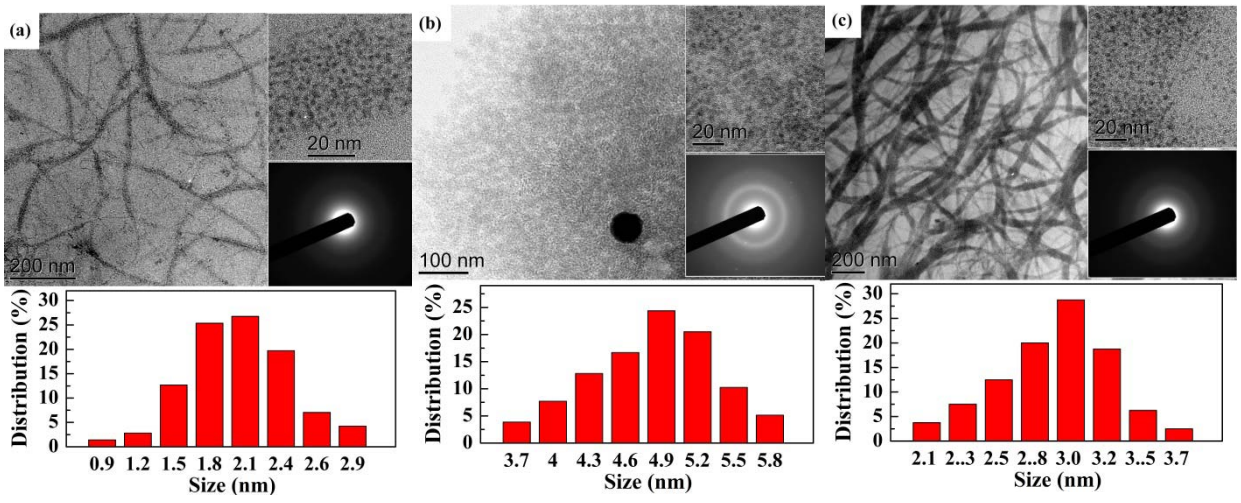

Figure 1 TEM images and size distribution of the samples of (a) $S_{\text{-160 °C-3 h}}$, (b) $S_{\text{-180 °C-3 h}}$ and (c) $S_{\text{-180 °C-1 h}}$.

In this work, we report a facile approach to prepare self-assembly nanobelts of bismuth oxide through thermal decomposition of bismuth oleate with oleylamine in 1-octadecylene. The obtained nanobelts were characterized by TEM, SEM, XRD, XPS and FTIR. We found that oleylamine and the size of nanoparticles play key roles in the self-assembly of nanoparticles. Based on the experimental results, a formation mechanism of the self-assembled nanobelts was suggested, in which the van der Waals interactions and dipolar forces between the molecules of capping ligands guide the self-assembly behavior of Bi_2O_3 nanoparticles.

Keywords: self-assembly, nanobelt, bismuth oxide, oleylamine

Reference

[1] PETERS, R. D., YANG, X. M., WANG, Q., DE PABLO, J. J. & NEALEY, P. F. 2000. Combining advanced lithographic techniques and self-assembly of thin films of diblock copolymers to produce templates for nanofabrication. *Journal of Vacuum Science & Technology B*, 18, 3530-3534.

[2] GOODMAN, R. P., SCHAAP, I. A., TARDIN, C. F., ERBEN, C. M., BERRY, R. M., SCHMIDT, C. F. & TURBERFIELD, A. J. 2005. Rapid chiral assembly of rigid DNA building blocks for molecular nanofabrication. *Science*, 310, 1661-1665.

[3] OZIN, G. A., HOU, K., LOTSCH, B. V., CADEMARTIRI, L., PUZZO, D. P., SCOTOGNELLA, F., GHADIMI, A. & THOMSON, J. 2009. Nanofabrication by self-assembly. *Materials Today*, 12, 12-23.

[4] QIU, Y., YANG, M., FAN, H., ZUO, Y., SHAO, Y., XU, Y., YANG, X. & YANG, S. 2011. Nanowires of α-and β-Bi2O3: phase-selective synthesis and application in photocatalysis. CrystEngComm, 13, 1843-1850.

[5] YANG, B., MO, M., HU, H., LI, C., YANG, X., LI, Q. & QIAN, Y. 2004. A Rational Self‐Sacrificing Template Route to β-Bi2O3 Nanotube Arrays. *European Journal of Inorganic Chemistry*, 2004**,** 1785-1787.

[6] WANG, C., SHAO, C., LIU, Y. & ZHANG, L. 2008. Photocatalytic properties BiOCl and Bi2O3 nanofibers prepared by electrospinning. *Scripta Materialia,* 59**,** 332-335.

[7] BHANDE, S. S., MANE, R. S., GHULE, A. V. & HAN, S.-H. 2011. A bismuth oxide nanoplate-based carbon dioxide gas sensor. *Scripta Materialia,* 65**,** 1081-1084.

Cuprous Oxide Nanoparticle Modified ZnO Nanowires for Photodegradation of Organic Dye and NO Gas Sensing

Cheng-En Tsai, Hsien-Wen Ke, Heh-Nan Lin

Department of Materials Science and Engineering, National Tsing Hua University, Hsinchu 30013, Taiwan

E-mail: hnlin@mx.nthu.edu.tw

We report on the growth of cuprous oxide nanoparticle modified ZnO nanowires (NWs) and their applications for photodegradation of organic dye and NO gas sensing. ZnO NWs are first synthesized on a substrate by low-temperature solution growth. Cuprous oxide nanoparticles are then created on the NW surfaces by photoreduction and subsequent thermal annealing. Transmission electron microscopy is utilized for analysis and the compositions of the ZnO NWs and cuprous oxide nanoparticles are both confirmed. For photocatalysis, NWs are grown on a 10 × 10 cm^2 fluorine-doped tin oxide substrate. The photodegradation of 100 mL and 10 μM rhodamine B solution under the illumination of a halogen lamp is investigated. For gas sensing, NWs are grown on a Si substrate with contact electrodes created by photolithography. By measuring the resistance change, NO gas sensing below 1 ppm level has been achieved under ambient environment.

Keywords: ZnO nanowire, cuprous oxide nanoparticle, photocatalysis, gas sensing

[1] CHIANG, M.-Y. & LIN, H.-N. 2015. Enhanced Photocatalysis of ZnO Nanowires Co-modified with Cuprous Oxide and Silver Nanoparticles. *Materials Letters*, 160, 440-443.

[2] CHANG, Y.-H., CHIANG, M.-Y., CHANG, J.-H. & LIN, H.-N. 2015. Enhanced Visible Light Photocatalysis of Cuprous Oxide Nanoparticle Modified Zinc Oxide Nanowires. *Materials Letters*, 138, 85-88.

1T'-enriched Transition Metal Dichalcogenides Intercalation Host for Zero Valent Metal Catalysts

Zhongxin Chen and Kai Leng and Kian Ping Loh

Department of Chemistry, National University of Singapore

Centre for Advanced Functional Materials, National University of Singapore

Abstract

The identification of a processing strategy to intercalate transition metal dichalcogenide (TMDC) with metal nanoparticles, allowing long-term operation with excellent catalytic activity for hydrogen production, is very important. Although TMDC can catalyze hydrogen evolution in principle via its edges or defective sites, its activity is not competitive with respect to noble metals. Solution deposition of metal nanoparticles on exfoliated TMDC nanosheets has been used conventionally to form hybrid structures, however, their long-term operation is usually poor due to the gradual loss of electrochemical active area of metal nanoparticles by dissolution and aggregation. Furthermore, the ability to make membrane-electrode assemblies (MEA) is critical for industrial operation and few recipes have been developed to make the powder samples or mm-sized films to membrane-type assemblies. Most current researches in this area are solely based on the electrochemical measurement of powder samples on glassy carbon electrode where the long-term stability as well as scalability are not examined and no methods have been developed to bridge the technological gap. This is a major gap between lab research and industry.

Our processing strategy allows a series of zero-valent metal nanoparticles, ***e.g.***, platinum, to be successfully intercalated into TMDC (such as MoS_2) layered structure (ternary structure), achieving unprecedented stability and activity for hydrogen evolution. Such MoS_2 catalysts with ~ 10 wt% platinum loading exhibits higher hydrogen evolution activity than the benchmark 40 wt% Pt/C catalyst, with an overpotential down to 20 mV and a Tafel slope of ~20 mV/dec. Even at a current density up to 50 mA/cm^2, the overpotential can still reach to ~48 mV *vs.* RHE and is stable for 120,000 s (~ 33.3 hours) operation. This is among the best performance reported to date for TMD and the first example for zero-valent intercalation in transition metal dichalcogenides. A 25 cm^2 membrane-electrode assemblies can be made by casting "catalyst inks" onto carbon papers/cloths and subsequent hot-pressing with Nafion® membrane, thus showing the scalability of our processing methods.

Cuprous Oxide Nanoparticle Modified ZnO Nanowires for Photodegradation of Organic Dye and NO Gas Sensing

Cheng-En Tsai, Hsien-Wen Ke, Heh-Nan Lin

Department of Materials Science and Engineering, National Tsing Hua University, Hsinchu 30013, Taiwan

E-mail: hnlin@mx.nthu.edu.tw

We report on the growth of cuprous oxide nanoparticle modified ZnO nanowires (NWs) and their applications for photodegradation of organic dye and NO gas sensing. ZnO NWs are first synthesized on a substrate by low-temperature solution growth. Cuprous oxide nanoparticles are then created on the NW surfaces by photoreduction and subsequent thermal annealing. Transmission electron microscopy is utilized for analysis and the compositions of the ZnO NWs and cuprous oxide nanoparticles are both confirmed. For photocatalysis, NWs are grown on a 10 × 10 cm^2 fluorine-doped tin oxide substrate. The photodegradation of 100 mL and 10 μM rhodamine B solution under the illumination of a halogen lamp is investigated. For gas sensing, NWs are grown on a Si substrate with contact electrodes created by photolithography. By measuring the resistance change, NO gas sensing below 1 ppm level has been achieved under ambient environment.

Keywords: ZnO nanowire, cuprous oxide nanoparticle, photocatalysis, gas sensing

[1] CHIANG, M.-Y. & LIN, H.-N. 2015. Enhanced Photocatalysis of ZnO Nanowires Co-modified with Cuprous Oxide and Silver Nanoparticles. *Materials Letters*, 160, 440-443.

[2] CHANG, Y.-H., CHIANG, M.-Y., CHANG, J.-H. & LIN, H.-N. 2015. Enhanced Visible Light Photocatalysis of Cuprous Oxide Nanoparticle Modified Zinc Oxide Nanowires. *Materials Letters*, 138, 85-88.

Electron beam irradiation effect on monolayer MoS_2 field-effect transistors

Shang-Chi Wu[1,2#], Ming-Yen Lu[1,2]*

[1]Graduate Institute of Opto-Mechatronics, National Chung Cheng University, Chia-Yi 62102, Taiwan
[2] Advanced Institute of Manufacturing with High-Tech Innovations, National Chung Cheng University, Chia-Yi 62102, Taiwan

[#]Presenting Author: wu80921@gmail.com
*Corresponding Author: mylu@ccu.edu.tw

In this work, we report the effects of electron beam irradiation to the properties of MoS_2 monolayer devices. The MoS_2 monolayer flakes were grown using chemical vapor deposition (CVD) method. Raman spectroscopy, Photoluminescence measurements and TEM were further implemented to confirm the number of layer, emission properties and crystal structure of MoS_2 flakes, respectively. After the device fabrication on 300 nm SiO_2/Si substrate by e-beam lithography and lift-off process, the MoS_2 field-effect transistors (FETs) were irradiated with electron beam of different doses. The results showed that the conductivity of MoS_2 increased and the threshold voltages shifted to negative gate voltage regime with increasing electron beam doses. The variations are attributed to the oxygen-trap charge in SiO_2. Interestingly, the mobility of MoS_2 FETs increased from 0.00148 to 0.178 $cm^2v^{-1}s^{-1}$ after electron beam irradiation. The electron beam irradiation on MoS_2 FETs can be the promising strategy to modulate the performances of MoS_2 FETs.

Keywords: 2D material, MoS_2, CVD, FET, E-beam irradiation

Evaluation of Metal Chloride, Molecular, and Metal Oxide Doping of Graphene Electrode for Schottky Junction Solar Cells

Chandramohan Samygounder[1], Tae Hoon Seo[2], Janardhanam Vallivedu[1], Chang-Hee Hong[1], Eun-Kyung Suh[1]

[1] School of Semiconductor and Chemical Engineering, Semiconductor Physics Research Center, Chonbuk National University, Jeonju 54896, Republic of Korea.

[2] Soft Innovative Materials Research Center, Korea Institute of Science and Technology, Jeonbuk 55324, Republic of Korea.

E Mail: eksuh@jbnu.ac.kr; chandra79@jbnu.ac.kr

The low intrinsic carrier concentration of graphene confines the electrical conductivity, a key problem limiting wider implementation of graphene as a next-generation transparent conductive electrode in energy devices, and research to overcome this constraint is undertaken by many groups [1-3]. Charge transfer doping has been widely adopted to realize low sheet resistance with a simultaneous work function regulation. Numerous studies have been conducted using different metal chlorides, strong acids, and organic molecules. However, majority of such dopants have been found unstable upon exposure to organic or acidic solvents, inhibiting their use in device manufacturing that involves lithography and etching processes. Alternatively, wide band gap metal oxides are considered promising as they can be thermally deposited onto graphene to give conformal coverage with high ambient and thermal stability [1]. Among the various metal oxides studied, molybdenum trioxide (MoO_3) has unique characteristics such as large electron affinity of 6.8 eV and oxygen-vacancy-derived semi-metallic character. Motivated by a series of recent research on graphene doping, here we study how factors such as the surface chemistry of graphene, post-transfer thermal annealing, ambient conditions, and dopant morphology influences the doping efficiency and stability of single layer graphene grown by chemical vapor deposition and subsequently doped using dopants of common interest such as gold chloride ($AuCl_3$), bis(trifluoromethanesulphonyl)imide (TFSA), and MoO_x. Experiments performed on various graphene films showed a reduction in the sheet resistance up to 79%, 69%, and 56% upon doping with $AuCl_3$, TFSA, and MoO_3, respectively. Single layer graphene films with sheet resistance values

between 100 and 200 ohm/square were consistently produced without losing the optical transparency by implementing a two-step growth and doping approaches. Graphene/Si solar cells with power conversion efficiencies as high as 8% were realized and the origin of efficiency degradation is investigated with respect to stability of graphene doping and oxidation of Si under illumination conditions. The potential of MoO_x as a stable dopant and conformal antireflection coating to preserve the stability of chemical dopants are also addressed.

Keywords: graphene, chemical vapor deposition, doping, molybdenum trioxide, Si solar cell

[1] MEYER, J., KIDAMBI, P. R., BAYER, B. C., WEIJTENS, C., KUHN, A., CENTENO, A., PESQUERA, A., ZURUTUZA, A., ROBERTSON, J. & HOFMANN, S. 2014. Metal oxide induced charge transfer doping and band alignment of graphene electrodes for efficient organic light emitting diodes. *Sci. Rep.*, 4, 5380.

[2] BOINTON, T. H., JONES, G. F., SANCTIS, A. D., HILL-PEARCE, R., CRACIUN, M. F. & RUSSO, S. 2015. Large-area functionalized CVD graphene for work function matched transparent electrodes. *Sci. Rep.*, 5, 16464.

[3] CHANDRAMOHAN, S., KANG, J. H., KATHARRIA, Y. S., HAN, N., BEAK, Y. S., KO, K. B., PARK, J. B., RYU, B. D., KIM, H. K., SUH, E. K. & HONG, C. H. 2012. Chemically modified multilayer graphene with metal interlayer as an efficient current spreading electrode for InGaN/GaN blue light-emitting diodes. *J. Phys. D: Appl. Phys.* 45, 145101.

Influence of Self Alignment and Orientation of ZnO Nanorods on the Performance of Field Effect Transistors

Ashish Kumar[1], Tejendra Dixit[1], Kshitij Bhargava[1], I. A. Palani[2] and Vipul Singh[1*]
[1]Molecular and Nanoelectronics Research Group (MNRG), Department of Electrical Engineering
[2]Mechatronics and Instrumentation Lab, Department of Mechanical Engineering
Indian Institute of Technology Indore, Indore, Madhya Pradesh, India 453441
Email: *vipul.iiti@gmail.com

Abstract: ZnO field effect transistors were demonstrated on SiO_2/Si^{++} substrate using self-aligned nanorods network synthesized by hydrothermal process. To control the alignment and orientation of nanorods two additives potassium permanganate ($KMnO_4$) and Potassium Dichromate ($K_2Cr_2O_7$) were added in precursor solution. The effect of the additive was studied through structural and optical characterization. Further, these nanorods were used as active layer in FETs and the estimated mobility and On-OFF ratio of the devices were 0.0032cm^2/V-s and 1×10 for vertical aligned and 0.51 cm^2/V-s and 6×10^3 for lateral aligned NRs network respectively. The possible mechanism of charge transport in network path was also discussed.

Keywords: Field Effect Transistors, Alignment,, Hydrothermal, Nanorods, ZnO.

Introduction: In recent years**,** nanowire/nanorods network based field effect transistors have been explored by different research groups [1-4] to overcome the limitation of single nanowire/ nanorods based FETs viz. poor integration, and precisely assembling of single nanowire/nanotube which are time consuming [4-5]. Several methods in the past have demonstrated improvement of the performance of FETs based on networks based on direct growth of network on the substrate, transfer of the network on the substrate and substrate modification [1-4]. However the orientation and alignment of the ZnO NR network was rarely related to the performance of FETs.

Fabrication and Characterization: Heavily doped silicon (Si) substrate with 200 nm thick silicon dioxide (SiO_2) was used as substrate having a gate insulator on top, for the fabrication FETs. Similar procedure as described elsewhere [4], was utilized for fabrication of ZnO NR networks. After formation of ZnO NR networks, patterned Source/Drain electrodes of 80 nm thick Aluminum (Al), to make Ohmic contact were coated on top of the ZnO NR networks using shadow masking technique, having a typical channel length (L) and width (W) of 100 µm and 2mm respectively.

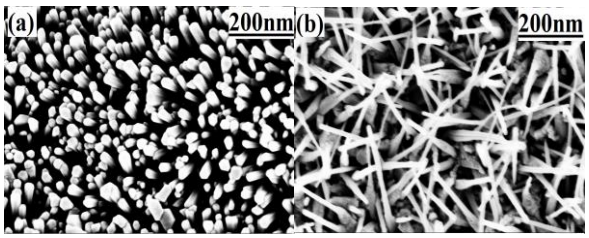

Fig. 1 FESEM images (a) vertically aligned ($KMnO_4$) and (b) lateral aligned ($K2Cr_2O_7$) ZnO NRs network

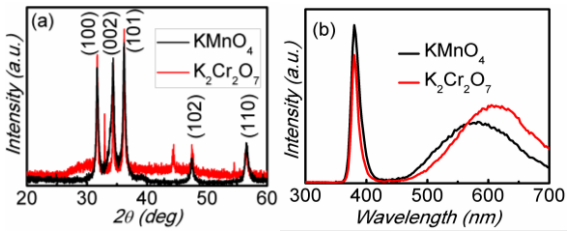

Fig. 2 (a) XRD patterns (b) PL spectra of ZnO NRs Network

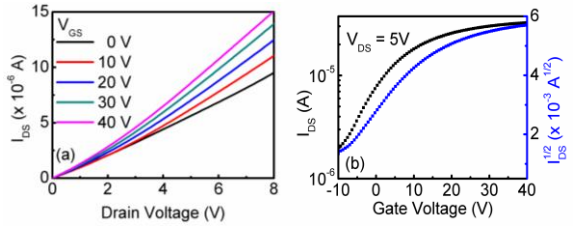

Fig. 3 Output characteristics of FETs based on vertical aligned NRs (a) I_{DS}-V_{DS} curves (b) I_{DS}-V_{GS} curve

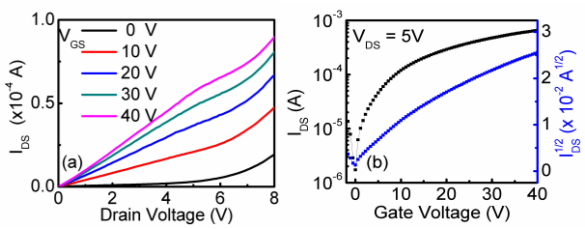

Fig. 4 Output characteristics of FETs based on lateral aligned NRs (a) I_{DS}-V_{DS} curves (b) I_{DS}-V_{GS} curve

Results and Discussion: Morphological properties of the ZnO NR network grown on Si substrate are shown in Fig. 1 (a) and (b). The effect the additive can be seen clearly in structure of NRs, the additive $KMnO_4$ facilitates the alignment of the NRs in vertical direction while lateral alignment was facilitated by the in situ addition of $K_2Cr_2O_7$.XRD pattern of the NRs networks is shown in Fig.2 (a). Looking at the XRD spectra as a whole, it is confirmed that all diffraction peaks can be indexed to ZnO with Wurtzite structure (space group: p63mc (180): a=3.2512 Å and c=5.2109 Å) and are in good agreement with the JCPDS file of ZnO (JCPDS 01-089-7102). In addition to the well indexed peaks, the peak observed 31.65° and at 44.5° can be assigned to Cr impurity and $Zn(OH)_2$ respectively. Fig. 2(b) shows the PL spectra, consisting of sharp UV emission peak around 380 nm and visible emission corresponding to near band edge (NBE) and deep level defects respectively for both un-annealed as well as annealed ZnO NRs.Moreover, the obtained values of the transistor performance parameter such as saturation field-effect mobility and current on/off current ratio were estimated to be 0.51 cm^2/V-s and 6×10^3 respectively for lateral aligned NRs network while these parameters for vertical aligned NR network from transfer characteristics as shown in Figure 3 (a) and (b). The results pave way of for realization of cost effective ZnO NW network based FETs. Figure 5 shows the schematic representation of charge transport path in vertical aligned (a) and lateral aligned (b) NRs network and corresponding band diagram at the junction of NRs/NRs is discussed in Fig. 6 (a and b).

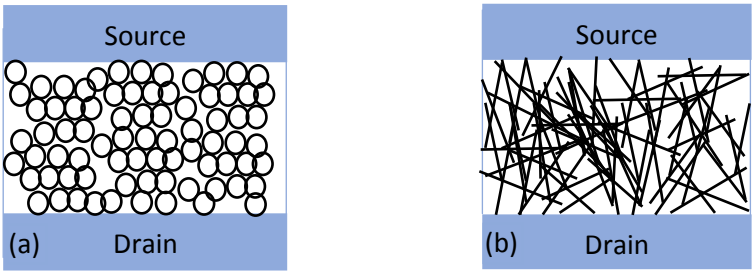

Fig. 5 Network path to flow the electron in (a) vertical aligned (b) lateral aligned ZnO NRs network

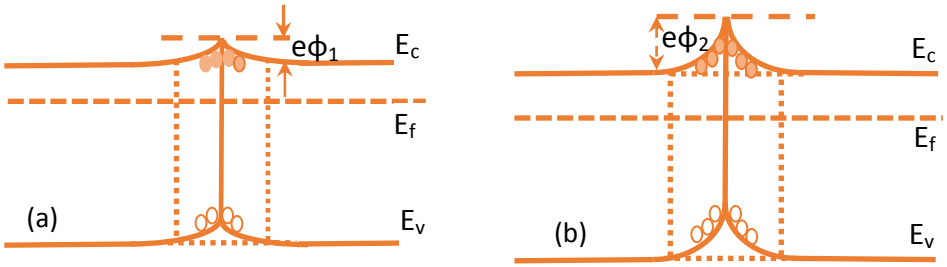

Fig. 6 Schematic diagram of band structure at the NRs/NRs interface (a) without any bias (b) under the bias

Conclusion: In summary we have shown how alignment of the NRs and interface interaction of NRs affect the performance of network based FETs. Better performance of FETs in term of higher mobility and I_{ON}/I_{OFF} ratios is achieved from lateral aligned NRs. Low cost and simple fabrication method has high potential for the large-area production of transistor which paves new way for ZnO based optoelectronic and sensing devices.

Acknowledgement: Author A. Kumar would like to thank the Ministry of human resource dept., Govt. of India, for financial support. Authors are also grateful to Sophisticated Instrument Centre, IIT Indore for FESEM, XRD, and PL facilities**.**

References: [1] B. Sun, and H. Sirringhaus, 2005. Nano letters, 5, 2408. [2] S. Thiemann, *et al.*, 2013. ACS applied materials & interfaces, 5, 1656-1662. [3] T. Dixit, *et al.* 2015. Journal of Materials Science: Materials in Electronics 26, 821. [4] A. Kumar *et. al.* 2016 Adv. Sci. Eng. Med. 8, 49-56. [5]. A. Kumar and M. S. Baghini, 2014.Electronics Letters 50 1547-1549. [6] T. Dixit, *et al.* 2015 J. Sol-Gel Scie. Tech. 75, 693.

Preparation and Employment of the Functional Hybrid Nanomaterials on the Metal-Organic Framework (MOF) Basis

V. Isaeva [1], A. Kudelin [1], and L. Kustov [1]

[1]National Engineering Technological University of Steel and Alloys,

Leninsky prospect, 2, 119991 Moscow, Russia.

v_isaeva@inbox.ru

The novel type of hybrid nanoporous coordination polymers - metal-organic frameworks (MOFs) assembled by metal cations/metal oxide clusters and organic linkers) - are now explored in catalysis, gas storage/separation, drug delivery, as sensors, and so on. Currently, the investigation related to MOF using as the components of functional materials, fabrication of which allows to combine the advantages of MOFs (record high suface area and porosity, high crystallinity degree, chemical composition diversity etc.) with useful characteristics of other type matrices. For instance, by preparation of polycrystalline MOF coating the surface of porous substrates the membrane materials with supported selective layer can be synthesized. Mixed matrix membranes (MMM membranes) in the form of MOF nanoparticles embedded in the polymer matrices represent other type of hybrid materials. Another examples of MOF exploitation as a platform for the preparation of functional materials are the composites with hierarhical pore structure obtained by the intrusion of metal-organic framwork crystallites in the mesopores of inorganic matrices of MCM type. The adsorbents synthesized according this approach can feature an enhanced shape-size selectivity in respect of representative set of gases and hydrocarbons. In this contribution will be discissed the mentioned above types of functional nanomaterials on MOF basis, which are successfully explored in our laboratory. The examples of employment of these systems as the effective adsorbents and membranes will also presented.

Keywords: Functional materials, hybrid materials, metal-organic frameworks, hierarchical structures, membranes

Low temperature chemically reduced graphene oxide encapsulated in polymer matrix for high performance EMI Shielding

Faisal Shahzad,[1,2] Seunghwan Lee,[1] Soon Man Hong[1,2] and Chong Min Koo[*1,2]

[1] Materials Architecturing Research Center, Korea Institute of Science and Technology, Hwarangno 14-gil 5, Seongbuk-gu, Seoul 136-791, Republic of Korea.

[2]Nanomaterials Science and Engineering, University of Science and Technology, 176 Gajung-dong, 217 Gajungro, Yuseong-gu, Daejeon 305-350, Republic of Korea

*Corresponding author. Tel.: +8229586872; Fax: +8229585309.

E-mail address: koo@kist.re.kr (C.M. Koo).

ABSTRACT

We report the synthesis of a graphene/polymer composite via a facile and straightforward approach for electromagnetic Interference shielding applications. Polystyrene (PS) beads were added in graphene oxide (GO)/water solution followed by the addition of Hydroiodic acid (HI) for in-situ reduction of GO. The reduced graphene oxide (rGO) sheets encapsulating the PS beads were tested for EMI shielding and dielectric measurements. A 2mm thick sample with 5 vol% filler loading yield a high EMI shielding value of 26.2 dB and AC electrical conductivity of 21.8 S m^{-1} which was well above the commercial requirement for EMI shielding applications. For comparison with the rGO/PS beads approach, a control sample with thermally reduced graphene oxide (reduced at 600^0C) mixed with PS/Dimethylformamide solution followed by coagulation in methanol was prepared. The as-synthesized product yield an EMI shielding value of 13.5dB and AC conductivity of 11.3 S m^{-1}. The high EMI shielding of rGO/PS bead approach originates from the better connection of graphene layers surrounded by PS bead and due to the better reduction and preservation of graphene structure during reduction process which makes the low temperature chemically reduced rGO/PS bead approach a viable route compared to high temperature thermally reduced rGO/PS solution approach.

Keywords: Graphene, polystyrene, dielectric, Electromagnetic Interference Shielding, conductivity

Topography-induced cell morphology and migration on near-field electrospun alginate/poly(ethylene oxide) nanofiber-textured substrates

Yiin Kuen Fuh[1,2], ZheYu He [1]

[1] Department of Mechanical Engineering, National Central University, Taoyuan City, Taiwan.

[2] Institute of Energy Engineering, National Central University, Taoyuan City, Taiwan.

mikefuh@cc.ncu.edu.tw/ 300 Jhongda road, Jhongli, Taoyuan City, Taiwan

It is highly desirable of functional nanofibers and relevant nanofibrous structures fabricated by electrospinning due to the simple and versatile process. Nevertheless, precise geometric and morphological control and preferred orientation is a great barrier for electrospun nanofibrous mats. Near-field electrospinning (NFES) process has been demonstrated to be able to accurately achieve direct-write and well-aligned alginate/poly(ethylene oxide)(PEO) nanofibers in the microscale. The ability to precisely control and deposit alginate-based nanofibers in a direct-write manner is biologically favorable in manipulating cells attachment and proliferation in a preferred position. A direct-write NFES process is used to fabricate highly-aligned and 3D geometrically complicated functionalities as well as various patterned thick nanofibrous patterns, without resorting to any expensive mask and aligning process. Consequently, diverse pre-patterned nanofibrous mats were used for cell patterning. The experimental results showed that aligned nanofibrous array (ANA) with repeatedly accumulated thickness has an enhanced effects on cellular behavior of elongation and cell spreading. Therefore, it is believed that NFES direct-write method is a promising tool to systematically investigate the cell-based research such as cell spreading, adhesion and tissue architecture.

Keywords: ***Near-field electrospinning (NFES), alginate/poly(ethylene oxide)(PEO) nanofibers, aligned nanofibrous array (ANA), cell spreading, adhesion***

[1] FUH Y.K., CHEN S.Z., JANG J.S.C. 2012. Direct-write, Well-aligned Chitosan-poly(ethylene oxide) Nanofibers Deposited via Near-field Electrospinning. *J. Macromol.Sci. A.* 49(10), 845–850

[2] FUH Y.K., CHEN S.Z., HE Z.Y. 2013. Direct-write, Highly-aligned Chitosan-poly (ethylene oxide) Nanofiber Patterns for Cell Morphology and Spreading Control. *Nanoscale Res. Lett.* 8(1), 97

Transferable, Transparent and Functional Polymer@Graphene 2D Objects

Sze-Wing (NG) [1], Tingting (GAO) [1, 2, 3], Zijian (ZHENG) [1]*

[1] Institute of Textiles and Clothing, The Hong Kong Polytechnic University, Hong Kong, China.

[2] State Key Laboratory of Solid Lubrication, Lanzhou Institute of Chemical Physics, Chinese Academy of Sciences, Lanzhou, China

[3]Graduate School of Chinese Academy of Sciences, Beijing, China

E-mail: miyaa.ng@connect.polyu.hk

Compared with inorganic two-dimensional (2D) materials, such as graphene and transition metal dichalcogenides, organic 2D materials are believed to possess more interesting chemical and biological properties for certain applications, such as separation membranes, smart surfaces, sensors and drug delivery[1,2]. However, the 2D polymers reported to date are only limited to very specific building blocks and microscale sizes because of the lack of robust methods to produce them. On the other hand, the preparation of quasi-2D polymers either requires the undesirable crosslinking of the materials, using expensive and opaque novel metal supports, or high-energy electron beams[6]. Therefore, the investigation of the fundamental properties as well as practical applications of these organic 2D materials have remained largely hindered.

Here we report the development of a new type of functional organic 2D material, namely 'polymer@graphene 2D objects', which are synthesized via a high-througput and cost-effective manner. The polymer@graphene 2D objects are made of functional polymer brushes that tether one end of the polymer chain on the surface of

graphene sheets via non-covalent π-π stacking interactions. Graphene acts as a mechanical support in this 2D object because of its atomic thickness, ultra flexibility, superb optical transparency (>97% in visible and infrared range), mechanical durability (Young's modulus: ~1 TPa; tensile strength: ~100 GPa), stability in air and moisture below 300 °C[3-5] Meanwhile, polymer brushes tethered on the graphene surface provide desirable chemical and biological functionalities. Importantly, as π-π stacking interactions are selected to immobilize functional polymer brushes, it do not require a harsh reaction environment but offer remarkable stability for tethering the polymer chains on the graphene surface even using good solvents.

The 'polymer@graphene 2D objects' are therefore transparent, mechanically freestanding, lightweight, flexible and transferable to various substrates, even flexible ones. The lateral size of the 2D objects can be readily scaled to be as large as the size of the graphene support and was demonstrated by preparing a 3-in sample. The polymer@graphene 2D objects were also be patterned into different structures or smaller pieces using conventional lithography and soft lithography; and they were found to have good solvent stability after transferring to target substrates. For their functionalities, a wide variety of chemical and biological functionalities can be achieved on these 2D objects by simply changing the polymer brushes that are immobilized. We also demonstrated the application of these 2D objects in the smart control of surface wettability and immobilizing DNA oligonucleotide arrays.

Importantly, this approach is an effective direct-transfer method of rendering functionality to substrates that are otherwise difficult to modify using traditional wet chemistry.

Keywords: Functional, transferrable, freestanding, graphene, polymer brushes

References:

[1] COLSON, J. W. & DICHTEL, W. R. 2013. Rationally synthesized two-dimensional polymers. Nature Chemistry, 5, 453-465.

[2] KISSEL, P., ERNI, R., SCHWEIZER, W. B., ROSSELL, M. D., KING, B. T., BAUER, T., GOETZINGER, S., SCHLUETER, A. D. & SAKAMOTO, J. 2012. A two-dimensional polymer prepared by organic synthesis. Nature Chemistry, 4, 287-291.

[3] GEIM, A. K. & NOVOSELOV, K. S. 2007. The rise of graphene. Nature Materials, 6, 183-191.

[4] BAE, S., KIM, H., LEE, Y., XU, X., PARK, J.-S., ZHENG, Y., BALAKRISHNAN, J., LEI, T., KIM, H. R., SONG, Y. I., KIM, Y.-J., KIM, K. S., OZYILMAZ, B., AHN, J.-H., HONG, B. H. & IIJIMA, S. 2010. Roll-to-roll production of 30-inch graphene films for transparent electrodes. Nature Nanotechnology, 5, 574-578.

[5] LEE, C., WEI, X., KYSAR, J. W. & HONE, J. 2008. Measurement of the elastic properties and intrinsic strength of monolayer graphene. Science, 321, 385-388.

[6] AMIN, I., STEENACKERS, M., ZHANG, N., BEYER, A., ZHANG, X., PIRZER, T., HUGEL, T., JORDAN, R. & GOELZHAEUSER, A. 2010. Polymer Carpets. Small, 6, 1623-1630.

Electrospraying Fabrication and Characterization of Zein/Silver Nanospheres for Antibacterial Applications

Seong Baek Yang[1], Sung Hun Yoo[1], Dae Won Jeong[1], Hyun Ji Lee[2],

Byung Chul Ji[1], Jeong Hyun Yeum[1,2]

[1]Department of Advanced Organic Materials Science and Engineering, Kyungpook National University, Daegu 702-701, Korea

[2]Department of Bio-fibers and materials Science, Kyungpook National University, Daegu 702-701, Korea

E Mail :ysb@knu.ac.kr, jhyeum@knu.ac.kr

Zein/silver (Ag) composite nanoparticles with various Ag contents have been fabricated using electrospinning technique. The effect of Ag nanoparticles on the morphologies and properties of zein nanoparticles has been investigated using different amount of Ag contents. The prepared zein/Ag composite nanoparticles have been characterized by field-emission scanning electron microscopy (FE-SEM), transmission electron microscopy (TEM), X-ray diffraction (XRD), and thermogravimetric analysis (TGA). The antibacterial activity of zein/Ag composite nanoparticles has also been investigated.

Acknowledgments: This research was supported by Technology Commercialization Support Program (113042-3), Ministry of Agriculture, Food, and Rural Affairs. In addition, this work was partially supported by the Human Resource Training Program for Regional Innovation and Creativity through the Ministry of Education and the National Research Foundation of Korea (2015H1C1A1035576).

Keywords: Zein, silver, electrospraying, nanospheres

[1] RENEKER, D. H., CHUN, I. 1996. Nanometre Diameter Fibres of Polymer, Produced by Electrospinning. *Nanotechnology*, 7, 216-223.

Influence of phonon confinement on the optically-detected electro-phonon resonance line-width in GaAs quantum wells

Tran Cong Phong[a], Huynh Vinh Phuc[b] Nguyen Dinh Hien[c] Vo Thanh Lam[d]

[a)] Vietnam Institute of Educational Sciences, 101 Tran Hung Dao, Hanoi 10000, Vietnam
[b)] Division of Theoretical Physics, Dong Thap University, Dong Thap 93000, Vietnam
[c)] Hue University's College of Education, 34 Le Loi, Hue City, Vietnam
[d)] Department of Physics, Sai Gon University, 273 An Duong Vuong, Ho Chi Minh City, Vietnam

We investigate the effect of phonon confinement on the optically-detected electro-phonon resonance (ODEPR) effect and ODEPR line-width in GaAs quantum wells. The ODEPR conditions as functions of the well's width and the photon energy are also obtained. The shifts of ODEPR peaks caused by the confined phonon are discussed. The numerical result for the specific GaAs quantum well shows that in the two cases of confined and bulk phonons, the line-width (LW) decreases with increasing well's width and increases with increasing temperature. Furthermore, in the small range of the well's width the influence of phonon confinement plays an important role and cannot be neglected in reaching the ODEPR line-width

Interfacial assembly of Mxene-based nanoblocks

Ruizhi Lin, Dongyu Cai Institute of Advanced Materials, NanjingTech University, No.5 Xinmofan Road, Nanjing, 210009, China. Email:rzhlin@njtech.edu.cn
Chenxi Xu, School of Materials Science and Engineering, Hefei University of Technology, No 193 Tunxi Road, Hefei, 230009, China.

The MAX phases are a group of layered ceramics (ternary carbide and nitride) with metallic properties, which have the general formula $M_{n+1}AX_n$ with n=1-3. In this formula, M represents an early transition metal, A is an A-group (mostly IIIA and IVA) element and X is either carbon or nitrogen.[1] In 2011, the researchers from Drexel University, for the first time, synthesized a new 2D material, called Mxene, through selectively etching A element using strong acids.[2] Mxene not only exhibits high conductivity comparable to graphene but also has hydrophilic surface like clay. [3] This characteristic seems to open an easy way for assembling Mxene blocks into 3D bulk materials such as thin films [4,5] for energy storage devices. In this poster, we will present our study on controlling the surface chemistry of Mxene-based blocks and interfacial behavior of these blocks at water-oil interface. Based on this, we will further show our approach for building Mxene-based 3D structures at water-oil interface and also preliminary results of their potential application in fuel cells.

[1] M. W. Barsoum, *Prog. Solid State Chem.* **2000**, 28, 201.
[2] M. Naguib, M. Kurtoglu, V. Presser, J. Lu, J. Niu, M. Heon, L. Hultman, Y. Gogotsi, M. W. Barsoum, *Adv. Mater.* **2011**, 23, 4248.
[3] M. Ghidiu, M. R. Lukatskaya, M. Q. Zhao, Y. Gogotsi, M. W. Barsoum, *Nature* 2014, 516, 78-81.
[4] M.Q. Zhao, C.E. Ren, Z. Ling, M.R. Lukatskaya, C. Zhang, K.L.V. Aken, M.W. Barsoum and Y. Gogotsi, *Adv. Mater.* **2015**, 27, 339-345. 27. Z.
[5] Z. Ling, C.E. Ren, M.Q. Zhao, J. Yang, J.M. Giammarco, J. Qiu, M.W. Barsoum and Y. Gogotsi, PNAS, 2014, 111, 16676-16681.

Electronic Properties of Layered Materials: Inorganic Phosphorene Analogs to Organometallic Complexes

Fazel (Shojaei)[1] , Hong Seok (Kang)[2]

[1]Departme Department of Chemistry and Bioactive Material Sciences and Research Institute of Physics and Chemistry, Jeonbuk National University, Jeonju, Chonbuk 561-756, Republic of Korea

[2]Department of Nano & Advanced Materials, Jeonju University,

Chonju, Chonbuk 560-759, SOUTH KOREA

hsk@jj.ac.kr

Using first-principles calculations, we have investigated electronic structures of black (α) arsenic phosphoridene (AsP), which is a two-dimensional (2D) monolayer composed of equimolar mixture of phosphorus and arsenic. According to structure optimizations and phonon calculations, α phase branches into three distinguished ones.[1] Second, our calculations in collaboration with photoluminescence measurement indicate that oxygen adsorption can cause the direct/indirect band gaps of GaS monolayer to converge, resulting in a strong emission.[2] Third, the I-V measurement of metal-semiconductor-metal (MSM) photodetectors involving multilayer nanobelts or monolayers of GaS and GaSe can be understood in terms of Fermi level alignment based on our HSE06 calculation.[3] Fourth, the bilayer nanoribbons of α1 AsP experiences cooperativity in the substitutional Si doping in such a way that Si-Si bonds are formed.[4] The doped bilayer exhibits an indirect band gap, which can be turned into a direct gap by Stone-Wales deformation.[4] Finally, electronic and mechanical properties of recently synthesized 2D organometallic complexes of π-Conjugated M-Bis(dithiolene) (MC_4S_4) (M= Ni, Pd) are shown to depend on the kind of metal ions. [5] Band gap Tuning in mixed halide pervoskite [6] and Tetragonal Phase Germanium Nanocrystals in Lithium Ion Batteries[7] will be also discusseed.

Keywords: two-dimensional layered materials, black arsenic pohphide, GaS multilayer or monolayer, indirect-gap to direct-gap transition, π-Conjugated M-Bis(dithiolene) complex

[1] SHOJAEI, F.; KANG, H. S. 2015. Electronic Structure and Carrier Mobility of Two-Dimensional α Arsenic Phosphide. *J. Phyc. Chem. C,* 119, 20210-20216.
[2] JUNG, C. S et al. 2015. Red-to-Ultraviolet Emission Tuning of Two-Dimensional Gallium Sulfide/Selenide. *ACS Nano*, 9, 9585-9593.

[3] Kang, H. S.et al. *in preparation.*

[4] SHOJAEI, F.; KANG, H. S. *in preparation*.

[5] SHOJAEI, F.; HAHN, J. R.; KANG, H. S. 2014. Mechanical and Electronic Properties of π-Conjugated Metal Bis(dithiolene) Complex Sheets. *Chem. Mater*. 26, 2967-2976

[6] JANG, D. M. et al. 2015. Reversible Halide Exchange Reaction of Organometal Trihalide Perovskite Colloidal Nanocrystals for Full-Range Band Gap Tuning. *Nano Lett.* 15, 5191-5199.

[7] CHO, Y. J. et al. 2013, Tetragonal Phase Germanium Nanocrystals in Lithium Ion Batteries. *ACS Nano*, 7, 9075-9084.

Modeling of Polarizability of Fullerene-Based Compounds. Insights from Computational Chemistry to Materials Science

Denis Sabirov, Alina Tukhbatullina, and Anton Terentyev

Institute of Petrochemistry and Catalysis of RAS, Ufa, Russia.

E Mail : diozno@mail.ru

Fullerene derivatives are promising compounds for nano- and optical devices, medicine, electron-acceptor materials of organic solar cells, etc. Polarizability determines the intermolecular interactions, underlying the functioning of the mentioned applications, so its investigations are the base for understanding the mechanisms of processes in which fullerenes and its derivatives take part. This report is based on our review [1] and summarizes the results of computational studies on polarizability of diverse derivatives of C_{60}, C_{70} and other fullerenes performed by us and by other research groups.

Using the accurate DFT methods, we have obtained general regularities of fullerene derivatives polarizability. The most important among them are: *(a)* the mean polarizabilities of 5.6 open isomers are higher than those of respective 6.6 closed isomers [2]; *(b)* regio isomers of $C_{60/70}X_n$ are characterized with the approximately equal average polarizabilities and differ with the anisotropy values [3]; *(c)* the non-additivity of polarizability of polyadducts $C_{60/70}X_n$ with *n* increase [1–4]; *(d)* sheltering the encapsulated atoms and molecules by fullerene frameworks from the external electric fields [5]. A theoretical model of the fullerene derivatives polarizability has been proposed [1]. It allows explanation of the experimentally-measured mean polarizabilities of polyfluorofullerenes. Applications of polarizability to the following aspects of fullerene materials science are discussed: *(a)* the quenching of electronically-excited states by fullerenes [6]; *(b)* mechanical transformations of endofullerenes [7, 8]; *(c)* electron-acceptor properties of C_{60} bisadducts in organic solar cells [9, 10]; *(d)* molecular nanotechnologies [11–13]; nanocapillarity; orientation effects in composite carbon-based materials *etc*.

The work was financially supported by Russian Foundation for Basic Research (project number 16-03-00822 A).

Keywords: fullerenes, organic solar cells, molecular machinery, nanotechnology, polarizability.

[1] SABIROV, D. 2014. Polarizability as a Landmark Property for Fullerene Chemistry and Materials Science. *RSC Adv.*, 4, 44996.

[2] SABIROV, D. & BULGAKOV, R. 2011. Polarizability of Oxygen-Containing Fullerene Derivatives $C_{60}O_n$ and $C_{70}O$ with Epoxide/Oxidoannulene Moieties. *Chem. Phys. Lett*., 506, 52.

[3] SABIROV, D., TUKHBATULLINA, A. & BULGAKOV, R. 2012. Dependence of Static Polarizabilities of $C_{60}X_n$ Fullerene Cycloadducts on the Number of Added Groups X= CH_2 and NH (n = 1–30). *Comput. Theor. Chem.*, 993, 113.

[4] SABIROV, D., GARIPOVA, R. & BULGAKOV, R. 2012. Polarizability of C_{70} Fullerene Derivatives $C_{70}X_8$ and $C_{70}X_{10}$. *Fullerenes Nanotubes Carbon Nanostruct.*, 20, 386.

[5] SABIROV, D. & BULGAKOV, R. 2010. Polarizability Exaltation of Endofullerenes X@C_n (n = 20, 24, 28, 36, 50, and 60; X Is a Noble Gas Atom). *JETP Lett.*, 92, 662.

[6] BULGAKOV, R., GALIMOV, D. & SABIROV, D. 2007. New Property of the Fullerenes: The Anomalously Effective Quenching of Electronically Excited States Owing to Energy Transfer to the C_{70} and C_{60} Molecules. *JETP Lett.*, 85, 632.

[7] SABIROV, D. 2013. From Endohedral Complexes to Endohedral Fullerene Covalent Derivatives: A Density Functional Theory Prognosis of Chemical Transformation of Water Endofullerene $H_2O@C_{60}$ upon Its Compression. *J. Phys. Chem. C*, 117, 1178.

[8] SABIROV, D., TUKHBATULLINA, A. & BULGAKOV, R. 2015. Compression of Methane Endofullerene $CH_4@C_{60}$ as a Potential Route to Endohedral Covalent Fullerene Derivatives: A DFT Study. *Fullerenes Nanotubes Carbon Nanostruct.*, 23, 835.

[9] SABIROV, D. 2013. Anisotropy of Polarizability of Fullerene Higher Adducts for Assessing the Efficiency of Their Use in Organic Solar Cells. *J. Phys. Chem. C*, 117, 9148.

[10] SABIROV, D., TERENTYEV, A. & BULGAKOV, R. 2015. Counting the Isomers and Estimation of Anisotropy of Polarizability of the Selected C_{60} and C_{70} Bisadducts Promising for Organic Solar Cells. *J. Phys. Chem. A*, 119, 10697.

[11] SABIROV, D., GARIPOVA, R. & BULGAKOV, R. 2015. Density Functional Theory Study on the Decay of Fullerenyl Radicals and Polarizability of the Formed Fullerene Dimers. *J. Phys. Chem. A*, 117, 13176.

[12] SABIROV, D. 2013. Polarizability of C_{60} Fullerene Dimer and Oligomers: the Unexpected Enhancement and Its Use for Rational Design of Fullerene-Based Nanostructures with Adjustable Properties. *RSC Adv.*, 3, 19430.

[13] SABIROV, D., TERENTYEV, A. & BULGAKOV, R. 2014. Polarizability of Fullerene [2+ 2]-Dimers: A DFT Study. *Phys. Chem. Chem. Phys*., 16, 14594.

The band structure of defective Z-shaped graphene nanoribbon

Kazuma KIHIRA, Masato AOKI

Faculty of Engineering, Gifu University, Yanagido, Gifu 501-1193, Japan

kazumax.0122@gmail.com

In 2007, Z-shaped graphene nanoribbon (ZGNR) was reported as a new quantum dot device[1], which has two characteristic levels arising from localized states within the band gap. ZGNR has the structure that zigzag graphene nanoribbon connects at both ends to semi-infinite armchair ribbons. In the present work the calculations of the electronic structure of defective ZGNR, which consists of a vacancy-introduced zigzag ribbon of length 4 and semi-infinite perfect armchair ribbons of width 7, were performed within the orthogonal nearest neighbor tight-binding approximation using the recursive Green's function method and the density functional based tight-binding (DFTB) method. As a main result, it was found that an introduction of an atomic vacancy into the ZGNR could create an additional discrete level within the bandgap, and also that the position of the level depends on the choice of the defective lattice site. These results indicate the possibility to construct multilevel intermediate band structures for the high efficiency solar cell by using defective ZGNRs.

Keywords: graphene nanoribbon, vacancy, tight-binding, DFTB, solar cell

[1] Z. F. Wang et al., *Appl. Phys. Lett.* **91**, 053109 (2007).

The study of magnetic and electronic properties of Ni doped ZnO in low dimensional polar-surface structure by density functional theory

C. Supatutkul, Y. Laosiritaworn*

Department of Physics and Materials Science, Faculty of Science,

Chiang Mai University, Chiang Mai 50200, Thailand

** Corresponding author: Email: yongyut_laosiritaworn@yahoo.com; Tel.: +66 (0)53943367; Fax: +66 (0) 53943445; Postal address: Department of Physics and Materials Science, Faculty of Science, Chiang Mai University, Chiang Mai 50200, Thailand*)

The transition metal doped zinc oxide (ZnO) has shown high potential and interest in spintronics application because it exhibits both ferromagnetic and semiconductor states, which can enhance data accessing speed and digital data storage capacity. The reason that ZnO is considered as the host semiconductor is ZnO has wide band gap, non-toxic, low cost, and easy fabrication. Many magnetic transition metals, such as Mn, Fe, Co, and Ni, can also be candidate for the impurity doping in ZnO to introduce the magnetism properties, which is called diluted magnetic semiconductor (DMS) [1]. The Ni dopant atom is one of the most promising candidate for the high Curie temperature ferromagnetic materials [2]. The x-ray diffraction pattern of Ni doped ZnO (Ni:ZnO) shows the majority surface in (002) direction in wurtzite structure which is also a polar surface. This polar surface of ZnO is well-known to be structurally unstable in the low dimensional structure, the dipole moment lead to the surface reconstruction [3, 4], such as nanosheet, nanotube, or nanorod. Therefore, the foundation of ferromagnetic and semiconductor state in transition metal doped ZnO is well interested in this ZnO polar surface structure. To investigate the stability of transition metal doped ZnO, the density functional theory (DFT) is an appropriate tool as it provides insightful schemes to investigate spin-polarized electronic properties of this emerging doped-ZnO in microscopic details. In this work, the DFT calculation used generalized gradient approximation + Hubbrad (GGA+U) as exchanges correlation potential, while the periodic low-dimensional slab structure of ZnO was considered as the low dimensional structure model. In the calculation processes, the concentration of the Ni doped ZnO was varied between 1-5–%mole. The calculation results show that the Ni:ZnO polar surface is energetically more stable in ferromagnetic state than antiferromagnetic state for all considered

concentration at ground state. The ferromagnetic state is dominating because the substitution of Ni atom on the Zn site has only one sublattice. In addition, the substitution of Ni^{2+} atom on the Zn^{2+} atom of the slab surface contribute to the exhibition of spin-polarized electronic structure in Ni:ZnO. Moreover, the existing of semiconductor in majority spin carriers and metallic minority spin carriers suggest the potential application in spin based electronic device.

Keywords: Density Functional Theory, ZnO polar surface, Ni-dopped ZnO, slab structure

[1] B. Ul Haq, R. Ahmed, A. Shaari, N. Ali, Y. Al-Douri, and A. H. Reshak. Comparative study of Fe doped ZnO based diluted and condensed magnetic semiconductors in wurtzite and zinc-blende structures by first-principles calculations. *Mater. Sci. Semicond. Process.*, vol. 43, pp. 123-128, 2016.

[2] A. El haimeur, A. Ballouch, B. Benali, M. Addou, M. Eljaouad, Z. Sofiani, *et al.* Effect of Grain Size on Magnetic Properties of ZnO Doped with Nickel Single Impurities. *J. Supercond. Novel Magn.*, vol. 29, pp. 427-437, 2016.

[3] K. Mun Wong, S. M. Alay-E-Abbas, A. Shaukat, Y. Fang, and Y. Lei. First-principles investigation of the size-dependent structural stability and electronic properties of O-vacancies at the ZnO polar and non-polar surfaces. *J. Appl. Phys.*, vol. 113, 2013.

[4] B. Meyer and D. Marx. Density-functional study of the structure and stability of ZnO surfaces. *Phys. Rev. B: Condens. Matter.*, vol. 67, pp. 354031-3540311, 2003.

Ammonia Sensing of Silver Nanoparticles Synthesized using Tannic Acid Combined with UV Radiation

Vimolvan (Pimpan) [1,2], Thanawan (Ritthichai) [1,2]

[1]Department of Materials Science, Faculty of Science, and [2]Center of Excellence on Petrochemical and Materials Technology, Chulalongkorn University, Phayathai Rd., Pathumwan, Bangkok 10330, Thailand.

E Mail/ Contact Détails ***(thanawan.ri@student.chula.ac.th/ vimolvan.p@chula.ac.th)***

Green synthesis of silver nanoparticles were done using silver nitrate as a silver source and tannic acid as a reducing agent and a stabilizer with the assistance of UV radiation at room temperature and neutral condition. UV exposure times were varied from 15, 30, 45, 60, 90 to 120 minutes. The appearances of the main characteristic peak at 425 nm in UV-Vis spectra confirmed the formation of silver nanoparticles. While the peak intensities of the nanoparticles synthesized using the exposure times of 60, 90 and 120 minutes were comparable, they increased with increasing UV exposure times from 15 to 60 minutes. This indicates that the exposure time of 60 minutes is suitable for the synthesis of silver nanoparticles using this system. The spherical particles having the average sizes in the range of 8-30 nm were revealed by transmission electron microscope. All synthesized nanoparticles exhibited the color change from orange-yellow to yellowish-green after exposing to ammonia with the shifts of the wavelength in UV-Vis spectra to around 320 nm. Their color became darker with increasing the ammonia concentrations from 100 to 500 ppm. This suggests the possibility of using these nanoparticles as a colorimetric sensor for ammonia.

Keywords: Silver nanoparticles, tannic acid, UV radiation, ammonia, sensing

[1] TIMMER, B., OLTHUIS, W., & VAN DER BERG, A. 2005. Ammonia Sensors and Their Applications—A Review. *Sensors and Actuators B: Chemical*, 107, 666-677.

[2] DUBAS, S. T., & PIMPAN, V. 2008. Green Synthesis of Silver Nanoparticles for Ammonia Sensing. *Talanta*, 76, 29-33.

[3] MOLINS-LEGUA, C., MESEGUER-LLORET, S., MOLINER-MARTINEZ, Y., & CAMPÍNS-FALCÓ, P. 2006. A Guide for Selecting the Most Appropriate Method for

Ammonium Determination in Water Analysis. *TRAC Trends in Analytical Chemistry*, 25, 282-290.

[4] ZENG, S., BAILLARGEAT, D., HOD, H. P., & YONG, K. T. 2014. Nanomaterials Enhanced Surface Plasmon Resonance for Biological and Chemical Sensing Applications. *Chemical Society Reviews*, 43, 3426-3452.

[5] DUBAS, S. T., & PIMPAN, V. 2008. Humic Acid Assisted Synthesis of Silver Nanoparticles and its Application to Herbicide Detection. *Materials Letters*, 62, 2661–2663.

[6] YANG, N., WEI, X. F., & LI, W. H. 2015. Sunlight Irradiation Induced Green Synthesis of Silver Nanoparticles Using Peach Gum Polysaccharide and Colorimetric Sensing of H_2O_2. *Materials Letters*, 154, 21-24.

[7] WATCHARAPORN, K., OPAPRAKASIT, M., & PIMPAN, V. 2014. Effects of UV Radiation and pH of Tannic Acid Solution in the Synthesis of Silver Nanoparticles. *Advanced Materials Research*, 911, 110-114.

[8] YI, Z., LI, X., XU, X., LUO, B., LUO, J., WU, W., YI, Y., & TANG, Y. 2011. Green, Effective Chemical Route for the Synthesis of Silver Nanoparticles in Tannic Acid Aqueous Solution. *Colloid and Surfaces A: Physicochem and Engineering Aspects*, 392, 131-136.

An optical reflectivity-based in situ thickness measurement method for nanothick membranes using Fabry-Perot interference spectra

Cheng Li[1,*], Qianwen Liu[1], Xiaobin Peng[1], Shangchun Fan[1], Feifan Yu[2], Ruitao Lv[2]

[1]School of Instrumentation Science and Opto-electronics Engineering, Beihang University, Beijing, 100191, China.

[2]School of Materials Science and Engineering, Tsinghua University, Beijing, 100084, China.

*E-mail:liuqianwenok@163.com /*licheng@buaa.edu.cn* (*corresponding author*)

Summary

A simple in situ optical fiber Fabry-Perot (FP) interference method was demonstrated to determine the thickness of nanothick diaphragm by measuring its optical reflectivity. Four multilayer graphene and MoS_2 membranes with different thicknesses were suspendedly adhered onto the endface of a ferrule with a 125-μm inner diameter by van der Waals interactions to construct micro FP cavities. Along with the modeled reflection and refraction matrix of the diaphragm, working as a light reflector of a FP interferometer, the effects of layer thickness, optical absorption and measurement wavelength of membrane were explored to characterize the film thickness-dependent optical reflectivity. In this way, the optical reflectivities of two graphene membranes (6~8 layer and 10~15 layer) were extracted by the interference spectra and averaged to be 0.652% and 1.49% based on 3σ rule, respectively. The corresponding thicknesses were solved to be 2.68 nm and 4.02 nm, in exceeding agreement with those obtained by atomic force microscope (AFM) experiments. Accordingly, the thicknesses of the rest two MoS_2 membranes were determined as about 8.8 nm and 19.4 nm, respectively, in close proximity to the measured results (8.1 nm and 20.3 nm) using AFM. Hence, the highly consistent theoretical and experimental data confirmed the accuracy of our method, which could be further extended for measuring the thickness of other 2D membrane materials.

Motivation

Thickness measurement is very ciritcal for many 2D membrane materials, such as graphene and MoS_2, in order to investigate or predict their mechanical and optical behaviors. The common measurements are performed by AFM, X-ray reflectivity

experiments and imaging cross-sectional samples with conventional transmission electron microscopy [1]. However, specific measurement setups or complicated time-consuming sample test process as well as clean substrates with low surface roughness are generally needed for the aforemention methods. Moreover, there is the discrepancy in membrane thickness between material samples and micro/nano devices due to the imperfection in large-area, uniform and high-quality nanothick film preparation [2]. Here we presented a simple in situ optical reflectivity-based method for determinating the thickness of thin films by FP interference spectra.

Results

Figure 1 shows the temperature and thickness (layer number) dependence of optical reflectivity for graphene membrane at a typical wavelength of 1550nm. The simulation result verified the correlation between membrane thickness and optical reflectivity. By the experimental rig for the determination of thin film thickness shown in Fig.2, the measured membrane thicknesses of a 6~8-layer graphene diaphragm in the tested range of 20-60℃ are demonstrated in Fig.3. And the solved thickness achieved an exceedingly low fitted sensitivity of 0.0045 nm/℃. Then Fig. 4 depicts the measured thicknesses of 8.1 nm and 20.3 nm for MoS_2 diaphragms using AFM, which well conformed to the derived values with the proposed method.

Keywords: Graphene, membrane thickness, optical reflectivity, Fabry-Perot interference, in situ measurement

[1] KUMAR, A., AGRAWAL, K. V., TSAPATSIS, M. & MKHOYAN, K. A. 2015. Quantification of Thickness and Wrinkling of Exfoliated Two-Dimensional Zeolite Nanosheets. *Nature Communications*, 6, 7128.

[2] LIU, W., LI, H., XU, C. KHATAMI Y. & BANERJEE, K. 2011. Synthesis of High-Quality Monolayer and Bilayer Graphene on Copper Using Chemical Vapor Deposition. *Carbon*, 49, 4122-4130.

Figures

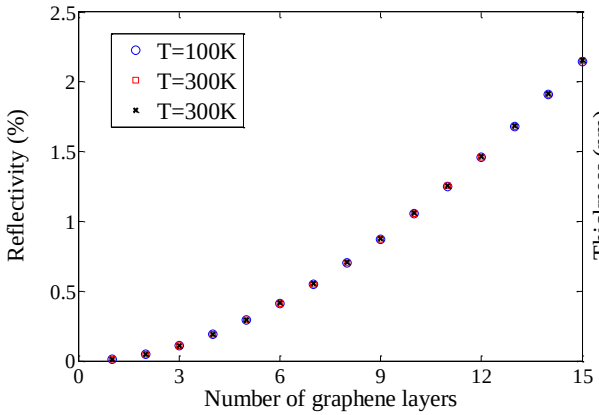

Fig. 1 The temperature and layer number dependence of optical reflectivity.

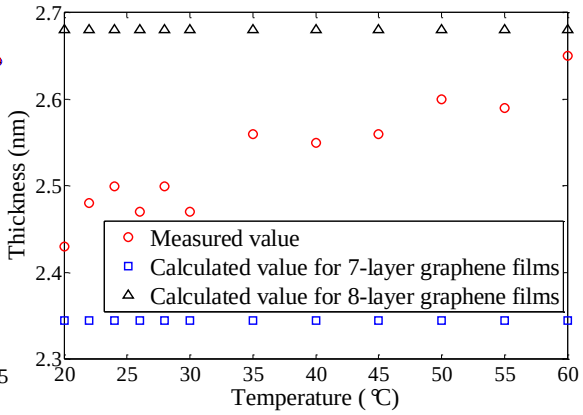

Fig. 3 The measured thickness of graphene membrane verse temperature.

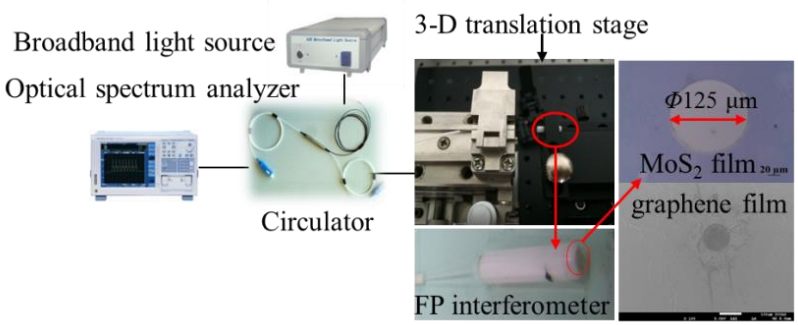

Fig. 2 Schematic diagram of experimental rig for FP interference measurement.

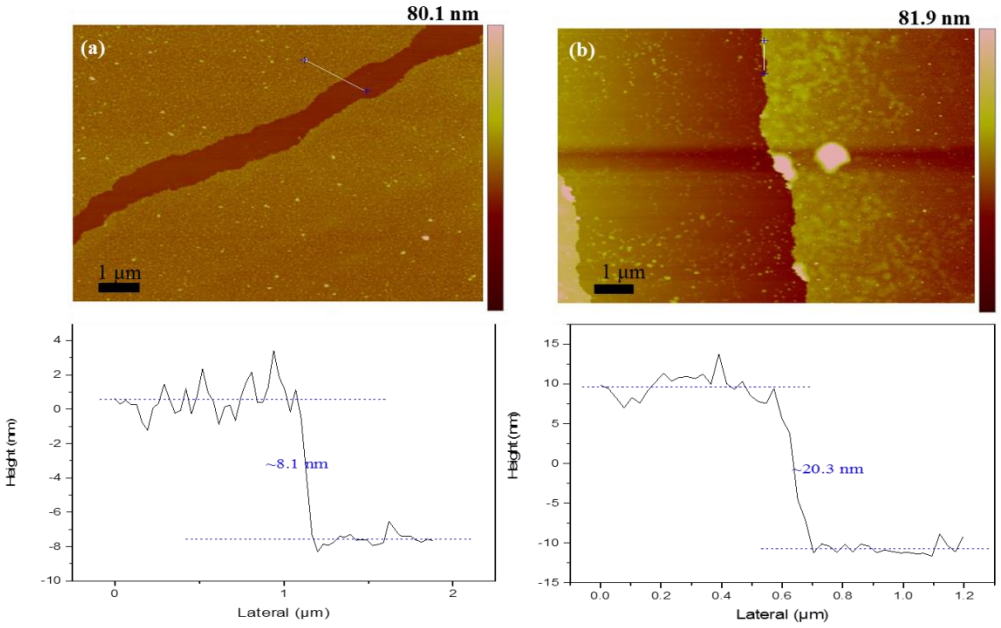

Fig. 4 The measured thickness results of (a) few layer and (b) multilayer MoS_2 diaphragms using AFM.

Anisotropic Carbon Nanotube for new type of angle sensor development

Mohd Asyraf[a], M. Masud Rana[a], T. Saleh[a]*, Harrison D. E. Fan[b], Andrew T. Koch[b], Alireza Nojeh[b], Kenichi Takahata[b] and Asan GA Muthalif[a]

a Department of Mechatronics Engineering, Faculty of Engineering, International Islamic University Malaysia, Kuala Lumpur, 50728, Malaysia

b Department of Electrical and Computer Engineering, University of British Columbia, Vancouver BC, V6T 1Z4, Canada.

Vertically Aligned Carbon Nanotubes (VACNTs) has captured attention by the researchers because of their flexibility and other attractive engineering properties. They are promising to be used as a functional bulk material in MEMS as well **[1]**. VACNT array (CNT forest) is known to be the darkest material on Earth because of their unique absorption index. However, this author has shown and explained that tip bent carbon nanotube forest can reflect light like mirror **[2]**.This paper reports that selectively tip bent CNT forest act as an anisotropic mirror, and this property can be exploited to fabricate CNT-based flexible angle sensor that is first of its kind.

In this report, we presented a method that can bend the tips of the CNT inside a VACNT array as described in Fig. 1(a). A rigid cylindrical tool rolls over the CNT forest to bend and align the CNTs in the direction of the tool motion. The alignment of the CNTs after process can be observed in Fig. 1(b). Later optical characterization was carried out (on the bent CNT zone) using a polarized laser source as explained in Fig. 1(c). It was observed that if we rotate the sample from 0 to 90 degree, the reflectance is decreasing; this is because the polarization reflection changes from along the nanotube to the perpendicular direction of the nanotubes which is also supported by the findings of Deheer et.al **[3].** The result of this analysis is shown in Fig. 1(d). It can be seen that from 10-90 degree the graph is quite linear and the hysteresis of the curve is minimal. The average sensitivity was found to be 0.155%/degree rotation. This finding opens the gateway to fabricate a new CNT-based flexible and miniaturize angle sensor.

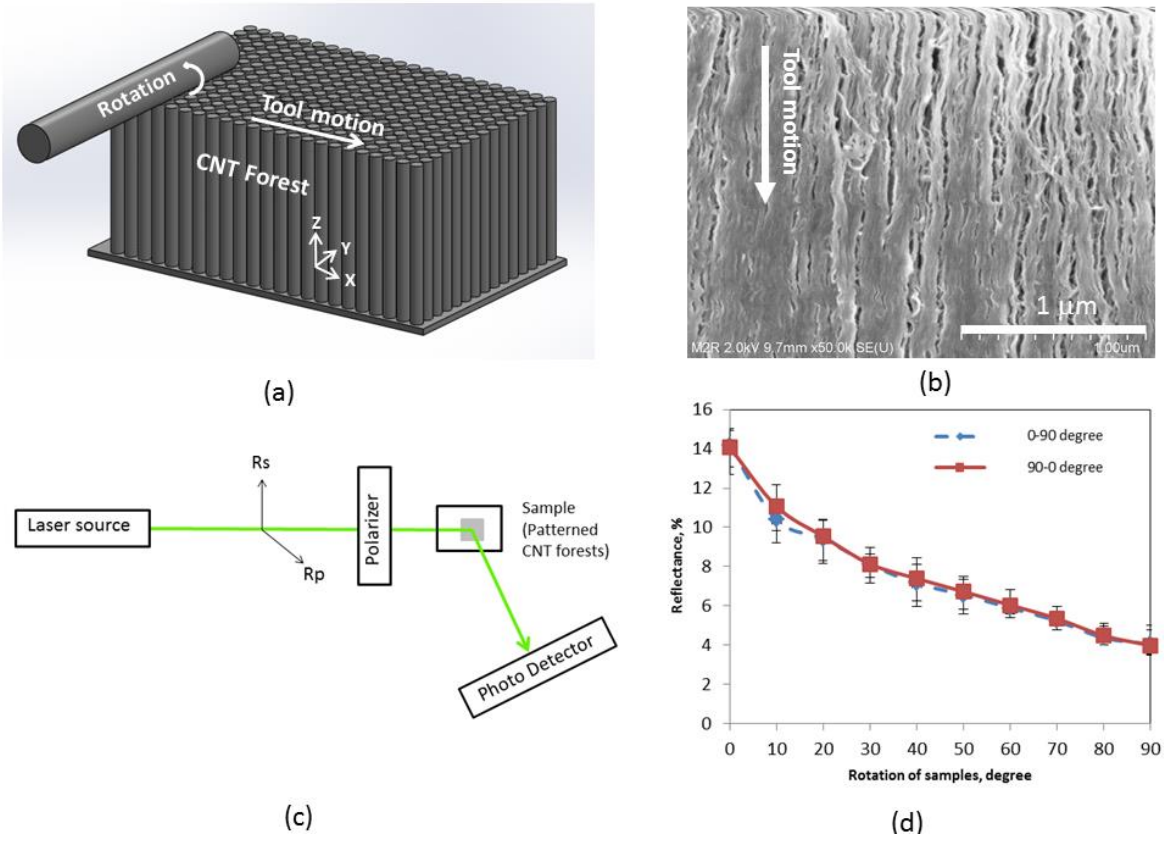

Fig. 1: (a) Description of the 'tip bending' process of CNTs along the direction of the tool motion. (b) SEM image shows the alignment of tip bent CNTs along the direction of the tool motion. (c) Optical characterization of the bent CNT zone. (d) Variation of the reflectance from the sample as the sample is rotated from 0 to 90 degree.

References:

[1] Yuhei Hayamizu, Takeo Yamada, Kohei Mizuno, Robert C. Davis, Don N. Futaba, Motoo Yumura & Kenji Hata, Nature Nanotechnology 3, 289 - 294 (2008)

[2] .Saleh, T., Moghaddam, M. V., Mohamed Ali, M. S., Dahmardeh, M., Foell, C. A., Nojeh, A., and Takahata, K. Appl. Phys. Lett., 101(6): 061913. (2012)

[3] W. A. Deheer, W. S. Bacsa, A. Chatelain, T. Gerfin, R. Humphrey-Baker, L. Forro, and D. Ugarte, Science **268**, 845 (1995)

Flexible Silver Nanowires Electrodes Based on Roll Coating Process for Dynamic Flow Sensing

Yan-Ren Chen, Tong-Miin Liou, Chien-Chong Hong

Dept. of Power Mechanical Engineering, National Tsing Hua University, Hsinchu, Taiwan.

Email: bread12035@gmail.com

Summary

Silver nanowire electrode represents a mass-manufacturable way toward transparent flexible electrode for organic photovoltaics (OPV), organic light emitting (OLED), and other sensors. Here this paper presents a flexible silver nanowire electrode based on roll coating process for dynamic flow sensing. The as coated silver nanowire electrodes suffer from tremendous contact resistance owing to the capping insulated polymer: PVP. Two steps process eliminate the contact resistance between silver nanowires by water washing away capping polymer and light pressure (50 psi) and low temperature (60 degree) welding silver nanowires. Silver nanowire electrode with 91% transmittance and 10 Ω/□ are shown in this paper. After process, silver nanowire electrodes are patterned by custom tape as dynamic flow rate sensor. The flexible and transparent flow rate sensors on car windshield are able to monitor wind speed during driving. Furthermore, silver nanowire based dynamic flow sensor tube allows users to monitor flow inside the tube and observe the fluid at the same time. To prevent flow sensors from affecting the flow inside the tube, the surface of sensor must be smooth. The surface roughness after process is below 17 nm which can be ignored. The response resistance of silver nanowire flow sensor is about 1 ohm and the response time is less than 1 second. The sensitivity is 0.01 ohm/L.

Figure 1 shows a flexible transparent dynamic flow sensor in this paper. Silver nanowire electrode fabricated by a straightforward two steps process is shown in figure 2. Meyer-rod roll coated silver nanowire film on PET is immersed into water to wash away PVP residual and then press at low temperature and pressure for 3 minutes. The process can sinter silver nanowires and smooth the surface of silver nanowires film at the same time at relative low temperature (60°C) and pressure (50 psi). Silver nanowires film after process exhibits a high transmittance (91%) and a low sheet resistance (10 Ω/□). After process, silver nanowire electrode is patterned by custom tape shown in figure 3. Figure 4 shows SEM images before and after pressing and the performance of silver nanowires electrode after process is shown in figure 5. Silver nanowires stick together after pressing and the performance of electrode is competitive to commercial ITO while showing better flexibility for applications. Whole process is able to integrate into roll to roll process and consume less power than other sintering process such as intensity pulsed light sintering [1] or laser sintering [2]. Excellent electrical, optical and morphology performance are shown in this work. The performance of dynamic flow rate sensor is shown in figure 6.

Keyword: silver nanowires, sintering, smoothing, flow rate sensor

[1] JINTING, J., MASAYA, N., TOHRU, S., TAKEHIRO, T., TEPPEI, A., NATSUKI, K., KATSUAKI, S., HIROSHI, U. & KENJI, S. 2012. Strongly Adhesive and Flexible Transparent Silver Nanowire Conductive Films Fabricated with a High-Intensity Pulsed Light Technique. *J. Mater. Chem.,* 22, 23561-23567.

[2] JOSHUA, A. S., KEN, A. N., JAMES, C. S. & CRAIG, B. A. 2015.Improved Efficiency of Hybrid Organic Photovoltaics by Pulsed Laser Sintering of Silver Nanowire Network Transparent Electrode. *ACS Appl. Mater. Interfaces,* 7, 10556−10562.

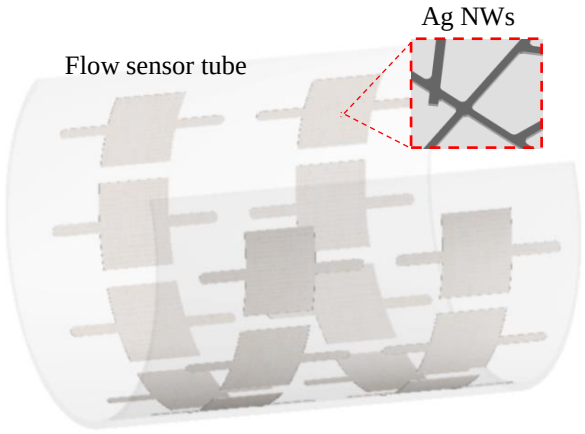

Figure 1. *Schematic drawing of heat sensitive flow rate sensor in this work.*

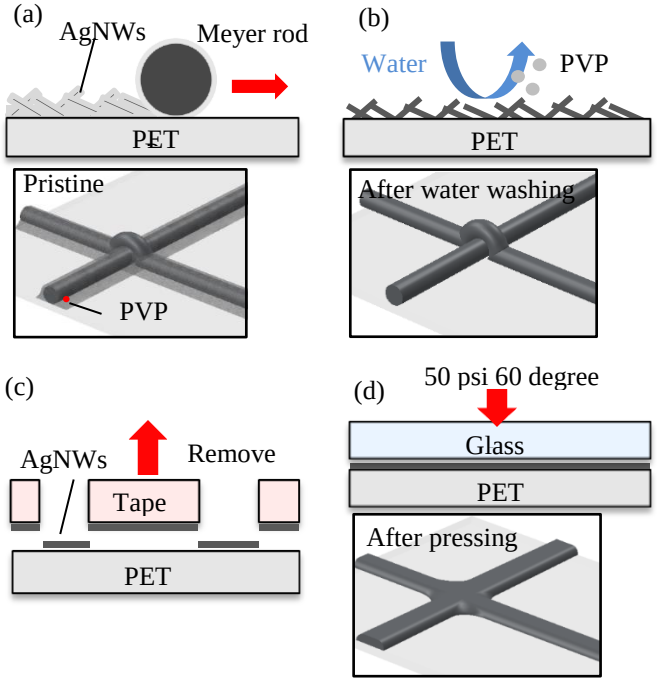

Figure 2. *Schematic drawing of low temperature low pressure process and fabrication of flow rate sensor, (a) roll coating AgNWs on PET, (b) water bath washing off PVP coating on AgNWs, (c) AgNWs patterned by tape, (d) low temperature and low pressure pressing process,*

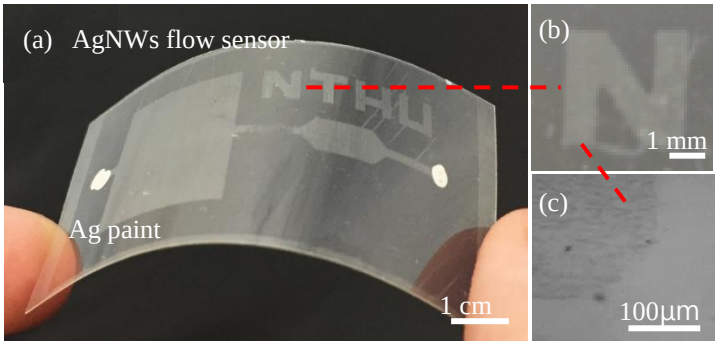

Figure 3. *Photograph of (a) silver nanowires based flow rate sensor, (b) tape for patterning.*

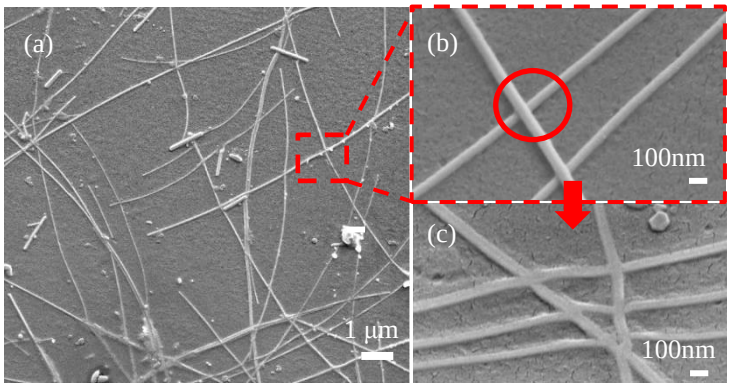

Figure 4. *SEM image of (a) silver nanowires (b) silver nanowires after washing off PVP, (c) silver nanowires after low temperature low pressure pressing .*

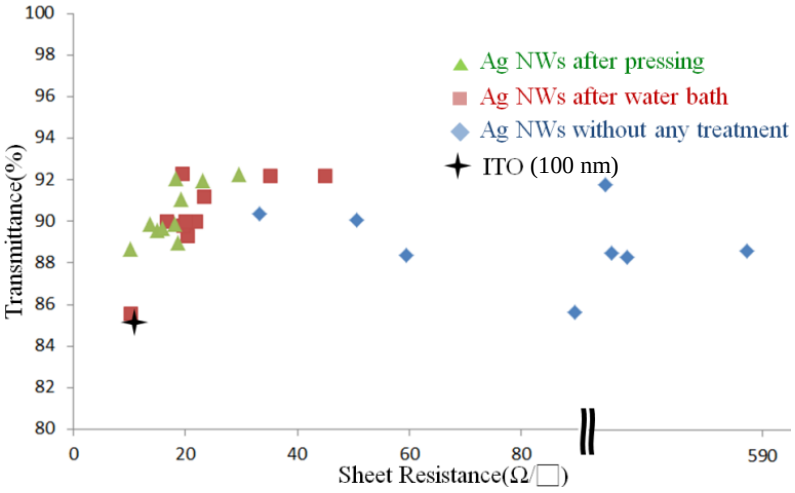

Figure 5. *Transmittance (at λ = 550 nm) vs. sheet resistance after roll coating, water washing, and low temperature low pressure pressing.*

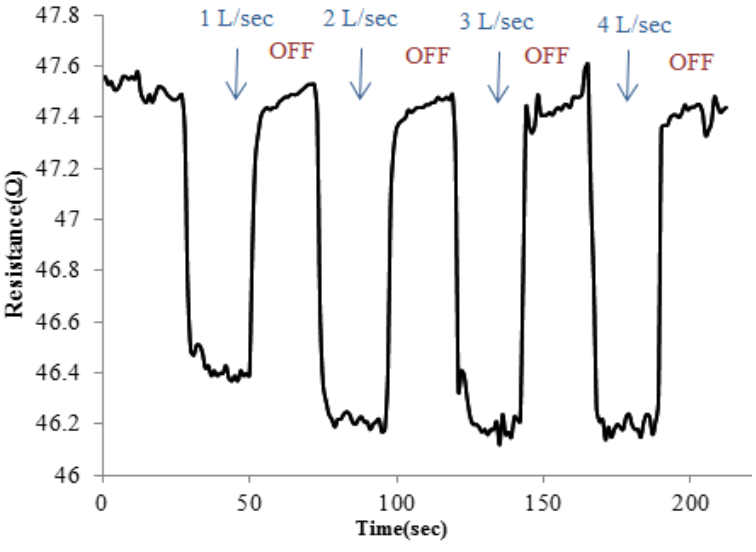

Figure 6. *Resistance of AgNWs electrode under different flow rate (20 seconds recovery after 20 second flow exerting)*

New Functionalities of Flexible Electronic and Photonic Devices Based on III-Nitride Semiconductor Heterostructures

Shahab Shervin[1], Seung-Hwan Kim[1,2], Mojtaba Asadirad[1], Keon-Hwa Lee[1], Jae-Hyun Ryou[1,3]

[1]Department of Mechanical Engineering and Materials Science and Engineering Program, University of Houston, Houston, Texas 77204-4006, USA.

[2] Metamaterial Electronic Device Research Center, Hongik University, Seoul 121-791, Korea.

[3]Texas Center for Superconductivity at the University of Houston (TcSUH), University of Houston, Houston, Texas 77204, USA.

jryou@uh.edu

Recent developments in flexible electronics demonstrate that semiconductor thin-film materials are flexible, deviating from bulk properties.[1,2] Especially, flexible devices based on Group III-nitride (III-N) heterostructures, which are a promising candidate for next-generation energy devices, have been developed using a layer-transfer technique for versatile applications of wearable and implantable electronics.[3] Authors recently demonstrated by numerical studies that flexible III-N devices can be more than just mechanically flexible devices.[4] They can be equipped with new functionalities. This work presents a new concept for flexible III-N light-emitting diodes (LEDs) and high electron mobility transistors (HEMTs) through theoretical calculations. The performance of this new type of transistor is based on applied external strain so called strain-effect LED and strain-effect transistors (SETs). For photonic devices, we have studied the effects of external bending strain on quantum-confined Stark effect (QCSE) of quantum wells (QWs) in wurtzite InGaN/GaN heterostructures on flexible substrates. Our results show internal quantum efficiency (IQE) improves significantly by applying external compressive strain in QW and QWB with bending-up. Our results also show that significant tunability in peak emission wavelength is achievable. The blue- and red- shift of the emission peaks achieved for flexible LEDs can produce red, green, and blue colors. This finding leads us to suggest a concept of photo-electro-mechanical (PEM) device. For electronic devices, we show that the electronic band structures of InAlGaN/GaN thin-film

heterostructures on flexible substrates can be modified by external bending with a high degree of freedom using polarization properties of the polar semiconductor materials. Transfer characteristics of the HEMT devices, including threshold voltage and transconductance, are controlled by varied external strain. Equilibrium 2-dimensional electron gas (2DEG) is enhanced with applied tensile strain by bending the flexible structure with the concave-side down (bend-down condition). 2DEG density is reduced and eventually depleted with increasing compressive strain in bend-up conditions. The operation mode of different HEMT structures changes from depletion- to enchantment-mode or vice versa depending on the type and magnitude of external strain. The results suggest that the operation modes and transfer characteristics of HEMTs can be engineered with an optimum external bending strain applied in the device structure. In addition, we show that drain currents of transistors based on flexible InAlGaN/GaN can be modulated only by external strain without applying electric field in the gate. The channel conductivity modulation that obtained by only external strain proposes an extended functional device, gate-free SETs.

Keywords: III-N semiconductors, flexible devices, light-emitting diodes, high-electron mobility transistors

[1] O. G. Schmidt and K. Eberl, 2001. Nanotechnology: Thin solid films roll up into nanotubes. *Nature* 410, 168.

[2] D. Shahrjerdi and S. W. Bedell, 2013. Extremely flexible nanoscale ultrathin body silicon integrated circuits on plastic. *Nano Lett.* 13, 315–320.

[3] Y. Jung, X. Wang, J. Kim, S. Hyun Kim, F. Ren, S. J. Pearton, and J. Kim, 2012. GaN-based light-emitting diodes on origami substrates. *Appl. Phys. Lett.* 100, 231113-1–3.

[4] J.-H. Ryou, S. Shervin, and S.-H. Kim, "Externally-strain-engineered semiconductor photonic and electronic devices and methods of making thereof and assemblies thereof," (Provisional patent application in Apr. 2015 (Application #: 62144715; Doc #: 2483-07000)).

Synthesis of Metal/Bimetal Nanowires and Their Application in Ultra-Stretchable Conductors

Ranran Wang, Xiao Wang, Yin Cheng and Jing Sun*

Shanghai Institute of Ceramics, Chinese Acadamy of Sciences, Shanghai 200050, China

wangranran@mail.sic.ac.cn jingsun@mail.sic.ac.cn

Stretchable electronics emerged as an intriguing, yet challenging research field and has gained some achievements in sophisticated applications like stretchable displays, skin-like sensors, implantable biomedical devices and so forth. The realization of stretchable electronics frequently involves the demanding for stretchable conductors utilized as stretchable electric circuiting. However, the fabrication of high-performance (working strain exceeding 150%) stretchable conductor through facile and scalable method is still a challenging task.

Metallic nanowires (NWs) could be very promising candidates for electrical conductive components in stretchable conductors due to their high conductivity and flexibility. In our work, we successfully synthesized metal/bimetal nanowires (Cu NWs, Ag NWs, CuNi NWs and CuAg NWs) and presented a novel, cost-effective, and scalable strategy for the manufacturing of composite fibers as stretchable conductors. The composite fiber possessed an artfully designed "twining spring" hierarchical architecture, based on materials of elastic yarns and metal nanowires. The conductivity of the composite fibers reached up to 4018 S/cm and remained as high as 688 S/cm at 500% tensile strain. The conductivity of composite fibers (initial conductivity of 4018 S/cm) kept perfectly stable after 1000 times bending, and leveled off at 183 S/cm after 1000 times cyclic stretching of 200% strain. Commercial electronic components (LED arrays) were integrated onto a transparent, foldable and stretchable substrate using the composite fibers as stretchable electric wiring, demonstrating the potential application in large-area stretchable electronics. The validation of the biocompatibility of the composite fiber also opened up its prospect in the field of implantable devices. Additionally, our fabrication strategy is versatile and can be extended to diverse materials for preparation of functionalized composite fibers with superb stretchability.

Keywords: Stretchable electronics, conductors, metal nanowires, synthesis

[1] WANG, X, WANG, R. R.* SHI, L. J. and SUN J.* 2015. Synthesis of Metal/Bimetal Nanowires and Their Applications as Flexible Transparent Electrodes. *Small*, 11, 4737–4744.

[2] CHENG, Y., WANG, R. R.*, SUN J.*, GAO, L. 2015. Highly Conductive and Ultrastretchable Electric Circuits from Covered Yarns and Silver Nanowires. *ACS Nano*, 4, 3887-3895.

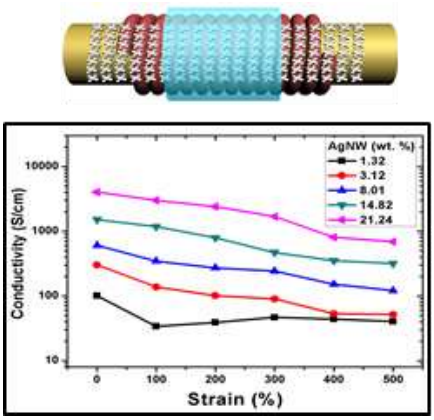

An optical fiber Fabry-Perot resonator with multilayer graphene diaphragm

Yumei She[1], Cheng Li[1,*], Shangchun Fan[1], Qianwen Liu[1], Tian Lan[1]

[1]School of Instrumentation Science and Opto-electronics Engineering, Beihang University, Beijing, 100191, China.

*E-mail:sheymbh@163.com /*licheng@buaa.edu.cn* (*corresponding author*)

Summary

We demonstrated a multilayer graphene mechanical resonator with optical excitation and detection. The effects of structural parameters for circular and square membranes on the frequency of the fundamental mode at different temperatures were analyzed based on a continuum model, which indicated that circular membrane could offer a better resonance. Then a 6~8-layer circular CVD graphene membrane was suspendedly adhered onto the endface of a ferrule with a 125-μm inner diameter by van der Waals interactions to construct a micro Fabry-Perot (FP) cavity. The modulated optical fields were coupled into the diaphragm causing amplified mechanical vibrations which were picked up by a FP interferometry. The resonator exhibited preferable resonances with an optimal frequency of 184 kHz in the tested range of 120-260 kHz. Although the change between measured resonance spectral and theoretical ones was observed primarily due to adhesive behaviors at the membrane-substrate interface and adsorbates imparting tension to the graphene in addition to air damping in the FP cavity, the experimental results confirmed the potential applicability of the FP graphene resonator for micro/nano pressure or mass sensors with high sensitivity and fast response. Further research on performance optimization will be performed in a wider frequency range.

Motivation

The combination of low mass density, high frequency and high quality-factor of mechanical resonators made of two-dimensional materials such as graphene make them attractive for applications in force sensing/ mass sensing [1]. Thus far, research has foucused primarily on electromechanical resoantors with smal cross-sectional dimensions made of single- and multilayer graphene sheets suspended over a trench [2] or ones with electrical drive and readout [3]. Although it is possible to improve the sensitivity of

resonators by reducing cross-sectional dimensions, the quality factor will decrease. Here we fabricated an optically actuated circluar mechanical resonator with a larger diameter of 125 μm from multilayer graphene using FP interferrometry.

Results

Figure 1 shows the frequency of the fundamental mode for circluar and square graphene membranes verse t/d^2 at different temperatures, where t and d are the thickness and the diameter (or edge length) of membrane, respectively. Due to the increased frequency with decreasing temperature for a ~7-layer circular graphene membrane with a diameter of 125 μm when air damping in FP cavity is considered in Fig.2, the simulation results indicated that the frequency shifts at different temperatures were avaliable to measure thermal expansion coefficients of graphene. By the experimental rig for FP graphene resonator optically actuated and detected in Fig.3, the amplitude versue frequency for the multilayer graphene resonator was measured in the range of 120-260 kHz as demonstrated in Fig.4. A fit to the Lorentzian resonance yielded an optimal resonant frequency f_0=184 kHz. Figure 5 depicts the optomechanical coupled resonance output in response to an optical excitation with a light intensity of -8.124 dBm at f_0.

Keywords: Graphene resonator, optomechanical coupling, Fabry-Perot interference, resonant frequency

[1] WEBER, P., GUTTINGER, J., TSIOUTSIOS, I., CHANG. D. E. & BACHTOLD, A. 2014. Coupling Graphene Mechanical Resonator to Superconducting Microwave Cavities. *Nano Letters*, 14, 2854-2860.

[2] BUNCH, J. S., VAN DER ZANDE, A. M., VERBRIDGE, S. S., FRANK, I. W., TANENBAUM, D. M., PARPIA, J. M., CRAIGHEAD, H. G. & MCEUEN, P. L. 2007. Electromechanical Resonators from Graphene Sheets. *Science*, 315, 490-493.

[3] CHEN, C. Y., ROSENBLATT, S., BOLOTIN, K. I., KALB, W., KIM, P., KYMISSIS, I., STORMER, H. L., HEINZ, T. F. & HONE, J. 2009. Performance of Monolayer Graphene Nanomechanical Resonators with Electrical Readout. *Nature Nanotechnology*, 4, 861-867.

Figures

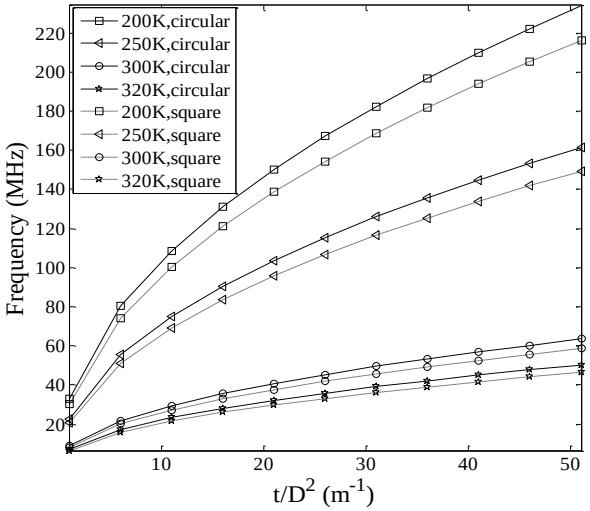

Fig. 1 Simulation on frequency of the fundamental mode verse t/d^2 at different temperatures.

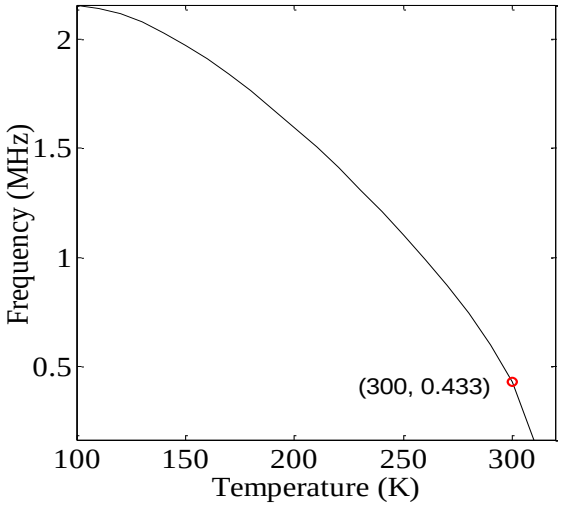

Fig. 2 Simulation on frequency of the fundamental mode verse temperature with air damping in FP cavity.

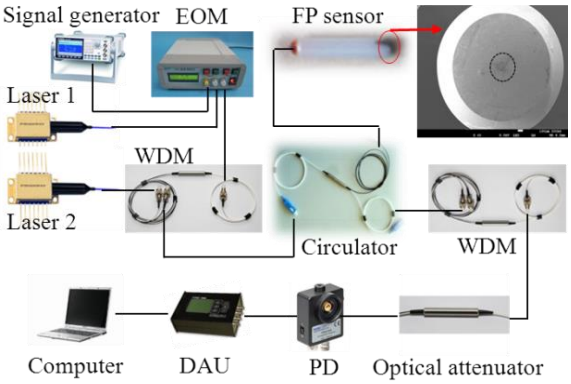

Fig. 3 Schematic diagram of experimental rig for FP graphene resonator.

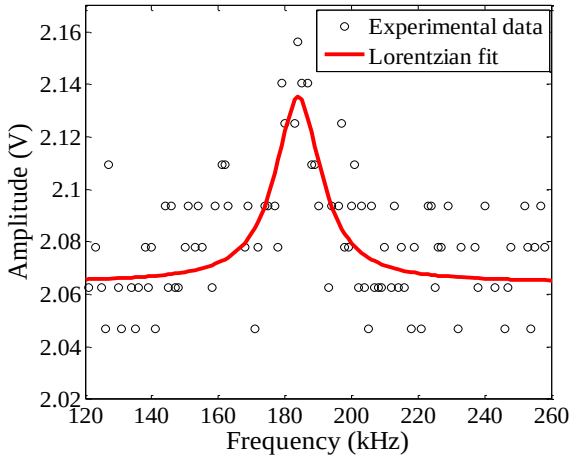

Fig. 4 Amplitude verse frequency of the fundamental mode.

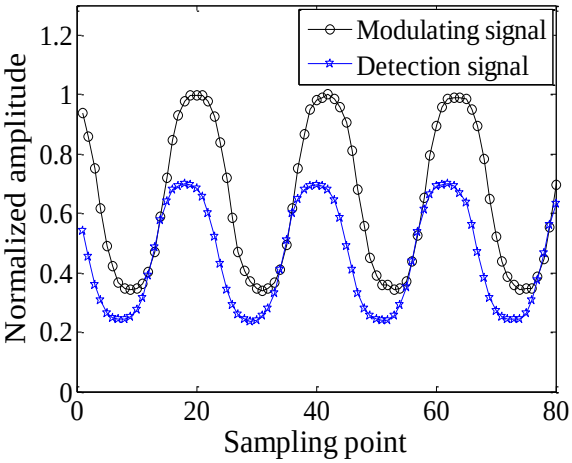

Fig. 5 The resonant signals taken with optical drive and detection at f_0.

Biomimetic Magnetic Nanoparticles as a Promising Building-Blocks for Magnonics

S. Mamica, M. Krawczyk

Faculty of Physics, Adam Mickiewicz University in Poznan,
ul. Umultowska 85, 61-614 Poznan, Poland.

mamica@amu.edu.pl

Biomimetic magnetic nanoparticles (NPs) have unusual physical properties as well as promising applications in a wide variety of fields that range from medicine to nanoelectronics. They are special not only because of the peculiar way of growing but mostly due to some extra properties inherited from the biological material. The use of protein cages as reaction chambers for the production of NPs has a number of advantages from a high level of homogeneity of the NPs to the possibility of producing highly ordered three-dimensional (3D) structures by self-assembly. E.g. the protein crystallization technique has been successfully used for the production of 3D fcc magnetoferritin crystals of highly ordered structure and the external size up to 400 μm [1]. An interesting effect is a substantial reduction of the lattice constant as a result of dehydration.

Magnonic crystals (MCs), the magnetic counterpart of photonic crystals, proved to be promising materials for the construction of new logic systems and improvement of parameters and functionalities of rf devices [2]. The realization of MCs with a lattice constant of tens of nanometers, though technologically possible, remains a challenge. The protein crystallization technique seems to open the prospect of realizing 3D MCs with a lattice constant of ten-odd nanometers. This would be an enormous step forward in magnonics, and would allow shifting the magnonic band gap to the subterahertz frequency range. Additionally, the self-assembly processes depend on the external surface of the protein cage, the characteristics of which can be modified without affecting those of the internal surface, involved in the biomineralization process. This allows to control the self-assembly of biomimetic particles without modifying the core obtained inside the protein cage.

In this work we consider magnonic crystals with magnetoferritine nanoparticles embedded in a ferromagnetic matrix and study numerically the width of the absolute magnonic gap versus magnetic and structural parameters. Our approach is based on Maxwell's equations for magnetostatics, solved by the plane wave method [3]. We show that the proper choice of the magnetic material as well as the interparticle distance can lead to the magnonic gap opening. Moreover, on the basis of our results the magnetoferritine crystals produced by the protein crystallization technique seem to be very promising building-blocks for magnonic crystals having the crystallographic structure and the lattice constant almost optimized for the occurrence of well-defined magnonic band gap of two types: complete or directional. The second kind of gap in photonic crystals was proved to leads to the negative refraction or self-collimation.

The project leading to this application has received funding from the European Union's Horizon 2020 research and innovation programme under the Marie Skłodowska-Curie grant agreement No 644348.

Keywords: Biomimetic, magnetic nanoparticles, magnonic crystals, band gap

[1] OKUDA, M., ELOI, J.-C., WARD JONES, S. E., SARUA, A., RICHARDSON, R. M. & SCHWARZACHER W. 2012. Fe_3O_4 nanoparticles: protein-mediated crystalline magnetic superstructures. Nanotechnology, 23, 415601.

[2] KRAWCZYK M. & GRUNDLER D. 2014. Review and prospects of magnonic crystals and devices with reprogrammable band structure. J. Phys.: Cond. Matter, 26, 123202.

[3] MAMICA, S., KRAWCZYK, M., SOKOLOVSKYY, M. L. & ROMERO-VIVAS, J. 2012. Large magnonic band gaps and spectra evolution in three-dimensional magnonic crystals based on magnetoferritin nanoparticles. Phys. Rev. B, 86, 144402.

Effect of Ni doping on Structural, optical and magnetic properties of ZnO nanostructure: Synthesis by wet chemical process

Amit Kumar Rana, Yogendra Kumar, Rajasree Das, Somaditya Sen and Parasharam Shirage*

Department of Physics & Centre for Materials Science and Engineering Indian Institute of Technology Indore, Khandwa Road, Simrol Campus, INDORE - 452020. INDIA

*Correspondence E-mail: pmshirage@iiti.ac.in , paras.shirage@gmail.com

Abstract:

$Zn_{1-x}Ni_xO$, ($0 < x < 12.5\%$) nanostructure thin film samples are prepared by simple wet chemical technique. Effect of Ni-doping on structural, optical and magnetic properties of ZnO is systematically investigated. Reitveld refinement of XRD shows that all the films belongs to P63mc space group followed by a change in lattice parameters confirm incorporation of Ni ions in ZnO lattice without any Ni related impurity. SEM confirm the nano-rods like morphology in pure and with Ni doping changes the morphology from rod to flakes like. EDS confirm the Ni doping in ZnO. UV–Vis absorption and Photoluminescence (PL) spectra measurements, demonstrate some modification in the absorption characteristics with change in band gap from 3.01 to 2.90 *eV* and show defect related strong visible emission, indicating the presence oxygen vacancy point defect with strong intensities in the Ni doped ZnO sample, which is believed to play a significant role in the ferromagnetic (FM) ordering. Raman spectra confirm the Ni doping in ZnO. The magnetic properties are measured at low (5K and 80K) and room temperature of the Ni doped ZnO nanostructure show ferromagnetic nature at room temperature, which increases with decrease in temperature.

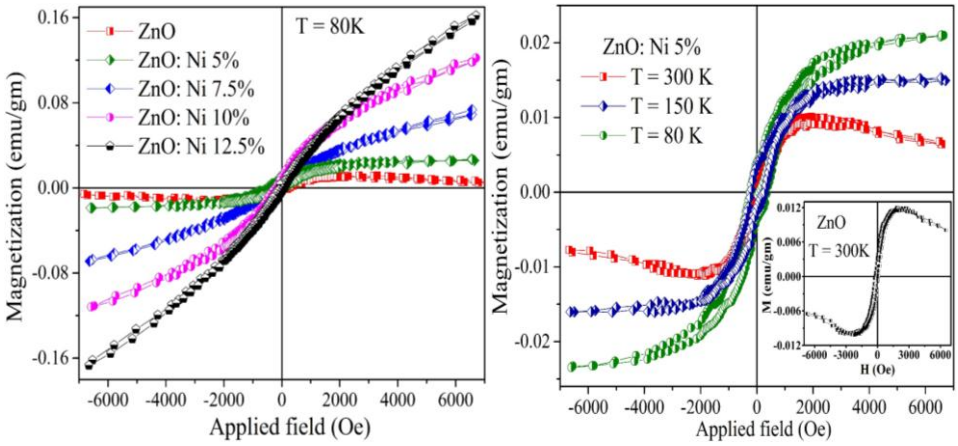

Fig.1 (a) M–H plot at 80 K showing the hysteresis loop for pure and Ni doped ZnO nano structure and (b) shows the M-H plot of Ni 5% doped ZnO at 80 K, 150 K and 300 and inset fig. shows room temperature M-H plot of ZnO.

Magnetic surfactants as a versatile tool for functional materials design

Sanghoon Kim[1], Christine Bellouard[2], Julian Eastoe[3], Nadia Canilho1, Andreea Pasc[1]

[1] SRSMC, UMR 7565, Université de Lorraine/CNRS, F-54506 Vandoeuvre-lès-Nancy, France

[2] Institut Jean Lamour, UMR 7198 , Université de Lorraine/CNRS, F-54506 Vandoeuvre-lès-Nancy, France

[3] School of Chemistry, University of Bristol, Cantock's Close, Bristol, BS8 1TS, United Kingdom

E-mail : andreea.pasc@univ-lorraine.fr

Magneto-responsive surfactants[1] are gathering increasing attention and were already use to design several molecularly organized systems such as magnetic micelles or microemulsion or to magnetize DNA. Moreover, magneto-responsive surfactants can also be used for material design. In this context, it will be firstly presented the structuring and the magnetization of hexagonally ordered mesoporous silica[2]. Starting porogens exhibit a paramagnetic behavior in the temperature range 2K-300K with a S = 5/2 spin state (Fe^{3+}), whereas magnetized silica, free of organic template, remains paramagnetic with a high spin- low spin transition below 15K. This temperature can be decreased by increasing the iron content.

Then, it will be shown that magneto-responsive surfactants combined with solid lipid nanoparticles (SLNs) can be used as colloidal tools for meso-macroporous supported catalyst[3]. The key point of this work is that the size of iron oxide nanoparticles embedded in the meso−macroporous matrices has been decreased to 15−20 nm in diameter to give high surface area of the active catalytic sites in comparison with the previous submicron scald iron oxide, As a matter of fact, the resulting material exhibits an excellent performance in a Fenton-like reaction for methylene blue degradation, even at low amount of iron oxide.

Finally, a novel system of paramagnetic vesicles was designed using ion pairs of iron-containing magnetic surfactants[4]. Unilamellar vesicles (diameter ~200 nm) formed spontaneously and were characterized by cryogenic transmission electron microscopy,

nanoparticle tracking analysis, light and small-angle neutron scattering. Moreover, for the first time, it is shown that magnetization measurements can be used to investigate self-assembly of such functionalized systems, giving information on the vesicle compositions and distribution of surfactants between the bilayers and the aqueous bulk.

Keywords: Magnetic surfactant, Vesicle, Spin crossover, Mesoporous silica, Catalysis

[1] Brown, P., Bushmelev, A., Butts, C. P., Cheng, J., Eastoe, J., Grillo, I., Heenan, R. K., Schmidt, A. M. 2012. Magnetic Control over Liquid Surface Properties with Responsive Surfactants. *Angew. Chem. Int. Ed.*, 51, 2414-2416.

[2] Kim, S., Bellouard, C., Pasc, A., Lamouroux, E., Blin, J. L., Carteret, C., Fort, Y., Emo, M., Durand, P., Stébé, M. J. 2013. Nanoparticle-Free Magnetic Mesoporous Silica with Magneto-Responsive Surfactants. *J. Mater. Chem. C.,* 1, 6930-6934.

[3] Kim, S., Durand, P., Roques-Carmes, T., Eastoe, J., Pasc, A. Metallo-Solid Lipid Nanoparticles as Colloidal Tools for Meso–Macroporous Supported Catalysts. 2015. *Langmuir*, 31, 1842-1849.

[4] Kim, S., Bellouard, C., Eastoe, J., Canilho, N., Roger, S. E., Ihiawakrim, D., Ersen, O., Pasc, A. 2016. Spin State as a Probe of Vesicle Self-Assembly. *J. Am. Chem. Soc.*, 2016 in press (doi: 10.1021/jacs.6b00537)

Size-dependent critical temperature of the nanoparticles

Petrov Aleksanr[1], Leonid Afremov[1]

[1]Far Eastern Federal University, 8 Sukhanova St., Vladivostok 690950, Russia

aleksandr.al.petrov@gmail.com

Magnetic phase transition's temperature varies by noticeable amount for nanoparticles (NPs), ultrathin films and nanowires compared with the bulk material. This is due to the nanostructure's size is commensurable number with the spin-spin correlation size. In this case nanodivides influence on the physical properties of the nanostructures so what is called size-effects to affect. There are many experimental studies [1-3] to show that phase transition critical temperature T_c decreases with size decreasing. Theoretical studies of the size-effect's influence on the phase transition's critical temperature based on d-f model and using Green's function technique [4], Monte-Carlo method [5] and average spin method [6,7] are in agreement with experimental data.

The aim of this work is to study the NP size dependence on the magnetic phase transition temperature. The study was based on "average spin" method developed earlier [6,7] and it main principles are given below:

1. N "magnetic atoms" are distributed uniformly over sites of cubic-shaped NP with L size;
2. Fields of interaction h between atom's spin magnetic moments are distributed randomly and there is direct exchange interaction between nearest neighbors only;
3. Atom's spin magnetic moments are oriented along axis oz (in the approximation of the Ising model).

Based on approximation this model self-consistent equations for magnetic moment μ_n of all atoms are written:

$$\mu_n = \int_{-\infty}^{\infty} \tanh\left(\frac{m_{n0}h}{k_B T}\right) W_n(h)dh, \quad 1 \le n \le N \ (1)$$

where $W_n(h)$- the distribution function of random fields of exchange interaction h with $n-th$ atom which calculation is presented in [7].

The calculation results of the relative Curie temperature $t_C = k_B T_C / J$ (J –the exchange interaction constant) on the atoms' number $N_a = L/a_0$ on the cube edge (a_0 – lattice constant, L-cube's length of the edge) for cubic-shaped NPs with different crystalline structure are shown in Fig. 1.

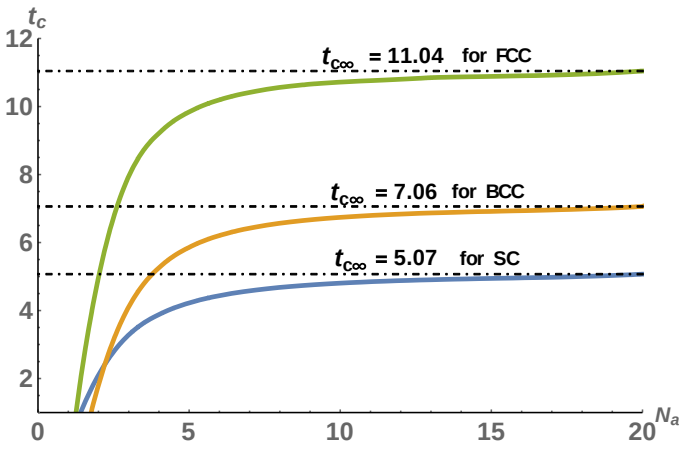

Fig. 1. The relative Curie temperature dependence t_C on the atoms' number on the cube edge N_a for NPs with different crystalline structure.

As could be expected the Curie temperature rather quickly increases to the bulk materials' values with atoms' number on the edge increase. So the limit relative Curie temperature is $t_C(N_a \to \infty) = 5.07$ for SC crystalline lattice, $t_C(N_a \to \infty) = 7.06$ for BCC crystalline lattice and $t_C(N_a \to \infty) = 11.04$ for FCC crystalline lattice.

Keywords: Curie temperature, finite-size effects, magnetic nanoparticles, "average spin"

[1] REGULACIO, M. D., BUSSMANN, K., LEWIS, B., STOLL, S. L. 2006. Magnetic Properties of Lanthanide Chalcogenide Semiconducting. *J. Am. Chem. Soc.*, 128 (34), 11173-11179.

[2] AMBROSE, T., CHIEN, C.L. 1996. Finite-Size Effects and Uncompensated Magnetization in Thin Antiferromagnetic CoO Layers. *Phys. Rev. Let.*, 76 (10), 1743-1746.

[3] LOPEZ-RUIZ, R., MAGEN, C., LUIS, F., BARTOLOME, J. 2012. High Temperature Finite-Size Effects in the Magnetic Properties of Ni Nanowires. *J. App. Phys.*, 112, 073906

[4] APOSTOLOVA, I., WESSELINOWA, J.M.. 2009. Composition Dependence of the Coercivity in the Magnetic Nanoparticles Suitable for Magnetic Hyperthermia. *Phys. Status Solidi B,* 246 (8), 1925-1930.

[5] LAOSIRITAWORN, Y., POULTER, J., STAUNTON, *J. B.* 2004. Magnetic Properties of Ising Thin Films with Cubic Lattices. *Phys. Rev. B*, 70, 104413

[6] BELOKON, V.I., SEMKIN, S.V. 1992. Random Field Method in the Ising Model of a Dilute Ferromagnet. *JETP*, 101, 1254-1258

[7] KIRIENKO, Y., AFREMOV, L. 2013. Modeling of the Magnetic Properties of Nanomaterials with Different Crystalline Structure. *J. of Ph.: Conference Series*, 410, 012017

Introducing Gd^{III} Ions to Linear [Mn3] System: The Remained Ferromagnetic Coupling and Enhanced Magnetocaloric Effect

Jian (Huang)[1], Fang (Wang)[1], Chengan (Tao)[1], Xiaorong (Zou)[1], Hui (Zhu)[1], Jianfang (Wang)[1*]

[1]College of Science, National University of Defense Technology, Changsha 410073, P. R. China

*E Mail/ Contact Details (***huangjian_kd314@126.com, wangjianfang@nudt.edu.cn**)

Magnetocaloric effect (MCE) has attracted considerable interest due to the potential applications in the ultra-low temperature refrigeration. [1] As a new type of refrigerants, high-spin molecules are crucial for the cryogenic refrigerators, which are energy-efficient and environmentally friendly. [2] Taking advantages of large spin ground state, negligible magnetic anisotropy and weak exchange interaction that might result in large MCE, Gd^{III} ions were used to construct 3d-Gd^{III} and pure Gd^{III} complexes, in which a breakthrough was achieved by M. Evangelisti *et. al*. [3] However, such strategy of introducing Gd^{III} ions to the multinuclear complex system to enhance the $-\Delta S_m$ value is not always successful. Ferro- or antferro-magnetic exchange interactions among Gd^{III} and other ions usually lead to different ends.

Generally, it is helpful to improve the $-\Delta S_m$ value via possessing a larger spin ground state of a complex by employing Gd^{III} ions to a high-spin system. Herein, we obtained a chain complex $[Mn^{III}Gd^{III}_2(L)_2(Br)(OAc)_2(MeOH)_6]$ (L = deprotonated 2,2-diphenyl-1,3-propanediol), by introducing Gd^{III} ions and replacing Mn^{II} vertexes, weak ferromagnetic exchange interactions were remained and $-\Delta S_m$ value was increased to 27 J K^{-1} kg^{-1}, which is two times than that of pure Mn chains.

Keywords: High-spin complex, ferromagnetic coupling, enhanced MCE, linear [Mn3]

[1] SESSOLI, R. 2012. Chilling with Magnetic Molecules. *Angew. Chem., Int. Ed.,* 51, 43-45.

[2] ZHENG, Y. Z., EVANGELISTI, M., TUNA, F. & WINPENNY, R. E. P. 2012. Co-Ln Mixed-Metal Phosphonate Grids and Cages as Molecular Magnetic Refrigerants. *J. Am. Chem. Soc.,* 134, 1057-1065.

[3] LORUSSO, G., SHARPLES, J. W., PALACIOS, E., ROUBEAU, O., BRECHIN, E. K., SESSOLI, R., ROSSIN, A., TUNA, F., MCINNES, E. J. L., COLLISON, D. & EVANGELISTI, M. 2013. A Dense Metal-Organic Framework for Enhanced Magnetic Refrigeration. *Adv. Mater.,* 25, 4653-4656.

Investigation of perpendicular magnetic anisotropy at high annealing temperatures in CoFeSiB-Pd multilayers and co-deposited alloy film

Yong Jin Kim[1], Do Kyun Kim[1], Seung Hyun Kim[1], Ki Ha Kim[1], Jiung Cho[2], Young Keun Kim[1 *]

[1]Department of Materials Science and Engineering, Korea University, Seoul 02481 Korea

[2] Korea Basic Science Institute, Gangneung 25457 Korea

klloz@koera.ac.kr (Yong Jin Kim), ykim97@korea.ac.kr (Young Keun Kim)

Co- or Fe- based multilayers have attracted attentions for MRAM junctions with perpendicular magnetic anisotropy (PMA) because it is relatively easy to control the magnetic properties by changing ferromagnetic and nonmagnetic layer thicknesses and number of bilayers [1, 2]. But PMA of Co- or Fe based multilayer was degraded after high temperature annealing process due to intermixing at interface of multilayer. In our previous study, we reported the magnetic tunnel junctions (MTJs) using amorphous CoFeSiB film which have low saturation magnetization [3]. Here, we investigate the PMA in CoFeSiB-Pd multilayers (ML) and co-deposited alloy (CA) films which can be easily prepared by co-deposition of CoFeSiB and Pd targets by sputtering. All films were prepared by dc magnetron sputtering system under the base pressure below 5 x 10^{-9} Torr. The magnetic properties were measured by a vibrating sample magnetometer (VSM) at RT. The microstructure of films was characterized by X-ray diffraction (XRD) using Cu K_α radiation. The ML films show PMA at RT and all annealing temperatures whereas CA film does not. On the other hand, the CA films start to show PMA after 400^{o}C annealing and maintains it even after 500^{o}C annealing. After annealing, very high H_C and K_U were observed in both cases.

Keywords: CoFeSiB, Pd, multilayer, co-deposition, perpendicular magnetic anisotropy

[1] YAKUSHIJI K., SARUYA, T., KUBOTA, H., FUKUSHIMA, A., NAGAHAMA, T., YUASA, S. & ANDO, K. 2010. Ultrathin Co/Pt and Co/Pd Superlattice Films for MgO-Based Perpendicular Magnetic Tunnel Junctions. Applied Physics Letters, 87, 232508

[2] MIZUNUMA, K., YAMANOUCHI, M., IKEDA, S., SATA, H., YAMAMOTO, H., GAN, H. D., MIURA, K., HAYAKAWA, J., MATSUKURA, F. & OHNO, H. 2011. Pd Layer Thickness Dependence of Tunnel Magnetoresistance Properties in CoFeB/MgO-Based Magnetic Tunnel Junctions with Perpendicular Anisotropy CoFe/Pd Multilayers. Applied Physics Express, 4, 023002

[3] NOH, S. J., CHUN, B. S., KIM, Y. K. & WANG, T. 2011. Effect of Co Addition on Magneto-Transport Properties of Magnetic Tunnel Junction Consisting of CoFeB or CoFeSiB Free Layer. Journal of Applied Physics, 109, 07D346

Magnetic Solid Phase Extraction (MSPE) for Chromatographic Separation of Carbamates and Organophosphorus

Ramadan AA[1], Rakib MF[1], Abul Baker AA[1], Al-Saad KA[1]*

[1]Qatar University, Doha, Qatar, P.O. Box 2713

Presenting author: Ramadan AA, *E Mail:* ahmedissa@qu.edu.qa

***Corresponding author:** Al-Saad KA *E Mail:* kalsaad@qu.edu.qa

Pesticides such as organophosphorus and carbamates are heavily used worldwide in order to protect the crops and control disease-carrying insects, (WHO, 2008). Chromatographic methods are used for monitoring pesticides. The most difficulty faced in chromatography is the need of prior sample preparation, using liquid-liquid extraction (LLE), soxhlet, or solid phase extraction (SPE). The pre-column sample preparation can be necessary for several purposes such as elimination of the matrix effect, removing interferences, and pre-concentration of the analytes. LLE and soxhlet often require large volume of toxic organic solvents, and can be tedious and time consuming.

The objective of this work is to apply an environmentally friendly method, following previous works (Gdula et al., 2016, Zheng et al., 2014), in order to prepare a magnetic solid phase nanoparticles consisting of functionalized silicate groups. These prepared particles will be used for the extraction of organophosphorus and carbamates pesticides. The particles will then be separated from water using a neodymium magnet as shown in **Fig 1**. After that, the analyts that were adsorbed on the particles will be dissolved in a very small amount (1 mL) of organic solvent (n-hexane, acetone, or methylene chloride) before injection to GC/MS. In addition, in advanced stage of this work, the particles will be dried by nitrogen and directly and thermally desorbed in GC/MS.

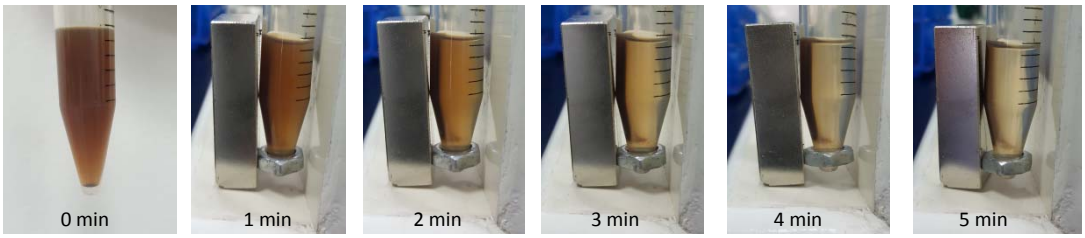

Fig 1. Magnetic nanoparticles moving to the neodymium magnet over time

The work can be summarized as i) preparation magnetic nanoparticles by using modified Massart method (Massart, 1981), ii) functionalize the magnetic Fe_3O_4 with octyl and cyno-propyl groups, by using Stober method (Stöber et al., 1968, Effati and Pourabbas, 2012) (iii) treatment of the contaminated samples with prepared particles, those particles are collected by neodymium magnet, extracted in n-hexane, and then the extracted analytes will be analyzed by using GC/MS(Liu et al., 2006). In step (ii), there are two approaches: In the first approach the magnetic core is covered by solid silicate layer then functionalized with target group. In the second approach, the magnetic core is covered by mesoporous layer from the target functional groups.

As preliminary experiment, several silicate functionalized nanoparticles were successfully prepared including cyano-propyl, and tri-methyl, using sol-gel methods. The SEM analysis of the two particles indicated the formation of relatively small (nano-size), which appeared to be uniformly and homogenously spherical (**Fig 2 a,b**). TEM micrograph of magnetic Fe_3O_4 in ethanol showed particles with less than 50 nm (**Fig 3**).

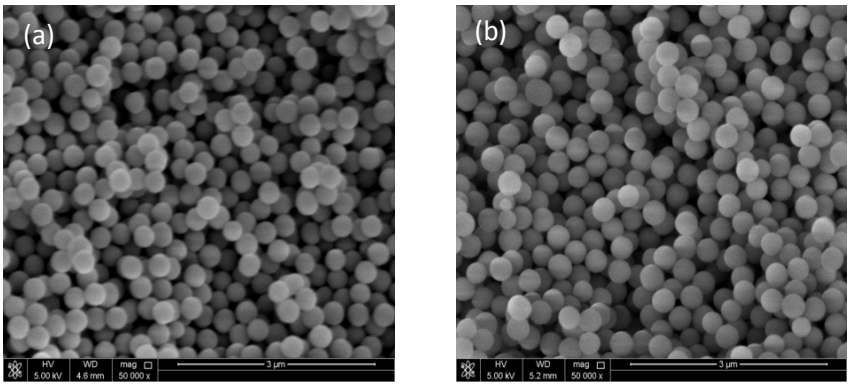

Fig 2. SEM images of silica particles functionalized with (**a**) CN-propyl (**b**) tri-methyl by using sol-gel methods

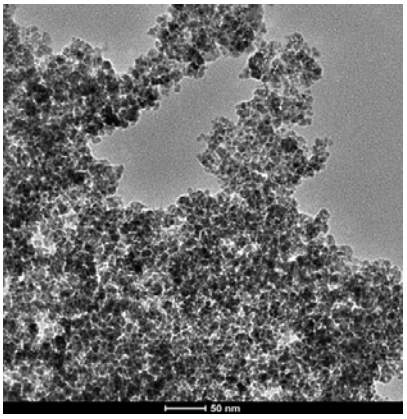

Fig 3. TEM micrograph of magnetic Fe_3O_4 nanoparticles in ethanol

Using the silicate functionalized particles for treating water artificially contaminated with nine types of carbamates indicated significant removal of these pesticides as indicated in **Table 1**, below:

Table 1. LC-MS/MS data for carbamate pesticides in water before treatment (control) and after treatment with the prepared particles.

RT	Pesticide name	Area of control	CN-propyl	Tri-methyl
4.25	aldicarb sulfoxide	2263486	1.49	1.70
5.438	aldicarb sulfone	12057785	0.76	0.26
6.146	methomyl	35514998	0.90	0.79
9.651	3-hydroxy carbofuran	9532232	0.44	0.00
13.566	aldicarb	16311302	0.82	0.88
16.975	propoxur	59736753	0.81	0.00
17.235	carbofuran	22457618	0.84	0.30
17.809	carbaryl	3865604	0.45	0.20
19.109	methiocarb	1909135	0.44	0.00

Keywords: *Functionalized silicate*, *Magnetic SPE*, *Magnetic iron (III) oxide*, *Octyl*, *Nanoparticles*, *Gas Chromatography*, *Pesticides*.

References

EFFATI, E. & POURABBAS, B. 2012. One-pot synthesis of sub-50 nm vinyl- and acrylate-modified silica nanoparticles. *Powder Technology,* 219**,** 276-283.

GDULA, K., DĄBROWSKI, A. & SKWAREK, E. 2016. Synthesis, surface characterization and electrokinetic properties of colloidal silica nanoparticles with magnetic core. *Adsorption***,** 1-8.

LIU, M., YUKI, H., SONG, Y. & LIN, J. 2006. Determination of Carbamate and Organophosphorus Pesticides in Fruits and Vegetables Using Liquid Chromatography-Mass Spectrometry with Dispersive Solid Phase Extraction. *Chinese Journal of Analytical Chemistry,* 34**,** 941-945.

MASSART, R. 1981. Preparation of aqueous magnetic liquids in alkaline and acidic media. *Magnetics, IEEE Transactions on,* 17**,** 1247-1248.

STÖBER, W., FINK, A. & BOHN, E. 1968. Controlled growth of monodisperse silica spheres in the micron size range. *Journal of Colloid and Interface Science,* 26**,** 62-69.

WHO, W. H. O.-. 2008. *Pesticides* [Online]. Available: http://www.who.int/ceh/capacity/Pesticides.pdf [Accessed 28-1-2016 2016].

ZHENG, X., HE, L., DUAN, Y., JIANG, X., XIANG, G., ZHAO, W. & ZHANG, S. 2014. Poly(ionic liquid) immobilized magnetic nanoparticles as new adsorbent for extraction and enrichment of organophosphorus pesticides from tea drinks. *Journal of Chromatography A,* 1358**,** 39-45.

The effects of magnetic field annealing on the magnetic properties of FeSiB amorphous powder cores

Zichao Li[1,2], Yaqiang Dong[1], Min Liu[1], Chuntao Chang[1], Fushan Li[2], Xin-Min Wang[1,3], Run-Wei Li[1]

[1]Zhejiang Province Key Laboratory of Magnetic Materials and Application Technology, Key Laboratory of Magnetic Materials and Devices, Ningbo Institute of Materials Technology & Engineering, Chinese Academy of Sciences. Ningbo, Zhejiang 315201

[2]School of Materials Science and Engineering, Zhengzhou University, Zhengzhou, Henan 450001

[3]Ningbo yunsheng co. ltd, Ningbo, Zhejiang 315201

Keywords:
magnetic field annealing; amorphous powder cores; permeability; core loss

Abstract:

$Fe_{78}Si_9B_{13}$ amorphous magnetic powders cores were produced from mixtures of the amorphous alloy powders and some insulating and bonding materials by mold compacting with a compact pressure of 1800 MPa. The dimension of the sample was 20.3 mm in outer diameter, 12.7 mm in inner diameter, and 6 mm in thickness (Φ 20.3 mm $\times\Phi$ 12.7 mm $\times$ t 6 mm). Then the effects of transverse magnetic field annealing on the soft magnetic properties of FeSiB amorphous powder cores were investigated. When the transverse magnetic field is 0.5 T and annealed at 673 K for 30 min, the soft magnetic properties of the amorphous powder core were improved. The permeability was improved from 75 to 79 and kept a constant value up to 2 MHz compared with zero field annealing, The core loss was decreased from 260 to 235 W/kg at B_m=0.1 T and f=100 kHz. Meanwhile, there is no distinguishable change on the DC bias property of the magnetic powder cores. The improvement of soft magnetic properties of the Fe-based amorphous powder cores is encouraging for future applications as functional materials.

Correlative imaging by NanoSIMS - TEM/X-EDS for nanometric investigation

Philippe Le Coustumer[1,2]*, Etienne Gontier[3], Florent Penen[1], Julien Malherbe[1], and Dirk Schaumlöffel[1]

1. Université de Pau et des Pays de l'Adour, CNRS, Institut des Sciences Analytiques et de Physico-Chimie pour l'Environnement et les Matériaux (IPREM), UMR 5254, 64000 Pau, France

2. Université de Bordeaux, UF STM, 33615 Pessac cedex, France

3. Université de Bordeaux, Bordeaux Imaging Center, 33076 Bordeaux

Recent developments in spectroscopic imaging techniques allow nanometric investigation of a wide range of materials such as biological ones up to nano engineered particles (NEPs). Our purpose is to present some relevant results using correlative imaging techniques. If Transmission Electron Microscopy (TEM) is a well-known technique, NanoSecondary Ion Mass Spectroscopy is more recent (1990s). Secondary ion mass spectrometry (SIMS) is an analytical technique which relies on the sputtering of ions from a solid surface by focused positive or negative primary ion beams and the subsequent analysis of the produced secondary ions by a mass spectrometer. Different combinations of primary ion sources (e.g. Ga^+, $B^{i+,}$ Cs^+, O^-, C_{60}^+) and mass spectrometers (quadrupole, time of flight, double sector) enables a wide range of applications for this technique. In the case of NanoSIMS (CAMECA), the primary ions beam (either Cs^+ and/or O^-) is scanned over the surface of the sample and the secondary ions are directed toward a double sector analyzer allowing elemental and isotopic images in 2D and 3D at nanometric scale (around 50 nm).

Correlative techniques can be traduced as dual spectral images issued from different sources. NanoSIMS combined with TEM/X-EDS has been used to explore biological samples exposed to trace metals at low concentration. The goal is to image the elemental and isotopic distribution at nanometric scale. Shared sample preparation for both techniques has been optimized in order:

- to respect and conserve the structure and texture of biological samples,
- to stabilize the samples before beeing analyzed by probes generating heat and contamination
- to maintain shape and chemical composition in an ultra-high vacuum environment

- to provide elemental and isotopic set of data
- to localize metallic trace elements
- to build a 2D and 3D elemental map at nanometric scale

Thus the sampling protocols used for correlative images request thin/thick slices of the biological material investigated (unicellular green algae *Chlamydomonas reinhardtii* as biological model exposed to cadmium). The ultrastructure of a *C. reinhardtii* cell was directly related to the spatial distribution of macro and trace elements present at basal levels in the cell. Trace metals have been localized in different cell organelles (contractile vacuoles, acidocalcisomes, and the chloroplast).

This example reveals that a complex bio-inorganic matrix can be explored at nanometric scale using correlative approaches based on spectral images. The potential of NanoSIMS-TEM/X-EDS for NEPs, bio-NEPS, NEPs into biological samples changes the sciences borders. Dual techniques are complementary and can be applied in medical, material sciences, environmental sciences, biology, geology and cosmology.

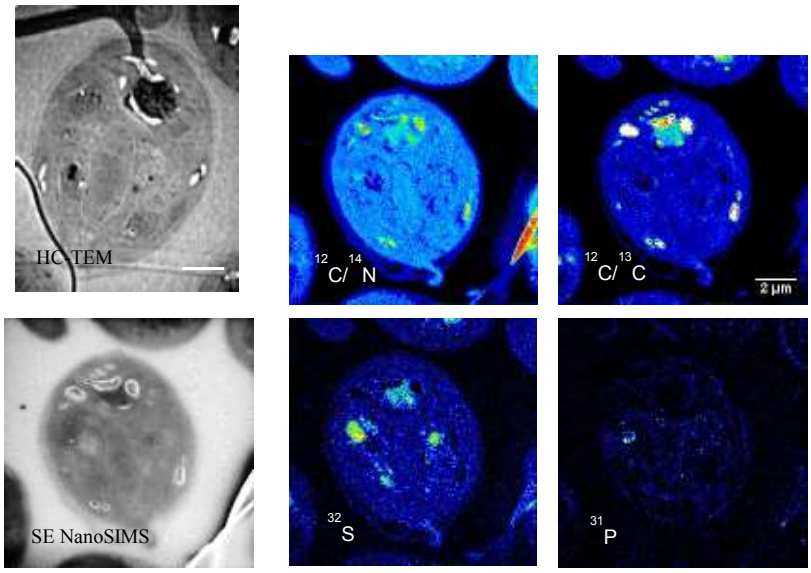

Fig.1: TEM and NanoSIMS correlative images of the ultra-structure and elemental/isotopic distribution

Covalent Immobilization of Trypsin onto Modified Magnetite Nanoparticles for Casein Digestion

Keziban Atacan[a*], Bekir Cakiroglu[a], Mahmut Ozacar[a,b]

[a]*Biomedical, Magnetic and Semiconductor Materials Research Center (BIMAS-RC), Sakarya University, Sakarya 54187, Turkey*

[b]*Department of Chemistry, Science & Arts Faculty, Sakarya University, Sakarya 54187, Turkey*

[*]corresponding author: keziiiban@gmail.com

Immobilization of enzymes on solid supports can enhance enzyme stability and proteolysis efficiency as well as it facilitates separation and recovery for reuse [1]. Magnetic iron oxide (Fe_3O_4) nanoparticles have been used in various fields owing to their unique properties including large specific surface area and simple separation with magnetic fields. The commonly used method for immobilization of enzymes on magnetic nanoparticles is covalent bonding. Covalent bonding is widely used for immobilization of enzymes on bare or modified magnetic nanoparticles, which can be achieved by creation of covalent bonds between the chemical groups on the particles and the chemical groups of enzymes [2].

The aim of this study was to immobilize the trypsin produced by bovine pancreas on Fe_3O_4 nanoparticles coated with tannic acid (TA) and digest casein from bovine milk protein. Firstly, the magnetic Fe_3O_4 nanoparticles were prepared according to solvothermal reaction [3,4]. Secondly, tannic acid was coated on magnetite nanoparticles and trypsin was immobilized on tannic acid modified Fe_3O_4 nanoparticles [5]. Finally, the enzymatic hydrolysis of casein by the immobilized and the free trypsin was investigated to determine whether more peptide fragments could be obtained by immobilized trypsin in terms of accurate protein identification. The improved stability of immobilized trypsin was demonstrated by SDS-PAGE and MS analysis of the peptides produced by the hydrolysis of casein carried out using similar amounts of native and immobilized trypsin.

Keywords: Fe_3O_4, trypsin immobilization, casein, digestion, SDS-PAGE.

References

[1] ANSARI, S.A., HUSAIN, Q. 2012. Potential Applications of Enzymes Immobilized on/in Nano Materials: A Review. Biotechnol. Adv., 30, 512–523.

[2] CAO, M., LI, Z., WANG, J., GE, W., YUE, T., LI, R., COLVIN, V.L., YU, W.W. 2012. Food Related Applications of Magnetic Iron Oxide Nanoparticles: Enzyme Immobilization, Protein Purification, and Food Analysis. Trends in Food Science & Technology, 27, 47−56.

[3] CHENG, G., WANG, Z.G., LIU, Y.L., ZHANG, J.L., SUN, D.H., and NI, J.Z. 2013. Magnetic Affinity Microspheres with Meso-/Macroporous Shells for Selective Enrichment and Fast Separation of Phosphorylated Biomolecules. Appl. Mater. Interfaces, 5, 3182−3190.

[4] CHENG, G., ZHOU, M.D., ZHENG, S.Y. 2014. Facile Synthesis of Magnetic Mesoporous Hollow Carbon Microspheres for Rapid Capture of Low-Concentration Peptides. Appl. Mater. Interfaces, 6, 12719−12728.

[5] ATACAN, K., OZACAR, M. 2015. Characterization and immobilization of trypsin on tannic acidmodified Fe_3O_4 nanoparticles. Colloids and Surfaces B: Biointerfaces, 128, 227–236.

Enhancement of self-renewal and differentiation capacities of stem cells using nanomaterials

Cho, Ssang-Goo
Department of Stem Cell and Regenerative Biology, Konkuk University, Seoul, Korea

Scientists have made amazing advances in regenerative medicine for treatment of many diseases and disorders. Laboratory and clinical research has shown that it is possible to use stem cells to restore lost, damaged or aging cells to effectively regenerate tissue and provide some patients with an alternative to surgery. Discovery of induced pluripotent stem cells (iPSCs) gave a new directional path to knock the disease world with new resource for cell transplantation and drug screening. Further progress and advances in iPSC generation technology kept adding feathers to the technology making it more feasible for clinical application. Previously, we generated iPSCs using DNA nanofection. Global gene-expression analysis revealed that these NiPSCs showed similar gene expression pattern with that of embryonic stem cells (ESCs). We also developed a simple RNA-based iPSC generation technique that utilizes a graphene oxide (GO)-polyethylenimine (PEI) complexes for efficient RNA delivery into the cells. The GO-PEI complex enriched in positively charges for effective loading of RNA and the GO-PEI-RNA complex showed strong protection from RNase attacks. The iPSC-generating GO-PEI-RNA complexes were prepared with RNAs from the reprogramming transcription factors and the GO-PEI complexes. We could successfully generate RNA-derived iPSCs which show all the hallmarks of pluripotent stem cells, including expression of pluripotency genes, epigenetic reprogramming, and differentiation into the three germ layers. Moreover, our laboratory could efficiently enhance the self-renewal or differentiation capacity of stem cells using nanomaterials or modulating the microenvironments (such as interaction with extracellular matrix), which will be ultimate use in stem cell therapies in regenerative medicine.

Key Words:
Regenerative medicine, Stem cells, induced pluripotent stem cells (iPSCs), Self-renewal and differentiation capacities, Microenvironments

Iron Based Oncotoxic Nanomaterials for in vivo Cancer Theranostics

Li-Xing Yang[1], Kuang-Jing Huang[1], Ya-Na Wu[2], Pei-Wen Wang[1], Dar-Bin Shieh[1,2, 3]

[1]Institute of Basic Medical Sciences, National Cheng Kung University College of Medicine, 1 University Rd., Tainan, Taiwan 70101.

[21]Institute of Oral Medicine and Department of Stomatology, National Cheng Kung University College of Medicine and Hospital, 1 University Rd., Tainan, Taiwan 70101.

darbinshieh@gmail.com/ National Cheng Kung University/ Taiwan

Nanoparticles have been developed to improve cancer therapeutics through effective passive targeting delivery by EPR or combination with active targeting though cancer specific surface molecule recognition. However, nanoparticles in these therapeutic designs mostly serve as naive carrier or external energy converter in hyperthermia therapy. We discovered previously that iron core gold shell nanoparticles (Fe@Au) effectively inhibit proliferation of cancer cell in vitro and dose dependently reduce tumor growth in vivo while spare the normal non-transformed cells. We further found that Fe@Au caused irreversible mitochondria membrane potential loss in cancer cells, but not in healthy control cells. Significant ROS production was observed in Fe@Au treated cancer cells while common ROS scavengers were unable to protect Fe@Au derived cancer cell death. Various other types of zero-valent iron-containing nanoparticles also demonstrated cancer-specific inhibition through similar mitochondria mediated pathway. And such cancer selectivity was found to be effective in both carcinoma and sarcoma types of malignancies. Further, we found that iron elements, before oxidation, triggered mitochondria-mediated autophagy was the key factor responsible for the selective growth inhibition observed between cancerous and healthy cells. These results suggest an universal cancer-mitochondria targeting based oncotoxic therapeutics that various zero-valent iron based nanoparticles may harbor. The endogenous magnetic property of such nanoparticles also enabled in vivo tracking by MRI imaging and holds great potential to become a new anti-cancer theranostic platform.

Keywords: Zero valent iron, nanoparticle, cancer, mitochondria, cytotoxicity

[1] WU YN, YANG LX, SHI XY, LI IC, BIAZIK JM, RATINAC KR, CHEN DH, THORDARSON P, SHIEH DB, BRAET F. 2011. The Selective Growth Inhibition of Cancer by Iron Core-gold Shell Nanoparticles through Mitochondria-Mediated Autophagy. *Biomaterials*, 32(20), 4565-4573.

[2] WU YN, WU PC, YANG LX, RATINAC KR, THORDARSON P, JAHN KA, CHEN DH, SHIEH DB, BRAET F. 2013. The Ant-cancer Properties of Iron Core-gold Shell Nanoparticles in Colorectal cancer Cells. *Int J Nanomedicine*, 8, 3321-3331.

Usage of the magnetic nanoparticles coated with tantalum oxide in radiotherapy

Apanasevich Vladimir[1], Lukyanenko Kseniya[2], Afremov Leonid[2]

[1] Pacific State Medical University, 2 Ostryakova Avenue, Vladivostok 690002, Russia.

[2] Far Eastern Federal University, 8 Sukhanova St., Vladivostok 690950, Russia.

ks.lukyanenko@gmail.com

Non-invasive imaging techniques including computed tomography are now essential tools for the detection of malignant tumors. Application of nanoparticles may increase sensitivity of the modern methods of tumor imaging in vivo based on contrasts with the selective localization in tumor tissues including through external magnetic. The effectiveness of radiotherapy is limited on the one hand radiosensitive tissues surrounding the tumor, on the other hand – radioresistance of the malignancy. Introduction of radiosensitizers into a tumor with subsequent irradiation results in secondary radiation inside the tumor, thus increasing the effect of radiotherapy [1]. Currently iodine-containing X-ray contrast agents and platinum based drugs are widely used for the contrasting of organs and for the treatment of malignant tumors but they have a number of disadvantages associated with their high toxicity.

The aim of this work is to investigate the possibility of the use of core-shell nanoparticles as radiopaque agents and radiomodifier in radiotherapy.

Core-shell nanoparticles were obtained in sole-gel process to increase the contrast and intensity of the radio and to increase the radiosensitivity of tumor cells; the core of the nanoparticles is magnetic material coated with tantalum oxide. The shell of the tantalum oxide is:

1) to visualize the core-shell nanoparticles;
2) to increase energy absorption effect during exposing with high-energy gamma rays;
3) not have any toxic effects.

Numerous studies show that the most frequently used iron and iron oxide nanoparticles are toxic towards the biological tissue. Therefore, the most probable carrier material of the magnetic properties can be two-phase (core-shell) particles, nanoparticles

with a magnetic core covered with a protective shell.

We have studied in vivo contrast properties of the synthesized substance namely tantalum oxide and bismuth as compared to saline. Bismuth was excluded from the experiment because its toxicity. Suspensions were prepared with concentration 2,5%. Compared X-ray contrast agents were injected intramuscularly into mice hind paw of 0,2ml. X-rays were performed on digital mammography “Senographe 200” (General Electric).

We studied the contrast (X-ray density) dependence on the time of the clearance for nanoparticles with different sizes. It is found that the tantalum oxide nanoparticles are X-ray contrast and completely remove from the body the next day after administration. This work was showed that the growth of the nanoparticles’ size increases the contrast for the suspension.

Keywords: core-shell nanoparticles, magnetic field, radiosensitivity

[1] RAHMAN, W. N., BISHARA, N. B., ACKERLY, T., He, C. F., JACKSON, P., WONG, C., DAVIDSON, R., GESO, M. 2009. Enhancement of Radiation Effects by Gold Nanoparticles for Superficial Radiation Therapy. Nanomedicine: Nanotechnology, Biology, and Medicine, 5, 136-142.

[2] CHERNICHENKO, A., FILIMONOV, A. 2008. Chemoradiotherapy Non-Small Cell Lung Cancer. Practical Oncology, 9 (1).

Antimicrobial and antioxidant activity of multifunctional ZnO@CA nanoparticles

Kyong-Hoon Choi[1], Jung Hyun Kim[2], Ho-Joong Kim[3,]*, Bong Joo Park[1,2]*

[1]Plasma Bioscience Research Center and [2]Department of Electrical & Biological Physics, Kwangwoon University, 20 Kwangwoongil, Nowon-gu, Seoul, 139-701, Republic of Korea

[3]Department of Chemistry, Chosun University, Gwangju 501-759, Korea

The synthesis of metal oxide nanoparticles attracts an increasing interest due to their new and different characteristics as compared with those of macroscopic phase, that allow attractive applications in various fields such as antimicrobials, medicine, biotechnology, optics, microelectronics, catalysis and energy conversion. ZnO nanoparticles have the properties of high surface area, very small size and high dispersion. ZnO is a safe and effective bactericidal metal because it is non-toxic to animal cells and highly toxic to bacteria. In the present study, we have synthesized a novel antioxidant ZnO nanoparticle that is newly designed and prepared by simple surface modification process. Antioxidative functionality is provided by the immobilization of antioxidant 3-(3,4-dihydroxyphenyl)-2-propenoic acid (caffeic acid, CA) onto the surface of ZnO nanoparticles. Microstructure and physical properties of the ZnO@CA nanoparticles were investigated by field emission scanning electron microscopy (FE-SEM), transmission electron microscopy (TEM), infrared spectroscopy (IR) and steady state spectroscopic methods. Antimicrobial Activities of ZnO@CA nanoparticles were measured against various bacterial strains using antibacterial testing methods.

Biomediated synthesis of silver nanoparticles using cell extracts of *Catharanthus roseus* and its antibacterial property

Dandy Osibe[1,2], Nneka Chiejina[2], Kazuyoshi Ogawa[1], Hideki Aoyagi[1*]

[1]Faculty of Life and Environmental Sciences, University of Tsukuba, 1-1-1, Tennodai, Tsukuba, Ibaraki 305-8572, Japan.

[2]Department of Plant Science and Biotechnology, University of Nigeria, Nsukka 410001, Nigeria.

*Corresponding author

E-mail address: dandy.osibe@unn.edu.ng (D. Osibe), aoyagi.hideki.ge@u.tsukuba.ac.jp (H. Aoyagi)

Abstract

Biogenic reduction of metal precursors to corresponding nanoparticles (NPs) has attracted much interest as it affords eco-friendly, sustainable, non-toxic, and cost-effective route. Here, we describe an unexplored green route using extracts of seed-derived callus of *Catharanthus roseus*, which offers well-dispersed, spherical silver nanoparticles (Ag-NPs) with consistent morphology as revealed by Transmission electron microscopy. That the formation of Ag-NPs indeed occurred was evident from UV-vis spectroscopic analysis, wherein the absorption maxima of the surface plasmon resonance featured at 425 nm, indicative of elemental silver. The stability against rapid aggregation of the Ag-NPs prepared by this method was confirmed over a period of 3 months. Fourier transform infrared spectroscopy elucidated the functional moieties associated with its surface stabilization. Significantly, we demonstrated a dose-dependent antibacterial property of the as-synthesised Ag-NPs using agar well diffusion and liquid-to-plate assays. The unique prospect of utilizing cultured plant callus derived extracts for the synthesis of functional NPs is highlighted.

Keywords: *Catharanthus roseus*, seed-derived callus, silver nanoparticles, green synthesis

High Performance Solar Thermal Effect by Spherical Shell-type Metallic Nanocomposites

Takuya Iida[1], Shiho Tokonami[2], Yojiro Yamamoto[3], Atsuko Kosuga[4]

[1]Department of Physical Science, Osaka Prefecture University.

[2] Department of Applied Chemistry, Osaka Prefecture University.

[3]GreenChem Inc.

[4]Nanoscience and Nanotechnology Research Center, Osaka Prefecture University.

E Mail/ Contact Détails: t-iida@p.s.osakafu-u.ac.jp

Strong and unique optical response of localized surface plasmon in metallic nanoparticles (NPs) is widely studied in the field of nanophotonics, bio-analytical chemistry, and environmental applications. Previously, it has been clarified a giant spectral broadening of the optical response of metallic NPs assembled on a plastic bead, i.e., metallic nanoparticle fixed bead (MNFB) [1]. Paying attention to such a anomalous optical property of MNFB, a photothermal film (PTF) with densely assembled gold nanoparticle-fixed beads on a polymer substrate was fabricated [2]. It has been clarified that PTF can exhibit a temperature rise higher than 40 °C with only 100 seconds of solar irradiation. Moreover, PTF enhanced the output power of the thermoelectric device to be one order higher, which will provide a guiding principle of a rapid solar thermoelectric device.

Acknowledgement: Authors would thank Mr. Y. Yamamoto, Ms. M. Miyai, Ms. M. Matsuzawa, Mr. Y. Nishimura, Mr. S. Hidaka, Mr. K. Yamamoto, Mr. S. Tanaka for their cooperation in this research.

Keywords: Metallic nanoparticle, nanophotonics, solar energy, thermoelectric effect

[1] Tokonami, S., Hidaka, S., Nishida, K., Yamamoto, Y., Nakao, H., Iida, T., 2013. Multipole Superradiance from Densely Assembled Metallic Nanoparticles", *The Journal of Physical Chemistry C*; 117, 15247-15252.

[2] Kosuga, A., Yamamoto, Y., Miyai, M., Matsuzawa, M., Nishimura, Y., Hidaka, S., Yamamoto, K., Tanaka, S., Yamamoto, Y. Tokonami, S. & Iida, T 2015. A high performance photothermal film with spherical shell-type metallic nanocomposites for solar thermoelectric conversion", *Nanoscale*; 7, 7580-7584.

A vanadium dioxide-based terahertz nano antennas for phase transition engineering

Young-Gyun Jeong[1], Sanghoon Han[2], Jiyeah Rhie[1], Ji-Soo Kyoung[1], Jae-Wook Choi[1], Namkyoo Park[2], Seunghun Hong[3], Bong-Jun Kim[4], Hyun-Tak Kim[4,5], and Dai-Sik Kim[1]

[1]Department of Physics and Astronomy and Center for Atom Scale Electromagnetism, Seoul National University, Seoul 08826, Republic of Korea.

[2]Photonic Systems Laboratory, School of EECS, Seoul National University, Seoul 08826, Republic of Korea.

[3]Department of Physics and Astronomy, Department of Biophysics and Chemical Biology, and Institute of Applied Physics, Seoul National University, Seoul 08826, Republic of Korea.

[4]Creative Research Center of Metal−Insulator Transition, Electronics and Telecommunications Research Institute, Daejeon 34129, Republic of Korea

[5]School of Advanced Device Technology, University of Science and Technology, Daejeon 34113, Republic of Korea

E Mail/ Contact Details **(dsk@phya.snu.ac.kr)**

We found a new approach towards engineering the apparent transition behavior in VO_2 without changing the material parameters themselves, simply by extreme nano-patterning tailored for millimeter wave applications. Having a semiconducting bandgap, even below the insulator-to-metal transition (IMT) temperature the number of electrons and holes keep increasing with temperature, with an $\exp(-\frac{E_g}{2k_BT})$ (E_g: bandgap energy, k_B: Boltzmann constant, T: Kelvin) dependence, although its influence to optical response is minimal. Armed with only conventional photolithography and atomic layer deposition methods, we fabricated negative square ring array structures of hybrid nanogap-strongly correlated systems entirely based upon this small change in dielectric constant. The effective transition temperature is lowered by 20 degrees and the switching action starts more than 40 degrees earlier than in a bare film. In a 5 nm gap-VO_2 hybrid film structure, we demonstrated a transition temperature engineering by utilizing the Boltzmann tail of semiconducting VO_2 at an extreme subwavelength regime. Strikingly, the IMT part is not

even needed for most of the device performance and the transmitting THz wave can be significantly controlled before the IMT. The overall thermal transition behavior of our hybrid film device is determined by the width of the nanogap with high modulation range enhanced by at least one order of magnitude than the bare film. We can engineer the onset of the *apparent* transition temperature by simply controlling the width of the nanogap. When we consider the generality of this phenomenon in VO_2 films, the transition temperature is expected to be further lowered in combination with other techniques such as doping, external strain, and substrate matching. These results will provide a wide potential in developing near room temperature phase transition devices combined with plasmonic nano structures.

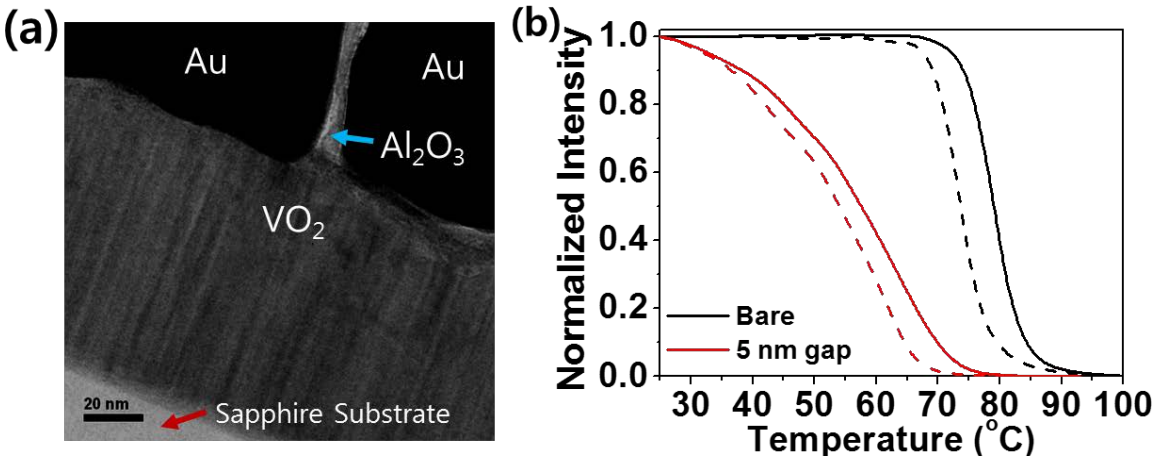

Figure 1 (a) Cross-section TEM image of a 5 nm gap fabricated on a 100 nm thick VO_2 film. (b) Thermal hysteresis curves of normalized THz transmission intensities for bare and 5 nm gap patterned VO_2 samples while being heated (solid line) and being cooled (dashed line).

Keywords: Vanadium dioxide, insulator to metal transition, Boltzmann tail, nanogap, terahertz

[1] JEONG, Y.-G., HAN, S., RHIE, J., KYOUNG, J.-S., CHOI, J.-W., PARK, N., HONG, S., KIM, B.-J., KIM, H.-T. & KIM, D.-S. 2015. A Vanadium Dioxide Metamaterial Disengaged from Insulator-to-Metal Transition. Nano Letters, 15, 6318-6323.

Synthesis and Characterization of Ag-TiO_2 Nanotubes as Photocatalyst using Hydrothermal Method

L. T. N.Tu[1,4], P. T. Thi[1], P. V. Hien[2], N. D. Nam[3], V. T. H. Thu[1]

[1]Faculty of Physics and Engineering Physics, University of Science, 227 Nguyen Van Cu Street, District 5, Ho Chi Minh City, Vietnam

[2]Department of Chemical Engineering, Ho Chi Minh City University of Technology, 268Ly Thuong Kiet Street, District 10, Ho Chi Minh City, Vietnam

[3]Petroleum Department, PetroVietnam University, 762 Cach Mang Thang Tam Street, LongToan Ward, Ba Ria City, Ba Ria - Vung Tau Province, Vietnam

[4]Dong Thap University, 783 Pham Huu Lau, Ward 6, Cao Lanh City, Dong Thap Province, Vietnam

*Email/Contact Details (*ltntu@dthu.edu.vn, phamvanhien240991@gmail.com, namnd@pvu.edu.vn and vththu@hcmus.edu.vn)

An improvement of the photocatalytic activity as semiconductor materials via using incorporation of the noble metals such as Ag, Au, and Pt is a promising technology. In this study, Ag nanoparticle -TiO_2 nanotube structures (Ag-TNTs) have been investigated as photocatalyst in different irradiation conditions. TiO_2 nanotubes were synthesized at 130°C during 22h by hydrothermal method. Ag-TNTs structures (2.5, 5.0, and 10.0 wt.%) were fabricated by a mix of an aqueous $AgNO_3$ solution and TNTs combined with UV irradiation and magnetic stirring. The morphology, chemical components, crystallinity and potential photocatalyst have been analyzed using transmission electron microscopy/energy dispersive X-ray spectroscopy, X-ray diffraction, and decoloration reaction of methylene blue in aqueous solution. The results indicated that Ag-nanoparticles dispersed uniformly on the TNTs' surface without any change in TNTs' morphology. In addition, Ag-TNTs exhibited lower photoactivity than that of based TiO_2 and TNTs under UV irradiation. In contrast, Ag-TNTs increased the photoactivity in comparison with based TiO_2, TNTs and the photocatalytic performance under dark and sunlight irradiation.

Keywords: TiO_2 nanotubes, Ag nanoparticles , hydrothermal, photocatalytic degradation.

Nanoporous gold film based evanescent wave sensor for detection of small molecules

Chen Chen, Li Wang, Dan-feng Lu, Zhi-mei Qi*
State Key Laboratory of Transducer Technology, Institute of Electronics, Chinese Academy of Sciences, No. 19 Beisihuan West Road, Beijing 100190, China
*e-mail: zhimei-qi@mail.ie.ac.cn

Nanoporous gold (NPG) is an advanced functional material with both propagating and localized surface plasmon resonance (PSPR and LSPR) characteristics. NPG films are usually prepared using commercial AuAg alloy foils with given thicknesses, and they have been widely studied for application as surface enhanced Raman scattering (SERS) substrates based on their LSPR property. In contrast, application of NPG films as PSPR-based bio-/chemical sensors has not yet attracted considerable attention. Since the evanescent field inside the NPG film enables to interact with analyte molecules adsorbed in its internal surface, it is anticipated that the NPG film can offer the PSPR-based sensors a high sensitivity.

In this work, NPG films with a desirable thickness being below 100 nm were prepared by slow dealloying of the sputtered AuAg alloy layers in nitric acid at low temperature. This sputtering-dealloying method allows us to easily control the film thickness and its pore size for optimizing the PSPR performance of NPG film. The as-prepared NPG films show the salient PSPR effect in the visible and near infrared wavelength range, and they were used as wavelength-interrogated PSPR sensor and PSPR-excited surface Raman spectroscopy based on Kretschmann configuration. The following experimental results were obtained: (1) with the NPG film the PSPR sensitivity to small molecule analyte is much higher than that with dense gold layer; (2) with the PSPR excitation the Raman signal emitted from NB molecules adsorbed in the NPG film is much stronger than that with the LSPR excitation; (3) with the NPG film the PSPR-excited Raman signal of NB is also much stronger than that with the dense gold layer; (4) the surface plasmon coupled directional emission of Raman signal was detected with the NPG film. The findings demonstrated that the NPG films with a desirable thickness can be used for sensitive, label-free and real-time detection of small molecules based on the PSPR-excited Raman spectroscopy and PSPR sensing technique.

Acknowledgments

This work was supported by the National Key Basic Research Program of China (No. 2015CB352100), the National Natural Science Foundation of China (No. 61377064), and the Research Equipment Development Project of Chinese Academy of Sciences (No. 2060303).

Optoelectronic devices based on two-dimensional metal chalcogenides and their p-n junctions

Zhenxing Wang, Kai Xu, Feng Wang, Xueying Zhan, Jun He

National Center for Nanoscience and Technology, Beijing, 100190, China
E-Mail address (corresponding author): wangzx@nanoctr.cn

Inspired by the success of graphene and especially its intrinsic shortcoming of zero band gap, research on two dimensional (2D) semiconductors has triggered tremendous worldwide interests over the past few years. 2D semiconductors have showed unique physical and chemical properties due to their ultrathin thickness, smooth surface, high flexibility and high compatibility with traditional micro-fabrication techniques as well. They may lead the next generation of electronics and optoelectronics. However, in order to realize the practical applications, we have to face the challenges from structure design, controllable growth, property modulation, and device optimization. In the past few years, we investigated a series of 2D metal chalcogenides, including GaTe, $MoTe_2$, HfS_2 and their p-n junctions. For instances, GaTe based phototransistor, short channel effects on GaTe, GaTe/MoS_2 p-n junctions and controllable growth of GaTe have been systematically studied. In addition, for optimizing the device, we investigated the metal contact effects on $MoTe_2$ and HfS_2 devices. Recently, we constructed an electrostatically tunable lateral p-n junction based on bipolar $MoTe_2$ and studied its photovoltaic performance. In this talk, I will present these recent works on controllable growth, property modulation and electronic applications based on 2D metal chalcogenides.

References

1. Z. X. Wang, F. Wang, L. Yin, Y. Huang, K. Xu, F. M. Wang, X. Y. Zhan and J. He*, Electrostatically tunable lateral $MoTe_2$ p-n junction for use in high-performance optoelectroncis, 2016, submitted.
2. L. Yin, X. Y. Zhan, K. Xu, F. Wang, Z. X. Wang*, Y. Huang, Q. S. Wang, C. Jiang and J. He*, Ultrahigh sensitive $MoTe_2$ phototransistors driven by carrier tunneling, *Appl. Phys. Lett.* 2016, 108, 043503.
3. Z. X. Wang, M. Safdar, M. Mirza, K. Xu, Q. Wang, Y. Huang, F. Wang, X. Zhan and J. He*, High-performance flexible photodetectors based on GaTe nanosheets, *Nanoscale* 2015, ***7***, 7252.
4. Z. X. Wang, K. Xu, Y. C. Li, X. Y. Zhan, M. Safdar, Q. S. Wang, F. M. Wang, J. He*, Role of Ga vacancy on a multilayer GaTe phototransisotor, *ACS Nano* 2014, **8**, 4859.
5. K. Xu, Z. X. Wang, F. Wang, Y. Huang, F. M. Wang, L. Yin, C. Jiang and J. He*, Ultrasensitive phototransistors based on few-layered HfS_2, *Adv. Mater.* 2015, **27**, 7881.
6. F. Wang, Z. X. Wang, K. Xu, F. M. Wang, Q. S. Wang, Y. Huang, L. Yin and J. He*, Tunable GaTe-MoS_2 van der Waals p-n junctions with novel optoelectronic performance, *Nano Lett.* 2015, **15**, 7558.
7. Z. Wang, M. Safdar, C. Jiang and J. He*, High-performance UV-visable-NIR broad spectral photodetectors based on one-dimensional In_2Te_3 nanostructres, *Nano Lett.* 2012, ***12***, 4715-4721.
8. J. Wang,[+] Z. Wang,[+] Q. Li, L. Gan, X. Xu, L. Li and X. Guo*, Revealing Interface-Assisted Charge Transfer Mechanisms Using Silicon Nanowires as Local Probes, *Angew. Chem. Int. Ed.* 2013, ***52***, 3369-3373. (+ equal contribution).

Optoelectronic properties analysis of ZnO p-n nanohomojunction by hydrothermal method

Chen-Yu Tsai[1,2],Yen-Ti Tseng[1,2], Ming-Yen Lu[1,2]

[1]Graduate Institute of Opto-Mechatronics, National Chung Cheng University, Chia-Yi 62102, Taiwan

[2]Advanced Institute of Manufacturing with High-Tech Innovations, National Chung Cheng University, Chia-Yi 62102, Taiwan

E Mail/ Contact Détails : andys87689@gmail.com and mylu@ccu.edu.tw

Abstract

In this work, we used hydrothermal method to grow well-aligned p-n ZnO nanorod (NR) arrays. Sb was used as dopants for p-ZnO NR arrays growth, X-ray photoelectron spectroscopy was used to analyze the atomic percentages and the chemical state of the Sb dopant in p-type ZnO NR arrays. Both of photoluminance (PL) and electrical measurements confirmed the p-type characteristics of Sb-doped ZnO NR arrays, the p-type characteristics of Sb-doped ZnO NR arrays were attributed to the formation of the acceptor-like (Sb_{Zn}-$2V_{Zn}$) complex defects. Moreover, the sequential growth of n-ZnO and p-ZnO were implemented to form the p-n ZnO nanojunction arrays. The photovoltaic properties using p-n ZnO nanojunction devices were investigated under 365 nm UV light with different incident power. The promising application of self-driven UV photodetectors were also investigated. The low-temperature growth of p-n ZnO nanojunctions provides facile strategy to fabricate the junctioned nanostructures for energy-harvesting optoelectronic applications.

Keywords: *ZnO, Hydrothermal method ,p-n junction , self-driven photodetectors*

PHOTONICS OF NOVEL ZINC(II) AND BORON(III) DIPYRROMETHENE COMPLEXES

A.A. Prokopenko[1], Iu.V. Aksenova[1], D.E. Bashkirtsev[1], R. T. Kuznetsova[1], M.B.Berezin[2]

[1]Tomsk State University, 634050, Lenin av.36, Tomsk, Russia

[2]Institute of solution chemistry of RAS, 153045, Akademicheskaya St., 1, Ivanovo, Russia

alexpr898@gmail.com

The photonics of the new organic luminophores – coordination compounds Zn(II) and B(III) (BODIPY) with dipyrromethenes are the one of the most actual nowadays. It is caused by the possibility of using these compounds as markers and fluorescence probes, optical sensors on oxygen and temperature, OLED-s, solar probes, laser media. Investigation into the photonics of these compounds is of great importance for effective uses in different optical devices.

Table. Spectral-luminescent and lasing properties of dipyrromethene complexes

Compound in ethanol solutions	λ_{abs}^{max}, nm, (ε, M^{-1}, cm^{-1})	λ_{fl}^{max}, nm (λ_{ex}, nm)	γ_{fl} (λ_{ex}, nm)	λ_{php}^{max}, nm* (*77K)
$(CH_3)_4$-BODIPY	504 (84000)	514 (440)	0.8 (440)	Lasing: λ_{las}=537 nm (λex=355 nm) Eff.=20%
$Zn[(CH_3)_4dpm]_2$	485 (146200)	491 (460)	0.008 (460)	740+820 (460)
$Br_2(CH_3)_4$BODIPY	526 (31370)	545 (470)	0.4 (485)	795 (485)
$Zn[Br_2(CH_3)_4dpm]_2$	504 (45750)	521 (465)	0.005 (465)	745 (475)
$Br_2(CH_3)_2(C_5H_{11})_2$ BODIPY	537 (49230)	551 (475)	0.5 (475)	802 (475)
$Zn[Br_2(CH_3)_2(C_5H_{11})_2dpm]_2$	510 (33300)	520 (475)	0.065 (475)	744 (475)

The aim of this work was to investigate the spectral-luminescent, lasing properties and stability in protic media properties of coordination compounds of Zn(II) with dipyrromethenes on the excitation parameters in comparison with the dipyrromethene BF_2 complexes with a similar ligand structure.

The analysis of the results shows that the spectral and luminescent parameters of BF_2 and Zn dipyrromethene complexes are determined by the structure of the ligand. As known, boron dipyrromethene (BODIPY) dyes are well-known for their intense fluorescence and have wide applications as unique active media with long time operation for liquid and solid state tunable lasers. We have studied a similar complex with high efficiency: $(CH_3)_4$-BODIPY (table). Introduction of heavy atoms into the dipyrromethene core enhances intersystem crossing, which leads to a long-lived emission. For such complexes we obtained characteristics of the spectra of long-lived emission of frozen ethanol solutions. The matching of the phosphorescence excitation spectra with absorption spectra of halogen-substituted complexes confirm that the phosphorescence belongs to the corresponding complexes.

Stability of fluorophores in acidic media is closely linked with the possibility of practical application. The complexes stabilities in the ground and excited states are estimated by spectrophotometric titration of ethanol solutions of compounds using water–ethanol solutions of hydrochloric acid. The results obtained in this work can be used as the basis for the design of optical devices.

Keywords: dipyrromethenes, BODIPY, protic media, complex stability

The effects of doping concentration to the photovoltaic property of CdS-Cu_2S core-shell nanodevices

Yen-Min Ruan[1,2], Meng-Hsiang Hong[1,2], Wen-Wei Wu[3], Ping-Hung Yeh[4], Ming-Yen Lu[1,2]

[1]Graduate Institute of Opto-Mechatronics, National Chung Cheng University, Chia-Yi 62102, Taiwan.

[2] Advanced Institute of Manufacturing with High-tech Innovations, National Chung Cheng University, Chia-Yi 62102, Taiwan

[3]Department Of Materials Science And Engineering, National Chiao Tung University

[4]Department of Physics, Tamkang University

E Mail : c7551140@hotmail.com.tw (presenting author)

mylu@ccu.edu (corresponding author)

Gallium (Ga) -doped cadmium sulfide (CdS) nanowires (NWs) were successfully grown by chemical vapor deposition (CVD) method. We could not only improve the conductivity of the CdS NWs, but also modulate the electrical properties of CdS NWs by different doping amounts. X-ray photoelectron spectroscopy (XPS) analysis and photoluminescence (PL) analysis verified that Ga has been incorporated into CdS NWs with the atomic percentages of 1.59%, 2.45%, and 3.59 %, when 0.1 g, 0.2 g, and 0.3 g Ga were used as the doping source, respectively. We further investigated the carrier transport properties of the Ga-doped CdS NWs, the results showed that the conductivities of NWs increased with the Ga doping source and the mobilities of CdS nanodevice with different Ga doping levels were significantly distinctive. Furthermore we fabricated the CdS/Cu_2S core-shell n-p hetrostructure using e-beam lithography and cation exchange technique and the photovoltaic properties of different Ga-doped CdS/Cu_2S core-shell n-p heterostructures were discussed.

Keywords: cadmium sulfide, cation exchange, p-n junction, solar cell.

Infrared and Terahertz Transmission properties of super-thin periodic multi-walled carbon nanotubes gratings

Yue Wang[1], Xin Liu[1], Liying Zhang[1]

[1]Key Laboratory of Engineering Dielectrics and Its Application of Ministry of Education, Harbin University of Science and Technology, Harbin, 150080, China

E Mail : wangyue@hrbust.edu.cn

The discovery of enhanced transmission of the visible light through sub-wavelength metal holes arrays on a metal thin film sparked extensive interest in surface plasmon polaritons (SPPs) related phenomena among the science community[1,2]. Many experimental and theoretical studies have been developed to find numerous applications in fields such as near field microscopy[3] and photolithography[4]. This unusual enhancement transmission through all kinds of arrays of sub-wavelength apertures has been also widely investigated in the range of terahertz band[5-7].

In this article, we report the extraordinary transmission of infrared and THz wave through super-thin multi-walled carbon nanotube films with the periodic gratings of patterns. The super-thin MWCNT films were prepared by being drawn out from vertical aligned carbon nanotubes fabricated through low pressure chemical vapor deposition (LPCVD) on Si wafer (Fig.1). We demonstrate that the THz transmission not only dependents on the orientation of the gratings, but also the direction of THz polarization.

We focus on the maxima in the transmittance spectra, which derive from a resonant interaction between SPPs and the incident THz wave in the interface of MWCNT films/Si. The measured peaks appear at 0.30 THz, corresponding to the SPPs [m, n] = [0, $\pm$1] mode of the sample A (3μm) and B (5μm) (Fig.2), respectively. The weak resonance peak near 0.49 THz corresponds to the SPPs [m, n] =[$\pm$1, $\pm$1] mode of the sample A and B, respectively.

Transmittance measurement of the CNTs films were carried out by a Varian Cary 5000 (UV-vis-NIR) spectrophotometer for wavelengths of 800-2500 nm (375-120 THz) at intervals of 1 nm. As we expect that the CNTs films exhibit polarization dependence of infrared signals because of their anisotropic property. Figure 3 shows the transmittance spectra as a function of infrared frequency of MWCNTs films. The experimental results demonstrate that the transmission intensity decreases with the

increasing of the infrared frequency when the MWCNTs alignment axis is a perpendicular direction. However, the transmission keeps no change in the parallel direction. It can be seen that the transmission increases sharply in the near of 1100 nm (272 THz) which is the Si band gap. The transmission properties of CNTs in the infrared band need further study in the future.

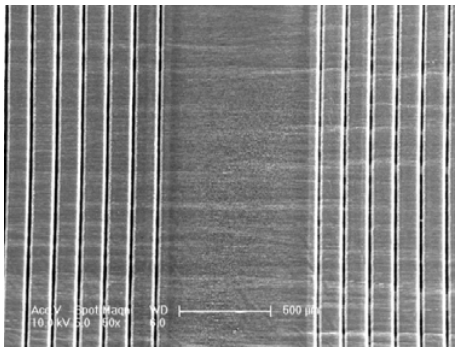

Fig.1 SEM image of MWCNTs film with period of 200μm.

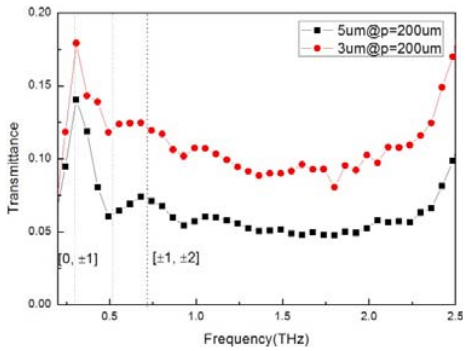

Fig.2 Transmittance of sample A and B.

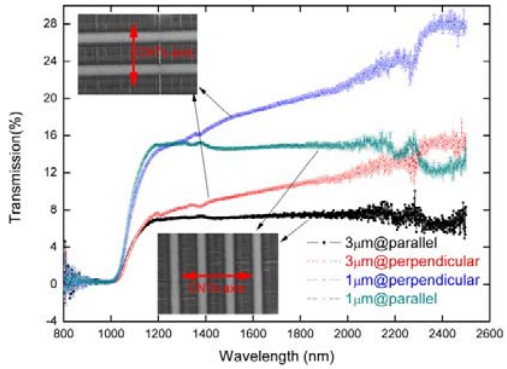

Fig. 3. Infrared transmission spectra as a function of wavelength for 1μm and 3 μm CNTs films.

Keywords: Multi-walled carbon nanotubes film, Infrared, Terahertz, Transmission

[1] EBBESEN, T. W., LEZEC, H. J., GHAEMI, H. F., THIO, T. & WOLFF, P. A. 1998. Extrordinary optical transmisson through sub-wavelength hole arrays. *Nature,* 391, 667-672.

[2] BARNES, W. L., MURRAY,W. A., DINTINGER, J., DEVAUX, E. &EBBESEN, T. W. 2004.

Surface plasmon polaritons and their role in the enhanced transmission of light through periodic arrays of subwavelength holes in a metal film. *Phys. Rev. Lett.*, 92, 170401-1-4.

[3] BAUMBERG, J. J., KELF, T. A., SUGAWARA, Y., CINTRA, S., ABDELSALAM, M. E., BARTLETT, P. & RUSSELL, A. E. 2005. Angel-resolved surface enhanced Raman scattering on metallic nanostructured plasmonic crystals. *Nano Lett.*, 5, 2262–2267.

[4] LIU, Z. W., WEI, Q. H. & ZHANG, X. 2005. Surface plasmon interference nanolithography. *Nano Lett.*, 5, 957–961.

[5] MONNAI, Y., JAHN, D., WITHAYAXHUMNANKUL, W., KOCH, M. & SHINODA H. 2015 Terahertz plasmonic Bessel beamformer. *Appl. Phys. Lett.*, 106, 021101

[6] JIMBA, Y., TAKANO, K., HANGYO, M. & MIYAZAKI, H. 2013. Extraordinary optical transmission through incommensurate metal hole arrays in the terahertz region. *J. Opt. Soc. Am. B*, 30, 2476-2482.

[7] ZHANG, Y., LIU, Y. K. & HAN, J. G. 2014. Electrically tunable resonant terahetz transmission in subwavelength hole arrays. *Chin. Phys. B*, 23, 067301.

Photoluminescence characteristics of CdSe quantum dots: Role of exciton-phonon coupling and defect/trap states

Dushyant Kushavah[1], P. K. Mohapatra[2], Mamraj Singh[2], Pintu Ghosh[2], P. Vasa[2], K. C. Rustagi[2], D. Bahadur[3] and B.P.Singh[2]

[1]*Centre for Research in Nanotechnology & Science, IIT Bombay-400076, Mumbai, India*
[2]*Department of physics, IIT Bombay, Mumbai-400076, India*
[3]*Department of Metallurgical Engineering and Materials Science, IIT Bombay, Mumbai-400076, India*
Email: dushyantkushavah@gmail.com, bhanups@iitb.ac.in

Colloidal semiconductor quantum dots (QDs) have attracted much attention for optoelectronic devices (LEDs, solar cells, single photon emitters, diode lasers etc.) and biological labelling. It is important to understand the basic interactions and processes affecting their spectral transitions characteristics. We report temperature dependent photoluminescence (PL) study of colloidal CdSe QDs. The role of exciton-phonon and defect/trap mediated radiative, nonradiative processes has been inferred from spectral behaviors of peak position, linewidth and PL intensity in 30 K to 300 K temperature range. We find that QDs lie in intermediate phonon dispersion regime where low energy acoustic phonons and high-energy longitudinal phonons have considerable effect on band gap shift. Temperature ranges over which the interaction of excitons with acoustic and longitudinal phonons dominate are clearly demarcated at 90 K. Former of the two is operative in lower temperature regime. While the exciton-acoustic-phonon coupling is strongly enhanced (~81 meV), reduction in exciton–longitudinal-optical phonon coupling (~29 meV) is observed, with respect to bulk CdSe due to quantum confinement. An increase in PL intensity in the temperature range 90-230 K with increasing temperature is observed. This intensity enhancement has been attributed to the detrapping of the charge carriers from localized CdSe QDs' surface states with potential depth of ~29.5 meV. It has been found that thermally activated carrier trapping by QDs' defect states play important role at low temperature, with an activation energy of about 12 meV. We also observe that at room temperature dominant quantum yield limiting process is thermal escape of charge carriers from QDs assisted by eight LO phonons scattering.

Keywords: Quantum Dots, phonon dispersion, exciton-phonon coupling, thermal escape

[1] D. Valerini, A. Cretí, M. Lomascolo, L. Manna, R. Cingolani, and M. Anni, Phys. Rev. B **71**, 235409 (2005).
[2] P. Jing, J. Zheng, M. Ikezawa, X. Liu, S. Lv, X. Kong, J. Zhao, and Y. Masumoto, J. Phys. Chem. C **113**, 13545-13550 (2009).
[3] Ong, X., Zhi, M., Gupta, S. and Chan, Y., ChemPhysChem. doi:10.1002/cphc.201500975, (2016).

Selective Dispersion of arc-discharged single-walled carbon nanotubes by polymethyl(cylic acidyl)silane

Jinling Gao[1,2], Yao Huang[1], Guoqiang Liu[1], Yongfu Lian[1]

[1]Key Laboratory of Functional Inorganic Material Chemistry, Ministry of Education, School of Chemistry and Materials Science, Heilongjiang University, Harbin 150080, China.
[2]Collage of science, Heilongjiang Bayi Agricultural University, Daqing, 163319, China

chyflian@hlju.edu.cn

Water soluble polymethyl(cylic acidyl)silane, synthesized by the hydrosilylation of cylic acid with polymethylsilane catalyzed by 2,2'-azobisisbutyronitrile, is first applied to the dispersion of the single-walled carbon nanotubes (SWNTs) produced by arc discharge method. After heating in air at a temperature of 673 K and treatment with concentrated acid, the arc-discharged SWNTs are ultrasonically dispersed in an aqueous solution of polymethyl(cylic acidyl)silane. Such obtained dispersions are subjected to ultracentrifugation, and then the supernatants are collected. Optical absorption spectra and Raman scattering evidence that polymethyl(cylic acidyl)silane demonstrate good selective dispersion ability towards the arc-discharged SWNTs. According to Naito *et al*, a fairly weak CH-π interaction plays key roles during the wrapping of poly(dialkylsilane) onto the CoMoCAT SWNTs SWNTs.[1] Therefore, the stiffness and length of main chains and side chains as well as the charge state of the polymethylsilane derivative play are assumed to be important for the dispersion of SWNTs.

Keywords: polymethyl(cylic acidyl)silane, dispersion, arc-discharged SWNTs

Reference

[1] NAITO, M., NOBUSAWA, K., ONOUCHI, H., NAKAMURA, M., YASUI, K. I., IKEDA, A., & FUJIKI, M. 2008. Stiffness-and conformation-dependent polymer wrapping onto single-walled carbon nanotubes. *Journal of the American Chemical Society*, 130, 16697-16703.

Specular Andreev reflection in graphene with the spin-orbit interaction

Yanling Yang[1,2], Chunxu Bai[2], and Xiaoguang Xu[1]

[1]*School of Materials Science and Engineering, University of Science and Technology Beijing, Beijing 100083, People's Republic of China*

[2]*School of Physics, Anyang Normal University, Anyang 455000, People's Republic of China*

Abstract

Based on the extended Blonder-Tinkham-Klapwijk (BTK) approach, the spin polarized transport properties through a ballistic graphene-based superconductor tunneling junction with the spin-orbit interaction have been investigated. We have presented a comparative study on two kinds of cases: in the presence and in the absence of specular Andreev reflection. It is shown that, in sharp contrast to the case of the retro Andreev reflection, the angularly averaged tunneling conductance for the case of specular Andreev reflection can be largely modulated by the incident energy and the spin-orbit interaction strength. Moreover, the effect of tunneling barrier on the tunneling conductance has also been taken into account. This effect is in sharp contrast to that in conventional superconductor structures. In addition, the Andreev reflections from different dispersion relations are revealed and contrasted with those in conventional semiconductor materials. Our work suggests that the graphene-based superconductor tunneling junction with the spin-orbit interaction opens a possible new route to diagnose specular Andreev reflection and access to new type nanoelectronic device.

Temperature dependence of graphene quantum dot photoluminescence

P. K. Mohapatra[1], Dushyant Kushavah[2], J. Mohapatra[2], P. Ghosh[1], P. Vasa[1], B. P. Singh[1]

[1]*Department of physics, IITBombay, Mumbai-400076, India*
[2] *Centre for Research in Nanotechnology & Science, IITBombay-400076, Mumbai, India*
Email: pranabmohapatra30@gmail.com, bhanups@iitb.ac.in

Graphene quantum dots (GQDs) have gained a significant attention in the field of biological and optoelectronic device applications for its non-toxicity and bio compatibility properties. In order to use this material for device purposes, a detail understanding of the optical processes is necessary. In our work, we report the temperature dependent photoluminescence study of GQDs prepared by thermolysis of glucose. The room temperature photoluminescence, when fitted with Gaussian functions, shows the presence of two emission bands, which can be attributed to the carbon core and the surface/edge state emission. Temperature dependent studies of photoluminescence intensity, spectral peak position and line width for these two bands are investigated in 30K to 300K temperature range. The large line width (FWHM) at 30K for the surface/edge (~ 837.7 meV) state as compared to the core (~ 504.7 meV) indicates a strong electron-electron interaction. It is observed that with increasing temperature the line width for the carbon core band increases by 37.2 meV. In stark contrast the edge/surface state band decreases by 57.2 meV, indicating strong electron-phonon interaction. The temperature dependence of photoluminescence peak energy suggests the phonon dispersion behavior for two bands are strikingly different. In case of the band associated with the carbon core the dispersion lies in the intermediate regime while for surface/edge state it is strongly dispersive. Photoluminescence quenches with the increasing temperature mainly on account of 2-phonon assisted thermal escape process. Our results suggest that the nature and strength of the interaction of electrons in the core and surface/edge states are significantly different in these quantum dots.

Keywords: Graphene Quantum Dots, Photoluminescence, Core state, surface/edge states

1. Yu, P., Wen, X., Toh, Y. R. and Jau Tang P. 2012 Temperature-Dependent Fluorescence in Carbon Dots, *J. Phys. Chem. C*, 116, 25552−25557.
2. Zhu, S., Song, Y., Zhao, X., Shao, J., Zhang, J. & Yang, B. 2015 The photoluminescence mechanism in carbon dots (graphene quantum dots, carbon nanodots, and polymer dots): Current state and future perspective. *Nano Research*, 8(2): 355–381.

Understanding the effect of water in the oxidation of graphene coated copper for dry delamination of graphene

Da Luo[1], Xueqiu You[1], Baowen Li[1], Xianjue Chen[1], Xiong Chen[1], Ming Huang[1], Sun Hwa Lee[1], Wolfgang Bacsa[2], Rodney S. Ruoff[1,3*]

[1]Center Center for Multidimensional Carbon Materials, Institute for Basic Science (IBS), Ulsan 44919, Republic of Korea

[2]CEMES-CNRS and University of Toulouse, 29 Jeanne Marvig, 31055 Toulouse, France

[3]Department of Chemistry and School of Materials Science, Ulsan National Institute of Science and Technology (UNIST), Ulsan 44919, Republic of Korea

E Mail/ Contact Details (luodarhoda@gmail.com, ruofflab@gmail.com)

The coating of graphene on Cu is known to protect Cu from thermal oxidation in air at 200 °C for hours [1], but can, such as in the presence of pinholes or grain boundaries, accelerate the corrosion of Cu after exposure to air for several days or months due to the electrochemical reactions through a galvanic corrosion process [2-3]. We have investigated the role of water vapor in the oxidation of Cu substrates coated by graphene. By introducing ^{18}O-labeled water and ^{18}O-labeled oxygen gas, we have found that the oxygen in the oxidized Cu (at the graphene interface) comes from the water only. A mechanism is proposed where the presence of graphene facilitates the reaction of water and the Cu surface. The oxidation of Cu via exposure to water vapor enables 'dry delamination' of CVD-grown graphene from the Cu substrate (with Poly(bisphenol A carbonate) as the support layer). The transferred graphene is clean and of high quality.

We have also recently studied the hydrogenation and oxidation of graphene on Cu foil using AFM lithography [4], and the functionalized graphene can be transferred to target substrates using the dry transfer method for further study; time permitting this will also be discussed. *This work was supported by IBS-R019-D1.*

Keywords: oxidation of Cu, water vapor, isotope-labeling, graphene, dry transfer

[1] Chen, S., Brown, L., Levendorf, M., Cai, W., Ju, S., Edgeworth, J., Li, X, Magnuson, C., Velamakanni, A., Piner, R., Kang, J., Park, J. & Ruoff, R. 2011. Oxidation resistance of graphene-coated Cu and Cu/Ni alloy. *ACS Nano*, 5, 1321–1327.

[2] Schriver, M., Regan, W., Gannett, W. J., Zaniewski, A. M., Crommie, M. F., & Zettl, A. 2013. Graphene as a long-term metal oxidation barrier: worse than nothing. *ACS Nano*, 7, 5763-5768.

[3] Zhou, F., Li, Z., Shenoy, G. J., Li, L., & Liu, H. 2013. Enhanced room-temperature corrosion of copper in the presence of graphene. *ACS Nano*, 7, 6939-6947.

[4] Byun, I. S., Yoon, D., Choi, J. S., Hwang, I., Lee, D. H., Lee, M. J., Kawai, T., Son, Y. W., Jia, Q., Cheong, H. & Park, B. H. 2011. Nanoscale lithography on monolayer graphene using hydrogenation and oxidation. *ACS Nano*, 5, 6417-6424.

Feasibility of 2D stacks based on hexagonal AlN sheets

R. B. dos Santos[1,2], F. de Brito Mota[1], R. Rivelino[1], A. Kakanakova-Georgieva[2], G. K. Gueorguiev[2]

[1]Instituto de Física, Universidade Federal da Bahia, 40210-340 Salvador, Bahia, Brazil

[2]Department of Physics, Chemistry and Biology, IFM, Linköping University, SE-58183 Linköping Sweden

gekos@ifm.liu.se

The intense research dedicated to graphene and its prospective applications motivated and triggered exploration into other two-dimensional (2D) systems. III-Nitride sheets such as 2D hexagonal-BN (h-BN), 2D hexagonal-GaN, and 2D hexagonal-AlN (h-AlN) are among the best candidates to be investigated in the pursuit of prospective graphene alternatives due to the electronic and optoelectronic applications for bulk III-Nitrides [1] on one side, and the structural similarity of their 2D phases to graphene, on the other.

Stability and reactivity issues as well as the electronic properties of 2D III-Nitrides are becoming a focal point of theoretical research. BN monolayers were first predicted theoretically [2] and later experimentally obtained by exfoliation [3].

We predicted the stability of 2D hexagonal-AlN sheets which emerge as a 2D analogue of technologically highly prospective wide-band gap semiconductor Aluminium Nitride.

By performing detailed modelling of the stability of hexagonal AlN (h-AlN) sheets and their structural and electronic properties within the framework of DFT at the GGA-PBE level of theory, we found a lattice parameter of 1.82 Å and an indirect band gap of 2.81 eV as well as a cohesive energy which is by 6% lower than that of the bulk AlN (wurtzite) which is suggestive for the feasibility/synthesizability of individual h-AlN sheets [4].

We also reported on h-AlN typical defects: vacancies, anti-site defects and impurities [4]. Such defects significantly change the band structure in the vicinity of the Fermi level in

comparison to the band structure of pristine h-AlN which can be used for deliberately tailoring the electronic properties of h-AlN sheets.

To address functional nanostructures based on h-AlN, we consider different stacking combinations of h-AlN sheets and graphene sheets. The structural and electronic properties of more complex stacks depend on the number of h-AlN/graphene sheets and on the stacking conuration [5]. We predict that the integrity of an h-AlN sheet and of 2D stacks based on h-AlN sheets is preserved upon oxidation by oxygen molecules. This is another indication for the feasibility of h-AlN-based stacks and even corresponding layered systems [5]

If synthesizable, the layered materials based on stacked hexagonal AlN sheets may play an essential role as substrates for growth of integrated nanostructures for optoelectronic applications, including LEDs and solar cells. They also may be prospective templates for novel hydrogen storage materials.

In this presentation we'll emphasize our encouraging theoretical findings on h-AlN in the context of the vast competence and experience on growth of III-Nitrides available in our group at Linköping University in Sweden [6, 7].

Keywords: III-Nitrides, 2D, stacks, LED, solar cell

[1] O. Ambacher, J. Phys. D: Appl. Phys. 31 (1998) 2653.

[2] S. Azevedo, J. R. Kaschny, Caio M. C. de Castilho, F. de Brito Mota, Nanotechnology 18, 495707 (2007).

[3] J.N. Coleman et al, Sci. 331 (2011) 568.

[4] Edward F. de Almeida Junior, Fernando de B. Mota, Caio M. C. de Castilho, A. Kakanakova-Georgieva and G. K. Gueorguiev, European Physical Journal B 85 (2012) 48.

[5] Renato B. dos Santos, F. de Brito Mota, R. Rivelino, A. Kakanakova-Georgieva, G. K. Gueorguiev, (2015), manuscript submitted to Nanotechnology.

[6] A. Kakanakova-Georgieva, R. R. Ciechonski, U. Forsberg, A. Lundskog and E. Janzén, Cryst. Growth & Design 9 (2009) 880.

[7] This work was supported by the Swedish Research Council (VR) (Swedish Research Links Project 348-2014-4249). G.K.G. and A.K.G. acknowledge support by the Linköping Linnaeus Initiative on Novel Functional Materials (VR). A.K.G. acknowledges support by the Swedish Governmental Agency for Innovation Systems (VINNOVA) and the Swedish Research Council (VR). R.R., R.B.S., and F.de B.M. acknowledge Conselho Nacional de Desenvolvimento Científico e Tecnológico (CNPq) for partial support. R.B.S. acknowledges support by Coordenação de Aperfeiçoamento de Pessoal de Nível Superior (CAPES).

Static and Dynamic Charge Transport of Atomically Thin $MoTe_2$ Transistors and Their Possible Applications

Yen-Fu Lin

Department of Physics, National Chung Hsing University, Taichung 40227, Taiwan

yenfulin@nchu.edu.tw

Here, atomically thin flaks were obtained to fabricate field-effect transistors by using mechanical exfoliation of 2H-type α-molybdenum ditelluride ($MoTe_2$) bulk crystal grown by chemical vapor transport. Both static and dynamic charge transport of these layered transistors were systematically investigated.[1-3] In the quasi-static measurements, charge transport ambipolarity was observed and originated from the formation of tunable Schottky barriers at the metal/$MoTe_2$ contacts. In the dynamic measurements, the low-frequency current fluctuations were monitored. The 1/*f* dependence of the noise was observed in the conducting channels in vacuum and followed the carrier number fluctuation model. More interestingly, the noise spectrum in ambient conditions changed to a Lorentzian, possibly because a large number of gas molecules absorbed at the chalcogen vacancies, enhancing the trapping and emission of carriers between two discrete energy states. Using such ambipolar $MoTe_2$ transistors, we further realized complementary-like inverters, amplifiers and environmental sensors, demonstrating their feasibility for future digital and analog circuit applications.

Keywords: two-dimensional electronics, transition metal dichalcogenide, molybdenum ditelluride, low-frequency noise, random telegraph signals, ambipolar transistors

[1] LIN, Y. F., XU, Y., WANG, S. T., LI, S. L., YAMAMOTO, M., APARECIDO-FERREIRA, A., LI, W., SUN, H., NAKAHARAI, S., JIAN, W. B., UENO, K. & TSUKAGOSHI, K. 2014. Ambipolar $MoTe_2$ Transistors and Their Applications in Logic Circuits. *Adv. Mater*. 26, 3263-3269.

[2] LIN, Y. F., XU, Y., LIN, C. Y., SUN, Y. W., YAMAMOTO, M., NAKAHARAI, S., UENO, K. & TSUKAGOSHI, K. 2015. Origin of Noise in Layered $MoTe_2$ Transistors and its Possible Use for Environmental Sensors. *Adv. Mater.* 27, 6612-6619.

Multi-wavelength Photoluminescence in CdS/CdSe Nanoheterostructures

Minh Tan Man and Hong Seok Lee*

Department of Physics, Chonbuk National University, Jeonju 54896, South Korea

*E Mail/ Contact Détails (**hslee1@ jejunu.ac.kr**)*

New composite materials and hybrid nanostructures are widely used as the basis for new-generation photonic, optoelectronic devices, and semiconducting cores, because of the unique optical properties of semiconductor nanocrystals and the possibility of their effective control owing to quantum size and shape effects. In particular, the processes and mechanisms of photoluminescence (PL) of spherical colloidal nanocrystals implanted into organic matrices are investigated intensely. In contrast to widely used spherical quantum dots hetero-nanostructures (tetrapod, nanoplatelets, etc.) with distinct regions of different material composition strongly depend on the fluorescence lifetime turns out to be extremely short due to the giant oscillator strength of the transition, and multiple wavelengths of emission due to radiative excitonic recombination in the different material regions. In this work, we have synthesized and analyzed hetero-nanostructures in the form of two components CdS/CdSe nanostructures. Comparable PL intensities were derived from the CdS core and CdSe under electrical excitation conditions. Given the large size of the CdSe shell, the absorption cross section at excitation energies smaller than the CdS band gap is dominated by the shell. Excitons generated in CdSe are rapidly localized in the CdS core, whereupon radiative recombination takes place. The unique optical properties obtained for these structures promise to offer great opportunities for biological labels, energy transfer pairs, new hybrid LEDs with a high external quantum efficiency and improved color purity, as well as effective photovoltaic elements.

Keywords: Heterostructures, CdS/CdSe, carrier dynamics, energy transfer pairs

[1] ITHURRIA, S., TESSIER, M. D., MAHLER, B., LOBO, R. P. S. M., DUBERTRER B. & EFROS, Al. L. 2011. Colloidal nanoplatelets with two-dimensional electronic structure. *Nat. Mater. 10, 936-941.*

Selective Area Growth of Semi-polar InGaN/GaN Core-Shell Light Emitting Diodes

Zhiqiang Liu[1,2], Zhi Li[1,2], Junjie Kang[1,2,] Xiaoyan Yi[1,2], Guodong Yuan[1,2], Junxi Wang[1,2], Jinmin Li[1,2], Luna[3], Ian Ferguson[4]

[1]*Research and Development Center for Solid State Lighting, Institute of Semiconductors, Chinese Academy of Science，Beijing, 100086,China*

[2]*State Key Laboratory of Solid State Lighting, Beijing, 100086,China*

[3]*Lyles School of Civil Engineering, Purdue University, West Lafayette, IN 47907, U.S.A*

[4]*College of Engineering and Computing, Missouri University of Science and Technology, 305 McNutt Hall, 1400 N. Bishop, Rolla, MO 65409, U.S.A*

The hexagonal GaN pyramids structures were grown on a (0001) oriented SiO2/GaN/sapphire patterned substrate by selective area growth via metal-organic chemical deposition. The LEDs with semi-polor InGaN multiquantum well (MQW) structures were prepared on these GaN microstructures. The dimensions of the hexagonal GaN pyramids were determined by scanning electron microscopy. The basic understanding for the growth kinetics of hexagonal GaN pyramids structure was analyzed via the total surface energy calculation. Furthermore, pyramid arrays InGaN/GaN core-shell light emitting diodes (LEDs) were fabricated using a highly homogeneous multilayer graphene transparent conductive electrode, which exhibited excellent optical, structural and electrical properties. Our results provide the basic understanding for controlled growth of hexagonal GaN pyramid structures and demonstrate that graphene offers an excellent current spreading and transparent conductive properties for nano-or micro-scale photoelectric devices.